UNIVERSITAT DE BARCELONA

Novel molecular alterations in amyotrophic lateral sclerosis and frontotemporal lobar degeneration spectrum

Pol Andrés Benito

Novel molecular alterations in amyotrophic lateral sclerosis and frontotemporal lobar degeneration spectrum

Doctoral thesis in Biomedicine
Specialty Neuroscience
School of Pharmacy

Institute of Neuropathology - Bellvitge University Hospital (HUB), Bellvitge Biomedical Research Institute (IDIBELL)
Department of Pathology and Experimental Therapeutics - School of Medicine, University of Barcelona (UB)
Network Center for Biomedical Research in Neurodegenerative Diseases (CIBERNED)

Pol Andrés Benito

Thesis directors:
Prof. Isidro Ferrer Abizanda and Prof. Ester Aso Pérez

UNIVERSIDAD DE BARCELONA

Facultad de Farmacia

Programa de Doctorado en Biomedicina

Novel molecular alterations in amyotrophic lateral sclerosis and frontotemporal lobar degeneration spectrum

Memoria presentada por Pol Andrés Benito para optar al título de Doctor por la Universidad de Barcelona. Esta tesis ha sido realizada bajo la dirección y supervisión del Prof. Isidro Ferrer Abizanda y la Prof. Ester Aso Pérez en el Instituto de Neuropatología del Hospital Universitario de Bellvitge (IDIBELL), en el Departamento de Patología y Terapéutica Experimental de la Universidad de Barcelona y Centro de Investigación Biomédica en Red sobre Enfermedades Neurodegenerativas (CIBERNED).

Director/Tutor
Dr. Isidro Ferrer Abizanda

Directora
Dra. Ester Aso Pérez

Doctorando
Pol Andrés Benito

“Let us keep looking in spite of everything. Let us keep searching
It is indeed the best method of finding, and perhaps thanks to our efforts,
the verdict we will give such a patient tomorrow
will not be the same we must give this patient today.”

Jean-Martin Charcot


P

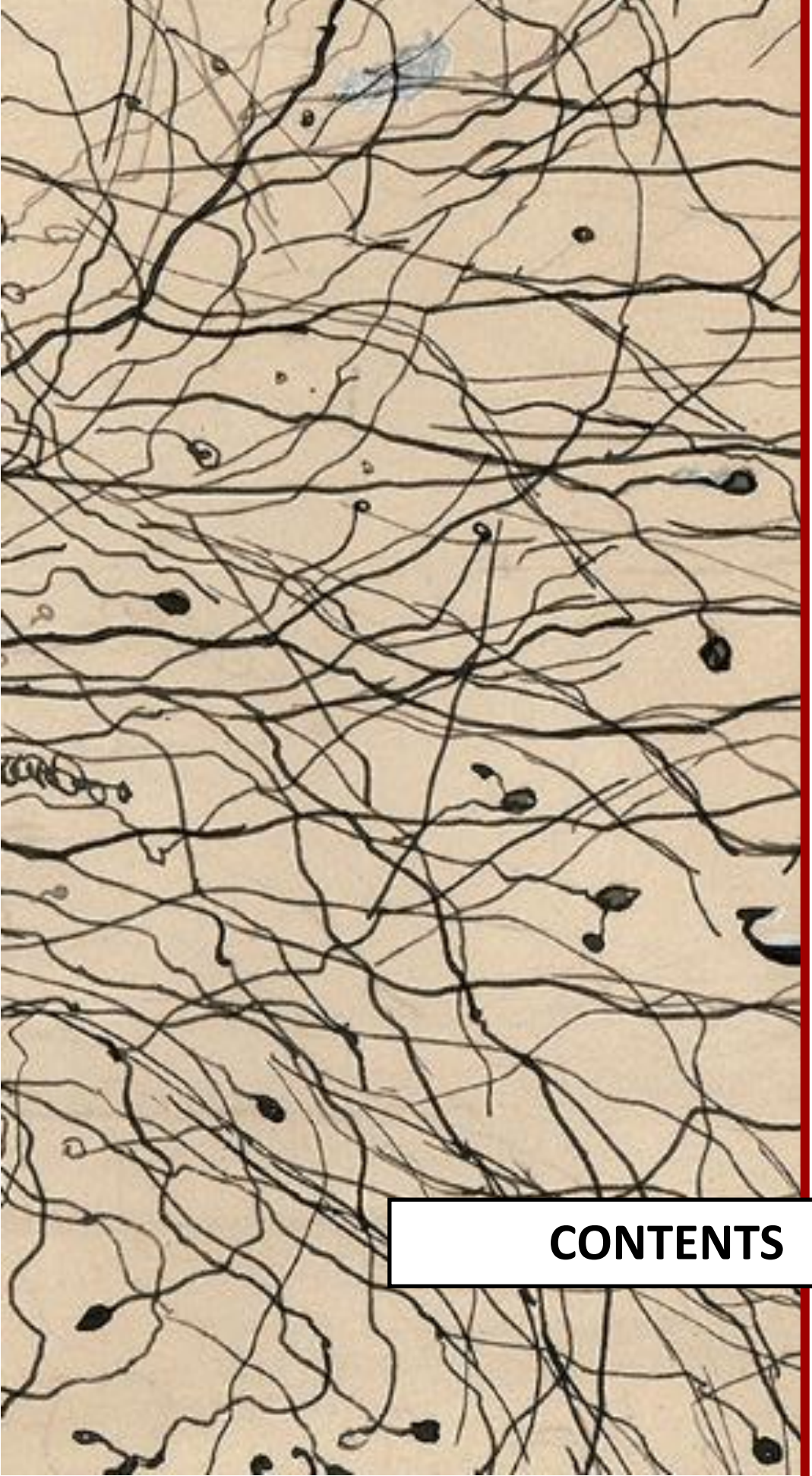

CONTENTS

CONTENTS

CONTENTS

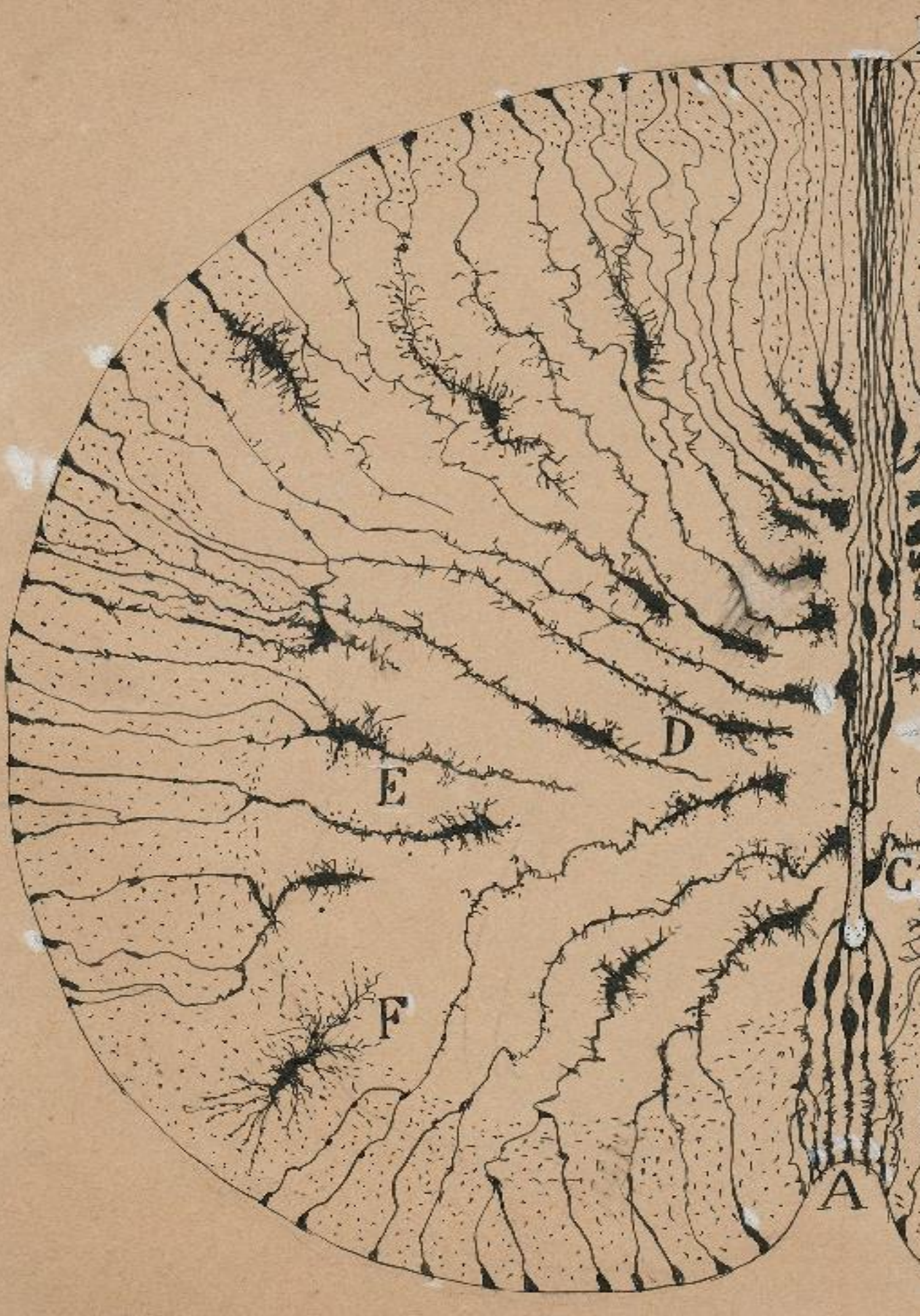
D
E
C
F
A

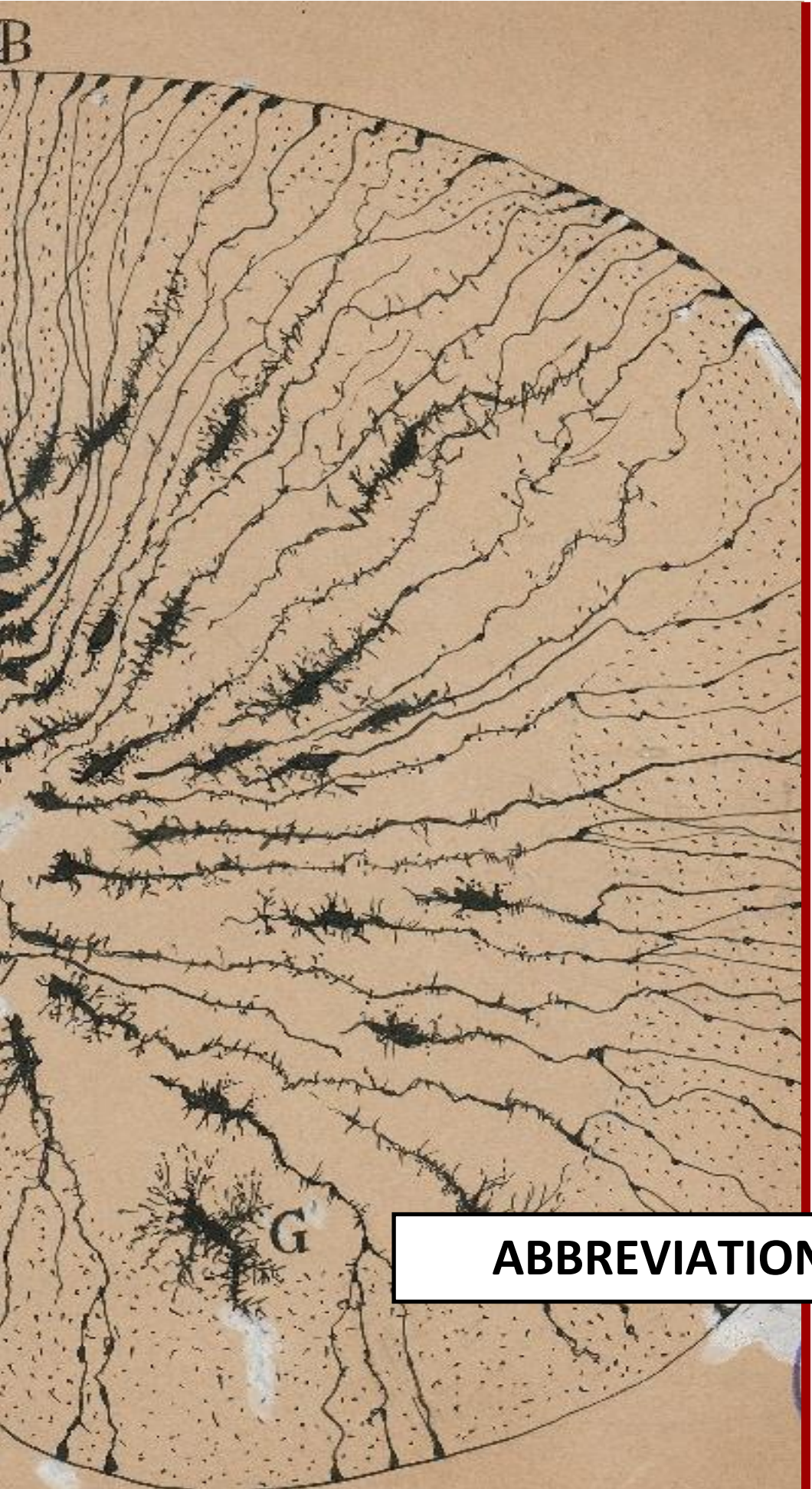

ABBREVIATIONS

Abbreviations

A

AD
Alzheimer's disease
ADP
adenosine diphosphate
AMPAr
α-amino-3-hydroxy-5-methylisoxazole-4-propionate receptor
ALS
amyotrophic lateral sclerosis
ATP
adenosine triphosphate

B

BB
Bunina bodies
bvFTLD
behavioural-variant frontotemporal dementia

C

C9ORF72
chromosome 9 open reading frame 72
c9FTLD
familial frontotemporal lobar degeneration linked to chromosome 9 open reading frame 72 expansion
C-I
complex I
C-II
complex II
C-III
complex III
C-IV
complex IV
C-V
complex V
CBS
corticobasal syndrome
CHCHD10
coiled-coil-helix-coiled-coil-helix domain containing 10
COX
cytochrome C oxidase
CSF
cerebrospinal fluid
CNS
central nervous system
CSI
Crescent-shaped inclusions
CTF
C-terminal fragment

D

DNA
deoxyribonucleic acid
DNAAF1
dynein axonemal assembly factor 1
DNs
dystrophic neurites

E

ETC
electron transport chain

F

fALS
familial amyotrophic lateral sclerosis
fFTLD
familial frontotemporal lobar degeneration
FTD
frontotemporal dementia
FTLD
frontotemporal lobar degeneration
FUS
Fused in sarcoma

G

GCIs
glial cytoplasmic inclusions

H

HD
Huntington's disease
HI
hyaline inclusions
hnRNP
heterogeneous nuclear ribonucleoprotein

I

IFs
intermediate filaments
IMM
inner mitochondrial membrane
IMS
intermembrane space

K

KA
kainic acid

L

LBHI
Lewy body-like hyaline inclusions
LMN
lower motor neurons
LRRC50
leucine-rich repeat-containing protein 50

M

MND(s)
motor-neuron disease(s)
MTs
microtubules

N

NCIs
neuronal cytoplasmatic inclusions
NDD
neurodegenerative disease
NES
nuclear export signal
NFH
neurofilament heavy
NFL
neurofilament light
NFM
neurofilament medium
nfvPPA
nonfluent variant of primary progressive aphasia
NIIs
neuronal intranuclear inclusions
NLS
nuclear localization signal
NMDAr
N-methyl-D-aspartic acid receptor

O

OMM
outer mitochondrial membrane
OPCs
oligodendrocyte progenitor cells
OXPHOS
oxidative phosphorylation

P

PD
Parkinson's disease
PSP
progressive supranuclear palsy

R

RBPs
RNA-binding proteins
RNA
ribonucleic acid
RNS
reactive nitrogen species
ROS
reactive oxygen species

S

sALS
sporadic amyotrophic lateral sclerosis
sFTLD
sporadic frontotemporal lobar degeneration
sFTLD-TDP
sporadic frontotemporal lobar degeneration TDP-43 immunoreactive
SGs
stress granules
SLI
skein-like inclusions
SOD1
superoxide dismutase 1
svPPA
semantic variant of primary progressive aphasia

T

TDP-43
TAR DNA-binding protein 43
TLR
toll-like receptor

U

UMN
upper motor-neurons
UPS
ubiquitin-proteosome system

V

VCP
valosin-containing protein
VDAC
Voltage-dependent anion-selective channel


c
c
c

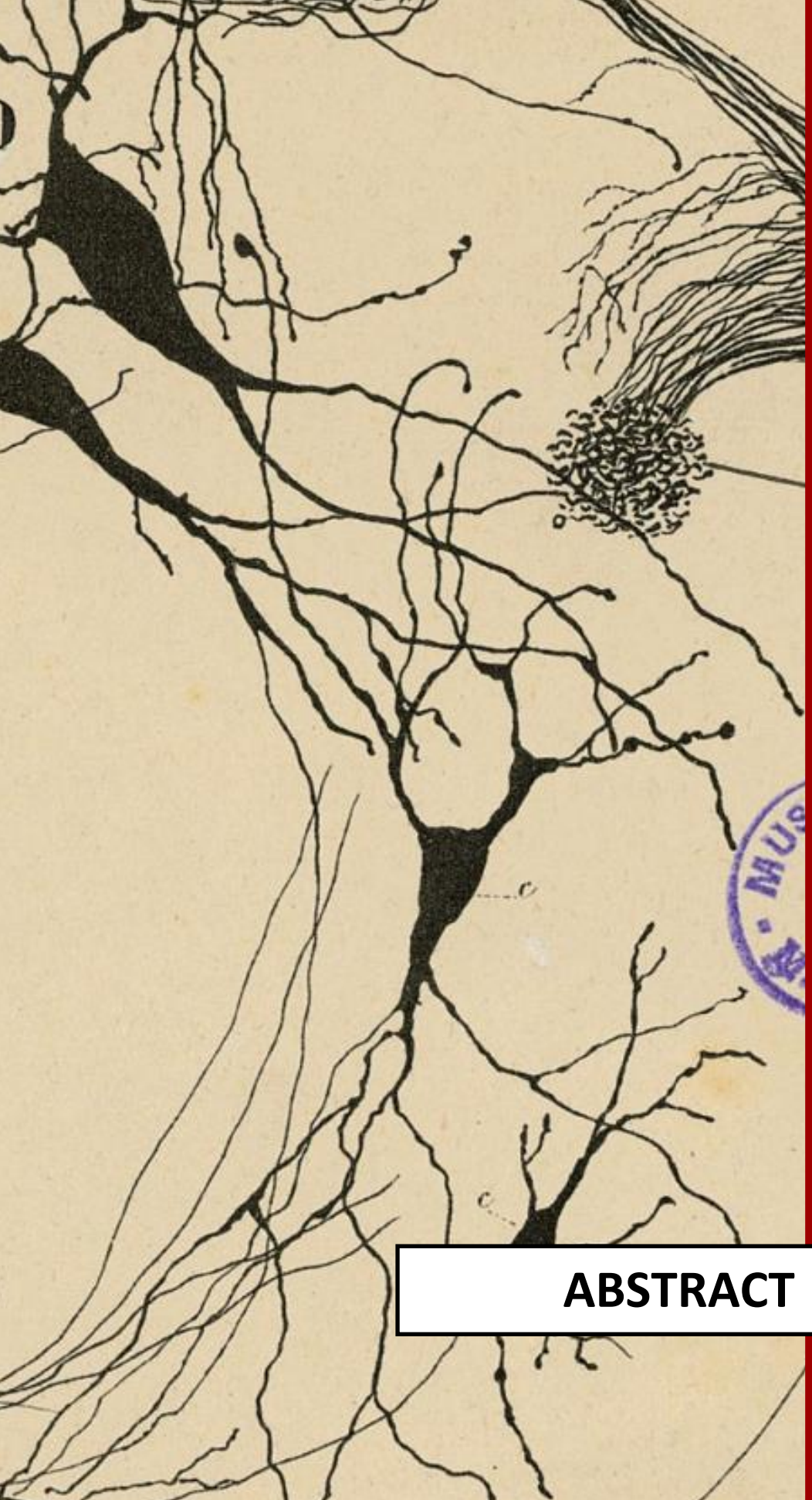

ABSTRACT

Abstract

Amyotrophic lateral sclerosis (ALS) and frontotemporal lobar degeneration (FTLD) are clinically distinct neurodegenerative diseases that are connected by genetic and pathological overlap. ALS patients present with muscle weakness and spasticity associated with degeneration of motor neurons in the motor cortex, brainstem, and spinal cord that ultimately leads to death. In contrast, patients with FTLD display cognitive dysfunction associated with degeneration of neurons in the frontal and temporal lobes of the brain. Despite being clinically distinct, 15% of individuals presenting FTLD also have ALS, whereas 30% of individuals with ALS will develop FTLD. This implies that these two neurodegenerative diseases are part of a shared clinical spectrum. In recent years, several mechanisms have been proposed as contributory factors in the pathogenesis of neuron damage in ALS and FTLD, including excitoxicity, mitochondrial and energy metabolism failure, oxidative stress damage, altered glial cells, inflammation, cytoskeletal abnormalities, alterations in RNA metabolism, and altered TDP-43 metabolism, among others. However, it is poor known about the etiology of these disorders and their possible treatment. The objective of the investigations presented in this doctoral thesis is focused in the identification of new molecular alterations underlying motor and cognitive changes in *post-mortem* human spinal cord and brain samples of ALS patients and brain samples of FTLD-TDP patients compared with controls, combining microarray, mRNA, protein and enzyme assays studies. The obtained results have identified molecular alterations in ALS and FTLD of different biological functions and cellular pathways including changes in mitochondrial energy metabolism, neuroinflammation, neuronal structure, neurotransmission, axonal transport mechanisms and oligodendrocyte function; allowing in turn, the screening and identification of new candidate molecules as biomarkers for these disorders.

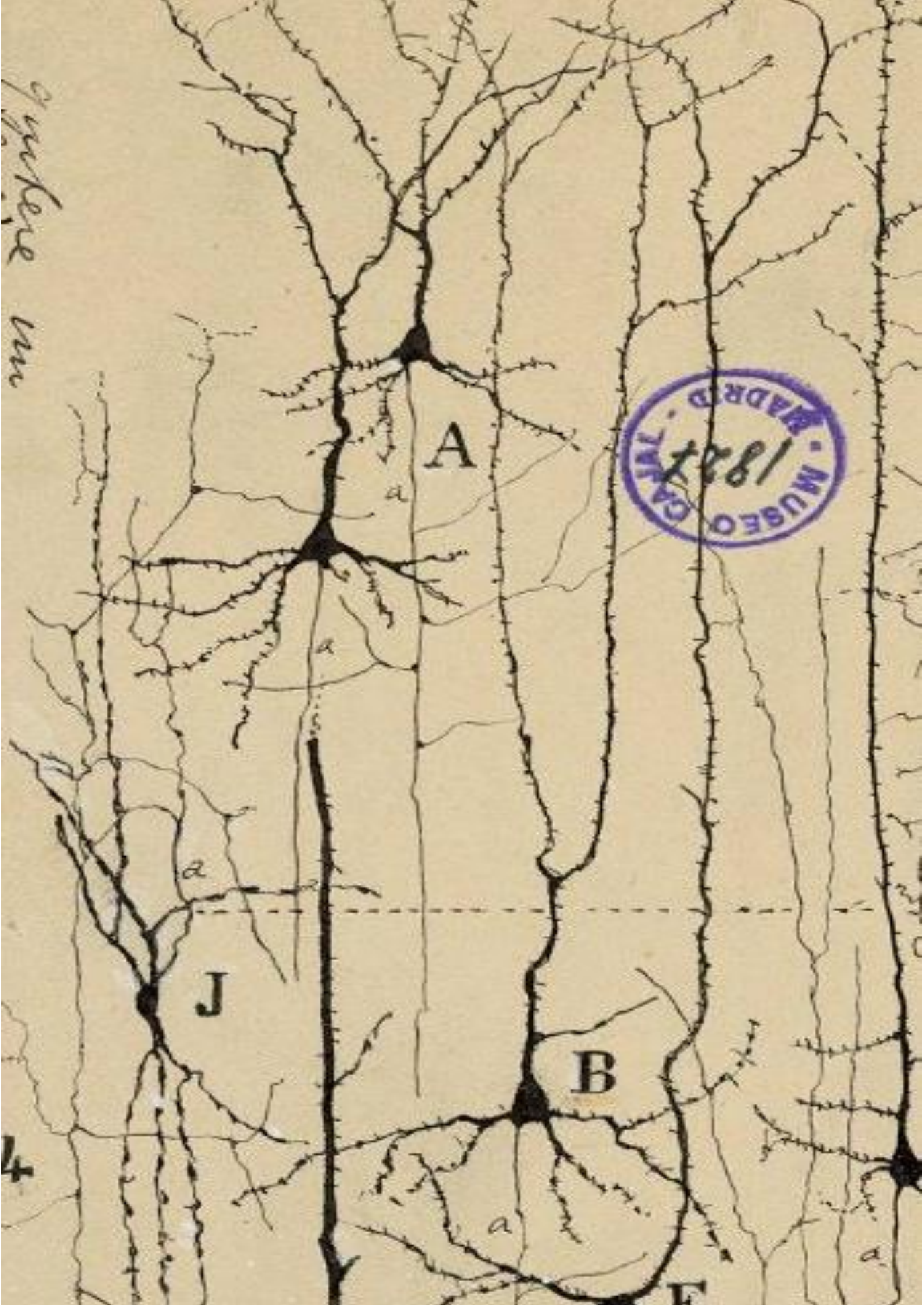
A
a
J
B
E
a
a
a

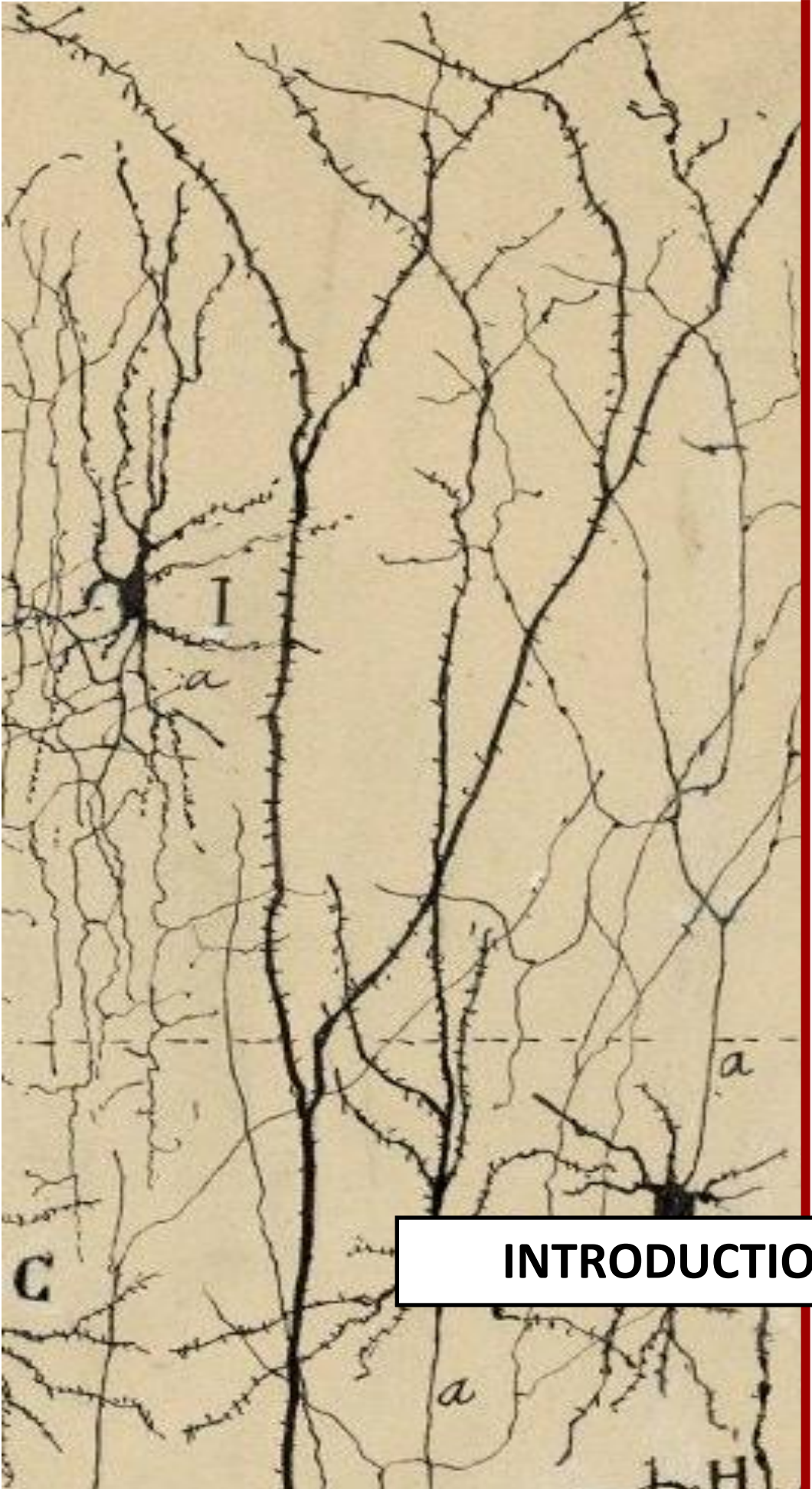

INTRODUCTION

1 Neurodegenerative diseases

1.1. Overview

Ageing, which all creatures must encounter, is a challenge to every living organism. In the human body, it is estimated that cell division and metabolism occur exuberantly until about twenty-five years of age. Beyond this time, subsidiary products of metabolism and cell damage accumulate and the phenotypes of ageing appear, causing appearance of disease in the long term. Among age-related diseases, neurodegenerative diseases (NDD) have drawn a lot of attention due to their lack of effective treatment, their irreversibility and the economic and social cost that they represent (Hung *et al.*, 2010). *Neurodegenerative disease* is an umbrella term for a range of conditions that primarily affect the neurons in the human brain. Etymologically, the word neurodegeneration is composed of the prefix “neuro-,” which designates nerve cells, and “degeneration,” which refers to, in the case of tissues or organs, a process of losing structure or function, including death of neurons. In practice, NDD represent a large group of heterogeneous neurological disorders with variegated clinical and pathological expressions affecting specific subsets of neurons in specific functional anatomic systems, which arise for reasons that are not well-understood and progress in a relentless manner, affecting the structure and function of the central nervous system and/or peripheral nervous system (Przedborski *et al.*, 2003).

Intracellular protein aggregates are a common neuropathological feature of all neurodegenerative diseases, suggesting that these disorders might share cellular and molecular alterations (Bayer, 2013). These disorders are caracterized by the aberrant aggregation of a protein with physiological function in normal states. In all cases, proteins aggregate due to several combined factors including mutations in specific genes, changes in alternative splicing, enhanced protein production, aberrant post-translational modifications (e.g. phosphorylation, advanced glycation, deamidation, truncation) and altered protein clearance, which result in a change in the conformation of the protein different from its native condition with loss of binding partners, and leading to reticular stress, oxidative damage and inflammatory responses, among other reactions (Carrel and Lomas, 1997; Kovacs *et al.*, 2010).

Thus, altered proteins become pathologically active, aggregating and accumulating at different subcellular locations and resulting in a toxic gain or loss of function by interference with normal cellular processes (Nijholt *et al.*, 2011). It is important to note that the risk of self-association and aggregation, associated or not with a genetic mutation, is largely increased by proteins which are inherently able to undergo radical changes in their conformation (Carrel and Lomas, 1997).

In addition to proteostasis network disturbances, proteinopathies include fundamental molecular abnormalities involved in basic mechanisms of neuronal loss and selective vulnerability. These include oxidative stress and free radical formation, mitochondrial dysfunction and impaired energectic metabolism, deoxyribonucleic acid (DNA) damage, neuroinflammation and neuroimmune processes, alterations in synaptic systems and disruption of

axonal transport, among other mechanisms (Jellinger, 2010; Nijholt *et al.*, 2011).

These common features allow grouping of these NDD under the term of "protein misfolding diseases" or "proteinopathies", characterized either by a single type of proteinaceous aggregate or by two different aggregated proteins. However, proteinopathies are often mixed, making a definite diagnosis and therapy difficult.

The period between the first events initiating neurodegeneration and the clinical manifestation may last for decades. The aggregates accumulate early in the lifetime of the individual, but only manifest clinically in middle or late life (Skovronsky *et al.,* 2006). Major clinical symptoms are cognitive decline, dementia and movement disorders, and combinations of them. Most cases are sporadic, but the evidence for genetic causative factors is very strong, as many of the disorders are closely linked to mutations that make the mutated protein more prone to misfold and aggregate (Bertram and Tanzi, 2005). Neverthless, the most common risk factors are ageing (Walker and LeVine, 2000) and sometimes traumatic brain injury (DeKosky *et al.*, 2010) in combination with other environmental and endogenous factors (Skovronsky *et al.,* 2006).

The most prevalent proteinopathy is Alzheimer's disease (AD) although many more exist, such as Parkinson's disease (PD), Lewy body disease (LBD), prion diseases, tauopathies, amyotrophic lateral sclerosis (ALS), frontotemporal lobar degeneration (FTLD), Huntigton's disease, certain familial hereditary spinocerebellar ataxias, and many other disorders like familial British and Danish dementias (Table I).

Protein	Disease type
Aβ	Alzheimer's Disease (AD)
Tau	Globular glial tauopathy (GGT), Corticobasal degeneration (CBD), Progressive supranuclear palsy (PSP), Argyrophilic grain disease (AGD), Pick disease (PiD), FTD and PD linked to chr-17 tauopathy (FTDP-17T), Primary age-related tauopathy (PART)
TDP-43	Frontotemporal lobar degeneration TDP-43 (FTLD-TDP), Motor neuron disease TDP-43 (MND-TDP/ALS), Frontotemporal lobar degeneration with motor neuron disease TDP-43 (FTLD-MND-TDP)
FUS	Motor neuron disease FUS (MND-FUS), Atypical FTLD with ubiquitinated inclusions (aFTLD-U), Neurofilament intermediate filament inclusion disease (NIFID), Basophilic inclusion body disease (BIBD)
α-syn	Parkinson's disease (PD), Dementia with Lewy bodies (DLB), Multiple system atrophy (MSA)
PrP	Creutzfeldt-Jakob disease (CJD), fatal insomnia (FI), Kuru, Gerstmann-Sträussler-Scheinker disease (GSS), variably protease-sensitive prionopathy (vPSPr)
TRD	Huntington's Disease (HD), Spinocerebellar ataxia (SCA), Fragile X associated tremor and ataxia syndrome (FXTAS), Spinal and bulbar muscular atrophy (SBMA), Dentatorubral-pallidoluysian atrophy (DRPLA)
Others	Neuroserpinopathy, Heredetiray ferritinopathy, neurodegeneration with brain iron accumulation (NBIA), Hereditary amyloidoses

Table I. List of major neurodegenerative disorders classified on the basis of their characteristic protein alterations. Abbreviations: alpha-synuclein (α-syn); Beta-amyloid (Aβ); Fused in sarcoma (FUS); Prion protein (PrP); triplet repeat diseases (TRD); modified from Kovacs 2016.

As mentioned above, among the different protein aggregates, neuronal intracytoplasmic transactive response (TAR) DNA binding protein 43 (TDP-43)-immunoreactive inclusions are neuropathological hallmarks of the majority of cases with ALS and, by definition, of all cases of FTLD-TDP, including cases with *C9ORF72* mutated forms in both diseases.

The present thesis is focused on the study of ALS, FTLD-TDP and c9FTLD (as a particular form of genetic FTLD-TDP), which are classified according to the major component of their deposits, phosphorylated TDP-43 protein, as TDP-43pathies, and more specifically included into the spectrum of ALS-FTLD-TDP43 diseases.

1.2. TDP-43 proteinopathies

Despite significant clinical, genetic and neuropathological overlapping, frontotemporal lobar degeneration (FTLD) with or without motor neuron disease and amyotrophic lateral sclerosis (ALS) have been historically considered as separate entities (Mackenzie and Feldman, 2005). However, this axiom changed when Neumann and colleagues (2006) revealed trans-activation response element (TAR) DNA binding protein-43 (TDP-43) to be the major pathological protein in the inclusions of frontotemporal lobar degeneration with ubiquitin-positive inclusions (FTLD-U) with or without motor neuron disease, and in amyotrophic lateral sclerosis (ALS) (Neumann *et al.*, 2006).

This discovery provided the strongest evidence to date that these conditions are part of the same clinicopathological spectrum of disease unifying the majority of cases of FTLD with ubiquitin inclusions (FTLD-U) and ALS cases within the same spectrum (Neumann *et al.*, 2006). Aggregates of TDP-43 have been identified in multiple brain areas in ALS as well as in FTLD-TDP throughout the central neurvous system (Brandmeir *et al.*, 2008; Nishihira *et al.*, 2009). Different studies have confirmed TDP-43 pathology in large cohorts of cases representing the most common forms of TDP-43 proteinopathy according to their clinical phenotype as well as to their morphological subtypes. The most common phenotypes are (i) pure ALS, (ii) pure FTD-TDP, and (iii) a combination of both in FTLD-MND (Geser *et al.*, 2009). In addition, detailed reviews of the significance of clinical overlap and transition forms among ALS, ALS-FTLD-TDP, FTLD-MND and FTLD-TDP have been published (Strong, 2008; Elman *et al.*, 2008).

1.2.1. TAR DNA-binding protein 43 structure

Transactive response DNA-binding protein 43 (TDP-43) is a 414 amino acid nuclear protein encoded by the *TARDBP* gene on human chromosome 1 (1p36.22) which contains six transcribed exons. The major protein form of TDP-43 is translated from exons 2–6, resulting in a 414 amino acid protein (Figure 1A). It is highly conserved and ubiquitously expressed in a variety of tissues including the nuclei of neurons and glial cells in the central nervous system (Buratti *et al*., 2001).

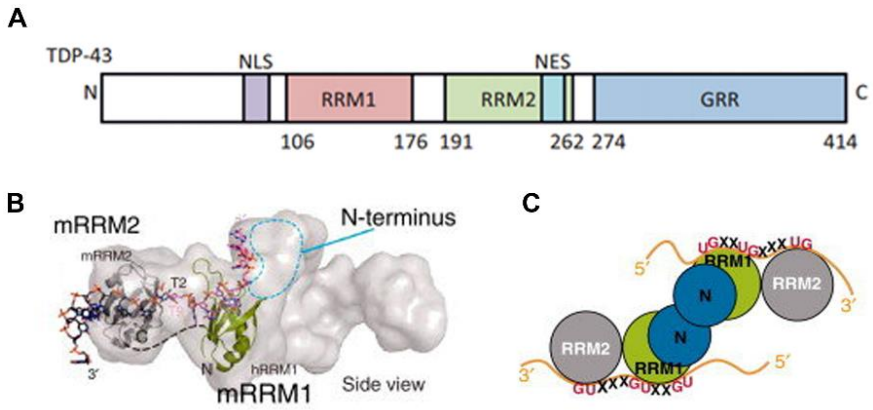

Figure 1. Structure of TDP-43 protein. (A) Schematic representation of TDP-43 aminoacid sequence. **(B)** TDP-43 binds to both DNA and to RNA. The small angle X-ray scattering (SAXS) envelope of TDP-43 dimer is fitted with the crystal structure of RNA recognition motif (hRRM1)-DNA and mRRM2-DNA in the orientation allowing the DNA to form a continuous 5'–3' strand, as it is bound from hRRM1 to mRRM2 in TDP-43. **(C)** Schematic representation of the domain structure of TDP-43 homodimer, which binds to a long UG-rich RNA via its RRM1 and RRM2 domains. Adapted from Lee and McMurray, 2014.

TDP-43 is physiologically active as a homodimer (Figure 1B and 1C). Each monomer contains two RNA-recognition motifs (RRM1: ~aa 106–176 and RRM2: ~aa 191–262) and a glycine-rich C-terminal region (GRR: ~aa 274–414) containing a Q/N-rich prion-like domain that allows it to bind single nucleic acid strands and proteins, respectively (Buratti *et al*., 2001; Wang *et al*., 2004). TDP-43 protein also contains both nuclear localization signal (NLS) and nuclear

export signal (NES), which allows it to shuttle between the nucleus and the cytoplasm, although the protein is predominantly located in the nucleus (Coehn *et al.,* 2011) (Figure 1A).

1.2.2. TAR DNA-binding protein 43 function

TDP-43 is a highly conserved, ubiquitously expressed heterogeneous nuclear ribonucleoprotein (hnRNP), mainly present in the nucleus, but it shuttles in and out of the cytoplasm and along axons. The physiological functions of TDP-43 protein are wide and variegated, including its role in different cellular functions such as mRNA stability (Volkening *et al.,* 2009; Ayala *et al.,* 2011b), mRNA and miRNA processing (Buratti *et al*., 2010; Kawahara and Mieda-Sato, 2012), mRNA transport (Godena *et al.*, 2011; Wang *et al.,* 2008) and negative regulation of alternative splicing (Buratti *et al*., 2001) (Figure 2). TDP-43 regulates many non-coding and protein-coding RNAs, covering proteins involved in neuronal survival, and modulating the expression of genes relevant in neurodegenerative diseases (Tollervey *et al*., 2011), as well as mitochondrial transcripts which play a role in maintaining mitochondrial homeostasis (Izumikawa *et al*., 2017). Recently it has suggested that it may act as a neuronal activity-response factor, involved in the regulation of neuronal plasticity (Sephton *et al.,* 2012). Moreover, thousands of RNAs are bound by TDP-43 in neurons (Sephton *et al.*, 2011). For example, in human spinal motor neurons, TDP-43 acts as a low molecular weight neurofilament (hNFL) mRNA-binding protein (Strong *et al*., 2007). TDP-43 also acts as a neuronal activity response factor in dendrites of hippocampal neurons, suggesting possible roles in regulating mRNA stability, transport and local translation in neurons (Wang *et al*., 2008).

Additionally, in response to an oxidative insult or under stress conditions, TDP-43 may contribute to cell survival, associating with stalled translation initiation complexes localized in stress granules (SGs) which are transient, dense, non-membrane-bound aggregations (100-200 nm) in the cytosol composed of proteins and RNAs that appear when the cell is under stress, acting as sorting stations for mRNAs (Figure 2) (Nover *et al.*, 1989). Nevertheless, stress granules can also precipitate the formation of toxic protein aggregates such as those seen during the progression of certain types of neurological disease (Colombrita *et al.*, 2009; Higashi *et al.*, 2013).

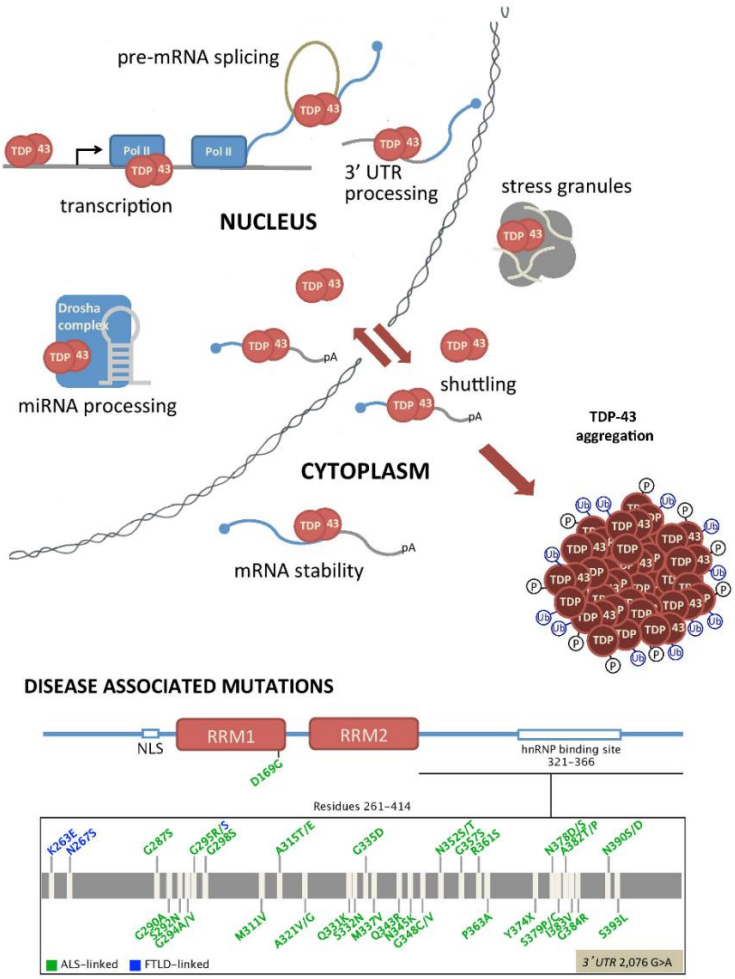

Figure 2. Schematic representation of TDP-43 functions in physiological conditions and main mutations in TARDBP gene located in the C-terminal glycine-rich domain. Modified from Ayala, 2008.

TDP-43 protein acts via its two RNA recognition motifs (RRM1 and RRM2), binding both mRNA and DNA molecules, predominantly within long introns and in the 3'UTR region of mRNAs, whereas the exon skipping, splicing and inhibitory activity, and SGs formation, require the glycine-rich C-terminal domain of TDP-43 that binds to several proteins, such as other members of the heterogeneous nuclear ribonucleoprotein family (Wang *et al.*, 2004; Buratti *et al.*, 2005). Notably, the identification of missense mutations in *TARDBP* gene in patients with ALS and FTLD has revealed that several mutations are located in the C-terminal glycine-rich domain, most of which is localized within the prion-like domain (Barmada *et al.*, 2010), and encoded by exon 6 (Figure 2). It is worth stressing that exon 6 encodes ∼60% of the TDP-43 protein and more than 70% of the entire mRNA transcript. In light of these observations, it is clear that exon 6 and its encoded glycine-rich domain are critical components of the TDP-43 protein (Pesiridis *et al.*, 2009).

1.2.3. TAR DNA-binding protein 43 regulation

Little information exists about the factors that regulate TDP-43, and how post-translational modifications affect TDP-43 function. Preliminary research identified specific TDP-43 residues that undergo phosphorylation under physiological conditions as well as multiple other predicted phosphosites. Based on their positions, the reported and predicted phosphosites may affect key TDP-43 processes, e.g. cellular trafficking and RNA interactions. Thus, it is hypothesized that TDP-43 is regulated by phosphorylation and that several disease-associated mutations or insults have the capacity to change the phosphorylation profile with deleterious consequences on protein function (Li *et al.*, 2017).

Given its crucial function in the processing of thousands of RNA transcripts, the levels of TDP-43 protein are tightly controlled through autoregulation mechanisms, as the protein binds to and edits its own 3' untranslated region mRNA leading to degradation of the TDP-43 transcript. A decrease in the cellular levels of TDP-43 results in decreased transcript editing and increased translation of TDP-43 protein. Similarly, if the levels of TDP-43 are too high, TDP-43 will bind to more transcripts and induce their degradation, thus decreasing the levels of soluble TDP-43 (Ayala *et al.,* 2011b).

1.2.4. TAR DNA-binding protein 43 oligomerisation and aggregation

As a neurodegenerative disorder, the central histopathological hallmark of ALS and FTLD spectrum is the presence of TDP-43-immunoreactive inclusions or aggregates in degenerating neurons and oligodendrocytes. The origin of TDP-43-positive histopathological inclusions *in vivo* is poorly understood. Under an acute insult, the recruitment of TDP-43 containing RNA complexes into SGs via a TDP-43 Q/N-rich C-terminal targeting domain is promoted. TDP-43 is selectively recruited into specific SGs depending on the type of stress condition. Once recruited to SGs, TDP-43 might have a physiological role in the regulation of TDP-43-dependent RNAs during acute stress. However, it is hypothesized that pathological factors such as prolonged stress or ageing could induce the formation of pathological SGs, representing persistent accumulation of coalesced SGs that form TDP-43 positive inclusions, characterized pathologically as TDP-43 aggregates in ALS and FTLD-TDP. The formation of pathological SGs can inhibit TDP-43 function via cytoplasmic sequestration of normal TDP-43 and/or initiate a toxic gain or loss of function leading to mitochondrial damage and other neuronal dysfunctions (Liu-Yesucevitz *et al*., 2010; Coehn *et al.,* 2011)

Biochemical analysis of insoluble protein extracts isolated from affected FTLD-U and ALS tissue revealed a characteristic biochemical profile of TDP-43 with detection of disease-specific bands at ~25 kDa, ~45 kDa and a smear of high-molecular-mass proteins in addition to the normal 43 kDa band (Zhang *et al.,* 2007). Further analysis demonstrated that this profile is due to N-terminal truncation, hyperphosphorylation and ubiquitination of TDP-43 in FTLD-U and ALS (Neumann *et al.*, 2006), which shows characteristics of amyloid (Bigio *et al.,* 2013).

The abnormal TDP-43 together with normal TDP-43 translocates from the nucleus to the cytoplasm, giving rise to intracytoplasmic neuronal inclusions and aberrant neurites (Barmada *et al.*, 2010). The mechanism behind this redistribution is not known, and it could either be due to the translocation of TDP-43 from the nuclei to the cytoplasm, or to impaired TDP-43 cytoplasm to the nucleus shuttling process (Thorpe *et al.*, 2008; Mackenzie *et al.*, 2011; Geser *et al.*, 2011). Additionally, CTF TDP-43 contains conformationally unstable structures that correspond to the prion-like domain and the glycine-rich region with aggregation-prone properties (Zhang *et al.*, 2009). Indeed, expression of an insoluble TDP-43 C-terminal fragment is sufficient for the recruitment to SGs (Liu-Yesucevitz *et al.*, 2010). In this line, several studies have indicated that the glycine-rich C-terminal region mutations are required for TDP-43 association with SGs, most of which are localized in a prion-like domain (Barmada *et al.*, 2010).

Thus, SGs may represent a functional intersection of normal TDP-43 function and the pathological accumulation of TDP-43 inclusions, reflecting the potential for both loss and gain of function toxicity associated with TDP-43 aggregation in ALS and FTLD-TDP.

1.2.5. TAR DNA-binding protein 43 aggregates and Bunina bodies

In sporadic and most familial ALS as well as in FTLD-TDP cases, there is a loss of nuclear TDP-43 and formation of pathological aggregates mislocalized in the cytoplasm (Giordana *et al.*, 2010)**.** Inclusions are widespread and not restricted to the spinal cord, motor nuclei of the brainstem, or frontal and temporal cortices, but also present in other brain regions such as hippocampus (Al-Chalabi *et al.*, 2012). Neuronal cytoplasmic TDP-43-immunoreactive inclusions (NCIs) and glial cytoplasmic inclusions (GCIs) in oligodendrocytes are present in the majority of cases with ALS (Neumann *et al.*, 2006). Three types of neuronal TDP-43-immunoreactive inclusions have been described in FTLD with TDP-43 proteinopathy: (1) neuronal cytoplasmic inclusions (NCIs), (2) dystrophic neurites (DNs) and (3) neuronal intranuclear inclusions (NIIs). FTLD cases with MND overlap, also presenting glial cytoplasmic inclusions (GCIs) (Brandmeir *et al.*, 2008). Three different types of TDP-43-immunoreactive cytoplasmic inclusions have been described in the upper and lower motor neurons, and other regions in patients with ALS-FTLD: skein-like inclusions (SLIs), round hyaline inclusions (HIs) and dot-like inclusions (Figure 3) (Mori *et al*., 2008).

- Skein-like inclusions (SLI) are immunostained by anti-phospho-TDP-43 and anti-ubiquitin antibodies. The SLI is basically a thready structure of a bundle of thick filaments. The threads may be present singly or in the form of networks or aggregates, occasionally forming single larger inclusions that resemble hyaline inclusions (HIs) (Figure 4A and 4B). These features indicate that HIs and SLIs may be closely related (Mizusawa, 1993). The exact composition of such inclusions is not known, although proteins identified so far include, in varying amounts, phospho-TDP-43, ubiquitin, SOD1, FUS, dorfin and

peripherin, with the most prevalent being phospho-TDP-43 protein (Okamoto *et al.*, 2008). This is the most common form of TDP-43-positive inclusion in the lower motor neurons. They are found in the anterior horn cells of the spinal cord in patients with ALS and, to a lesser extent, in the hypoglossal and facial nuclei (Mori *et al.*, 2008). Skein-like inclusions can be found in other brain regions and have been observed in certain spinocerebellar ataxias.

- Round hyaline inclusions (HI) are usually round eosinophilic structures about 5-15 µm in diameter, with occasional spiculae in the marginal portion, that show immunoreactivitiy for TDP-43 and ubiquitin (Figure 3C) (Mizusawa, 1993; Piao *et al.*, 2003). Hyaline inclusions are chiefly observed within the perikarya of both normal-looking and chromatolytic anterior horn cells in the lumbar spinal cord, but some are detected in the axons and dendrites. Usually, a single inclusion is found in the perikaryon, but in rare cases two or more are noted (Sasaki *et al*., 1989). HIs are composed of various amounts of granule-associated thick filaments and neurofilaments, and are heterogeneous (Mizusawa, 1993). Several investigators have suggested that round hyaline inclusions may arise from dense compact areas of skein-like inclusions because of the ultrastructural and antigenic similarities between the two. HIs consist of dense cores with a rough peripheral halo lacking a limiting membrane, called Lewy body-like hyaline inclusions (LBHIs). LBHIs are found in a small proportion of sALS cases as well as in patients with familial ALS (fALS) due to mutations in the Cu/Zu superoxide dismutase (*SOD1*) gene. LBHIs in sALS are immunopositive for TDP-43 and those in fALS with *SOD1* mutations are immunoreactive for SOD1 but not for TDP-43 (Mizusawa, 1993).

- Dot-like inclusions are small round perinuclear aggregates composed of granulo-filamentous structures that are immunoreactive to ubiquitin and TDP-43 and approximately 1-3 µm diametre, from which round inclusions appear to arise as mature inclusions (Figure 3D) (Mori *et al.*, 2008).

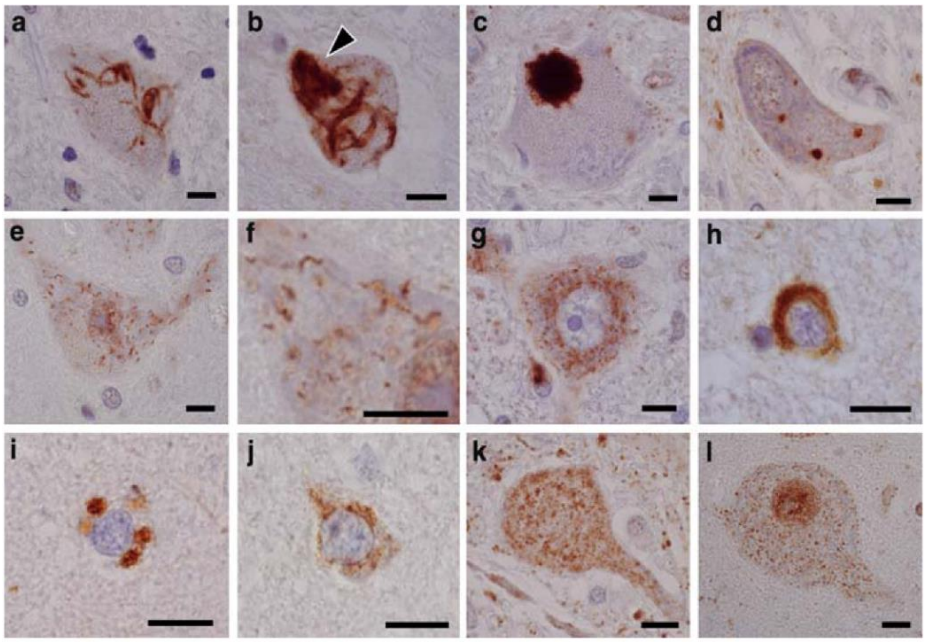

Figure 3. TDP-43 immunohistochemistry in the brain and spinal cord of patients with amyotrophic lateral sclerosis (ALS) and control subjects. (**a**) and (**b**) skein-like inclusions in the anterior horn cells. Dense compacted area (arrowhead) is also evident (**b**). (**c**) Round hyaline inclusion, spicular inclusion in the anterior horn cell. (**d**) Dot-like inclusions in the anterior horn cell. (**e**) Early thread-like structures scattered in the cytoplasm of anterior horn cell. (**f**) Higher magnification view of the area in (**e**) showing straight or wavy linear wisps. (**g**) Punctate granules in the spinal anterior horn. Note that nuclear TDP-43 immunoreactivity is absent. (**h**) Circular inclusion in the putamen. (**i**) and (**j**) Granular cytoplasmic staining in the neostriatal small neurons. Punctate granules in the spinal anterior horn (**k**) and motor cortex (**l**). Note that nuclear TDP-43 immunoreactivity is preserved (**l**) (bars 10 µm). Adapted from Mori *et al.*, 2008.

In some cases, TDP-43 proteinopathy is manifested as clearing of the nucleus and/or diffuse, or as granular cytoplasmic TDP-43 despite the absence of clearly cytoplasmic inclusions (Figure 3E-K) (Alves-Rodrigues *et al.*, 1998; Neumann *et al.*, 2006). Morphologically, the diffuse cytoplasmic TDP-43 immunoreactivity may be divided into two types: (i) diffuse punctate cytoplasmic staining as punctate structures diffusely scattered in the

cytoplasm in the brainstem and spinal cord (Figure 3G), and (ii) granular cytoplasmic immunoreactivity as a fine or coarse granular perikaryal staining in the cerebral cortex and basal ganglia (Figure 3I-J) (Cairns *et al.*, 2007; Brandmeir *et al.*, 2008). Both 'diffuse punctate cytoplasmic staining' and 'granular cytoplasmic immunoreactivity may represent incipient TDP-43 inclusion formation or 'pre-inclusions' (Cairns *et al.*, 2007; Davison *et al.*, 2007; Dickson *et al.*, 2007; Brandmeir *et al.*, 2008; Fujita *et al.*, 2008).

Additionally, other structures called Bunina bodies (BBs) may be found in the cell bodies of motor neurons in ALS (Okamoto *et al.*, 1993; Sasaki and Maruyama, 1994) and occasionally in dendrites (Kuroda *et al.*, 1990). BBs consist of small round eosinophilic inclusions with a diameter of 1-5 µm, surrounded by tubular and vesicular structures (Okamoto *et al.*, 2008).

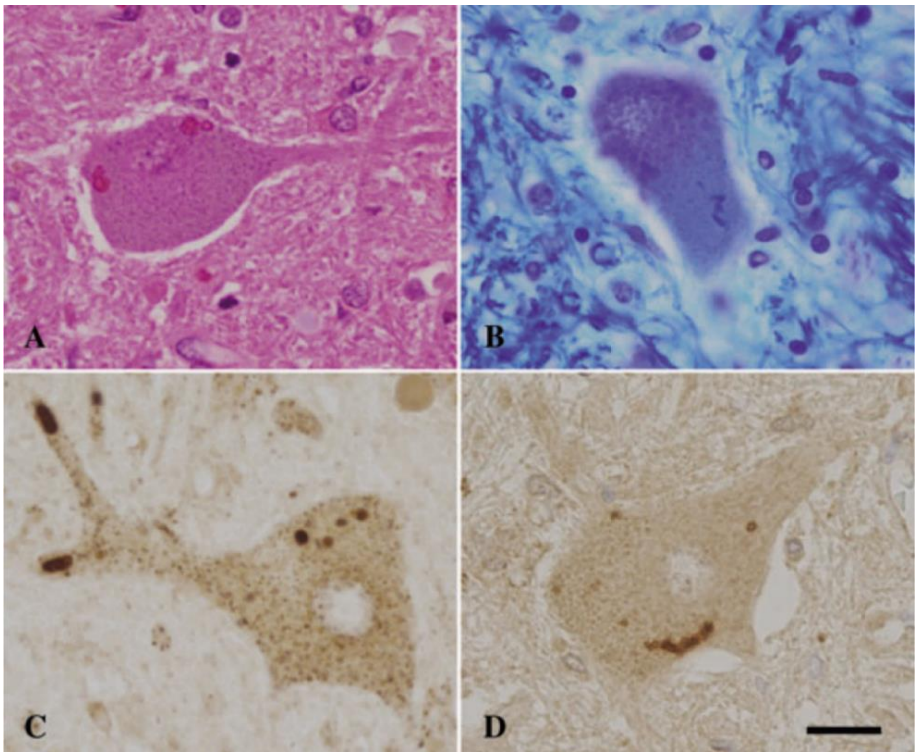

Figure 4: Bunina bodies in the anterior horn cells in the lumbar cord of amyotrophic lateral sclerosis. (A) HE staining; (B) Klüver-Barrera staining; (C) cystatin C immunoreactivity is seen in the Bunina bodies in an anterior horn cell and its dendrites; (D) transferrin immunoreactivities are seen in the Bunina bodies. (Scale bar = 20 mm). Adapted from Okamoto *et al.*, 2008.

These aggregates are composed of cystatin C, transferrin- and sortilin-related receptor CNS expressed 2 (SorCS2), and they partially colocalize with peripherin, but are negative for TDP-43 (Figure 4) (Okamoto *et al.*, 1993; Mizuno *et al.*, 2011; Miki *et al*., 2018). Ultrastructurally, these inclusions consist of electron-dense, granular material with membranous vesicular structures, and they are thought to originate in the Golgi apparatus or rough endoplasmic reticulum (Miki *et al*., 2018).

2 Amyotrophic lateral sclerosis

2.1. Discovery of ALS

ALS is considered the third most common adult-onset neurodegenerative disease (Hirtz *et al.*, 2007). It is described as a progressive, paralytic disorder characterized by degeneration of motor neurons in the primary motor cortex, motor neurons of the lower brainstem and spinal cord (Rowland and Shneider, 2001; Al-Chalabi *et al.*, 2016). The first reports of this disorder in terms of motor symptoms bring us back to the second half of the 1800s. The first description of the disease, by Charles Bell, dates back to at least 1824 (Rowland, 2001). In 1869, Jean-Martin Charcot, through careful clinical observation and meticulous work in the laboratory detailing the pathophysiology of the illness, deduced the relationship between the clinical signs and neuropathological findings at autopsy.

Charcot's work on amyotrophic lateral sclerosis classified neurological entities formerly considered as unrelated disorders to be expressions of the same disease, including primary amyotrophy and primary lateral sclerosis. In addition, these studies contributed to understanding of spinal cord and brain stem anatomy, and to the organization of the normal nervous system (Goetz, 2000). The term amyotrophic lateral sclerosis was introduced in 1874, when Charcot's works were compiled into a collection entitled 'Oeuvres Completes'

(Rowland, 2001; Kumar *et al.*, 2011). The term 'amyotrophic' comes from the Greek word *amyotrophia*, where a- means 'no', myo- refers to 'muscle', and trophia to 'nourishment'. Amyotrophia therefore means 'no muscle nourishment' which describes the characteristic atrophy of the disused muscle tissue. The second term, 'lateral', identifies the motor tracts of the spinal cord. Finally, 'sclerosis' describes the scarring that degeneration leads to in the motor tracts (Rowland, 2001; Ferrari *et al.*, 2011).

Nowadays, ALS is still referred to as Charcot's disease worldwide, as the original description of the clinical and pathological findings has virtually remained unaltered (Tan and Shigaki, 2007). In the United States it is commonly referred to as 'Lou Gehrig's disease', for the baseball great who succumbed to the illness in 1941.

2.2. Epidemiology of ALS and nomenclature of MNDs

ALS has an annual incidence of 3 to 5 cases per 100,000 people, and it is globally fairly uniform, although there are rare foci in which ALS is more common (Robberecht and Philips, 2013). There appears to be no ethnic or racial predisposition to ALS. Prior to the age of 65 or 70, the incidence of ALS is higher in men than in women, but thereafter the gender incidence is equal. ALS has an age distribution that peaks in the seventh to eighth decades.

Therefore, the incidence and prevalence of ALS increase with age. However, many different etiologies of ALS have been described including juvenile forms (Elman and McCluskey, 2012). The following scheme summarizes different ALS types and the main human motor neuron diseases (Table II).

Idiopatic motor neuron disease
- **Sporadic amyotrophic lateral sclerosis (sALS).** - sALS with frontotemporal lobar degeneration. - sALS-parkinsonism-dementia complex Western Pacific. - Parkinsonism-dementia-sALS Guadeloupe forms. - Monomeric motor neuron disease. - 'Madras-type' motor neuron disease. - Post-polio syndrome.
Autosomal dominant
- **Familial ALS (fALS).** Distal spinal muscular atrophy. Juvenile-onset ALS. fALS with frontotemporal lobar degeneration.
Autosomal recessive
- Spinal muscular atrophy (SMA) linked to chromosome 5q13. Deletions of exons 7 and 8 of the SMN1 gene; clinical manifestations depend on the number of copies of the SMN2 gene. Type I: Werdnig-Hoffmann disease. Type II: Intermediate. Type III: Kugelberg-Welander disease. - Fazio-Londe disease (FLD). - Juvenile forms of ALS.
X-linked
- Kennedy syndrome (spinal and bulbar muscular atrophy with gynaecomastia, testicular atrophy and reduced fertility): expansion at the CAG trinucleotide repeat in exon 1 of the androgen receptor (AR) located at Xq11-q12157t.
Autosomal dominant, recessive or X-linked
- Non.5q SMA (autosomal dominant or recessive: SMA-plus: with pontocerebellar hypoplasia, with respiratrory distress, with myoclonus eiplepsy, distal, scapulohumeral). - Hereditary spastic paraplegia (HSP) or Strümpell-Lorrain syndrome. Heterogeneous group associated with mutations in 19 different genes: restricted involvement of the upper motorneuron.

Table II. List of main motor neuron diseases classified on the basis of their etiology. Abbreviations: SMN1, Survival of Motor Neuron 1; SMN2, Survival of Motor Neuron 2.

2.3. Clinical symptoms of classical ALS forms

The clinical hallmark of ALS is the combination of upper and lower motor neuron signs and symptoms. Motor neurons are grouped into upper populations (UMN) in the motor cortex, and lower populations in the brain stem and spinal cord (LMN) which innervate muscle. When the failing of corticospinal (upper) motor neurons happens, weakness with slowness, hyperreflexia, abnormal reflex such as Babinski's sign, and spasticity result from degeneration of frontal motor neurons located in the motor strip (Brodman area 4) and their axons traversing the corona radiata, internal capsule, cerebral peduncles, pontine base, medullary pyramids, and corticospinal tracts of the spinal cord (Rowland, 1998; Ferguson and Elman, 2007; Elman and McCluskey, 2012). When lower motor neurons become affected in the brainstem and spinal cord, excessive electrical irritability, leading to spontaneous muscle twitching (fasciculations) is followed by neuron degeneration and loss of synaptic connectivity with target muscles, all of which results in muscular weakness and atrophy (Rowland, 1998; Ferguson and Elman, 2007; Elman and McCluskey, 2012). Usually, these clinical signs begin insidiously with focal weakness but spread relentlessly to involve most muscles. Patients experience difficulty in moving, swallowing (dysphagia), and speaking or forming words (dysarthria), culminating in diaphragm involvement that leads to death due to respiratory paralysis after 3 to 5 years from the onset of symptoms (Elman and McCluskey, 2012).

The start of ALS may be so subtle that the symptoms are overlooked (Kiernan *et al.*, 2011). Differences in site and segment of onset, pattern and speed of spread, and the degree of upper and/or lower motor neuron dysfunction produce a disorder that is remarkably variable among individuals (Elman and McCluskey, 2012). Most commonly, in about 70% of cases, the limbs are

affected first, with this debut known as 'limb onset', in which neurons in the brain and in the spinal cord start to die first. People first experience awkwardness when walking or running; tripping or stumbling may be experienced and this is often marked by walking with a 'dropped foot' which drags gently on the ground. Or there may be arm onset, marked by difficulty with tasks requiring manual dexterity such as buttoning a shirt, writing, or turning a key in a lock (Turner *et al.*, 2010). In about 25% of cases, muscles in the throat are affected initially because motor neurons in the medulla oblongata start to die first. This form is called 'bulbar onset'. Initial symptoms include difficulty in speaking and swallowing. Speech may become slurred, nasal in character, or quieter. The difficulty in swallowing may be accompanied by loss of tongue mobility (Jawdat *et al*., 2015). Finally, a smaller proportion of patients, about 5% of cases, experience a respiratory debut ('respiratory-onset'), in which the intercostal muscles that support breathing are affected first (Kiernan *et al.*, 2011).

In addition, during the past two decades, a link between ALS and frontotemporal executive dysfunction that may precede or follow the onset of upper and/or lower motor neuron dysfunction has been called ALS or MND with dementia: ALS-D or MND-D (Ringholz *et al.*, 2005; Murphy *et al.*, 2007a and 2007b; Takeuchi *et al.*, 2016). It has been recognized that up to 50% of patients with ALS have at least some evidence of frontal-executive cognitive deficits and behavioural abnormalities (Phukan *et al.*, 2007) leading ultimately to dementia in about 15-20% of patients. The presentation of dementia may be dramatic and initially suggestive of a psychiatric disorder because of change in personality, impairment of judgment and development of obsessive behavior. It may also manifest as a disorder of language in the form of primary progressive aphasia (also semantic aphasia or semantic dementia). Short-term memory and spatial abilities are usually spared early in the course of the

disease (Phukan *et al.*, 2007; Logroscino *et al.*, 2010; Bang *et al.*, 2015; Ng *et al.*, 2015). Since these behavioral alterations correlate with autopsy evidence of degeneration of the frontal and temporal lobes, the condition is designated frontotemporal dementia (FTD).

In contrast, certain motor neurons are usually spared in ALS, which means that some functions are preserved. Most patients retain extraocular movements, and bowel and bladder control. With disease progression, patients may develop problems with urge incontinence and constipation because of weak abdominal musculature, but sphincter control generally is unaffected. Since the disease primarily involves motor neurons, sensory function typically is preserved, although a minority of patients complain of some numbness and paresthesia. Abnormalities have been reported in sensory nerve conduction studies in a small number of patients with ALS, but these findings often reflect the presence of an unrelated, coexistent condition (Isaacs *et al.*, 2007). Involvement of other spinal tracts, in addition to the pyramidal pathways, is not unocommon in certain familial forms linked to SOD1 mutations.

2.4. Diagnosis and treatment of ALS

ALS diagnosis is based primarily on clinical examination in conjunction with electromyography, to confirm the extent of denervation, and laboratory testing, to rule out reversible disorders that may resemble ALS (Armon, 2018). When the disease has progressed clinical symptoms and signs and neurologic examination may provide sufficient evidence for the diagnosis. Specifically, the diagnosis of ALS is made possible by: (1) history, physical and appropriate neurological examinations to ascertain clinical findings which may suggest suspected, possible, probable or definite ALS; (2) electrophysiological examinations to ascertain findings which confirm LMN degeneration in

clinically involved regions, identify LMN degeneration in clinically uninvolved regions and exclude other disorders; (3) neuroimaging examinations to ascertain findings which may exclude other disease processes; (4) clinical laboratory examinations, determined by clinical judgement, to ascertain possible ALS related syndromes; (5) neuropathologic examinations, where appropriate, to ascertain findings which may confirm or exclude sporadic ALS, coexistent sporadic ALS, ALS-related syndromes or ALS variants; and (6) repetition of clinical and electrophysiological examinations at least six months apart to ascertain evidence of progression (Brooks *et al.*, 1994).

The criteria for the diagnosis of ALS was stablished in a consensus document called the “El Escorial ALS Diagnostic Criteria” in 1990. In accordance with this document formulated by the World Federation of Neurologists in 1994 and modified in 1998, the definitive diagnosis of ALS is based on clinical and electrophysiological examination; in addition to the required clinical criteria, laboratory and imaging tests (Escorial Revisited) (Brooks *et al.*, 1994 and 2001). Essentially, the criteria classify patients into four categories of certainty: 'definite', `probable' and `possible', by taking into account their clinical, electrophysiological, neuroimaging, laboratory and neuropathological information (Table III).

Criteria	Clinical presentation
Definite ALS	It is defined on clinical grounds alone by the presence of UMN as well as LMN signs in the bulbar region and at least two of the other spinal regions or the presence of UMN and LMN signs in three spinal regions (cervical, lumbosacral and thoracic). The important determinants of the diagnosis of definite ALS in the absence of electrophysiological, neuroimaging and laboratory examinations are the presence of UMN and LMN signs together in multiple regions.
Probable ALS	It is defined on clinical grounds alone by UMN and LMN signs in at least two regions. While the regions may be different, some UMN signs must be rostral (above) the LMN signs. Multiple different combinations of UMN and LMN signs may be present in patients with probable ALS.

Probable ALS, laboratory results supported	It is defined when clinical signs of UMN and LMN dysfunction are in only one region, or when UMN signs alone are present in one region, and LMN signs defined by EMG criteria are present in at least two regions, with proper application of neuroimaging and clinical laboratory protocols to exclude other causes. Monomelic ALS, progressive bulbar palsy without spinal UMN and/or LMN signs and progressive primary lateral sclerosis without spinal LMN signs constitute special cases which may develop LMN or UMN signs to meet the criteria for probable ALS with time or be subsequently confirmed at autopsy by specific LMN and UMN neuropathologic findings.
Possible ALS	It is defined when clinical signs of UMN and LMN dysfunction are found together in only one region or UMN signs are found alone in two or more regions; or LMN signs are found rostral to UMN signs and the diagnosis of Clinically Probable ALS-Laboratory-supported cannot be proven by evidence on clinical grounds in conjunction with electrodiagnostic, neurophysiologic, neuroimaging or clinical laboratory studies. Other diagnosys must have been excluded to accept a diagnosis of Clinically possible ALS.

Table III. Diagnostic certainty based on Revised El Escorial criteria. Abbreviations: LMN: lower motor neuron; UMN: upper motor neuron. Adapted from Brooks *et al.*, 1994 and 2001.

Although there is no known cure for ALS, the drugs Rilutek (riluzole) and Radicava (edavarone) may slow the progression of the disease. Rilutek is indicated to buffer glutamate excitotoxic pulses in ALS, whereas Radicava is used to counteract the excessive oxidative stress observed in this disorder. These are short-term treatments with a slight effect on disease progression; they do not reverse the damage caused by the disease but they can slow the deterioration of function, prevent complications, and increase the comfort and independence of patients.

In the years that followed the discovery of these two drugs, over 60 molecules have been investigated as possible treatments for ALS (Table IV). Despite significant research efforts, the majority of human clinical trials have failed to demonstrate clinical efficacy. Only oral masitinib and intravenous edaravone have emerged as promising new drugs with beneficial effects in clinical trials (Petrov *et al.*, 2017).

Compound	Route	Endpoint	Phase	Outcome	Reference
Anti-glutamatergic					
Ceftriaxone	i.v.	ALSFRS-R; DTP	1-2; 3	Failure	Berry et al., 2013; Cudkowicz M. et al., 2013
Memantine	Oral	ALSFRS	2-3	Failure	de Carvalho et al., 2010
Riluzole	Oral	Survival	3	Mixed*	Bensimon et al., 1994, 2002; Lacomblez et al., 1996
Talampanel	Oral	ALSFRS-R	2	Failure	Pascuzzi et al., 2010; Teva, 2010
Anti-inflammatory					
Celecoxib	Oral	MVIC	2-3	Failure	Cudkowicz et al., 2006
Erythropoietin	i.v.	DTP	2; 3	Failure	Lauria et al., 2009
Copaxone	s.c.	ALSFRS-R	2; 2-3	Failure	Gordon et al., 2006; Meininger et al., 2009
Minocycline	Oral	ALSFRS-R	1-2; 3	Failure	Gordon et al., 2004, 2007; Pontieri et al., 2005
NP001	i.v. infusion	ALSFRS-R	1; 2	Failure	Miller et al., 2014, 2015
Pioglitazone	Oral	Survival	2	Failure	Dupuis et al., 2012
Valproic acid	Oral	DTP	3	Failure	Piepers et al., 2009
Anti-oxidative					
Coenzyme Q10	Oral	ALSFRS-R	2	Failure	Ferrante et al., 2005; Kaufmann et al., 2009
Creatine	Oral	DTP; MVIC	2; 2-3; 3	Failure	Rosenfeld, 2001; Groeneveld et al., 2003; Shefner et al., 2004; Rosenfeld et al., 2008; Pastula et al., 2012
Edaravone	i.v. infusion	ALSFRS-R	2; 3	Mixed**	Yoshino and Kimura, 2006; Abe et al., 2014; Palumbo et al., 2016; Sakata et al., 2016; Tanaka et al., 2016 a,b
Neuroprotective					
Dexpramipexole	Oral	CAFS	2; 3	Failure	Cudkowicz et al., 2011; Cudkowicz et al., 2013; Bozik et al., 2014
Olesoxime	Oral	Survival	2-3	Failure	Lenglet et al., 2014
TCH346	Oral	ALSFRS-R	2-3	Failure	Miller et al., 2007
Xaliproden	Oral	MMT; DTP	2; 3	Failure	Lacomblez et al., 2004; Meininger et al., 2004
Neurotrophic factors					
BDNF	i.v.	Survival; %FVC	1-2; 3	Failure	Bradley, 1995; Kasarskis et al., 1999
CNTF	s.c.	MVIC	1; 1-2; 2-3; 3	Failure	Miller et al., 1993, 1996; ALS CNTF Treatment Study Group, 1995, 1996

IGF-1	s.c.	AALS; MMT	3	Failure	Lai et al., 1997; Borasio et al., 1998; Sorenson et al., 2008
CSF1R inhibition					
Masitinib	Oral	ALSFRS-R	2-3	Positive$	AB Science
Other					
Lithium	Oral	ALSFRS-R; Survival	2; 2-3; 3	Failure£	Fornai et al., 2008; Verstraete et al., 2012; Morrison et al., 2013
Tirasemtiv	Oral	ALSFRS-R	2	Failure	Shefner et al., 2016

Table IV. List of drugs and compounds tested in human ALS clinical trials. *Two out of three late-stage trials reported negative results; **: two out of three Phase 3 trials reported negative results; $: statistical significance reached on multiple efficacy endpoints based on the results of interim analysis with 192 patients (50% of enrolled patients); £: only one pilot early phase trial reported statistical significance on efficacy endpoints, all subsequent large-scale follow-up studies failed to reproduce these positive results. Abbreviations: AALS, Appel ALS Rating Scale; ALSFRS-(R), The ALS Functional Rating Scale (Revised); CAFS, combined assessment of function and survival; DTP, time to death, tracheostomy or persistent assisted ventilation; %FVC, forced vital capacity; MMT, manual muscle test; MVIC, maximum voluntary isometric contraction; CSF1R, colony stimulating factor 1 receptor; i.m., intramuscular i.v., intravenous; s.c., subcutaneous. Adapted from Petrov *et al.*, 2017.

Generally, complementary treatment is used in ALS to help control symptoms, including treatment with drugs such as baclofen or diazepam, which may help control spasticity; gabapentin, which may be prescribed to help control pain; and trihexyphenidyl or amitriptyline, which may help patients swallow saliva, among other drugs or functional adapatations indicated for other possible symptoms. Control of respiration with respiratory assistance devices, and control of alimentation using gastrostomy and alimentary perfusion, are usually employed at advanced stages of the disease. Various devices are used to facilitate communication in the absence of oral language and very reduced hand movement.

2.5. Neuropathology of ALS

In most ALS cases, no gross abnormalities are observed in the brain. In contrast, the spinal cord often reveals atrophy of the anterior nerve roots and lateral spinal tracts (Ellison *et al.*, 2012; Kassubek *et al.*, 2005). Some cases

show atrophy of the precentral gyrus (Ellison *et al.*, 2012). In patients with dementia, atrophy of the frontal and/or temporal cortex may be seen (Murphy *et al.*, 2007a,b; Ellison *et al.*, 2012); the atrophy is more marked in patients with overlapping ALS-frontotemporal lobar degeneration (ALS-FTLD). The core pathological finding in ALS is motor neuron death in the motor cortex and spinal cord including degeneration and loss of Betz cells in the motor cortex, large motor neurons in the anterior horn of the spinal cord and cranial motor nuclei of the lower brainstem (Hammer *et al*., 1979; Nihei *et al.*, 1993). Although it is known that motor neurons degenerate and die in ALS, it is not clear how this degeneration begins and progresses (Saberi *et al.*, 2015). Microscopic changes include loss of myelinated axons in the lateral and anterior pyramidal tracts of the spinal cord, reduced number of fibers in the anterior roots of the spinal cord and cranial motor nerves of the lower brainstem, and altered nerve-motor junctions in skeletal muscles (Ellison *et al.*, 2012). These observations are in agreement with morphometric studies of the spinal anterior horn that show a global reduction of all neurons in the anterior horn including large alpha motor neurons (Stephens *et al.*, 2006). Other pathological features of ALS include vacuolization, large empty spaces near neurons and spongiosis. These changes in neurons are accompanied by astrocytic gliosis, oligodendroglial alterations, and microglial activation in target regions. Axonal balloons filled with aggregates of abnormal filaments are particularly common in the anterior horn of the spinal cord in rapid forms.

As detailed above, the central histopathological hallmark of ALS is the presence of cytoplasmic inclusions composed of abnormal forms of TDP-43 protein. Staging of TDP-43 pathology in ALS has been proposed in line with similar categorization stages in other neurodegenerative disorders (Brettschneider *et al.*, 2013). In stage 1, abnormal TDP-43 inclusions are restricted to motorneurons of the primary motor cortex, motorneurons of the

anterior horn of the spinal cord and certain motor nuclei of the brain stem. In stage 2, abnormal TDP-43 extends to neurons of the reticular formation of the brain stem and deep nuclei of the cerebellum. In stage 3, TDP-43-immunoreactive inclusions are also noted in the prefrontal cortex and basal ganglia. In stage 4, the hippocampal formation and the anteromedial areas of the temporal cortex show TDP-43-immunoreactive inclusions. However, recent refinements of this staging identify oligodendroglial TDP-43-immunoreactive inclusions as early pathological events in the spinal cord in ALS. Involvement of the oculomotor nuclei and Onuf's nucleus may occur at advanced stages of the disease categorized as stage 5 (Brettschneider *et al.*, 2014b). Brainstem nuclei that remain free of pTDP-43 pathology include the noradrenergic locus coeruleus and the serotoninergic nuclei of the raphe.

2.6. Etiology: sporadic and familial ALS

ALS is categorized into two forms. The most common form is sporadic (90–95%) which has no obvious genetically inherited component (sALS), although mutations in selected genes may occur in some patients. The remaining 5-10% of cases make up familial-type ALS (fALS) linked to mutations in various genes (Greenway *et al*., 2006; Abhinav *et al.*, 2007; Valdmanis *et al.*, 2008). The pattern of inheritance varies depending on the gene involved. The inheritance in most cases is autosomal dominant. However, some carriers do not develop clinical symptoms, and variability exists among unaffected individuals within the same family. ALS may be inherited with an X-linked dominant pattern. In these cases, males tend to develop the disease earlier and have a decreased life expectancy compared with females. Less frequently, ALS is inherited in an autosomal recessive pattern. Since parents of a particular affected person may be not affected, autosomal recessive ALS is often mistaken for sporadic ALS (Lattante *et al.*, 2015; Marangi and Traynor, 2015). About 20% of fALS is

caused by mutations in *SOD1*, 4-5% of fALS results from mutations in *TARDBP* and *FUS* genes, more than 30% of fALS cases are associated with *C9ORF72* repeat expansions, and the remaining genetic cases are caused by mutations in alsin (*ALSIN*), senataxin (*SETX*), spatacsin (*SPG11*), vesicle associated membrane protein associated protein B (*VAPB*), angiogenin (*ANG*), factor induced gene 4 (*FIG4*) and optineurin (*OPTN*) genes, among other genes summarized in Table V (Chen *et al.*, 2013).

fALS	Chr. locus	Gene	Protein	Onset	Inheritance
ALS1	21q22.1	*SOD1*	Cu/Zn SOD-1	Adult	AD/AR
ALS2	2q33-2q35	*ALSIN*	Alsin	Juv	AR
ALS3	18q21	Unknown	Unknown	Adu	AD
ALS4	9q34	*SETX*	Senataxin	Juv	AD
ALS5	15q15-21	*SPG11*	Spatacsin	Juv	AR
ALS6	16p11.2	*FUS*	Fused in Sarcoma	Juv/Adu	AD/AR
ALS7	20ptel-p13	Unknown	Unknown	Adu	AD/AR
ALS8	20q13.3	*VAPB*	VAPB	Adu	AD
ALS9	14q11.2	*ANG*	Angiogenin	Adu	AD
ALS10	1p36.2	*TARDBP*	DNA-binding protein	Adu	AD
ALS11	6q21	*FIG4*	PI 5-phosphatase	Adu	AD
ALS12	10p13	*OPTN*	Optineurin	Adu	AD/AR
ALS14	9p13.3	*VCP*	VCP	Adu	AD
ALS15	Xp11	*UBQLN2*	Ubiquilin 2	Adu/Juv	XD
ALS16	9p13.2-21.3	*SIGMAR1*	SIGMAR1	Juv	AR
ALS-FTD1	9q21-22	unknown	unknown	Adu	AD
ALS-FTD2	9p21	*C9ORF72*	C9ORF72	Adu	AD

Table V. Several mutated genes have been identified in fALS patients. Abbreviations: VAPB Vesicle associated membrane protein associated protein B, VCP valosin-containing protein, SIGMAR1 Sigma non-opiod intracellular receptor, C9ORF72 Chromosome 9 open reading frame 72, AD Autosomal dominant, AR Autosomal recessive.

2.6.1. ALS1/ *Superoxide dismutase 1 (SOD1)*

SOD1, which maps to chromosome 21q22.1, was the first gene identified as causative of fALS, as revealed by linkage analysis in autosomal dominant fALS pedigrees (Turner *et al.*, 2013). Individuals with mutant *SOD1* (mSOD1) usually

present with limb onset, starting predominantly in the lower limbs rather than the upper. A few cases also start with bulbar symptoms. However, SOD1 mutant ALS cases show wide individual variation regarding the age of onset, severity, rate of disease progression, and duration. Several mutations have been found in all 5 exons affecting the functional domains of *SOD1,* predominantly in patients bearing missense mutations, followed by a small percentage of nonsense mutations, insertions and deletions. Mutations in *SOD1* have been reported in ~20% of fALS and in ~1-4% of sALS (Pasinelli and Brown, 2006).

2.6.2. ALS6/*fused in sarcoma (FUS)* mutations

ALS patients with ALS6 mutations are characterized by variable age at onset from 26 to 80 years (Pasinelli and Brown, 2006). Most cases show LMN predominance without bulbar region involvement, and no cognitive impairment. The locus for ALS6 has been mapped to chromosome 16p11.2 encoding *FUS* (Sapp *et al.*, 2003). *FUS* gene encodes for a DNA/RNA binding protein that has multiple domains; the domain at N-terminus plays a role in transcriptional activation of the gene. Mutations at the C-terminus disrupt the transport of FUS protein into the nucleus, which leads to cytoplasmic localization of FUS and to the formation of stress granules (Bosco *et al.*, 2010; Dormann *et al*., 2010). To date, more than 50 *FUS* mutations have been identified in ~4% cases of fALS and ~1% of sALS cases (Lanson and Pandey, 2012). Histopathological analysis of this type of ALS case with mutant FUS illustrates distinctive FUS positive and TDP-43 negative inclusions (Bäumer *et al.*, 2010).

2.6.3. ALS10/ *TAR DNA binding protein (TARDBP)* mutations

Mutations of gene *TARDBP* were first reported in fALS cases in 2008. TARDBP-related ALS patients present autosomal dominant ALS with predominant limb

onset. The age of onsert is variable (30–77 years), as is disease duration. Since its discovery, more than 40 mutations have been identified in various ethnic groups, with an incidence of ~4-5% in fALS and up to 2% in sALS. However, it is not clear how *TARDBP* mutations cause motor neuron degeneration, although mechanisms of loss of nuclear function and gain of toxic function have been proposed (Sreedharan *et al.*, 2008).

2.6.4. *ALS-FTD1* and *ALS-FTD2* (*C9ORF72* mutations)

ALS-FTD1 is an adult-onset, autosomal dominant disorder linked to chromosome 9q21-q22 which presents with the symptoms of both fALS and fFTD (Hosler *et al.*, 2000; Pasinelli and Brown, 2006). The causal genetic defect is variable hexanucleotide GGGGCC repeat expansions in the chromosome 9 open reading frame 72 (*C9ORF72*) gene (DeJesus-Hernandez *et al.*, 2011). Cases with ALS-FTD2 mutation have both p62/ubiquitin- and TDP-43-positive inclusions. p62-ubiquitin inclusions are particularly visible in the cerebellar cortex. C9ORF72 repeat expansions are the most frequent genetic cause of fALS and fFTD-TDP, accounting for approximately 34.2% and 25.9% of the cases, respectively (Van Blitterswijk *et al.*, 2012). Patients bearing C9ORF72 mutations manifest FTD and ALS as well as other features including psychosis, akinetic-rigid symptoms and cerebellar signs (Rademakers *et al.*, 2012). Detailed description of this mutated gene is provided in the Part 3 of this thesis.

2.7. Animal models of ALS

Animal models of ALS provide a unique opportunity to uncover the molecular players involved in the pathology, which might be amenable to therapeutic intervention. Although much work has been carried out to generate new animal models based on identified ALS-causing mutations, there is no model

that enterely recapitulates the human disease. Therefore, although various animal models have been developed to investigate ALS disease, human post-mortem tissue remains the gold standard.

Small-animal models, such as *Caenorhabditis elegans*, *Drosophila* and zebrafish, can be used for unbiased forward genetic screens. However, rodent models are believed to mimic human disease more closely (Van Damme *et al.*, 2017). The transgenic rodent models most commonly used in ALS reaserch are those bearing mutations in *SOD1*, *TARDBP*, *FUS* and *C9ORF72* (Turner and Talbot *et al.*, 2008; Gendron and Petrucelli, 2011; Philips and Rothstein, 2015; Nolan *et al.*, 2016) , as described below.

2.7.1. SOD1-G93A transgenic mice

The first breakthrough in the development of rodent models to study ALS came in the early 1990s with the identification of missense mutations in *SOD1* as a cause of autosomal dominant fALS (Rosen *et al.*, 1993). SOD1 is a 153 amino acid located in the cytoplasm and mitochondria which functions in a dimeric state. SOD1 protein attaches to copper and zinc to catalyse the breakdown of harmful reactive oxygen species (ROS), and converts superoxide radicals to hydrogen peroxide, thereby preventing oxidative stress (Roberts *et al.*, 2007). Due to the damaging effects of ROS and their association with neurodegenerative diseases, it was originally proposed that pathogenic mutations in SOD1 might cause ALS because of decreased dismutase activity. Subsequent investigation failed to correlate mutant SOD1 activity with pathogenicity (Borchelt *et al.*, 1995). Deficiency of SOD1 in *Sod1* knock-out mice (Sod1−/−) does not result in motor dysfunction, at least up to 6 months of age (Reaume *et al.*, 1996). Thus, the significant loss of motor neurons in transgenic mice expressing mutant SOD1 is likely to result from a toxic gain-

of-function. Accordingly, with this gain of function, wild type SOD1 may play a role in ALS pathogenesis (Deng *et al.*, 2006; Bosco *et al.*, 2010; Graffmo *et al.*, 2012); over-expression of human wild-type SOD1, at a level similar to that seen in the SOD1G93A mouse model, can cause progressive motor neuron degeneration (Graffmo *et al.*, 2012), and abnormal axonal and mitochondrial structure (Jaarsma *et al.*, 2000 and 2006).

More than 150 different mutations have been found in this gene throughout all coding regions (Battistini *et al.*, 2005) but animal model studies have been focused on the mutation containing a substitution of glycine to alanine at position 93, abbreviated as SOD1-G93A, which is overexpressed (15-20 copies) under control of the human SOD1 promoter (Gurney *et al.*, 1994). This mutation retains SOD1 enzymatic activity (Gurney *et al.*, 1994) although it does not bind copper ions as effectively as wild-type SOD1 (Pratt *et al.*, 2014). For the past twenty years, since the first of such models became available in 1994, SOD1 transgenic mice, mainly SOD1-G93A, followed by G37R, G85R and G86R models, have been used extensively to characterize the biology of ALS as well as to explore specific benefits of potential therapies, albeit with questionable success (Gurney *et al.*, 1994). More particularly, SOD1 G93A has been widely used to study motor neuron cell death.

The original SOD1 mutant lines have diverged into a family of strains with different genetic backgrounds manifested with particular clinical aspects such as variable age of onset and rate of disease progression (Gurney *et al.*, 1994). Development of ALS-like symptoms in these mice is known to be largely dependent on four factors: (i) SOD1 mutation; (ii) transgene expression level; (iii) gender and (iv) genetic background (Heiman-Patterson *et al.*, 2011; Mancuso *et al.*, 2012a and 2012b). In our experiments, we used the well-characterized mouse model SOD1-G93A with C57BL/6J background, which

shows a milder phenotype and relative long survival rate compared with mice with SJL/J background. The later show aggressive phenotype and shorter lifespan.

Although the SOD1-G93A transgene is widely expressed, pathology in this model is largely restricted to the spinal cord, especially in the lumbar region, the brainstem, the descending spinal tracts and the neuromuscular junctions. Various pathogenic mechanisms have been recognized including protein misfolding and aggregation precedening MN death (Johnston *et al.*, 2000; Chattopadhay and Valentine, 2009), together with mitochondrial vacuolization (Dal Canto and Gurney, 1995), Lewy body-like inclusions (Dal Canto and Gurney, 1995), aberrant neurofilamant processing, neurofilament-positive inclusions (Tu *et al.*, 1996), axonal transport deficits, Golgi fragmentation (Mourelatos *et al.*, 1996), astrogliosis and microgliosis (Philips and Rothstein, 2014), glutamate-mediated excitotoxocity and reduced metabolic support to motor neurons from their surrounding glial cells (Boillée *et al.*, 2006). SOD1-G93A mutant mice also show degeneration of neuromuscular junctions at the age of about 47 days (Frey *et al.*, 2000; Pun *et al.*, 2006). This is followed by spinal motor neuron death with about a 50% reduction in the cervical and lumbar segments at the end-stage of the disease (Chiu *et al.*, 1995; Bento-Abreu *et al.*, 2010).

2.8. Molecular pathways affected in ALS

Several molecular and cellular mechanisms, such as oligodendrocyte dysfunction, oxidative stress, excitotoxicity, proteostasis disturbance, mitochondrial dysfunction, defective axonal transport, alteration in RNA/DNA mechanisms and glial activation, have been proposed as key players in ALS pathogenesis (Ferraiuolo *et al.*, 2011; Taylor *et al.*, 2016). Nevertheless, how

these mechanisms precisely contribute to selective motor neuron vulnerability and degeneration is not understood. The mechanisms are not mutually exclusive and it seems probable that they all participate to some extent in disease progression, suggesting that ALS is a multifactorial disorder with a poorly understood primary factor.

2.8.1. Glial cells: microglia, astrocytes and oligodendrocytes

The central nervous system is a complex organ composed of neurons, which represent 10% of the total number of cells, and glia, representing 90% of the total cell number. Glial cells were discovered in 1856 by the pathologist Rudolf Virchow in his search for a 'connective tissue' in the brain. The term derives from Greek word *γλία* that means 'glue' and suggests the original impression that they were the glue of the nervous system (Purves *et al.*, 2001). Glia play an active role in many processes, maintaining tissue homeostasis, supplying nutrients and oxygen to neurons, supporting neurotransmission, participating in adult neurogenesis, and providing immune surveillance, among a pleiad of functions (Rasband, 2016; Jäkel and Dimou, 2017).

Glial cells in the central nervous sytem are subdivided into four major groups: (A) astrocytes, (B) oligodendrocytes, (C) microglia and (D) ependymal cells (Figure 5) (Von Bartheld *et al*., 2016; Jäkel and Dimou, 2017). These different types of cells participate in these processes in a coordinated form, interacting with neurons and infiltrating peripheral immune cells as part of their regulation of inflammatory responses in the central nervous system. In the brain, this inflammatory response, termed neuroinflammation, is a fundamental response generated to protect the central nervous system. However, uncontrolled or prolonged neuroinflammation is potentially harmful and can result in cellular damage (Frank-Cannon *et al.*, 2009). After

injury, there is a non-specific reactive change in glial cells in response to damage, called gliosis, which is one of the most important features in neuroinflammation and includes proliferation or hypertrophy of several different types of glial cells (McMillian *et al.*, 1994; Fawcett and Asher, 1999).

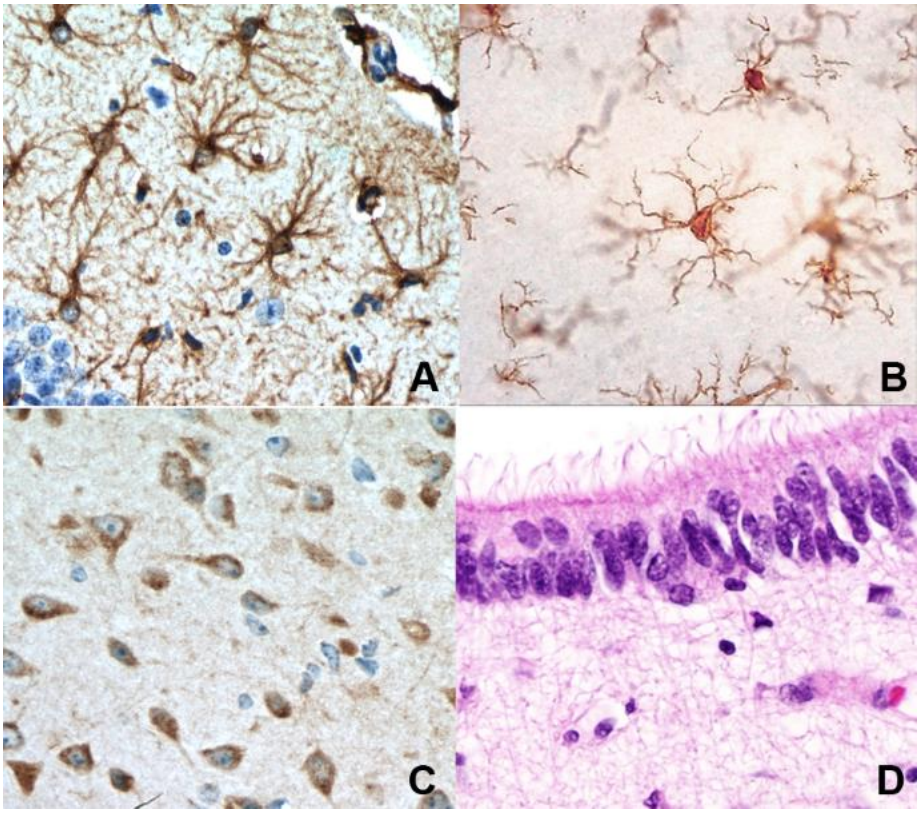

Figure 5: Glial cells of the CNS. Representative drawings of four different types of glial cells in central nervous system: (A) astrocytes (IHC anti-GFAP), (B) microglia (IHC anti-IBA1), (C) oligodendrocytes (IHC anti-MOG) and (D) ependymal cells (H&E stain). Abbreviations: GFAP-glial fibrillary acidic protein; H&E-hematoxylin and eosin; IHC-immunohistochemistry; IBA1-ionized calcium-binding adapter molecule 1; MOG- myelin oligodendrocyte glycoprotein.

Microglia

Microglia play an important role as resident immunocompetent and phagocytic cells in the central nervous system in the event of injury and disease (Kim and de Vellis, 2005). Microglia were first recognized in 1899 by

Franz Alexander Nissl who named them 'rod cells' for their rod-shaped nuclei and considered them as reactive neuroglia. However, Pío del Rio Hortega was who advanced microglia as a distinct cell type apart from astrocytes and oligodendrocytes after his studies of brains from young animals using his silver carbonate staining method in 1919, recognizing them as cells of mesodermal origin (Del Rio-Hortega, 1919). Microglia emerge from two sources: erythromyeloid precursors of the embryonic yolk sac, and myeloid progenitors. These precursor cells invade the developing brain during the embryonic, fetal, or perinatal stages, and they are transformed from actively phagocytic globoid-ameboid cells into resting ramified microglia (Sievers et al., 1994; Ginhoux *et al.*, 2013). These cells are identified by the expression of monocytic markers, such as α-M-β2 integrin (or CD11b/CD18 and MAC-1), IgG receptors (CD16/CD32), ionized calcium-binding adaptor protein-1 (Iba-1), and the major histocompatibility complex (MHC) (Hendrickx *et al.*, 2017).

In agreement with Hortega's original description, microglia have been classically described as existing in two states, resting and activated. 'Resting' microglia exhibit a highly ramified morphology characterized by motile processes that constantly monitor their immediate surroundings by extending and retracting their processes to maintain homeostasis (Davalos *et al.*, 2005; Nimmerjahn *et al.*, 2005). This constant movement of microglial processes while the soma remains stationary is called microglial motility. The unexpected finding of microglial process motility led scientists to investigate and identify new roles in the non-pathological brain (Kettenmann *et al.*, 2013), showing active involvement in the phagocytosis of synaptic elements during the entire lifespan, and the formation of learning-dependent synapses in the mature brain, as well as in the maturation and plasticity of excitatory synapses (Figure 6) (Hristovska and Pascual, 2016).

In contrast, when microglia encounter a substance that they sense is foreign or indicative of harm, they enter into an 'activated' state with ameboid morphology. As macrophage-like cells of the brain, active microglia regulate innate central nervous system immunity and initiate appropriate responses. Concretely, the term activation includes a range of different 'activated' states. It is now recognized that activated microglia can exist broadly in two different states (Colton *et al.*, 2009). The first is classical activation (phenotype M1), which is identified by the production of inflammatory cytokines and reactive oxygen species (ROS).

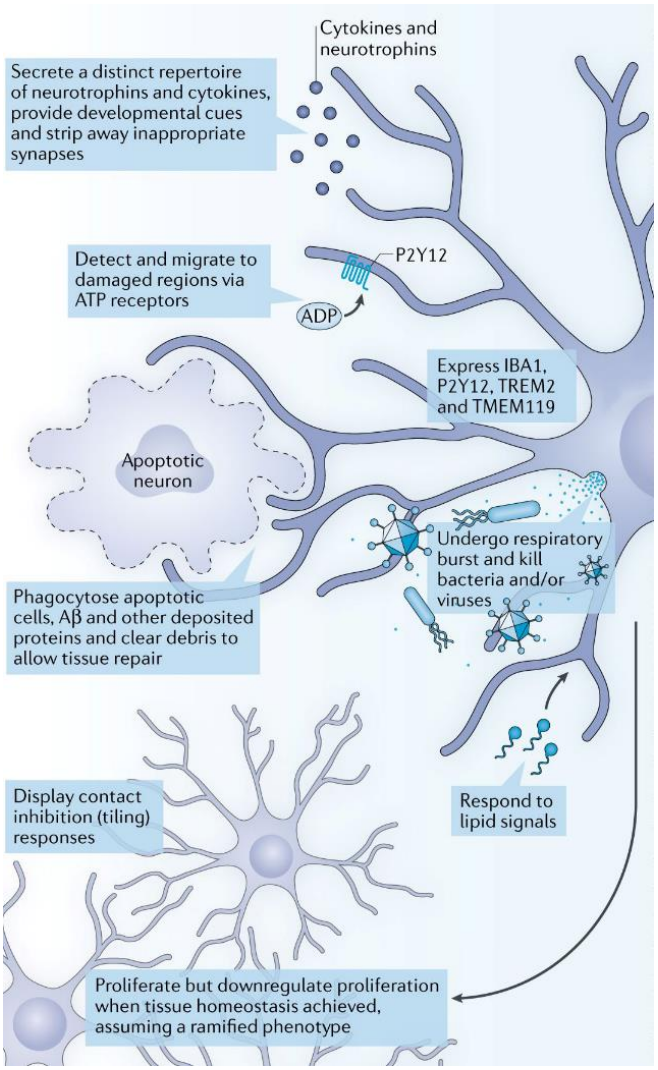

Figure 6. The schematic image illustrates most of the physiological functions of microglia. Microglia contribute to healthy nervous system physiology in several ways. They provide cues and remove inappropriate synapses during development, and they secrete neurotrophins and cytokines to support and maintain neural networks in the mature nervous system. In addition, they rapidly sense ATP signalling via receptors such as P2Y purinoceptor 12 (P2Y12) and migrate to areas of damage, where they proliferate and phagocytose apoptotic cells and any other damaged tissue to aid repair. Indeed, activation of microglia following CNS damage or disease induces a respiratory burst, which is necessary for an efficient innate immune response. Adapted from Pocock and Piers, 2018.

Using a full array of immune receptors, such as toll-like receptors (TLRs), nucleotide-binding oligomerization domains (NODs), NOD-like receptors and many scavenger receptors (Ransohoff and Perry, 2009; Ransohoff and Brown, 2012), microglia are able to recognize harmful stimuli and respond by producing inflammatory cytokines such as TNFα, IL-6, IL-1β, interferon-γ (IFNγ), and several chemokines (Boche *et al.*, 2013). Further, there is a state of alternative activation (phenotype M2) in which microglia take an anti-inflammatory phenotype involved in wound repair and debris clearance (Gordon, 2003). In contrast with proinflammatory M1 cells, alternatively activated macrophages express cytokines and receptors that are involved in inhibiting inflammation and restoring homeostasis. This includes production of IL-10 to downregulate inflammatory cells, extracellular matrix protecting proteins like YM1, a heparin-binding lectin (Chang *et al.*, 2001); FIZZ1, which promotes deposition of extracellular matrix (Raes *et al.*, 2002); ornithine, which promotes proliferation; CD206, a mannose receptor for phenotype M2 inducer IL-4 (Stein *et al.*, 1992); polyamines for wound repair; and higher levels of receptors associated with phagocytosis, such as scavenger receptors (CD68 antigen) (Martinez *et al.*, 2009; Varin and Gordon, 2009). Thus, it makes sense that during neurodegenerative disease, in which neuroinflammation is a prominent feature and potential contributor to disease, the alternatively activated microglia would be beneficial in resolving pathology.

Astrocytes

Astrocytes are arguably the most numerous and diverse neuroglial cells in the central nervous system, compromising nearly 35% of the total cell population (Liberto *et al.*, 2004; Sofroniew, 2005). After the first description of glial cells by Virchow in 1856, the cellular nature of glial cells was recognized soon after and different types of these cells were morphologically characterized (Parpura

and Verkhratsky, 2012). Nevertheless, the detailed morphological analysis of glial cells began after Camillo Golgi's had developed black staining reaction and produced drawings of stained glial cells in 1872 (Golgi, 1873 and 1903).I It was not until 1891 that Michael von Lenhossek introduced the term astrocyte, in which *astron* means 'star' while *kytos* means 'cell, to define the star-like cells.

Astrocytes are present in all regions of the central nervous system. However, they are not uniform; their functions and morphology differ depending largely on their location, subtypes, and developmental stage. In healthy brain, the most prevalent are the protoplasmic astrocytes that are found throughout the grey matter and, as first demonstrated using classical silver impregnation techniques, they exhibit several stem branches that give rise to many finely branching processes in a uniform globoid distribution (Ramon y Cajal, 1909). In contrast, fibrous astrocytes are found throughout the white matter and exhibit many long fiber-like processes, and are in physical contact with oligodendrocytes while playing a crucial role in myelinization and support of the white matter (Ramon y Cajal, 1909; Lundgaard *et al.*, 2013).

Although originally defined as gap fillers for the neuronal network, astrocytes play a number of active roles in the brain (Figure 7). They provide trophic and metabolic support for neurons in conditions of energy depletion, when glucose expenditure exceeds availability, by releasing lactate from glycogen stores, forming the astrocyte neuron lactate shuttle (Zwingmann *et al.*, 2000; Bouzier-Sore *et al.*, 2002). Astrocytes also have high concentrations of anti-oxidant molecules such as vitamin E, ascorbate, and glutathione (GSH) (Dringen *et al.*, 2000; Shih *et al.*, 2003). The interaction between astrocytes and neurons is required for the maintainence of the synaptic homeostasis, clearing away glutamate and other neurotransmitters and ions from synapses

(Bergami *et al.*, 2008; Bogen *et al.*, 2008). Although astrocytes are electrically nonexcitable, with a constant resting membrane potential, contact at the synaptic level is necessary in the assembly of tripartite synapses along with the pre- and postsynaptic neurons. Astrocytes modulate transmission by releasing chemical transmitters (Araque *et al.*, 2001; Fields and Stevens-Graham, 2002). The interaction between developing neurons and astrocytes plays an important role in neuronal replacement, including dendritic growth and axon guidance, effective synapse formation and removal of unwanted synapses (Seri *et al*., 2001; Bundesen *et al.*, 2003; Sanai *et al.*, 2004; Petros *et al.*, 2006; Hu *et al*., 2007; Araque, 2008).

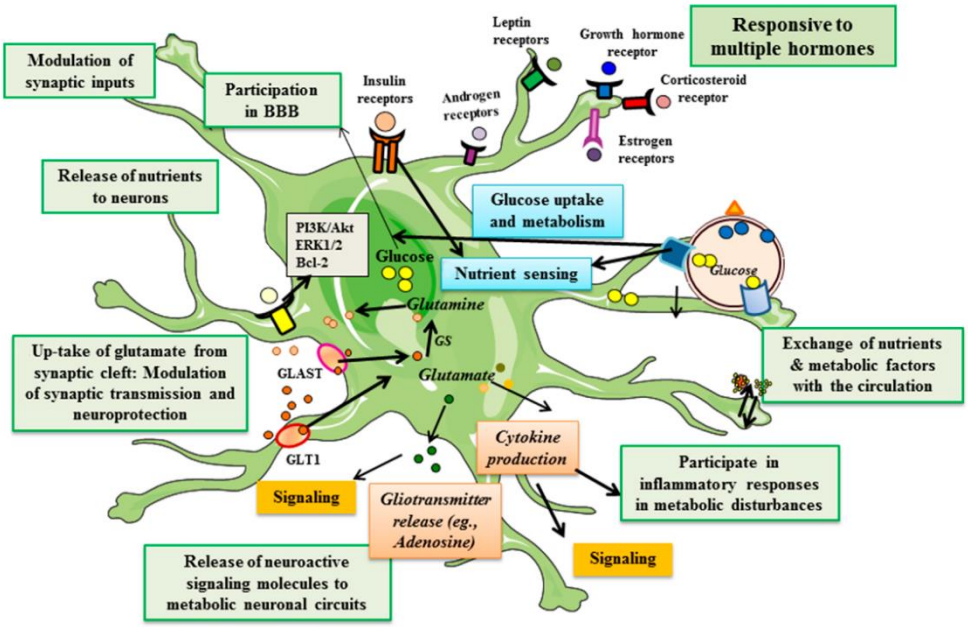

Figure 7. Schematic representation of the various functions attributed to astrocytes. Abbreviations: BBB: blood-brain barrier, GS: glutamine synthetase, GLAST: glutamate aspartate transporter, GLT1: glutamate transporter 1; adapted from Frago and Chowen, 2017.

Moreover, astrocyte contact with other central nervous system cells is important for several biological functions in the brain. Astrocytes are able to regulate the specialized roles of the endothelial cells that line cerebral microvessels and form part of the BBB (Abbott *et al.*, 2006), modifying barrier

permeability to nutrients such as glucose (Leybaert, 2005). Astrocytes regulate the function of oligodendrocytes (Ishibashi *et al.*, 2006; Yamaguchi *et al.*, 2008). In addition, astrocytes respond to all forms of nervous system damage and disease, showing a variety of changes in gene expression, cellular structure and function in the processes of 'astrogliosis' and 'reactive astrocytosis' (Sofroniew, 2014).

Reactive astrocytes increase cell body size and thickness of astrocytic processes. In addition, branching of astrocyte processes becomes complex and is reorganized with increasing reactivity (Wilhelmsson *et al.*, 2006). Increased numbers of astrocyte processes and a polarization occur toward the injury site or toxic aggregates (Bardehle *et al.*, 2013). Reactive astrocytes show a broad heterogeneous graded spectrum of reactivity that in function of the inury can be classified into two main types, 'A1' and 'A2'. A1 astrocytes are partially induced by micrcoglial secreted cytokines, such as the interleukin 1α (Il-1α), tumour necrosis factor (TNF) and complement component 1, subcomponent q (C1q) (Zhang *et al.*, 2014; Bennett *et al.*, 2016). A1 astrocytes highly upregulate many classical complement cascade genes, rapidly killing neurons and mature differentiated 'harmful' oligodendrocytes.By contrast, A2 reactive astrocytes upregulate many neurotrophic factors, which promote survival and growth of neurons, as well as thrombospondins, which promote synapse repair. This upregulation suggests that A2s might have 'helpful' or reparative functions.

The first modern description of a 'reactive astrocyte' occurred during the 1970s, after the discovery of the intermediate filament protein glial fibrillary acidic protein (GFAP)- a routine identifier of astrocytes in the healthy and the pathological central nervous system. Histologically, astrocytes can be visualized by immunolabeling for other filamentous proteins in addition to

GFAP, such as vimentin or other markers such as the astrocyte specific glutamate transporters, glial L-glutamate transporter 1 (GLT1) and L-glutamate/L-aspartate transporter (GLAST) (also known as EAAT1) (Walz, 2000). Other markers for astrocytes have varying specificities: S-100b (calcium binding protein), aquaporin 4 (AQ4), brevican, G-protein coupled receptor 37-like1 (gpr371R), aldehyde dehydrogenase 1 family-member L1 (ALDH1L1), and anti-low-affinity nerve growth factor receptor-p75 (NGFRp75), among others (Bachoo *et al*., 2004; Cahoy *et al*., 2008).

Oligodendrocytes

Oligodendrocytes represent highly specialized glial cells in the central nervous system that closely interact with the axons of neurons. The first systematic description of oligodendrocytes was provided by Pío Del Río Hortega in an article published in 1928 (Del Río Hortega, 1928). However, the complete story of this discovery begun in 1921 when he described microglia as the third element, mentioning the existence of oligodendrocytes as a new neuroglia cell type , the interfascicular glia, made up of cells showing very fine processes and arranged in groups along axonal tracts (Del Río Hortega, 1921). He used the term 'oligodendroglia' as in his observervations, glial cells with very few processes or branches, present in white matter, were also diffusely distributed in all regions of the central nervous system, and commonly grouped next to neurons in grey matter. Four different types were described by Pio del Río-Hortega as detailed in recent reviews (Pérez-Cerdá *et al.*, 2015; Ferrer, 2018):

- Type I: small round cell bodies and large numbers of very fine cellular processes associated with thin myelinated fibers in the grey matter and interfascicular white matter.

- Type II: cuboidal with a few thick processes which trap axons longitudinally in the white matter.
- Type III: one or two long cellular processes and present in the brain stem and spinal cord.
- Type IV: elongated cell body and unique long processes running in parallel to thick axons in the white matter of the brain stem and spinal cord.

Perineuronal oligodendroglial cells are called 'perineuronal satellites' whereas another subtype includes oligodendroglial cells localized in the proximity of small blood vessels and called, for this reason, 'perivascular satellites'.

One year later, using metallic silver impregnations, Del Río Hortega proposed that these cells were functionally similar to Schwann cells in the central nervous system (Del Río Hortega, 1922), and he predicted their relationship with myelination processes, their involvement in neuronal trophism, and their ectodermal origin (Del Río Hortega, 1928).

The most typical characteristic of this cell type is the ability to generate a compact multilayered myelin sheath around the axon (Figure 8) (Nonneman *et al.*, 2014). The myelin sheath is made up of thick concentric membrane bilayers of about 12 nm in periodicity formed by alternating electron-dense (major dense line of myelin) and electron-light (intra-period line of cytoplasm) membranes tightly connected at their edges by thigh junctions between the electron-dense layers (Baumann and Pham-Dinh, 2001; Simons and Trotter, 2007). Myelin is composed of lipids, including cholesterol (26%); glycosphingolipids, in particular galactocerebrosides and sulphatides (24%); plasmalogens (20%); phospholipids and gangliosides, particularly GM4; and proteins (30%) (Kursula, 2001 and 2008; Chrast *et al.*, 2011; Saher and Stumpf, 2015; Schmitt *et al.*, 2015). The most abundant protein components of the

myelin sheath are proteolipid protein (PLP), including its isoform DM20, and myelin basic protein (MBP). Other less abundant proteins are 2',3'-cyclic nucleotide-3'phosphodiesterase (CNP), myelin oligodendrocyte glycoprotein (MOG), myelin-associated glycoprotein (MAG), myelin/oligodendrocyte basicprotein (MOBP), oligodendrocyte myelin glycoprotein (OMgp), myelin/oligodendrocyte specific protein (MOSP), transferrin (TF), carbonic anhydrase, claudin 11, connexins 32 and 47 (Cx32 and Cx47) and tetraspan-2, among other minor proteins (Figure 8) (Jahn and Surrey, 2009; Ferrer, 2018).

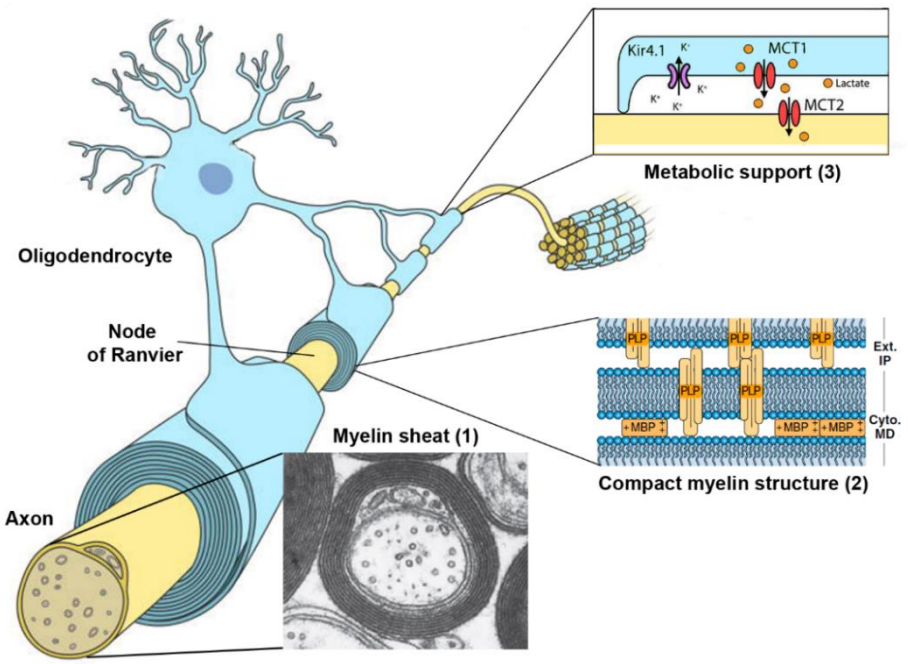

Figure 8: Schematic representation of oligodendrocyte structure and functions. (1) A typical CNS myelinated fiber from the spinal cord observed by transmission electron microscopy (TEM). **(2)** Diagrammatic representation of current concepts of the molecular organization of compact CNS myelin. The apposition of the extracellular (Ext) surfaces of the oligodendrocyte cell membranes to form the intraperiod (IP) line is shown in the upper part of the figure. The apposition of the cytoplasmatic (Cyto) surfaces of the membranes of the myelin-forming cells with the major dense (MD) line are shown in the lower part of the figure. This diagram does not include CNP, MAG and other quantitatively minor proteins of isolated myelin, because they do not play a major structural role in most of the compact myelin. **(3)** Oligodendrocytes provide lactate to axons via the periaxonal space and remove K+ ions. Abbreviations: PLP: proteolipid protein; MBP: myelin basic protein; MCT1/2: monocarboxylate transporter ½. Adapted from Mount and Monje, 2017 and Siegel *et al.,* 2011.

Individual neuronal axons are myelinated by consecutive oligodendrocytes arranged in line, separating each segment from the next by a gap, the so-called node of Ranvier. Ranvier's nodes are enriched in certain myelin- and axon-derived proteins, such as netrin, contactin 1 and 2, neurofascin 155, neurofascin 186 and contactin-associated proteins (Caspr), which interact to bind the myelin sheath to the axon at the free borders of myelin, together with extracellular matrix proteins (Rasband, 2011; Thaxton, 2011; Arancibia-Carcamo and Attwell, 2014).

Myelin sheath makes fast and efficient propagation of action potentials possible over long distances along the axons through saltatory conduction due to the interruption of the myelin sheath at regular distances by the nodes of Ranvier. At these nodes of Ranvier, electrical activity can be generated in order to propagate the action potential efficiently from one node of Ranvier to the next (Poliak and Peles, 2003). Nodes are enriched in voltage-gated sodium channels and potassium-gated channels Nav 1.6, Nav 1.1, KCNQ2/3, Kv 3.1, Kv1.1/1.2; and postsynaptic density protein 93/95 (PSD 93/95) which are all crucial for saltatory nerve conduction (Poliak and Peles, 2003).

Another important function of the oligodendrocytes is their ability to provide neurons with energy support. Monocarboxylates, including lactate, pyruvate and keton bodies, are a class of essential energy substrates for the central nervous system. These energy substrates are transported across membranes by monocarboxylate transporters (MCTs). The most abundant lactate transporter in the CNS is monocarboxylate transporter-1 (MCT1), mainly expressed by oligodendrocytes at high levels (Lee *et al.*, 2012; Morrison *et al.*, 2012). Abnormalities in one of these two functions cause a number of neurodegenerative diseases (Nave, 2010a and 2010b).

Most oligodendrocytes develop during embryogenesis and early postnatal life in restricted periventricular germinal regions. In the adult brain, oligodendrocyte formation is associated with glial-restricted progenitor cells, known as oligodendrocyte progenitor cells (OPCs), that may be called NG2-glia because of their expression of proteoglycan GSPG4 (NG2) (Dawson *et al.*, 2003). Differentiation of OPCs to oligodendrocytes depends on the availability of certain growth and survival factors, such as platelet-derived growth factor A (PDGF)-A, fibroblast growth factor 2 (FGF-2), insulin-like growth factor 1 (IGF-1), ciliary neurotrophic factor (CNTF) and neurotrophin 3 (NT-3) (Barres *et al.*, 1992). Early stages of oligodendrocyte lineage are identified by the expression of Olig1, Olig2 and Nkx2.2 (Liu *et al.*, 2007). PDGF-Rα, NG2, Olig1, Olig2, Sox 10 and A2B5 are OPC differentiation and pre-oligodendrocyte markers. Loss of PDGF-Rα and NG2, and increased expression of surface lipid sulfatide, galactocerebroside and CNP, together with Olig1 and Olig2 transcription factor, are characteristic markers of immature oligodendrocytes (Marinelli *et al.*, 2016). After oligodendrocyte differentiation, myelination is triggered by myelin regulatory factor (MYRF) which is expressed in post-mitotic oligodendrocytes (Cahoy *et al.*, 2008), loosing the expression of myelin proteins that have MYRF binding motifs in their promoters (Emery *et al.*, 2009). At this time, oligodendrocytes also produce sulfatides and galactocerebrosides as the main lipid components of myelin (Bradl and Lassmann, 2010).

2.8.1.1. Neuroinflammation in ALS

A common characteristic of neurodegenerative disorders is the occurrence of a neuroinflammatory reaction consisting of activated glial cells, mainly microglia and astrocytes, and infiltrated active T cells, evidencing the important role neuroinflammation plays in disease pathology, even during the

presymptomatic phase of ALS (Kang *et al*., 2013; Philips and Rothstein, 2014; Komine and Yamanaka, 2015; Liu and Wang, 2017). In neurodegenerative diseases, the neuroinflammatory reaction is not transient, but sustained, probably because of the persistent presence of precipitating factors, turning it into a hazardous process and contributing to neuronal damage. Chronically activated microglia and astrocytes, as well as infiltrating immune cells, represent prominent pathological findings in affected central nervous system areas of patients and animal models of neurodegenerative disorders such as ALS (McCombe and Henderson, 2011).

Despite not being immune cells, astrocytes are a potential source of both pro- and anti-inflammatory cytokines, actively contributing to the immune response. Data in *post-mortem* tissues of ALS patients reveal changes in the morphology of astrocytes together with reactive astrogliosis surrounding both upper and lower motor neurons (Schiffer *et al.*, 1996). Increased numbers of GFAP- and ALDH1L1-immunoreactive astrocytes locate in the dorsal horn and at sites where fibres of the corticospinal tract enter the grey matter; and they are particularly notable in the grey matter of the ventral horn of the spinal cord where astrocytes normally express GFAP at very low levels (Philips and Robberecht, 2011). In the brain, astrocytosis occurs in both cortical grey matter and subcortical white matter, and it is not restricted to the motor cortex (Kushner *et al*., 1991; Nagy *et al.*, 1994).

Additionally, reactive astrocytes in *post-mortem* tissue from ALS cases also show increased immunoreactivity for calcium-binding protein S100, and they express inflammatory mediators (Shobha *et al.*, 2010), such as cyclo-oxygenase-2 (COX-2), prostaglandin E2, leukotriene B4, nitric oxide (NO), inducible nitric oxide synthase (iNOS) and neuronal nitric oxide synthase (nNOS) that exert toxic effects on MNs (Haidet-Phillips *et al.*, 2011).

Corroborating these data, mutant hSOD1 transgenic mice show a similar pattern of reactive astrogliosis, although the time course of astrogliosis, relative to motor neuron degeneration and the onset of symptoms, seems to vary in different models (Wong *et al*., 1995; Bruijn *et al*., 1997; Hall *et al.*, 1998; Howland *et al.*, 2002).

Microgliosis occurs in the motor cortex, the motor nuclei of the brainstem, along the corticospinal tract, and in the ventral horn of the spinal cord where microglia might interact with T-cell infiltrates (Kawamata *et al.*, 1992). It has been reported that injured MNs and astrocytes in ALS release misfolded proteins and activate, through CD14, toll-like receptor (TLR) 2, TLR4, and scavenger receptor dependent pathways (Appel *et al.*, 2011; Zhao *et al.*, 2013). Once microglia are activated, they display distinct plastic phenotypes, with either neurotoxic or neuroprotective function, depending on the state of activation and disease stage. At early slow progressive stages of ALS, microglia display an M2 phenotype with upregulated expression of tissue repair and regeneration molecules, like CD206 and Ym1; overexpression of neurotrophic factors such as IGF-1, BDNF or GDNF and secretion of anti-inflammatory mediators IL-10 and TGFB; and interaction with protective signals such as CD200 and fractalkine (CX3CL1) (Appel *et al.*, 2011; Blasco *et al.*, 2013). As ALS progresses, MNs release signals which induce microglia to acquire M1 phenotype which enhances the secretion of NOX2, ROS and proinflammatory cytokines (e.g., TNF-α, IL-1, INFy and IL-6) (Beers *et al*., 2011; Liao *et al*., 2012).

Microglial activation is associated with infiltration of helper T cells and cytotoxic T cells. Concomitant with increased infiltration of inflammatory T cells, parenchymous microglia acquire properties of antigen-presenting cells, as revealed by the upregulation of certain expression markers such as CD11c (also known as ITGAX), CD86, and intracellular adherin molecule 1 (ICAM1).

This suggests that these microglial cells interact closely with the T-cell infiltrates (Philips and Robberecht, 2011). Infiltrated T cells can both damage and protect neurons. At early stages of ALS, the immune profile is characterised by increased regulatory T cells, upregulation of anti-inflammatory cytokines and activation of neuroprotective microglia (M2) cells. Transition to pro-inflammatory effector T cells and cytokines along with activation of neurotoxic microglia (M1) cells occurs with disease progression (Holmøy, 2008).

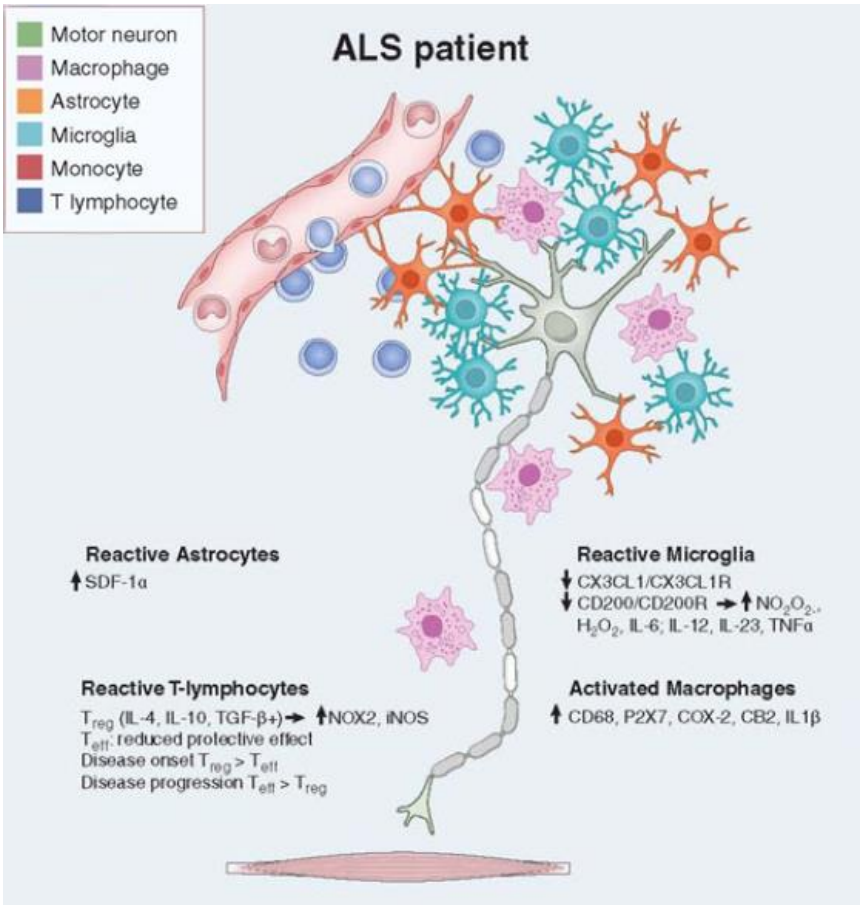

Figure 9. General overview of the cross-talk between motor neurons, astrocytes, and immune cells in ALS context. Neuroinflammation, characterized by the appearance of reactive astrocytes and microglia as well as macrophage and T-lymphocyte infiltration, appears to be highly involved in the disease pathogenesis, highlighting the involvement of non-neuronal cells in neurodegeneration. There appears to be cross-talk between motor neurons, astrocytes, and immune cells, including microglia and T-lymphocytes, which are subsequently activated. Adapted from Rizzo *et al.*, 2014.

Thus, in ALS, astrocytes, microglia and peripheral immune cells are involved exerting either deleterious or protective effects on MN survival depending on the stage of the disease, but the mechanism is far from being fully elucidated (Figure 9). Moreover, it remains to be clarified whether neuroinflammation is a consequence of motor neuron injury or actively contributes to the development and progression of the disease.

2.8.1.2. Myelin and oligodendrocyte alterations in ALS

The involvement of non-neuronal glial cells, such as microglia and astrocytes, is a well-studied aspect of ALS pathology. However, the oligodendrocytes and their progenitor cells are glial cell types that have been largely ignored for years in the context of ALS (Nonneman *et al.*, 2014). However, recent studies have demonstrated that motor neuron degeneration in ALS is intimately linked to oligodendroglial cell dysfunction.

Recent studies have postulated oligodendroglial TDP-43-immunoreactive inclusions to be an early pathological event in the spinal cord in ALS (Brettschneider *et al.*, 2014a). Specifically, oligodendroglial TDP-43-immunoreactive inclusions are present in the anterior horn of the spinal cord and in the motor, sensory and premotor cortex, but not in the *corpus callosum*, *cingulum* or lateral tracts of the spinal cord (Fatima *et al.*, 2015).

In addition to the presence of inclusions, myelin abnormalities and demyelination are present in the motor cortex and grey matter of the ventral spinal cord of ALS patients, in both sporadic and familial ALS patients (Kang *et al.*, 2013). The levels of myelin-related proteins progressively decrease during disease (Niebroj-Dobosz *et al.*, 2007), most prominently the decrease in MBP. However, the absence of myelin alone is not sufficient for axonal

degeneration, unless it occurs in combination with oligodendroglial injury or inflammation (Nave, 2010b).

Besides myelin defects, oligodendrocytes also fail to supply axons with metabolic energy substrates. MCT1 expression levels are predominantly decreased in the ventral horn of the spinal cord grey matter of symptomatic SOD1-G93A mice and significally decreased in the motor cortex of ALS patients, while unaffected brain regions show normal MCT1 levels (Lee *et al.*, 2012).

Furthermore, in mutant SOD1-G93A mice, evidence indicates that oligodendrocytes start to degenerate before the first symptoms of motor neuron degeneration become apparent, increasing with disease progression, and showing oligodendrocytes with thickened, irregularly shaped cell bodies, enlarged cytoplasm and elongated reactive processes, known as dysmorphic oligodendrocytes. In addition, clear markers of the apoptotic state are observed in dysmorphic oligodendrocytes, such as cleaved caspase-3 immunoreactivity and chromatin condensation (Kang *et al.*, 2013).

Nevertheless, mature oligodendrocytes are not the only cells in their lineage affected in ALS patients. NG2+ oligodendroglial precursor cells also show reactive changes, with augmentation of NG2 immunoreactivity and thick hypertrophic NG2+ processes (Philips *et al.*, 2013). Oligodendrocyte degeneration with disease progression is offset by increased proliferation and differentiation of NG2+ glial cells into oligodendrocytes, thereby maintining the overall number of oligodendrocytes. In this manner, the density of oligodendrocytes remains constant in ALS, although newly generated oligodendrocytes are dysfunctional (Kang *et al.*, 2013).

2.8.2. Mitochondria

The brain, which accounts for only 2% of body weight, consumes 20% of the total oxygen (O_2) breathed in. A major reason for the high oxygen uptake by the brain is the vast amounts of ATP needed for its normal activity, maintaining the intracellular ion homeostasis and powering its ~86 billion neurons and their unfathomably complex connectome spanning trillions of synapses abetted by ~250–300 billion glial cells (Carey, 2002; Cobley *et al.*, 2018).

Mitochondria are responsible for the production of most of the cell's 'energy currency' in the form of ATP, the end-product of pathways involving oxidation of substrates. The mitochondrion is a double-membrane-bound organelle found in most eukaryotic organisms. The term 'mitochondrion' is derived from a Greek words 'mitos', which means 'thread', and 'chondrion', which means 'granule'. The first observations of intracellular structures that probably represented mitochondria were published in the 1840s (Ernster and Schatz, 1981), but it was not until 1957 that, based on evidence accumulated over years by different authors about its different functions, Philip Siekevitz dubbed them 'powerhouse of the cell' (Siekevitz, 1957).

Mitochondria, frequently 0.75 and 3µm in diameter, vary considerably in size, structure and number, depending on the organism, tissue, and cell type. The organelle is composed of compartments that carry out specialized functions (Wiemerslage and Lee, 2016). These compartments include (Figure 10):

(i) Outer mitochondrial membrane (OMM) is a smooth lipid bilayer composed of equal amounts of phospholipids and proteins, specifically a large number of transport proteins, such as translocase of outer

mitochondrial membrane -40 (TOMM40) or -70 (TOMM70), with most of them being porins, like the voltage-dependent anion channel (VDAC). OMM is freely permeable to nutrient molecules, ions and energy molecules like the ATP and ADP.

(ii) Inner mitochondrial membrane (IMM) is a phospholipid bilayer with a complex structure turned into a number of repeated folds known as the cristae. This folding helps to increase the surface area inside the organelle hosting the main proteins of ETC involved in the production of ATP. IMM is strictly permeable to oxygen and ATP, and also helps regulate the transfer of some metabolites.

(iii) Intermembrane space (IMS) is the space between the outer and inner membrane of the mitochondria; it has the same composition as the cell's cytoplasm. It tends to have a low pH because of the proton gradient, which occurs when protons are pumped from the mitochondrial matrix into the intermembrane space during ETC.

(iv) Matrix is the viscous space within the IMM. The mitochondrial matrix contains the mitochondria's DNA, ribosomes and molecules linked to energy production, such as soluble enzymes, small organic molecules, nucleotide cofactors and inorganic ions.

Additionally, the mitochondrion contains mitochondrial DNA (mtDNA), which is organized as several copies of a single, usually circular, chromosome, coding information for 13 mitochondrial proteins (Friedman and Nunnari, 2014). Mitochondria are involved in a myriad of functions, including biosynthesis of amino acids and steroids, β-oxidation of fatty acids, maintenance of cytosolic calcium homeostasis, buffering of calcium fluctuations, production and

modulation of reactive oxygen species (ROS) and acting centrally in apoptosis, among others (Davis and Williams, 2012). However, as noted before, the most important function of the mitochondrion is to produce energy (Friedman and Nunnari, 2014).

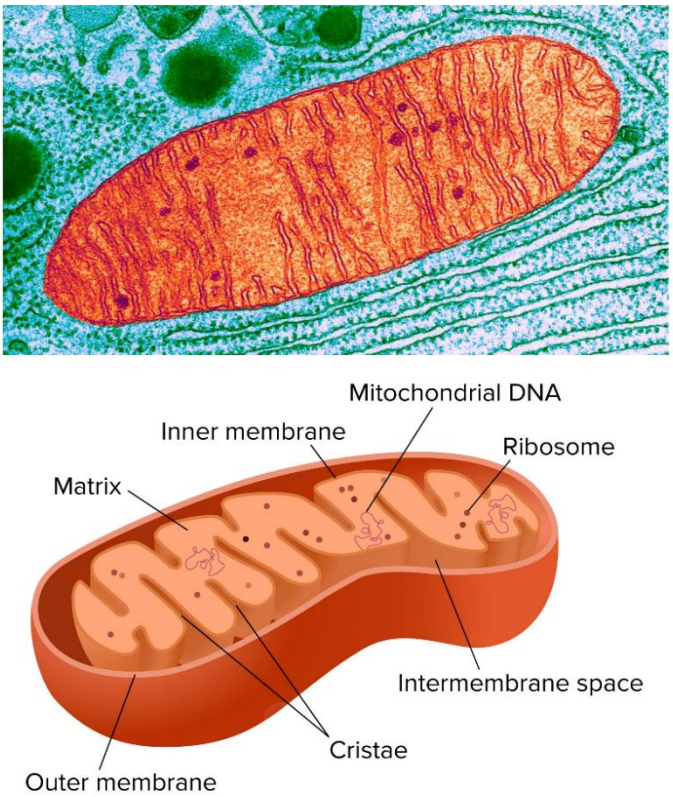

Figure 10: Mitochondrion structure. (A) Coloured transmission electron microscope image of a thin section of mammalian tissue; mitochondria displaying their matrix, membranes and ribosomes. **(B)** Schematic structure of a mitochondrion, showing its two specialized membranes. The inner membrane is highly convoluted so that a large number of infoldings called cristae are formed.

2.8.2.1. Mitochondria's energy metabolism

Energy production is accomplished through the mitochondrial electron transport chain (ETC) which consists of four enzyme complexes (complex I to complex IV) embedded in the IMM that transfer electrons from donors like NADH/FADH to oxygen, the ultimate electron acceptor. During electron

transfer, the ETC pumps protons into the IMS, generating a gradient across the IMM that the ATP synthase exploits to drive adenosine triphosphate (ATP) synthesis (chemiosmosis) (Mitchell, 1961; Wallace, 2013; Birsoy *et al.*, 2015). This process is called oxidative phosphorylation (OXPHOS) and is fueled using electron donors generated in the mitochondrial matrix by the tricarboxylic acid (TCA) cycle and fatty acid β-oxidation or by cytosolic glycolysis (Birsoy *et al.*, 2015). The five components of the ETC are (Figure 11):

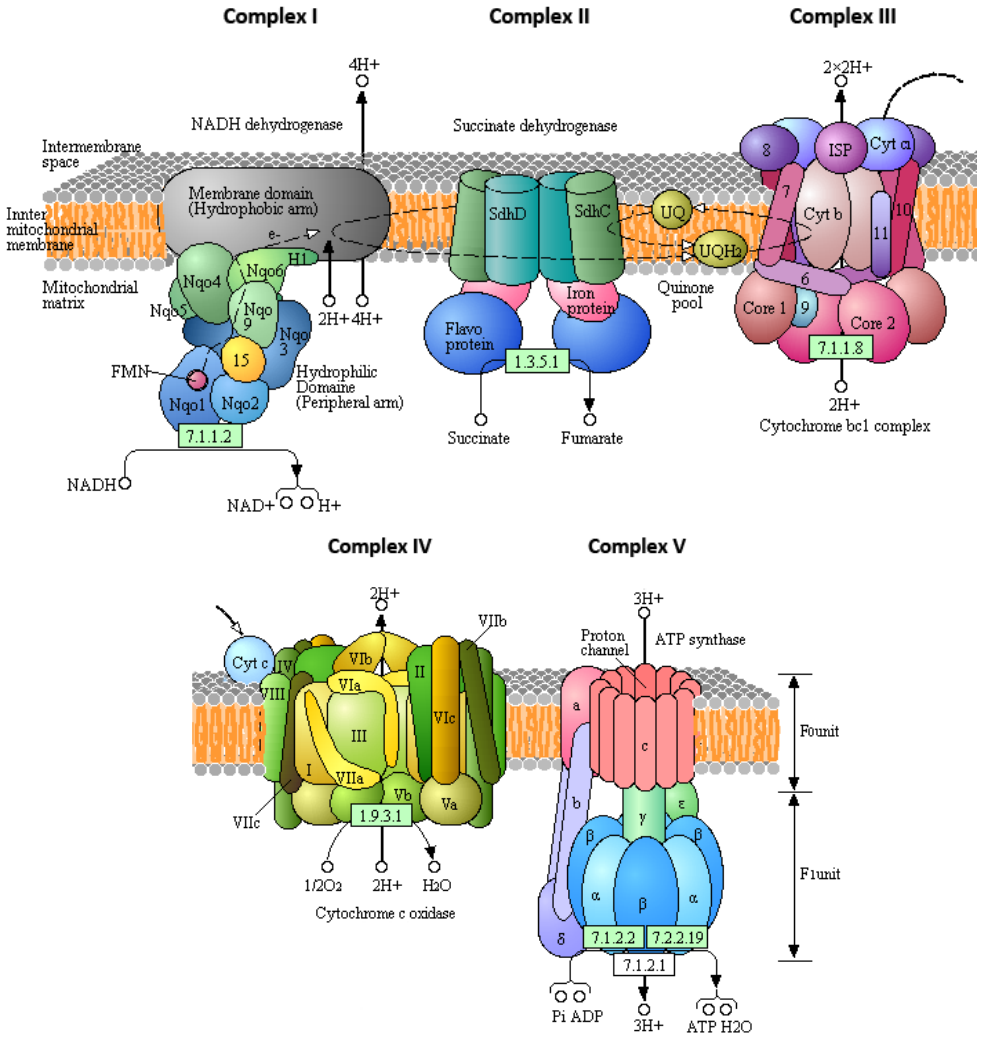

Figure 11: The electron transport chain has four protein complexes (C-I to C-V). The transfer of electrons creates hydrogen ions that get pumped across a proton gradient in the mitochondrial matrix and the intermembrane space. During chemiosmosis, there are more hydrogen ions in the intermembrane mitochondrial space than the mitochondrial matrix. Thus,

these ions will travel across ATP synthase, catalyzing the phosphorylation of ADP to ATP. Legend: (7.1.1.2) NADH dehydrogenase (ubiquinone); (1.3.5.1) succinate dehydrogenase; (7.1.1.8) cytochrome bc1 complex; (1.9.3.1) cytochrome C oxidase; (7.1.2.2) ATP synthase; (7.2.2.19) proton pump; (7.1.2.1) proton transport ATPase.

1. Complex I (C-I) receives two electrons from NADH molecule. C-I is composed of flavin mononucleotide (FMN), a prosthetic group derived from vitamin B2 also called riboflavin, and an iron-sulfur (Fe-S)-containing enzyme, known as NADH dehydrogenase (Sharma *et al.*, 2009). Fourteen central subunits represent the minimal form of C-I; these are assigned to functional modules for NADH oxidation and ubiquinone reduction, and they pump hydrogen ions across the membrane from the matrix into the intermembrane space, establishing and maintaining an ion gradient between the two compartments separated by the inner mitochondrial membrane. The enzymatic core is composed of seven hydrophobic subunits (ND1–ND6 and ND4L) encoded by the mitochondrial genome (Chomyn *et al*., 1985) in combination with seven nuclear-encoded subunits (NDUF) divided into different subtypes (Iα, Iβ, Iλ, and Iγ) (Sazanov *et al.*, 2000). In addition, there are assembly proteins, which mediate complex I assembly and maintain the complex I stability including NDUFAF1, NDUFAF12L, AIF, NDUFS4, ECSIT and C6orf66, among others.

2. Complex II (C-II), also known as succinate dehydrogenase (SDH) complex, directly receives FADH2 from mitochondrial matrix, which does not pass through C-I. SDH is comprised of four subunits (SDHA, SDHB, SDHC, and SDHD) encoded by nuclear DNA, and unlike other mitochondrial complexes, lacks subunits encoded by the mitochondrial genome. SDH transfers electrons from succinate via its [Fe–S] clusters to ubiquinone (UbQ). Thus, UbQ receives the electrons derived from complex II but also receives electrons derived from NADH from C-I. Once ubiquinone is reduced to ubiquinol (QH2), ubiquinone delivers its electrons to the next

complex in the electron transport chain (Kluckova *et al.*, 2013; Bezawork-Geleta *et al.*, 2017). C-II has also a role in the ETC and the tricarboxylic acid (TCA) cycle where SDH oxidises the metabolite succinate to fumarate, thus linking the two essential energy-producing processes of the cell (Kluckova *et al.*, 2013).

3. Complex-III (C-III), also called cytochrome oxidoreductase, is a multiheteromeric enzyme composed of 11 different subunits (Schagger *et al*., 1986), one encoded by mitochondrial DNA and 10 by nuclear genes. These 11 subunits constitute the monomeric module of a symmetric dimer, which constitutes the functionally active form of the enzyme. The complex is embedded in the mitochondrial inner membrane, spanning from the matrix to the inter-membrane space. Three of these subunits contain the catalytic centers: cytochrome b (MT-CYB), cytochrome c1 (CYC1) and the Rieske protein (UQCRFS1). Additionally, cytochrome b contains two heme moieties, the low potential (bL) and the high potential (bH) heme b; CYC1 binds a c-type heme group and the Rieske Iron Sulfur Protein subunit (ISP) that contains a 2Fe-2S cluster (UQCRFS1). Heme groups act as prosthetic groups, helping in the electron transition process (Fernández-Vizarra and Zeviani, 2015). The exact function of the other eight supernumerary subunits (UQCRC1, UQCRC2, UQCRH, UQCRB, UQCRQ, Subunit 9, UQCR10 and UQCR11) remains to be established (Xia *et al.*, 2013).

C-III shunts the electrons coming from ubiquinol across the intermembrane space to cytochrome c, which brings electrons to the next complex. Oxidation of ubiquinol at C-III requires the donation of those two electrons to the single electron carrier cytochrome *c*. The first electron transfer at complex III is to the Reiske iron-sulfur center protein (RISP). This electron is then transferred to cytochrome *c1* and subsequently to cytochrome *c*.

This one electron transfer from ubiquinol results in the unstable radical ubisemiquinone ($Q^{\bullet-}$) which can donate its unpaired electron to oxygen to generate superoxide within the Q-cycle. However, under most circumstances, the unpaired electron of ubisemiquinone is transferred to the two heme groups of cytochrome *b* (Heme b_L and Heme b_H). The two hemes have different electron affinities because they are located in different polypeptide environments. Heme b_L is located closer to the intermembrane space and has a lower affinity for electrons than Heme b_H, which is located closer to them matrix side. Ubisemiquinone transfers its electron to b_L to form ubiquinone. Heme b_L in turn donates an electron to Heme b_H, which subsequently reduces another molecule of ubiquinone, forming ubisemiquinone. The Q-cycle at this stage is only half complete as only one electron from ubiquinol has been transferred to cytochrome *c*. After a second round of the Q-cycle, two molecules of ubiquinol have been oxidized on the intermembrane side of the inner membrane and two molecules of cytochrome *c* have been reduced on the matrix side of the inner membrane. The total balance produces the exchange of 4H+ to the mitochondrial intermembrane space (Kramer *et al.*, 2004; Chandel, 2010).

4. Complex IV (C-IV) or cytochrome C oxidase (COX) is the last electron acceptor of the respiratory chain. COX is a multimeric complex formed by 14 polypeptide subunits, three of which are encoded by mitochondrial DNA and which are the catalytic subunits that carry out the electron transport function (MT-CO1, MT-CO2 and MT-CO3), whereas the remaining 11 are encoded by nuclear DNA (COX4-COX8, some of them with different forms) (Balsa *et al.*, 2012). Subunits are combined with prosthetic groups (heme *a* and heme a_3, one in each of the two cytochromes), three ion copper metallic centers, and three copper ions (a pair of CuA and one CuB in cytochrome a3) to perform their function (Mansilla *et al.*, 2018). COX

receives an electron from each complex III molecule, and transfers these to one oxygen molecule, converting molecular oxygen to two molecules of water. The cytochromes hold an oxygen molecule very tightly between the iron and copper ions until the oxygen is completely reduced. The free energy released as the electrons move to an even lower energy state is used to pump even more protons into the intermembrane space, further strengthening the transmembrane difference of proton electrochemical potential that the ATP synthase then uses to synthesize ATP (McEwen *et al.*, 2011).

5. Complex V (C-V), also known as ATP synthase or FoF1 ATPase, consists of two main subunits, Fo and F1, which have a rotational motor mechanism allowing for ATP production. Fo and F1 create a pathway for proton movement across the membrane. The flow of these protons down the gradient turns the rotor and stalk of the ATP synthase, which makes it possible for a phosphate group to join with adenosine diphosphate (ADP), forming ATP (Velours *et al*., 2000).

F1 is composed of three copies of each of subunits α (ATP5A1, ATPAF2) and β (ATP5B, ATPAF1, C16orf7), and one each of subunits γ (ATP5C1), δ (ATP5D) and ε (ATP5E) (Jonckheere *et al.*, 2012). There is a substrate-binding site on each of the α and β subunits; those on β subunits are catalytic, while those on α subunits are regulatory. The remaining F1 subunits (γ, δ, ε) form part of the stalks with diverse regulatory functions. The α/β subunits undergo a sequence of conformational changes, induced by the rotation of the γ subunit, leading to the formation of ATP (Leyva *et al.*, 2003). In contrast, Fo has mainly hydrophobic regions that consist of 8 *c* subunits forming a ring and one copy each of *a* (ATP6, ATP8), *b* (ATP5F1), *c* (ATP5G1, ATP5G2, ATP5G3), *d* (ATP5PD), F6 and oligomycin sensitivity-

conferring protein (OSCP) subunits, together with the accessory subunits *e* (ATP5ME), *f* (ATP5MF), *g* (ATP5MG) and A6L (ATP8) that form the peripheral stalk which lies to one side of the complex. The ring has a tetramer shape with a helix-loop-helix protein that goes though conformational changes when protonated and deprotonated, pushing neighboring subunits to rotate andcausing the spinning of Fo which then also affects conformation of F1, resulting in the switching of states of α and β subunits (Jonckheere *et al.*, 2012).

Considering the intense energy demands and limited regenerative capacity of neurons, improper functioning of mitochondria energy mechanisms and the remaining biological functions can trigger devastating effects on neuronal survival.

2.8.2.1.1. Energy failure in ALS

Besides their ability to convert nutrients into ATP, mitochondia are crucial in intermediate metabolism, maintaining cellular calcium homeostasis and functioning as gatekeepers in the intrinsic apoptotic pathways. Because of the multiple functions of mitochondria, alteration of their properties might confer an intrinsic susceptibility to long-lived post-mitotic cells, such as motor neurons, and to aging and cellular stress (Cozzolino and Carrì, 2012).

Mitochondrial abnormalities are pathological hallmarks in spinal cord of ALS patients (Afifi *et al.*, 1966). Specific, structurally altered and aggregated mitochondria with swollen and vacuolated appearance were one of the first changes observed in ALS patient motor neurons and in Bunina body-containing cells (Hart *et al*., 1977; Atsumi, 1981; Sasaki and Iwata, 2007). sALS occasionally display axonal swellings containing enlarged mitochondria and

neurofilaments. Morphologically, abnormal mitochondria are also consistently reported in animal and cell models of ALS, mainly manifested as mitochondrial fragmentation (Jaarsma *et al.*, 2000; Bendotti *et al*., 2001; Martin *et al.*, 2007; Martin, 2007).

Direct evidence that disruption of mitochondrial structure may contribute to ALS comes from the discovery of causative mutations in the mitochondrial protein coiled-coil-helix-coiled-coil-helix domain containing 10 (CHCHD10) which is localised to contact sites between the inner and outer mitochondrial membranes (Bannwarth *et al.*, 2014). ALS-associated mutations in CHCHD10 disrupt mitochondrial cristae and have profound effects on mitochondrial structure (Genin *et al*., 2016). Deformation and loss of mitochondrial cristae have also been reported in C9orf72-related ALS and FTD (c9ALS/FTD) patient fibroblasts (Dafinca *et al.*, 2016; Onesto *et al.*, 2016), and *in vitro* and *in vivo* in SOD1-G93A mouse (Kirkinezos *et al.*, 2005). In addition, part of misfolded mutant SOD1 protein is located on the cytoplasmic surface of mitochondria. Axonal mitochondria of motor neurons are primary targets (Vande Velde *et al.*, 2011). Mutant SOD1 motor neurons have impaired mitochondrial fusion processes in cell bodies and axons, showing smaller mitochondrial size, reduced density and defective membrane (Magrané *et al.*, 2012).

The electron transport chain is also affected in ALS patients, although the well-known difficulty in obtaining well-conserved, large collections of samples and the heterogeneity of tissues have, at times, complicated the interpretation of results. For instance, increased activity of complex I was found in a first study on post-mortem brain tissue (Bowling *et al.*, 1993) which may represent a compensatory event against the deficiency of mtDNA encoded enzyme cytochrome c oxidase observed in some ALS patients (Yamamoto *et al*., 1989; Borthwick *et al.*, 1999). However, in *post-mortem* spinal cord tissue from sALS

and fALS patients, the decrease in citrate synthase activity parallels the decrease in the activity of respiratory chain complexes (Fujita *et al.*, 1996; Borthwick *et al.*, 1999; Wiedemann *et al.*, 2002). This suggests loss of mitochondria in ALS spinal cords and increased mitochondrial DNA damage (Swerdlow *et al.*, 1998). Alteration of ETC also occurs in ALS skeletal muscle, mainly manifested by severe deficiency of respiratory chain complex I and complex IV. This has been interpreted to mean either that sALS patients have primary mitochondrial DNA damage in muscle fibers or that these alterations are secondary to muscle fiber denervation and atrophy (Wiedemann *et al.*, 1998).

Mitochondria are also key players in the buffering of intracellular calcium, which in prolonged excess results in the activation of pro-oxidant and apoptotic factors (Choi, 1988; Dawson *et al.*, 1991). Depletion of mitochondrial calcium-buffering ability is particularly deleterious to neurons and skeletal muscle, whose normal functioning involves frequent influxes of calcium to generate action potentials. Likewise, both ALS patients and mouse models have increased intracellular calcium concomitant with mitochondrial damage (Curti *et al.*, 1996; Siklos *et al.*, 1996; Damiano *et al.*, 2006). It is not clear whether decreased mitochondrial buffering capacity precedes cytosolic Ca2+ overload or *vice-versa*, since these processes reciprocally enhance each other (Dykens, 1994; Carriedo *et al.*, 2000). Indeed, glutamate-receptor mediated neurotoxicity has been linked to overload of mitochondrial calcium and ROS production in cultured spinal motor neurons from transgenic ALS animals (Carriedo *et al.*, 2000).

Together, these studies demonstrate that changes in mitochondrial function and dynamics are common central features of the pathogenesis of ALS.

2.8.2.2. Mitochondria and oxidative stress

Under normal physiological conditions, the mitochondrial electron flow leads to the formation of superoxide anion (O_2^-) subproduct, the primary oxygen free radical produced by mitochondria. Superoxide is a reactive oxygen species (ROS), a natural product of the oxygen metabolism that has important roles in cell signaling and homeostasis (Devasagayam *et al.*, 2004). Reactive oxygen molecules include superoxide radical (O_2^-), hydroxyl radical (OH^-) and hydrogen peroxide (H_2O_2) (Chandra *et al.*, 2015). However, under environmental stress, ROS levels can increase dramatically, triggering the deleterious condition known as oxidative stress (OS), which reflects an imbalance between the systemic manifestation of ROS and a biological system's ability to readily detoxify the reactive intermediates and to repair the resulting damage (Figure 12) (Betteridge, 2000). In the case of oxidative stress induced by superoxide molecule, it interferes with the electron transport chain, dramatically increasing superoxide production. Mitochondria are highly vulnerable to the action of ROS, which are able to interfere with multiple components of the respiratory chain (Murphy, 2009), with the heme-containing molecule COX1 of the complex 4 of the respiratory chain being the most vulnerable (Mahad *et al.*, 2008). Oxidation of respiratory chain components results either in functional inhibition or in increased degradation of the respective proteins, leading to partial dysfunction of energy metabolism. In addition, mitochondrial DNA mutations and deletions may be induced by free radicals (Campbell *et al.*, 2010). Moreover, superoxide radicals can rapidly react with nitric oxide (NO) to generate cytotoxic peroxynitrite anions ($ONOO^-$) (Figure 12). Peroxynitrite anions belong to reactive nitrogen species (RNS) that act together with reactive oxygen species to damage cells, causing nitrosative stress. Peroxynitrite can react with carbon dioxide, leading

to protein damage via the formation of nitrotyrosine and lipid oxidation (Barber *et al.*, 2006).

While these partially reduced oxygen species can attack iron sulfur centers in a variety of enzymes, superoxide is rapidly converted within the cell to hydrogen peroxide (H_2O_2) by the superoxide dismutase enzymes (SOD1, SOD2 and SOD3) (Figure 12). However, hydrogen peroxide can react with reduced transition metals, via the Fenton reaction, to produce the highly reactive hydroxyl radical (OH), a far more damaging molecule to the cell (Yim *et al.*, 1990). Oxidative injury leads to tissue degeneration in the central nervous system through various mechanisms. First, it may directly oxidize lipids, proteins and DNA, thus interfering with the function of these molecules and propagating their degradation (Wang and Michaelis, 2010).

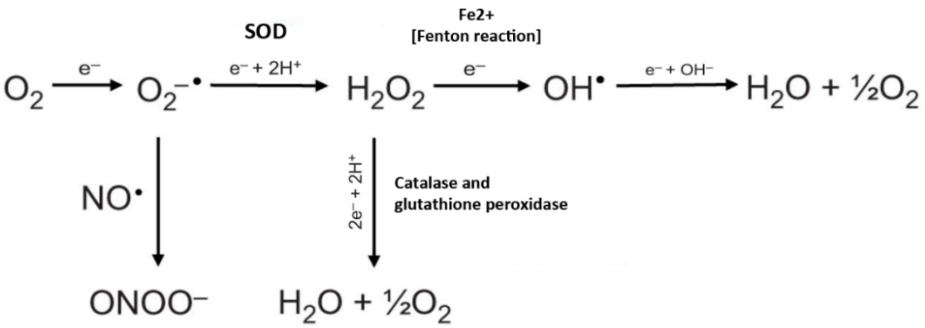

Figure 12. Generation of reactive oxygen and nitrogen species (ROS and RNS). This overview shows the major reactions (not fully balanced) generating ROS and RNS (only peroxynitrite) and the antioxidant (scavenging) proteins catalyzing the reduction of superoxide anion (O2-) and hydrogen peroxide (H_2O_2). It also indicates that ferrous iron (Fe^{2+}) contributes to catalyzing the formation of hydroxyl radicals; SOD, superoxide dismutase; OH- , hydroxyl radical; NO- , nitric oxide; ONOO-, peroxynitrite. Adapted from Tomanek, 2015.

The oxidative stress can be effectively neutralized by enhancing cellular defenses in the form of antioxidants. Certain enzymatic antioxidants work by breaking down and removing free radicals, converting dangerous oxidative products to hydrogen peroxide and then to water, in a multi-step process in the presence of cofactors such as copper, zinc, manganese, and iron. For

example, to reduce hydroxyl radical damage, the antioxidant enzymes catalase and glutathione peroxidase act on hydrogen peroxide molecules, converting them to oxygen and water (Figure 12) (Lü *et al.*, 2009; Nimse and Pal, 2015).

Other antioxidants are those compounds which act by raising the levels of endogenous antioxidant defenses, such as the expression of gene coding for detoxyfing enzymes like superoxide dismutase (SOD), catalase (CAT) and glutathione peroxidase (GSHPx), or by directly interfering with free radical chain reactions (Nimse and Pal, 2015). Examples of non-enzymatic antioxidants are vitamin C, vitamin E, plant polyphenol, carotenoids and glutathione, among others (Lü *et al.*, 2009).

2.8.2.2.1. Oxidative stress in ALS

The vast majority of neurons are more susceptible to oxidative stress than other cellular populations because they are post mitotic cells, and damage accumulates throughout life (Shaw and Eggett, 2000). Markers of oxidative stress are found in post-mortem brains from patients with different neurodegenerative disorders (Sayre *et al.*, 2001). However, motor neurons in particular are highly specialised cells; likely, this specialisation renders them vulnerable to oxidative stress injury. The unusually high energy demand of the motor neuron must be supported by mitochondria with the side-effect of increased ROS generation (Shaw and Eggett, 2000). In addition, free radical production is a major cause of aging (Lenaz *et al.*, 2002).

In ALS, there is substantial evidence to support the hypothesis that oxidative stress is one mechanism by which motor neuron death may occurs. In sporadic ALS tissue samples, elevated protein carbonyl levels in both spinal cord (Shaw

et al., 1995) and motor cortex (Ferrante *et al.*, 1997), and increased 3-nitrotyrosine levels, a marker for oxidative damage mediated by peroxynitrite, are observed in both sporadic and SOD1 familial ALS patients (Beal *et al.*, 1997). Protein and lipid oxidation markers are localised in motor neurons, reactive astrocytes and microglia/macrophages in the grey matter neuropil of sporadic ALS patients (Shibata *et al.*, 2001). Oxidative damage to DNA, measured by levels of 8-hydroxy-2'-deoxyguanosine (8-OHdG), are found elevated in whole cervical spinal cord from ALS patients (Fitzmaurice *et al.*, 1996). These facts became more persuasive with the discovery of superoxide dismutase 1 (SOD1) mutations that cause disease in a significant minority of fALS cases. However, the precise mechanism(s) by which mutant SOD1 leads to motor neuron degeneration has not been defined, and the results of trials with anti-oxidant therapies have been disappointing (Barber *et al.*, 2006).

2.8.3. Excitotoxicity

Neuronal excitotoxicity that culminates in neuronal death is a hallmark of cellular responses to major stresses such as those that occur in hypoxia/ischemia injury and in neurodegenerative diseases (Prentice *et al.*, 2015). The excitotoxicity concept was coined by John Olney in 1969 (Olney, 1969), based on the observations that those amino acids that induce neuronal death were the ones known to activate excitatory amino acid (EAA) receptors (Olney, 1978). Overactivation of these receptors causes excitotoxicity by allowing high levels of calcium ions to enter the cell (Manev *et al.*, 1989). The excitatory effects of glutamate are exerted via the activation of three major types of ionotropic receptors and several classes of metabotropic receptors linked to G-proteins. The major ionotropic receptors activated by glutamate are N-methyl-D-aspartic acid (NMDA), α-amino-3-hydroxy-5-methylisoxazole-4-propionate (AMPA) and kainic acid (KA) receptors, which are ligand-gated

ion channels permeable to various cations (Danysz and Parsons, 2003). As to metabotropic (mGluR) receptors, they mediate slow synaptic responses, owing to their coupling with intracellular G-proteins. For example, the mGluR1 and mGluR5 subunit subtypes are coupled to the inositol trisphosphate (IP3)/Ca^{2+} signal transduction pathway and can thus affect protein kinase activation and stimulation of Ca^{2+} release from neuronal stores, both of which can trigger delayed cell death processes (Friedman, 2006). Excessive calcium influx into cells activates a number of enzymes, including phospholipases, endonucleases and proteases, such as calpain. These enzymes go on to damage cell structures such as components of the cytoskeleton, membranes and DNA (Berliocchi *et al.*, 2005), leading to cell death (Figure 13).

Under physiological conditions, during glutamatergic neurotransmission, a depolarizing impulse on the presynaptic neuron triggers a transient spike in the concentration of glutamate in the synaptic cleft that activates ionotropic glutamate receptors present on the postsynaptic neuron. Activation of these glutamate receptors results in the influx of sodium ions into the cell, leading to depolarization and ultimately, if the threshold is achieved, to the generation of an action potential at the axon hillock of the postsynaptic neuron (Van Den Bosch *et al.*, 2006; Sirohi and Kuhn, 2017). In addition to Na-K channel activation, activation of NMDA receptors also allows conductivity of Ca^{2+} ions that trigger a signaling cascade which helps to modulate the strength of the synapse. Additionally, NMDA receptors may also be hyperactivated if the ambient glycine levels in the synaptic cleft are disturbed due to malfunctioning of the glycine transporters (GlyT1) (Sirohi and Kuhn, 2017).

Thus, regulation of glutamatergic transmission is a complex process, dependent on fine-tuning of extracellular glutamate levels-reuptake and resynthesis-excitatory/inhibitory balance and the firing thresholds of

individual neurons. Neurons have evolved to finely regulate their excitability and maintain appropriate output, although a dramatic or prolonged disturbance to any of these processes may disrupt this control (King *et al.*, 2016).

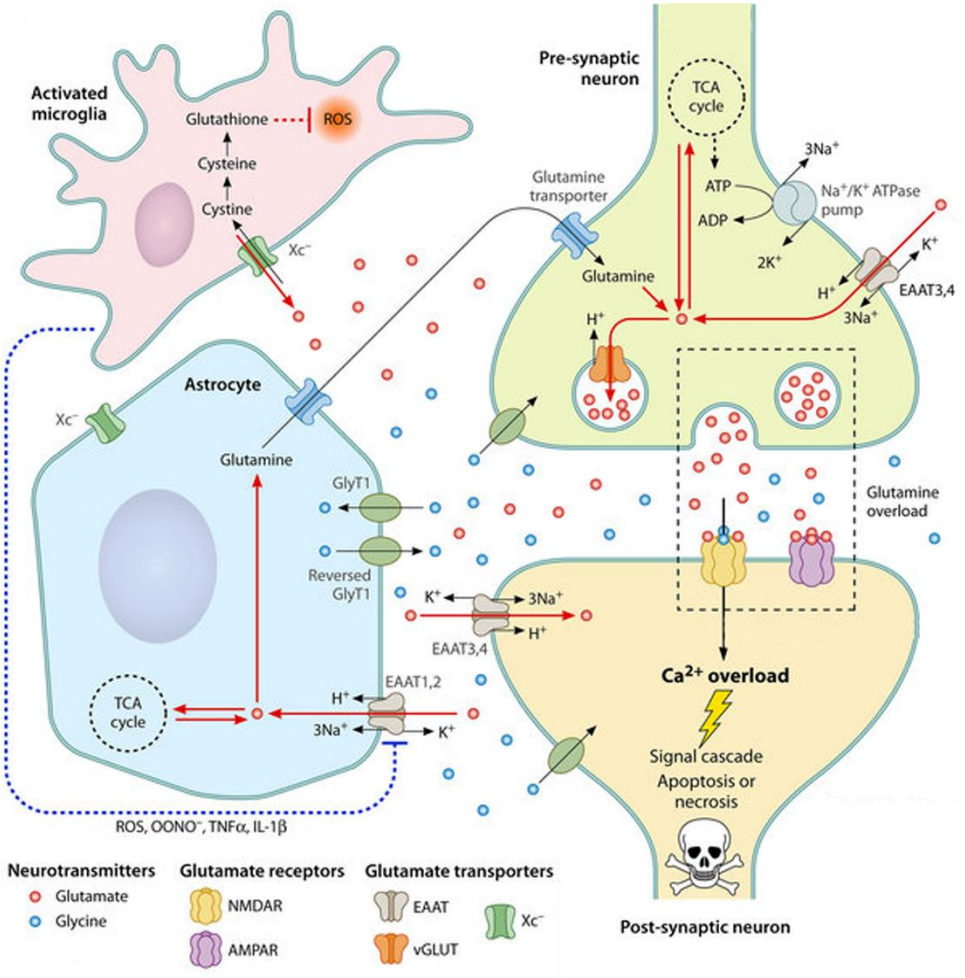

Figure 13. Glutamate neurotransmission, homeostasis, and excitotoxicity in the brain. A glutamate-driven chemical synapse along with a neighboring astrocyte and an activated microglia is shown. Different pathological insults, many of them occurring in ALS, lead to the unprovoked and sustained presence of glutamate in the synaptic cleft and chronic activation of NMDAR, resulting in neuronal damage. Abbreviations: (NMDAR) N-methyl-d-aspartate receptor; (AMPAR) α-amino-3-hydroxy-5-methyl-4-isoxazolepropionic acid receptor; (EAAT) excitatory amino acid transporter; (vGLUT) vesicular glutamate transporter; (Xc^-) cystine-glutamate antiporter; (GlyT1) glycine transporter; (TCA) tricarboxylic acid (cycle); (ROS) reactive oxygen species; ($OONO^-$) peroxynitrite; (TNF-α) tumor necrosis factor alpha; (IL-1β) interleukin-1β; (H^+) hydrogen; (Ca^{2+}) calcium; (Na^+) sodium; (K^+) potassium. Adapted from Sirohi and Kuhn, 2017.

In neurodegenerative conditions, such as those associated with ALS and other neurodegenerative disorders, glutamate homeostasis may be disturbed by a variety of mechanisms such as (i) oxidative stress, mitochondrial dysfunction, or energy deficiency (via loss of ATP-dependent Na^+/K^+ pumps), which may cause chronic or excessive release of glutamate from presynaptic neurons; (ii) release of large amounts of glutamate from activated microglia mediated by Xc antiporters; and (iii) reduction of glutamate clearance from synaptic clefts due to compromised activity of EAATs on astrocytes, either due to the presence of ROS and inflammatory cytokines produced by activated microglia or to damage in the astrocytes themselves (Sirohi and Kuhn, 2017).

The excess of glutamate overactivates glutamatergic receptors, including NMDA receptors, leading to Ca^{2+} overload in cells, and in consecuence, causing excitotoxicity which rapidly leads to cell death or prolonged pathologic changes via calcium-dependent effectors. These efectors include endoplasmic reticulum (ER) stress and mitochondrial overload (Van Damme *et al.*, 2005), high level generation of ROS and RNS, and loss of mitochondrial membrane potential which in turn increase cell vulnerability (Le Masson *et al.*, 2014).

2.8.3.1. Excitotoxicity in ALS

Motor neuron injury caused by EAA may explain how motor neurons can be selectively damaged by a disturbance of the glutamate neurotransmitter system, in spite of the fact that EAA receptors are widely distributed throughout the central nervous system. Three cell-specific molecular features of human motor neurons may render this cell group particularly susceptible to calcium-mediated toxic events following glutamate receptor activation (Shaw and Ince, 1997). The first feature is the low expression of mGluR2 and the resulting possibility that human motor neurons express atypical calcium-

permeable AMPA receptors (Tomiyama *et al.*, 2001). mGluR2 may help to mediate the survival of neurons, as activation of mGluR2 increases the phosphorylation of tau and reduces oxidative stress-mediated cytotoxicity in neuronal cells (Lee *et al.*, 2009). The second feature is the fact that human motor neurons that are vulnerable in ALS do not express the calcium-binding proteins parvalbumin and calbindin D28K (Ince *et al.*, 1993). These proteins buffer intracellular calcium and protect neurons from calcium-mediated injury following activation of glutamate receptors. A direct relationship exists between cellular calcium buffering capacity and resistance to glutamate neurotoxicity (Mattson *et al.*, 1989). Finally, the third fact is linked to selective reduced expression of the astrocytic glutamate transporter EAAT2, which mediates prompt clearance of glutamate from the synaptic cleft after firing (Maragakis *et al.*, 2004). Both sALS and fALS patients, and mutant SOD1 mice, have decreased levels of functional EAAT2 protein (also known as GLT1), and increased circulating glutamate in the CSF (Rothstein *et al.*, 1995; Fray *et al.*, 1998; Sasaki *et al.*, 2000; Howland *et al.*, 2002). Work in transgenic mice confirms the importance of EAAT2/GLT1-mediated glutamate clearance to motor neuron health. Deletion of this gene is sufficient to induce progressive neurodegeneration (Rothstein *et al.*, 1996), and genetically encoded (Guo *et al.*, 2003) or exogenously stimulated EAAT2/GLT1 overexpression (Rothstein *et al.*, 2005) delays the onset of clinical symptoms in ALS mouse models. The mechanisms by which EAAT2/GLT1 is downregulated in ALS are not yet understood, and it is not clear whether decreased mRNA synthesis/stability is a factor.

These three molecular features may, in combination, render human motor neurons particularly susceptible to calcium toxicity following AMPA receptor activation (Shaw and Ince, 1997). The most important argument for the role of excitotoxicity in ALS is that riluzole, the only drug with proven effective

properties against disease progression, has anti-excitotoxic properties and inceases survival by a few months (Bensimon *et al.*, 1994; Lacomblez *et al.*, 1996). However, the properties of riluzole are not limited to anti-excitotoxic activity.

2.8.4. Axonal transport

Intracellular trafficking of cargoes is an essential process in maintaining the structure and function of all mammalian cell types, but especially of neurons because of their extreme axon/dendrite polarization (De Vos and Hafezparast, 2017). Motor neurons are highly specialized cells with extensive dendritic arbors and axonal processes that can extend up to 1 m from the cell body (Ström *et al.*, 2008). The ability of motor neurons to maintain this specialized morphology depends on the cytoskeletal structure and the continous transport of proteins and organelles for long distances to and from the cell body.

Microtubules (MTs), intermediate filaments (IF) and microfilaments, as components of the cytoskeleton, contribute to the morphology and function of neurons, but it is almost entirely on microtubules that axonal transport depends (Maday *et al.*, 2014; Clark *et al.*, 2016). Microtubules are polarized tubulin polymers with fast growing plus ends and more stable minus ends, organized in a generally radial array in the soma with plus ends directed toward the cell surface. In the axon, parallel microtubules form a unipolar array with plus-ends oriented outward (Burton and Paige, 1981; Stepanova *et al.*, 2003), while in dendrites microtubule organization is more complex, with microtubules often organized in arrays with mixed polarity (Kwan *et al.*, 2008).

Neurofilaments (NF), a type of intermediate filament abundantly found in neuronal cytoplasm, also act as structural components assembled into an intracellular scaffold, which provides mechanical stability to axons. Moreover, neurofilaments determine axonal caliber, which in turn is essential for the rapid speed of neuronal signal propagation (Lobsiger and Cleveland, 2009). In a pathological context, NF are also important because their accumulation is one of the pathological hallmarks of various MNDs including ALS (Ikenaka *et al.*, 2012). Neurofilaments consist of light (NF-L), medium (NF-M), and heavy (NF-H) subunits, in equal proportion, and their assembly mainteins vulnerable large-caliber motor axons (Kawamura *et al*., 1981; Julien, 1997).

Thus, using cytoskeletal rails, axonal transport is able to mediate the movement of cargoes, such as proteins, mRNA, lipids, membrane-bound vesicles and organelles mostly synthesised in the cell body (De Vos and Hafezparast, 2017). In the axon and dendrites, transport occurs bidirectionally, depending on the polarity of the rails being transported from the cell body to the periphery, in a process known as anterograde transport, and from the periphery to the cell body, in a molecular system called retrograde transport. The major components of axonal transport are a group of specialized motor proteins that govern cargo transport along the cytoskeletal networks of microtubules and actin filaments. These are kinesin, dyenin and myosin proteins (Hirokawa, 1998; Cheney and Baker, 1999).

The human kinesin superfamily contains 45 members (Hirokawa *et al.*, 2009), subdivided into 15 subfamilies, which are termed kinesin 1 to kinesin 14B according to the results of phylogenetic analyses (Lawrence *et al.*, 2004; Hirokawa *et al.*, 2009). Kinesin acts as a tetramer of two heavy chains (KHC) and two light chains (KLC) mainly composed of motor and coiled-coil/cargo binding domains, respectively (Figure 14A) (Hirokawa and Noda, 2008).

Kinesin components comprise three major groups depending on the position of the motor domain within the molecule: N-terminal motor domain KIFs (N-KIFs), middle motor domain KIFs (M-KIFs) and C-terminal motor domain KIFs (C-KIFs) (Figure 14B) (Miki *et al.*, 2001; Hirokawa *et al.*, 2009).

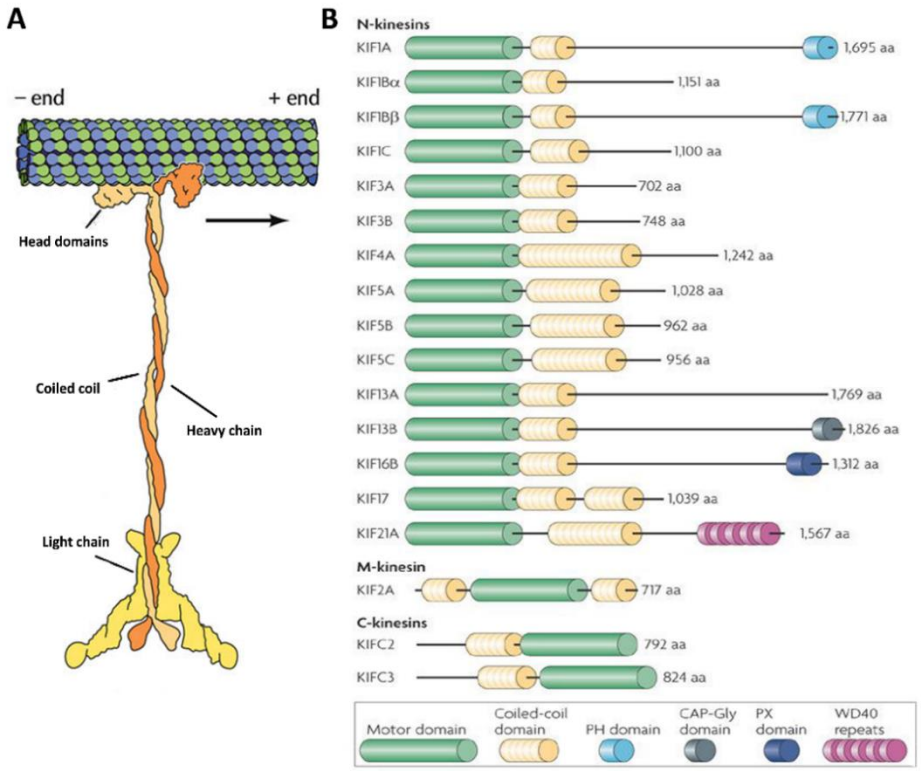

Figure 14. Kinesin protein. (**A**) Kinesin tetrameric structure. (**B**) The domain structure of the major kinesins. In general, kinesins comprise a kinesin motor domain and a coiled-coil domain. There are also gene specific domains, such as the pleckstrin homology (PH) domain of KIF1A and KIF1Bβ, the CAP-Gly domain of KIF13B and the WD40 repeats of KIF21A. N-kinesins drive microtubule plus end-directed transport, while C-kinesins drive minus end-directed transport and M-kinesins depolymerize microtubules. Only the kinesin 13 family contains M-kinesins and only the kinesin 14A and 14B families contain C-kinesins. All other families consist of N-kinesins. Abbreviattions: (aa) amino acids; (PX) phox homology. Adapted from Cooper and Hausman, 2006 and Hirokawa *et al*., 2009.

Kinesin is the major motor for anterograde transport supplying distal axons with newly synthesized proteins and lipids, like synaptic proteins and neurite elongation components (Hirokawa *et al.*, 1991); kinesin also participates in the transport of a number of organelles such as mitochondria, endosomes,

lysosomes, membrane organelles, and granular-like particles (Hirokawa *et al.*, 2009; Maday *et al.*, 2014).

Dyneins are a superfamily of cytoskeletal mechanoenzymes that move along microtubules in cells, converting the chemical energy stored in ATP to mechanical work, allowing the transport of various cellular cargos. Dyenins comprise two major groups: (i) axonemal dyneins and (ii) cytoplasmic dyneins (Karki and Holzbaur, 1999). Axonemal dyneins regulate microtubule sliding in the axonemes of cilia and flagella, whereas cytoplasmic dynein facilitates movement of organelles and other cargo necessary for cellular function. Each molecule of the dynein motor is a complex protein assembly composed of many smaller polypeptide subunits. Dynein consists of a huge protein complex containing multiple polypeptide subunits: two heavy chains (~520 kDa) with ATPase activity and generating movement along the microtubules, two intermediate chains (~74 kDa), four intermediate light chains (~33–59 kDa) and several light chains (~10–14 kDa) (Figure 15A) (Pfister *et al.*, 2005).

Cytoplasmic and axonemal dynein contain some of the same components, but they also contain some unique subunits. Axonemal dyneins might include as subunits the axonemal dynein heavy chain subunits (DNAH1, DNAH2, DNAH3, DNAH5, DNAH6, DNAH7, DNAH8, DNAH9, DNAH10, DNAH11, DNAH12, DNAH13, DNAH14, DNAH17), the axonemal dynein intermediate chain subunits (DNAI1, DNAI2), the axonemal dynein light intermediate chain subunits (DNALI1) and the axonemal dynein light chain subunits (DNAL1, DNAL4), whereas cytoplasmatic dyneins may include as subunits the cytoplasmic dynein heavy chain subunits (DYNC1H1, DYNC2H1), the cytoplasmic dynein intermediate chain subunits (DYNC1I1, DYNC1I2), the cytoplasmic dynein light intermediate chain subunits (DYNC1LI1, DYNC1LI2,

DYNC2LI1) and the cytoplasmic dynein light chain subunits (DYNLL1, DYNLL2, DYNLRB1, DYNLRB2, DYNLT1, DYNLT3) (Lee *et al.*, 2005).

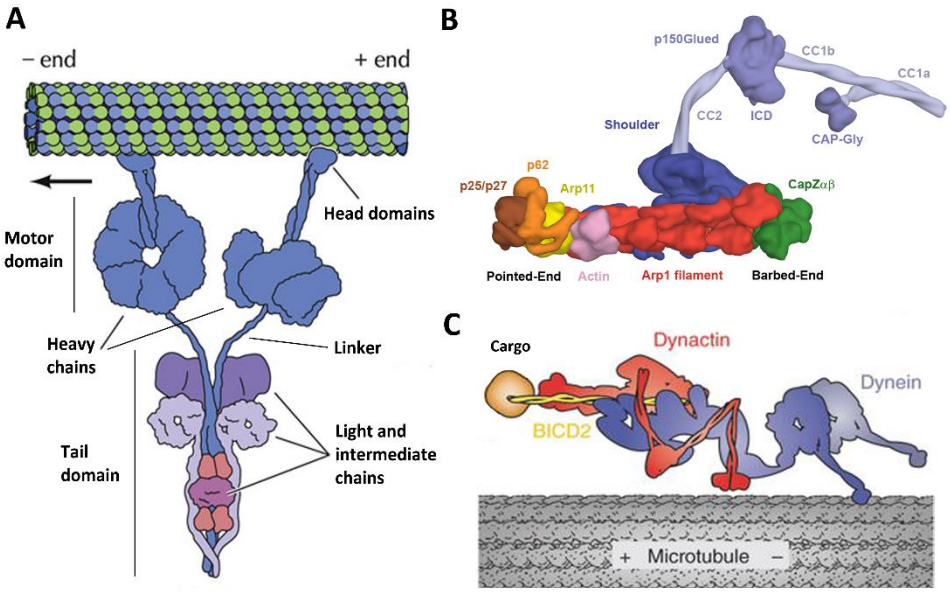

Figure 15. Dynein protein. (**A**) Dynein complex tetrameric structure. (**B**) Representation of dynactin complex tetrameric structure. The dynactin filament is shown by Arp1 (red) and β-actin (light purple). It is capped by Arp11 (yellow) and p62 (orange) and p25/p27 (brown) on the pointed end and by CapZ α–β (green) on the barbed end. p150 is found both in the shoulder complex (blue) and in the extended coiled coil (CC) (gray), at the end of which is its microtubule-binding CAP-Gly domain (blue). (**C**) Cartoon of the functional complex between dynein and dynactin complexes moving a cargo toward microtubule minus end. The dynein motor domains (blue) point toward the minus end of the microtubule, whereas the rest of the dynein motor and dynactin (red) extends toward the microtubule plus end. BICD2 (yellow) stabilizes the interaction between dynein and dynactin and also provides a link to cargo. Adapted from Cooper and Hausman, 2006 and Reck-Peterson, 2015.

Cytoplasmic dynein moves toward the minus ends of microtubules. Therefore, it conveys cargo retrogradely in the axon and distal dendrites, while in the proximal dendrites it conveys cargo to both the periphery and the cell center because of the mixed polarity of the microtubules (Hirokawa *et al.*, 1990; Kamiya, 2002). Retrograde transport is required to maintain homeostasis by removing aging proteins and organelles from the distal axon for degradation and recycling of components (Maday *et al.*, 2014). In other settings, dynein is

also important to provide forces and displacements in mitosis, and drive the beat of eukaryotic cilia and flagella (Roberts *et al.*, 2013).

Dynein often works in association with dynactin (Schroer, 2004), a 23-subunit protein complex that acts as a co-factor of the microtubule motor cytoplasmic dynein-1. Dynactin consists of three major structural domains: (1) sidearm-shoulder: DCTN1/p150Glued, DCTN2/p50/dynamitin, DCTN3/p24/p22; (2) the Arp1 filament: ACTR1A/Arp1/centractin, actin, CapZ; and (3) the pointed end complex: Actr10/Arp11, DCTN4/p62, DCTN5/p25, and DCTN6/p27 (Figure 15B and C) (Schroer, 2004). Dynactin can be considered as a 'dynein receptor' that modulates binding of dynein to cell organelles that are to be transported along microtubules (Vaughan and Vallee, 1995).

Myosin superfamily motor proteins use the energy of ATP hydrolysis to generate force and movement along actin filaments for short-range, dispersive distribution of vesicles, and/or organelles to the cell periphery. They are classified into 18 classes (Foth *et al.*, 2006). Concretely, myosin motor proteins play significant roles in cell movement, muscle contraction, cytokinesis, membrane trafficking and signal transduction. Most myosins form a dimer and consist of a motor domain, a neck region, and a tail region (Hirokawa *et al.*, 2010). Actin filaments also have a polarity; the barbed end (the growing end) points to the plasma membrane in the presynaptic and postsynaptic regions (Hirokawa *et al.*, 2010).

2.8.4.1. Axonal transport impairment in ALS

Because of the decreased motility of motor proteins or their decreased binding to motor proteins, various cargos of motor proteins are accumulated in degenerated motor neurons in ALS. Decreased kinesin-mediated and

dynein-mediated axonal transport occurs in ALS patients and in transgenic animal models (Breuer *et al.*, 1987; Breuer and Atkinson, 1988; Collard *et al.*, 1995; Sasaki and Iwata, 1996; Williamson and Cleveland, 1999; Ligon *et al.*, 2005). Among related genes with dysregulated expressions, *dynactin-1* is also markedly and widely downregulated in sALS motor neurons (Jiang *et al.*, 2005). Furthermore, dynactin-1 downregulation precedes the accumulation of phosphorylated-neurofilament (Jiang *et al.*, 2007). This change in sALS seems to be specific to motor neurons, as dynactin-1 expression is preserved in neurons in the dorsal nucleus of Clarke and the intermediolateral nucleus in the spinal cord, Purkinje cells of the cerebellum, and cortical neurons in the occipital cortex (Ikenaka *et al.*, 2012).

Additionally, mutations in the retrograde motor complex dynein and in the dynein interacting complex dynactin cause motor neuron degeneration in humans and mice (Hafezparast *et al.*, 2003; Puls *et al.*, 2005). For example, the potential involvement of cytoplasmic dynein in ALS is further highlighted by the identification of a number of alterations in the motor-binding domain of dynactin subunit p150^{Glued} (*DTCN1*) in ALS patients (Münch *et al.*, 2004). Other mutations associated with fALS and axonal transport are found in genes coding for charged multivesicular body protein 2B (CHMP2B) and synaptobrevin-associated membrane protein B (VAPB) (Nishimura *et al.*, 2004; Parkinson *et al.*, 2006).

Accumulation of neurofilaments is a long-recognized hallmark of ALS pathology in humans and mouse models and contributes to the selective vulnerability of long, large-caliber motor axons (Carpenter, 1968; Gurney *et al.*, 1994; Bruijn *et al.*, 2004). Concretely, SOD1 mutants have impaired slow axonal transport with axonal accumulations of neurofilaments and tubulin (Borchelt *et al.*, 1998). Similarly, large axonal swellings with neurofilament

accumulations, consistent with a failure in axonal transport, are observed in patients with ALS (Muñoz *et al.*, 1988). Thus, misassembly of neurofilaments due to altered expression, mutation or deficient transport of individual subunits results in their accumulation, further hindrance of axonal transport, and eventual motor neuron death (Beaulieu *et al.*, 1999; Millecamps *et al.*, 2006).

Defects in kinesin and the dynein/dynactin axonal transport also result in abnormal accumulation of mitochondria and autophagosomes, among others (Hirokawa *et al.*, 2010). Mitochondria accumulate in the axons of spinal motor neurons in mouse mutant SOD1 models (Collard *et al.*, 1995; Magrané and Manfredi, 2009), and in sALS patients (Sasaki and Iwata, 1996), suggesting an impairment of axonal transport in ALS. Indeed, defective axonal transport of mitochondria in sciatic nerves is observed during the presymptomatic stage in mutant SOD1 models (Bilsland *et al.*, 2010). Something similar happens with the accumulations of autophagosomes in sALS human *post-mortem* tissue and animal models of ALS (Sasaki, 2011).

2.8.5. Proteostasis clearance systems

Protein homeostasis, also known as proteostasis, is the correct balance between production and degradation of proteins that is essential for the health and survival of cells. Proteostasis requires an intricate network of protein quality control pathways that works to prevent protein aggregation and maintain proteome health throughout the lifespan of the cell (Webster *et al.*, 2017).

Proteins are only slightly stable at physiological temperatures. This fact, together with the nature of protein folding and the cellular environment

means that proteins are constantly exposed to the high probability of unfolding and misfolding; in consequence, the process of cellular proteostasis is highly demanding (Schubert *et al.*, 2000; Hipp *et al.*, 2014). Proteins are constantly turned over to ensure a steady supply of functional proteins. Newly synthesized proteins fold into their specific three-dimensional shape co-translationally as the nascent polypeptide chain emerges from the ribosome. The specific three-dimensional structure of a protein, which is in part determined by its amino acid sequence, is crucial to its function (Webster *et al.*, 2017).

Under normal conditions, cells have efficient protein quality control machinery that is able to detect and handle misfolded proteins. This is accomplished by a number of cytosolic and endoplasmatic reticulum resident folding factors that aid in this calibrated system, including effectors such as chaperones and co-chaperones of the heat shock protein (Hsp) family, peptidyl prolyl cis/trans isomerases, and oxidoreductases (Braakman and Bulleid, 2011), which recognize wrongly folded proteins, help in their refolding, prevent their aggregation and provide aid to repair damaged proteins. In the event that all attempts to repair and correctly refold the proteins fails, then these chaperones also actively mediate their removal to prevent protein aggregation and proteotoxic stress (Ruegsegger and Saxena, 2016).

Eukaryotic cells have two major pathways of protein degradation: (i) the proteasome and (ii) the lysosome. The proteasome is a multimeric ATP-dependent protease complex that selectively recognizes ubiquitinated substrates, forming the ubiquitin-proteosome system (UPS). Degradation by the proteasome requires protein unfolding and relies on chaperones to prevent proteins from aggregating (Hershko and Ciechanover, 1998).

Concretely, UPS employs polyubiquitin chains to label proteins for proteolysis and a vast array of ubiquitin-activating (E1), ubiquitin-conjugating (E2), and ubiquitin-ligase (E3) enzymes to assure protein turnover in a tightly regulated spatio-temporal manner (Figure 16) (Glickman and Ciechanover, 2002).

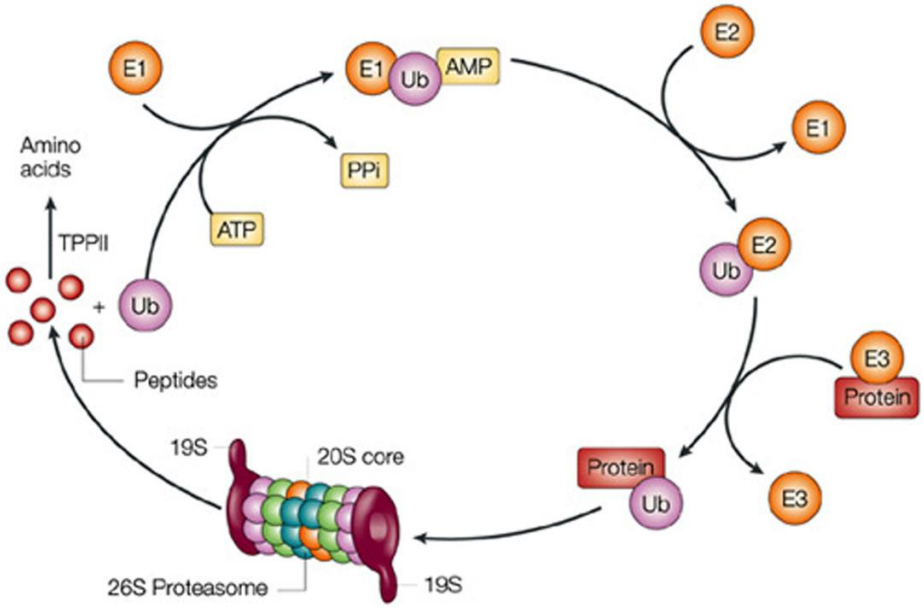

Figure 16. The scheme shows the main steps of the ubiquitin-proteasome pathway. 1) E1 binds to ubiquitin by consumption of one ATP to AMP in order to activate it. 2) The ubiquitin-carrier enzyme E2 takes over the ubiquitin from E1. 3) E2 transfers the ubiquitin to a protein substrate bound to the ubiquitin ligase, E3. 4) The ubiquitin chain is extended. Each step of the extension can be reversed by a deubiquitinating enzyme. 5) A ubiquitinated protein bound with either 1, 2, 3 or 4 ubiquitin molecules binds to the 26 S proteasome in order to be degraded. At degradation of the substrate the ubiquitin molecules are released by deubiquitinating enzymes. Adapted from Sino Biological web.

Autophagy is a crucial lysosome-dependent protein degradation process, in which cytosolic materials such as long-lived proteins and aggregate-prone pathogenic proteins, as well as damaged organelles, are eliminated by enclosing them within a double membrane vesicle termed as an 'autophagosome'. The autophagosome ultimately fuses with lysosome to degrade the isolated materials (Mizushima and Komatsu, 2011). Autophagy is classified into three major types: macroautophagy, microautophagy and

chaperone-mediated autophagy (CMA). Macroautophagy (here onwards termed autophagy) is associated with the bulk degradation of cytoplasmic components via the formation of autophagosomes, whereas microautophagy is a process that involves the direct uptake and degradation of cytoplasmic components by lysosomes, without the formation or involvement of transport vesicles (Glick *et al.*, 2010). In the case of CMA, the presence of a consensus pentapeptide sequence, Lys-Phe-Glu-Arg-Gln, is required in the substrate protein to which the chaperone Hsp70 binds, followed by the recognition of the substrate-chaperone complex by LAMP2A. The entire complex is then unfolded, moved across lysosomal membranes and eventually degraded within the lysosome (Figure 17) (Arias and Cuervo, 2011; Cuervo, 2011).

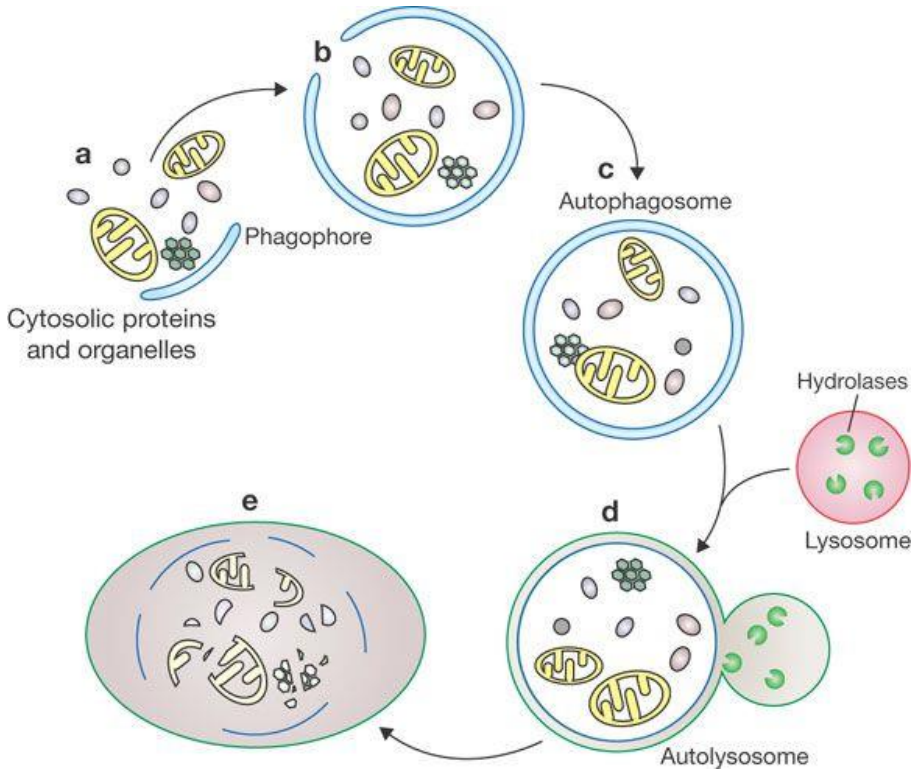

Figure 17. The scheme shows the autophagy mechanism. (a, b) Cytosolic material is sequestered by an expanding membrane sac, the phagophore, (c) resulting in the formation of a double-membrane vesicle, an autophagosome; (d) the outer membrane of the autophagosome subsequently fuses with a lysosome, exposing the inner single membrane of the autophagosome to lysosomal hydrolases; (d) the cargo-containing membrane compartment is then lysed, and the contents are degraded. Adapted from Xie and Klionsky, 2007.

Taking into account the important role played by autophagy and proteosome in the clearance of damaged or misfolded proteins, it is not surprising that disturbances in any of the mechanisms described above induce the cellular stress that is commonly observed in neurodegenerative disorders (Koga and Cuervo, 2011). Moreover, the ability of cells to maintain proteostasis declines with aging, thereby promoting the aberrant protein folding and aggregate deposition and facilitating the development and progression of various diseases, including neurodegenerative diseases (Takalo *et al.*, 2013). Furthermore, neuronal cells appear to be particularly vulnerable to disturbances in proteostasis because they are long-lived post-mitotic cells that are not able to dilute out protein aggregates during cell divisions (Son *et al.*, 2012).

2.8.5.1. Proteoasis disturbance in ALS

A hallmark feature in affected tissues of ALS is the presence of pathological protein aggregates. This fact suggests defective proteostasis mechanisms as possible causative players in ALS pathology. The discovery of ALS genes linked to UPS and autophagy (*C9ORF72*, *VCP*, *UBQLN2*, *OPTN*, and *TBK1*) supports its dysfunction as part of the etiology of the disease, explaining alterations in protein quality control, trafficking and degradation, and maintaining protein homeostasis (Blokhuis *et al.*, 2013; Peters *et al.*, 2015).

The insoluble protein aggregates observed in ALS and FTD are mainly composed of TDP-43 and, in a low percentatge of cases, FUS protein (Neumann *et al*., 2006; Vance *et al.*, 2009). Upon stress by missfolding, mutant forms of both proteins are ubiquitinated and recruited into cytoplasmic stress granules, where they aggregate with stress granule components in an irreversible manner to give rise to pathological inclusions (Vance *et al.*, 2013;

Chen *et al.*, 2016). The accumulation of these ubiquitin-positive inclusion bodies in sALS and fALS cases, also observed in several disease models, has been linked to UPS dysfunction (Bendotti *et al.*, 2012), due to the catalytic activity of the proteasome shown to be significantly reduced in sALS tissue (Kabashi *et al.*, 2012). In addition, there are several pieces of evidence, accumulated over years, that mutant SOD1 models also present proteoasis disturbances. Aggregation of SOD1 has toxic effects on the two major protein degradation mechanisms. Mutant SOD1 also forms toxic oligomers (Urushitani *et al.*, 2002), which further adopt a conformation to prevent ubiquitin-mediated degradation and accumulate as aggregates to induce stress response in cells (Atkin *et al.*, 2006; Niwa *et al.*, 2007).

Other ALS-associated proteins are involved in proteoastasis impairment, such as valosin-containing protein (VCP), which functions as an ATP-driven chaperon involved in the maturation of ubiquitin containing autophagosomes, playing an important role in the regulation of ER stress. VCP mutations lead to suboptimal functioning of these quality control mechanisms, thereby damaging proteostasis (Wojcik *et al.*, 2006; Yamanaka *et al.*, 2012). Another example is mutations in *VAPB* gene, coding for Vesicle-Associated Membrane Protein-Associated Protein B/C, causing ER stress and impairment of proteasome function (Moumen *et al.*, 2011).

Autophagy enhancement has been reported in ALS patients and mouse models (Morimoto *et al.*, 2007; Li *et al.*, 2008; Hetz *et al.*, 2009; Sasaki, 2011) accompanied by alterations at different steps of this pathway either in transport of cargo in autophagosome formation or in lysosome-mediated degradation (Zhang *et al.*, 2011). A direct role for TDP-43 has been identified in regulating transcription factor EB (*TFEB*) gene expression (Xia *et al.*, 2006), a master gene for lysosomal biogenesis, coordinating the expression of

lysosomal hydrolases, membrane proteins and other genes involved in autophagy (Sardiello *et al.*, 2009). Under physiological conditions, both UPS and autophagy are actively involved in the clearance of TDP-43, which is dependent on the solubility of TDP-43. Soluble form of TDP-43 is preferentially degraded by the UPS, whereas the removal of oligomeric TDP-43 and TDP-43 aggregates is achieved via autophagy. In fact, functional UPS and autophagy are able to clear macro-aggregates *in vitro* that mimic the pathological features of the aggregates in patients (Scotter *et al.*, 2014). Yet loss of TDP-43 leads to enhanced nuclear translocation of TFEB, thereby impairing the fusion of autophagosomes with lysosomes (Xia *et al.*, 2006).

Similarly, loss of optineurin function, which occurs in membrane and vesicle trafficking, results in protein aggregation that in turn leads to the appearance of severe motor axonopathy. Mutations in optineurin impair autophagy-facilitated degradation of misfolded proteins, as well as inhibiting autophagosome formations, thereby contributing to proteostasis impairment and concomitant aggregate formation and accumulation (Shen *et al.*, 2015). In the same manner, mutations in *C9ORF72* gene result in defective regulation of endosomal trafficking and autophagy. Loss of C9orf72 function diminishes the transport of proteins from the plasma membrane to the Golgi, and changes the ratio of autophagosome marker light chain 3 (LC3-II):(LC3-1) (Farg *et al.*, 2014).

2.8.6. RNA processing

Gene expression is tightly regulated by complex pathways by which RNA is generated, stored, transported, and translated (Lagier-Tourenne and Cleveland, 2009; Verma, 2011; Ling *et al.*, 2013). Transcription is the first step of RNA generation, in which a particular segment of DNA gene serves as a

template for complementary base-pairing, when an enzyme called RNA polymerase II catalyzes the formation of a pre-mRNA molecule, which is then processed to form mature mRNA (Clancy and Brown, 2008). After transcription, alternative splicing occurs in cellular machines called spliceosomes, which are a complex of small nuclear ribonucleoproteins (snRNPs) and additional proteins. Alternative splicing is a regulated process during gene expression that results in a single gene coding for multiple proteins. In this process, particular exons of a gene may be included within or excluded from the final processed messenger RNA produced from that gene (Black, 2003). The resulting mRNA is a single-stranded copy of the gene, which must then be translated into a protein molecule. Consequently, the proteins translated from alternatively spliced mRNAs will contain differences in their amino acid sequence and, often, in their biological functions. Specifically, neurons and glial cells in the brain take great advantage of these different strategies to diversify their repertoires.

After the process of transcription in the cell's nucleus, mature mRNA molecules must leave the nucleus and travel to the cytoplasm, where the ribosomes are located. Translation machinery resides within a specialized organelle called the ribosome. The ribosome molecules translate this code to a specific sequence of amino acids. The ribosome is a multi-subunit structure containing rRNA and proteins. It is the 'factory' where amino acids are assembled into proteins.

2.8.6.1. Aberrant RNA processing in ALS

RNA processing is essential for normal and properly regulated gene expression; therefore, defects at all or some levels of gene regulation can contribute to disease-RNA specific alterations (Belzil *et al.*, 2013a and 2013b;

Bentmann *et al.*, 2013; Anderson and Ivanov, 2014). Recent studies have shown that mutations in RNA-binding proteins (RBPs) are a key cause of several human neuronal-based diseases (Liu *et al.*, 2017). RBPs are essentially required at all levels of RNA processing in both the nucleus and cytoplasm where transcription, splicing, RNA stabilization and RNA degradation occur. A notable example of RBP defects is found in familial and sporadic cases of ALS and FTD, the TDP-43 protein. The involvement of TDP-43 in RNA-related pathways is strong. Since its discovery, TDP-43 has been described as an RNA-processing protein with roles in multiple steps of RNA regulation including RNA transcription, splicing, transport, translation and microRNA production (Lagier-Tourenne *et al.*, 2010).

TDP-43 participates in RNA transcription in human brain (Thorpe *et al.*, 2008; Lagier-Tourenne *et al.*, 2010) and in several cell culture systems (Ayala *et al.*, 2008); this is conducted by direct interaction with RNA through two RNA recognition motif (RRM) protein domains, used to mediate their binding to euchromatin in nuclear DNA. TDP-43 directly interacts with the heterogeneous nuclear ribonucleoprotein complex, which regulates RNA splicing and transport (D'Ambrogio *et al.*, 2009). TDP-43 is associated with other splicing factors in the spliceosome, and its depletion or overexpression affects the splicing pattern of specific targets (De Conti *et al.*, 2015).

Furthermore, TDP-43's major interactor protein, hnRNP A2, is a crucial component of splicing regulation. TDP-43 is known to affect the splicing of apolipoprotein A-II (APOA2) and survival motor neuron (SMN) transcripts. SMN mutation is the underlying cause of human spinal muscular atrophies, another form of MND (Bose *et al.*, 2008). Notably, TDP-43's RNA targets also include genes linked to synaptic function, neurotransmitter release and the neurodegeneration-related genes progranulin (GRN), α-synuclein (SNCA), tau

(MAPT) and ataxin 1 and 2 (ATXN1/2). However, the magnitude of its specific RNA targets in nerve cells remains poorly understood. Approximately,1/3 of all transcribed RNAs harbor TDP-43 binding sites, which is consistent with the critical functions of TDP-43 in regulating RNA splicing and transport (Luquin *et al.*, 2009). However, the mechanism of protein-RNA interaction is not known (Polymenidou and Cleveland, 2011; Sephton *et al.*, 2011).

Heterokaryon assays have also demonstrated the function of TDP-43 as shuttle between the nucleus and the cytoplasm (Belly *et al.*, 2005; Feiguin *et al.*, 2009; Lagier-Tourenne *et al.*, 2010). Indeed, TDP-43 is present in variable amounts in the cytoplasm, where it is involved in regulating mRNA's fate in space and time, controlling its subcellular localization, translation and degradation. In the neuronal cytoplasm, TDP-43 is found in RNA-transporting granules that translocate to dendritic spines upon specific neuronal stimuli (Belly *et al.*, 2005; Fujii *et al.*, 2005). The loss of TDP-43 reduces branching as well as synaptic formation in Drosophila neurons, suggesting that TDP-43 also plays a role in the modulation of neuronal plasticity by altering mRNA transport and local protein translation in the neurons (Feiguin *et al.*, 2009).

2.8.6.2. Dysfunctional miRNA processing in ALS

miRNAs are defined as 21-25 nucleotide single-stranded RNAs (ssRNAs), which are produced from hairpin shaped precursors (Ambros *et al.*, 2003). A number of miRNAs are known for functions in diverse processes including cell proliferation, cell death, fat metabolism, neuronal patterning, hematopoietic differentiation and immunity (He and Hannon, 2004).

miRNAs are synthesized from primary miRNAs (pri-miRNAs) in two stages by the action of two RNase III-type proteins: Drosha in the nucleus, and Dicer in

the cytoplasm (Kim *et al.*, 2009). The pri-miRNA is processed within the nucleus to a precursor miRNA (pre-miRNA) by Drosha enzyme. Next, the transport of pre-miRNAs to the cytoplasm is mediated by exportin-5 (EXP-5). In the cytoplasm, pre-miRNA are further processed to become mature miRNAs by Dicer and, subsequently, loaded onto the Argonaute (Argo) protein to be incorporated into the effector RNA-induced silencing complex (RISC), which degrades or translationally silences mRNA (Verma, 2011).

In the context of ALS, TDP-43 associates with DROSA (Hicks *et al.*, 2000; Feiguin *et al.*, 2009). Additionally, TDP-43 is involved in the cytoplasm cleavage step of miRNA biogenesis as evidenced by its association with proteins known to be part of the Dicer complex (Feiguin *et al.*, 2009).

3 Frontotemporal lobar degeneration

3.1. FTLD definition

Frontotemporal lobar degeneration (FTLD) is a pathological process underlying frontotemporal dementia (FTD); FTLD is the second most common cause of early-onset dementia after Alzheimer disease (Forman *et al.*, 2006). FTLD is clinically and pathologically a heterogeneous syndrome, characterized by progressive decline in behaviour and/or language associated with degeneration of the frontal and anterior temporal lobes (Forman *et al.*, 2006a; Rabinovici and Miller, 2010).

3.2. Epidemiology of FTLD

FTD prevalence ranges from four to fifteen per 100,000 inhabitants under the age of 65, as reported in European and US epidemiological studies (Rabinovici and Miller, 2010). The age of onset can vary widely from the third to the ninth decade (Ratnavalli *et al.*, 2002; Hodges *et al.*, 2003; Johnson *et al.*, 2005; Dickerson, 2016). Median survival in FTLD is 6-11 years from symptom onset, and 3-4 years from diagnosis, with a shorter survival and more rapid cognitive and functional decline than in Alzheimer's disease (Hodges *et al.*, 2003; Roberson *et al.*, 2005). Sex distribution in FTLD appears to vary depending on the clinical syndrome, with most studies reporting a male preponderance in

behavioural-variant, whereas others report male predominance in the semantic-variant and female predominance in the nonfluent variant (Ratnavalli *et al.*, 2002; Hodges *et al.*, 2003; Roberson *et al.*, 2005).

3.3. Clinical symptoms of FTLD

FTD usually presents in the patient's mid-life, preserving, at the beginning, memory, navigational skills and other aspects of general intellect. Three main clinical syndromes of FTD have been defined (Warren *et al.*, 2013):

(i) Behavioural-variant frontotemporal dementia (bvFTLD) manifests with progressive decline in interpersonal and executive skills with altered emotional reactions and a variety of abnormal behaviours such as apathy, disinhibition, obsessions, rituals and stereotypies. This clinical syndrome is closely associated with frontal-predominant cortical degeneration (Rascovsky *et al.*, 2011).

(ii) Semantic variant of primary progressive aphasia (svPPA) manifests with progressive breakdown of semantic memory that stores knowledge about objects and concepts. Typically, semantic dementia initially affects highly elaborate knowledge of vocabulary as well as the meaning of words. This syndrome is associated with bilateral anterior temporal degeneration (Hodges and Patterson, 2007).

(iii) Nonfluent variant of primary progressive aphasia (nfvPPA) manifests with progressive breakdown in language output with effortful non-fluent speech (Rohrer *et al.*, 2010). In some patients, speech sound (phonemic) or articulatory (phonetic, speech apraxic) errors are the dominant feature, whereas in others, the syndrome is dominated by expressive agrammatism

with terse telegraphic phrases. This syndrome is associated with left perisylvian cortical atrophy (Rabinovici and Miller, 2010).

Additionally, disturbances of motor function are common, including clinical symptoms and signs of three disorders that are part of the FTD spectrum: corticobasal syndrome (CBS), progressive supranuclear palsy (PSP), and amyotrophic lateral sclerosis (ALS) (Bott *et al.*, 2014). Therefore, ALS may be associated with cognitive impairment characteristics of FTLD, thus suggesting that ALS and FTLD might be different manifestations of a single disorder.

FTD decline differs from one person to another. Persons suffering from FTD show muscle weakness and coordination problems, leaving them in need of a wheelchair or remaining bedbound. Muscular alterations may cause problems of swallowing, chewing, moving and controlling bladder and/or bowels. Causes of death include urinary tract and/or lung infections (Bott *et al.*, 2014).

3.4. Diagnosis and treatment of FTLD

FTD diagnosis is based on clinical examination, followed by complementary analysis including magnetic resonance imaging (MRI) and positron emission tomography (PET) (Kipps *et al.*, 2009). Nowadays, there is no treatment for any of the frontotemporal subtypes. Selective serotonin re-uptake inhibitors can be used to control disinhibition and compulsive behavior (Swartz *et al.*, 1997).

3.5. Neuropathology of FTLD

Neuropathological changes in brains affected by FTD are atrophy in the frontal lobe and temporal lobe of the brain, resulting from neuronal loss and

spongiosis in the upper cortical layers, and astrocytic gliosis; the white matter shows variable reduction and myelin pallor.

FTLD was initially classified into two different types: (a) FTLD-MAPT, linked to the presence of tau-positive inclusions, and (b) FTLD-U, linked to tau-negative, ubiquitin-positive inclusions. However, this classification has been refined, establishing three main different types of FTLD: (1) FTLD-MAPT, (2) FTLD-TDP and (3) FTLD-FUS. Before the discovery of TDP-43 agreggates in 2006, most tau-negative FTLD cases were collectively termed FTLD-U. After the discovery, the majority of cases became FTLD-TDP43 because TDP43 was the main protein accumulated in ubiquitin-positive inclusions.

In 2009, mutations in FUS were identified as causative in some familial ALS cases; further studies demonstrated that most tau-negative and TDP-43-negative inclusions were FUS positive, thereby establishing the third group, FTLD-FUS (Hasegawa, 2017). Notably, the neuropathology underlying FTLD is a tauopathy (tau-positive) in approximately 45% of patients, while in about 50% of patients the underlying pathology is FTLD-TDP (ubiquitin-positive but tau- and α-synuclein-negative); a minority of cases are FUS-positive or positive for other proteins (Geser *et al.*, 2009). Thus, the most common form of tau-negative FTLD is associated with neuronal inclusions composed of TDP-43 (FTLD-TDP-43) (Josephs *et al.*, 2009).

3.5.1. Histopathology of FTLD-TDP

TDP-43 is the most specific and sensitive marker to detect the characteristic protein aggregates of FTLD-TDP, forming neuronal cytoplasmic inclusions (NCIs), dystrophic neurites (DNs) and neuronal intranuclear inclusions (NIIs) (Figure 18).

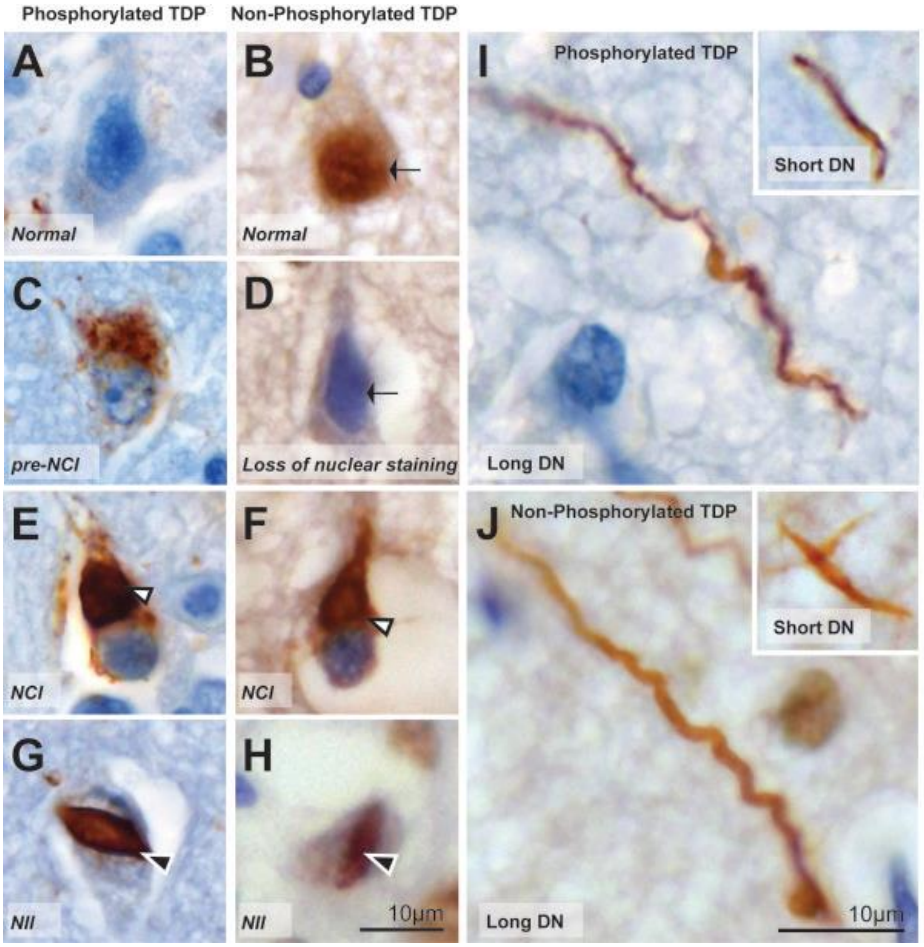

Figure 18. Typical examples of TDP43-immunoreactivity with pTDP43 and iTDP43 in FTLD. In sections immunostained with anti-phosphorylated TDP43 antibodies (pTDP43), nuclear staining is not observed in normal neurons (A). Typical examples of pTDP43-immunoreactive pre-inclusions (C), NCI I, NII (G) and long DN (I, the inset shows a short DN) are seen in FTLD-TDP43 cases. In sections stained with anti-non-phosphorylated TDP43 antibodies, normal neurons demonstrate TDP43 nuclear staining (B). Loss of nuclear staining is accompanied by NCIs and NIIs in FTLD-TDP43 cases (D, F, H). TDP43-immunoreactive long DN (J, inset shows a short DN). Scale in H (equivalent for A-G), scale in J (equivalent for I). Adapted from Tan *et al.*, 2013.

FTLD-TDP is categorized into four subtypes depending on the morphology of TDP-43 inclusions, laminar distribution, and relative proportion of dystrophic neurites versus neuronal cytoplasmic inclusions (Figure 19) (Mackenzie *et al.*, 2006a; Sampathu *et al.*, 2006; Mackenzie *et al.*, 2011; Tan *et al.*, 2013):

- Type A shows abundant short dystrophic neurites (DN) and compact oval or crescent-shaped neuronal cytoplasmic inclusions (NCI), predominantly in layer II/III of the neocortex. Moderate numbers of granular NCI are present in the dentate granule cells of the hippocampus. TDP-43-immunoreactive glial cytoplasmic inclusions (GCI) are present in the cerebral white matter, and in affected subcortical regions including the striatum, thalamus and substantia nigra. Cases with this pathology usually present with either bvFTD or nfvPPA.

- Type B shows moderate numbers of compact or granular neuronal cytoplasmic inclusions (NCI) in both superficial and deep cortical layers with few or no pre-inclusions and delicate wispy neurites which are often more abundant in the superficial cortical laminae. Characteristic, and almost exclusive to type B, is the presence of neuronal cytoplasmic inclusions (NCI) in lower motor neurons (LMN), even in the absence of clinical features of ALS. Glial cytoplasmic inclusions (GCI) in oligodendrocytes of the cerebral white matter, medulla and spinal cord are common.

- Type C includes abundance of tortuously long neurites, predominantly in the superficial cortical laminae, with few or no neuronal cytoplasmic inclusions (NCI). Neuronal intranuclear inclusions (NII) and glial cytoplasmic inclusions (GCI) are uncommon. Variable numbers of neuronal cytoplasmic inclusions (NCI) are present in the hippocampus, usually with a compact round morphology. This is the most common pathology found in cases presenting with svPPA.

- **Type D** shows abundance of lentiform neuronal intranuclear inclusions (NII) and few short dystrophic neurites (DN) in the neocortex, not restricted to any cortical layer, with only rare neuronal cytoplasmic inclusions (NCI).

Recently, the sequential distribution of TDP-43 pathology has been proposed in a few cases of bvFTD (Brettschneider *et al.*, 2014b)

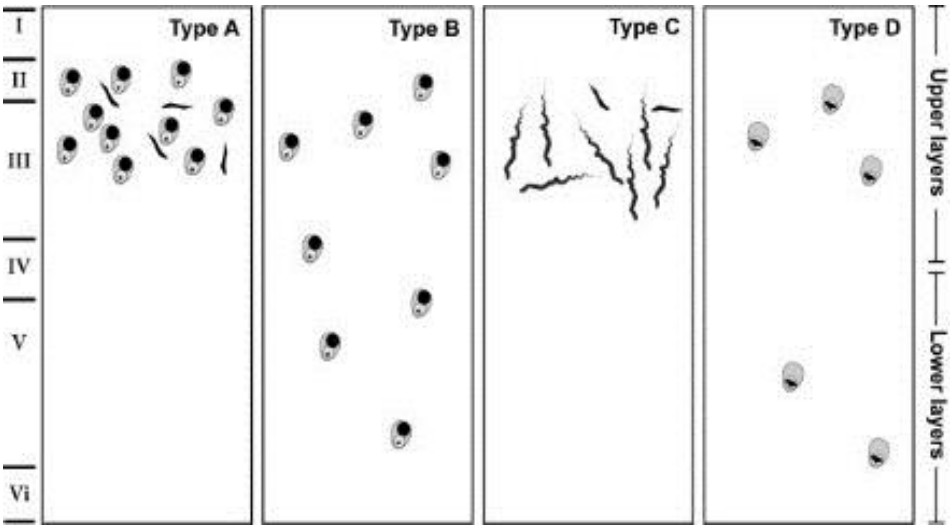

Figure 19. Ilustration of the harmonized classification system used for FTLD-TDP subtyping. Cases with moderate-to-numerous TDP43-immunoreactive NCI and short DN predominantly in the cortical layers II/III are assigned to type **A.** Cases with moderate to numerous TDP43-immunoreactive NCIs and sparse DNs across all cortical layers are assigned to type **B.** Cases with long dystrophic neurites in the upper layers, and NCIs, are assigned to type **C.** Cases with numerous lentiform NII are assigned to type **D**. From Tan *et al.,* 2013.

3.5.1.1. Genetics of frontotemporal lobar degeneration TDP-43

FTD is genetically complex and can present as sporadic or familial, often with autosomal dominant inheritance (Chow *et al.*, 1999). Conventional linkage studies have identified different chromosomal loci and a number of mutated genes including those coding for TAR DNA-binding protein (*TARDBP*), progranulin (*PGRN*), valosin containing protein (*VCP*), and charged multivesicular body protein 2B (*CHMP2B*), as well as those linked to

chromosome 9p (*C9ORF72*), among other minoritary mutations in other genes.

3.5.1.1.1. *TARDBP* mutations

TDP-43 gene mutations are rare in FTLD, despite this protein's being present in the pathological inclusions of most cases (FTLD-U) (Neumann *et al.*, 2006). Mutations in *TARBP* are more common in fALS.

3.5.1.1.2. *PGRN* mutations

Mutations in *PGRN* account for ~5–10% of all FTLD cases (Baker *et al.*, 2006; Cruts *et al.*, 2006). *PGRN*, located on chromosome 17q21, is composed of a noncoding region and 12 coding exons. *PGRN* encodes a 593 amino acid precursor protein having a signal peptide followed by 7.5 tandem repeats of 12 cysteinyl granulin motifs (He and Bateman, 2003). The secreted progranulin is subjected to proteolysis by extracellular proteases like elastase that cleave progranulin to generate granulin, a process regulated by secretory leukocyte protease inhibitor (SLPI) (Zhu *et al.*, 2002; He and Bateman, 2003). PGRN protein is a widely expressed, multifunctional, high molecular weight secreted growth factor, which plays significant roles in development, tumorigenesis, wound repair and inflammation by activating signaling pathways that control cell cycle progression and cell motility (Ahmed *et al.*, 2007). In the periphery, progranulin and granulin regulate the inflammatory cascade through opposing effects, with progranulin being anti-inflammatory while granulin is pro-inflammatory. The exact function of *PGRN* in CNS is unknown, although it may be involved in neurotrophic activity and neuroinflammation (He *et al.*, 2003; Ahmed *et al.*, 2007).

To date, more than 60 different pathogenic mutations in 163 families have been described worldwide (Gijselinck *et al.*, 2008). Almost all

pathogenic *PGRN* mutations including heterozygous deletions create functional null alleles and retain or degrade the unspliced transcript within the nucleus, preventing the translation of PGRN, and thus ultimately resulting in the reduction of secreted PGRN. Nevertheless, the ubiquitinated neuronal inclusions in the affected regions of brain do not show immunoreactivity to PGRN but to TDP-43-immunoreactivity in NCIs, NIIs and DNs (Baker *et al.*, 2006; Cruts *et al.*, 2006; Mackenzie *et al.*, 2006b).

3.5.1.1.3. *VCP* mutations

FTD associated with inclusion body myopathy and Paget's disease of bone (IBMPFD) is a rare multi-system disorder linked to chromosome 9p21-12. The gene responsible for this is *VCP*; the coding protein acts as a molecular chaperone associated with several cellular functions including ubiquitin-dependent protein degradation, cell cycle regulation and apoptosis (Watts *et al.*, 2004). Most of the VCP mutations are located within or near the ubiquitin-binding domain (Watts *et al.*, 2004). VCP mutations produce numerous lentiform NIIs and DNs (Forman *et al.*, 2006b). Similar to other FTLD-U subtypes, TDP-43 is the major protein constituent of these inclusions (Neumann *et al.*, 2006).

3.5.1.1.4. *CHMP2B* mutations

Genome-wide linkage analysis in different families with dementia has revealed rare complex mutations in the *CHMP2B* gene on chromosome 3p11 (Skibinski *et al.*, 2005). The protein encoded by this gene is a component of the endosomal secretory complex required for transport (ESCRT) type III (Skibinski *et al.*, 2005; Momeni *et al.*, 2006). The disease segregating mutation results in aberrant splicing of exon 6, producing a truncated protein (Skibinski *et al.*, 2005). Dysfunction of the ESCRT results in the inability of multi-vesicular bodies to internalize membrane-bound cargoes, leading to distorted

endosomes and reduced protein turnover (Babst *et al.*, 2002). Carriers of *CHMP2B* mutations show ubiquitinated inclusions negative for TDP-43 (Holm *et al.*, 2007). Besides FTD, CHMP2B mutations can also cause additional phenotypes including ALS and FTD-ALS (Parkinson *et al.*, 2006).

The identification of a common genetic locus for FTD and ALS (shown above) reinforces the molecular link between FTD and ALS. Thus, the genetic overlap between these two clinical entities suggests that diagnostic genetic screening in FTD-ALS should include both FTD-related and ALS-related genes including, *PGRN*, *VCP*, *CHMP2B* and *TARDBP* gene, among other minor prevalent genes (Aswathy *et al.*, 2010). Among these, the strongest link between the two disorders is mutations located in C9ORF72 gene, causing ALS, FTLD and concomitant forms.

3.5.1.1.5. *C9ORF72* mutations

Phenotypical overlap exists between FTD and amyotrophic lateral sclerosis, with as many as 30% of FTD patients developing clinical symptoms of motor neuron dysfunction (Lomen-Hoerth *et al.*, 2002), and 50% of ALS cases displaying at least some evidence of frontal-executive cognitive deficits (Phukan *et al.*, 2007). The link between ALS and FTD is supported by the identification of a non-coding "GGGGCC" (G_4C_2) hexanucleotide repeat expansion in the first intron or promoter region of the *C9ORF72* gene on chromosome 9p21 in fALS and fFTD. Mutations in *C9ORF72* are the most common genetic abnormality in familial and sporadic FTLD/ALS, being found in at least 8% of sALS and sFTLD cases and more than 40% of fALS and fFTLD cases (Dejesus-Hernandez *et al.*, 2011; Renton *et al.*, 2011).

In a normal population, wild-type alleles are, on average, three of these hexanucleotide-repeat units, ranging from two to 23 repeats. However, in

persons with the repeat expansion mutation, expansion sizes vary considerably between individual cases, with tens, hundreds or even thousands of these repeat units being present (Dejesus-Hernandez *et al.*, 2011; Renton *et al.*, 2011). Nevertheless, the lower threshold required to initiate pathogenesis is poorly defined. An individual with intermediate repeat length (30 units) exhibits some C9orf72-associated pathological phenotypes in the absence of clinical manifestations (Gami *et al.*, 2015), suggesting that 30 repeats may lie on the border between mild abnormalities and full-blown disease. Expansions of less than 30 repeats are not typically associated with disease, but a minority of ALS cases with 20-22 repeats have been described (Byrne *et al*., 2014). The inheritance of the *C9ORF72* mutation is autosomal dominant, although reduced penetrance occurs in some cases (Bigio, 2012; Van Blitterswijk *et al.*, 2012). Repeat expansion is unstable, increasing in repeat number over generations (Vance *et al.*, 2006).

C9orf72 repeat expansions also manifest pathologically as proteinaceous inclusions of the RNA/DNA-binding protein TDP-43, as in other forms of the clinicpathological spectrum. Thus, C9orf72 repeat expansion as a common genetic cause of ALS of FTD further highlights the extensive clinical, genetic and pathological overlap between these two conditions, suggesting that the two diseases represent opposite ends of a continuous clinical spectrum, with C9orf72 mutations at the heart of this spectrum, increasing the risk of developing FTD and/or ALS (Barker *et al*., 2017). In addition to TDP-43-positive inclusions, patients with C9orf72 mutations show TDP-43-negative and p62-positive inclusions mainly in the cerebellum. C9orf72-immunoreactive inclusions also occur in the CNS.

- **C9orf72 function**

C9orf72 protein is found in many regions of the brain, in the cytoplasm of neurons as well as in presynaptic terminals. Differential use of transcription alternative start and termination sites generates three RNA transcripts from C9orf72 DNA. These encode two protein isoforms consisting of a long isoform (isoform A) of approximately 54 kDa derived from variants 2 and 3, and a short isoform (isoform B) of approximately 24 kDa derived from variant 1 (Figure 20) (Barker *et al*., 2017).

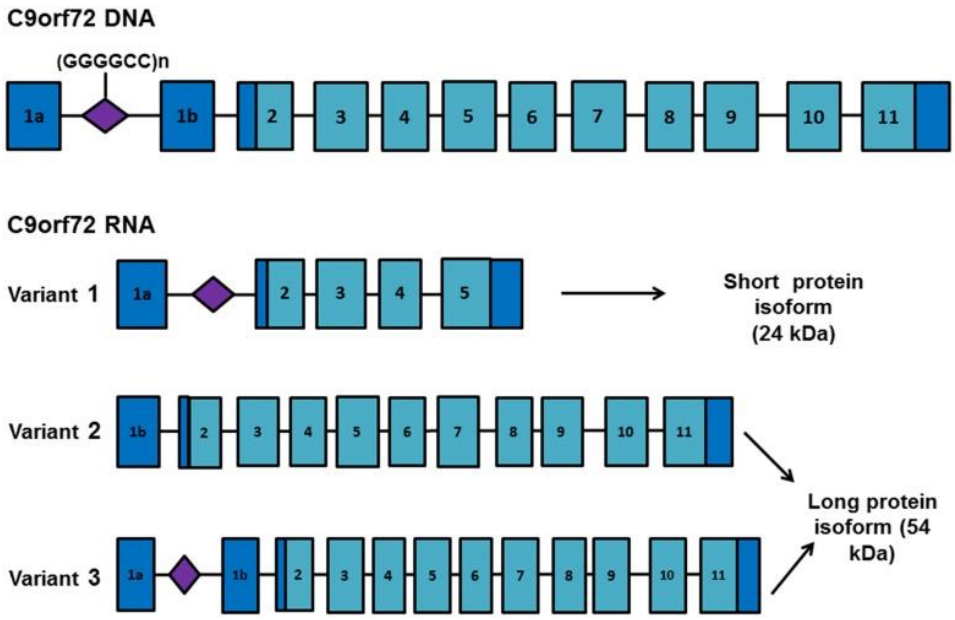

Figure 20. *C9orf72* RNA transcript variants. Schematic representation of the *C9orf72* gene and RNA transcript variants. Exons are depicted as blue boxes and the location of the GGGGCC repeat expansion is shown in purple. Differential selection of transcription start and termination sites generates three different RNA transcripts. Variant 1 encodes a short protein isoform (isoform B) whereas variants 2 and 3 encode a longer protein isoform (isoform A). Presence of the repeat expansion favors transcription from exon 1a, increasing the proportion of transcripts containing the repeat expansion. Adapted from Barker *et al*., 2017.

The normal function of the C9orf72 protein remains obscure, but the major predicted structural feature is a DENN (differentially expressed in normal and

neoplastic cells) domain. DENN-domain containing proteins function as guanine nucleotide exchange factors (GEFs), regulating GTPase-mediated membrane trafficking pathways. In cells, C9orf72 co-localizes with Rab proteins 7 and 11 suggesting its involvement in the regulation of vesicular membrane traffic (Zhang *et al.*, 2012; Levine *et al.*, 2013). C9orf72 is also implicated in the formation of autophagosome (Webster *et al.*, 2016) and in the removal of aggregated proteins via the autophagy receptor p62 (Sellier *et al.*, 2016).

Recent genetic and cell biological studies indicate that C9orf72 protein functions in lysosomes as part of a tri-molecular complex with Smith-Magenis chromosome region 8 (SMCR8) (Amick and Ferguson, 2017) and WD repeat-containing protein 41 (WDR41) proteins (Sullivan *et al.*, 2016), both regulators of autophagy. The important role for C9orf72 in lysosomes is supported by defects in the lysosome morphology and mTOR complex-1 (mTORC1) signaling arising from knocking out C9orf72 in diverse model systems. Moreover, C9orf72 knockdown in murine models produces an altered immune response (Atanasio *et al*., 2016) characterized by the accumulation of lysosomal vesicles within macrophages, implying a role for the C9orf72 protein in the regulation of late endosomal/lysosomal trafficking in macrophages and microglia (O'Rourke *et al*., 2016). Collectively, these findings define C9orf72-containing protein complex and lysosomal sites of action as central to C9orf72 function (Amick and Ferguson, 2017).

- **C9orf72 repeat toxicity**

There are currently three major hypotheses to explain how such repeat expansions could be pathogenic in fALS and fFTLD. The presence of a large "GGGGCC" repeat expansion may cause down-regulation in *C9ORF72* gene

expression leading to loss of C9orf72s still undefined normal cellular function. Several groups have shown that mRNA levels of at least one *C9ORF72* transcript are decreased in fFTLD and fALS (Dejesus-Hernandez *et al.*, 2011; Renton *et al.*, 2011; Gijselinck *et al.*, 2012), suggesting a potential loss of function.

In addition, RNA-mediated toxicity contributes to disease pathophysiology. C9orf72 repeat RNA is bidirectionally transcribed, from both the sense $(G_4C_2)n$ and the antisense $(G_2C_4)n$ DNA strand (Zu *et al.*, 2013), forming punctate nuclear aggregates termed RNA foci. Early reports indicate that transcribed repeats lead to accumulation of repeat-containing RNA foci in patient tissues (Dejesus-Hernandez *et al.*, 2011). Multiple nuclear, and more rarely, cytoplasmic, sense and anti-sense RNA foci have been identified in patient-derived cells throughout the CNS in expansion carriers (Gendron *et al.*, 2013; Lagier-Tourenne *et al*., 2013; Mizielinska *et al*., 2013; Zu *et al*., 2013).

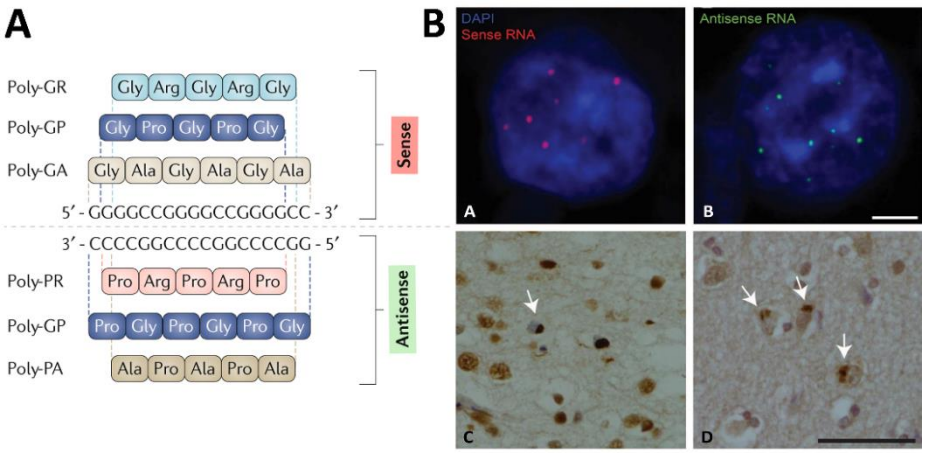

Figure 21. (A) Dipeptide repeat proteins. The figure shows the dipeptide repeat proteins generated by GGGGCC repeat-associated non-ATG (RAN) translation. The sense strand generates poly-GA, poly-GP and poly-GR , and the antisense strand generates poly-GP, poly-PA and poly-PR. **(B) c9FTD/ALS neuropathology.** Sense and antisense RNA foci are a common feature in the brains of patients with c9FTLD and/or c9ALS. a,b) Representative images show neurons from the frontal cortex of a patient with C9FTD/ALS, containing multiple sense (red; part A) and antisense (green; part B) foci in nuclei (stained blue with DAPI). Scale bar: 2.5 µm. c) TAR DNA-binding protein 43 (TDP-43) pathology in a patient with C9FTD/ALS. Arrow indicates a neuronal cytoplasmic TDP-43-immunoreactive inclusion in the frontal cortex, with

concomitant depletion of nuclear TDP-43. Scale bar: 50 µm. d) Dipeptide repeat protein (DPR) pathology in a patient with C9FTD/ALS. Inclusions consisting of sense and antisense DPRs. Arrows indicate neuronal cytoplasmic inclusions of poly-GA protein. Scale bar: 50 µm. Adapted from Barker *et al*., 2017.

The RNA toxicity hypothesis postulates that sense and antisense G_4C_2 repeats accumulate in nuclear RNA foci where they sequester essential RBPs (hnRNP-A1, hnRNP-A3, hnRNP-H, ADARB2, Pur-a, ASF/SF2, ALYREF and nucleolin), thus impairing their ability to regulate their RNA targets and culminating in a range of RNA misprocessing events.

Additionally, sense and antisense *C9ORF72* RNA repeats translate by an unconventional form of translation, repeat-associated non-AUG initiated translation (RAN translation). RAN translation of (G_4C_2) and (C_4G_2) results in the synthesis of five dipeptide repeat protein (DPR) species: poly-GA, poly-GP and poly-GR, from the sense transcript, and poly-GP, poly-PR and poly-PA, from the antisense transcript (Figure 21A). All five DPR species form ubiquitinated inclusions, which spread in different brain regions; these inclusions are more abundant in the cerebellum, hippocampus and neocortex, less frequent in subcortical regions, and rare in the brainstem and spinal cord (Figure 21B) (Ash *et al.*, 2013; Gendron *et al*., 2013; Mann *et al*., 2013). They produce toxic effects *in vitro* and *in vivo* (Kwon *et al.*, 2014; Mizielinska *et al*., 2014; Wen *et al*., 2014). Analyses of DPR interactomes reveal preferential interactions between proteins involved in proteasomal degradation (May *et al.*, 2014; Zhang *et al.*, 2018), RBPs, and components of membrane-less organelles, such as RNA stress granules, nucleoli, spliceosomes and the nuclear pore complex (NPC) (Lee *et al.*, 2016; Boeynaems *et al.*, 2017). A significant number of these organelle-related proteins, such as FUS, hnRNP-A1 and TIA1, possess low complexity sequence domains (LCDs) which mediate the assembly of membrane-less organelles. In order for membrane-less organelles to form, they must separate from the liquid cytoplasm which is

achieved by the concentration of the organelle components and the formation of a network of weak multi-valent interactions, a process known as liquid-liquid phase separation (LLPS) (Hyman *et al*., 2014). DPRs are able to interact with the LCD of these proteins, thus disrupting LLPS and altering their biophysical properties (Lee *et al*., 2016). Therefore, DPRs may contribute to toxicity by upsetting the composition of membrane-less organelles.

Both RNA foci and protein aggregates may produce gain of function toxicity in neurons, which, in addition to the *C9ORF72* transcript reduction, may promote neurodegeneration. Reduced *C9ORF72* expression in sALS and sFTLD with normal repeat ranges implies that reduced C9orf72 levels may be a common pathogenic factor in ALS or a consequence of the disease process (Ciura *et al.*, 2013). Several studies support the idea that we cannot conclusively prove that RNA foci or DPRs alone or in combination act as the main drivers of C9orf72 toxicity (Mackenzie *et al*., 2013; Davidson *et al*., 2014 and 2016; Gami *et al.*, 2015; Gomez-Deza *et al*., 2015; Schuldi *et al.*, 2015). Rather, a combination of the two, together with other factors, contributes to the pathogenesis.

3.6. Animal models of FTLD-TDP

Several models recapitulate the initial proteinopathy and other pathological features linked to the human disorder. A summary of different C9orf72 FTLD animal models is shown in Table VI (Picher-Martel *et al.*, 2016). Some models develop neurodegenerative cascades, but it remains uncertain whether the entire sequence of pathophysiologic events that occur in the human disease is fully captured (Dawson *et al.*, 2018).

Studies in the nematode *C. elegans* have contributed to our understanding of basic physiological processes such as aging, sensory processing and

programmed cell death, and to mechanisms underlying human diseases such as cancer and neurodegeneration. The genes linked to familial forms of FTLD including PGRN, VCP and TDP-43, have homologs in *C. elegans* (only CHMP2B and FUS do not) (Boxer *et al.*, 2012).

Homologues of several genes causing human autosmal FTD syndromes including valosin-containing protein (VCP) and TDP-43 occur in *Drosophila*. *Drosophila* models are particularly useful for dissecting the pathogenic mechanisms associated with particular mutations and identifying possible therapeutic targets, because they are relatively inexpensive to produce and have rapid life cycles (Boxer *et al.*, 2012).

Species	Nº repeats	Promoter	Onset time (weeks)	Survival (weeks)	Phenotype			
					P	CS	NPF and particularities	G
Mice	80	TRE	none	normal	N	N	Ubiquitin-positive inclusion, no DPR, no TDP43 inclusion	nd
	66 (injection of AVV2/9 at PND0)	nd	24	nd	nd	Y	Nuclear RNA foci, pTDP43 inclusions, cytosolic and nuclear DPR, anxiety and social abnormalities, motor impairment	Y
	100-1000	BAC	none	normal	N	N	RNA foci, DPR, no NCI	N
	500	BAC	none	normal	N	N	RNA foci, DPR, no NCI	N
	450	BAC	52	normal	N	Y	RNA foci, DPR, age-dependent protein accumulation, no motor deficits or MN loss, age dependent cognitive deficit, no TDP43 mislocalitzation	N
	500	BAC	16	20-40	Y	Y	NMJ loss, reduced axonal size, MN loss, RNA foci, DPR, TDP43 NCI	Y
Fruit flies	36-103	elav-GS	nd	4	nd	nd	RNA foci, DPR, toxicity linked to DPR	nd
	160	actin5C-Gal4	none	normal	N	nd	RNA foci, DPR, toxicity linked to DPR	nd

	30	Ok371-Gal4	4	nd	nd	nd	Decreased locomotor activity	nd
	58	Ok371-Gal4	nd	nd	nd	nd	Decreased locomotor activity, NMJ loss DPR	nd
Nematodes	n/a	alfa-1	2	nd	Y	nd	MN loss, paralysis in 60% of worms	nd
Zebrafish	C9ORF72-KO	n/a	nd	nd	nd	nd	MN axons shortening, reduced swimming	nd

Table VI. Summary of C9ORF72 animal models. Abbreviations: Y: yes; N: no; nd: not described; n/a: not applicable, BAC: Bacterial artificial chromosome (include C9ORF72 exons with promoter); CS: cognitive symptoms; DPR: dipeptide repeat; G: gliosis; NCI: neuron cytoplasmatic inclusions; MN: motor neuron; NMJ: neuromuscular junction; P: paralysis; PND: post-natal day. Adapted from Picher-Martel *et al.*, 2016.

However, among the different FTLD animal models, C9orf72 mutants have acquired relevance due to the high prevalence of this mutation in ALS and FTLD. In recent years, mice carrying 80 "GGGGCC" repeat expansions controlled under *TRE* promoter have been generated (Hukema *et al.*, 2014). After doxycycline induction, mice develop ubiquitin-positive inclusion but not DPR; however, behavioral analyses are not available on these mice. Additionally, knockout of C9orf72 in mice does not result in any motor neuron degeneration or modification in life expectancy, thus suggesting that loss of function is not sufficient to cause disease (Koppers *et al.*, 2015).

More recently, an AAV vector expressing either 2 or 66 repeats of G_4C_2 was injected into the CNS of postnatal-day-0 mice (Chew *et al.*, 2015). RNA nuclear foci occurred in mice carrying 66 repeats but not in mice carrying only two repeats. Moreover, rare pTDP-43 aggregates occurred in the nucleus and cytosol of cortex and hippocampus regions. These aggregates were not positive for poly(GA) but 75% of cells containing TDP-43 NCI were positive for poly(GA) inclusions. (G_4C_2)66 mice exhibit anxiety behavior in an open field test and motor impairment in the second day of rotarod testing at 6 months of age as compared to control mice.

3.7. Molecular alterations in FTLD-TDP

ALS, FTLD and ALS-FTLD reflect a clinicopathological spectrum sharing similar disease mechanisms linked to pathological TDP-43 (Lomen-Hoerth *et al.*, 2002). Consequently, a wide range of cellular pathways linked to ALS occurs in FTLD-TDP. C9orf72 loss of function and toxic gain of function mechanisms and TDP-43 alterations in sporadic forms can affect RNA processing and metabolism pathways, with alterations in transport granule function and stress granule formation and vesicular trafficking. They can lead to nucleolar dysfunction, affecting RNA splicing and transcription, and causing DNA damage. Proteostasis pathways including autophagy and lysosomal function impairment, unfolded protein response, endoplasmic reticulum, and ubiquitin-proteasome system altered in ALS also occur in FTLD. Other cellular processes, including mitochondrial function, can be impaired. In addition, neuron-specific processes, such as hyperexcitability and hypoexcitability, glutamate excitotoxicity, axonal transport, and neuronal branching defects, occur in C9orf72-associated FTLD and c9FTD/ALS. Finally, loss of C9orf72 function alters immune system and microglial function (Balendra and Isaacs, 2018).

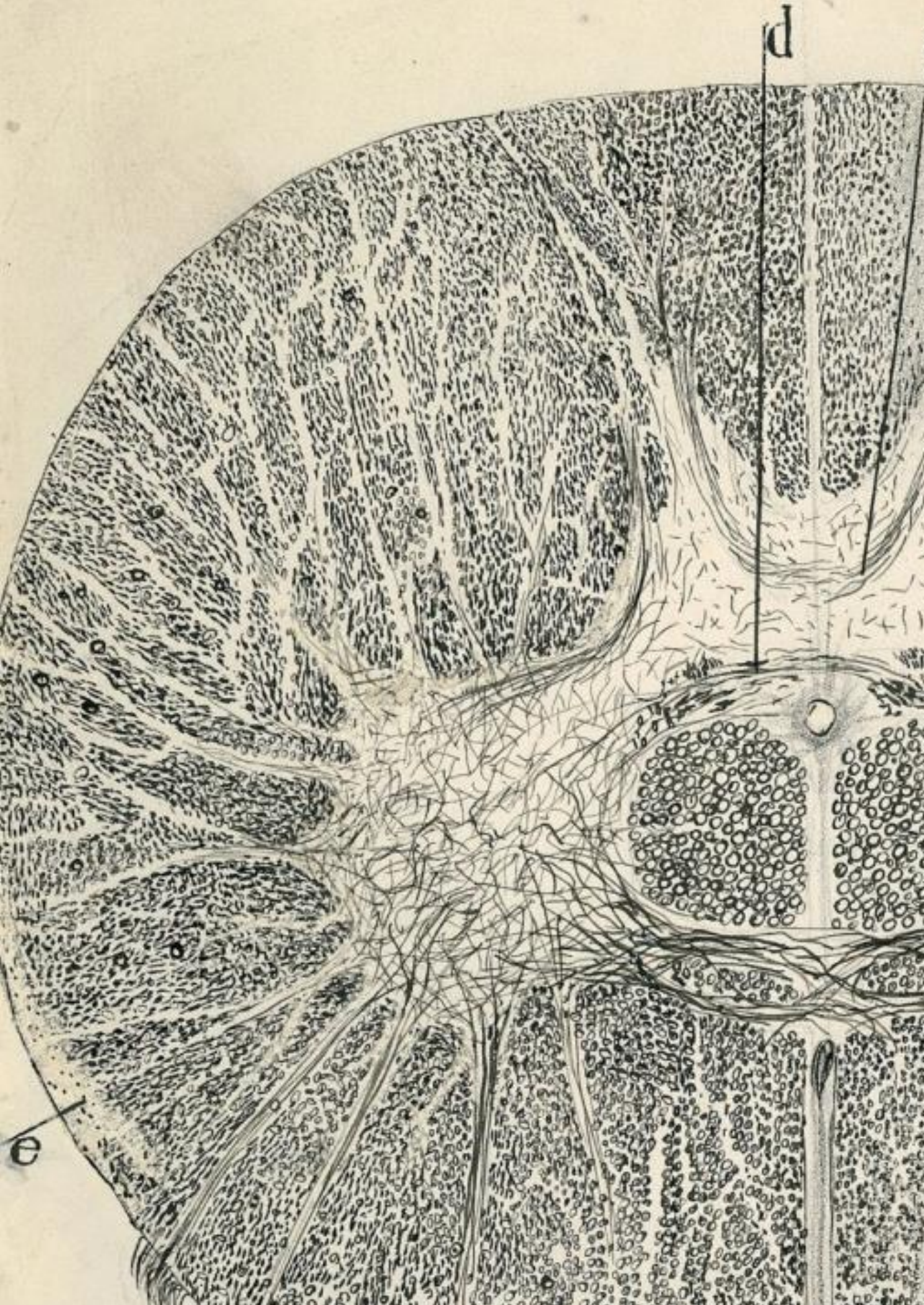
d
e

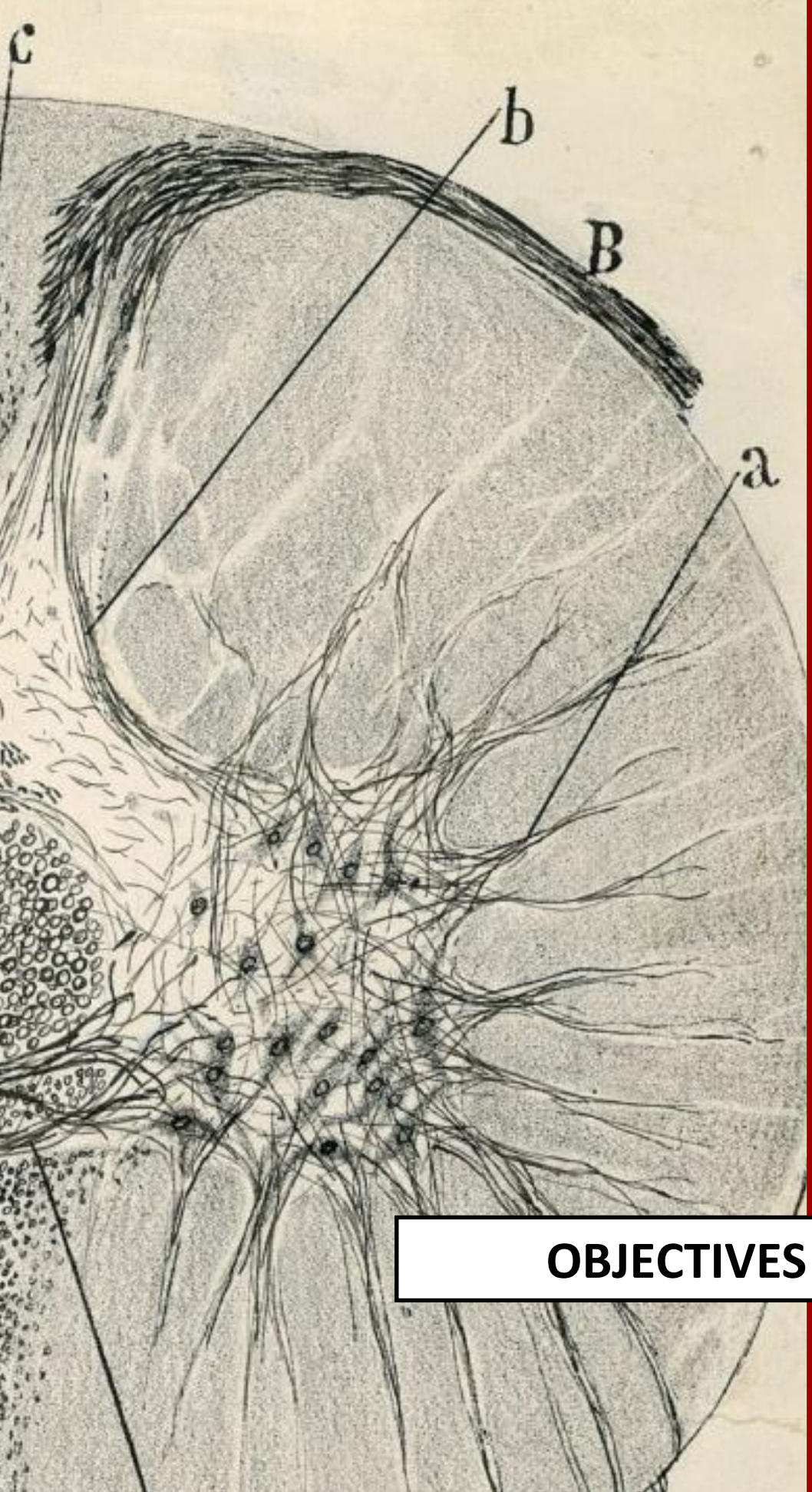

OBJECTIVES

2. General objective

The main aim of this doctoral thesis is the identification of new molecular alterations underlying motor and cognitive changes in *post-mortem* human spinal cord and frontal cortex in amyotrophic lateral sclerosis and in the frontal cortex in frontotemporal lobar degeneration TDP-43, both diseases within the spectrum of TDP-43 proteinopathies.

2.1. Specific objectives

Objective 1: To identify molecular alterations underlying brain alterations in frontal cortex of sporadic amyotrophic lateral sclerosis without frontotemporal dementia and their possible implications in frontotemporal lobar degeneration.

- To identify transcriptomic alterations using microarray technology in the spinal cord and frontal cortex area 8 in sALS without cognitive alterations.
- To validate altered pathways at mRNA and protein levels in the spinal cord and frontal cortex area 8, using RT-qPCR, western blotting and immunohistochemistry.
- To analyze whether alterations in spinal cord samples are similar to those found in frontal cortex area 8 of the same cases.
- To identify effectors of altered pathways as key players in disease etiology and/or disease progression, and at the same time postulating their possible role as potential biomarkers.

Objective 2: To identify and evaluate the possible alterations of the immune response at early stages of sALS in blood samples to learn about systemic responses to the disease.

- To identify alterations in the peripheral immune response by detecting altered mRNA levels in samples of peripheral whole-blood cells from patients with sALS at early stage of the disease.
- To analyze the predictive capacities of the possible alterations as biomarkers of disease progression.
- To identify possible therapeutic candidates in peripheral blood samples at early stages of the disease.

Objective 3: To evaluate and validate the chitinase-3-like protein 1/YKL-40 molecule in the CSF as a possible biomarker in sALS.

- To identify and characterize YKL-40 molecule by detecting mRNA and protein levels in *post-mortem* tissue of sALS, including spinal cord and frontal cortex area 8 compared with values in healthy controls.
- To quantify and establish YKL-40 protein levels in cerebrospinal fluid of sALS cases as a diagnostic or prognostic marker of the disease.
- To correlate YKL-40 levels with different clinical and biochemical parameters to promote its possible validity as a biomarker.

Objective 4: To evaluate and validate axonemal transport effectors as possible biomarkers in sALS based on the axonal transport alterations previously observed in the spinal cord in sALS cases (objective 1) when compared with control cases.

- To identify and characterize *DNAAF1* by detecting mRNA and LRRC50 protein levels in spinal cord of sALS cases compared with healthy controls.
- To characterize LRRC50 alterations in different neuronal nuclei, including dorsal nucleus of the vagus nerve, hypoglossal nuclei and oculomotor nuclei of the brain stem at terminal stages of ALS compared to controls.
- To characterize LRRC50 in the spinal cord of hSOD1-G93A transgenic mice at pre-clinical and clinical stages of ALS, and study its possible implication in disease pathogenesis.

Objective 5: To characterize molecular alterations in frontal cortex area 8 in sFTLD-TDP cases compared to control cases, and establish their possible relationship with cognitive alterations in sALS.

- To identify transcriptomic alterations using microarray techniques in frontal cortex area 8 *post-mortem* samples of sFTLD-TDP.
- To validate the altered pathways at mRNA and protein levels.
- To verify enzymatic alterations by assessing enzymatic activity of complexes of the electron transport chain.
- To explore possible relationships between alterations in sFTLD-TDP and sALS in frontal cortex area 8.

Objective 6: To characterize molecular alterations in frontal cortex area 8 of fFTLD-TDP linked to C9orf72 mutations.

- To identify mRNA and protein alterations using combined 'omics' in frontal cortex area from *post-mortem* samples of FTLD-TDP linked to C9orf72 mutations.

- To validate the altered pathways by measuring mRNA and protein levels using RT-qPCR and western blotting.
- To determine possible correlations between transcriptomics and proteomics in the same region (area 8) and in the same individuals
- To establish a possible relationship between fFTLD-TDP linked to C9orf72 mutations and alterations in sALSs and sFTLD-TDP frontal cortex area 8.

gutere
un tercio

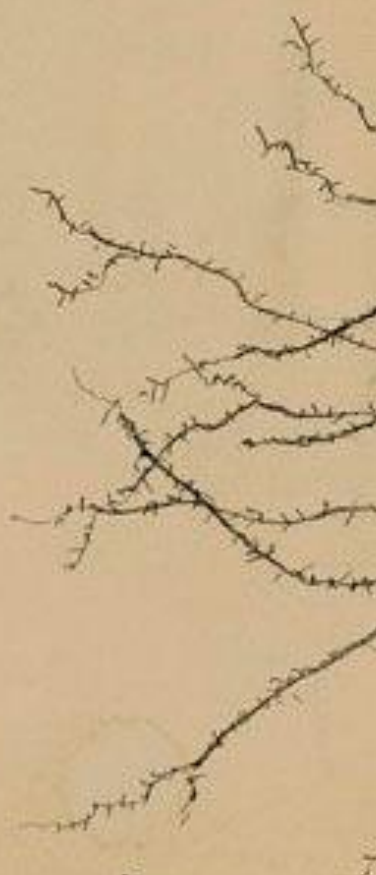

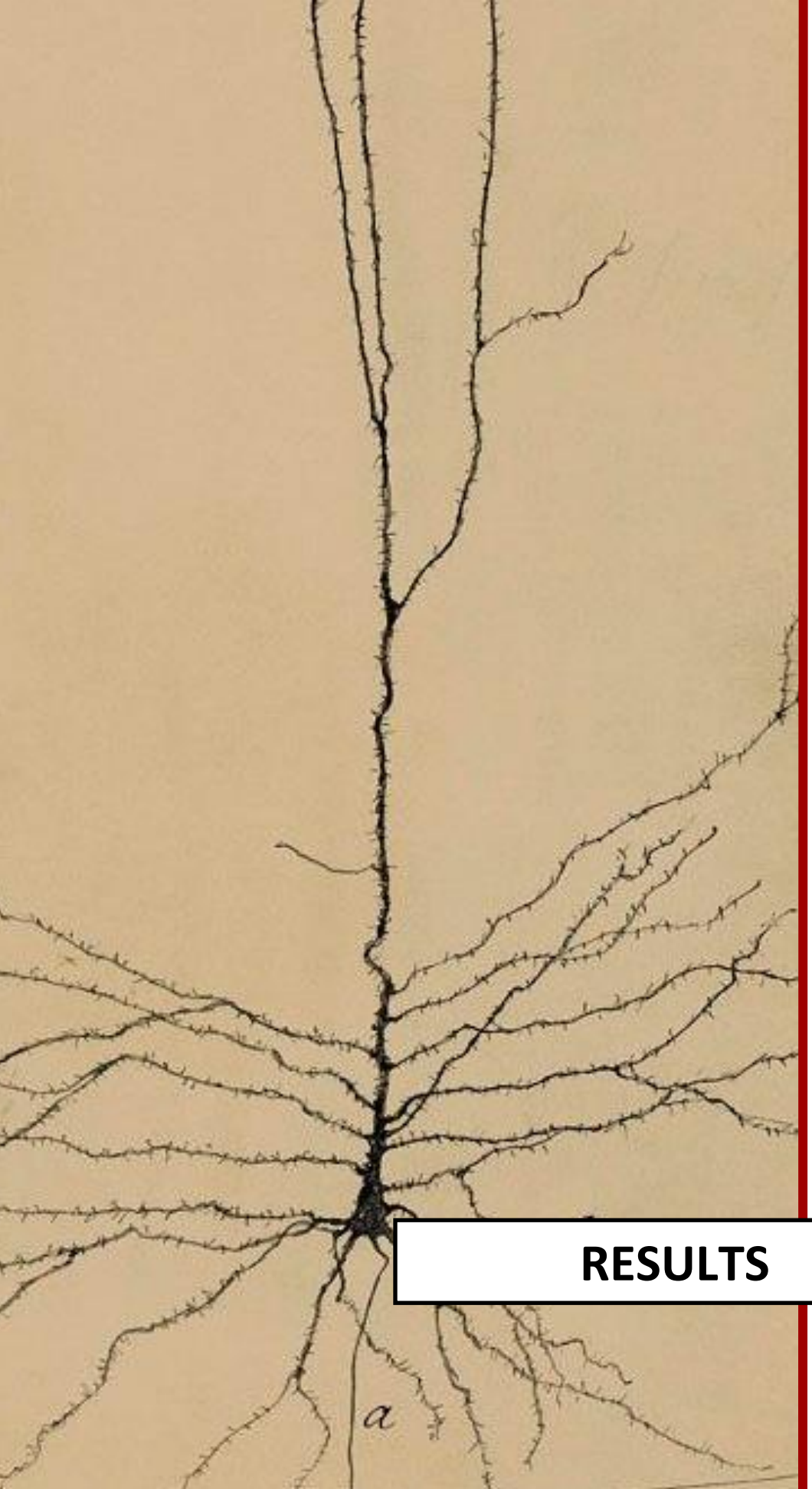

RESULTS

Article I

Amyotrophic lateral sclerosis, gene deregulation in the anterior horn of the spinal cord and frontal cortex area 8: Implications in frontotemporal lobar degeneration

Pol Andrés Benito, Jesús Moreno, Ester Aso, Mònica Povedano and Isidro Ferrer

Aging (Albany NY) 2017 Mar 9; 9(3): 823-851.

www.aging-us.com AGING 2017, Vol. 9, No. 3

Research Paper

Amyotrophic lateral sclerosis, gene deregulation in the anterior horn of the spinal cord and frontal cortex area 8: implications in frontotemporal lobar degeneration

Pol Andrés-Benito[1], Jesús Moreno[1], Ester Aso[1], Mónica Povedano[2], Isidro Ferrer[1, 3, 4, 5]

[1]Institute of Neuropathology, Pathologic Anatomy Service, Bellvitge University Hospital, IDIBELL, Hospitalet de Llobregat, Spain
[2]Service of Neurology, Bellvitge University Hospital, Hospitalet de Llobregat, Spain
[3]Department of Pathology and Experimental Therapeutics, University of Barcelona, Spain
[4]Institute of Neurosciences, University of Barcelona, Barcelona, Spain
[5]Biomedical Network Research Center on Neurodegenerative Diseases (CIBERNED), Institute Carlos III, Hospitalet de Llobregat, Spain

Correspondence to: Isidre Ferrer; **email:** 8082ifa@gmail.com
Keywords: amyotrophic lateral sclerosis, frontal cortex, spinal cord, frontotemporal lobar degeneration, excitotoxicity, neuroinflammation
Received: November 17, 2016 **Accepted:** February 27, 2017 **Published:** March 9, 2017

ABSTRACT

Transcriptome arrays identifies 747 genes differentially expressed in the anterior horn of the spinal cord and 2,300 genes differentially expressed in frontal cortex area 8 in a single group of typical sALS cases without frontotemporal dementia compared with age-matched controls. Main up-regulated clusters in the anterior horn are related to inflammation and apoptosis; down-regulated clusters are linked to axoneme structures and protein synthesis. In contrast, up-regulated gene clusters in frontal cortex area 8 involve neurotransmission, synaptic proteins and vesicle trafficking, whereas main down-regulated genes cluster into oligodendrocyte function and myelin-related proteins. RT-qPCR validates the expression of 58 of 66 assessed genes from different clusters. The present results: a. reveal regional differences in de-regulated gene expression between the anterior horn of the spinal cord and frontal cortex area 8 in the same individuals suffering from sALS; b. validate and extend our knowledge about the complexity of the inflammatory response in the anterior horn of the spinal cord; and c. identify for the first time extensive gene up-regulation of neurotransmission and synaptic-related genes, together with significant down-regulation of oligodendrocyte- and myelin-related genes, as important contributors to the pathogenesis of frontal cortex alterations in the sALS/frontotemporal lobar degeneration spectrum complex at stages with no apparent cognitive impairment.

INTRODUCTION

Amyotrophic lateral sclerosis (ALS) is a progressive age-dependent neurodegenerative disease characterized by degeneration and death of upper (motor cortex) and lower (brain stem and spinal cord) motor neurons, resulting in muscle atrophy, together with variable frontotemporal lobar degeneration (FTLD). ALS may be sporadic (sALS) with unknown cause, in up to 90%-92% of cases, or inherited (fALS), accounting for about 8-10% of cases, most of them transmitted as autosomal dominant but also recessive and X-linked in some families. However, about 13% of sALS cases bear a gene mutation linked to fALS. Main pathological features in sALS are loss of myelin and axons in the pyramidal tracts and anterior spinal roots, chromatolysis of motor neurons, axonal spheroids in the anterior horn, cystatin C-containing Bunina bodies in motor neurons, ubiquitin-immunoreactive TDP-43-positive skein-like and spherical inclusions in motor neurons, and TDP-43 inclusions in oligodendroglial cells. In many cases, the frontal cortex shows cytoplasmic TDP-43-immuno-

reactive intracytoplasmic inclusions in neurons and oligodendrocytes, and neuropil threads. Neuron loss and spongiosis in the upper cortical layers are usually restricted to cases with severe cognitive impairment and frontotemporal dementia [1, 2].

Several mechanisms have been proposed as contributory factors in the pathogenesis of motor neuron damage in sALS including excitoxicity, mitochondrial and energy metabolism failure, oxidative stress damage, altered glial cells, inflammation, cytoskeletal abnormalities, alterations in RNA metabolism, and altered TDP-43 metabolism, among others [3-16]. Increased understanding on the pathogenesis of sALS has emerged from the use of transcriptome analysis of the spinal cord and motor cortex [17-26]. Previous transcriptomic studies center in the spinal cord and motor cortex in separate groups of patients, cover a limited number of cases, identify and validate a few genes not coincidental among the different studies. Selection of the sample may account for these differences. Further microarray studies carried out on isolated motor neurons of the spinal cord obtained by laser micro-dissection in sALS cases have revealed up-regulation of genes associated with cell signalling and cell death and down-regulation of genes linked to transcription and composition of the cytoskeleton [27]. Curiously, similar studies performed on samples from individuals bearing mutations linked to ALS show different regulated transcripts, thus suggesting gene expression variants in the spinal cord in fALS [28, 29].

Importantly, no gene expression analyses are available in the frontal cortex area 8 in sALS in spite that frontal alterations are common in this disease. Moreover, ALS and FTLD with TDP inclusions (FTLD-TDP) are within the same disease spectrum [1].

The present study analyzes gene expression in the anterior horn of the spinal cord and frontal cortex area 8 in a series of 18 sALS cases and 23 controls. The main goals of the present study are to analyze and compare gene expression in these two regions, and more specifically to identify altered gene expression and clusters with specific functions in the anterior horn and frontal cortex area 8. Thus, the present study focuses on the pathogenesis of motor neuron damage responsible of altered motor function, and frontal cortex at preclinical stages of cognitive impairment.

RESULTS

Microarray analysis

Cofactors age and gender were not relevant for the analysis. 9,563 gene sequences were detected across all samples. Heat map indicates differences in transcripts expression levels between control and ALS cases in the anterior cord of the spinal cord and in frontal cortex area 8 (Figure 1). We identified 747 genes differentially expressed with p-value lower than or equal to 0.05 in the anterior horn of the spinal cord (up: 507 and down: 240) and 2,300 genes differentially expressed in the frontal cortex area 8 (up: 1,409 and down: 891) in sALS (Figure 1).

Supplementary Tables 1 and 2 identify all de-regulated genes. Post-analysis microarray data of differentially expressed genes assessed with enrichment analysis against Go Ontology database are shown in Tables 1 and 2.

Table 1. Main significant clusters of altered genes in spinal cord of ALS samples.

Cluster	Gene names	Size	Count	Odds Ratio	p-value	Deregulation
Activation of blood coagulation via clotting cascade	*F3, ANO6*	2	2	Inf	0.000574	Up
Antigen processing and presentation of exogenous peptide antigen	*CTSS, FCER1G, FCGR1A, HLA-A, HLA-B, HLA-C, HLA-DMA, HLA-DMB, HLA-DQA1, HLA-DQA2, HLA-DQB1, HLA-DQB2, HLA-DRB1, HLA-DRB5, HLA-F, HLA-G, NCF2, PSMB8, PSMB9, PSMD5, TAP1, IFI30*	165	22	6.58	6.84e-11	Up
Antigen processing and presentation of exogenous peptide antigen via MHC class I	*CTSS, FCER1G, FCGR1A, HLA-A, HLA-B, HLA-C, HLA-F, HLA-G, NCF2, PSMB8, PSMB9, PSMD5, TAP1, IFI30*	75	14	9.66	2.45e-09	Up
Antigen processing and presentation of exogenous peptide antigen via MHC class I, TAP-independent	*CTSS, HLA-A, HLA-B, HLA-C, HLA-F, HLA-G*	9	6	82.7	1.45e-08	Up
Antigen processing and presentation of exogenous peptide antigen via MHC class II	*CTSS, FCER1G, HLA-DMA, HLA-DMB, HLA-DQA1, HLA-DQA2, HLA-DQB1, HLA-DQB2, HLA-DRB1, HLA-DRB5, IFI30*	92	11	5.66	1.24e-05	Up
Antigen processing and presentation of peptide antigen via MHC class I	*CTSS, FCER1G, FCGR1A, HLA-A, HLA-B, HLA-C, HLA-F, HLA-G, NCF2, PSMB8, PSMB9, PSMD5, TAP1, IFI30*	97	14	7.09	7.58e-08	Up

Cluster	Gene names	Size	Count	Odds Ratio	p-value	Deregulation
Apoptotic process	*AHR, APOE, FAS, BCL2A1, BCL6, BMP2, BTK, CAMK2D, CASP1, CASP4, TNFSF8, CDKN1A, CTSC, DAB2, NQO1, ECT2, EDN1, F3, FCER1G, HCK, HGF, HIF1A, HMOX1, ICAM1, IFI16, IL1A, ITGA5, JAK3, LMNB1, LYN, MNDA, MYC, NCF2, NOS3, P2RX4, PLAGL1, PLAUR, PLSCR1, PRLR, PSMB8, PSMB9, PSMD5, PTPN2, CCL2, CCL19, SNAI2, STAT1, TEK, TGFB2, TLR2, TLR3, GPR65, YBX3, NOL3, SOCS3, LY86, IKBKE, CHI1, PPP1R15A, RRM2B, SHISA5, TNFRSF12A, ACSL5, FNIP2, DNASE2B, ZMAT3, NOA1, FGD3, IL33, DEDD2, ANO6*	1745	71	1.89	5.22e-06	Up
Apoptotic signaling pathway	*FAS, BCL2A1, BTK, CASP4, CDKN1A, CTSC, ECT2, HGF, HIF1A, HMOX1, ICAM1, IFI16, IL1A, NOS3, P2RX4, PLAUR, PTPN2, SNAI2, TGFB2, TLR3, YBX3, NOL3, IKBKE, PPP1R15A, RRM2B, SHISA5, TNFRSF12A, ACSL5, FNIP2, FGD3, IL33, DEDD2*	596	32	2.43	1.88e-05	Up
Axonemal dynein complex assembly	*DNAH5, DNAI1, TEKT2, ZMYND10, ARMC4, DNAH7, CCDC114, CCDC151, DNAAF1, CCDC39*	21	10	175	8.54e-18	Down
Axoneme	*DNAH5, DNAH9, SPAG6, DNAI1, DCDC2, HYDIN, CFAP46, ARMC4, MNS1, DNAH7, CFAP74, CCDC114, CCDC151, DNAAF1, CFAP54, DNAH2, SPAG17, CFAP221, CCDC39, RSPH4A*	89	20	52.5	1.31e-25	Down
Axoneme assembly	*DNAH5, DNAI1, TEKT2, ZMYND10, HYDIN, CFAP46, ARMC4, DNAH7, CFAP74, RSPH1, CCDC114, CCDC151, DNAAF1, SPAG17, CCDC39, RSPH4A*	42	16	128	5.9e-26	Down
B cell mediated immunity	*FAS, BCL6, BTK, C1QB, C1QC, C7, FCER1G, HLA-DMA, HLA-DQB1, HLA-DRB1, HLA-DRB5, CFI, IL4R, CD226, TLR8*	103	15	7.18	2.28e-08	Up
Cellular protein modification process	*IL12RB1, INS, KCNE1, MAK, CFP, RASA4, TRAK2, MYLK3, NEK5, C17orf97, PPIAL4A*	3527	11	0.473	0.00885	Down
Cellular response to interferon-gamma	*CAMK2D, EDN1, FCGR1A, GBP1, HCK, HLA-A, HLA-B, HLA-C, HLA-DQA1, HLA-DQA2, HLA-DQB1, HLA-DQB2, HLA-DRB1, HLA-DRB5, HLA-F, HLA-G, ICAM1, IRF8, OAS2, PTPN2, CCL2, CCL19, STAT1, SOCS3, IFI30, TRIM38, TRIM5*	126	27	11.9	1.95e-18	Up
Clathrin-coated endocytic vesicle membrane	*FCGR1A, HLA-DQA1, HLA-DQA2, HLA-DQB1, HLA-DQB2, HLA-DRB1, HLA-DRB5*	49	7	7.32	0.000108	Up
Copper ion import	*ATP7B, SLC31A1, STEAP4*	7	3	30.7	0.000446	Up
Cytokine production involved in immune response	*BCL6, BTK, FCER1G, HLA-A, HMOX1, JAK3, SLC11A1, TEK, TGFB2, TLR2, TLR3, TREM1*	69	12	8,81	7,87E-08	Up
Endolysosome membrane	*TLR3, TLR7, TLR8*	4	3	131	4.51e-05	Up
Fc receptor mediated stimulatory signaling pathway	*FCER1G, FCGR1A, FCGR2A, FGR, HCK, ITPR3, LYN, PLSCR1, CD226, MYO1G*	77	10	6.21	1.47e-05	Up
Humoral immune response mediated by circulating immunoglobulin	*C1QB, C1QC, C7, HLA-DQB1, HLA-DRB1, HLA-DRB5, CFI*	46	7	7.42	0.000103	Up
Igg binding	*FCER1G, FCGR1A, FCGR2A, FCGR2B*	10	4	28.3	5.42e-05	Up
Immunoglobulin production	*FAS, BCL6, CD37, HLA-DQB1, HLA-DRB1, HLA-DRB5, IL4R, TNFSF13B, POLM, IL33*	87	10	5.4	4.34e-05	Up
Inner dynein arm assembly	*TEKT2, ZMYND10, DNAI1, DNAAF1, CCDC39*	10	5	182	1.44e-09	Down
Integral component of lumenal side of endoplasmic reticulum membrane	*HLA-A, HLA-B, HLA-C, HLA-DQA1, HLA-DQA2, HLA-DQB1, HLA-DQB2, HLA-DRB1, HLA-DRB5, HLA-F, HLA-G*	28	11	28.8	1.04e-11	Up
Interferon-alpha production	*TLR3, NMI, TLR7, TLR8*	18	4	11.7	0.000764	Up
Interferon-beta biosynthetic process	*TLR3, NMI, TLR7, TLR8*	8	4	41.1	2.12e-05	Up
Interferon-gamma biosynthetic process	*TLR3, EBI3, TLR7, TLR8*	16	4	13.7	0.000472	Up
Interleukin-10 production	*FCER1G, HLA-DRB1, HLA-DRB5, JAK3, TLR2, PDCD1LG2*	42	6	6.87	0.000463	Up
Intrinsic apoptotic signaling pathway	*BCL2A1, CASP4, CDKN1A, HIF1A, HMOX1, IFI16, PLAUR, PTPN2, SNAI2, YBX3, NOL3, IKBKE, PPP1R15A, RRM2B, SHISA5, FNIP2*	284	16	2.49	0.00143	Up
Macrophage activation	*IL4R, SLC11A1, TLR1, SBNO2, CD93, TLR7, TLR8, IL33*	48	8	8.29	1.66e-05	Up
Mast cell cytokine production	*BCL6, FCER1G, HMOX1*	7	3	30.7	0.000446	Up
MHC class II receptor activity	*HLA-DQA1, HLA-DQA2, HLA-DQB1, HLA-DQB2, HLA-DRB1*	11	5	35.4	2.73e-06	Up
MHC protein complex	*HLA-A, HLA-B, HLA-C, HLA-DMA, HLA-DMB, HLA-DQA1, HLA-DQA2, HLA-DQB1, HLA-DQB2, HLA-DRB1, HLA-DRB5, HLA-F, HLA-G*	25	13	48.4	1.34e-15	Up

Cluster	Gene names	Size	Count	Odds Ratio	p-value	Deregulation
Microtubule bundle formation	*DNAH5, DNAI1, TEKT2, ZMYND10, HYDIN, CFAP46, ARMC4, DNAH7, CFAP74, RSPH1, CCDC114, CCDC151, DNAAF1, SPAG17, CCDC39, RSPH4A*	63	16	70.7	1.18e-22	Down
Monocyte chemotaxis	*CCR1, LYN, CCL2, CCL19, PLA2G7, ANO6*	49	6	5.75	0.00107	Up
Outer dynein arm assembly	*DNAH5, DNAI1, ZMYND10, ARMC4, CCDC114, CCDC151, DNAAF1*	11	7	325	5.6e-14	Down
Peptide antigen binding	*HLA-A, HLA-B, HLA-C, HLA-DQA1, HLA-DQB1, HLA-DRB1, HLA-DRB5, HLA-F, HLA-G, TAP1*	26	10	26.9	1.57e-10	Up
Platelet-derived growth factor receptor binding	*TYMP, ITGA5, ITGB3, LYN*	12	4	21.2	0.000123	Up
Positive regulation of Fc receptor mediated stimulatory signaling pathway	*LYN, CD226*	2	2	Inf	0.000574	Up
Positive regulation of interleukin-6 production	*FCER1G, TLR1, TLR2, TLR3, TLR7, IL33*	55	6	5.05	0.00197	Up
Positive regulation of interleukin-8 production	*TLR2, TLR3, TLR5, TLR7, TLR8*	42	5	5.56	0.00318	Up
Positive regulation of tumor necrosis factor production	*FCER1G, CCL2, CCL19, TLR1, TLR2, TLR3*	51	6	5.5	0.00133	Up
Protection from natural killer cell mediated cytotoxicity	*HLA-A, HLA-B, TAP1*	5	3	61.5	0.000132	Up
Regulated secretory pathway	*ANXA3, FCER1G, FGR, HCK, HMOX1, IL4R, LYN, STX11, CD300A, RAB11FIP2, RAB11FIP1*	73	11	7.4	1.23e-06	Up
Regulation of apoptotic process	*APOE, FAS, BCL2A1, BCL6, BMP2, BTK, CAMK2D, CASP1, CASP4, CDKN1A, CTSC, DAB2, NQO1, ECT2, EDN1, F3, FCER1G, HCK, HGF, HIF1A, HMOX1, ICAM1, IL1A, ITGA5, JAK3, LYN, MNDA, MYC, NCF2, NOS3, PLAUR, PRLR, PSMB8, PSMB9, PSMD5, PTPN2, CCL2, CCL19, SNAI2, STAT1, TEK, TGFB2, TLR3, YBX3, NOL3, SOCS3, CHL1, RRM2B, TNFRSF12A, ACSL5, ZMAT3, FGD3, DEDD2, ANO6*	1344	54	1.82	0.000117	Up
Regulation of B cell apoptotic process	*BCL6, BTK, LYN*	16	3	9.45	0.00608	Up
Regulation of coagulation	*APOE, EDN1, F3, FCER1G, LYN, NOS3, PLAU, PLAUR, THBD, HPSE, ADAMTS18, ANO6*	85	12	6.87	8.31e-07	Up
Regulation of cytokine biosynthetic process	*CD86, HMOX1, IL1A, TLR1, TLR2, TLR3, NMI, EBI3, TLR7, TLR8*	93	10	5.01	7.72e-05	Up
Regulation of extrinsic apoptotic signaling pathway	*FAS, HMOX1, ICAM1, IL1A, NOS3, SNAI2, TGFB2, NOL3, TNFRSF12A, ACSL5, DEDD2*	155	11	3.17	0.0013	Up
Regulation of Fc receptor mediated stimulatory signaling pathway	*LYN, PLSCR1, CD226*	5	3	61.5	0.000132	Up
Regulation of hemostasis	*APOE, EDN1, F3, FCER1G, LYN, NOS3, PLAU, PLAUR, THBD, HPSE, ADAMTS18, ANO6*	81	12	7.27	4.87e-07	Up
Regulation of leukocyte apoptotic process	*BCL6, BTK, FCER1G, HIF1A, JAK3, LYN, CCL19, TGFB2*	74	8	5.02	0.000386	Up
Regulation of lipid kinase activity	*FGR, LYN, CCL19, TEK, NRBP2*	47	5	4.89	0.0052	Up
Regulation of mast cell activation	*FCER1G, FGR, HMOX1, IL4R, LYN, PLSCR1, CD226, CD300A*	31	8	14.4	4.96e-07	Up
Regulation of mast cell degranulation	*FCER1G, FGR, HMOX1, IL4R, LYN, CD300A*	24	6	13.8	1.71e-05	Up
Regulation of microtubule movement	*DNAH11, ARMC4, DNAAF1, CCDC39*	18	4	51.3	3.03e-06	Down
Regulation of natural killer cell mediated immunity	*HLA-A, HLA-B, PVR, TAP1, CD226*	27	5	9.36	0.000405	Up
Regulation of protein metabolic process	*FOXJ1, INS, CFP, RASA4, NEK5, DTHD1*	2448	6	0.381	0.00803	Down
Regulation of protein modification process	*INS, RASA4*	1641	2	0.192	0.00288	Down
Regulation of T-helper 1 cell differentiation	*HLX, IL4R, JAK3, CCL19*	9	4	32.9	3.74e-05	Up
T cell costimulation	*CD86, HLA-DQA1, HLA-DQA2, HLA-DQB1, HLA-DQB2, HLA-DRB1, HLA-DRB5, LYN, CCL19, TNFSF13B, PDCD1LG2*	71	11	7.65	9.25e-07	Up
TAP binding	*HLA-A, HLA-B, HLA-C, HLA-F, TAP1*	7	5	106	1.34e-07	Up
T-helper 2 cell differentiation	*BCL6, CD86, HLX, IL4R*	14	4	16.4	0.00027	Up

Up-regulated genes in ALS anterior horn of the spinal cord cluster into inflammatory responses, metal ion regulation and hemostasis; whereas down-regulated genes cluster into neuronal axonal cytoskeleton and apoptosis.

In contrast, clusters of up-regulated genes were involved in neurotransmission, ion channels and ion transport, synapses, maintenance of axons and dendrites, intracellular signaling and synaptic vesicle mechanisms. The majority of down-regulated genes were encoded for proteins associated with myelin and glial cell regulation (Figure 2).

A

	Spinal cord (SC)	Frontal cortex (FC)
	Amyotrophic lateral sclerosis vs. Control	Amyotrophic lateral sclerosis vs. Control
up-regulated. p-value < 0.05	507	1409
down-regulated. p-value < 0.05	240	891

B

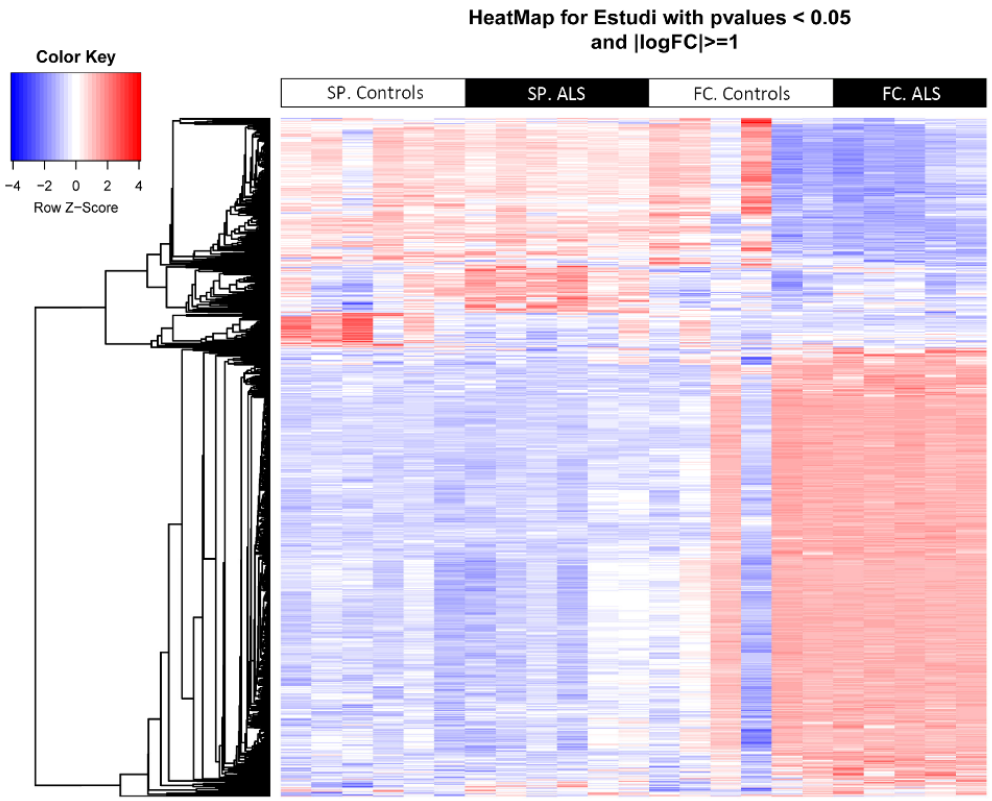

Figure 1. (A) Total number of significantly different expressed genes comparing transcriptomic profiles between groups and regions. (B) Hierarchical clustering heat map of expression intensities of mRNA array transcripts reflect differential gene expression profiles in the anterior horn of the spinal cord and frontal cortex area 8 in ALS compared with controls. Differences between groups are considered statistically significant at p-value ≤ 0.05. Abbreviations: ALS: amyotrophic lateral sclerosis; FC: frontal cortex area 8; mRNA: messenger RNA; SP: anterior horn of the spinal cord lumbar level.

Table 2. Main significant clusters of altered genes in frontal cortex of ALS samples.

Cluster	Gene names	Size	Count	Odds Ratio	p-value	Deregulation
Adenylate cyclase-inhibiting G-protein coupled receptor signaling pathway	*ADCY1, CHRM1, CHRM3, GNAI3, MCHR1, GRM8, HTR1B, HTR1E, IITR1F, NPY1R, OPRK1, OPRM1, SSTR2*	64	13	3.79	0.000164	Up
Astrocyte differentiation	*ABL1, MAG, NKX2-2, NOTCH1, POU3F2, S100B, TAL1, CNTN2, SOX8*	53	9	5.12	0.000184	Down
Axolemma	*KCNC1, KCNC2, KCNH1, ROBO2, SLC1A2*	14	5	8.26	0.00124	Up
Axon	*DAGLA, CAMK2D, CCK, CHRM1, CHRM3, AP1S1, CTNNA2, DLG4, DRD1, EPHA4, PTK2B, FGF13, GAP43, GARS, GRIA1, GRIK5, GRIN2A, HTR2A, KCNB1, KCNC1, KCNC2, KCNH1, KCNK2, KCNMA1, KCNQ2, KCNQ3, MYH10, NPY1R, NRCAM, NRGN, OPRK1, PAK1, PFN2, MAP2K1, PTPRN2, ROBO2, SCN1A, SCN1B, SCN2A, SCN8A, CCL2, SLC1A2, SNCA, STXBP1, SYN1, KCNAB1, FZD3, GLRA3, PRSS12, CNTNAP1, KCNAB2, NRP1, CDK5R1, BSN, SYT7, SYNGR1, DGKI, NRXN1, HOMER1, KATNB1, SEMA3A, OLFM1, SLC9A6, CPLX1, AAK1, ADGRL1, TPX2, UNC13A, MYCBP2, NCS1, PACSIN1, STMN3, SEPT11, SLC17A7, TBC1D24, NDEL1, LMTK3, MTPN, CNTN4, LRRTM1, HCN1*	358	81	4.6	1.68e-24	Up
Axon extension	*BMPR2, NRCAM, PPP3CB, SLIT1, CDKL5, NRP1, CDK5R1, LHX2, SEMA3A, OLFM1, SLC9A6, BCL11A, ISLR2, NDEL1*	91	14	2.7	0.00176	Up
Axon hillock	*CCK, TPX2, NDEL1*	7	3	11.1	0.00729	Up
Cadherin binding	*CDH13, CTNNA2, TRPC4, CDK5R1, AKAP5, MMP24, PTPRT*	29	7	4.81	0.00167	Up
Calcineurin complex	*ITPR1, PPP3CA, PPP3CB, PPP3R1*	4	4	Inf	1.59e-05	Up
Calcium channel regulator activity	*CACNB2, FKBP1B, ITPR1, PRKCB, STX1A, NRXN1, TSPAN13, HPCAL4, CACNA2D3*	36	9	5.05	0.000281	Up
Calcium ion-dependent exocytosis of neurotransmitter	*CACNA1A, SYT1, SYT5, DOC2A, SYT7, RIMS2, RAB3GAP1, RIMS1, SYT13, SYT12*	28	10	8.25	4.76e-06	Up
Calmodulin binding	*ADCY1, ADD2, ATP2B1, ATP2B2, CACNA1C, CAMK4, CAMK2A, CAMK2B, CAMK2D, GAP43, ITPKA, KCNH1, KCNN1, KCNQ3, MAP2, MYH10, MYO5A, NOS2, NRGN, PDE1B, PPP3CA, PPP3CB, PPP3R1, RGS4, RIT2, RYR2, SLC8A2, SLC8A1, AKAP5, CAMKK2, ARPP21, PLCB1, KCNH5, CAMK1D, CAMK1G, CAMKV, CAMKK1, PNCK, CFAP221, RHAD1*	176	40	4.57	5.38e-13	Up
Calmodulin-dependent protein kinase activity	*CAMK4, CAMK2A, CAMK2B, CAMK2D, PTK2B, ITPKA, CAMKK2, CAMK1D, CAMK1G, CAMKK1, PNCK*	32	11	7.95	2.02e-06	Up
Camp binding	*PDE2A, PDE4A, PRKAR1B, PRKAR2B, RAPGEF2, RAPGEF4, HCN1*	24	7	6.23	0.000487	Up
Central nervous system neuron axonogenesis	*EPHA4, SCN1B, NR2E1, MYCBP2, PRDM8, ARHGEF28, NDEL1*	29	7	4.71	0.00187	Up
Chloride channel activity	*CLIC2, GABRA1, GABRA2, GABRA3, GABRA4, GABRA5, GABRB2, GABRB3, GABRD, GABRG3, GLRB, SLC26A4, GLRA3, SLC17A7, SLC26A8, ANO5*	78	16	3.93	2.05e-05	Up
Clathrin binding	*SYT1, SYT5, DOC2A, SYT7, SNAP91, HIMP19, SYTL2, CEMIP, SYT13, SMAP1, SYT16, SYT12*	56	12	4.14	0.000141	Up
Compact myelin	*MAG, SIRT2, JAM3*	12	3	8.38	0.00957	Down
Cyclin-dependent protein serine/threonine kinase activity	*CDK14, CDKL5, CDKL1, CDK5R1, CDKL2, CDK20*	29	6	3.94	0.008	Up
Cytoskeleton of presynaptic active zone	*BSN, PCLO*	2	2	Inf	0.004	Up
Dendrite	*BMPR2, CACNA1A, CACNA1B, CACNA1C, CCK, CHRM1, CHRM3, CRMP1, DLG3, DLG4, DRD1, EPHA4, EPHA7, PTK2B, FGF13, GABRA5, GRIA1, GRIA2, GRIA3, GRIK5, GRIN2A, GRM1, GRM5, HTR2A, ITPKA, KCNB1, KCNC1, KCNC2, KCND3, KCNH1, KCNJ4, KCNQ3, MAP2, MYH10, NELL2, NRGN, OPRK1, PAK1, PRKAR2B, PRKCG, MAP2K1, RARA, RGS7, SCN8A, CCL2, SLC8A1, CDKL5, SYN1, KCNAB1, FZD3, PRSS12, CDK5R1, BSN, NEURL1, DGKI, HOMER1, CABP1, AKAP5, ARHGAP32, FRMPD4, SEMA3A, BAIAP2, SLC9A6, ARFGEF2, CHL1, PLK2, CPLX1, LZTS1, CPEB3, NCS1, NSMF, SHANK1, IFT57, SEPT11, ANKS1B, SLC4A10, TENM2, DLGAP3, JPH4, PPP1R9B, SHANK3, LMTK3, GRIN3A, SNAP47, CNIH2, HCN1*	406	86	4.24	7.25e-24	Up

Cluster	Gene names	Size	Count	Odds Ratio	p-value	Deregulation
Dendrite development	*ADGRB3, CACNA1A, CAMK2B, CTNNA2, DLG4, EPHA4, HPRT1, ITPKA, MAP2, MEF2C, PAK1, PAK3, PPP3CA, CDKL5, NR2E1, NRP1, CDK5R1, NEURL1, AKAP5, RAPGEF2, KIAA0319, SEMA3A, BAIAP2, SLC9A6, PLK2, CIT, LZTS1, CPEB3, NEDD4L, MAPK8IP2, RBFOX2, NGEF, NSMF, SLITRK5, PACSIN1, SHANK1, DCDC2, BCL11A, FEZF2, CAMK1D, SHANK3, GRIN3A, FMN1*	178	43	4.85	1.44e-14	Up
Dendrite extension	*PARK2, SYT1, RIMS2, SLC9A6, RIMS1, UNC13A, NEDD4L, CPNE5*	21	8	9.12	2.53e-05	Up
Dendrite morphogenesis	*ADGRB3, CACNA1A, CAMK2B, CTNNA2, DLG4, EPHA4, HPRT1, ITPKA, MAP2, PAK3, PPP3CA, CDKL5, NR2E1, CDK5R1, AKAP5, RAPGEF2, SEMA3A, BAIAP2, CIT, LZTS1, NEDD4L, MAPK8IP2, RBFOX2, NGEF, NSMF, SLITRK5, SHANK1, DCDC2, SHANK3, FMN1*	109	30	5.73	4E-12	Up
Dendritic shaft	*CACNA1C, DLG3, DRD1, GRM5, HTR2A, MAP2, PRKAR2B, SLC8A1, HOMER1, AKAP5, LZTS1, JPH4, CNIH2*	37	13	8.11	2.07e-07	Up
Dendritic spine development	*CAMK2B, DLG4, EPHA4, ITPKA, MEF2C, PAK1, PAK3, CDK5R1, NEURL1, BAIAP2, SLC9A6, PLK2, CPEB3, NGEF, SHANK1, SHANK3*	58	16	5.68	4.06e-07	Up
Dendritic spine membrane	*ATP2B1, GRIA1, ITGA8, AKAP5, DDN*	9	5	18.6	0.000102	Up
DNA metabolic process	*BMPR2, CDKN2D, CIDEA, DACH1, HGF, IGF1, KCNK2, KPNA2, MAS1, KITLG, ORC4, PAK3, PIK3CA, PRKCG, CHAF1B, CDC7, NPM2, PPARGC1A, PARM1, CHD5, UBE2W, FBXW7, TSPYL2, BCL11B, SLF1, TBRG1, MAEL, XRCC6BP1, ZBED9, KLHDC3, STOX1, KIAA2022*	867	32	0.549	0.000264	Up
Ensheathment of neurons	*MYRF, LPAR1, KCNJ10, KEL, MAG, MAL, NGFR, CLDN11, PMP22, POU3F2, KLK6, CNTN2, QKI, ARHGEF10, OLIG2, NDRG1, SIRT2, PARD3, FA2H, SH3TC2, JAM3, NKX6-2, SERINC5*	101	23	7.53	4.57e-12	Down
Excitatory postsynaptic potential	*DLG4, PTK2B, GRIK5, GRIN2A, GRIN2B, MEF2C, PPP3CA, SNCA, STX1A, DGKI, NRXN1, RIMS2, RAB3GAP1, RIMS1, MAPK8IP2, SHANK1, CELF4, SLC17A7, NETO1, SHANK3*	50	20	9.99	7.46e-12	Up
GABA receptor activity	*GABRA1, GABRA2, GABRA3, GABRA4, GABRA5, GABRB2, GABRB3, GABRD, GABRG3, GABBR2*	22	10	12.6	2.77e-07	Up
GABA receptor binding	*GABRA5, AKAP5, ARFGEF2, JAKMIP1*	14	4	6.03	0.0091	Up
Glial cell development	*MYRF, GSN, KCNJ10, NKX2-2, POU3F2, CNTN2, ARHGEF10, NDRG1, SIRT2, PHGDH, PARD3, FA2H, SH3TC2, NKX6-2*	71	14	6.19	4.84e-07	Down
Glutamate receptor activity	*PTK2B, GRIA1, GRIA2, GRIA3, GRIK5, GRIN2A, GRIN2B, GRM1, GRM5, GRM8, GRIN3A*	27	11	10.4	2.72e-07	Up
Innervation	*GABRA5, GABRB2, GABRB3, PRKCG, NRP1, SEMA3A, UNC13A*	23	7	6.47	0.000412	Up
Inositol phosphate metabolic process	*PTK2B, ITPKA, MAS1, OCRL, SNCA, INPP4B, SYNJ1, PPIP5K1, PLCH1, PLCB1, NUDT11*	65	11	3.02	0.00247	Up
Ionotropic glutamate receptor activity	*PTK2B, GRIA1, GRIA2, GRIA3, GRIK5, GRIN2A, GRIN2B, GRIN3A*	19	8	11	9.08e-06	Up
JNK cascade	*ADORA2B, EPHA4, PTK2B, FGF14, MAP3K9, MAP3K10, GADD45B, PAK1, PARK2, MAPK9, CCL19, MAP2K4, MAP3K6, RB1CC1, RASGRP1, PLCB1, MAPK8IP2, KIAA1804, DUSP19, ZNF675, MAGI3*	185	21	1.9	0.00716	Up
Lipid binding	*ABCA1, ANXA5, APOD, AR, C3, LPAR1, HSD17B10, HIP1, HSPA2, KCNJ2, MAL, MYO1E, NPC1, P2RX7, PLD1, PTGS1, SELL, SNX1, ACOX2, IQGAP1, HIP1R, CYTH1, STARD3, FNBP1, RASGRP3, LDLRAP1, GLTP, ANKFY1, PXK, ADAP2, PARD3, PREX1, WDFY4, PLEKHF1, PRAM1, PAQR8, MVB12B, SNX29, SYTL4, ARAP1, FRMPD2, AMER2, NCF1C, C8orf44-SGK3*	601	44	2.07	2.63e-05	Down
Mrna processing	*LGALS3, CELF2, PPARGC1A, CELF3, CPEB3, RBFOX2, RBFOX1, MTPAP, CELF4, CELF5, SRRM4, LSM11, RBFOX3*	417	13	0.466	0.00202	Up
Myelin maintenance	*MYRF, NDRG1, FA2H, SH3TC2*	11	4	14.2	0.000601	Down
Myelin sheath	*CA2, CNP, CRYAB, GSN, HSPA2, MAG, MOBP, MOG, MYO1D, CLDN11, RDX, CNTN2, NDRG1, SIRT2, PHGDH, GJC2, ERMN, MYH14, JAM3, SERINC5*	156	20	3.77	2.29e-06	Down
Myelination	*MYRF, LPAR1, KCNJ10, KEL, MAG, MAL, NGFR, PMP22, POU3F2, KLK6, CNTN2, QKI, ARHGEF10, OLIG2, NDRG1, SIRT2, PARD3, FA2H, SH3TC2, JAM3, NKX6-2, SERINC5*	98	22	7.38	1.81e-11	Down
Negative regulation of neuron apoptotic process	*CACNA1A, PTK2B, GABRA5, GABRB2, GABRB3, MEF2C, PARK2, PIK3CA, PRKCG, CCL2, SNCB, SNCA, STAR, STXBP1, NRP1, CHL1, PPARGC1A, OXR1, AGAP2*	128	19	2.59	0.000465	Up

Cluster	Gene names	Size	Count	Odds Ratio	p-value	Deregulation
Negative regulation of transcription, DNA-templated	*ARNTL, RUNX1T1, CRYM, CYP1B1, DACH1, FGF9, FOXG1, H2AFZ, MEF2C, MAP3K10, TRIM37, PDE2A, RARA, RORB, SATB1, SNCA, SOX5, TBX15, THRB, NR2E1, WNT10B, CDK5R1, LRRFIP1, ZBTB33, BASP1, ZBTB18, KLF12, CPEB3, PLCB1, SATB2, NEDD4L, SIRT5, RBFOX2, ATAD2, TAGLN3, BCL11A, FEZF2, SMYD2, PRDM8, TENM2, MTA3, SCRT1, MAEL, PRICKLE1, EID2, ARX, ZNF675, KCTD1*	1135	48	0.632	0.00083	Up
Neuron apoptotic process	*CACNA1A, EPHA7, PTK2B, GABRA5, GABRB2, GABRB3, GRIK5, KCNB1, MEF2C, PAK3, PARK2, PIK3CA, PRKCG, SCN2A, CCL2, SNCB, SNCA, STAR, STXBP1, NRP1, CDK5R1, CHL1, PPARGC1A, NSMF, OXR1, FBXW7, AGAP2, SDIM1*	206	28	2.35	0.000117	Up
Neuron spine	*DLG4, DRD1, EPHA4, GRIA1, GRM5, ITPKA, MYH10, NRGN, PRKAR2B, SLC8A1, CDK5R1, NEURL1, DGKI, AKAP5, ARHGAP32, FRMPD4, BAIAP2, SLC9A6, ARFGEF2, LZTS1, SHANK1, SEPT11, ANKS1B, TENM2, DLGAP3, PPP1R9B, SHANK3, CNIH2*	104	28	5.57	3.28e-11	Up
Neuronal postsynaptic density	*ADD2, ATP1A1, BMPR2, CAMK2A, CAMK2B, CTNNA2, DLG4, DMTN, GAP43, GRIN2B, MAP2, PAK1, PRKCG, BSN, DGKI, DLGAP1, HOMER1, BAIAP2, CAP2, CNKSR2, CLSTN1, MAPK8IP2, SHANK1, CLSTN2, SHANK3*	64	25	9.69	3.02e-14	Up
Neuron-neuron synaptic transmission	*CA7, CACNA1A, CACNB4, CAMK4, DRD1, PTK2B, GABRA1, GABRB2, GLRB, GRIA1, GRIA2, GRIA3, GRIK5, GRIN2A, GRM1, GRM5, GRM8, HRH2, HTR1B, HTR2A, MEF2C, NPY5R, PAK1, PARK2, PRKCE, PTGS2, SNCA, STXBP1, SYT1, GLRA3, DGKI, DLGAP2, NRXN1, RAB3GAP1, UNC13A, MAPK8IP2, RASD2, TMOD2, SHC3, SLC17A7, SHANK3, GRIN3A, CNIH2*	136	43	7.06	2.63e-19	Up
Neurotransmitter secretion	*CACNA1A, CACNA1B, CAMK2A, GAD1, GLS, GRIK5, MEF2C, PAK1, PARK2, PFN2, SLC1A1, SLC1A2, SNCA, STX1A, STXBP1, SYN1, SYN2, SYT1, SYT5, DOC2A, PPFIA4, PPFIA2, PPFIA3, CADPS, LIN7A, SYNJ1, SYT7, DGKI, BZRAP1, NRXN1, RIMS2, RIMS3, CPLX1, HRH3, ADGRL1, RAB3GAP1, RIMS1, UNC13A, PCLO, SYTL2, SLC17A7, SYT13, SYT16, SYT12, CADPS2, SNAP47*	154	46	6.52	1.93e-19	Up
Node of Ranvier	*KCNQ2, KCNQ3, SCN1A, SCN1B, SCN2A, SCN8A*	15	6	9.92	0.000193	Up
Nucleic acid metabolic process	*ABCA2, ABL1, PARP4, AR, ATM, BMP8B, MYRF, CAPN3, CAT, CBFB, CCNA2, CDKN1C, CENPB, ELF1, EYA4, ERF, FGF1, FGFR2, GDF1, HSD17B10, HDAC1, HIP1, HOXA1, HOXA2, HOXA5, HOXB2, HOXB5, HOXD1, HOXD3, HSPA1A, FOXN2, JUP, SMAD5, SMAD9, MCM7, MEIS1, CIITA, FOXO4, NKX2-2, NOTCH1, YBX1, PBX3, PDE8A, ENPP2, POLR2L, POU3F2, PSEN1, RNH1, RPLP0, RPS5, RXRG, SALL1, SGK1, SOX10, SREBF1, STAT2, SYK, TAL1, TCF12, TRAF1, TRPS1, ZNF3, ZNF69, VEZF1, FZD5, ARHGEF5, HIST1H2AC, HIST1H3E, HIST1H4H, HIST1H4B, RNASET2, CCNE2, QKI, LITAF, ST18, ZNF536, DDX39A, OLIG2, HMG20B, SEMA4D, TXNIP, DMRT2, TCFL5, ATF7, IKZF2, ZNF652, SIRT2, SAMD4A, KANK1, HEY2, BAMBI, ZNF521, ZBTB20, GREM1, CECR2, HIPK2, KLF15, BAZ2B, SLC40A1, SOX8, ZBTB7B, RRNAD1, KLF3, DDIT4, ZNF280D, TRIM62, CHD7, SLF2, ZNF83, SLC2A4RG, OTUD7B, BBX, MAVS, SFMBT2, NCOA5, TP53INP2, ZNF462, ARHGAP22, CREB3L2, CRTC3, TRAK2, BILLIE41, DBF4B, TSC22D4, NKX6-2, ZBTB37, LOXL3, OLIG1, ZSWIM7, GABPB2, CC2D1B, ZBTB12, ZNF844, ZNF326, FRYL, C9orf142, ZNF710, GTF2IRD2B, DBX2, HIST2H4B, ZNF812, TMEM229A, GTF2H2C_2, C8orf44-SGK3*	4679	144	0.718	0.000284	Up
Oligodendrocyte development	*MYRF, GSN, KCNJ10, NKX2-2, CNTN2, FA2H, NKX6-2*	32	7	6.99	0.000187	Down
Oligodendrocyte differentiation	*BOK, MYRF, CNP, GSN, KCNJ10, NKX2-2, NOTCH1, SOX10, CNTN2, OLIG2, SOX8, FA2H, NKX6-2*	75	13	5.27	5.64e-06	Down
Phosphatase activity	*ALPL, ATP1A1, CDKN3, DUSP8, OCRL, PPP2R5D, PPP3CA, PPP3CB, PPP3R1, MAP2K1, PTPN3, PTPN4, PTPRN2, PTPRR, INPP4B, SYNJ1, PIP5K1, LPPR4, PTPRT, PTP4A3, NT5DC3, PDP1, LPPR3, PTPN5, DUSP19, PPM1L, PPM1J*	254	27	1.81	0.00475	Up
Phosphatidylinositol binding	*HIP1, KCNJ2, MYO1E, PLD1, SNX1, IQGAP1, HIP1R, LDLRAP1, ANKFY1, PXK, ADAP2, PARD3, PLEKHF1, SNX29, ARAP1, FRMPD2, AMER2, NCF1C, C8orf44-SGK3*	187	19	2.92	9.82e-05	Down

Cluster	Gene names	Size	Count	Odds Ratio	p-value	Deregulation
Phospholipase C-activating G-protein coupled receptor signaling pathway	*ADRA1B, CCKBR, CHRM1, CHRM3, DRD1, GRM1, GRM5, HRH2, HTR2A, OPRK1, OPRM1, HOMER1, MCHR2*	81	13	2.84	0.00172	Up
Phospholipid binding	*ABCA1, ANXA5, LPAR1, HIP1, KCNJ2, MYO1E, PLD1, SNX1, IQGAP1, HIP1R, LDLRAP1, ANKFY1, PXK, ADAP2, PARD3, PREX1, WDFY4, PLEKHF1, SNX29, SYTL4, ARAP1, FRMPD2, AMER2, NCF1C, C8orf44-SGK3*	332	25	2.1	0.000966	Down
Phospholipid translocation	*ABCA1, P2RX7, ATP10B, ATP11A*	20	4	6.21	0.00667	Down
Positive regulation of RNA metabolic process	*ACVR1B, ARNTL, BMPR2, CAMK4, CAMK2A, CDH13, ETV1, H2AFZ, HGF, IGF1, KRAS, LUM, MEF2C, TRIM37, PPP1R12A, NEUROD2, PARK2, PLAGL1, PPP3CA, PPP3CB, PPP3R1, PRKCB, MAPK9, MAP2K1, RARA, RORB, SOX5, STAT4, THRB, NR2E1, TRAF5, WNT10B, ITGA8, LMO4, LDB2, LHX2, MICAL2, CAMKK2, TBR1, PPARGC1A, MLLT11, CELF3, KLF12, CPEB3, MAPRE3, DDN, PLCB1, SATB2, ATAD2, BCL11A, TESC, FEZF2, FBXW7, DCAF6, CELF4, ARNTL2, ATXN7L3, CAMK1D, MKL2, NEUROD6, BCL11B, CSRNP3, MED12L, RHEBL1, MTPN, SOHLH1*	1455	66	0.678	0.0011	Up
Postsynapse	*ADD2, ATP1A1, BMPR2, CACNA1C, CAMK2A, CAMK2B, CHRM1, CHRM3, CTNNA2, DLG3, DLG4, DRD1, DMTN, EPHA4, EPHA7, PTK2B, GABRA1, GABRA2, GABRA3, GABRA4, GABRA5, GABRB2, GABRB3, GABRD, GABRG3, GAP43, GLRB, GRIA1, GRIA2, GRIA3, GRIK5, GRIN2A, GRIN2B, GRM1, GRM5, ITPKA, ITPR1, KCNB1, KCNC2, KCNJ4, KCNMA1, MAP2, MYH10, NRGN, PAK1, PRKAR2B, PRKCG, SLC8A1, GLRA3, KCNAB2, ITGA8, LIN7A, CDK5R1, BSN, NEURL1, DGKI, DLGAP2, DLGAP1, HOMER1, CABP1, AKAP5, GABBR2, ARHGAP32, FRMPD4, LZTS3, BAIAP2, CAP2, ARFGEF2, LZTS1, CNKSR2, CLSTN1, RIMS1, SYNE1, NCS1, MAPK8IP2, NSMF, PCLO, SHANK1, SEPT11, ANKS1B, TENM2, LRFN2, KCTD16, LRRC7, DLGAP3, CACNG8, CLSTN2, LRRTM4, NETO1, PPP1R9B, SHANK3, CADPS2, GRIN3A, GRASP, CNIH2, LRRTM1, LRRTM3, IQSEC3*	341	98	6.47	7.81e-39	Up
Postsynaptic membrane	*CHRM1, CHRM3, DLG3, DLG4, EPHA4, EPHA7, GABRA1, GABRA2, GABRA3, GABRA4, GABRA5, GABRB2, GABRB3, GABRD, GABRG3, GLRB, GRIA1, GRIA2, GRIA3, GRIK5, GRIN2A, GRIN2B, KCNB1, KCNC2, KCNJ4, KCNMA1, GLRA3, LIN7A, NEURL1, DLGAP2, DLGAP1, HOMER1, CABP1, GABBR2, ARHGAP32, LZTS3, LZTS1, CNKSR2, CLSTN1, SYNE1, NCS1, NSMF, SHANK1, ANKS1B, TENM2, LRFN2, KCTD16, LRRC7, DLGAP3, CACNG8, CLSTN2, LRRTM4, NETO1, SHANK3, CADPS2, GRIN3A, GRASP, CNIH2, LRRTM1, LRRTM3, IQSEC3*	197	61	6.98	1.99e-26	Up
Potassium channel activity	*KCNB1, KCNC1, KCNC2, KCND3, KCNF1, KCNH1, KCNJ3, KCNJ4, KCNJ6, KCNJ9, KCNK2, KCNMA1, KCNN1, KCNQ2, KCNQ3, KCNS1, KCNS2, KCNAB1, KCNAB2, KCNAB3, KCNH4, KCNH3, KCNV1, KCNH5, KCNIP2, KCNQ5, KCNT1, KCNK15, KCNIP4, KCNH7, KCNG3, KCNT2, HCN1*	119	33	5.93	1.53e-13	Up
Presynapse	*DLG4, GABRA2, GRIA1, GRIA2, GRIN2B, ICA1, NPY1R, SNCA, STX1A, SYN1, SYN2, SYT1, SYT5, SLC30A3, FZD3, DOC2A, PPFIA4, PPFIA2, PPFIA3, BSN, SYT7, SYNGR1, DGKI, RIMS2, RIMS3, SV2B, DNM1L, RIMS1, UNC13A, DMXL2, ERC2, PCLO, SVOP, SLC17A7, SYT12, TPRG1L, SYNPR, STXBP5, SCAMP5, SLC6A17, UNC13C*	142	41	6.21	5.89e-17	Up
Presynaptic active zone	*SYN1, FZD3, PPFIA4, PPFIA2, PPFIA3, BSN, DGKI, RIMS2, RIMS3, RIMS1, UNC13A, ERC2, PCLO, SLC17A7, UNC13C*	24	15	25	7.23e-13	Up
Protein kinase C-activating G-protein coupled receptor signaling pathway	*CCK, CHRM1, DGKB, GAP43, GRM1, GRM5, HTR1B, DGKZ, DGKE, DGKI*	32	10	6.74	1.85e-05	Up
Protein lipidation	*ABCA1, ZDHHC9, PIGT, HHATL, ZDHHC14, ZDHHC11, MAP6D1, ATG4C, PIGM, ZDHHC20*	84	10	3.38	0.00152	Down
Regulation of axon guidance	*BMPR2, NRP1, SEMA3A, TBR1, FEZF2*	18	5	5.68	0.00441	Up
Regulation of neuron apoptotic process	*CACNA1A, EPHA7, PTK2B, GABRA5, GABRB2, GABRB3, GRIK5, KCNB1, MEF2C, PAK3, PARK2, PIK3CA, PRKCG, CCL2, SNCB, SNCA, STAR, STXBP1, NRP1, CDK5R1, CHL1, PPARGC1A, NSMF, OXR1, FBXW7, AGAP2*	183	26	2.47	9.7e-05	Up

Cluster	Gene names	Size	Count	Odds Ratio	p-value	Deregulation
Regulation of neurotransmitter levels	*DAGLA, CACNA1A, CACNA1B, CAMK2A, DRD1, GABRA2, GAD1, GLS, GRIK5, MEF2C, PAK1, PARK2, PDE1B, PFN2, SLC1A1, SLC1A2, SNCA, STX1A, STXBP1, SYN1, SYN2, SYT1, SYT5, DOC2A, PPFIA4, PPFIA2, PPFIA3, CADPS, LIN7A, SYNJ1, SYT7, DGKI, BZRAP1, NRXN1, RIMS2, RIMS3, CPLX1, HRH3, ADGRL1, RAB3GAP1, RIMS1, UNC13A, PCLO, SYTL2, SLC17A7, SYT13, SYT16, SYT12, CADPS2, SNAP47*	192	50	5.4	3.37e-18	Up
Regulation of postsynaptic membrane potential	*DLG4, PTK2B, FGF14, GABRB3, GRIK5, GRIN2A, GRIN2B, MEF2C, PPP3CA, SNCA, STX1A, DGKI, NRXN1, RIMS2, RAB3GAP1, RIMS1, MAPK8IP2, SHANK1, CELF4, SLC17A7, NETO1, SHANK3*	59	22	8.92	3.58e-12	Up
Regulation of synaptic plasticity	*ATP2B2, CAMK2A, CAMK2B, DLG4, DRD1, PTK2B, FGF14, GRIA1, GRIN2A, GRIN2B, GRM5, HRH2, ITPKA, KCNB1, MEF2C, NEUROD2, NRGN, PAK1, PPP3CB, PTGS2, PTN, SNCA, STAR, STXBP1, NR2E1, PPFIA3, SYNGAP1, SYNGR1, NEURL1, DGKI, RAPGEF2, BAIAP2, PLK2, CPEB3, RAB3GAP1, RIMS1, UNC13A, NSMF, NPTN, JPH3, NETO1, JPH4, SHANK3, SNAP47, CNTN4, LRRTM1*	132	46	8.2	1.48e-22	Up
Regulatory region nucleic acid binding	*ARNTL, ETV1, H2AFZ, HIVEP2, MEF2C, NEUROD2, PLAGL1, RARA, SATB1, SNCA, SOX5, STAT4, TBX15, LMO4, ZBTB33, BASP1, TBR1, KLF12, DDN, BCL11A, FEZF2, ARNTL2, PKNOX2, DMRTC1, NEUROD6, BCL11B, ZNF831, ZNF519, ARX, ZNF675, STOX1, SOHLH1, DMRTC1B*	790	33	0.643	0.00634	Down
Release of cytochrome c from mitochondria	*CCK, IFI6, HGF, IGF1, PARK2, MAPK9, HRK, DNM1L, MLLT11, GGCT*	55	10	3.29	0.00222	Up
SNARE binding	*CACNA1A, STX1A, STXBP1, SYT1, SYT5, DOC2A, NAPG, SYT7, STXBP5L, CPLX1, UNC13A, SYTL2, SYT13, NAPB, SYT16, SYT12, SNAP47, STXBP5*	112	18	2.91	0.000188	Up
Sodium channel activity	*SHROOM2, SCN1A, SCN1B, SCN2A, SCN2B, SCN8A, SCN3B, HCN1*	36	8	4.32	0.00141	Up
Synapse	*ADD2, ATP1A1, ATP2B1, ATP2B2, BMPR2, CACNA1C, CACNB4, CAMK2A, CAMK2B, CAMK2D, CCK, CHRM1, CHRM3, AP1S1, CTNNA2, DLG3, DLG4, DRD1, DMTN, EPHA4, EPHA7, PTK2B, GABRA1, GABRA2, GABRA3, GABRA4, GABRA5, GABRB2, GABRB3, GABRD, GABRG3, GAP43, GLRB, GRIA1, GRIA2, GRIA3, GRIK5, GRIN2A, GRIN2B, GRM1, GRM5, GRM8, ICA1, ITPKA, ITPR1, KCNB1, KCNC2, KCNH1, KCNJ4, KCNMA1, MAP2, MYH10, NPY1R, NRCAM, NRGN, OPRK1, PAK1, PDE2A, PFN2, PRKAR2B, PRKCG, PTPRN2, CCL2, SLC8A1, SNCB, SNCA, STX1A, STXBP1, SYN1, SYN2, SYT1, SYT5, SLC30A3, FZD3, GLRA3, DOC2A, PRSS12, PPFIA4, PPFIA2, KCNAB2, ITGA8, PPFIA3, CADPS, LIN7A, CDK5R1, BSN, WASF1, SYT7, SYNGR1, NEURL1, DGKI, DLGAP2, DLGAP1, NRXN1, HOMER1, CABP1, AKAP5, GABBR2, RAPGEF2, RIMS2, ARHGAP32, FRMPD4, LZTS3, RIMS3, SV2B, DNM1L, OLFM1, BAIAP2, SLC9A6, CAP2, ARFGEF2, CPLX1, LZTS1, AAK1, CPEB3, ADGRL1, CNKSR2, CLSTN1, RIMS1, PDZRN3, UNC13A, NMNAT2, DDN, DMXL2, SYNE1, NCS1, MAPK8IP2, FRRS1L, MYRIP, NSMF, ERC2, CYFIP2, NPTN, PCLO, PACSIN1, SHANK1, NRN1, SVOP, SEPT11, SEPT3, ANKS1B, SLC17A7, TENM2, TBC1D24, LRFN2, KCTD16, LRRC7, DLGAP3, CACNG8, CLSTN2, LRRTM4, NETO1, PPP1R9B, SHANK3, SYT12, CADPS2, PRRT2, GRIN3A, OLFM3, TPRG1L, SYNPR, STXBP5, CBLN4, GRASP, SCAMP5, PHACTR1, CNIH2, LRRTM1, LRRTM3, VWC2, SLC6A17, IQSEC3, UNC13C*	658	173	6.11	1.15e-62	Up
Synapse maturation	*CAMK2B, NEUROD2, NEURL1, NRXN1, ADGRL1, SHANK1*	18	6	7.39	0.000626	Up
Synaptic transmission	*ADCY1, ATP2B2, CA7, CACNA1A, CACNA1B, CACNA1C, CACNB1, CACNB2, CACNB4, CAMK4, CAMK2A, CAMK2B, CAMK2D, CHRM1, CHRM3, DLG3, DLG4, DRD1, EGR3, PTK2B, FGF14, GABRA1, GABRA2, GABRA3, GABRA4, GABRA5, GABRB2, GABRB3, GABRD, GABRG3, GAD1, GLRB, GLS, GNAI3, GRIA1, GRIA2, GRIA3, GRIK5, GRIN2A, GRIN2B, GRM1, GRM5, GRM8, HRH2, HTR1B, HTR1E, HTR1F, HTR2A, ITPKA, KCNB1, KCNC1, KCNC2, KCND3, KCNF1, KCNH1, KCNJ3, KCNJ4, KCNJ6, KCNJ9, KCNK2, KCNMA1, KCNN1, KCNQ2, KCNQ3, KCNS1, KCNS2, KIF5A, MEF2C, MYO5A, NEUROD2, NPY5R, OPRK1, OPRM1, PAK1, PARK2, PFN2, PPP3CA, PPP3CB, PRKCB, PRKCE, PRKCG, PTGS2, PTN, RIT2, SCN1B, SCN2B, CCL2, SLC1A1, SLC1A2, SNCB, SNCA, SSTR2, SSTR4, STAR,*	702	184	6.18	1.54e-66	Up

Cluster	Gene names	Size	Count	Odds Ratio	p-value	Deregulation
	STX1A, STXBP1, SYN1, SYN2, SYT1, SYT5, NR2E1, VIPR1, KCNAB1, GLRA3, DOC2A, PPFIA4, PPFIA2, KCNAB2, PPFIA3, CADPS, LIN7A, SYNGAP1, SYNJ1, BSN, SYT7, SYNGR1, NEURL1, DGKI, KCNAB3, DLGAP2, DLGAP1, BZRAP1, NRXN1, HOMER1, AKAP5, GABBR2, RAPGEF2, RIMS2, RIMS3, SNAP91, CACNG3, BAIAP2, CSPG5, PLK2, CPLX1, HRH3, CPEB3, ADGRL1, CLSTN1, RAB3GAP1, RIMS1, UNC13A, PLCB1, KCNH4, KCNH3, MAPK8IP2, RASD2, NSMF, SLITRK5, KCNV1, NPTN, KCNH5, PCLO, TMOD2, KCNIP2, SHANK1, SHC3, SYTL2, PCDHB13, KCNQ5, CELF4, SLC17A7, JPH3, SYT13, CACNG8, CLSTN2, NETO1, SYT16, CAMKK1, JPH4, PPP1R9B, SHANK3, KCNH7, SYT12, CADPS2, BTBD9, GRIN3A, SNAP47, CNTN4, KCNG3, CNIH2, LRRTM1, HCN1, UNC13C					
Synaptic transmission, glutamatergic	*CACNA1A, CACNB4, DRD1, PTK2B, GRIA1, GRIA2, GRIA3, GRIK5, GRIN2A, GRM1, GRM5, GRM8, HTR1B, HTR2A, MEF2C, PAK1, PARK2, PTGS2, SYT1, DGKI, NRXN1, RAB3GAP1, UNC13A, MAPK8IP2, SHC3, SLC17A7, SHANK3, GRIN3A, CNIH2*	78	29	8.94	1.42e-15	Up
Synaptic vesicle exocytosis	*GRIK5, PFN2, STX1A, STXBP1, SYN1, SYT1, SYT5, DOC2A, CADPS, SYNJ1, SYT7, RIMS3, CPLX1, ADGRL1, RIMS1, UNC13A, PCLO, SYTL2, SYT13, SYT16, SYT12, CADPS2, SNAP47*	76	23	6.51	1.59e-10	Up
Synaptic vesicle localization	*FGF14, GRIK5, PARK2, PFN2, SH3GL2, SNCA, STX1A, STXBP1, SYN1, SYT1, SYT5, AP3B2, DOC2A, CADPS, LIN7A, SYNJ1, SYT7, NRXN1, RIMS3, CPLX1, ADGRL1, RIMS1, UNC13A, PCLO, PACSIN1, SYTL2, SYT13, SYT16, SYT12, CADPS2, BTBD9, SNAP47*	120	32	5.49	1.97e-12	Up
Synaptic vesicle membrane	*ICA1, STX1A, SYN1, SYN2, SYT1, SYT5, SLC30A3, DOC2A, SYT7, SYNGR1, SV2B, DNM1L, DMXL2, SVOP, SLC17A7, SYT12, SYNPR, SCAMP5, SLC6A17*	55	19	7.94	4.52e-10	Up
Synaptic vesicle priming	*STX1A, STXBP1, CADPS, SYNJ1, CADPS2, SNAP47*	12	6	14.8	4.34e-05	Up
Synaptic vesicle recycling	*FGF14, SH3GL2, SNCA, SYT1, SYT5, SYNJ1, PACSIN1, BTBD9*	29	8	5.64	0.000338	Up
Synaptic vesicle transport	*FGF14, GRIK5, PARK2, PFN2, SH3GL2, SNCA, STX1A, STXBP1, SYN1, SYT1, SYT5, AP3B2, DOC2A, CADPS, LIN7A, SYNJ1, SYT7, RIMS3, CPLX1, ADGRL1, RIMS1, UNC13A, PCLO, PACSIN1, SYTL2, SYT13, SYT16, SYT12, CADPS2, BTBD9, SNAP47*	116	31	5.51	4.11e-12	Up
Syntaxin binding	*CACNA1A, STXBP1, SYT1, SYT5, DOC2A, NAPG, SYT7, STXBP5L, CPLX1, UNC13A, SYTL2, SYT13, NAPB, SYT16, SYT12, SNAP47, STXBP5*	78	17	4.24	4.82e-06	Up
Terminal bouton	*CCK, AP1S1, GRIK5, GRIN2A, KCNC2, KCNMA1, PFN2, PTPRN2, SNCA, STXBP1, SYN1, PRSS12, SYT7, SYNGR1, CPLX1, AAK1, TBC1D24*	61	17	5.8	1.39e-07	Up

RT-qPCR validation

Sixty-six genes from different pathways were selected for validation by RT-qPCR.

Inflammatory gene expression in the anterior horn of the spinal cord

No modifications in the expression levels of glial fibrillary acidic protein gene (*GFAP*) or prostaglandin-endoperoxide synthase 2 gene *(PTGS2*) occurred in ALS when compared with controls (p=0.31 and p=0.55, respectively). However, expression levels of *AIF1* and *CD68* were significantly increased in the anterior horn of the spinal cord in ALS (p=0.044 and p=0.00023, respectively). Gene expression of toll-like receptors (TLRs) *TLR2, TLR and TLR7* was significantly increased in the spinal cord in ALS cases (p=2.48E-05, p=0.00011 and p=0.00074, respectively), but *TLR4* was not (p=0.669). *IL1B* was up-regulated (p=0.005), but *IL6* and *IL6ST* were not (p=0.26 and p=0.76, respectively). In contrast, the expression of *IL10* and its corresponding receptors *IL10RA* and *IL10RB* was increased in ALS (p=0.00046, p=0.022 and p=3.23E-05, respectively). *TNFA* expression was significantly increased whereas a trend was found for *TNFRSF1B* (p=0.04 and p=0.08, respectively). The expression of *CTSC* and *CTSS* was significantly increased in spinal cord in ALS (p=5.82204E-05 and p=0.00014, respectively). Levels of *SLC11A1* were also significantly increased in spinal cord of ALS (p=0.014). *HLA-DRB1*, a protein coding gene for the Major Histocompatibility Complex Class II (MHC-II) DR β1 protein was markedly up-regulated in ALS (p=0.004365).

PDCD1LG2, IFNγ and *IL33* were significantly up-regulated in the anterior horn of the spinal cord in ALS (p=0.00153, p=0.03 and p=0.0032, respectively).

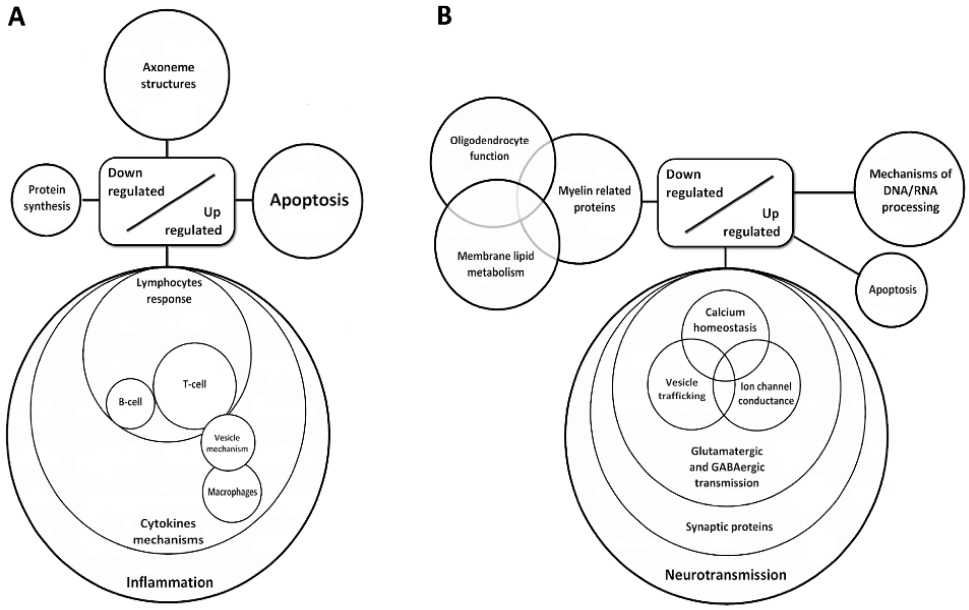

Figure 2. Diagram showing de-regulated gene clusters in the anterior horn of the spinal cord (**A**) and frontal cortex area 8 in ALS (**B**) as revealed by whole transcriptome arrays.

Finally, *IL8* (interleukin 8) and *ITGB4* (integrin subunit beta 4) expression was similar in control and ALS cases (p=0.92 and p=0.40, respectively) (Figure 3).

Axonemal gene expression in anterior horn of the spinal cord

No modifications in the expression levels of *NEFH*, which codes for neurofilament heavy polypeptide protein, was seen in ALS when compared with controls (p=0.30). However, *DNAAF1* levels were significantly reduced (p=0.019). Expression of *DNAH2*, *DNAH5*, *DNAH7* and *DNAH11* mRNA was significantly reduced in ALS (p=0.029, p=0.012, p=0.005 and p=0.023, respectively), whereas *DNAH9* mRNA was not altered (p=0.14). *DNAI1* mRNA expression was also significantly reduced in ALS (p=0.0086) (Figure 3).

SLC1A2 and SC17A7 expression in anterior horn of the spinal cord

SLC1A2 and SLC17A7 expression levels were significantly decreased in the anterior horn of the spinal cord in ALS anterior (p=0.000115 and p=0.000125, respectively). See Figure 3.

Neurotransmission-related gene expression in frontal cortex area 8

GRIA1, which codes for the ionotropic glutamate receptor AMPA 1, and *GRIN2A* and *GRIN2B*, coding for NMDA receptors, were significantly up-regulated (p=0.018, p=0.018 and p=0.029, respectively) in frontal cortex in ALS cases. *GRM5*, which codes for the glutamate metabotropic receptor 5, was also up-regulated (p=0.0079). However, no significant alteration was seen in the expression of *NETO1* (p=0.165).

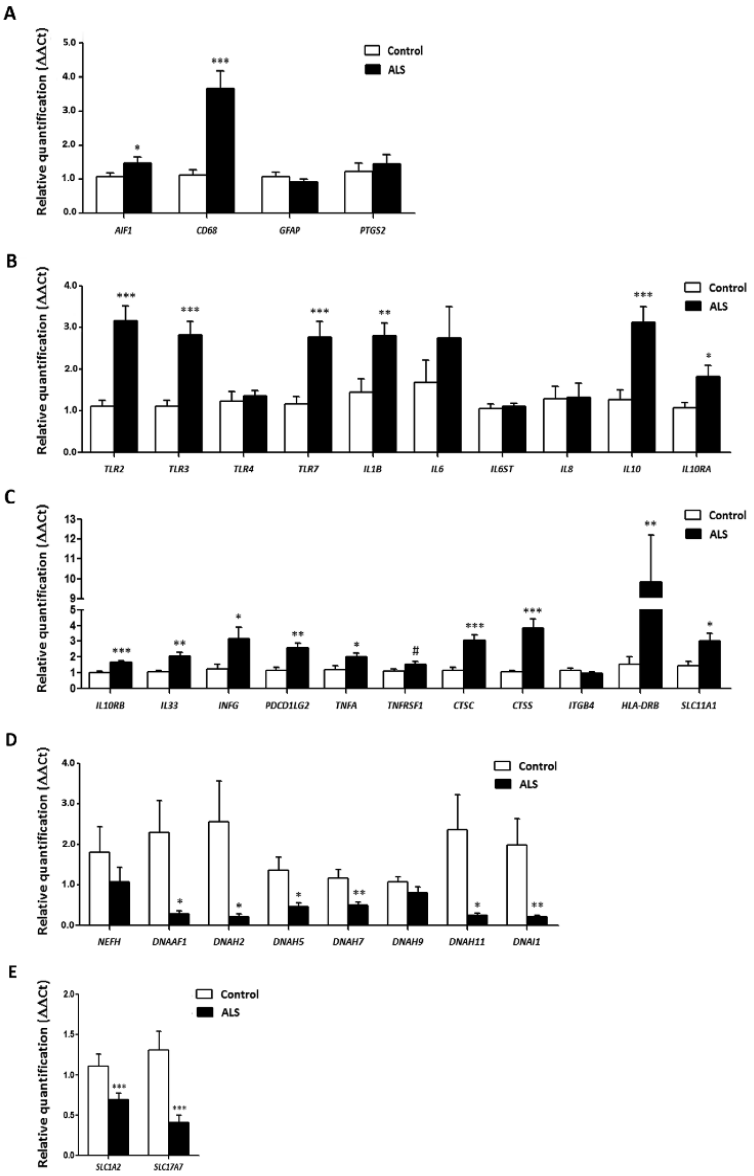

Figure 3. mRNA expression levels of selected deregulated genes identified by microarray analysis in the anterior horn of the spinal cord in ALS determined by TaqMan RT-qPCR assays. (**A**) general glial markers; (**B-C**) mediators of the inflammatory response; and (**D**) axolemal components. Up of AIGF1 and CD68, toll-like receptors, cytokines and receptors, chemokines and other mediators of the innate and adaptative inflammatory responses. Axolemal genes, excepting NEFH, which shows a non-significant trend to decrease, are significantly down-regulated. (**E**) glutamate transporter coding genes. The significance level is set at * $p < 0.05$, ** $p < 0.01$ and *** $p < 0.001$.

Regarding the GABAergic system, *GAD1* was up-regulated in ALS (p=0.034). Gene expression of GABA receptors *GABRA1*, *GABRD*, *GABRB2* was increased (p=0.09, tendency, p=0.006 and p=0.0029, respectively). *GABBR2* mRNA levels were also significantly elevated in the frontal cortex in ALS (p=0.01) (Figure 4).

Synaptic cleft gene expression in frontal cortex area 8

BSN, which codes for Bassoon, a pre-synaptic cytoskeletal matrix, was up-regulated in ALS (p=0.04). mRNA levels of *PCLO*, coding gene for Piccolo protein, and *FRMPD4* were also increased in ALS (p=0.036 and p=0.029, respectively), Finally, *NRN1*, which codes for

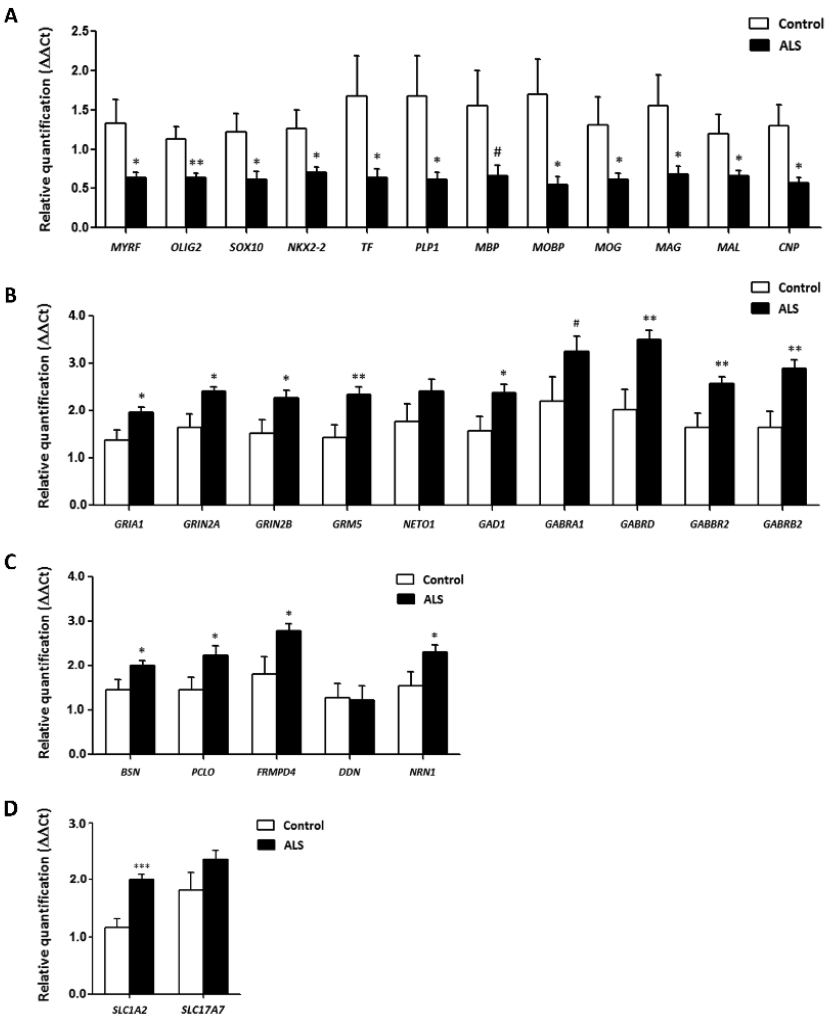

Figure 4. mRNA expression levels of selected deregulated genes identified by microarray analysis in frontal cortex area 8 of ALS cases determined by TaqMan RT-qPCR assays. (**A**) oligodendroglial and myelin-related genes; (**B**) glutamatergic and GABAergic-related genes and corresponding ionotropic and metabotropic receptors; (**C**) genes coding for synaptic cleft proteins. Significant up of genes linked to neurotransmission and synapses, and significant down of genes linked to oligodendroglia and myelination. (**D**) Glutamate transporter coding genes. The significance level is set at * p < 0.05, ** p < 0.01 and *** p < 0.001, and tendencies at # < 0.1.

neuritin 1, but not DDN, which codes for dendrin protein, was up-regulated in the frontal cortex in ALS (p=0.04 and p=0.92, respectively) (Figure 4).

Myelin- and oligodendrocyte-related gene expression in frontal cortex area 8

Significant decrease in mRNA expression of myelin transcription factor (*MYRF*) (p= 0.028), *OLIG2* (p = 0.009), *SOX10* (p = 0.02), *NKX2-2* (p = 0.032), transferring (TF) (p=0.5), proteolipid protein 1 (*PLP1*) (p=0.040), myelin basic protein (*MBP*) (p=0.061), myelin-associated oligodendrocyte basic protein (*MOBP*) (p=0.019), oligodendrocyte glycoprotein (*MOG*) (p=0.05), Mal T-cell differentiation protein (*MAL*) (p=0.039), myelin associated glycoprotein (*MAG*) (p=0.035), and 2',3'-cyclic nucleotide 3' phosphodiesterase (*CNP1*) (p=0.017) was seen in frontal cortex in ALS cases compared with controls (Figure 4).

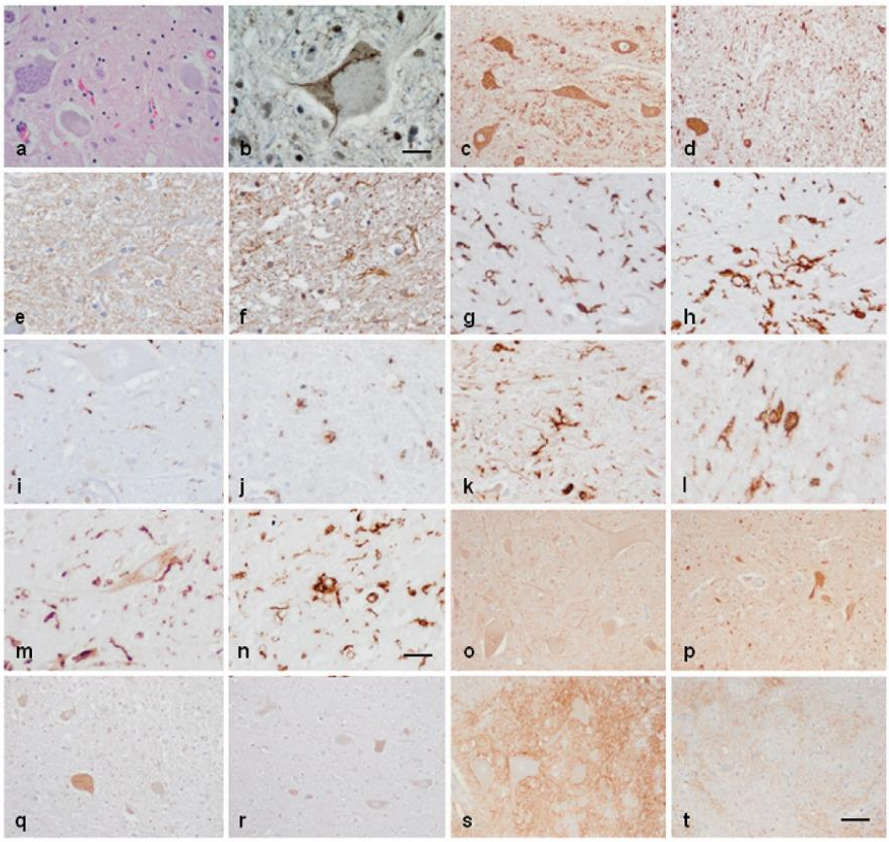

Figure 5. Anterior horn of the spinal cord. Haematoxilin and eosin staining showing damaged neurons in ALS (**a**). Immunohistochemistry to TDP-43 showing skein-like intracytoplasmic inclusions (**b**), VDAC (**c**, **d**), GFAP (**e**, **f**), IBA-1 (**g**, **h**), CD68 (**i**, **j**), HLA-DRB1 (**k**, **l**), HLA-DRB5 (**m**, n), IL-10 (**o**, **p**), TNF-α (**q**, **r**) and GluT (SLC1A2) (**s**, **t**) in the anterior horn of the lumbar spinal cord in control (**c**, **e**, **g**, **I**, **k**, **m**, **o**, **q**, **s**) and sALS (**a**, **b**, **d**, **f**, **h**, **j**, **l**, **n**, **p**, **r**, **t**) cases. TDP-43-immunoreactive cytoplasmic inclusions are seen in motor neurons in sALS. GFAP is increased in reactive astrocytes; microglial cells have a round, amoeboid morphology as seen with IBA-1, CD-68, HLA-DRB1, and HLA-DRB5 antibodies. VDAC immunoreactivity is decreased whereas IL-10 and TNF-α is increased in remaining motor neurons in sALS. SLC1A2 immunoreactivity is reduced in the membrane of neurons and in neuropil of the anterior horn in sALS. Paraffin sections, slightly counterstained with haematoxylin; a, c-d, o-t, bar in t = 40μm; e-n, bar in = 20μm; bar in b = 10μm.

SLC1A2 and *SLC17A7* expression in frontal cortex area 8

SLC1A2 expression was significantly increased (p=5.25e-5) whereas *SLC17A7* mRNA showed a non-significant increase (p=0.42) in frontal cortex area 8 in ALS (Figure 4).

Immunohistochemistry in spinal cord

The anterior horn of the spinal cord in ALS cases showed decreased number of neurons and altered morphology of most remaining motor neurons including loss of endoplasmic reticulum (chromatolysis) and axonal ballooning (Figure 5a) and intracytoplasmic TDP-43-immunoreactive inclusions (Figure 5b). Immunohistochemistry was carried out in the lumbar spinal cord in control and sALS cases (Figure 5a and b). VDAC was reduced in a subpopulation of neurons in the anterior horn in ALS, but not in neurons of the Clarke's column and posterior horn, when compared with controls (Figure 5c and d). Increased expression of GFAP was found in reactive astrocytes in the lateral columns and anterior horn of the spinal cord in ALS cases (Figure 5e and f). Marked differences were seen regarding microglial cell markers: IBA-1 and CD68 immunoreactivity was dramatically increased in the pyramidal tracts and anterior horn in ALS; moreover the morphology of microglia was modified in pathological cases with predominance of round, amoeboid microglia (Figure 5g-j). Similar immunoreactivity, distribution and morphology were found in reactive microglia using antibodies against HLA-DRB1 and HLA-DRB5 (Figure 5k-n). In contrast IL-10 and TNF-α immunoreactivity predominated in neurons; immunoreactivity was increased in neurons in ALS cases compared with controls (Figure 5o-r). Finally, GluT (SLC1A2), the transporter of glutamate from the extracellular space at synapses, was expressed in the membrane of neurons and in the neuropil; SLC1A2 immunoreactivity was decreased in neurons and neuropil of the anterior horn in ALS (Figure 5s, t).

Gel electrophoresis and western blotting in frontal cortex area 8

A few tested antibodies were eventually suitable for western blotting studies. No differences in the expression levels of glutamate receptor ionotropic, NMDA 2A (NMDAR2A) and glutamate decarboxylase

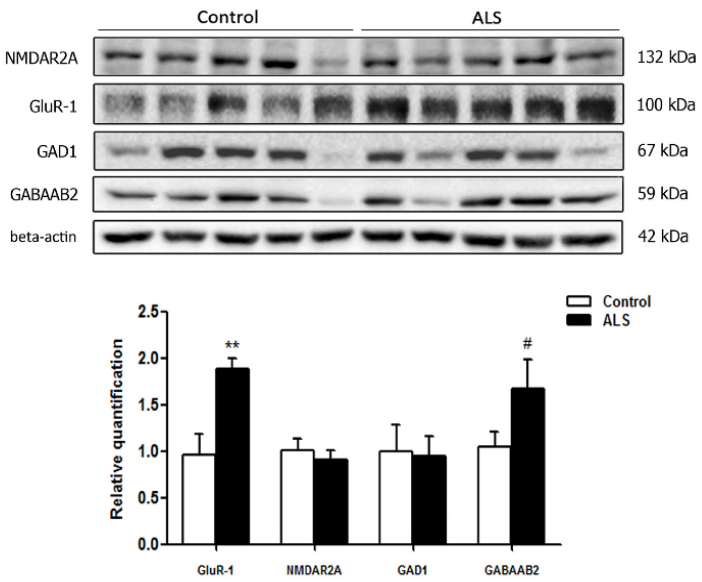

Figure 6. Gel electrophoresis and western blotting to glutamate receptor ionotropic, NMDA 2A (NMDAR2A), α-amino-3-hydroxy-5-methyl-4-isoxazolepropionic acid receptor 1 (GluR-1), glutamate decarboxylase 1 (GAD1) and gamma-aminobutyric acid receptor subunit beta-2 (GABAAB2) in the frontal cortex area 8 of control and ALS. Significant increased levels of GluR-1 and a tendency to increased levels of GABAAB2 are seen in ALS when compared with controls. The significance level is set at ** $p < 0.01$ and tendencies at # < 0.1.

1 (GAD1) were observed between control and ALS cases. However, a significant increase in α-amino-3-hydroxy-5-methyl-4-isoxazolepropionic acid receptor 1 (AMPAR GluR-1) ** $p < 0.01$ and a tendency to increase in the expression of gamma-aminobutyric acid receptor subunit beta-2 (GABAAB2) (# $p < 0.1$) was found in the frontal cortex in ALS when compared to controls (Figure 6).

DISCUSSION

Transcriptomic profiles in ALS are region-dependent when comparing the anterior horn of the lumbar spinal cord and frontal cortex area 8 in the same individuals. As an important regional difference related to excitotoxicity, the expression of glutamate transporters is markedly different in the anterior horn of the spinal cord and the frontal cortex area 8. *SLC1A2* and *SLC17A7* mRNA expression is significantly decreased in the anterior horn of the spinal cord, whereas *SLC1A2* is significantly increased in frontal cortex area 8. *SLC1A2* encodes the solute carrier family 1 member 2 or excitatory amino-acid transporter 2 (EAAT2) which clears glutamate from the extracellular space at synapses in the central nervous system. Immunohistochemistry has shown decreased SLC1A2 protein expression in the membrane of neurons and neuropil of the anterior horn in ALS. *SLC17A7* encodes the vesicular glutamate transporter 1 (VGLUT1) which is a vesicle-bound, sodium-dependent phosphate glutamate transporter expressed in the synaptic vesicles. Decreased expression of these proteins is linked to increased excitotoxity which is postulated as primary factor triggering motor neuron degeneration in ALS [30, 31].

Whole transcriptome arrays show that major up-regulated clusters in the anterior horn are related with innate inflammatory and adaptative inflammatory responses. Genes involved in hemostasis and ion transport forms a small up-regulated group. The major group of down-regulated genes is linked to the neuronal cytoskeleton. The majority of significantly differentially up-regulated transcripts in sALS in frontal cortex area 8, as revealed by whole transcriptome arrays, code for proteins linked with neurotransmission, ion channels and ion transport, synapses, and axon and dendrite maintenance, whereas down-regulated genes code for proteins involved in oligodendrocyte development and function, myelin regulation and membrane lipid metabolism.

Altered gene expression as revealed by whole transcriptome arrays has been validated by RT-qPCR in 58 of 66 assessed genes. These observations increase the list of genes which are de-regulated in the anterior spinal cord and provide, for the first time, robust evidence of gene de-regulation in frontal cortex area 8 in sALS. Increased inflammatory response in the anterior horn and increased expression of selected neurotransmitter markers in frontal cortex has been further assessed using immunohistochemistry and western blotting, respectively.

Inflammation in the anterior horn of the spinal cord

AIF1 gene codes for the Allograft Inflammatory Factor 1, a protein induced by cytokines and interferon which promotes macrophage and glial activation [32, 33]. *CD68* codes for the macrophage antigen CD68 glycoprotein which is expressed by microglial cells [35-37], the principal resident immune cell population in brain [38, 39]. Microglia pro-inflammatory state activation can be initiated by engagement of germline-encoded pattern-recognition receptors such as Toll-like receptors (TLRs) which are expressed in glial cells [40]. TLR activation, in turn, activates phagocytosis [41-43] and pro-inflammatory responses [44]. Up-regulated interleukins in ALS are *IL1B*, the coding gene for interleukin 1B an important mediator of the inflammatory response [45], interleukin 10 (encoded by *IL10)* which has pleiotropic effects down-regulating the expression of Th1 cytokines, MHC class II antigens and co-stimulating the production of several molecules by macrophages through the activation of IL10 receptor subunit α and subunit β (encoded by *IL10RA* and *IL10RB*, respectively) [46]. However, IL6 mRNA, which encodes a specific pro-inflammatory cytokine with regenerative and anti-inflammatory activities in particular settings [47-50] is not modified. Tumor Necrosis Factor Receptor Superfamily Member 1A (encoded by *TNFA*) is involved in the regulation of a wide spectrum of biological processes including cell proliferation, cell differentiation, apoptosis, lipid metabolism and coagulation [50, 51]. *CTSC* gene encodes Cathepsin C which is central coordinator of activation of many serine proteinases in immune cells [52]. *CTSS* codes for a protein of the same family, Cathepsin S, which acts as a key protease responsible for the removal of the invariant chain from MHC class II antigens [53]. *SLC11A1* encodes natural resistance-associated macrophage protein 1, which acts as a host resistance to certain pathogens [54].

Major Histocompatibility Complex Class II (MHC-II) DR β1 protein, encoded by *HLA-DRB-1,* plays a central role in the immune system by presenting peptides derived from extracellular proteins [55, 56] and participate in the activation of autophagosomes [57]. *PDCD1LG2* codes for Programmed Cell Death 1 Ligand 2, a protein involved in co-stimulatory signals essential for T-cell proliferation and IFN-γ production

[58]. *IFNγ* gene, which codes for the cytokine interferon-γ, is key player in antigen-specific immune responses [59]. Finally, interleukin 33, encoded by *IL33*, acts as a chemo-attractant for Th2 cells and functions as an 'alarm' that amplifies immune responses during tissue injury [60].

Increased inflammatory response in the anterior horn of the spinal cord has been further documented by immunohistochemistry showing increased expression of IBA-1, the protein encoded by *AIF1*, CD68, and HLA-DRB1 and HLA-DRB5 in reactive microglia. Reactive microglia has a round, amoeboid morphology and is also localized, as expected in the lateral and anterior pyramidal tracts. IL-10 and TNF-α are mainly localized in neurons of the spinal cord, and its expression is increased in remaining motor neurons of the spinal cord in ALS. These findings indicate a parallelism between gene expression and protein expression regarding inflammatory responses of assessed molecules. On the other hand the different localization of microglial markers, and IL-10 and TNF-α in neurons points to a cross-talk between microglia and neurons in the anterior horn of the spinal cord in ALS.

This is in contrast with other markers as glial fibrillary acidic protein and voltage dependent anion channel in which levels of mRNA differ from levels (or intensity) of protein expression. No modifications in the expression of *GFAP* mRNA are observed in the present study, but GFAP immunoreactivity is clearly increased in reactive astrocytes, as already reported in classical neuropathological studies. *VDAC* mRNA is not abnormally regulated in gene arrays; yet VDAC is decreased in motor neurons, but not in neurons of the Clarke's column and neurons of the posterior horn, of the spinal cord in ALS. VDAC immunohistochemistry is in line with observations in human sALS showing deficiencies in mitochondria and energy metabolism [61, 62].

Reduced expression of axolemal genes in anterior horn of the spinal cord

The expression levels of *NEFH*, which codes for neurofilament heavy polypeptide protein [63], are preserved in ALS. However, *DNAAF1,* which encodes dynein (axonemal) assembly factor 1, and mRNAs encoding several dynein axonemal heavy chains (DHC) are down-regulated thus suggesting impairment of motor ATPases involved in the transport of various cellular cargoes by 'walking' along cytoskeletal microtubules towards the minus-end of the microtubule [64-66].

Up-regulation of neurotransmission-related genes and synaptic cleft genes in frontal cortex

Genes involved in glutamatergic and GABAergic transmission are up-regulated in the frontal cortex in ALS. This applies to genes encoding the ionotropic glutamate receptor AMPA 1 (*GRIA1*), glutamate ionotropic receptor NMDA type subunit 2A (*GRIN2A*), the glutamate ionotropic receptor NMDA type subunit 2B (*GRIN2B)*, and glutamate metabotropic receptor 5 (*GRM5*). Regarding the GABAergic system, *GAD1*, coding for glutamate decarboxylase 1, a rate-limiting enzyme that acts in the decarboxylation of glutamate essential for the conversion reaction of GABA from glutamate [67, 68], is up-regulated, as are *GABRA1*, *GABRD, GABRB2,* which code for different subunits of ionotropic GABA-A receptors. *GABBR2,* which codes for the metabotropic receptor component Gamma-Aminobutyric Acid Type B Receptor Subunit 2 and forms heterodimers with GABBR1, thus resulting in the formation of the G-protein coupled receptor for GABA [69], is also up-regulated in ALS.

In line with increased expression of neurotransmitter-related genes, several genes encoding molecules linked with the synaptic cleft are also up-regulated in ALS. *BSN* codes for Bassoon, a pre-synaptic cytoskeletal matrix (PCM) protein acting as a scaffolding protein and essential for the regulation of neurotransmitter release in a subset of synapses [70, 71]. *PCLO* codes for Piccolo protein, a component of the PCM assembled in the active zone of neurotransmitter release [72, 73]. *FRMPD4* codes for PSD-95-interacting regulator of spine morphogenesis protein which regulates dendritic spine morphogenesis and is required for the maintenance of excitatory synaptic transmission [74]. *DDN* and *NRN1* code for dendrin protein and neuritin 1 protein, respectively which are involved in the remodeling of the postsynaptic cytoskeleton and neuritic outgrowth [75-77].

De-regulation of neurotransmitters and receptors is further supported by the demonstration of significant increase in the levels of GluR-1 and a tendency in those of GABAAB2 in the frontal cortex area 8 in ALS when compared with controls. It is worth stressing that only a few antibodies of the total assessed (eight) were suitable for western blotting.

Myelin and oligodendrocyte genes in frontal cortex area 8

Myelin transcription factor (encoded by *MYRF*) regulates oligodendrocyte differentiation and is required for central nervous system myelination [78-81]. The basic loop- helix protein OLIG2 mediates motor neuron

and oligodendrocyte differentiation [22, 82]. High mobility group protein SOX10 modulates myelin protein transcription [83, 84]. NKX2.2 homeodomain transcription factor is a key regulator of oligodendrocyte differentiation [85]. Transferrin encoded by *TF* participates in the early stages of myelination [86, 87]. Proteolipid protein 1 (encoded by *PLP1*) plays a role in the compaction, stabilization, and maintenance of myelin sheaths, as well as in oligodendrocyte development and axonal survival [88, 89]. Myelin basic protein (encoded by *MBP*) is the second most abundant myelin-associated protein, constituting about 30% of total myelin protein [90]. Myelin-associated oligodendrocyte basic protein (encoded by *MOBP*) constitutes the third most abundant protein in CNS myelin and it acts by compacting and stabilizing myelin sheaths [91]. Myelin oligodendrocyte glycoprotein (encoded by *MOG*) is a cell surface marker of oligodendrocyte maturation [92]. Myelin associated glycoprotein (encoded by *MAG*) is a type I membrane protein and member of the immunoglobulin super-family involved in the process of myelination and certain myelin-neuron cell-cell interactions [93]. Mal T-cell differentiation protein (encoded by *MAL*) is involved in myelin biogenesis [94]. Finally, 2',3'-cyclic nucleotide 3' phosphodiesterase (encoded by *CNP1*) participates in early oligodendrocyte differentiation and myelination [95-97].

Concluding comments

Results of the present study validate gene expression of individual studies performed in a limited number of samples identifying a limited number of de-regulated genes in the anterior horn of the spinal cord [17, 20, 21, 25]. Present results are more close to those carried out by using laser micro-dissection of anterior horn spinal motor neurons [27] thus reinforcing the consistence of observations in both studies. Whether some changes are related to the variable progression of the disease need further study with a larger number of cases of rapid or slow clinical course. In this line, altered mitochondria, protein degradation and axonal transport predominate in the 129Sv-SOD1(G93A) transgenic mouse with rapidly progressive motor neuron disease, whereas increased immune response is found in the C57-SOD1(G93A) transgenic mouse with more benign course [98].

The most important aspect of the present study is the description of altered gene expression and identification of altered clusters of genes in the frontal cortex area 8 in sALS cases without apparent cognitive impairment. It is worth stressing that altered clusters differ in the spinal cord and frontal cortex in sALS at terminal stages thus providing valuable information of molecular abnormalities which can also be present within the spectrum of FTLD-TDP. Noteworthy, altered regulation of transcription related to synapses and neurotransmission covering neurotransmitter receptors, synaptic proteins and ion channels in the frontal cortex in the absence of overt clinical symptoms of cognitive impairment are particularly important to identify early molecular alterations in frontal cortex with the spectrum of ALS/FTLD-TDP.

MATERIALS AND METHODS

Tissue collection

Post-mortem fresh-frozen lumbar spinal cord (SC) and frontal cortex (FC) (Brodmann area 8) tissue samples were from the Institute of Neuropathology HUB-ICO-IDIBELL Biobank following the guidelines of Spanish legislation on this matter and the approval of the local ethics committee. The post-mortem interval between death and tissue processing was between 2 and 17 hours. One hemisphere was immediately cut in coronal sections, 1-cm thick, and selected areas of the encephalon were rapidly dissected, frozen on metal plates over dry ice, placed in individual air-tight plastic bags, numbered with water-resistant ink and stored at -80°C until use for biochemical studies. The other hemisphere was fixed by immersion in 4% buffered formalin for 3 weeks for morphologic studies. Transversal sections of the spinal cord were alternatively frozen at -80°C or fixed by immersion in 4% buffered formalin. The whole series included 18 sALS cases and 23 controls. The anterior horn of the spinal cord was examined in 14 sALS (mean age 57 years; 6 men and 8 women) and the frontal cortex area 8 in 15 sALS (mean age 54 years; 11 men and 4 women). Spinal cord and frontal cortex were available in 11 cases. Lumbar anterior spinal cord was dissected on a dry-ice frozen plate under a binocular microscope at a magnification x4. TDP-43-immunoreactive small dystrophic neurites and/or TDP-43-positive granules and/or small cytoplasmic globules in cortical neurons in the contralateral frontal cortex area 8 were observed in 11 of 18 cases, but only abundant in three cases (cases 29, 30 and 31 in Table 3). Spongiosis in the upper cortical layers was found only in one case (case 28 in Table 3). Cases with frontotemporal dementia were not included in the present series. Patients with associated pathology including Alzheimer's disease (excepting neurofibrillary tangle pathology stages I-II of Braak and Braak), Parkinson's disease, tauopathies, vascular diseases, neoplastic diseases affecting the nervous system, metabolic syndrome, hypoxia and prolonged axonal states such as those occurring in intensive care units were excluded. Cases with infectious, inflammatory and autoimmune diseases, either systemic or limited to the nervous system were not included.

Table 3. Summary of the fifty six cases analyzed including frontal cortex area 8 of 14 controls and 15 ALS cases, and anterior horn of the spinal cord of 13 controls and 14 ALS cases.

						RIN value	
Case	Age	Gender	Diagnosis	PM delay	Initial symptoms	SC	FC
1	49	F	Control	07 h 00 min	-	-	7.2
2	75	F	Control	03 h 00 min	-	-	7.2
3	55	M	Control	05 h 40 min	-	-	7.7
4	59	M	Control	12 h 05 min	-	6.4	-
5	59	M	Control	07 h 05 min	-	-	7.8
6	43	M	Control	05 h 55 min	-	6.6	7.7
7	53	M	Control	07 h 25 min	-	-	5.3
8	56	M	Control	03 h 50 min	-	-	7.6
9	47	M	Control	04 h 55 min	-	5.6	7.7
10	64	F	Control	11 h 20 min	-	6.2	-
11	46	M	Control	15 h 00 min	-	5.9	7.9
12	56	M	Control	07 h 10 min	-	6.1	-
13	71	F	Control	08 h 30 min	-	5.9	-
14	64	F	Control	05 h 00 min	-	7.0	-
15	79	F	Control	06 h 25 min	-	6.7	-
16	75	M	Control	07 h 30 min	-	5.0	-
17	55	M	Control	09 h 45 min	-	5.3	-
18	52	M	Control	03 h 00 min	-	-	8.3
19	52	M	Control	04 h 40 min	-	-	6.3
20	76	M	Control	06 h 30 min	-	6.6	-
21	60	F	Control	11 h 30 min	-	-	7.5
22	51	F	Control	04 h 00 min	-	6.3	7.9
23	54	M	Control	08 h 45 min	-	-	7.0
24	56	M	ALS	10 h 50 min	NA	7.1	-
25	70	M	ALS	03 h 00 min	Respiratory	7.3	7.0
26	77	M	ALS	04 h 30 min	NA	7.4	-
27	56	F	ALS	03 h 45 min	NA	8.2	7.7
28	59	M	ALS	03 h 15 min	NA	7.5	7.7
29	63	F	ALS	13 h 50 min	Bulbar	6.8	8.2
30	59	F	ALS	14 h 15 min	NA	6.4	6.7
31	54	M	ALS	04 h 50 min	Spinal	-	7.8
32	76	M	ALS	12 h 40 min	Spinal	-	7.4
33	64	M	ALS	16 h 30 min	NA	6.3	7.3
34	57	F	ALS	04 h 00 min	Bulbar	6.2	8.6
35	75	F	ALS	04 h 05 min	Bulbar	6.8	6.8
36	79	F	ALS	02 h 10 min	NA	7.0	-
37	57	F	ALS	10 h 00 min	Bulbar	6.5	7.1
38	50	M	ALS	10 h 10 min	Spinal	-	5.9
39	59	F	ALS	02 h 30 min	Spinal	-	7.5
40	46	M	ALS	07 h 00 min	Spinal	7.0	8.0
41	69	F	ALS	17 h 00 min	Spinal	6.4	6.3

Abbreviations: ALS: amyotrophic lateral sclerosis; F: female; M: male; PM: post-mortem delay (hours, minutes); SC: anterior horn of the spinal cord lumbar level; FC: frontal cortex area 8; RIN: RNA integrity

Age-matched control cases had not suffered from neurologic or psychiatric diseases, and did not have abnormalities in the neuropathologic examination, excepting sporadic neurofibrillary tangle pathology stages I-II of Braak and Braak. No *C9ORF72*, *SOD1*, *TARDBP* and *FUS* mutations occurred in any case. Table 3 shows a summary of cases.

Whole-transcriptome array

RNA from frozen anterior horn of the lumbar spinal cord and frontal cortex area 8 was extracted following the instructions of the supplier (RNeasy Mini Kit, Qiagen® GmbH, Hilden, Germany). RNA integrity and 28S/18S ratios were determined with the Agilent Bioanalyzer (Agilent Technologies Inc, Santa Clara, CA, USA) to assess RNA quality, and the RNA concentration was evaluated using a NanoDrop™ Spectrophotometer (Thermo Fisher Scientific). Selected samples were analyzed by microarray hybridization with GeneChip® Human Gene 2.0 ST Array and WT Labeling Kit and microarray 7000G platform from Affymetrix® (Santa Clara, CA, USA). Microarray service was carried out at the High Technology Unit (UAT) at Vall d'Hebron Research Institute (VHIR), Barcelona, Spain.

Microarray data and statistical analysis

Microarray data quality control, normalization and filtering were performed using bioconductor packages in an R programming environment for genes [99] which enabled data preprocessing for differential gene expression analysis and enrichment analysis. Gene selection was based upon their values using a test for differential expression between two classes (Student's t-test). Genes differentially expressed showed an absolute fold change > 2.0 in combination with a p-value ≤ 0.05.

RT-qPCR validation

Complementary DNA (cDNA) preparation used High-Capacity cDNA Reverse Transcription kit (Applied Biosystems, Foster City, CA, USA) following the protocol provided by the supplier. Parallel reactions for each RNA sample run in the absence of MultiScribe Reverse Transcriptase to assess the lack of contamination of genomic DNA. TaqMan RT-qPCR assays were performed in duplicate for each gene on cDNA samples in 384-well optical plates using an ABI Prism 7900 Sequence Detection system (Applied Biosystems, Life Technologies, Waltham, MA, USA).

Table 4. Genes, gene symbols and TaqMan probes used for the study of gene expression in the anterior horn of the spinal cord and frontal cortex area 8 in ALS cases and controls including probes for normalization (*AARS*, *GUS-B*, *HPRT-1* and *XPNPEP-1*).

Gene	Gene symbol	Reference
2',3'-Cyclic Nucleotide 3' Phosphodiesterase	*CNP*	Hs00263981_m1
Alanyl-TRNA Synthetase	*AARS*	Hs00609836_m1
Allograft Inflammatory Factor 1	*AIF1*	Hs00741549_g1
Bassoon Presynaptic Cytomatrix Protein	*BSN*	Hs01109152_m1
Cathepsin C	*CTSC*	Hs00175188_m1
Cathepsin S	*CTSS*	Hs00356423_m1
C-X-C Motif Chemokine Ligand 8	*IL8*	Hs00174103_m1
Dendrin	*DDN*	Hs00391784_m1
Dynein (Axonemal) Assembly Factor 1	*DNAAF1*	Hs00698399_m1
Dynein Axonemal Heavy Chain 11	*DNAH11*	Hs00361951_m1
Dynein Axonemal Heavy Chain 2	*DNAH2*	Hs00325838_m1
Dynein Axonemal Heavy Chain 5	*DNAH5*	Hs00292485_m1
Dynein Axonemal Heavy Chain 7	*DNAH7*	Hs00324265_m1
Dynein Axonemal Heavy Chain 9	*DNAH9*	Hs00242096_m1
Dynein Axonemal Intermediate Chain 1	*DNAI1*	Hs00201755_m1

Gamma-Aminobutyric Acid Type A Receptor Alpha 1 Subunit	*GABRA1*	Hs00971228_m1
Gamma-Aminobutyric Acid Type A Receptor Beta 2 Subunit	*GABRB2*	Hs00241451_m1
Gamma-Aminobutyric Acid Type A Receptor Delta Subunit	*GABRD*	Hs00181309_m1
Gamma-Aminobutyric Acid Type B Receptor Subunit 2	*GABBR2*	Hs01554996_m1
Glial Fibrillary Acidic Protein	*GFAP*	Hs00909240_m1
Glutamate Decarboxylase 1	*GAD1*	Hs01065893_m1
Glutamate Ionotropic Receptor AMPA Type Subunit 1	*GRIA1*	Hs00181348_m1
Glutamate Ionotropic Receptor NMDA Type Subunit 2A	*GRIN2A*	Hs00168219_m1
Glutamate Ionotropic Receptor NMDA Type Subunit 2B	*GRIN2B*	Hs01002012_m1
Glutamate Metabotropic Receptor 5	*GRM5*	Hs00168275_m1
Hypoxanthine Phosphoribosyltransferase 1	*HPRT1*	Hs02800695_m1
Integrin Subunit Beta 4	*ITGB4*	Hs00173995_m1
Interferon, Gamma	*IFNG*	Hs00989291_m1
Interleukin 1 Beta	*IL1B*	Hs01555410_m1
Interleukin 10	*IL10*	Hs00961622_m1
Interleukin 10 Receptor Subunit Alpha	*IL10RA*	Hs00155485_m1
Interleukin 10 Receptor Subunit Beta	*IL10RB*	Hs00988697_m1
Interleukin 33	*IL33*	Hs00369211_m1
Interleukin 6	*IL6*	Hs00985639_m1
Interleukin 6 Signal Transducer	*IL6ST*	Hs00174360_m1
Macrophage Antigen CD68	*CD68*	Hs02836816_g1
Major Histocompatibility Complex, Class II, DR Beta 1/4/5	*HLA-DRB*	Hs04192463_mH
Mal T-Cell Differentiation Protein	*MAL*	Hs00360838_m1
Myelin Associated Glycoprotein	*MAG*	Hs01114387_m1
Myelin Basic Protein	*MBP*	Hs00921945_m1
Myelin Oligodendrocyte Glycoprotein	*MOG*	Hs01555268_m1
Myelin Regulatory Factor	*MYRF*	Hs00973739_m1
Myelin-Associated Oligodendrocyte Basic Protein	*MOBP*	Hs01094434_m1
Neuritin 1	*NRN1*	Hs00213192_m1
Neurofilament, Heavy Polypeptide	*NEFH*	Hs00606024_m1
Neuropilin And Tolloid Like 1	*NETO1*	Hs00371151_m1
NK2 Homeobox 2	*NKX2-2*	Hs00159616_m1
Oligodendrocyte Lineage Transcription Factor 2	*OLIG2*	Hs00377820_m1
Piccolo Presynaptic Cytomatrix Protein	*PCLO*	Hs00382694_m1
Programmed Cell Death 1 Ligand 2	*PDCD1LG2*	Hs01057777_m1
Prostaglandin-Endoperoxide Synthase 2	*PTGS2*	Hs00153133_m1

Proteolipid Protein 1	*PLP1*	Hs00166914_m1
PSD-95-Interacting Regulator Of Spine Morphogenesis	*FRMPD4*	Hs01568794_m1
Solute Carrier Family 1 (Glial High Affinity Glutamate Transporter), Member 2 (EAAT-2)	*SLC1A2*	Hs01102423_m1
Solute Carrier Family 11 Member 1	*SLC11A1*	Hs01105516_m1
Solute Carrier Family 17 (Vesicular Glutamate Transporter), Member 7 (VGLUT-1)	*SLC17A7*	Hs00220404_m1
SRY (Sex Determining Region Y)-Box 10	*SOX10*	Hs00366918_m1
Toll Like Receptor 2	*TLR2*	Hs00610101_m1
Toll Like Receptor 3	*TLR3*	Hs01551078_m1
Toll Like Receptor 4	*TLR4*	Hs01060206_m1
Toll Like Receptor 7	*TLR7*	Hs00152971_m1
Transferrin	*TF*	Hs01067777_m1
Tumor Necrosis Factor Receptor Superfamily Member 1A	*TNFRSF1*	Hs01042313_m1
Tumor Necrosis Factor-Alpha	*TNFa*	Hs01113624_g1
X-prolyl aminopepidase P1	*XPNPEP1*	Hs00958026_m1
β-glucuronidase	*GUS-β*	Hs00939627_m1

For each 10μL TaqMan reaction, 4.5μL cDNA was mixed with 0.5μL 20x TaqMan Gene Expression Assays and 5μL of 2x TaqMan Universal PCR Master Mix (Applied Biosystems). Table 4 shows identification numbers and names of TaqMan probes. The mean value of one house-keeping gene, hypoxanthine-guanine phosphoribosyltransferase (*HPRT1*), was used as internal control for normalization of spinal cord samples, whereas the mean values of the three house-keeping genes, alanyl-transfer RNA synthase (*AARS*), glucuronidase Beta (*GUS-β*) and X-prolyl amino-peptidase (aminopeptidase P) 1 (*XPNPEP1*) were used as internal controls for normalization of frontal cortex samples [100, 101]. The parameters of the reactions were 50°C for 2 min, 95°C for 10 min, and 40 cycles of 95°C for 15 sec and 60°C for 1 min. Finally, capture of all TaqMan PCR data used the Sequence Detection Software (SDS version 2.2.2, Applied Biosystems). The double-delta cycle threshold (ΔΔCT) method was used to analyze the data; results with T-student test. The significance level was set at * $p < 0.05$, ** $p < 0.01$ and *** $p < 0.001$, and tendencies at # < 0.1. Pearson's correlation method assessed a possible linear association between TDP-43 pathology in frontal cortex area 8 and gene deregulation in the same region; significant correlations were not found.

Immunohistochemistry

De-waxed sections, 4μm thick, of the lumbar spinal cord from control and ALS cases were processed in parallel for immunohistochemistry. Endogenous peroxidases were blocked by incubation in 10% methanol-1% H_2O_2 for 15 min followed by 3% normal horse serum. Then the sections were incubated at 4°C overnight with one of the primary antibodies: rabbit polyclonal antibodies to IBA-1 (019-19749, Wako Chemicals Gmbh, Neuss, GE) were used at a dilution of 1:1,000; VDAC (voltage dependent anion channel, ab15895, Abcam, Cambridge, UK) at 1:100; HLA-DRB1 (GTX104919, GeneTex, Barcelona, Spain) at 1:100; HLA-DRB5 (NBP2, Novusbio, Littleton, Colorado, USA) at 1:100; IL-10 (AP52181PU, ACRIS, ProAlt, Madrid, Spain) at 1:100; and GFAP (glial fibrillary acidic protein, RP014-S, Diagnostic Biosystem, Palex Medica, Sant Cugat, Spain) at 1:400. Mouse monoclonal antibodies to CD68 (ab955, Abcam, Cambridge, UK) and TNF-α (ab1793, Abcam, Cambridge, UK), were used at dilutions of 1:200 and 1:150, respectively. Antibodies to GluT: SLC1A2 (ab1783, Millipore, Billerica, MA, USA) were used at a dilution of 1:100. Following incubation with the primary antibody, the sections were incubated with EnVision + system peroxidase (Dako, Agilent, Santa Clara, CA,

USA) for 30 min at room temperature. The peroxidase reaction was visualized with diamino-benzidine and H_2O_2. Control of the immunostaining included omission of the primary antibody; no signal was obtained following incubation with only the secondary antibody. Sections were slightly stained with haematoxylin.

Gel electrophoresis and western blotting

Frozen samples of the somatosensory cortex were homogenized in RIPA lysis buffer composed of 50mM Tris/HCl buffer, pH 7.4 containing 2mM EDTA, 0.2% Nonidet P-40, 1mM PMSF, protease and phosphatase inhibitor cocktail (Roche Molecular Systems, USA). The homogenates were centrifuged for 20 min at 12,000 rpm. Protein concentration was determined with the BCA method (Thermo Scientific). Equal amounts of protein (20μg) for each sample were loaded and separated by electrophoresis on 10% sodium dodecyl sulfate polyacrylamide gel electrophoresis (SDS-PAGE) gels and transferred onto nitrocellulose membranes (Amersham, Freiburg, GE). Non-specific bindings were blocked by incubation in 3% albumin in PBS containing 0.2% Tween for 1 h at room temperature. After washing, membranes were incubated overnight at 4°C with antibodies against glutamate receptor ionotropic, NMDA 2A (NMDAR2A, 130 kDa, rabbit, 1:200, Abcam, Cambridge, UK), α-amino-3-hydroxy-5-methyl-4-isoxazolepropionic acid receptor 1 (AMPAR GluR-1, 100 kDa, rabbit, 1:200, Cell Signaling Technology, Danvers, MA, USA), glutamate decarboxylase 1 (GAD1, 67 kDa, rabbit, 1:200, Cell Signaling Technology, Danvers, MA, USA) and gamma-aminobutyric acid receptor subunit beta-2 (GABAAB2, 59 kDa, mouse, 1:1000, Abcam, Cambridge, UK). Protein loading was monitored using an antibody against β-actin (42 kDa, 1:30,000, Sigma). Membranes were incubated for 1 h with appropriate HRP-conjugated secondary antibodies (1:2,000, Dako); the immunoreaction was revealed with a chemiluminescence reagent (ECL, Amersham). Densitometric quantification was carried out with the ImageLab v4.5.2 software (BioRad), using β-actin for normalization. Seven samples of FC area 8 per group were analyzed. These antibodies were selected on the basis of a larger screening which included antibodies against proteins whose RNA levels were de-regulated as revealed by RT-qPCR. Only antibodies working for western blotting were eventually assessed. The significance level was set at ** $p < 0.01$ and tendencies at # < 0.1.

AUTHOR CONTRIBUTIONS

PA-B carried out gene expression studies and validation of gene expression; JM prepared the samples for morphological and biochemical studies; EA helped in the bioinformatics analysis; MP was in charge of the clinical studies; IF designed and supervised the study and wrote the advanced version of the manuscript which was then circulated among the contributors. All the authors agree with the final version of the manuscript.

ACKNOWLEDGEMENTS

We wish to thank the High Technology Unit (HTU) and Statistics and Bioinformatics Unit (SBU) of the Vall d'Hebron Research Institute (VHIR) (Barcelona, Spain), and particularly Ricardo Gonzalo and Ferran Briansó for the array procedure and data processing, respectively, and T. Yohannan for editorial help.

CONFLICTS OF INTEREST

The authors declare no conflict of interest.

FUNDING

This study was supported by grants from CIBERNED and Instituto de Salud Carlos III, and co-funded by FEDER funds/European Regional Development Fund (ERDF) – a way to build Europe PIE14/00034 and PI14/00757, and intra-CIBERNED project to IF, and IFI15/00035 fellowship to PA-B.

REFERENCES

1. Horobágyi T, Cairns NJ. Amyotrophic lateral sclerosis and frontotemporal lobar degeneration. In: Kovacs GG (ed) Neuropathology of neurodegenerative diseases: a practical guide. Cambridge Press, Cambridge, 2015; pp 209-248.

2. Strong MJ, Hortobágyi T, Okamoto K, Kato S. Amyotrophic lateral sclerosis, primary lateral sclerosis, and spinal muscular atrophy. In: Dickson DW (ed) Neurodegeneration: the molecular pathology of dementia and movement disorders, 2nd ed. Wiley-Blackwell, Oxford, 2011; pp: 418-433.

3. Boillée S, Vande Velde C, Cleveland DW. ALS: a disease of motor neurons and their nonneuronal neighbors. Neuron. 2006; 52:39–59. doi: 10.1016/j.neuron.2006.09.018

4. Calvo A, Moglia C, Balma M, Chiò A. Involvement of immune response in the pathogenesis of amyotrophic lateral sclerosis: a therapeutic opportunity? CNS Neurol Disord Drug Targets. 2010; 9:325–30. doi: 10.2174/187152710791292657

5. D'Amico E, Factor-Litvak P, Santella RM, Mitsumoto H. Clinical perspective on oxidative stress in sporadic amyotrophic lateral sclerosis. Free Radic Biol Med. 2013; 65:509–27.

doi: 10.1016/j.freeradbiomed.2013.06.029

6. Evans MC, Couch Y, Sibson N, Turner MR. Inflammation and neurovascular changes in amyotrophic lateral sclerosis. Mol Cell Neurosci. 2013; 53:34–41. doi: 10.1016/j.mcn.2012.10.008

7. Hooten KG, Beers DR, Zhao W, Appel SH. Protective and toxic neuroinflammation in amyotrophic lateral sclerosis. Neurotherapeutics. 2015; 12:364–75. doi: 10.1007/s13311-014-0329-3

8. King AE, Woodhouse A, Kirkcaldie MT, Vickers JC. Excitotoxicity in ALS: Overstimulation, or overreaction? Exp Neurol. 2016; 275:162–71. doi: 10.1016/j.expneurol.2015.09.019

9. Lin CL, Bristol LA, Jin L, Dykes-Hoberg M, Crawford T, Clawson L, Rothstein JD. Aberrant RNA processing in a neurodegenerative disease: the cause for absent EAAT2, a glutamate transporter, in amyotrophic lateral sclerosis. Neuron. 1998; 20:589–602. doi: 10.1016/S0896-6273(00)80997-6

10. Maragakis NJ, Rothstein JD. Glutamate transporters in neurologic disease. Arch Neurol. 2001; 58:365–70. doi: 10.1001/archneur.58.3.365

11. Peters OM, Ghasemi M, Brown RH Jr. Emerging mechanisms of molecular pathology in ALS. J Clin Invest. 2015; 125:1767–79. doi: 10.1172/JCI71601

12. Philips T, Robberecht W. Neuroinflammation in amyotrophic lateral sclerosis: role of glial activation in motor neuron disease. Lancet Neurol. 2011; 10:253–63. doi: 10.1016/S1474-4422(11)70015-1

13. Philips T, Rothstein JD. Glial cells in amyotrophic lateral sclerosis. Exp Neurol. 2014; 262:111–20. doi: 10.1016/j.expneurol.2014.05.015

14. Rossi S, Cozzolino M, Carrì MT. Old versus new mechanisms in the pathogenesis of ALS. Brain Pathol. 2016; 26:276–86. doi: 10.1111/bpa.12355

15. Strong MJ, Leystra-Lantz C, Ge WW. Intermediate filament steady-state mRNA levels in amyotrophic lateral sclerosis. Biochem Biophys Res Commun. 2004; 316:317–22. doi: 10.1016/j.bbrc.2004.02.051

16. Taylor JP, Brown RH Jr, Cleveland DW. Decoding ALS: from genes to mechanism. Nature. 2016; 539:197–206. doi: 10.1038/nature20413

17. Dangond F, Hwang D, Camelo S, Pasinelli P, Frosch MP, Stephanopoulos G, Stephanopoulos G, Brown RH Jr, Gullans SR. Molecular signature of late-stage human ALS revealed by expression profiling of postmortem spinal cord gray matter. Physiol Genomics. 2004; 16:229–39. doi: 10.1152/physiolgenomics.00087.2001

18. Heath PR, Kirby J, Shaw PJ. Investigating cell death mechanisms in amyotrophic lateral sclerosis using transcriptomics. Front Cell Neurosci. 2013; 7:259. doi: 10.3389/fncel.2013.00259

19. Henriques A, Gonzalez De Aguilar JL. Can transcriptomics cut the gordian knot of amyotrophic lateral sclerosis? Curr Genomics. 2011; 12:506–15. doi: 10.2174/138920211797904043

20. Ishigaki S, Niwa J, Ando Y, Yoshihara T, Sawada K, Doyu M, Yamamoto M, Kato K, Yotsumoto Y, Sobue G. Differentially expressed genes in sporadic amyotrophic lateral sclerosis spinal cords--screening by molecular indexing and subsequent cDNA microarray analysis. FEBS Lett. 2002; 531:354–58. doi: 10.1016/S0014-5793(02)03546-9

21. Malaspina A, Kaushik N, de Belleroche J. Differential expression of 14 genes in amyotrophic lateral sclerosis spinal cord detected using gridded cDNA arrays. J Neurochem. 2001; 77:132–45. doi: 10.1046/j.1471-4159.2001.t01-1-00231.x

22. Lederer CW, Torrisi A, Pantelidou M, Santama N, Cavallaro S. Pathways and genes differentially expressed in the motor cortex of patients with sporadic amyotrophic lateral sclerosis. BMC Genomics. 2007; 8:26. doi: 10.1186/1471-2164-8-26

23. Li H, de Faria JP, Andrew P, Nitarska J, Richardson WD. Phosphorylation regulates OLIG2 cofactor choice and the motor neuron-oligodendrocyte fate switch. Neuron. 2011; 69:918–29. doi: 10.1016/j.neuron.2011.01.030

24. Wang XS, Simmons Z, Liu W, Boyer PJ, Connor JR. Differential expression of genes in amyotrophic lateral sclerosis revealed by profiling the post mortem cortex. Amyotroph Lateral Scler. 2006; 7:201–10. doi: 10.1080/17482960600947689

25. Offen D, Barhum Y, Melamed E, Embacher N, Schindler C, Ransmayr G. Spinal cord mRNA profile in patients with ALS: comparison with transgenic mice expressing the human SOD-1 mutant. J Mol Neurosci. 2009; 38:85–93. doi: 10.1007/s12031-007-9004-z

26. Woodruff RH, Tekki-Kessaris N, Stiles CD, Rowitch DH, Richardson WD. Oligodendrocyte development in the spinal cord and telencephalon: common themes and new perspectives. Int J Dev Neurosci. 2001; 19:379–85. doi: 10.1016/S0736-5748(00)00083-6

27. Jiang YM, Yamamoto M, Kobayashi Y, Yoshihara T, Liang Y, Terao S, Takeuchi H, Ishigaki S, Katsuno M, Adachi H, Niwa J, Tanaka F, Doyu M, et al. Gene expression profile of spinal motor neurons in sporadic amyotrophic lateral sclerosis. Ann Neurol. 2005; 57:236–51. doi: 10.1002/ana.20379

28. Cox LE, Ferraiuolo L, Goodall EF, Heath PR, Higginbot-

tom A, Mortiboys H, Hollinger HC, Hartley JA, Brockington A, Burness CE, Morrison KE, Wharton SB, Grierson AJ, et al. Mutations in CHMP2B in lower motor neuron predominant amyotrophic lateral sclerosis (ALS). PLoS One. 2010; 5:e9872. doi: 10.1371/journal.pone.0009872

29. Kirby J, Halligan E, Baptista MJ, Allen S, Heath PR, Holden H, Barber SC, Loynes CA, Wood-Allum CA, Lunec J, Shaw PJ. Mutant SOD1 alters the motor neuronal transcriptome: implications for familial ALS. Brain. 2005; 128:1686–706. doi: 10.1093/brain/awh503

30. Rothstein JD. Excitotoxic mechanisms in the pathogenesis of amyotrophic lateral sclerosis. Adv Neurol. 1995; 68:7–20.

31. Rothstein JD. Current hypotheses for the underlying biology of amyotrophic lateral sclerosis. Ann Neurol. 2009 (Suppl 1); 65:S3–9. doi: 10.1002/ana.21543

32. Chen X, Kelemen SE, Autieri MV. AIF-1 expression modulates proliferation of human vascular smooth muscle cells by autocrine expression of G-CSF. Arterioscler Thromb Vasc Biol. 2004; 24:1217–22. doi: 10.1161/01.ATV.0000130024.50058.de

33. Kelemen SE, Autieri MV. Expression of allograft inflammatory factor-1 in T lymphocytes: a role in T-lymphocyte activation and proliferative arteriopathies. Am J Pathol. 2005; 167:619–26. doi: 10.1016/S0002-9440(10)63003-9

34. Schulze JO, Quedenau C, Roske Y, Adam T, Schüler H, Behlke J, Turnbull AP, Sievert V, Scheich C, Mueller U, Heinemann U, Büssow K. Structural and functional characterization of human Iba proteins. FEBS J. 2008; 275:4627–40. doi: 10.1111/j.1742-4658.2008.06605.x

35. Beranek JT. CD68 is not a macrophage-specific antigen. Ann Rheum Dis. 2005; 64:342–43.

36. Gottfried E, Kunz-Schughart LA, Weber A, Rehli M, Peuker A, Müller A, Kastenberger M, Brockhoff G, Andreesen R, Kreutz M. Expression of CD68 in non-myeloid cell types. Scand J Immunol. 2008; 67:453–63. doi: 10.1111/j.1365-3083.2008.02091.x

37. Holness CL, Simmons DL. Molecular cloning of CD68, a human macrophage marker related to lysosomal glycoproteins. Blood. 1993; 81:1607–13.

38. Colton C, Wilcock DM. Assessing activation states in microglia. CNS Neurol Disord Drug Targets. 2010; 9:174–91. doi: 10.2174/187152710791012053

39. Heneka MT, Kummer MP, Latz E. Innate immune activation in neurodegenerative disease. Nat Rev Immunol. 2014; 14:463–77. doi: 10.1038/nri3705

40. Arroyo DS, Soria JA, Gaviglio EA, Rodriguez-Galan MC, Iribarren P. Toll-like receptors are key players in neurodegeneration. Int Immunopharmacol. 2011; 11:1415–21. doi: 10.1016/j.intimp.2011.05.006

41. Chen K, Iribarren P, Hu J, Chen J, Gong W, Cho EH, Lockett S, Dunlop NM, Wang JM. Activation of Toll-like receptor 2 on microglia promotes cell uptake of Alzheimer disease-associated amyloid β peptide. J Biol Chem. 2006; 281:3651–59. doi: 10.1074/jbc.M508125200

42. Iribarren P, Zhou Y, Hu J, Le Y, Wang JM. Role of formyl peptide receptor-like 1 (FPRL1/FPR2) in mononuclear phagocyte responses in Alzheimer disease. Immunol Res. 2005; 31:165–76. doi: 10.1385/IR:31:3:165

43. Tahara K, Kim HD, Jin JJ, Maxwell JA, Li L, Fukuchi K. Role of toll-like receptor signalling in Abeta uptake and clearance. Brain. 2006; 129:3006–19. doi: 10.1093/brain/awl249

44. Facci L, Barbierato M, Marinelli C, Argentini C, Skaper SD, Giusti P. Toll-like receptors 2, -3 and -4 prime microglia but not astrocytes across central nervous system regions for ATP-dependent interleukin-1β release. Sci Rep. 2014; 4:6824. doi: 10.1038/srep06824

45. Lane T, Lachmann HJ. The emerging role of interleukin-1β in autoinflammatory diseases. Curr Allergy Asthma Rep. 2011; 11:361–68. doi: 10.1007/s11882-011-0207-6

46. Pestka S, Krause CD, Sarkar D, Walter MR, Shi Y, Fisher PB. Interleukin-10 and related cytokines and receptors. Annu Rev Immunol. 2004; 22:929–79. doi: 10.1146/annurev.immunol.22.012703.104622

47. Schellera J, Chalarisb A, Schmidt-Arrasb D, Rose-Johnb S. The pro- and anti-inflammatory properties of the cytokine interleukin-6. Biochim Biophys Acta - Mol. Cell Res. 2011; 1813:878–88.

48. Simpson RJ, Hammacher A, Smith DK, Matthews JM, Ward LD. Interleukin-6: structure-function relationships. Protein Sci. 1997; 6:929–55. doi: 10.1002/pro.5560060501

49. Pal M, Febbraio MA, Whitham M. From cytokine to myokine: the emerging role of interleukin-6 in metabolic regulation. Immunol Cell Biol. 2014; 92:331–39. doi: 10.1038/icb.2014.16

50. Locksley RM, Killeen N, Lenardo MJ. The TNF and TNF receptor superfamilies: integrating mammalian biology. Cell. 2001; 104:487–501. doi: 10.1016/S0092-8674(01)00237-9

51. Olszewski MB, Groot AJ, Dastych J, Knol EF. TNF trafficking to human mast cell granules: mature

chain-dependent endocytosis. J Immunol. 2007; 178:5701–09. doi: 10.4049/jimmunol.178.9.5701

52. McGuire MJ, Lipsky PE, Thiele DL. Purification and characterization of dipeptidyl peptidase I from human spleen. Arch Biochem Biophys. 1992; 295:280–88. doi: 10.1016/0003-9861(92)90519-3

53. Small DM, Burden RE, Scott CJ. The emerging relevance of the cysteine protease cathepsin S in disease. Clin Rev Bone Miner Metab. 2011; 9:122–32. doi: 10.1007/s12018-011-9095-5

54. Archer NS, Nassif NT, O'Brien BA. Genetic variants of SLC11A1 are associated with both autoimmune and infectious diseases: systematic review and meta-analysis. Genes Immun. 2015; 16:275–83. doi: 10.1038/gene.2015.8

55. Villadangos JA. Presentation of antigens by MHC class II molecules: getting the most out of them. Mol Immunol. 2001; 38:329–46. doi: 10.1016/S0161-5890(01)00069-4

56. Hahn M, Nicholson MJ, Pyrdol J, Wucherpfennig KW. Unconventional topology of self peptide-major histocompatibility complex binding by a human autoimmune T cell receptor. Nat Immunol. 2005;

6:490–96. doi: 10.1038/ni1187

57. Menéndez-Benito V, Neefjes J. Autophagy in MHC class II presentation: sampling from within. Immunity. 2007; 26:1–3. doi: 10.1016/j.immuni.2007.01.005

58. Saunders PA, Hendrycks VR, Lidinsky WA, Woods ML. PD-L2:PD-1 involvement in T cell proliferation, cytokine production, and integrin-mediated adhesion. Eur J Immunol. 2005; 35:3561–69. doi: 10.1002/eji.200526347

59. Schoenborn JR, Wilson CB. Regulation of interferon-gamma during innate and adaptive immune responses. Adv Immunol. 2007; 96:41–101. doi: 10.1016/S0065-2776(07)96002-2

60. Miller AM. Role of IL-33 in inflammation and disease. J Inflamm (Lond). 2011; 8:22. doi: 10.1186/1476-9255-8-22

61. Ruffoli R, Bartalucci A, Frati A, Fornai F. Ultrastructural studies of ALS mitochondria connect altered function and permeability with defects of mitophagy and mitochondriogenesis. Front Cell Neurosci. 2015; 9:341. doi: 10.3389/fncel.2015.00341

62. Carrì MT, D'Ambrosi N, Cozzolino M. Pathways to mitochondrial dysfunction in ALS pathogenesis. Biochem Biophys Res Commun. 2016.

63. Figlewicz DA, Krizus A, Martinoli MG, Meininger V, Dib M, Rouleau GA, Julien JP. Variants of the heavy neurofilament subunit are associated with the development of amyotrophic lateral sclerosis. Hum Mol Genet. 1994; 3:1757–61. doi: 10.1093/hmg/3.10.1757

64. Asai DJ, Brokaw CJ. Dynein heavy chain isoforms and axonemal motility. Trends Cell Biol. 1993; 3:398–402. doi: 10.1016/0962-8924(93)90090-N

65. Chapelin C, Duriez B, Magnino F, Goossens M, Escudier E, Amselem S. Isolation of several human axonemal dynein heavy chain genes: genomic structure of the catalytic site, phylogenetic analysis and chromosomal assignment. FEBS Lett. 1997; 412:325–30. doi: 10.1016/S0014-5793(97)00800-4

66. McKenney RJ, Huynh W, Tanenbaum ME, Bhabha G, Vale RD. Activation of cytoplasmic dynein motility by dynactin-cargo adapter complexes. Science. 2014; 345:337–41. doi: 10.1126/science.1254198

67. Giorda R, Peakman M, Tan KC, Vergani D, Trucco M. Glutamic acid decarboxylase expression in islets and brain. Lancet. 1991; 338:1469–70. doi: 10.1016/0140-6736(91)92781-V

68. Kaufman DL, McGinnis JF, Krieger NR, Tobin AJ. Brain glutamate decarboxylase cloned in lambda gt-11: fusion protein produces gamma-aminobutyric acid. Science. 1986; 232:1138–40.

doi: 10.1126/science.3518061

69. Burmakina S, Geng Y, Chen Y, Fan QR. Heterodimeric coiled-coil interactions of human GABAB receptor. Proc Natl Acad Sci USA. 2014; 111:6958–63. doi: 10.1073/pnas.1400081111

70. Hallermann S, Fejtova A, Schmidt H, Weyhersmüller A, Silver RA, Gundelfinger ED, Eilers J. Bassoon speeds vesicle reloading at a central excitatory synapse. Neuron. 2010; 68:710–23. doi: 10.1016/j.neuron.2010.10.026

71. Davydova D, Marini C, King C, Klueva J, Bischof F, Romorini S, Montenegro-Venegas C, Heine M, Schneider R, Schröder MS, Altrock WD, Henneberger C, Rusakov DA, et al. Bassoon specifically controls presynaptic P/Q-type Ca(2+) channels via RIM-binding protein. Neuron. 2014; 82:181–94. doi: 10.1016/j.neuron.2014.02.012

72. Fenster SD, Garner CC. Gene structure and genetic localization of the PCLO gene encoding the presynaptic active zone protein Piccolo. Int J Dev Neurosci. 2002; 20:161–71. doi: 10.1016/S0736-5748(02)00046-1

73. Fenster SD, Chung WJ, Zhai R, Cases-Langhoff C, Voss B, Garner AM, Kaempf U, Kindler S, Gundelfinger ED, Garner CC. Piccolo, a presynaptic zinc finger protein structurally related to bassoon. Neuron. 2000; 25: 203 – 14. doi: 10.1016/S0896-6273(00)80883-1

74. Matosin N, Green MJ, Andrews JL, Newell KA, Fernandez-Enright F. Possibility of a sex-specific role for a genetic variant in FRMPD4 in schizophrenia, but not cognitive function. Neuroreport. 2016; 27:33–38. doi: 10.1097/WNR.0000000000000491

75. Kremerskothen J, Kindler S, Finger I, Veltel S, Barnekow A. Postsynaptic recruitment of Dendrin depends on both dendritic mRNA transport and synaptic anchoring. J Neurochem. 2006; 96:1659–66. doi: 10.1111/j.1471-4159.2006.03679.x

76. Naeve GS, Ramakrishnan M, Kramer R, Hevroni D, Citri Y, Theill LE. Neuritin: a gene induced by neural activity and neurotrophins that promotes neuritogenesis. Proc Natl Acad Sci USA. 1997; 94:2648–53. doi: 10.1073/pnas.94.6.2648

77. Shimada T, Yoshida T, Yamagata K. Neuritin mediates activity-dependent axonal branch formation in part via FGF signaling. J Neurosci. 2016; 36:4534–48. doi: 10.1523/JNEUROSCI.1715-15.2016

78. Cahoy JD, Emery B, Kaushal A, Foo LC, Zamanian JL, Christopherson KS, Xing Y, Lubischer JL, Krieg PA, Krupenko SA, Thompson WJ, Barres BA. A transcriptome database for astrocytes, neurons, and oligodendrocytes: a new resource for understanding brain development and function. J Neurosci. 2008; 28:264–78. doi: 10.1523/JNEUROSCI.4178-07.2008

79. Emery B, Agalliu D, Cahoy JD, Watkins TA, Dugas JC, Mulinyawe SB, Ibrahim A, Ligon KL, Rowitch DH, Barres BA. Myelin gene regulatory factor is a critical transcriptional regulator required for CNS myelination. Cell. 2009; 138:172–85. doi: 10.1016/j.cell.2009.04.031

80. Li Z, Park Y, Marcotte EM. A Bacteriophage tailspike domain promotes self-cleavage of a human membrane-bound transcription factor, the myelin regulatory factor MYRF. PLoS Biol. 2013; 11:e1001624. doi: 10.1371/journal.pbio.1001624

81. Koenning M, Jackson S, Hay CM, Faux C, Kilpatrick TJ, Willingham M, Emery B. Myelin gene regulatory factor is required for maintenance of myelin and mature oligodendrocyte identity in the adult CNS. J Neurosci. 2012; 32:12528–42. doi: 10.1523/JNEUROSCI.1069-12.2012

82. Sun Y, Meijer DH, Alberta JA, Mehta S, Kane MF, Tien AC, Fu H, Petryniak MA, Potter GB, Liu Z, Powers JF, Runquist IS, Rowitch DH, Stiles CD. Phosphorylation state of Olig2 regulates proliferation of neural progenitors. Neuron. 2011; 69:906–17. doi: 10.1016/j.neuron.2011.02.005

83. LeBlanc SE, Ward RM, Svaren J. Neuropathy-associated Egr2 mutants disrupt cooperative activation of myelin protein zero by Egr2 and Sox10. Mol Cell Biol. 2007; 27:3521–29. doi: 10.1128/MCB.01689-06

84. Li H, Lu Y, Smith HK, Richardson WD. Olig1 and Sox10 interact synergistically to drive myelin basic protein transcription in oligodendrocytes. J Neurosci. 2007; 27:14375–82. doi: 10.1523/JNEUROSCI.4456-07.2007

85. Zhu Q, Zhao X, Zheng K, Li H, Huang H, Zhang Z, Mastracci T, Wegner M, Chen Y, Sussel L, Qiu M. Genetic evidence that Nkx2.2 and Pdgfra are major determinants of the timing of oligodendrocyte differentiation in the developing CNS. Development. 2014; 141:548–55. doi: 10.1242/dev.095323

86. Connor JR. Iron acquisition and expression of iron regulatory proteins in the developing brain: manipulation by ethanol exposure, iron deprivation and cellular dysfunction. Dev Neurosci. 1994; 16:233–47. doi: 10.1159/000112115

87. Erikson KM, Pinero DJ, Connor JR, Beard JL. Regional brain iron, ferritin and transferrin concentrations during iron deficiency and iron repletion in developing rats. J Nutr. 1997; 127:2030–38.

88. Diehl HJ, Schaich M, Budzinski RM, Stoffel W. Individual exons encode the integral membrane domains of human myelin proteolipid protein. Proc Natl Acad Sci USA. 1986; 83:9807–11. doi: 10.1073/pnas.83.24.9807

89. Griffiths I, Klugmann M, Anderson T, Yool D, Thomson C, Schwab MH, Schneider A, Zimmermann F, McCulloch M, Nadon N, Nave KA. Axonal swellings and degeneration in mice lacking the major proteolipid of myelin. Science. 1998; 280:1610–13. doi: 10.1126/science.280.5369.1610

90. Marty MC, Alliot F, Rutin J, Fritz R, Trisler D, Pessac B. The myelin basic protein gene is expressed in differentiated blood cell lineages and in hemopoietic progenitors. Proc Natl Acad Sci USA. 2002; 99:8856–61. doi: 10.1073/pnas.122079599

91. Montague P, McCallion AS, Davies RW, Griffiths IR. Myelin-associated oligodendrocytic basic protein: a family of abundant CNS myelin proteins in search of a function. Dev Neurosci. 2006; 28:479–87. doi: 10.1159/000095110

92. Roth MP, Malfroy L, Offer C, Sevin J, Enault G, Borot N, Pontarotti P, Coppin H. The human myelin oligodendrocyte glycoprotein (MOG) gene: complete nucleotide sequence and structural characterization. Genomics. 1995; 28:241–50. doi: 10.1006/geno.1995.1137

93. Lossos A, Elazar N, Lerer I, Schueler-Furman O, Fellig Y, Glick B, Zimmerman BE, Azulay H, Dotan S, Goldberg S, Gomori JM, Ponger P, Newman JP, et al.

Myelin-associated glycoprotein gene mutation causes Pelizaeus-Merzbacher disease-like disorder. Brain. 2015; 138:2521–36. doi: 10.1093/brain/awv204

94. Kim T, Fiedler K, Madison DL, Krueger WH, Pfeiffer SE. Cloning and characterization of MVP17: a developmentally regulated myelin protein in oligodendrocytes. J Neurosci Res. 1995; 42:413–22. doi: 10.1002/jnr.490420316

95. Kasama-Yoshida H, Tohyama Y, Kurihara T, Sakuma M, Kojima H, Tamai Y. A comparative study of 2', 3'-cyclic-nucleotide 3'-phosphodiesterase in vertebrates: cDNA cloning and amino acid sequences for chicken and bullfrog enzymes. J Neurochem. 1997; 69:1335–42. doi: 10.1046/j.1471-4159.1997.69041335.x

96. Kursula P. Structural properties of proteins specific to the myelin sheath. Amino Acids. 2008; 34:175–85. doi: 10.1007/s00726-006-0479-7

97. Lappe-Siefke C, Goebbels S, Gravel M, Nicksch E, Lee J, Braun PE, Griffiths IR, Nave KA. Disruption of Cnp1 uncouples oligodendroglial functions in axonal support and myelination. Nat Genet. 2003; 33:366–74. doi: 10.1038/ng1095

98. Nardo G, Iennaco R, Fusi N, Heath PR, Marino M, Trolese MC, Ferraiuolo L, Lawrence N, Shaw PJ, Bendotti C. Transcriptomic indices of fast and slow disease progression in two mouse models of amyotrophic lateral sclerosis. Brain. 2013; 136:3305–32. doi: 10.1093/brain/awt250

99. Gentleman RC, Carey VJ, Bates DM, Bolstad B, Dettling M, Dudoit S, Ellis B, Gautier L, Ge Y, Gentry J, Hornik K, Hothorn T, Huber W, et al. Bioconductor: open software development for computational biology and bioinformatics. Genome Biol. 2004; 5:R80. doi: 10.1186/gb-2004-5-10-r80

100. Barrachina M, Castaño E, Ferrer I. TaqMan PCR assay in the control of RNA normalization in human post-mortem brain tissue. Neurochem Int. 2006; 49:276–84. doi: 10.1016/j.neuint.2006.01.018

101. Durrenberger PF, Fernando FS, Magliozzi R, Kashefi SN, Bonnert TP, Ferrer I, Seilhean D, Nait-Oumesmar B, Schmitt A, Gebicke-Haerter PJ, Falkai P, Grünblatt E, Palkovits M, et al. Selection of novel reference genes for use in the human central nervous system: a BrainNet Europe Study. Acta Neuropathol. 2012; 124:893–903. doi: 10.1007/s00401-012-1027-z

SUPPLEMENTARY MATERIAL

Please browse the Full text version to see Supplementary Tables 1 and 2 identifying all de-regulated genes.

Article II

Inflammatory gene expression in whole peripheral blood at early stages of sporadic Amyotrophic lateral sclerosis

Pol Andrés Benito, Jesús Moreno, Raúl Domínguez, Ester Aso, Mònica Povedano and Isidro Ferrer

Frontiers in Neurology. 2017 Oct 13; 8: 546.

frontiers in Neurology

ORIGINAL RESEARCH
published: 13 October 2017
doi: 10.3389/fneur.2017.00546

Inflammatory Gene Expression in Whole Peripheral Blood at Early Stages of Sporadic Amyotrophic Lateral Sclerosis

*Pol Andrés-Benito[1,2], Jesús Moreno[2], Raúl Domínguez[3], Ester Aso[1,2], Mónica Povedano[2,3] and Isidro Ferrer[1,2,4,5]**

[1] Neuropathology, Pathologic Anatomy Service, Bellvitge University Hospital, IDIBELL, Hospitalet de Llobregat, Spain, [2] Biomedical Network Research Center on Neurodegenerative Diseases (CIBERNED), Institute Carlos III, Hospitalet de Llobregat, Spain, [3] Functional Unit of Amyotrophic Lateral Sclerosis (UFELA), Service of Neurology, Bellvitge University Hospital, Hospitalet de Llobregat, Spain, [4] Department of Pathology and Experimental Therapeutics, University of Barcelona, Hospitalet de Llobregat, Spain, [5] Institute of Neurosciences, University of Barcelona, Hospitalet de Llobregat, Spain

Objective: Characterization of altered expression of selected transcripts linked to inflammation in the peripheral blood of sporadic amyotrophic lateral sclerosis (sALS) patients at early stage of disease to increase knowledge about peripheral inflammatory response in sALS.

Methods: RNA expression levels of 45 genes were assessed by RT-qPCR in 22 sALS cases in parallel with 13 age-matched controls. Clinical and serum parameters were assessed at the same time.

Results: Upregulation of genes coding for factors involved in leukocyte extravasation (*ITGB2*, *INPP5D*, *SELL*, and *ICAM1*) and extracellular matrix remodeling (*MMP9* and *TIMP2*), as well as downregulation of certain chemokines (*CCL5* and *CXC5R*), anti-inflammatory cytokines (*IL10*, *TGFB2*, and *IL10RA*), pro-inflammatory cytokines (*IL-6*), and T-cell regulators (*CD2* and *TRBC1*) was found in sALS cases independently of gender, clinical symptoms at onset (spinal, respiratory, or bulbar), progression, peripheral leukocyte number, and integrity of RNA. *MMP9* levels positively correlated with age, whereas *CCR5*, *CCL5*, and *TRBC1* negatively correlated with age in sALS but not in controls. Relatively higher *TNFA* expression levels correlate with higher creatinine kinase protein levels in plasma.

Conclusion: Present findings show early inflammatory responses characterized by upregulation of factors enabling extravasation of leukocytes and extracellular matrix remodeling in blood in sALS cases, in addition to increased *TNFA* levels paralleling skeletal muscle damage.

Keywords: amyotrophic lateral sclerosis, blood, cytokines, extracellular matrix, leukocyte extravasation

OPEN ACCESS

Edited by:
Ghazala Hayat, Saint Louis University, United States

Reviewed by:
Sebastian Aleksander Lewandowski, Karolinska Institute (KI), Sweden
Janice C. Wong, Brigham and Women's Hospital, United States

Correspondence:
Isidro Ferrer
8082ifa@gmail.com

Specialty section:
This article was submitted to Neuromuscular Diseases, a section of the journal Frontiers in Neurology

Received: *30 May 2017*
Accepted: *27 September 2017*
Published: *13 October 2017*

Citation:
Andrés-Benito P, Moreno J, Domínguez R, Aso E, Povedano M and Ferrer I (2017) Inflammatory Gene Expression in Whole Peripheral Blood at Early Stages of Sporadic Amyotrophic Lateral Sclerosis. Front. Neurol. 8:546. doi: 10.3389/fneur.2017.00546

INTRODUCTION

Increase in the number of astrocytes and microglia, and activation of inflammatory responses are major pathological marks in the anterior horn of the spinal cord in amyotrophic lateral sclerosis (ALS). Chronic inflammation plays the principal role in motor neuron demise and parallels the severity of motor neuron damage. A plethora of receptors, modulatory factors, chemokines,

and anti- and pro-inflammatory cytokines are involved in this process at advanced stages of the disease (1–7). Inflammatory responses in the central nervous system are accompanied by modifications in blood and serum which may indicate a systemic inflammatory response in ALS (8–11). Peripheral nerves, autonomic nervous system, and muscle are involved in ALS, and they are putative targets of inflammatory reactions (12–18). Recent studies have also shown modifications in the intestinal microbiota in ALS (19, 20), thus categorizing ALS as a disease with multisystem involvement.

The majority of studies of blood and serum in ALS are at middle or advanced stages of the disease with or without treatment (10, 17, 21–26), but information about early stages at the time when the patient first asks for medical counseling and the disease is then diagnosed is limited (27). The purpose of the present study was to increase knowledge about expression of transcripts linked to inflammation in whole blood samples of sporadic ALS (sALS) patients at initial clinical stages of the disease. The selection of genes was conducted including representative pro- and anti-inflammatory cytokines, chemokines, cytokine modulators, extracellular matrix remodeling-related factors, molecules involved in extravasation mechanisms, oxidative stress markers, and T-cell regulators. The expression of these molecules was assessed considering the variables RNA integrity, gender, clinical symptoms at onset (spinal, respiratory, or bulbar), disease progression, peripheral leukocyte number, and creatinine kinase protein levels in plasma.

MATERIALS AND METHODS

Sample Description

Whole peripheral blood samples for mRNA expression and biochemical studies were obtained within the two first months after the diagnosis. Samples were obtained from 22 sALS patients (mean age at plasma sampling 62.5 years; 16 men and 6 women) and 13 healthy age-matched controls (mean age at plasma sampling 65 years; 11 men and 4 women). sALS patients were selected on the basis of early stage at the diagnosis with homogenous parameters of gender, age, and treatment, whereas controls were recruited on the basis of homogenous parameters of gender and age. Patients were evaluated clinically according to the main signs at onset (spinal, bulbar, and respiratory) and categorized according to disease progression as fast, expected, and slow progression depending on the survival or the clinical evolution in those still alive. Fast progression was considered in patients who survived less than 3 years; expected progression was considered between 3 and 5 years, and slow for those still alive after 5 years. The ALS Functional Rating Scale Revised (ALSFRS-R, version May 2015) was currently used in every case. No ALS cases or controls suffered from infection or inflammatory disorder at the time of sampling. None of them complained of systemic disease and none received any treatment related to ALS. No familial forms of ALS for *C9ORF72*, *SOD1*, *TARDBP*, and *FUS* mutations were detected when DNA of each patient was sequenced. Blood samples from sALS cases and age-matched controls were obtained following signed informed consent and approval by Clinical Research Ethics Committee (CEIC) of the Bellvitge University Hospital. A summary of cases is shown in **Table 1**.

Blood Collection

In addition to current blood samples for hemogram and biochemical parameters, whole blood samples were collected using PAXgene Blood RNA Tube (PAXgene Blood RNA Tube, PreAnalytiX, Qiagen© GmbH, Hilden, GE) collecting system. Two PAXgene Blood RNA tubes were obtained per case. Samples were collected at the first visit once the clinical diagnosis was established. Tubes were kept for 2 h at room temperature to ensure lysis of blood cells and then stored at −20°C for 24 h. Thereafter, tubes were transferred to −80°C for at least 7 days prior to processing.

White Blood Cells (WBC) Counting

Blood was collected in EDTA 3 mL tubes and analyzed using flow-cytometry equipment. Technicon H-1, H-2, and H-3 apparatuses

TABLE 1 | Summary of cases analyzed in the present study.

Case	Age at plasma sampling	Gender	Diagnosis	Initial symptoms	RIN value
1	60	M	Control	–	9.1
2	68	M	Control	–	9.2
3	66	F	Control	–	9.0
4	N/A	M	Control	–	8.9
5	74	M	Control	–	8.0
6	N/A	F	Control	–	8.3
7	76	F	Control	–	7.8
8	67	M	Control	–	6.1
9	72	F	Control	–	6.0
10	44	F	Control	–	6.0
11	66	F	Control	–	6.1
12	62	F	Control	–	6.5
13	63	F	Control	–	6.0
14	60	M	ALS	Spinal	7.4
15	63	M	ALS	Spinal	8.7
16	66	F	ALS	Bulbar	8.9
17	53	F	ALS	Bulbar	7.3
18	73	M	ALS	Bulbar	8.6
19	65	M	ALS	Spinal	8.9
20	43	M	ALS	Bulbar	8.6
21	57	F	ALS	Bulbar	7.4
22	65	M	ALS	Bulbar	7.1
23	67	M	ALS	Bulbar	7.4
24	73	M	ALS	Spinal	6.1
25	73	F	ALS	Spinal	6.0
26	59	F	ALS	Spinal	8.7
27	65	M	ALS	Respiratory	7.1
28	42	M	ALS	Bulbar	9.2
29	75	M	ALS	Respiratory	8.1
30	75	M	ALS	Bulbar	7.9
31	29	M	ALS	Spinal	8.3
32	77	M	ALS	Spinal	7.4
33	55	M	ALS	Spinal	8.5
34	69	M	ALS	Spinal	8.6
35	71	F	ALS	Spinal	8.7

ALS, amyotrophic lateral sclerosis; M, male; F, female; RIN, RNA integrity number.

are discrete analyzers that perform complete blood and platelet counts, and leukocyte differential count. The instrument has a tungsten halogen light source and cytometer for leukocyte peroxidase analysis, with the addition of a helium-neon red laser for RBC/platelet and basophil determinations. Red blood cells are lysed, and fixed leukocytes flow in a stream sheath—a layer of inert liquid of the same refractive index. The stream sheath serves to narrow the sample stream, which prevents clogging and keeps the flow cell clean. Within the cell flow, cells are classified one by one on the basis of size (determined by a dark-field light scatter detector) and cytochemical peroxidase reaction. Measurement of the peroxidase activity is sufficient for most of the WBC differential classification. Lymphocytes are identified as small, unstained cells. Large atypical lymphocytes, plasma cells, and some blasts are characterized as "large unstained cells" (LUCs). Eosinophils exhibit the strongest peroxidase activity and appear smaller than neutrophils because they absorb some of their own scatter signal. Neutrophils are large and have moderate peroxidase activity. Monocytes have somewhat weaker peroxidase staining and are, therefore, in the area to the left of the neutrophils and to the right of the LUCs. The instrument's computer automatically performs cluster analysis of the WBC subpopulations. The Technicon systems provide both relative (per cent) and absolute ($\times 10^9$ cells/L) cell counts for neutrophils, eosinophils, basophils, monocytes, and LUCs.

Quantitative Determination of Creatine Kinase (CK) in Blood Samples

Kinetic determination of CK was based upon IFCC (International Federation of Clinical Chemistry and Laboratory Medicine) and DGKC (Deutsche Gesellschaft für Klinische Chemie). The principle of the method is based on the ability of CK to catalyze the conversion of creatine phosphate and ADP to creatine and ATP. ATP and glucose are converted to ADP and glucose-6-phosphate by hexokinase. Glucose-6-phosphate dehydrogenase oxidizes glucose-6-phosphate to 6-phosphogluconate, reducing NADP to NADPH. The rate of conversion of NADP/NADPH, monitored at 340 nm, is proportional to CK activity. *N*-acetyl cysteine (NAC) is added as an activator of CK (28, 29).

RNA Extraction and RT-qPCR

PAXgene Blood RNA tubes were incubated overnight at 4°C in a shaker-plate to equilibrate the temperature and increase yields and then at room temperature for 2 h before starting the procedure. RNA from frozen whole blood samples was extracted following the instructions of the supplier (PAXgene Blood RNA kit, PreAnalytiX, Qiagen© GmbH, Hilden, GE). RNA integrity number (RIN) and 28S/18S ratios were determined with the Agilent Bioanalyzer (Agilent Technologies Inc., Santa Clara, CA, USA) to assess RNA quality. RNA concentration was evaluated using a NanoDrop™ Spectrophotometer (Thermo Fisher Scientific, Carlsbad, CA, USA). RIN values are shown in **Table 1**. Complementary DNA (cDNA) was prepared using the High-Capacity cDNA Reverse Transcription kit (Applied Biosystems, Foster City, CA, USA) following the protocol provided by the supplier. Parallel reactions for each RNA sample were run in the absence of MultiScribe Reverse Transcriptase to assess lack of genomic DNA contamination. TaqMan RT-qPCR assays were performed in duplicate for each gene on cDNA samples in 384-well optical plates using an ABI Prism 7900 Sequence Detection system (Applied Biosystems, Life Technologies, Waltham, MA, USA). For each 10 µL TaqMan reaction, 4.5 µL cDNA was mixed with 0.5 µL 20× TaqMan Gene Expression Assays and 5 µL of 2× TaqMan Universal PCR Master Mix (Applied Biosystems). The identification numbers and names of TaqMan probes are shown in **Table 2**. Probes were selected on the basis of our previous observations of inflammatory changes in the spinal cord and frontal cortex in sALS (7) together with additional markers linked to extravasation mechanisms and extracellular matrix remodeling. Mean values of two house-keeping genes, glucuronidase beta (*GUS-β*) (30) and glyceraldehyde 3-phosphate dehydrogenase (*GAPDH*) (31), were used as internal controls for normalization. The reactions were carried out using the following parameters: 50°C for 2 min, 95°C for 10 min, and 40 cycles at 95°C for 15 s, and at 60°C for 1 min. Finally, all TaqMan PCR data were captured using the Sequence Detection Software (SDS version 2.2.2, Applied Biosystems). Samples were analyzed with the double-delta cycle threshold (ΔΔCT) method.

Statistical Analysis

The normality of distribution of fold change values was analyzed with the Kolmogorov–Smirnov test. The non-parametric Mann–Whitney test was performed to compare each group when values did not follow a normal distribution, whereas the unpaired *t*-test was used for normal variables. Statistical analysis and graphic design were performed with GraphPad Prism version 5.01 (La Jolla, CA, USA). Results were analyzed with Student's *t*-test. Outliers were detected using the GraphPad software QuickCalcs ($p < 0.05$). The data were expressed as mean ± SEM and significance levels were set at $^*p < 0.05$ and $^{**}p < 0.01$ and $^{***}p < 0.001$, and tendencies at $^{\circ}<0.1$. Pearson's correlation coefficient was used to assess a possible linear association between two continuous quantitative variables.

RESULTS

General Clinical and Hematological Findings

Amyotrophic lateral sclerosis progression was heterogeneous in the present series. Hemogram was not altered in sALS patients with the exception of a few cases in whom slight increase of neutrophils and low levels of lymphocytes was observed. CK levels were out of range in some patients and moderately increased in a few sALS cases. Clinical, hematological, and biochemical data are summarized in **Table 3**.

Gene Expression Levels

Anti-inflammatory Cytokines

IL10, coding for interleukin 10, and *TGFB2*, coding for transforming growth factor beta 1, mRNA levels were significantly reduced in sALS, whereas *IL10RA* which codes for interleukin

TABLE 2 | Genes, gene symbols, and references in the present series.

Gene	Gene symbol	Reference
Catalase	*CAT*	Hs00156308_m1
Cathepsin C	*CTSC*	Hs00175188_m1
Cathepsin S	*CTSS*	Hs00356423_m1
CD4 molecule/T-cell surface glycoprotein CD4	*CD4*	Hs01058407_m1
CD44 molecule	*CD44*	Hs01075861_m1
CD8a molecule/T-cell surface glycoprotein CD8a Chain	*CD8A*	Hs00233520_m1
Chemokine (C–C motif) ligand 5	*CCL5*	Hs00982282_m1
Chemokine (C–C motif) receptor 5	*CCR5*	Hs00152917_m1
Chemokine (C–X–C motif) receptor 5	*CXCR5*	Hs00173527_m1
Colony stimulating factor 1 receptor	*CSF1R*	Hs00911250_m1
Colony stimulating factor 3 receptor (granulocyte)	*CSF3R*	Hs00167918_m1
C-type lectin domain family 7 member A	*CLEC7A*	Hs01124746_m1
C–X–C motif chemokine ligand 8	*CXC8*	Hs00174103_m1
Glyceraldehyde-3-phosphate dehydrogenase	*GAPDH*	Hs02786624_g1
Inositol polyphosphate-5-phosphatase D	*INPP5D*	Hs00183290_m1
Integrin subunit beta 2	*ITGB2*	Hs00164957_m1
Integrin subunit beta 4	*ITGB4*	Hs00173995_m1
Intercellular adhesion molecule 1	*ICAM-1*	Hs00164932_m1
Intercellular adhesion molecule 5	*ICAM-5*	Hs00170285_m1
Interferon, gamma	*INFG*	Hs00989291_m1
Interleukin 1 beta	*IL1B*	Hs01555410_m1
Interleukin 10	*Il 10*	Hs00961622_m1
Interleukin 10 receptor subunit alpha	*IL10RA*	Hs00155485_m1
Interleukin 10 receptor subunit beta	*IL10RB*	Hs00988697_m1
Interleukin 6	*IL6*	Hs00985639_m1
Interleukin 6 signal transducer	*IL6ST*	Hs00174360_m1
LFA-3 receptor	*CD2*	Hs00233515_m1
Lymphocyte function-associated antigen 1	*LFA-1*	Hs00158218_m1
Macrophage inflammatory protein 1-alpha	*CCL3*	Hs00234142_m1
Membrane-associated ring finger (C3HC4) 9	*MARCH9*	Hs04189729_m1
Monocyte chemotactic and activating factor	*CCL2*	Hs00234140_m1
Metallopeptidase-9	*MMP9*	Hs00234579_m1
Osteopontin	*SPP1*	Hs00959010_m1
Programmed cell death 1 ligand 2	*PD1L2*	Hs01057777_m1
Selectin L	*SELL*	Hs00174151_m1
Superoxide dismutase 1, soluble	*SOD1*	Hs00533490_m1
Superoxide dismutase 2, mitochondrial	*SOD2*	Hs00167309_m1
T cell receptor beta constant 1	*TRBC1*	Hs01588269_g1
TIMP metallopeptidase inhibitor 1	*TIMP-1*	Hs00171558_m1
TIMP metallopeptidase inhibitor 2	*TIMP-2*	Hs01091317_m1
Toll-like receptor 2	*TLR2*	Hs00610101_m1
Toll like receptor 3	*TLR3*	Hs01551078_m1
Toll-like receptor 4	*TLR4*	Hs01060206_m1
Toll-like receptor 7	*TLR7*	Hs00152971_m1
Tumor growth factor B1	*TGFB1*	Hs00998133_m1
Tumor growth factor B2	*TGFB2*	Hs00234244_m1
Tumor necrosis factor receptor superfamily member 1A	*TNFRSF1*	Hs01042313_m1
Tumor necrosis factor-alpha	*TNFA*	Hs01113624_g1
Vascular endothelial growth factor A	*VEGFA*	Hs00900055_m1
β-Glucuronidase	*GUS-β*	Hs00939627_m1

10 receptor subunit alpha showed a tendency to decrease. Expression levels of *IL10RB* and *TGFB1* encoding interleukin 10 receptor subunit beta and transforming growth factor beta 1, respectively, were not modified (**Figure 1A**).

Chemokines

Expression levels of *CCL5* and *CXC5R*, which code for C-C motif chemokine ligand 5 and C-X-C motif chemokine receptor 5, respectively, were significantly decreased; *CCR5* coding for C-C motif chemokine receptor 5 showed a tendency to decrease. No modifications were seen for C-C motif chemokine ligand 2 (*CCL2*) and 3 (*CCL3*), and C-X-C motif chemokine 8 (*CXC8*) (**Figure 1B**).

Cytokine Modulators

Toll like receptors *TLR2* and *TLR4* mRNA expression showed a tendency to increase, whereas *TLR3* mRNA expression was significantly decreased in sALS. *TLR7* and other genes involved in cytokine modulation such as C-type lectin domain family 7 member A (*CLEC7A*), colony stimulating factor 1 receptor (*CSF1R*), and colony stimulating factor 3 receptor (*CSF3R*) were not altered (**Figure 1C**).

Extracellular Matrix Remodeling

MMP9, coding for matrix metallopeptidase 9, and *TIMP2*, coding for its inhibitor protein, TIMP metallopeptidase inhibitor 2, were significantly increased in sALS. The expression levels of *CTSC*, *CTSS*, *TIMP1*, and *SPP1*, coding for cathepsin C, cathepsin S, TIMP metallopeptidase inhibitor 1, and osteopontin, respectively, were similar in sALS and controls (**Figure 1D**).

Extravasation Mechanisms

ITGB2, coding for integrin subunit beta 2, and *INPP5D*, coding for inositol polyphosphate-5-phosphatase D, were upregulated in sALS. Tendency to increase was found for *SELL* and *ICAM1*, coding for selectin-L and intercellular adhesion molecule 1, respectively. No changes were detected in the expression of *ICAM5*, *ITGB4*, *LFA1*, and *MARCH9* encoding, respectively, intercellular adhesion molecule 5, integrin subunit beta 4, lymphocyte function-associated antigen 1, and membrane associated ring-CH-type finger 9 (**Figure 1E**).

Oxidative Stress Markers

Expression of catalase (*CAT*) and superoxide dismutase 1 (*SOD1*) genes was not modified. Superoxide dismutase 2 (*SOD2*) showed a tendency to increase in sALS (**Figure 1F**).

Pro-inflammatory Cytokines

IL6, coding for interleukin-6, was significantly downregulated in sALS cases. TNF-α coding gene *TNFA* showed a tendency to decrease. In contrast, *TNFR1S*, the gene coding for its receptor, was significantly increased. No alterations were found in the remaining assessed genes *IL1B*, *IL6ST*, *INFG*, *PD1L2*, and *VEGFA*, coding for interleukin 1B, interleukin 6 signal transducer, interferon gamma, programmed cell death 1 ligand 2, and vascular endothelial growth factor A, respectively (**Figure 1G**).

T Cell Markers

Expression of *CD2*, coding for CD2 molecule; *CD8A*, coding for T-Cell Surface Glycoprotein CD8 Alpha Chain; and *TRBC1*, coding for T-cell receptor beta constant 1, was significantly decreased in sALS cases. The expression of *CD44* and T-cell surface glycoprotein CD4 gene (*CD4*) was not modified (**Figure 1H**).

TABLE 3 | Biochemical alterations in blood samples of sporadic amyotrophic lateral sclerosis (sALS) cases.

sALS case	Clinical progression	Creatinine kinase (CK) (μkat/L)	Leukocyte populations (×10E9cells/L)				
			Neutrophil (1.5–5.7)	Lymphocyte (1.3–3.4)	Monocyte (0.31–0.92)	Eosinophil (0.03–0.39)	Basophil (0.01–0.09)
14	Expected	13.9[a] (≤4.50)	3.7	1.4	0.48	0.02[b]	0.02
15	Expected	5.5[a] (≤4.50)	3.4	2.1	0.46	0.21	0.04
16	Expected	3.5[a] (≤2.30)	6.9[a]	0.8[b]	0.37	0.04	0.04
17	Fast	5.0[a] (≤2.30)	4.2	1.0[b]	0.34	0.1	0.05
18	Fast	3.5 (≤4.50)	N/A	N/A	N/A	N/A	N/A
19	Slow	0.8 (≤4.50)	4.3	1.2	0.44	0.16	0.04
20	Fast	4.6[a] (≤4.50)	N/A	N/A	N/A	N/A	N/A
21	Expected	5.9[a] (≤4.50)	3.3	1.0[b]	0.30[b]	0.15	0.04
22	Expected	2.2 (≤4.50)	3.9	2.5	0.56	0.34	0.01
23	Expected	2.6 (≤4.50)	7.8[a]	1.0[b]	0.6	0.01[b]	0.03
24	Expected	2.8 (≤4.50)	6.6[b]	1.8	0.6	0.15	0.06
25	Fast	0.7 (≤4.50)	5.6	1.4	0.87	0.39	0.09
26	Fast	N/A	3.6	1.6	0.49	0.11	0.02
27	Expected	8.3[a] (≤4.50)	7.0[a]	1.7	0.53	0.11	0.07
28	Fast	1.8 (≤4.50)	4.2	3.1	0.76	0.28	0.04
29	Fast	N/A	6.0[a]	0.9[b]	0.74	0.08	0.03
30	Fast	3.0 (≤4.50)	4.3	1.4	0.77	0.04	0.04
31	Fast	2.1 (≤4.50)	4.2	2.1	0.63	0.19	0.08
32	Fast	N/A	N/A	N/A	N/A	N/A	N/A
33	Slow	2.0 (≤4.50)	3.8	2.5	0.44	0.55	0.06
34	Slow	3.5 (≤4.50)	3.5	1.8	0.38	0.19	0.06
35	Fast	11.6[a] (≤4.50)	N/A	N/A	N/A	N/A	N/A

N/A, data not available; μkat/L, microkatals/litor.

Normal CK levels in brackets (these are variable depending on the method used; CK values in every ALS case are evaluated according to the method used).

[a]*Above normal range.*

[b]*Below normal range.*

Correlation between Clinical Parameters and Gene Transcription

Gender, ALS form of onset (spinal, bulbar, and respiratory), clinical progression, leukocyte counts and leukocyte types, and RIN values did not correlate with modifications in gene expression. However, *MMP9* levels in sALS cases positively correlated with age ($p = 0.046$) (**Figure 2A**). *CCR5* ($p = 0.0307$), *CCL5* ($p = 0.016$), and *TRBC1* ($p = 0.0076$) negatively correlated with age (**Figure 2A**) in sALS. These changes were not observed in the control group. Importantly, patients with sALS showed significant relation between elevated levels of *TNFA* gene and creatinine kinase (CK) values, which were out of the normal range ($p = 0.025$) (**Figure 2B**).

DISCUSSION

Peripheral inflammatory responses are common, but poorly defined, in human neurodegenerative diseases. Several studies focus on inflammatory responses in spinal cord and blood in sALS (1–11). The present study was geared to gain information about inflammatory gene expression profiles in the whole blood in a series of sALS patients at the beginning of clinical symptoms and non-treated with riluzole in order to avoid bias related to the treatment.

Present observations complement data from previous studies and point to the activation of mechanisms facilitating extravasation of WBC to target organs.

Neutrophil recruitment is supported by leukocyte adhesion molecules, chemokines, and cytokines (32, 33). Increased expression of *ITGB2* and a tendency of *ICAM1* to increase in blood suggest that adhesion and trans-endothelial migration of leukocytes is facilitated in sALS (34–36). Selectin 1, encoded by *SELL*, participates in leukocyte binding to endothelial cells and facilitates migration of WBC (37, 38); *SELL* expression has a tendency to increase in sALS. Increased expression of *MMP9* favors degradation of extracellular matrix components and facilitation of leukocyte migration (39). MMP9 is usually secreted in conjunction with TIMP-1, a specific inhibitor, which controls its proteolytic activity (40). A balance between MMP9 and TIMP-1 proteins regulates excessive tissue degradation in chronic inflammation (41). However, mRNA expression levels of cathepsins, also involved in extracellular matrix degradation (42), are not modified in blood of ALS cases when compared with blood samples from controls.

Expression levels of *CCL2* and *CCL3* v, the products of which modulate monocyte attraction (43, 44) are not modified in sALS. Moreover, reduced expression of *CCR5*, *CCL5*, and *CXCR5* supports reduced activation of B-cells (45).

The product of *CD2* expressed in T-cells modulates T-cell proliferation (46), whereas the product of *TRBC1* is implicated in T-cell activation (47). *CCL5* and *CCR5* encode T-cell chemoattractant and regulatory molecules (48, 49). Reduced mRNA expression of these markers suggests inhibition of T-cell signaling.

Finally, increased *INPP5D* mRNA expression favors a negative regulation of myeloid cell proliferation (50).

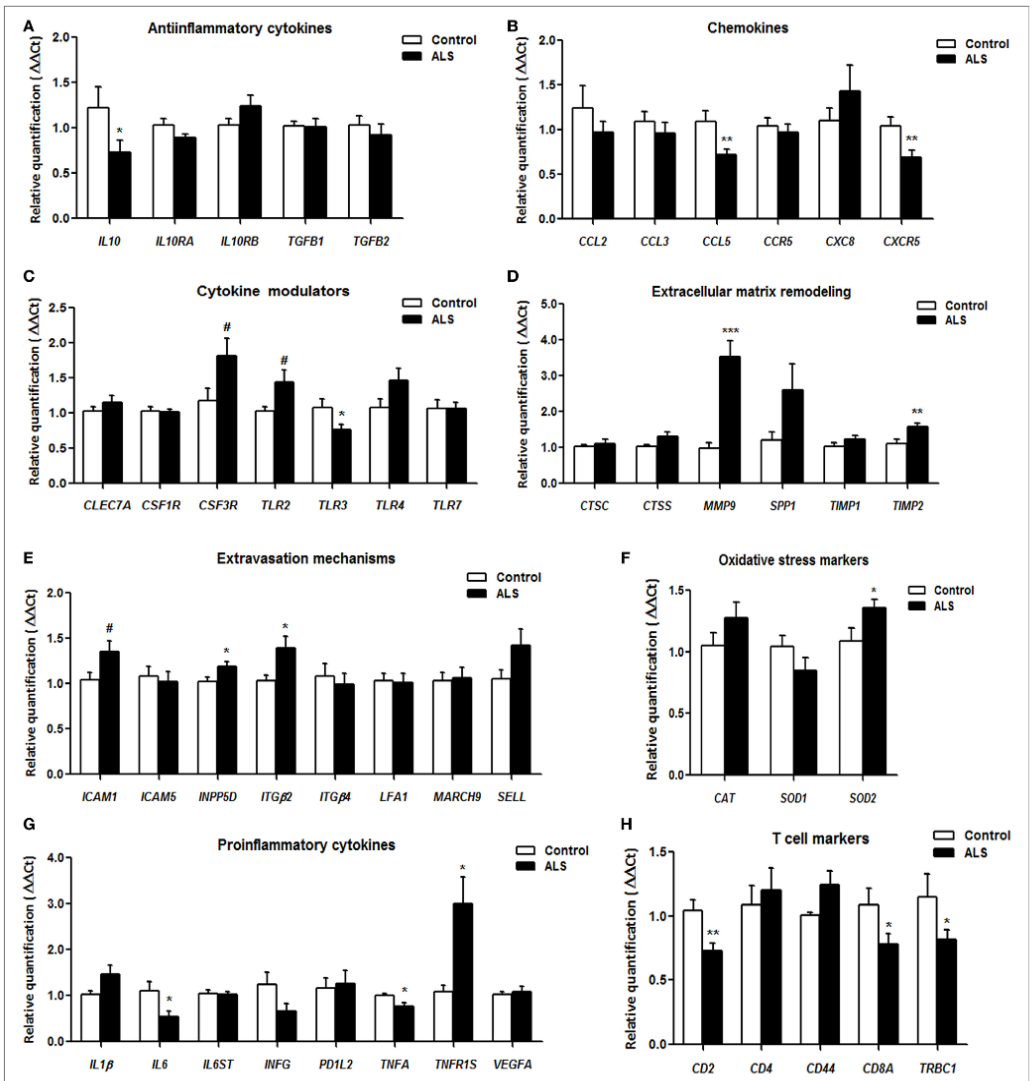

FIGURE 1 | Gene expression of anti-inflammatory cytokines **(A)**, chemokines **(B)**, cytokine modulators **(C)**, extracellular matrix remodeling-related factors **(D)**, molecules involved in extravasation mechanisms **(E)**, oxidative stress markers **(F)**, pro-inflammatory cytokines **(G)**, and T-cell markers **(H)**, as revealed by RT-qPCR, in blood from control and sporadic amyotrophic lateral sclerosis (sALS) cases. All data were expressed as the mean ± SEM. Statistical comparisons were performed using unpaired *t*-test; significance level was set at $^{*}p < 0.05$, $^{**}p < 0.01$ and $^{***}p < 0.001$, and tendencies at $^{\dagger}<0.1$. A total of 13 healthy samples and 22 sALS samples were included in RT-qPCR analysis.

Toll-like receptors are involved in the initiation of the inflammatory process (51). Reduced levels of *TLR3* accompanied by tendency to increased *TLR4* and *TLR2* mRNA expression point to ambiguous activation signaling by Toll-like receptors.

TGFB2, *IL10*, and *IL6* mRNAs are downregulated, and *IL10RA* and *TNFA* have tendency to decrease in blood in sALS when compared with controls. Expression levels of *IL10RB*, *TGFB1*, *IL1β*, *IL6ST*, *INFG* (coding for interferon γ), and *VEGFA* are not

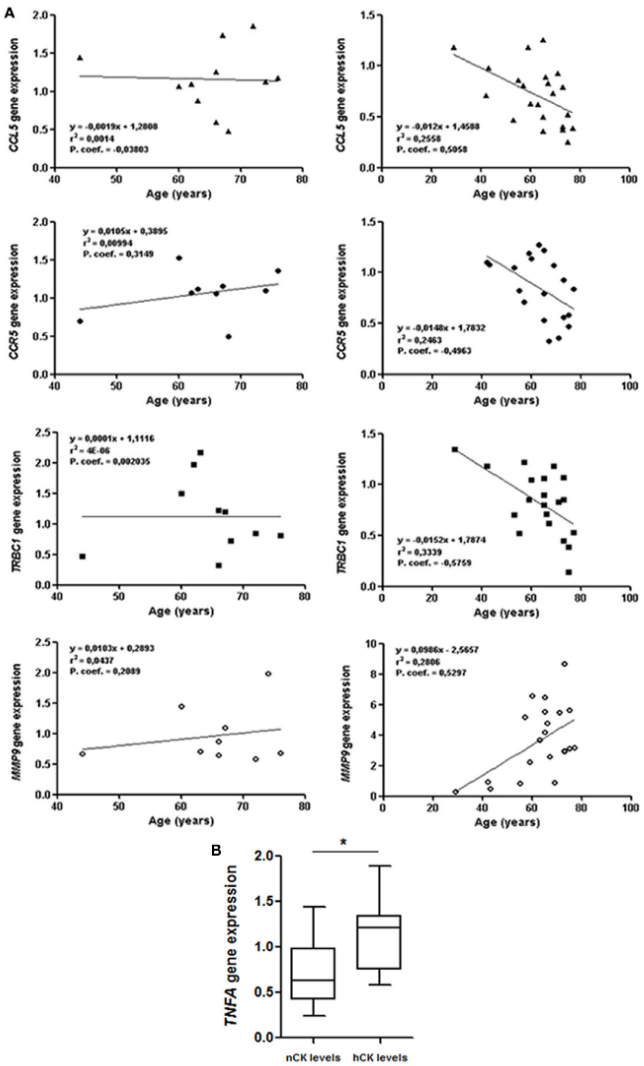

FIGURE 2 | (A) Positive correlation between *MMP9* and age at sampling, and negative correlation between age at sampling and *CCL5*, *CCR5*, and *TRBC1* in sporadic amyotrophic lateral sclerosis (sALS) (right graphs), but not in control cases (left graphs). **(B)** Relation between *TNFA* mRNA expression levels in blood and creatine kinase (CK) protein levels in serum in sALS (nCK, normal CK levels; hCK, high/out of range CK levels) using Student's *t*-test. Gene expression values correspond to fold change values of ΔΔCT.

modified in sALS. Expression levels of assessed colony-stimulating receptors and *CSF3R* do not differ from control values. Even considering the increased expression of *TNFR1S* mRNA, the final scenario is downregulation of pro- and anti-inflammatory cytokines in sALS.

SOD1 transgenic mice lacking functional CD4+ T cells show increased motor neuron damage which is reversed following bone marrow transplants thus suggesting a neuroprotective role of CD4+ T cells (52). On the other hand, SOD1 transgenic mice with additional depletion of the Rag2 gene (mSOD1/

RAG2−/− mice) show delayed motor neuron disease, thus suggesting that mature lymphocytes produce deleterious effects on vulnerable motor neurons (53).

Previous studies have shown a higher percentage of IL-13-positive CD4 and CD8 lymphocytes (8), increased numbers of peripheral CD8 cytotoxic T-cells and natural killer cells, together with decreased regulatory T (treg) lymphocytes (10) in ALS. Our observations show decreased expression of *CD2*, coding for CD2 molecule, *TRBC1*, coding for T-cell receptor beta constant 1 and *CD8* mRNA, and preserved *CD4* mRNA expression. Therefore, additional studies are necessary to elucidate these discrepancies in larger series.

The present findings show a complex scenario at early clinical stages of sALS, including on the one hand upregulation of genes whose products are involved in leukocyte extravasation and extracellular matrix remodeling, and on the other, downregulation of chemokines, anti- and pro-inflammatory cytokines, and lymphocyte modulators.

Positive correlation between *MMP9* and age, and negative correlation between age and *CCL5*, *CCR5*, and *TRBC1* has been observed in sALS but not in controls. No correlation has been found between present observations and first clinical manifestation, gender, and disease progression. Therefore, the present findings have little prognosis value.

There is only positive correlation between *TNFA* mRNA expression and CK levels. Although *TNFA* mRNA expression is lower in ALS when compared with controls, higher *TNFA* mRNA values correlate with higher CK protein levels. This observation points to the possibility of a link between *TNFA* and muscular damage in sALS. Previous studies have shown that muscular pathology is accompanied by increased expression of systemic inflammatory markers (17). Moreover, increased expression of inflammatory markers, including IL-1β and TNF-α, is found in the skeletal muscle at symptomatic and end-stages of SOD1(G93A) transgenic mice (18). However, these individual data are not sufficient to advance any definitive conclusion.

Transcriptome studies at early clinical stages in SOD1(G93A) transgenic mice have shown deregulated pathways common to spinal cord, muscle and sciatic nerve; two pathways are associated with T cell activation, two with macrophage activation, and one pathway contains genes involved in co-stimulatory regulation of the adaptive and innate immune systems; but blood did not show representation of these altered pathways (54). However, genetic ablation of IP3 receptor 2, which modulates inflammation and which expression is augmented in the spinal cord in ALS and related mice models, increases cytokines and decreases survival of SOD1G93A mice (55). These studies point to involvement of peripheral blood cells in the inflammatory response in the spinal cord in ALS. Present observations show systemic inflammatory responses linked to extravasation of leukocytes and remodeling of extracellular matrix at early stages of sALS. However, the observed changes do not indicate the primary or secondary origin, and the precise link between intrinsic and peripheral inflammatory responses in the pathogenesis of sALS.

ETHICS STATEMENT

Blood samples from sALS cases and age-matched controls were obtained following signed informed consent and approval by Clinical Research Ethics Committee (CEIC) of the Bellvitge University Hospital.

AUTHOR CONTRIBUTIONS

All the authors designed, supervised the study, and wrote the final version of the manuscript.

ACKNOWLEDGMENTS

We wish to thank T. Yohannan for editorial help.

FUNDING

This study was supported by grants from CIBERNED and Instituto de Salud Carlos III, and co-funded by FEDER funds/European Regional Development Fund (ERDF)—a way to build Europe; ALS intra-CIBERNED project to IF and IFI15/00035 fellowship to PA-B.

REFERENCES

1. Graves MC, Fiala M, Dinglasan LA, Liu NQ, Sayre J, Chiappelli F, et al. Inflammation in amyotrophic lateral sclerosis spinal cord and brain is mediated by activated macrophages, mast cells and T cells. *Amyotroph Lateral Scler Other Motor Neuron Disord* (2004) 5:213–9. doi:10.1080/14660820410020286
2. Henkel JS, Engelhardt JI, Siklós L, Simpson EP, Kim SH, Pan T, et al. Presence of dendritic cells, MCP-1, and activated microglia/macrophages in amyotrophic lateral sclerosis spinal cord tissue. *Ann Neurol* (2004) 55:221–35. doi:10.1002/ana.10805
3. Johann S, Heitzer M, Kanagaratnam M, Goswami A, Rizo T, Weis J, et al. NLRP3 inflammasome is expressed by astrocytes in the SOD1 mouse model of ALS and in human sporadic ALS patients. *Glia* (2015) 63:2260–73. doi:10.1002/glia.22891
4. Casula M, Iyer AM, Spliet WG, Anink JJ, Steentjes K, Sta M, et al. Toll-like receptor signaling in amyotrophic lateral sclerosis spinal cord tissue. *Neuroscience* (2011) 179:233–43. doi:10.1016/j.neuroscience.2011.02.001
5. Sta M, Sylva-Steenland RM, Casula M, de Jong JM, Troost D, Aronica E, et al. Innate and adaptive immunity in amyotrophic lateral sclerosis: evidence of complement activation. *Neurobiol Dis* (2011) 42:211–20. doi:10.1016/j.nbd.2011.01.002
6. Puentes F, Malaspina A, Van Noort JM, Amor S. Non-neuronal cells in ALS: role of glial, immune cells and blood-CNS barriers. *Brain Pathol* (2016) 26:248–57. doi:10.1111/bpa.12352
7. Andrés-Benito P, Moreno J, Aso E, Povedano M, Ferrer I. Amyotrophic lateral sclerosis, gene deregulation in the anterior horn of the spinal cord and frontal cortex area 8: implications in frontotemporal lobar degeneration. *Aging (Albany NY)* (2017) 9(3):823–51. doi:10.18632/aging.101195
8. Shi N, Kawano Y, Tateishi T, Kikuchi H, Osoegawa M, Ohyagi Y, et al. Increased IL-13-producing T cells in ALS: positive correlations with disease severity and progression rate. *J Neuroimmunol* (2007) 182:232–5. doi:10.1016/j.jneuroim.2006.10.001
9. Rentzos M, Evangelopoulos ME, Sereti E, Zouvelou V, Marmara S, Alexakis T, et al. Humoral immune activation in amyotrophic lateral sclerosis patients. *Neurol Int* (2013) 5:e3. doi:10.4081/ni.2013.e3
10. Rentzos M, Evangelopoulos E, Sereti E, Zouvelou V, Marmara S, Alexakis T, et al. Alterations of T cell subsets in ALS: a systemic immune

activation? *Acta Neurol Scand* (2012) 125:260–4. doi:10.1111/j.1600-0404.2011.01528.x

11. Henkel JS, Beers DR, Wen S, Rivera AL, Toennis KM, Appel JE, et al. Regulatory T-lymphocytes mediate amyotrophic lateral sclerosis progression and survival. *EMBO Mol Med* (2013) 5:64–79. doi:10.1002/emmm.201201544
12. Piccione EA, Sletten DM, Staff NP, Low PA. Autonomic system and amyotrophic lateral sclerosis. *Muscle Nerve* (2015) 51:676–9. doi:10.1002/mus.24457
13. Tian F, Yang W, Mordes DA, Wang JY, Salameh JS, Mok J, et al. Monitoring peripheral nerve degeneration in ALS by label-free stimulated Raman scattering imaging. *Nat Commun* (2016) 7:13283. doi:10.1038/ncomms13283
14. Schreiber S, Dannhardt-Stieger V, Henkel D, Debska-Vielhaber G, Machts J, Abdulla S, et al. Quantifying disease progression in amyotrophic lateral sclerosis using peripheral nerve sonography. *Muscle Nerve* (2016) 54:391–7. doi:10.1002/mus.25066
15. Vucic S. Sensory and autonomic nervous system dysfunction in amyotrophic lateral sclerosis. *Neuropathol Appl Neurobiol* (2017) 43(2):99 101. doi:10.1111/nan.12336
16. Nolano M, Provitera V, Manganelli F, Iodice R, Caporaso G, Stancanelli A, et al. Non-motor involvement in amyotrophic lateral sclerosis: new insight from nerve and vessel analysis in skin biopsy. *Neuropathol Appl Neurobiol* (2016) 43(2):119–32. doi:10.1111/nan.12332
17. Lu CH, Allen K, Oei F, Leoni E, Kuhle J, Tree T, et al. Systemic inflammatory response and neuromuscular involvement in amyotrophic lateral sclerosis. *Neurol Neuroimmunol Neuroinflamm* (2016) 3:e244. doi:10.1212/NXI.0000000000000244
18. Van Dyke JM, Smit-Oistad IM, Macrander C, Krakora D, Meyer MG, Suzuki M. Macrophage-mediated inflammation and glial response in the skeletal muscle of a rat model of familial amyotrophic lateral sclerosis (ALS). *Exp Neurol* (2016) 277:275–82. doi:10.1016/j.expneurol.2016.01.008
19. Fang X. Potential role of gut microbiota and tissue barriers in Parkinson's disease and amyotrophic lateral sclerosis. *Int J Neurosci* (2016) 126:771–6. doi:10.3109/00207454.2015.1096271
20. Zhang YG, Wu S, Yi J, Xia Y, Jin D, Zhou J, et al. Target intestinal microbiota to alleviate disease progression in amyotrophic lateral sclerosis. *Clin Ther* (2017) 39:322–36. doi:10.1016/j.clinthera.2016.12.014
21. Zhang R, Gascon R, Miller RG, Gelinas DF, Mass J, Lancero M, et al. MCP-1 chemokine receptor CCR2 is decreased on circulating monocytes in sporadic amyotrophic lateral sclerosis (sALS). *J Neuroimmunol* (2006) 179(1–2):87–93. doi:10.1016/j.jneuroim.2006.06.008
22. Mantovani S, Garbelli S, Pasini A, Alimonti D, Perotti C, Melazzini M, et al. Immune system alterations in sporadic amyotrophic lateral sclerosis patients suggest an ongoing neuroinflammatory process. *J Neuroimmunol* (2009) 210(1–2):73–9. doi:10.1016/j.jneuroim.2009.02.012
23. Zhao W, Beers DR, Hooten KG, Sieglaff DH, Zhang A, Kalyana-Sundaram S, et al. Characterization of gene expression phenotype in amyotrophic lateral sclerosis monocytes. *JAMA Neurol* (2017) 74(6):677–85. doi:10.1001/jamaneurol.2017.0357
24. Ikeda J, Kohriyama T, Nakamura S. Elevation of serum soluble E-selectin and antisulfoglucuronyl paragloboside antibodies in amyotrophic lateral sclerosis. *Eur J Neurol* (2000) 7(5):541–7. doi:10.1046/j.1468-1331.2000.t01-1-00114.x
25. Babu GN, Kumar A, Chandra R, Puri SK, Kalita J, Misra UK. Elevated inflammatory markers in a group of amyotrophic lateral sclerosis patients from northern India. *Neurochem Res* (2008) 33(6):1145–9. doi:10.1007/s11064-007-9564-x
26. Cereda C, Baiocchi C, Bongioanni P, Cova E, Guareschi S, Metelli MR, et al. TNF and sTNFR1/2 plasma levels in ALS patients. *J Neuroimmunol* (2008) 194(1):123–31. doi:10.1016/j.jneuroim.2007.10.028
27. Waller R, Goodall EF, Milo M, Cooper-Knock J, Da Costa M, Hobson E, et al. Serum miRNAs miR-206, 143-3p and 374b-5p as potential biomarkers for amyotrophic lateral sclerosis (ALS). *Neurobiol Aging* (2017) 55:123–31. doi:10.1016/j.neurobiolaging.2017.03.027
28. Hørder M, Elser RC, Gerhardt W, Mathieu M, Sampson EJ. Approved recommendation of IFCC methods for the measurement of catalytic concentration of enzymes, part 7 IFCC method for creatine kinase. *Eur J Clin Chem Clin Biochem* (1991) 29:435.
29. Young DS, Friedman RB. *Effects of Disease on Clinical Laboratory Tests*. 4th ed. Washington, DC: AACC Press (2001).
30. Zampieri M, Ciccarone F, Guastafierro T, Bacalini MG, Calabrese R, Moreno-Villanueva M, et al. Validation of suitable internal control genes for expression studies in aging. *Mech Ageing Dev* (2010) 131:89–95. doi:10.1016/j.mad.2009.12.005
31. Bayatti N, Cooper-Knock J, Bury JJ, Wyles M, Heath PR, Kirby J, et al. Comparison of blood RNA extraction methods used for gene expression profiling in amyotrophic lateral sclerosis. *PLoS One* (2014) 9:e87508. doi:10.1371/journal.pone.0087508
32. Ley K. Integration of inflammatory signals by rolling neutrophils. *Immunol Rev* (2002) 186:8–18. doi:10.1034/j.1600-065X.2002.18602.x
33. Nathan C. Neutrophils and immunity: challenges and opportunities. *Nat Rev Immunol* (2006) 6:173–82. doi:10.1038/nri1785
34. Smith CW, Marlin SD, Rothlein R, Toman C, Anderson DC. Cooperative interactions of LFA-1 and MAC-1 with intercellular adhesion molecule-1 in facilitating adherence and transendothelial migration of human neutrophils in vitro. *J Clin Invest* (1989) 83:2008–17. doi:10.1172/JCI114111
35. Lefort CT, Ley K. Neutrophil arrest by LFA-1 activation. *Front Immunol* (2012) 3:157. doi:10.3389/fimmu.2012.00157
36. Hua S. Targeting sites of inflammation: intercellular adhesion molecule-1 as a target for novel inflammatory therapies. *Front Pharmacol* (2013) 4:127. doi:10.3389/fphar.2013.00127
37. Ley K, Laudanna C, Cybulsky MI, Nourshargh S. Getting to the site of inflammation: the leukocyte adhesion cascade updated. *Nat Rev Immunol* (2007) 7:678–89. doi:10.1038/nri2156
38. Marki A, Esko JD, Pries AR, Ley K. Role of the endothelial surface layer in neutrophil recruitment. *J Leukoc Biol* (2015) 98:503–15. doi:10.1189/jlb.3MR0115-011R
39. Vandooren J, Van den Steen PE, Opdenakker G. Biochemistry and molecular biology of gelatinase B or matrix metalloproteinase-9 (MMP-9): the next decade. *Crit Rev Biochem Mol Biol* (2013) 48:222–72. doi:10.3109/10409238.2013.770819
40. Kurzepa J, Madro A, Czechowska G, Kurzepa J, Celiński K, Kazmierak W, et al. Role of MMP-2 and MMP-9 and their natural inhibitors in liver fibrosis, chronic pancreatitis and non-specific inflammatory bowel diseases. *Hepatobiliary Pancreat Dis Int* (2014) 13:570–9. doi:10.1016/S1499-3872(14)60261-7
41. Amalinei C, Caruntu ID, Giuşca SE, Balan RA. Matrix metalloproteinases involvement in pathologic conditions. *Rom J Morphol Embryol* (2010) 51:215–28.
42. Fonović M, Turk B. Cysteine cathepsins and extracellular matrix degradation. *Biochim Biophys Acta* (2014) 1840:2560–70. doi:10.1016/j.bbagen.2014.03.017
43. Paavola CD, Hemmerich S, Grunberger D, Polsky I, Bloom A, Freedman R, et al. Monomeric monocyte chemoattractant protein-1 (MCP-1) binds and activates the MCP-1 receptor CCR2B. *J Biol Chem* (1998) 273:33157–65. doi:10.1074/jbc.273.50.33157
44. Sanadgol N, Golab F, Mostafaie A, Mehdizadeh M, Abdollahi M, Sharifzadeh M, et al. Ellagic acid ameliorates cuprizone-induced acute CNS inflammation via restriction of microgliosis and down-regulation of CCL2 and CCL3 pro-inflammatory chemokines. *Cell Mol Biol* (2016) 62:24–30. doi:10.14715/cmb/2016.62.12.5
45. Le Y, Zhou Y, Iribarren P, Wang J. Chemokines and chemokine receptors: their manifold roles in homeostasis and disease. *Cell Mol Immunol* (2004) 1:95–104.
46. The SO, Killeen N, Tarakhovsky A, Littman DR, The HS. CD2 regulates the positive selection and function of antigen-specific CD4-CD8 T cells. *Blood* (1997) 89:1308–18.
47. MacLean SJ, Gibson DM. Identification of a predominant sequence variant of the T-cell receptor TCRBC1 gene. *Immunogenetics* (1997) 45:223–5. doi:10.1007/s002510050194
48. Siveke JT, Hamann A. T helper 1 and T helper 2 cells respond differentially to chemokines. *J Immunol* (1998) 160:550–4.
49. Rabin RL, Park MK, Liao F, Swofford R, Stephany D, Farber JM. Chemokine receptor responses on T cells are achieved through regulation of both receptor expression and signaling. *J Immunol* (1999) 162:3840–50.

50. Hakim S, Bertucci MC, Conduit SE, Vuong DL, Mitchell CA. Inositol polyphosphate phosphatases in human disease. *Curr Top Microbiol Immunol* (2012) 362:247–314. doi:10.1007/978-94-007-5025-8_12
51. Trinchieri G, Sher A. Cooperation of toll-like receptor signals in innate immune defence. *Nat Rev Immunol* (2007) 7:179–90. doi:10.1038/nri2038
52. Beers DR, Henkel JS, Zhao W, Wang J, Appel SH. CD4+ T cells support glial neuroprotection, slow disease progression, and modify glial morphology in an animal model of inherited ALS. *Proc Natl Acad Sci U S A* (2008) 105:15558–63. doi:10.1073/pnas.0807419105
53. Tada S, Okuno T, Yasui T, Nakatsuji Y, Sugimoto T, Kikutani H, et al. Deleterious effects of lymphocytes at the early stage of neurodegeneration in an animal model of amyotrophic lateral sclerosis. *J Neuroinflammation* (2011) 8:19. doi:10.1186/1742-2094-8-19
54. Lincecum JM, Vieira FG, Wang MZ, Thompson K, De Zutter GS, Kidd J, et al. From transcriptome analysis to therapeutic anti-CD40L treatment in the SOD1 model of amyotrophic lateral sclerosis. *Nat Genet* (2010) 42:392–9. doi:10.1038/ng.557
55. Staats KA, Humblet-Baron S, Bento-Abreu A, Scheveneels W, Nikolaou A, Deckers K, et al. Genetic ablation of IP3 receptor 2 increases cytokines and decreases survival of SOD1G93A mice. *Hum Mol Genet* (2016) 25:3491–9. doi:10.1093/hmg/ddw190

Conflict of Interest Statement: The authors declare that the research was conducted in the absence of any commercial or financial relationships that could be construed as a potential conflict of interest.

Article III

YKL40 in sporadic amyotrophic lateral sclerosis: cerebrospinal fluid levels as a prognosis marker of disease progression

Pol Andrés-Benito, Raúl Domínguez, María José Colomina, Franc Llorens, Mònica Povedano and Isidro Ferrer

Aging (Albany NY) 2018 Sep 13; 10(9): 2367-2382.

www.aging-us.com AGING 2018, Vol. 10, No. 9

Research Paper

YKL40 in sporadic amyotrophic lateral sclerosis: cerebrospinal fluid levels as a prognosis marker of disease progression

Pol Andrés-Benito[1,2,3], Raúl Domínguez[4], Maria J. Colomina[5], Franc Llorens[2,3], Mònica Povedano[4], Isidre Ferrer[1,2,3,6,7]

[1]Department of Pathology and Experimental Therapeutics, University of Barcelona, L'Hospitalet de Llobregat, Barcelona, Spain
[2]Biomedical Network Research Center on Neurodegenerative Diseases (CIBERNED), Institute Carlos III, L'Hospitalet de Llobregat, Barcelona, Spain
[3]Bellvitge Biomedical Research Institute (IDIBELL), L'Hospitalet de Llobregat, Barcelona, Spain
[4]Functional Unit of Amyotrophic Lateral Sclerosis (UFELA), Service of Neurology, Bellvitge University Hospital, L'Hospitalet de Llobregat, Barcelona, Spain
[5]Anesthesia and Critical Care Department, Bellvitge University Hospital - University of Barcelona L'Hospitalet de Llobregat, Barcelona, Spain
[6]Neuropathology, Pathologic Anatomy Service, Bellvitge University Hospital, IDIBELL, L'Hospitalet de Llobregat, Barcelona, Spain
[7]Institute of Neurosciences, University of Barcelona, Barcelona, Spain

Correspondence to: Isidro Ferrer; **email:** 8082ifa@gmail.com
Keywords: amyotrophic lateral sclerosis, chitinase-3-like protein 1, YKL40, spinal cord, frontal cortex area 8, NF-L, cerebrospinal fluid
Received: July 21, 2018 **Accepted:** September 6, 2018 **Published:** September 13, 2018

ABSTRACT

Amyotrophic lateral sclerosis (ALS) has variable clinical course and fatal outcome. Since inflammation plays a role in the pathogenesis of ALS, chitinase-3-like protein 1 or YKL40 has been assessed as putative biomarker of disease progression. YKL40 mRNA levels are increased in anterior horn of the spinal cord (*P*=0.004) in sporadic ALS (sALS) cases when compared with age-matched controls. These correlate with increased mRNA expression of microglial markers *AIF1* and *CD68* in the spinal cord in sALS (*P*=0.044 and *P*=0.000, respectively). YKL40 mRNA and protein expression had a tendency to increase in post-mortem frontal cortex area 8 (*P*=0.06 and *P*=0.08, respectively). Yet YKL40 immunoreactivity is restricted to a subpopulation of astrocytes in these regions. YKL40 protein levels, as revealed by enzyme-linked immunosorbent assay (ELISA), are significantly increased in the CSF in sALS (n=86) compared with age-matched controls (n=21) (*P*=0.045). Higher levels are found in patients with fast progression when compared with patients with slow and normal progression (*P*=0.008 and *P*=0.004, respectively), and correlates with ALS-FRS-R slope (*P*=0.000). Additionally, increased protein levels of neurofilament light chain (NF-L) are also found in sALS (*P*=0.000); highest values are found in patients with fast progression when compared with cases with slow and normal progression (*P*=0.005 and *P*=0.000, respectively), and also correlate with ALS-FRS-R slope (*P*=0.000). Pearson's correlation test linked positively the increased levels of YKL40 with increased NF-L levels (*P*=0.013). These data point to YKL40 and NF-L protein levels in the CSF as a good biomarker combination of disease progression in sALS.

INTRODUCTION

Chitinase-3-like protein 1 (CHI3L1) or YKL40 is a glycoprotein with a molecular weight of about 40 kDa that belongs to the family of chitinase-like proteins. Chitinases break down glycosidic bonds in chitin, a component of the cell wall of fungi and the exoskeleton of arthropods [1-5]. YKL40 and other chitinases are also localized in various tissues in vertebrates but their function is not known; YKL40 shows no chitinase activity. Increased expression levels of certain chitinases, and particularly of YKL40, are linked to inflammation, injury, tissue remodelling and regeneration, angiogenesis, and abnormal cell proliferation in tumours [6, 7]. Focusing on neurologic diseases, increased YKL40 expression levels have been observed in encephalitis, stroke, traumatic brain injury, multiple sclerosis, and glioblastomas [8-17]. YKL40 expression is also increased in the cerebrospinal fluid (CSF) in neurodegenerative diseases such as Alzheimer's disease, frontotemporal dementia, and Creutzfeldt-Jakob disease, but not in Parkinson disease or dementia with Lewy bodies [18-36]. For this reason, determination of YKL40 in the CSF has been postulated as a new biomarker that may guide diagnosis in par-ticular clinical settings. Since YKL40 is mainly expressed in astrocytes with only minor expression, if any, in microglia, increased YKL40 in CSF is inter-preted as a reactive response of astrocytes linked to inflammation and regeneration [33,37-40].

Chitinases have also been assessed in the brain and biological fluids in amyotrophic lateral sclerosis (ALS). Chitotriosidase (CHIT1) activity is increased in blood in ALS cases when compared with controls, and CHIT1 levels are higher in patients with rapid progression [41]. Furthermore, CHIT1 is increased in microglia and macrophages in spinal cord in ALS, and CSF levels correlate with disease severity and progression [42]. YKL40 and chitinase-3-like protein 2 (CHI3L2) mRNA levels are increased in the motor cortex in ALS [43]. Finally, as determined with liquid chromatography/ tandem mass spectrometry, elevated CHIT1, YKL40, and CHI3L2 levels in the CSF correlate with disease progression in ALS [44]. A parallel work presented by another group at the ALS Society Meeting (Amsterdam June 7-8, 2018) reported increased YKL40 in the CSF along the ALS-FTD spectrum [45].

The present study examines YKL40 mRNA and protein expression in brain, YKL40 mRNA levels in blood, and protein levels in the CSF in cases of sporadic ALS (sALS) to learn about the relation between mRNA and protein levels in the central nervous system, and those in CSF and peripheral blood. Based on the previous observations in several diseases, it is worth to have in mind that that YKL40 is not looked as a putative specific biomarker of ALS but as a potential biomarker of prognosis. Therefore, the present study was geared to learn about the use of YKL40 as a possible biomarker of progression in this disease.

RESULTS

Increased *CHI3L1* mRNA expression levels in the anterior horn of the spinal cord and frontal cortex in sALS

Significantly increased expression of *CHI3L1* was found in the anterior horn of the spinal cord (P=0.004) in sALS (Figure 1A). Levels of transcripts coding for the main markers of astrocytes and microglia were also assessed in the anterior horn of the spinal cord. Significantly up-regulated levels of microglial markers *AIF1* and *CD68* were detected in the spinal cord in sALS (P=0.044 and P=0.000, respectively) (Figure 1B), which significantly correlated with *CHI3L1* mRNA expression (P=0.043 and P=0.025, respectively). However, *GFAP* and *ALDH1L1* mRNA levels did not show differences between sALS and control cases (P=0.22 and P=0.77, respectively) (Figure 1B). No correlations were detected with *CHI3L1* expression (P=0.66 and P=0.88, respectively) in the spinal cord region.

CHI3L1 mRNA expression had a tendency to increase in the frontal cortex area 8 in sALS (P=0.06) (Figure 1A). No changes were observed in the mRNA levels of *AIF1* (P=0.32), *CD68* (P=0.89), *GFAP* (P=0.15), and *ALDH1L1* (P=0.15) in sALS (Figure 1B). Finally, no correlations were found between *CHI3L1* mRNA levels, and astrocytic and microglial markers in frontal cortex area 8 of sALS cases.

Protein levels of YKL40 are increased in frontal cortex area 8 in sALS

Western blotting showed a tendency to increase YKL40 and IBA1 protein levels in the anterior horn of the spinal cord of sALS when compared with controls (P=0.08 and P=0.07, respectively). GFAP protein levels were significantly increased, particularly breakdown products (BDP) (P=0.01) in the spinal cord of sALS when compared with controls (Figure 1C). Increased GFAP low molecular weight bands (BDPs) have been previously reported in ALS [46]. In contrast, a significant increase in YKL40 (P=0.03) and GFAP (P=0.02) levels, but not in IBA1 (P=0.62), was found in frontal cortex area 8 in sALS when compared with controls (Figure 1C). YKL40 immunoreactivity was restricted to astrocytes in the frontal cortex and spinal cord in sALS and control cases (Figure 1D).

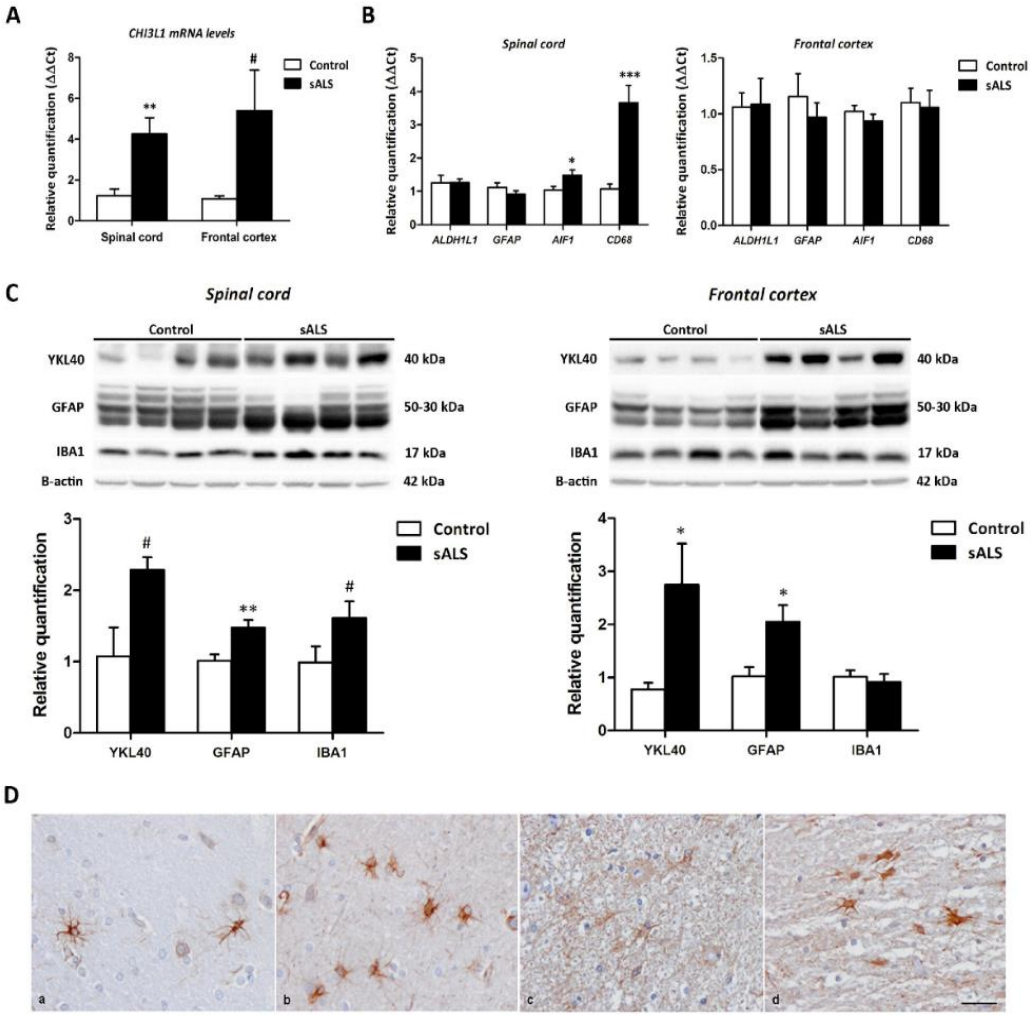

Figure 1. (**A**) *CHI3L1* mRNA expression levels in the anterior horn of the lumbar spinal cord and frontal cortex area 8 in sALS and control cases. *CHI3L1* is significantly up-regulated in the anterior spinal cord but has only a tendency to increase without significance in the frontal cortex in sALS compared with controls. (**B**) mRNA expression levels of microglial (*CD68* and *AIF1*) and astroglial (*GFAP* and *ALDH1L1*) markers in the anterior horn of lumbar spinal cord and frontal cortex area 8 in sALS and age-matched controls. Microglial markers CD68 and AIF1 are significantly up-regulated in the anterior horn of the spinal cord but not in the frontal cortex in sALS. The mRNA expression levels of astroglial markers in the spinal cord and frontal cortex are not modified in pathological cases when compared with controls. (**C**) Western blot analysis of YKL40 in the spinal cord (left panel) and frontal cortex area 8 (right panel) of control and sALS; β-actin was used for normalization. Graphical representation of western blot data; fold changes in the expression of protein are determined relative to the control cases. YKL40 and GFAP protein levels are increased in the spinal cord and frontal cortex in sALS when compared with controls. Due to individual variation, increased values in the anterior horn of the spinal cord showed only a tendency without statistical significance. In contrast, expression levels were not significantly modified in sALS. $^{*}P < 0.05$, $^{**}P < 0.01$, and $^{***}P < 0.001$, tendency #$P<0.1$. (**D**) YKL40 expression in frontal cortex area 8 (a, b) and spinal cord (c, d) in control (a, c) and sALS (b, d) cases) is found in astrocytes; immunohistochemical sections lightly counterstained with haematoxylin, bar = 25μm.

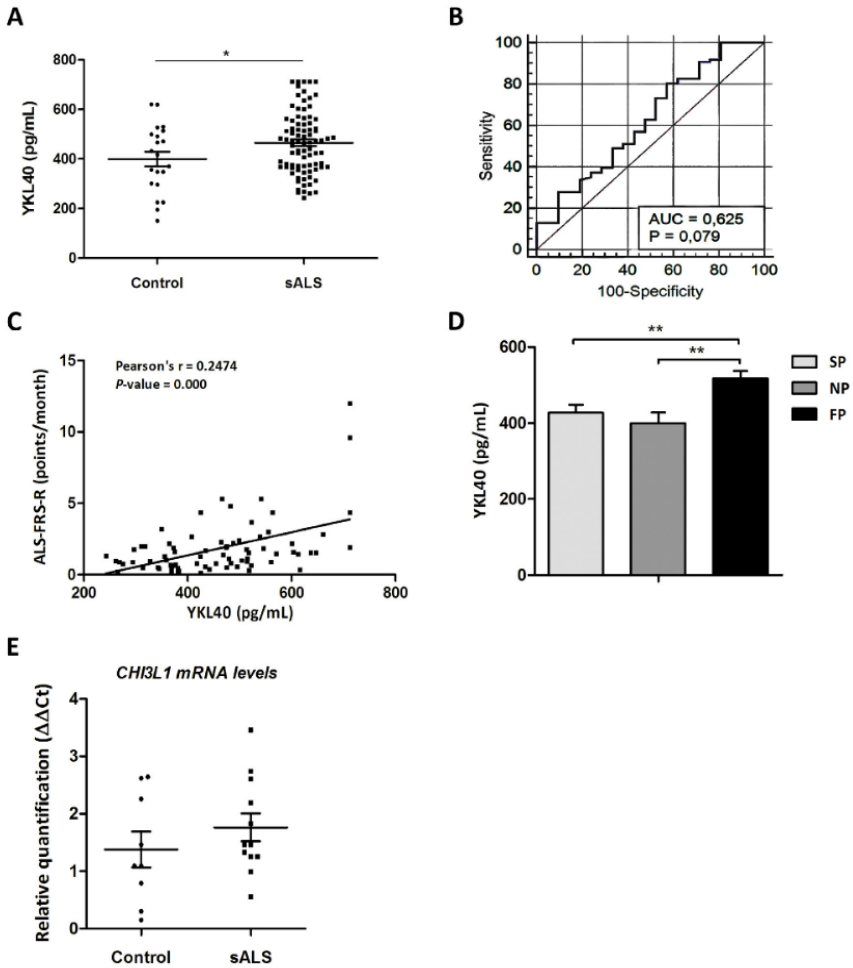

Figure 2. (**A**) Quantification of YKL40 protein levels in the CSF in sALS (n=85) and control (n=23) cases. (**B**) ROC curves for YKL-40 quantification in the differential diagnosis of sALS compared to control cases. In the legend, AUC values, corresponding to the area under ROC curves, and 95% confidence intervals are reported. (**C**) Positive correlation between ALS-FRS-R slope (point/month) and YKL40 levels (pg/mL) (Pearson's correlation, *P*=0.000). (**D**) Higher YKL40 protein levels in the CSF are found in cases with short survival (fast progression: FP) when compared with cases with slow and normal progression (SP and NP, respectively; *P* = 0.008, *P* = 0.004). (**E**) *CHI3L1* mRNA expression levels in whole-blood samples of sALS and control cases. *CHI3L1* is not deregulated in sALS.

Levels of YKL40 are increased in CSF of sALS patients and correlate with ALS-FRS evolution and fast disease progression

Significantly higher YKL40 levels were detected in sALS cases (465.41 ± 13.45 pg/mL) compared with controls (399 ± 29.52 pg/mL) (*P*=0.045) (Figure 2A).

To calculate the clinical accuracy of YKL-40 in discriminating between sALS and the control group, we estimated the AUC value (AUC: 0.6254, 95% CI: 0.52–0.72) (Figure 2B). Considering the optimal cut-off at 356.24pg/mL, defined by the Youden index, an overall sensitivity of 80% and specificity of 43% can be predicted. To demonstrate possible relations between

increased levels of YKL40 and the main clinical parameters, Pearson's correlation or parametric comparisons tests were applied. Clinical parameters such as age, gender, disease onset, disease progression, signs of frontotemporal lobar degeneration, and ALS-FRS-R score were examined. Pearson's correlation indicated a significant link between age and YKL40 levels, increasing with age in controls and sALS (P=0.000). Additionally, Pearson's correlation test demonstrated a positive correlation between ALS-FRS-R slope and YKL40 levels in CSF (P=0.004) (Figure 2C). Based on these observations, YKL40 levels were studied in function of the disease progression in every patient; a significant increase in YKL40 CSF levels was identified in those patients with fast progression when compared with patients with slow and normal progression (P=0.008 and P=0.004, respectively) (Figure 2D). Since at the end of the study only 28 of the 86 sALS cases assessed had died, no attempt was made to analyze the relationship between YKL40 levels in the CSF with survival.

CHI3L1 mRNA levels in blood

Additionally, *CHI3L1* mRNA levels were analyzed in whole peripheral blood samples of sALS at the time of diagnosis. Despite the relatively small number of control and disease cases, individual variations were frequent in the two groups and accounted for the lack of significant changes between control and sALS cases (Figure 2E).

Levels of NF-L are increased in CSF of sALS patients and correlate with ALS-FRS-R slope evolution, fast disease progression and YKL40 levels

Neurofilament light chain (NF-L) levels were quantified in CSF of the same cohort of control and sALS cases. Significant higher NF-L levels were detected in sALS cases (4637.55 ± 192.31pg/mL) compared with controls (610.36 ± 81.11pg/mL) (P=0.000) (Figure 3A). Additionally, NF-L levels were correlated with ALS-FRS-R slope using Pearson's test; positive correlation

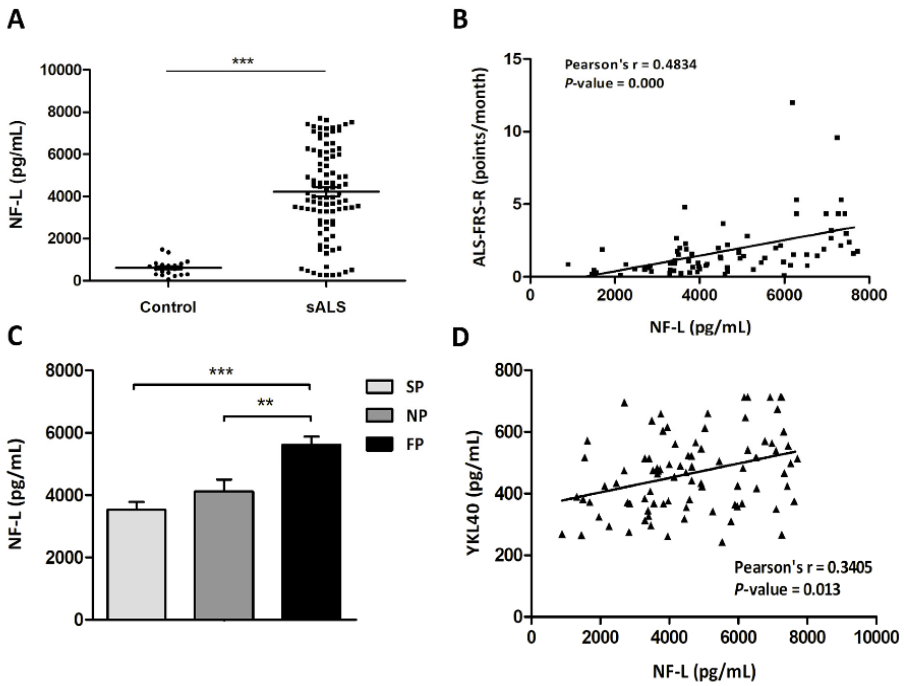

Figure 3. (**A**) Quantification of NF-L protein levels in the CSF in sALS (n=85) and control (n=23) cases. (**B**) Positive correlation between ALS-FRS-R slope (point/month) and NF-L levels (pg/mL) (Pearson's correlation, P=0.000). (**C**) Higher NF-L protein levels in the CSF are found in cases with fast progression (FP) when compared with cases with slow and normal progression (SP and NP, respectively; P = 0.000, P = 0.005). (**D**) Positive correlation between YKL40 levels (pg/mL) and NF-L levels (pg/mL) (Pearson's correlation, P=0.013).

was found between ALS-FRS-R and NF-L levels in CSF (P=0.000) (Figure 2B). NF-L levels were significantly increased in patients with fast progression when compared with patients with slow and normal progression (P=0.000 and P=0.005, respectively) (Figure 2C). Finally, positive significant correlation was observed between YKL40 and NF-L levels (Pearson's correlation test, P=0.013) (Figure 2D).

DISCUSSION

Inflammation involving microglial cells, macrophages, T cells, astrocytes, and neurons, and mediated by a plethora of mediators of the immune response including Toll-like receptors, members of the complement system, pro- and anti-inflammatory cytokines, chemoquines, and blood vessel factors, are activated in the anterior horn of the spinal cord and, to a lesser extent, in other brain regions in ALS [47-59].

Increased protein levels of several cytokines and mediators of the inflammatory response have also been reported in the CSF in ALS, including IL-1, IL-1β, IL-6, IL-8, IL-12, IL-15, IL-17A, IL-18BP, IL-23, RANTES, chemokines, and MCP1 [60-69]. This heterogeneous representation indicates variations depending on the methods and products employed in the different laboratories. Moreover, CSF profiles of angiogenic and inflammatory factors are, at least in part, dependent on the respiratory status of ALS patients [70].

Increased levels of selected inflammatory markers are found in blood and serum in ALS, thus suggesting systemic inflammatory responses which roughly correlate with disease progression [71-80].

All these observations strongly support a role of inflammation in the pathogenesis of sALS. However, the identification of a biomarker of inflammation with practical prognosis value has been limited because of individual variation and variations between methods and laboratories.

Previous studies in ALS have shown YKL40 mRNA up-regulation in the motor cortex [43] and increased YKL40 protein levels in the CSF correlating with disease progression [44, 45]. Regarding brain tissue, the present observations show significant YKL40 mRNA up-regulation in the anterior horn of the spinal cord and frontal cortex area 8, accompanied by significantly increased YKL40 protein levels in the frontal cortex and a tendency to increased YKL40 in the spinal cord in sALS. Importantly, YKL40 is expressed in astrocytes, in agreement with other observations [33, 36-40], but in contrast to another description ascribing YKL40 expression to brain macrophages [44].

Up-regulation and increased YKL40 expression occcurs in parallel with increased values of microglia markers in the spinal cord but not in the frontal cortex area in sALS, and with increased GFAP protein levels in the spinal cord and frontal cortex but not with GFAP mRNA up-regulation in these regions.

Together, these observations point to earlier responses in astrocytes when compared with microglial reactions in the frontal cortex in sALS, whereas microglial markers are strongly expressed in the spinal cord in the same group of patients.

Based on these findings, increased YKL40 protein levels in the CSF mirror YKL40 changes in the central nervous system, and they can be interpreted as the consequence of YKL40 delivery of astrocytes to the CSF. Unfortunately, no analysis of a possible correlation between YKL40 brain and spinal cord values, and disease progression/survival, was feasible in the present series because of the lack of sufficient clinical data. However, YKL40 CSF values negatively correlate with patient survival, thus indicating that higher YKL40 in the CSF likely occurs in patients with rapid disease progression.

We do not know at this time what the functional implications of elevated YKL40 expression in ALS and other neurological diseases are. Nor do we know whether YKL40, even considering this particular chitinase as a marker of astrocyte inflammation, has beneficial or deleterious effects. In this line, *chi3l1* KO mice have increased astrocytic responses (GFAP staining) and increased IBA1 microglial expression when compared with wild-type animals following traumatic brain injury, thus suggesting that YKL40 limits the extent of astroglial and microglial neuroinflammation [38]. If this is the case then increased YKL40 expression *per se* would not be dangerous but rather a manifestation of increased beneficial response in the face of a more aggressive facet of ALS in a subgroup of patients.

The present findings point to the likelihood that increased YKL40 levels in the CSF are not disease specific but they are good biomarker of disease progression in sALS.

Previous studies have shown increased levels of neurofilaments in the CSF of ALS cases [81-84]. NF heavy chain levels in CSF were negatively correlated disease duration and ALS-FRS-R slope, and NF-L levels in CSF were negatively correlated with disease duration. Thus, NF heavy and light chain levels have potential use as markers of neural degeneration in ALS [85, 86]. Increased NF-L in the CSF are not either

specific for the disease, but they are more likely used as measures of disease progression [85, 86].

In the present work, YKL40 levels in the CSF were assessed in parallel with levels of NF light chain. As expected, our results are in line with previous observations by other authors; NF-light chain levels are significantly increased in ALS and levels negatively correlate with disease progression and ALS-FRS-R slope in our series.

In summary, the present findings point that YKL40 and NF-L levels in CSF constitute valuable combination of biomarkers for improving accuracy in the prognosis of patients with sALS.

MATERIALS AND METHODS

Tissue samples

Post-mortem fresh-frozen lumbar spinal cord (SC) and frontal cortex (FC) (Brodmann area 8) tissue samples were obtained from the Institute of Neuropathology HUB-ICO-IDIBELL Biobank following the guidelines of Spanish legislation on this matter and the approval of the local ethics committee. The post-mortem interval between death and tissue processing was between 2h and 17h. One hemisphere was immediately cut in coronal sections, 1-cm thick, and selected areas of the encephalon were rapidly dissected, frozen on metal plates over dry ice, placed in individual air-tight plastic bags, numbered with water-resistant ink, and stored at -80°C until use for biochemical studies. The other hemisphere was fixed by immersion in 4% buffered formalin for 3 weeks for morphologic studies. Transversal sections of the spinal cord were alternatively frozen at -80°C or fixed by immersion in 4% buffered formalin. The anterior horn of the lumbar spinal cord was dissected on a dry-ice frozen plate under a binocular microscope at a magnification x4.

The neuropathological study was carried out on paraffin sections of twenty-six selected regions of the cerebrum, cerebellum, brain stem, and spinal cord which were stained with haematoxylin and eosin, Klüver Barrera, periodic acid shiff, and processed for immunohistochemistry with anti-β-amyloid, phospho-tau (clone AT8), α-synuclein, αB-crystallin, TDP-43, ubiquitin, p62, glial fibrillary acidic protein, CD68, and IBA1 [87]. All cases met the neuropathological criteria for classical ALS regarding involvement of motor cortex, pyramidal tracts, and selected motor nuclei of the cranial nerves and anterior horn of the spinal cord [88, 89]. In addition, TDP-43-immunoreactive small dys-trophic neurites and TDP-43-positive cytoplasmic neuronal inclusions in frontal cortex area 8 were observed in 11 of 18 cases, but they were abundant only in three cases (cases 29, 30, and 31). Spongiosis in the upper cortical layers was found in only one case (case 28). Frontotemporal dementia was found in no cases of the present series.

Patients with associated pathology including Alzheimer disease (excepting neurofibrillary tangle, NFT, pathology stages I-II of Braak and Braak), Parkinson disease, tauopathies, vascular diseases, neoplastic diseases affecting the nervous system, metabolic syndrome, hypoxia, and prolonged axonal states such as those occurring in intensive care units were excluded. Cases with infectious, inflammatory, or autoimmune diseases, either systemic or limited to the nervous system, were not included. Age-matched control cases had not suffered from neurologic or psychiatric diseases, and did not have abnormalities in the neuropathological examination excepting NFT pathology stages I-II of Braak and Braak. A summary of sALS and control cases is shown in Table 1.

CSF collection

Cerebrospinal fluid (CSF) was collected prospectively from patients undergoing lumbar puncture due to clinical suspicion of motor neuron disease at the functional unit of amyotrophic lateral sclerosis (UFELA) of the Neurology Service of the Bellvitge University Hospital. Samples were obtained from 86 sALS patients (Table 2). In these patients, 1.5 ± 0.5mL of CSF was collected in polypropylene tubes as part of the clinical routine investigation. CSF was centrifuged at 3,000 rpm for 15 min at room temperature. Supernatant was collected and aliquoted in volumes of 250µL and stored at -80ºC until use. All samples were analyzed after one freeze/thaw cycle.

Patients were evaluated clinically according to the main signs at onset (spinal, bulbar, and respiratory) and categorized according to disease progression as fast, expected, and slow progression depending on the survival or the clinical evolution in those still alive. Fast progression was considered in patients who survived less than 3 years; normal progression was considered between 3 and 5 years, and slow progression for those still alive after 5 years. The ALS Functional Rating Scale Revised (ALS-FRS-R, version May 2015) was used in every case. CSF from control cases was obtained from 21 healthy donors following the protocols for the use of biological samples for research (Table 2). No ALS cases or controls suffered from infection or inflammatory disorder at the time of sampling. CSF samples from sALS cases and age-matched controls were obtained after signed informed consent and approval by the Clinical Research Ethics Committee (CEIC) of the Bellvitge University Hospital.

Table 1. Summary of cases with tissue samples.

						RIN value	
Case	Age	Gender	Diagnosis	PM delay	Initial symptoms	SC	FC
1	49	F	Control	07 h 00 min	-	-	7.2
2	75	F	Control	03 h 00 min	-	-	7.2
3	55	M	Control	05 h 40 min	-	-	7.7
4	59	M	Control	12 h 05 min	-	6.4	-
5	59	M	Control	07 h 05 min	-	-	7.8
6	43	M	Control	05 h 55 min	-	6.6	7.7
7	53	M	Control	07 h 25 min	-	-	5.3
8	56	M	Control	03 h 50 min	-	-	7.6
9	47	M	Control	04 h 55 min	-	5.6	7.7
10	64	F	Control	11 h 20 min	-	6.2	-
11	46	M	Control	15 h 00 min	-	5.9	7.9
12	56	M	Control	07 h 10 min	-	6.1	-
13	71	F	Control	08 h 30 min	-	5.9	-
14	64	F	Control	05 h 00 min	-	7.0	-
15	79	F	Control	06 h 25 min	-	6.7	-
16	75	M	Control	07 h 30 min	-	5.0	-
17	55	M	Control	09 h 45 min	-	5.3	-
18	52	M	Control	03 h 00 min	-	-	8.3
19	52	M	Control	04 h 40 min	-	-	6.3
20	76	M	Control	06 h 30 min	-	6.6	-
21	60	F	Control	11 h 30 min	-	-	7.5
22	51	F	Control	04 h 00 min	-	6.3	7.9
23	54	M	Control	08 h 45 min	-	-	7.0
24	56	M	ALS	10 h 50 min	NA	7.1	-
25	70	M	ALS	03 h 00 min	Respiratory	7.3	7.0
26	77	M	ALS	04 h 30 min	NA	7.4	-
27	56	F	ALS	03 h 45 min	NA	8.2	7.7
28	59	M	ALS	03 h 15 min	NA	7.5	7.7
29	63	F	ALS	13 h 50 min	Bulbar	6.8	8.2
30	59	F	ALS	14 h 15 min	NA	6.4	6.7
31	54	M	ALS	04 h 50 min	Spinal	-	7.8
32	76	M	ALS	12 h 40 min	Spinal	-	7.4
33	64	M	ALS	16 h 30 min	NA	6.3	7.3
34	57	F	ALS	04 h 00 min	Bulbar	6.2	8.6
35	75	F	ALS	04 h 05 min	Bulbar	6.8	6.8
36	79	F	ALS	02 h 10 min	NA	7.0	-
37	57	F	ALS	10 h 00 min	Bulbar	6.5	7.1
38	50	M	ALS	10 h 10 min	Spinal	-	5.9
39	59	F	ALS	02 h 30 min	Spinal	-	7.5
40	46	M	ALS	07 h 00 min	Spinal	7.0	8.0
41	69	F	ALS	17 h 00 min	Spinal	6.4	6.3

Abbreviations: F: female; M: male; PM delay: post-mortem delay; SC: spinal cord; FC: frontal cortex; RIN: RNA integrity number.

Table 2. Summary of cases with CSF samples.

Group	n	Gender	Initial symptoms	
Control	21	9 (M) + 12 (F)	-	
sALS	86	47 (M) + 39 (F)	Spinal	55
			Bulbar	29
			Respiratory	2

Abbreviations: F: female; M: male; NA: not available.

Table 3. Summary of cases for whole peripheral blood mRNA studies.

Case	Age	Gender	Diagnosis	Initial symptoms	RIN value
1	60	M	Control	-	9.1
2	68	M	Control	-	9.2
3	66	F	Control	-	9.0
4	N/A	M	Control	-	8.9
5	74	M	Control	-	8.0
6	N/A	F	Control	-	8.3
7	67	M	Control	-	6.1
8	72	F	Control	-	6.0
9	44	F	Control	-	6.0
10	66	F	Control	-	6.1
11	60	M	ALS	Spinal	7.4
12	63	M	ALS	Spinal	8.7
13	66	F	ALS	Bulbar	8.9
14	53	F	ALS	Bulbar	7.3
15	73	M	ALS	Bulbar	8.6
16	65	M	ALS	Spinal	8.9
17	43	M	ALS	Bulbar	8.6
18	57	F	ALS	Bulbar	7.4
19	65	M	ALS	Bulbar	7.1
20	67	M	ALS	Bulbar	7.4
21	73	M	ALS	Spinal	6.1
22	73	F	ALS	Spinal	6.0

Abbreviations: F: female; M: male; NA: not available; RIN: RNA integrity value.

Whole blood samples were collected using PAXgene Blood RNA Tube (PAXgene Blood RNA Tube, PreAnalytiX, Qiagen® GmbH, Hilden, GE) collecting system. Two PAXgene Blood RNA tubes were obtained per case. Samples were collected at the first visit once the clinical diagnosis was established (n=12 sALS, n=10 controls).Tubes were kept for 2 h at room temperature to ensure lysis of blood cells, and then stored at −20°C for 24 h. Thereafter, tubes were stored at −80°C for at least 7 days prior to processing. A summary of sALS and control cases is shown in Table 3.

Genetic studies

Genetic testing was performed on genomic DNA isolated from blood or brain tissue. Informed consent for the chromosome9 open reading frame (*C9ORF72*), superoxide dismutase 1 (*SOD1*), TAR DNA binding protein (*TARDBP*), and FUS RNA binding protein (*FUS*) analysis was obtained from each patient or legal representative. Patients in this study did not show mutations in the assessed genes.

RNA extraction and RT-qPCR

RNA from dissected frozen anterior horn of the lumbar spinal cord (n=14 sALS, n=13 controls) and frontal cortex area 8 (n=15 sALS, n=14 controls) was extracted following the instructions of the supplier (RNeasy Mini Kit, Qiagen® GmbH, Hilden, Germany). PAXgene Blood RNA tubes were incubated overnight at 4°C in a shaker-plate to equilibrate the temperature and to increase yields, and then at room temperature for 2h before starting the procedure. RNA from frozen whole blood samples was extracted following the instructions of the supplier (PAXgene Blood RNA kit, PreAnalytiX, Qiagen® GmbH, Hilden, GE). RNA integrity and 28S/18S ratios were determined with the Agilent Bioanalyzer (Agilent Technologies Inc, Santa Clara, CA, USA) to assess RNA quality, and the RNA concentration was evaluated using a NanoDrop™ Spectrophotometer (Thermo Fisher Scientific). Complementary DNA (cDNA) preparation used the High-Capacity cDNA Reverse Transcription kit (Applied Biosystems, Foster City, CA, USA) following the protocol provided by the supplier. Parallel reactions for each RNA sample were run in the absence of MultiScribe Reverse Transcriptase to assess the lack of contamination of genomic DNA. TaqMan RT-qPCR assays were performed in duplicate for each gene on cDNA samples in 384-well optical plates using an ABI Prism 7900 Sequence Detection system (Applied Biosystems, Life Technologies, Waltham, MA, USA). For each 10µL TaqMan reaction, 4.5µL cDNA was mixed with 0.5µL 20x TaqMan Gene Expression Assays and 5µL of 2x TaqMan Universal PCR Master Mix (Applied Biosystems). Taqman probes used in expression assays were: allograft inflammatory factor (*AIF1*) (Hs00741549_g1) coding for IBA1, aldehyde dehydrogenase 1 family member L1 (*ALDH1L1*) (Hs01003842_m1), glial fibrillary acidic protein (*GFAP*) (Hs00909233_m1), and *CHI3L1* (Hs01072228_m1). Hypoxanthine-guanine phosphoribosyltransferase (*HPRT1*) was used as internal control for normalization of spinal cord samples, whereas β-glucuronidase (*GUS-β*) was used as the internal control for normalization of frontal cortex samples [90, 91]. Mean values of two house-keeping genes, glucuronidase beta (*GUS-β*) [92] and glyceraldehyde 3-phosphate dehydrogenase (*GAPDH*) [93], were used as internal controls for normalization of whole-blood mRNA expression studies.

The parameters of the reactions were 50°C for 2min, 95°C for 10min, and 40 cycles of 95°C for 15sec and 60°C for 1min. Finally, the capture of all TaqMan PCR data used the Sequence Detection Software (SDS version 2.2.2, Applied Biosystems). The double-delta cycle threshold (ΔΔCT) method was utilized to analyze the data results with Student's-*t* test.

Gel electrophoresis and immunoblotting

Frozen samples of frontal cortex area 8 (n=6 sALS, n=6 controls) and anterior horn of the spinal cord at the lumbar level (n=4 sALS, n=4 controls) were homogenized in RIPA lysis buffer composed of 50mM Tris/HCl buffer, pH 7.4 containing 2mM EDTA, 0.2% Nonidet P-40, 1mM PMSF, protease and phosphatase inhibitor cocktail (Roche Molecular Systems, USA). The homogenates were centrifuged for 20 min at 12,000 rpm. Protein concentration was determined with the BCA method (Thermo Scientific). Equal amounts of protein (12µg) for each sample were loaded and separated by electrophoresis on 10% sodium dodecyl sulfate polyacrylamide gel electrophoresis (SDS-PAGE) gels and then transferred onto nitrocellulose membranes (Amersham, Freiburg, GE). Non-specific bindings were blocked by incubation in 3% albumin in PBS containing 0.2% Tween for 1h at room temperature. After washing, the membranes were incubated overnight at 4°C with antibodies against glial fibrillary acidic protein (GFAP) (dilution of 1:500; rabbit polyclonal monoclonal, MO761, Dako, Agilent, Santa Clara, USA), ionized calcium binding adapter molecule 1 (IBA1) for microglia (diluted at 1:1,000; rabbit polyclonal, 019-19741, WAKO, Fujifilm, Tokyo, Japan), and YKL-40 (diluted 1:200; goat polyclonal, AF-2599, R&D Systems, Minneapolis, MN, USA). Protein loading was monitored using an antibody against β-actin (42 kDa, 1:30,000, Sigma). Membranes were incubated for 1h with appropriate HRP-conjugated secondary antibodies (1:2,000, Dako); the immunoreaction was revealed with a chemiluminescence reagent (ECL, Amersham). Densitometric quantification was carried out with the ImageLab v4.5.2 software (BioRad), using β-actin for normalization. Six samples per group were analyzed.

Immunohistochemistry

De-waxed sections, 4µm thick, of the lumbar spinal cord (n=6 sALS, n=6 controls) and frontal cortex area 8 (n=6 sALS, n=6 controls) were processed in parallel for immunohistochemistry. Endogenous peroxidases were blocked by incubation in 10% methanol-1% H_2O_2 for 15min followed by 3% normal horse serum. Then the sections were incubated at 4°C overnight with anti-YKL40 primary antibody (PA5-43746, ThermoFisher, Waltham, Massachusetts, USA) at a dilution of 1:200. Immediately afterwards, the sections were incubated with EnVision + system peroxidase (Dako, Agilent, Santa Clara, CA, USA) for 30min at room temperature. The peroxidase reaction was visualized with diaminobenzidine and H_2O_2. No signal was obtained following incubation with only the secondary antibody. Sections were slightly stained with haematoxylin.

Enzyme-linked immunosorbent assays (ELISA) in CSF

YKL40 protein levels were measured using the MicroVue YKL40 EIA ELISA kit (Quidel, San Diego, CA, USA) following the manufacturer's instructions. Receiver operating characteristic (ROC) curves and derived area under the curve (AUC) were calculated. The best cut-off value, sensitivity, and specificity were estimated based on the Youden index (point on a ROC curve providing the best balance of both sensitivity and specificity) [94]. NF-L levels were measured using the NF-light® (Neurofilament light) ELISA kit from UmanDiagnostics (Umea, Sweden) following the manufacturer's instructions.

Statistical analysis

The normality of distribution was analyzed with the Kolmogorov-Smirnov test. The unpaired Student's *t*-test was used to compare each group when values followed normal distribution, and statistical analysis of the CSF protein data between groups was carried out using one-way analysis of variance (ANOVA) followed by Tukey post-test, in both cases using the SPSS software (IBM Corp. Released 2013, IBM-SPSS Statistics for Windows, Version 21.0., Armonk, NY, USA). Graphic design was performed with GraphPad Prism version 5.01 (La Jolla, CA, USA). Outliers were detected using the GraphPad software QuickCalcs ($p < 0.05$). The data were expressed as mean ± SEM, and significance levels were set at $*P < 0.05$, $**P < 0.01$, and $***P < 0.001$, and tendencies at $\#P < 0.1$. Pearson's correlation coefficient was used to assess a possible linear association between two continuous quantitative variables.

AUTHOR CONTRIBUTIONS

PA-B carried out the analysis of YKL40 expression in brain tissue, CSF and peripheral blood; RD and MP examined the clinical characteristics and course of the patients, and obtained CSF and blood from sALS cases; MJC obtained the CSF from control individuals; FLI advised certain aspects of YKL40 in brain and CSF; IF directed and supervised the study, evaluated the results, and wrote the final version of the manuscript which was circulated for comments and suggestions, and approved by all the authors.

ACKNOWLEDGEMENTS

We wish to thank T. Yohannan for editorial assistance.

CONFLICTS OF INTEREST

The authors declare no conflicts of interest.

FUNDING

This study was supported by grants from CIBERNED and PI17/00809 Institute of Health Carlos III, and co-funded by FEDER funds/European Regional Development Fund (ERDF)—a way to build Europe; ALS intra-CIBERNED project to IF; IFI15/00035 fellowship to PA-B; Spanish Ministry of Health - Instituto Carlos III/ Fondo Social Europeo (CP16/00041) to FLI, and "Retos todos unidos contra la ELA" and "Proyecto DGeneración conexiones con sentido" to MP.

REFERENCES

1. Adrangi S, Faramarzi MA. From bacteria to human: a journey into the world of chitinases. Biotechnol Adv. 2013; 31:1786–95. https://doi.org/10.1016/j.biotechadv.2013.09.012

2. Karthik N, Akanksha K, Pandey A. Production, purification and properties of fungal chitinases--a review. Indian J Exp Biol. 2014; 52:1025–35.

3. Rathore AS, Gupta RD. Chitinases from bacteria to human: properties, applications, and future perspectives. Enzyme Res. 2015; 2015:791907. https://doi.org/10.1155/2015/791907

4. Di Rosa M, Distefano G, Zorena K, Malaguarnera L. Chitinases and immunity: ancestral molecules with new functions. Immunobiology. 2016; 221:399–411. https://doi.org/10.1016/j.imbio.2015.11.014

5. Langner T, Göhre V. Fungal chitinases: function, regulation, and potential roles in plant/pathogen interactions. Curr Genet. 2016; 62:243–54. https://doi.org/10.1007/s00294-015-0530-x

6. Shao R, Hamel K, Petersen L, Cao QJ, Arenas RB, Bigelow C, Bentley B, Yan W. YKL-40, a secreted glycoprotein, promotes tumor angiogenesis. Oncogene. 2009; 28:4456–68. https://doi.org/10.1038/onc.2009.292

7. Lee CG, Da Silva CA, Dela Cruz CS, Ahangari F, Ma B, Kang MJ, He CH, Takyar S, Elias JA. Role of chitin and chitinase/chitinase-like proteins in inflammation, tissue remodeling, and injury. Annu Rev Physiol. 2011; 73:479–501. https://doi.org/10.1146/annurev-physiol-012110-142250

8. Pelloski CE, Mahajan A, Maor M, Chang EL, Woo S, Gilbert M, Colman H, Yang H, Ledoux A, Blair H, Passe S, Jenkins RB, Aldape KD. YKL-40 expression is associated with poorer response to radiation and shorter overall survival in glioblastoma. Clin Cancer Res. 2005; 11:3326–34. https://doi.org/10.1158/1078-0432.CCR-04-1765

9. Bonneh-Barkay D, Bissel SJ, Wang G, Fish KN, Nicholl

GC, Darko SW, Medina-Flores R, Murphey-Corb M, Rajakumar PA, Nyaundi J, Mellors JW, Bowser R, Wiley CA. YKL-40, a marker of simian immunodeficiency virus encephalitis, modulates the biological activity of basic fibroblast growth factor. Am J Pathol. 2008; 173:130–43. https://doi.org/10.2353/ajpath.2008.080045

10. Bonneh-Barkay D, Wang G, Starkey A, Hamilton RL, Wiley CA. In vivo CHI3L1 (YKL-40) expression in astrocytes in acute and chronic neurological diseases. J Neuroinflammation. 2010a; 7:34. https://doi.org/10.1186/1742-2094-7-34

11. Bonneh-Barkay D, Zagadailov P, Zou H, Niyonkuru C, Figley M, Starkey A, Wang G, Bissel SJ, Wiley CA, Wagner AK. YKL-40 expression in traumatic brain injury: an initial analysis. J Neurotrauma. 2010b; 27:1215–23. https://doi.org/10.1089/neu.2010.1310

12. Horbinski C, Wang G, Wiley CA. YKL-40 is directly produced by tumor cells and is inversely linked to EGFR in glioblastomas. Int J Clin Exp Pathol. 2010; 3:226–37.

13. Comabella M, Fernández M, Martin R, Rivera-Vallvé S, Borrás E, Chiva C, Julià E, Rovira A, Cantó E, Alvarez-Cermeño JC, Villar LM, Tintoré M, Montalban X. Cerebrospinal fluid chitinase 3-like 1 levels are associated with conversion to multiple sclerosis. Brain. 2010; 133:1082–93. https://doi.org/10.1093/brain/awq035

14. Iwamoto FM, Hormigo A. Unveiling YKL-40, from serum marker to target therapy in glioblastoma. Front Oncol. 2014; 4:90. https://doi.org/10.3389/fonc.2014.00090

15. Burman J, Raininko R, Blennow K, Zetterberg H, Axelsson M, Malmeström C. YKL-40 is a CSF biomarker of intrathecal inflammation in secondary progressive multiple sclerosis. J Neuroimmunol. 2016; 292:52–57. https://doi.org/10.1016/j.jneuroim.2016.01.013

16. Mañé-Martínez MA, Olsson B, Bau L, Matas E, Cobo-Calvo Á, Andreasson U, Blennow K, Romero-Pinel L, Martínez-Yélamos S, Zetterberg H. Glial and neuronal markers in cerebrospinal fluid in different types of multiple sclerosis. J Neuroimmunol. 2016; 299:112–17. https://doi.org/10.1016/j.jneuroim.2016.08.004

17. Quintana E, Coll C, Salavedra-Pont J, Muñoz-San Martín M, Robles-Cedeño R, Tomàs-Roig J, Buxó M, Matute-Blanch C, Villar LM, Montalbán X, Comabella M, Perkal H, Gich J, Ramió-Torrentà L. Cognitive impairment in early stages of multiple sclerosis is associated with high cerebrospinal fluid levels of chitinase 3-like 1 and neurofilament light chain. Eur J Neurol. 2018; 25:1189–91. https://doi.org/10.1111/ene.13687

18. Craig-Schapiro R, Perrin RJ, Roe CM, Xiong C, Carter D, Cairns NJ, Mintun MA, Peskind ER, Li G, Galasko DR, Clark CM, Quinn JF, D'Angelo G, et al. YKL-40: a novel prognostic fluid biomarker for preclinical Alzheimer's disease. Biol Psychiatry. 2010; 68:903–12. https://doi.org/10.1016/j.biopsych.2010.08.025

19. Perrin RJ, Craig-Schapiro R, Malone JP, Shah AR, Gilmore P, Davis AE, Roe CM, Peskind ER, Li G, Galasko DR, Clark CM, Quinn JF, Kaye JA, et al. Identification and validation of novel cerebrospinal fluid biomarkers for staging early Alzheimer's disease. PLoS One. 2011; 6:e16032. https://doi.org/10.1371/journal.pone.0016032

20. Olsson B, Constantinescu R, Holmberg B, Andreasen N, Blennow K, Zetterberg H. The glial marker YKL-40 is decreased in synucleinopathies. Mov Disord. 2013a; 28:1882–85. https://doi.org/10.1002/mds.25589

21. Olsson B, Hertze J, Lautner R, Zetterberg H, Nägga K, Höglund K, Basun H, Annas P, Lannfelt L, Andreasen N, Minthon L, Blennow K, Hansson O. Microglial markers are elevated in the prodromal phase of Alzheimer's disease and vascular dementia. J Alzheimers Dis. 2013b; 33:45–53. https://doi.org/10.3233/JAD-2012-120787

22. Antonell A, Mansilla A, Rami L, Lladó A, Iranzo A, Olives J, Balasa M, Sánchez-Valle R, Molinuevo JL. Cerebrospinal fluid level of YKL-40 protein in preclinical and prodromal Alzheimer's disease. J Alzheimers Dis. 2014; 42:901–08. https://doi.org/10.3233/JAD-140624

23. Wildsmith KR, Schauer SP, Smith AM, Arnott D, Zhu Y, Haznedar J, Kaur S, Mathews WR, Honigberg LA. Identification of longitudinally dynamic biomarkers in Alzheimer's disease cerebrospinal fluid by targeted proteomics. Mol Neurodegener. 2014; 9:22. https://doi.org/10.1186/1750-1326-9-22

24. Alcolea D, Carmona-Iragui M, Suárez-Calvet M, Sánchez-Saudinós MB, Sala I, Antón-Aguirre S, Blesa R, Clarimón J, Fortea J, Lleó A. Relationship between β-Secretase, inflammation and core cerebrospinal fluid biomarkers for Alzheimer's disease. J Alzheimers Dis. 2014; 42:157–67. https://doi.org/10.3233/JAD-140240

25. Rosén C, Andersson CH, Andreasson U, Molinuevo JL, Bjerke M, Rami L, Lladó A, Blennow K, Zetterberg H. Increased levels of chitotriosidase and YKL-40 in cerebrospinal fluid from patients with Alzheimer's disease. Dement Geriatr Cogn Disord Extra. 2014; 4:297–304. https://doi.org/10.1159/000362164

26. Kester MI, Teunissen CE, Sutphen C, Herries EM, Ladenson JH, Xiong C, Scheltens P, van der Flier WM,

Morris JC, Holtzman DM, Fagan AM. Cerebrospinal fluid VILIP-1 and YKL-40, candidate biomarkers to diagnose, predict and monitor Alzheimer's disease in a memory clinic cohort. Alzheimers Res Ther. 2015; 7:59. https://doi.org/10.1186/s13195-015-0142-1

27. Alcolea D, Vilaplana E, Pegueroles J, Montal V, Sánchez-Juan P, González-Suárez A, Pozueta A, Rodríguez-Rodríguez E, Bartrés-Faz D, Vidal-Piñeiro D, González-Ortiz S, Medrano S, Carmona-Iragui M, et al. Relationship between cortical thickness and cerebrospinal fluid YKL-40 in predementia stages of Alzheimer's disease. Neurobiol Aging. 2015; 36:2018–23. https://doi.org/10.1016/j.neurobiolaging.2015.03.001

28. Wennström M, Surova Y, Hall S, Nilsson C, Minthon L, Hansson O, Nielsen HM. The inflammatory marker YKL-40 is elevated in cerebrospinal fluid from patients with Alzheimer's but not Parkinson's disease or dementia with Lewy bodies. PLoS One. 2015; 10:e0135458. https://doi.org/10.1371/journal.pone.0135458

29. Gispert JD, Monté GC, Falcon C, Tucholka A, Rojas S, Sánchez-Valle R, Antonell A, Lladó A, Rami L, Molinuevo JL. CSF YKL-40 and pTau181 are related to different cerebral morphometric patterns in early AD. Neurobiol Aging. 2016; 38:47–55. https://doi.org/10.1016/j.neurobiolaging.2015.10.022

30. Janelidze S, Hertze J, Zetterberg H, Landqvist Waldö M, Santillo A, Blennow K, Hansson O. Cerebrospinal fluid neurogranin and YKL-40 as biomarkers of Alzheimer's disease. Ann Clin Transl Neurol. 2015; 3:12–20. https://doi.org/10.1002/acn3.266

31. Teunissen CE, Elias N, Koel-Simmelink MJ, Durieux-Lu S, Malekzadeh A, Pham TV, Piersma SR, Beccari T, Meeter LH, Dopper EG, van Swieten JC, Jimenez CR, Pijnenburg YA. Novel diagnostic cerebrospinal fluid biomarkers for pathologic subtypes of frontotemporal dementia identified by proteomics. Alzheimers Dement (Amst). 2016; 2:86–94. https://doi.org/10.1016/j.dadm.2015.12.004

32. Baldacci F, Toschi N, Lista S, Zetterberg H, Blennow K, Kilimann I, Teipel S, Cavedo E, Dos Santos AM, Epelbaum S, Lamari F, Dubois B, Floris R, et al. Two-level diagnostic classification using cerebrospinal fluid YKL-40 in Alzheimer's disease. Alzheimers Dement. 2017; 13:993–1003. https://doi.org/10.1016/j.jalz.2017.01.021

33. Llorens F, Thüne K, Tahir W, Kanata E, Diaz-Lucena D, Xanthopoulos K, Kovatsi E, Pleschka C, Garcia-Esparcia P, Schmitz M, Ozbay D, Correia S, Correia Â, et al. YKL-40 in the brain and cerebrospinal fluid of neurodegenerative dementias. Mol Neurodegener. 2017; 12:83. https://doi.org/10.1186/s13024-017-0226-4

34. Alcolea D, Vilaplana E, Suárez-Calvet M, Illán-Gala I, Blesa R, Clarimón J, Lladó A, Sánchez-Valle R, Molinuevo JL, García-Ribas G, Compta Y, Martí MJ, Piñol-Ripoll G, et al. CSF sAPPβ, YKL-40, and neurofilament light in frontotemporal lobar degeneration. Neurology. 2017; 89:178–88. https://doi.org/10.1212/WNL.0000000000004088

35. Vijverberg EG, Schouws S, Meesters PD, Verwijk E, Comijs H, Koene T, Schreuder C, Beekman A, Scheltens P, Stek M, Pijnenburg Y, Dols A. Cognitive deficits in patients with neuropsychiatric symptoms: A comparative study between behavioral variant frontotemporal dementia and primary psychiatric disorders. J Clin Psychiatry. 2017; 78:e940–46. https://doi.org/10.4088/JCP.16m11019

36. Bonneh-Barkay D, Zagadailov P, Zou H, Niyonkuru C, Figley M, Starkey A, Wang G, Bissel SJ, Wiley CA, Wagner AK. YKL-40 expression in traumatic brain injury: an initial analysis. J Neurotrauma. 2010; 27:1215–23. https://doi.org/10.1089/neu.2010.1310

37. Bonneh-Barkay D, Bissel SJ, Kofler J, Starkey A, Wang G, Wiley CA. Astrocyte and macrophage regulation of YKL-40 expression and cellular response in neuroinflammation. Brain Pathol. 2012; 22:530–46. https://doi.org/10.1111/j.1750-3639.2011.00550.x

38. Wiley CA, Bonneh-Barkay D, Dixon CE, Lesniak A, Wang G, Bissel SJ, Kochanek PM. Role for mammalian chitinase 3-like protein 1 in traumatic brain injury. Neuropathology. 2015; 35:95–106. https://doi.org/10.1111/neup.12158

39. Querol-Vilaseca M, Colom-Cadena M, Pegueroles J, San Martín-Paniello C, Clarimon J, Belbin O, Fortea J, Lleó A. YKL-40 (Chitinase 3-like I) is expressed in a subset of astrocytes in Alzheimer's disease and other tauopathies. J Neuroinflammation. 2017; 14:118. https://doi.org/10.1186/s12974-017-0893-7

40. Ferrer I. Diversity of astroglial responses across human neurodegenerative disorders and brain aging. Brain Pathol. 2017; 27:645–74. https://doi.org/10.1111/bpa.12538

41. Pagliardini V, Pagliardini S, Corrado L, Lucenti A, Panigati L, Bersano E, Servo S, Cantello R, D'Alfonso S, Mazzini L. Chitotriosidase and lysosomal enzymes as potential biomarkers of disease progression in amyotrophic lateral sclerosis: a survey clinic-based study. J Neurol Sci. 2015; 348:245–50. https://doi.org/10.1016/j.jns.2014.12.016

42. Steinacker P, Verde F, Fang L, Feneberg E, Oeckl P, Roeber S, Anderl-Straub S, Danek A, Diehl-Schmid J, Fassbender K, Fliessbach K, Foerstl H, Giese A, et al, and FTLDc study group. Chitotriosidase (CHIT1) is

increased in microglia and macrophages in spinal cord of amyotrophic lateral sclerosis and cerebrospinal fluid levels correlate with disease severity and progression. J Neurol Neurosurg Psychiatry. 2018; 89:239–47. https://doi.org/10.1136/jnnp-2017-317138

43. Sanfilippo C, Longo A, Lazzara F, Cambria D, Distefano G, Palumbo M, Cantarella A, Malaguarnera L, Di Rosa M. CHI3L1 and CHI3L2 overexpression in motor cortex and spinal cord of sALS patients. Mol Cell Neurosci. 2017; 85:162–69. https://doi.org/10.1016/j.mcn.2017.10.001

44. Thompson AG, Gray E, Thézénas ML, Charles PD, Evetts S, Hu MT, Talbot K, Fischer R, Kessler BM, Turner MR. Cerebrospinal fluid macrophage biomarkers in amyotrophic lateral sclerosis. Ann Neurol. 2018; 83:258–68. https://doi.org/10.1002/ana.25143

45. Illán-Gala I, Alcolea D, Montal V, Dols O, Muñoz L, de Luna N, Turón-Sans J, Cortés-Vicente E, Sánchez-Saudinós B, Subirana A, Sala I, Blesa R, Clarimón J, et al. CSF sAPPβ, YKL-40, and NfL along the ALS-FTD spectrum. Neurology. 2017; 89:178-88. https://doi.org/10.1212/WNL.0000000000004088

46. Fujita K, Kato T, Yamauchi M, Ando M, Honda M, Nagata Y. Increases in fragmented glial fibrillary acidic protein levels in the spinal cords of patients with amyotrophic lateral sclerosis. Neurochem Res. 1998; 23:169–74. https://doi.org/10.1023/A:1022476724381

47. Graves MC, Fiala M, Dinglasan LA, Liu NQ, Sayre J, Chiappelli F, van Kooten C, Vinters HV. Inflammation in amyotrophic lateral sclerosis spinal cord and brain is mediated by activated macrophages, mast cells and T cells. Amyotroph Lateral Scler Other Motor Neuron Disord. 2004; 5:213–19. https://doi.org/10.1080/14660820410020286

48. Henkel JS, Engelhardt JI, Siklós L, Simpson EP, Kim SH, Pan T, Goodman JC, Siddique T, Beers DR, Appel SH. Presence of dendritic cells, MCP-1, and activated microglia/macrophages in amyotrophic lateral sclerosis spinal cord tissue. Ann Neurol. 2004; 55:221–35. https://doi.org/10.1002/ana.10805

49. Calvo A, Moglia C, Balma M, Chiò A. Involvement of immune response in the pathogenesis of amyotrophic lateral sclerosis: a therapeutic opportunity? CNS Neurol Disord Drug Targets. 2010; 9:325–30. https://doi.org/10.2174/187152710791292657

50. Casula M, Iyer AM, Spliet WG, Anink JJ, Steentjes K, Sta M, Troost D, Aronica E. Toll-like receptor signaling in amyotrophic lateral sclerosis spinal cord tissue. Neuroscience. 2011; 179:233–43. https://doi.org/10.1016/j.neuroscience.2011.02.001

51. Sta M, Sylva-Steenland RM, Casula M, de Jong JM, Troost D, Aronica E, Baas F. Innate and adaptive immunity in amyotrophic lateral sclerosis: evidence of complement activation. Neurobiol Dis. 2011; 42:211–20. https://doi.org/10.1016/j.nbd.2011.01.002

52. McCombe PA, Henderson RD. The Role of immune and inflammatory mechanisms in ALS. Curr Mol Med. 2011; 11:246–54. https://doi.org/10.2174/156652411795243450

53. Philips T, Robberecht W. Neuroinflammation in amyotrophic lateral sclerosis: role of glial activation in motor neuron disease. Lancet Neurol. 2011; 10:253–63. https://doi.org/10.1016/S1474-4422(11)70015-1

54. Evans MC, Couch Y, Sibson N, Turner MR. Inflammation and neurovascular changes in amyotrophic lateral sclerosis. Mol Cell Neurosci. 2013; 53:34–41. https://doi.org/10.1016/j.mcn.2012.10.008

55. Hooten KG, Beers DR, Zhao W, Appel SH. Protective and toxic neuroinflammation in amyotrophic lateral sclerosis. Neurotherapeutics. 2015; 12:364–75. https://doi.org/10.1007/s13311-014-0329-3

56. Komine O, Yamanaka K. Neuroinflammation in motor neuron disease. Nagoya J Med Sci. 2015; 77:537–49.

57. Puentes F, Malaspina A, van Noort JM, Amor S. Non-neuronal cells in ALS: role of glial, immune cells and blood-CNS barriers. Brain Pathol. 2016; 26:248–57. https://doi.org/10.1111/bpa.12352

58. Andrés-Benito P, Moreno J, Aso E, Povedano M, Ferrer I. Amyotrophic lateral sclerosis, gene deregulation in the anterior horn of the spinal cord and frontal cortex area 8: implications in frontotemporal lobar degeneration. Aging (Albany NY). 2017; 9:823–51. https://doi.org/10.18632/aging.101195

59. Liu J, Wang F. Role of neuroinflammation in amyotrophic lateral sclerosis: cellular mechanisms and therapeutic implications. Front Immunol. 2017; 8:1005. https://doi.org/10.3389/fimmu.2017.01005

60. Sekizawa T, Openshaw H, Ohbo K, Sugamura K, Itoyama Y, Niland JC. Cerebrospinal fluid interleukin 6 in amyotrophic lateral sclerosis: immunological parameter and comparison with inflammatory and non-inflammatory central nervous system diseases. J Neurol Sci. 1998; 154:194–99. https://doi.org/10.1016/S0022-510X(97)00228-1

61. Rentzos M, Nikolaou C, Rombos A, Boufidou F, Zoga M, Dimitrakopoulos A, Tsoutsou A, Vassilopoulos D. RANTES levels are elevated in serum and cerebrospinal fluid in patients with amyotrophic

lateral sclerosis. Amyotroph Lateral Scler. 2007; 8:283–87.
https://doi.org/10.1080/17482960701419232

62. Kuhle J, Lindberg RL, Regeniter A, Mehling M, Steck AJ, Kappos L, Czaplinski A. Increased levels of inflammatory chemokines in amyotrophic lateral sclerosis. Eur J Neurol. 2009; 16:771–74.

https://doi.org/10.1111/j.1468-1331.2009.02560.x

63. Mitchell RM, Freeman WM, Randazzo WT, Stephens HE, Beard JL, Simmons Z, Connor JR. A CSF biomarker panel for identification of patients with amyotrophic lateral sclerosis. Neurology. 2009; 72:14–19. https://doi.org/10.1212/01.wnl.0000333251.36681.a5

64. Rentzos M, Rombos A, Nikolaou C, Zoga M, Zouvelou V, Dimitrakopoulos A, Alexakis T, Tsoutsou A, Samakovli A, Michalopoulou M, Evdokimidis I. Interleukin-15 and interleukin-12 are elevated in serum and cerebrospinal fluid of patients with amyotrophic lateral sclerosis. Eur Neurol. 2010; 63:285–90. https://doi.org/10.1159/000287582

65. Rentzos M, Rombos A, Nikolaou C, Zoga M, Zouvelou V, Dimitrakopoulos A, Alexakis T, Tsoutsou A, Samakovli A, Michalopoulou M, Evdokimidis J. Interleukin-17 and interleukin-23 are elevated in serum and cerebrospinal fluid of patients with ALS: a reflection of Th17 cells activation? Acta Neurol Scand. 2010; 122:425–29. https://doi.org/10.1111/j.1600-0404.2010.01333.x

66. Fiala M, Chattopadhay M, La Cava A, Tse E, Liu G, Lourenco E, Eskin A, Liu PT, Magpantay L, Tse S, Mahanian M, Weitzman R, Tong J, et al. IL-17A is increased in the serum and in spinal cord CD8 and mast cells of ALS patients. J Neuroinflammation. 2010; 7:76. https://doi.org/10.1186/1742-2094-7-76

67. Tateishi T, Yamasaki R, Tanaka M, Matsushita T, Kikuchi H, Isobe N, Ohyagi Y, Kira J. CSF chemokine alterations related to the clinical course of amyotrophic lateral sclerosis. J Neuroimmunol. 2010; 222:76–81.
https://doi.org/10.1016/j.jneuroim.2010.03.004

68. Italiani P, Carlesi C, Giungato P, Puxeddu I, Borroni B, Bossù P, Migliorini P, Siciliano G, Boraschi D. Evaluating the levels of interleukin-1 family cytokines in sporadic amyotrophic lateral sclerosis. J Neuroinflammation. 2014; 11:94.
https://doi.org/10.1186/1742-2094-11-94

69. Martínez HR, Escamilla-Ocañas CE, Camara-Lemarroy CR, González-Garza MT, Moreno-Cuevas J, García Sarreón MA. Increased cerebrospinal fluid levels of cytokines monocyte chemoattractant protein-1 (MCP-1) and macrophage inflammatory protein-1β (MIP-1β) in patients with amyotrophic lateral sclerosis. Neurologia. 2017 Epub ahead of print. https://doi.org/10.1016/j.nrl.2017.07.020

70. Moreau C, Gosset P, Brunaud-Danel V, Lassalle P, Degonne B, Destee A, Defebvre L, Devos D. CSF profiles of angiogenic and inflammatory factors depend on the respiratory status of ALS patients. Amyotroph Lateral Scler. 2009; 10:175–81.
https://doi.org/10.1080/17482960802651725

71. Zhang R, Gascon R, Miller RG, Gelinas DF, Mass J, Hadlock K, Jin X, Reis J, Narvaez A, McGrath MS. Evidence for systemic immune system alterations in sporadic amyotrophic lateral sclerosis (sALS). J Neuroimmunol. 2005; 159:215–24.
https://doi.org/10.1016/j.jneuroim.2004.10.009

72. Shi N, Kawano Y, Tateishi T, Kikuchi H, Osoegawa M, Ohyagi Y, Kira J. Increased IL-13-producing T cells in ALS: positive correlations with disease severity and progression rate. J Neuroimmunol. 2007; 182:232–35.
https://doi.org/10.1016/j.jneuroim.2006.10.001

73. Cereda C, Baiocchi C, Bongioanni P, Cova E, Guareschi S, Metelli MR, Rossi B, Sbalsi I, Cuccia MC, Ceroni M. TNF and sTNFR1/2 plasma levels in ALS patients. J Neuroimmunol. 2008; 194:123–31.
https://doi.org/10.1016/j.jneuroim.2007.10.028

74. Mantovani S, Garbelli S, Pasini A, Alimonti D, Perotti C, Melazzini M, Bendotti C, Mora G. Immune system alterations in sporadic amyotrophic lateral sclerosis patients suggest an ongoing neuroinflammatory process. J Neuroimmunol. 2009; 210:73–79.
https://doi.org/10.1016/j.jneuroim.2009.02.012

75. Rentzos M, Evangelopoulos E, Sereti E, Zouvelou V, Marmara S, Alexakis T, Evdokimidis I. Alterations of T cell subsets in ALS: a systemic immune activation? Acta Neurol Scand. 2012; 125:260–64.
https://doi.org/10.1111/j.1600-0404.2011.01528.x

76. Rentzos M, Evangelopoulos E, Sereti E, Zouvelou V, Marmara S, Alexakis T, Evdokimidis I. Alterations of T cell subsets in ALS: a systemic immune activation? Acta Neurol Scand. 2012; 125:260–64.
https://doi.org/10.1111/j.1600-0404.2011.01528.x

77. Henkel JS, Beers DR, Wen S, Rivera AL, Toennis KM, Appel JE, Zhao W, Moore DH, Powell SZ, Appel SH. Regulatory T-lymphocytes mediate amyotrophic lateral sclerosis progression and survival. EMBO Mol Med. 2013; 5:64–79.
https://doi.org/10.1002/emmm.201201544

78. Zhao W, Beers DR, Hooten KG, Sieglaff DH, Zhang A, Kalyana-Sundaram S, Traini CM, Halsey WS, Hughes AM, Sathe GM, Livi GP, Fan GH, Appel SH. Characterization of gene expression phenotype in amyotrophic lateral sclerosis monocytes. JAMA Neurol. 2017; 74:677–85.

https://doi.org/10.1001/jamaneurol.2017.0357

79. Sidaway P. Motor neuron disease: peripheral immune cell levels correlate with disease progression in ALS. Nat Rev Neurol. 2017; 13:708. https://doi.org/10.1038/nrneurol.2017.149

80. Andrés-Benito P, Moreno J, Domínguez R, Aso E, Povedano M, Ferrer I. Inflammatory Gene expression in whole peripheral blood at early stages of sporadic amyotrophic lateral sclerosis. Front Neurol. 2017; 8:546. https://doi.org/10.3389/fneur.2017.00546

81. Weydt P, Oeckl P, Huss A, Müller K, Volk AE, Kuhle J, Knehr A, Andersen PM, Prudlo J, Steinacker P, Weishaupt JH, Ludolph AC, Otto M. Neurofilament levels as biomarkers in asymptomatic and symptomatic familial amyotrophic lateral sclerosis. Ann Neurol. 2016; 79:152–58. https://doi.org/10.1002/ana.24552

82. Steinacker P, Feneberg E, Weishaupt J, Brettschneider J, Tumani H, Andersen PM, von Arnim CA, Böhm S, Kassubek J, Kubisch C, Lulé D, Müller HP, Muche R, et al. Neurofilaments in the diagnosis of motoneuron diseases: a prospective study on 455 patients. J Neurol Neurosurg Psychiatry. 2016; 87:12–20. https://doi.org/10.1136/jnnp-2015-311387

83. Oeckl P, Jardel C, Salachas F, Lamari F, Andersen PM, Bowser R, de Carvalho M, Costa J, van Damme P, Gray E, Grosskreutz J, Hernández-Barral M, Herukka SK, et al. Multicenter validation of CSF neurofilaments as diagnostic biomarkers for ALS. Amyotroph Lateral Scler Frontotemporal Degener. 2016; 17:404–13. https://doi.org/10.3109/21678421.2016.1167913

84. Feneberg E, Oeckl P, Steinacker P, Verde F, Barro C, Van Damme P, Gray E, Grosskreutz J, Jardel C, Kuhle J, Koerner S, Lamari F, Amador MD, et al. Multicenter evaluation of neurofilaments in early symptom onset amyotrophic lateral sclerosis. Neurology. 2018; 90:e22–30. https://doi.org/10.1212/WNL.0000000000004761

85. Xu Z, Henderson RD, David M, McCombe PA. Neurofilaments as biomarkers for amyotrophic lateral sclerosis: A systematic review and meta-analysis. PLoS One. 2016; 11:e0164625. https://doi.org/10.1371/journal.pone.0164625

86. Rossi D, Volanti P, Brambilla L, Colletti T, Spataro R, La Bella V. CSF neurofilament proteins as diagnostic and prognostic biomarkers for amyotrophic lateral sclerosis. J Neurol. 2018; 265:510–21. https://doi.org/10.1007/s00415-017-8730-6

87. Ferrer I. Brain Banking. In: Aminoff MJ, Daroff RB (eds.) Encyclopedia of the Neurological Sciences, 2nd edition. Oxford: Academic Press 2014; 1, pp. 467-473.

88. Ince PG, Highley JR, Wharton SB. Motor neuron disorders. In: Love S, Budka H, Ironside JW, Perry A (eds.). Greenfield's Neuropathology, Ninth edition. Boca Raton: CRC Press, Taylor and Francis Group. 2015, pp. 817-848.

89. Strong MJ, Hortobágyi T, Okamoto K, Kato S. Amyotrophic lateral sclerosis, primary lateral sclerosis, and spinal muscular atrophy. In: Dickson DW, Weller R.O (eds.) Neurodegeneration: the molecular pathology of dementia and movement disorders. 2nd edition. Oxford: Wiley-Blackwell. 2011, pp. 418-433.

90. Barrachina M, Castaño E, Ferrer I. TaqMan PCR assay in the control of RNA normalization in human post-mortem brain tissue. Neurochem Int. 2006; 49:276–84. https://doi.org/10.1016/j.neuint.2006.01.018

91. Durrenberger PF, Fernando FS, Magliozzi R, Kashefi SN, Bonnert TP, Ferrer I, Seilhean D, Nait-Oumesmar B, Schmitt A, Gebicke-Haerter PJ, Falkai P, Grünblatt E, Palkovits M, et al. Selection of novel reference genes for use in the human central nervous system: a BrainNet Europe Study. Acta Neuropathol. 2012; 124:893–903. https://doi.org/10.1007/s00401-012-1027-z

92. Zampieri M, Ciccarone F, Guastafierro T, Bacalini MG, Calabrese R, Moreno-Villanueva M, Reale A, Chevanne M, Bürkle A, Caiafa P. Validation of suitable internal control genes for expression studies in aging. Mech Ageing Dev. 2010; 131:89–95. https://doi.org/10.1016/j.mad.2009.12.005

93. Bayatti N, Cooper-Knock J, Bury JJ, Wyles M, Heath PR, Kirby J, Shaw PJ. Comparison of blood RNA extraction methods used for gene expression profiling in amyotrophic lateral sclerosis. PLoS One. 2014; 9:e87508. https://doi.org/10.1371/journal.pone.0087508

94. Youden WJ. Index for rating diagnostic tests. Cancer. 1950; 3:32–35. https://doi.org/10.1002/1097-0142(1950)3:1<32::AID-CNCR2820030106>3.0.CO;2-3

Article IV

Altered dynein axonemal assembly factor 1 expression in spinal cord motor neurons in sporadic amyotrophic lateral sclerosis

Pol Andrés Benito, Mònica Povedano, Pascual Torres, Manuel Portero Otín and Isidro Ferrer

Journal of Neuropathology and Experimental Neurology. 2019 May 1; 78(5): 416-425.

J Neuropathol Exp Neurol
Vol. 0, No. 0, 2019, pp. 1–10
doi: 10.1093/jnen/nlz019

OXFORD

ORIGINAL ARTICLE

Altered Dynein Axonemal Assembly Factor 1 Expression in C-Boutons in Bulbar and Spinal Cord Motor-Neurons in Sporadic Amyotrophic Lateral Sclerosis

Pol Andrés-Benito, Mr, Mònica Povedano, MD, Pascual Torres, Mr, Manuel Portero-Otín, PhD, and Isidro Ferrer, MD, PhD

Abstract

Dyneins are major components of microtubules. Dynein assembly is modulated by a heterogeneous group of dynein axonemal assembly factors (DNAAFs). The present study analyzes dynein axonemal assembly factor 1 (*DNAAF1*) and leucine-rich repeat-containing protein 50 (LRRC50), the corresponding encoded protein, in lower motor neurons in spinal cord of sALS postmortem samples and *hSOD1-G93A* transgenic mice compared with controls. *DNAAF1* mRNA is significantly reduced in the anterior horn in sALS, and LRRC50 immunoreactivity is significantly reduced in C-boutons of the remaining motor neurons of the anterior horn, dorsal nucleus of the vagus nerve, and hypoglossal nuclei at terminal stages of ALS. LRRC50 immunoreactivity has a perinuclear distribution in motor neurons in sALS thus suggesting a disorder of transport. The number of LRRC50-/S1R-immunoreactive structures is also significantly decreased in *hSOD1-G93A* transgenic mice at the age of 90 days (preclinical stages), and the number of motor neurons with LRRC50-immunoreactive structures is significantly reduced in animals aged 150 days (clinical stages). These observations suggest cholinergic denervation of motor neurons as a pathogenic factor in motor neuron disease. LRRC50 protein levels were not detected in human CSF.

From the Department of Pathology and Experimental Therapeutics, University of Barcelona (PAB, IF); Institute Carlos III, Biomedical Network Research Center on Neurodegenerative Diseases (CIBERNED) (PAB, IF), Hospitalet de Llobregat, Spain; Bellvitge Biomedical Research Institute (IDIBELL), Hospitalet de Llobregat, Barcelona, Spain (PAB, IF); Functional Unit of Amyotrophic Lateral Sclerosis (UFELA), Service of Neurology, Bellvitge University Hospital, Hospitalet de Llobregat, Spain (MP); Departament Medicina Experimental, Facultat de Medicina, Universitat de Lleida, IRBLLEIDA, Lleida, Spain (PT, MPO); Neuropathology, Pathologic Anatomy Service, Bellvitge University Hospital, IDIBELL, L'Hospitalet de Llobregat, Spain (IF); and Institute of Neurosciences, University of Barcelona, Barcelona, Spain (IF).

Send correspondence to: Isidro Ferrer, MD, PhD, Department of Pathology and Experimental Therapeutics, University of Barcelona, Campus Bellvitge, c/Feixa Llarga sn, 08907 L'Hospitalet de Llobregat, Spain; E-mail: 8082ifa@gmail.com

This study was supported by grants from CIBERNED and PI17/00809 Institute of Health Carlos III, and cofunded by FEDER funds/European Regional Development Fund (ERDF)—a way to build Europe; ALS intraCIBERNED project to IF; IF115/00035 fellowship to PA-B; Fundació Miquel Valls, and "Retos todos unidos contra la ELA" and "Proyecto DGeneración conexiones con sentido" to MP.

The authors have no duality or conflicts of interest to declare.

Key Words: Amyotrophic lateral sclerosis, Biomarkers, Dynein axonemal assembly factor 1, LRRC50, Motor-neurons, Spinal cord.

INTRODUCTION

Neuronal microtubules are intracellular structures that facilitate a myriad of neuronal functions, including activity-dependent axonal transport (1), which is governed by the dynein/kinesin system (2, 3). Anterograde transport, mediated by kinesins, supplies distal axons with newly synthesized proteins and lipids, including synaptic components required to maintain presynaptic activity, whereas retrograde transport, mediated by dyneins, is required to maintain homeostasis by removing aging proteins and organelles from the distal axon for degradation and recycling of components (1, 3).

Dynein is a dimer composed of the motor-containing heavy chain and the distal tail formed by intermediate chains, light intermediate chains, and light chains. The motor domain is in the C-terminus and is responsible for microtubule binding, inasmuch as the N-terminal tail domain is responsible for dimerization, dynein interaction with other proteins (e.g. dynactin), and cargo interaction (3–6).

Amyotrophic lateral sclerosis (ALS) is a multifactorial disease characterized by the degeneration of motor neurons, their axons, and neuromuscular synapses (7, 8). Microtubule alterations, including abnormal kinesin/dynein and related interactors, are critical factors in the pathogenesis of this disease (9–18). In addition, Golgi complex disruption results from abnormal dynein/dynactin interactions (6). Since recent transcriptomics observations have identified significant reduction in the expression of a cluster involving several axonemal dynein transport components in the anterior horn of the spinal cord (SC) in sporadic ALS (sALS) (19), the ensuing study analyzes dynein axonemal assembly factor 1 (*DNAAF1*) and leucine-rich repeat-containing protein 50 (LRRC50), the corresponding encoded protein, in lower motor neurons in sALS compared with controls. LRRC50 is a dynein up-stream effector that participates in the cytoplasmic preassembly of dynein arms and is involved in the regulation of microtubule-based cilia and actin-based brush border microvilli. Different mutations in LRRC50 result in distinct clinical syndromes,

including abnormal assembly of cilia in respiratory epithelia producing primary ciliary dyskinesia, altered cardiac laterality, and polycystic kidney (20–22). The distribution and localization of LRRC50 in the nervous system is not known. The present study has identified LRRC50 in C-boutons of motor neurons of the SC and selected motor nuclei of the brain stem in sALS, and decreased LRRC50 immunoreactivity in sALS and in SOD1 transgenic mice as a model of unrelated motor neuron disease.

MATERIALS AND METHODS

Human Tissue Samples

Paraffin-embedded postmortem fresh-frozen and 4% formalin-fixed samples of the lumbar SC and medulla oblongata were obtained from the Institute of Neuropathology HUB-ICO-IDIBELL Biobank following the guidelines of the Spanish legislation (Real Decreto de Biobancos 1716/2011) and the approval of the local ethics committee of the Bellvitge University Hospital-Institute of Biomedical Research IDIBELL. The postmortem interval between death and tissue processing was from 2 to 17 hours. Transversal sections of the SC were alternatively frozen at –80°C or fixed by immersion in 4% buffered formalin. Age-matched control cases had not suffered from neurologic or psychiatric diseases and did not have neuropathologic lesions. Genetic testing, using genomic DNA isolated from blood or brain tissue, revealed no mutations in the chromosome 9 open reading frame (*C9orf72*), superoxide dismutase 1 (*SOD1*), TAR DNA binding protein (*TARDBP*), or FUS RNA binding protein (*FUS*). Cases in the present series used for biochemical studies (i.e. quantitative reverse transcription PCR [RT-qPCR]) are summarized in the Table. Cases used for immunohistochemical studies did not correspond always with those of the biochemical series; this group was composed of 16 sALS 10 age-matched controls as described in the corresponding section. Variable numbers of TDP-43-P-immunoreactive neuronal and oligodendroglial inclusions and neuropil threads were found in the anterior horn of the SC in every ALS case. Neuronal inclusions were small, round intracytoplasmic deposits, large globular inclusions and skein-like inclusions. Neuronal inclusions were present in only ~20% of the remaining motor neurons in ALS.

TABLE. Summary of Cases Used for Biochemical Study

Case	Age	Gender	Diagnosis	PM Delay	Initial Symptoms	RIN Value SC
1	59	M	Control	12 h 05 min	–	6.4
2	43	M	Control	05 h 55 min	–	6.6
3	47	M	Control	04 h 55 min	–	5.6
4	64	F	Control	11 h 20 min	–	6.2
5	46	M	Control	15 h 00 min	–	5.9
6	56	M	Control	07 h 10 min	–	6.1
7	71	F	Control	08 h 30 min	–	5.9
8	64	F	Control	05 h 00 min	–	7.0
9	79	F	Control	06 h 25 min	–	6.7
10	75	M	Control	07 h 30 min	–	5.0
11	55	M	Control	09 h 45 min	–	5.3
12	76	M	Control	06 h 30 min	–	6.6
13	51	F	Control	04 h 00 min	–	6.3
14	56	M	sALS	10 h 50 min	N/A	7.1
15	70	M	sALS	03 h 00 min	Respiratory	7.3
16	77	M	sALS	04 h 30 min	N/A	7.4
17	56	F	sALS	03 h 45 min	N/A	8.2
18	59	M	sALS	03 h 15 min	N/A	7.5
19	63	F	sALS	13 h 50 min	Bulbar	6.8
20	59	F	sALS	14 h 15 min	N/A	6.4
21	64	M	sALS	16 h 30 min	N/A	6.3
22	57	F	sALS	04 h 00 min	Bulbar	6.2
23	75	F	sALS	04 h 05 min	Bulbar	6.8
24	79	F	sALS	02 h 10 min	N/A	7.0
25	57	F	sALS	10 h 00 min	Bulbar	6.5
26	46	M	sALS	07 h 00 min	Spinal	7.0
27	69	F	sALS	17 h 00 min	Spinal	6.4

Abbreviations: sALS, sporadic amyotrophic lateral sclerosis cases; M, male; F, female; PM delay, postmortem delay (hours, minutes); N/A, not available; RIN, RNA integrity number.

Animal Model hSOD1-G93A

Transgenic mice expressing high copy numbers of the mutated form of human SOD1 (hSOD1), B6SJL-Tg(SOD1*G93A)1Gur/J (*hSOD1-G93A*) were obtained from The Jackson Laboratories (Bar Harbor, ME). The colony was maintained by breeding male hemizygous carriers with nontransgenic B6SJL females. Offspring were identified by PCR, and non-transgenic G93A littermates were used as wild-type controls. In addition, unrelated WT mice were examined. Animals were maintained under standard animal housing conditions (static isolation caging, 3–4 animals per cage) in a 12-hour dark-light cycle with free access to food and water. The first series of immunohistochemical studies was performed on 5 *hSOD1-G93A* mice, 3 control littermates, and 3 WT aged 150 days. The second series of histochemical studies was carried out on the SCs of 5 animals per stage: 90 days (preclinical), 120 (early clinical), and 150 (late clinical). Genotyped mice were dissected for immunohistochemical studies. All the procedures were carried out after the approval of the Animal Ethics Committee of the University of LLeida.

RNA Extraction and RT-qPCR

RNA from dissected human frozen anterior horn of the lumbar SC of 14 sALS (mean age 61 years; 6 men and 8 women) and 13 age-matched controls (mean age 59 years; 8 men and 5 women) was extracted following the instructions of the supplier (RNeasy Mini Kit, Qiagen, Hilden, Germany). RNA integrity and 28S/18S ratios were determined with the Agilent Bioanalyzer (Agilent Technologies, Santa Clara, CA) to assess RNA quality, and the RNA concentration was evaluated using a NanoDrop Spectrophotometer (Thermo Fisher Scientific, Waltham, MA). Complementary DNA (cDNA) preparation used the High-Capacity cDNA Reverse Transcription kit (Applied Biosystems, Foster City, CA) following the protocol provided by the supplier. Parallel reactions for each RNA sample were run in the absence of MultiScribe Reverse

Transcriptase to assess the lack of contamination of genomic DNA. TaqMan RT-qPCR assays for *DNAAF1* (Hs00698399_m1) were performed as detailed elsewhere (19). Hypoxanthine-guanine phosphoribosyltransferase (*HPRT1*) was used as internal control for normalization of SC samples. The double-delta cycle threshold (ΔΔCT) method was utilized to determine the fold change values. The obtained data were analyzed with the *t*-test.

Immunohistochemistry

Dewaxed 4-µm-thick sections of the SC and medulla oblongata in human cases and SC in mice were processed for immunohistochemistry. The human series included 16 sALS (mean age 57 years; 6 men and 8 women) and 10 age-matched controls (mean age 62 years; 6 men and 4 women). Immunohistochemistry in murine SCs was performed in 5 × 3 transgenic mice (5 animals at the ages of 90, 120, and 150 days) and 3 × 2 controls (3 control littermates and 3 WT aged 150 days). The sections were boiled in citrate buffer (20 minutes) to retrieve protein antigenicity. Endogenous peroxidases were blocked by incubation in 10% methanol-1% H_2O_2 solution (15 minutes) followed by 3% normal horse serum solution. Then the sections were incubated at 4°C overnight with one of the primary antibodies: LRRC50 (1/200, polyclonal rabbit, Abcam, Cambridge, UK); vesicular acetylcholine transporter: VAChT (1/100, polyclonal guinea pig, Synaptic Systems, Goettingen, Germany); and sigma 1 receptor: S1R (1/100, monoclonal mouse, Santa Cruz Biotechnology, Santa Cruz, CA). Following incubation with the primary antibody, the sections were incubated with EnVision + system peroxidase (Dako, Agilent Technologies) for 30 minutes at room temperature. The peroxidase reaction was visualized with diaminobenzidine and H_2O_2. Control of the immunostaining included omission of the primary antibody; no signal was obtained following incubation with only the secondary antibodies. No positive controls were used.

Double-Labeling Immunofluorescence and Confocal Microscopy

Dewaxed 4-µm-thick sections of human and mouse control SCs were stained with a saturated solution of Sudan black B (Merck, Glostrup, Denmark) for 15 minutes to block the autofluorescence of lipofuscin granules present in cell bodies, and then rinsed in 70% ethanol and washed in distilled water. The sections of human cases were incubated at 4°C overnight with double combinations (double-labeling) of LRRC50 (1/200, polyclonal rabbit, Abcam, Cambridge, UK) and VAChT (1/100, polyclonal guinea pig, Synaptic Systems) or S1R (1/100, monoclonal mouse, Santa Cruz Biotechnology) or synaptophysin (monoclonal mouse antibody used at 1/500, Leica Biosystems, Wetzlar, Germany) or TDP43-P Ser409/Se410 (1:200, MABN14 rat, Millipore, Burlington, MA). Other sections were triple labeled with LRRC50, VAChT, and S1R. The sections of mice were processed for double-labeling immunofluorescence with antiLRRC50 and antiS1R antibodies. After washing, the sections were incubated with the respective fluorescence secondary antibodies Alexa555, Alexa488, and/or Alexa657 (1:400, Molecular Probes, Eugene, OR) against the corresponding host species. Nuclei were stained with DRAQ5 (dilution 1:2000, BioStatus, Loughborough, UK). After washing, the sections were mounted in Immuno-Fluore mounting medium (ICN Biomedicals, Irvine, CA), sealed, and dried overnight. Sections were examined with a Leica TCS-SL confocal microscope. Control of the immunostaining included omission of the primary antibody; no signal was obtained following incubation with only the secondary antibodies.

Quantification and Statistical Analysis

Quantification of LRRC50 expression in human histological sections was made directly from the ocular of the microscope at a magnification of ×200 by counting the number of motor-neurons containing LRRC50-positive boutons in (i) the whole anterior horn of the lumbar SC, (ii) motor nucleus of the vagus nerve, and (iii) hypoglossal nucleus (HN) in 3 different sections separated 100 µm for every region in every sALS and control case. A similar approach was used to quantify motor-neurons with VAChT- and S1R-positive structures. Quantitative studies in mice were carried out only in the ventral horn of the SC following the same protocol. Quantification was made by one person blinded to the clinical status. The normality of distribution of counted cell number was analyzed with the Kolmogorov-Smirnov test. The unpaired *t*-test was performed to compare each group when values followed a normal distribution. Statistical analysis and graphic design were performed with GraphPad Prism version 5.01 (La Jolla, CA). Results were analyzed with the Student *t*-test. Outliers were detected using the GraphPad software QuickCalcs ($p < 0.05$). The data were expressed as mean ± SEM and significance levels were set at $*p < 0.05$, $**p < 0.01$, and $***p < 0.001$.

ELISA in CSF

Samples were obtained from sALS patients and controls as detailed elsewhere (23). CSF (1.5 ± 0.5 mL) was collected in polypropylene tubes as part of the clinical routine investigation. CSF was centrifuged at 3000 rpm for 15 minutes at room temperature. Supernatant was collected and aliquoted in volumes of 250 µL and stored at –80°C until use. All samples were analyzed after one freeze/thaw cycle. Quantification of LRRC50 was performed using the Human Dynein assembly factor 1, axonemal, LRRC50 ELISA Kit (Catalogue N° MBS9317767, MyBiosource, San Diego, CA) following the manufacturer's instructions.

RESULTS

In agreement with a previous study (19), *DNAAF1* mRNA expression levels in the anterior horn of the SC were significantly reduced in sALS compared with controls ($p = 0.019$; Fig. 1A).

LRRC-50 immunoreactivity in the human control SC and brainstem was restricted to immunoreactive boutons in motor neurons, and walls in the blood vessels. Such boutons were elongated, oval-shaped, 1–5 µm in length, and mainly localized at the periphery of the cytoplasm near the plasma

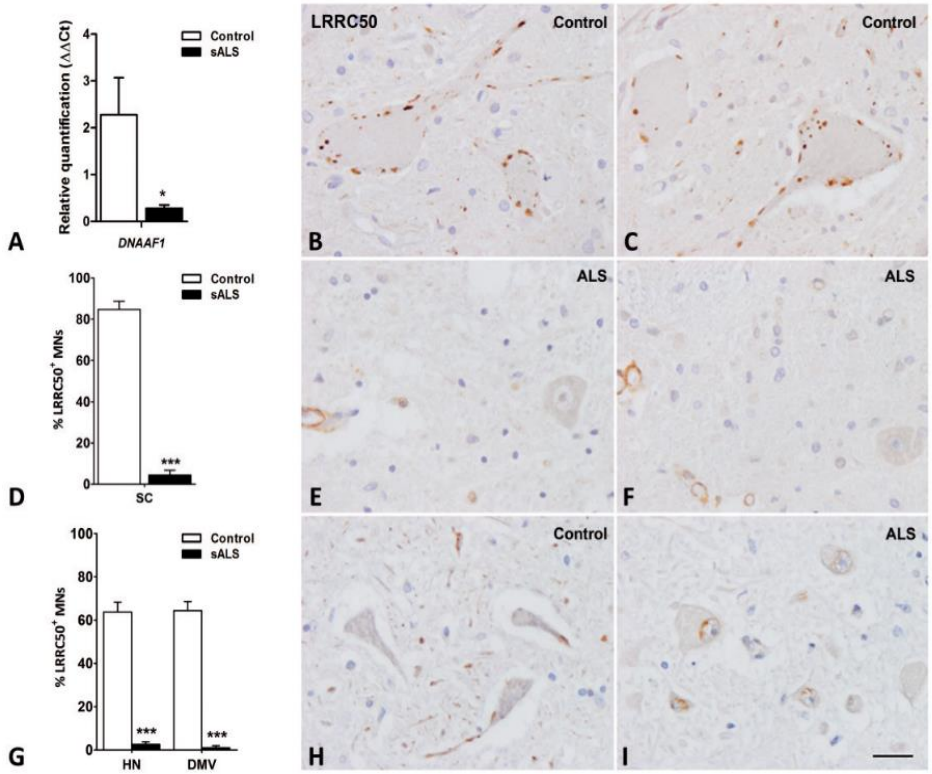

FIGURE 1. *DNAAF1* and LRRC50 expression in human control and sALS lower motor neurons. **(A)** Reduced *DNAAF1* mRNA expression in the anterior horn of the lumbar spinal cord in sALS compared with age-matched controls. **(B, C)** LRRC50 immunoreactivity in anterior horn motor neurons in controls identifies oval-shaped structures (boutons) at the periphery of the cytoplasm and proximal dendrites. **(D)** The percentage of motor neurons with LRRC50-immunoreactive dots is significantly decreased in the anterior horn of the spinal cord (SC) in sALS when compared with controls. **(E, F)** This decrease is due to the almost total absence of LRRC50-positive boutons in the remaining sALS motor neurons. **(G)** Similar reduction is found in the hypoglossal nucleus (HN) and motor nucleus of the vagus nerve (DNV) in sALS when compared with controls. **(H, I)** Representative images of the motor nucleus of the vagus nerve in control and sALS showing marked reduction, almost absence of LRRC50-immunoreactive boutons. Note perinuclear LRRC50 immunoreactivity in some motor neurons in sALS (arrows) but not in controls. LRRC50 immunoreactivity is also present in capillaries (ca). Paraffin sections slightly counterstained with hematoxylin; scale bar = 25 μm. Unpaired *t*-test, $*p < 0.05$, $***p < 0.001$.

membrane of the cell body and proximal dendrites (Fig. 1B, C). The number of LRRC50-immunoreactive boutons per neuron was as high as twenty-five in a single paraffin section. However, the number of LRRC50-immunoreactive boutons was markedly reduced in the remaining motor neurons in the anterior horn of the SC in sALS cases ($p = 1.10 \times 10^{-18}$; Fig. 1D–F). Similar LRRC50-immunoreactive boutons were found in contact with the cytoplasm and proximal dendrites of motor neurons in the dorsal motor nucleus of the vagus nerve and the HN in control cases, but their number was smaller in comparison with anterior horn motor neurons. A similar reduction in the number of LRRC50-immunoreactive boutons was found in the remaining motor neurons in the dorsal motor nucleus of the vagus nerve ($p = 1.2 \times 10^{-7}$) and in the HN ($p = 4.3 \times 10^{-8}$) in sALS (Fig. 1G–I). Curiously, LRRC50 in several motor neurons in sALS had a perinuclear distribution instead of its presence in boutons (Fig. 1I).

In contrast to the motor nuclei of the hypoglossal nuclei and vagus nerves, LRRC50-positive boutons were absent in the oculomotor nuclei of the brainstem in normal (control) brains (data not shown).

LRRC50 structures were similar in morphology to C-boutons on motor neurons of the spinal horn, as revealed by vesicular acetylcholine transporter (VAChT) and sigma 1 receptor (S1R) immunohistochemistry (Fig. 2). Moreover, VAChT- and S1R-positive motor neuron boutons were largely decreased in sALS cases ($p = 8.75 \times 10^{-6}$ and $p = 1.15 \times 10^{-12}$, respectively; Fig. 2E, H).

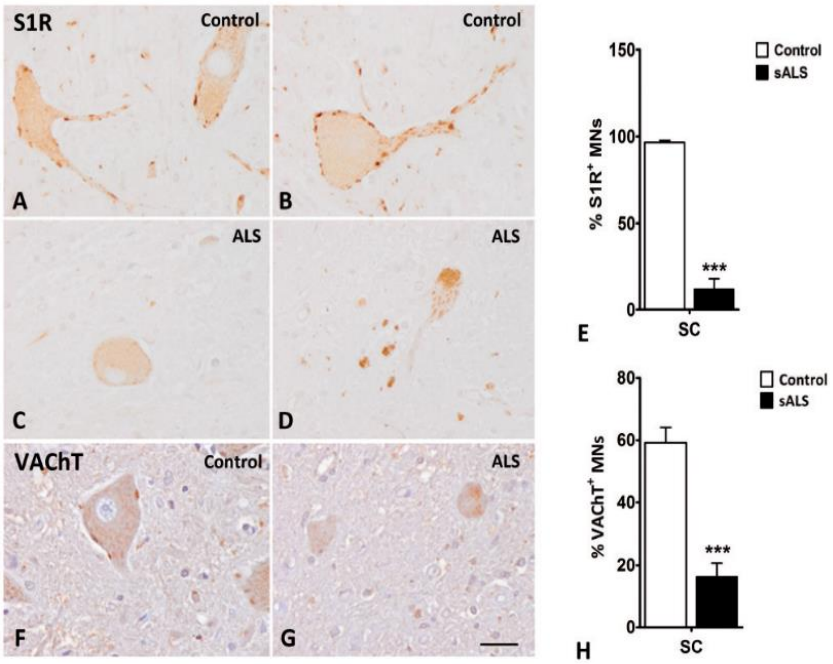

FIGURE 2. Sigma 1 receptor (S1R) and vesicular acetylcholine transporter (VAChT) immunoreactivity in motor neurons of the spinal cord in control and sALS. **(A, B)** S1R-immunoreactive C-boutons are found at the surface of the cytoplasm and proximal dendrites in controls. **(C, D)** Immunoreactive C-boutons practically disappear in the remaining motor neurons in sALS. **(E)** The graph illustrates that the percentage of neurons with S1R-positive C-boutons is significantly decreased in sALS compared with controls. **(F, G)** Representative images of VAChT-immunoreactive C-boutons in control and ALS; remaining ALS motor neurons are almost devoid of VAChT C-boutons. **(H)** The graph illustrates the significant reduction of the percentage of neurons with VAChT-positive C-boutons in sALS compared with controls. Paraffin sections slightly counterstained with hematoxylin; scale bar = 25 μm. Unpaired *t*-test, ***$p < 0.001$.

Double- and triple-labeling immunofluorescence to LRRC50 and S1R, VAChT, and synaptophysin in controls showed that LRRC50-immunoreactive boutons colocalized or were in close contact with VAChT or with S1R and synaptophysin-immunoreactive C-boutons (Fig. 3), thus supporting the idea that LRRC50 was a component of C-boutons. Double-labeling immunofluorescence and confocal microscopy to LRRC50 and TDP-43-P showed that loss of C-boutons was found equally in neurons with and without TDP-43-P-imunoreactive inclusions. This was not unexpected as TDP-43-P inclusions were observed in a minority of remaining motor neurons in ALS whereas loss of LRRC50 boutons was generalized in the anterior horn of the SC in ALS (data not shown).

Motor neurons of the SC in control mice (SOD1 littermates and WT mice) showed similar oval or round LRRC50-immunoreactive structures in the cytoplasm (Fig. 4). LRRC50-positive structures were in close proximity or colocalized with S1R as revealed by double-labeling immunofluorescence and confocal microscopy (Fig. 4). No differences were seen between control littermates and WT mice at the age of 150 days. However, LRRC50 positivity was significantly decreased in motor neurons in *hSOD1-G93A* transgenic mice aged 150 days ($p = 0.001$; Fig. 4).

To learn whether loss of LRRC50 immunoreactivity was an early or a late event in the progression of motor neuron degeneration, *hSOD1-G93A* transgenic mice at preclinical and early clinical stages, 90 and 120 days old, respectively, were examined. As shown in Figure 5, the number of positive structures per neuron was already decreased at the age of 90 days (preclinical stage) in hSOD1-G93A transgenic mice compared with controls ($p = 0.03$). The reduction was still noted at the age of 120 days although it was not significant ($p = 0.14$).

Finally, to test whether LRRC50 in the CSF might serve as a complementary biomarker in sALS, LRRC50 levels were measured using a commercial quantitative sandwich ELISA kit. The detection range was from 3.12 ng/mL to 100 ng/mL. Levels of LRRC50 were not detectable in the CSF of controls and sALS cases.

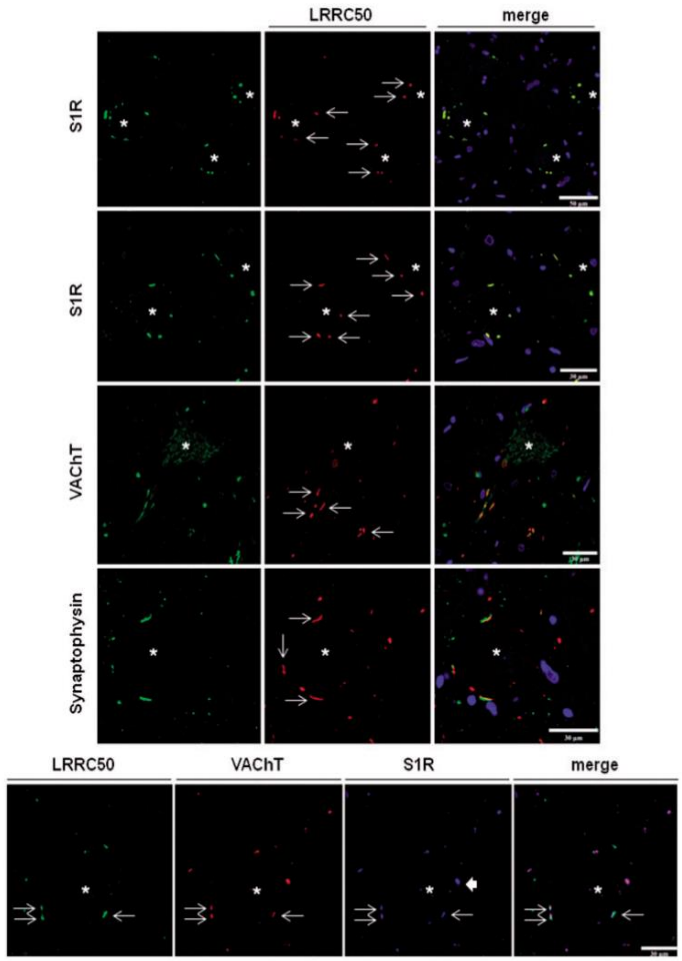

FIGURE 3. Double-labeling (upper panel) and triple-labeling (lower panel) immunofluorescence and confocal microscopy to LRRC50 and sigma 1 receptor (S1R), vesicular acetylcholine transporter (VAChT) or synaptophysin (SYN) in normal motor neurons of the human lumbar spinal cord. Upper panel: LRRC50-immunoreactive boutons (red) colocalize S1R-immunoreactive C-boutons (green), VAChT-positive C-boutons (green), and large synaptophysin terminals (green) at the periphery of the cytoplasm and proximal dendrites (arrows) of motor neurons (asterisks). Merge shows, in addition, nuclei stained with DRAQ5 (blue). Lower panel: LRRC50 (green) colocalizes VAChT (red) and S1R (blue) in C-boutons (long arrows: merge: white); some structures colocalize VAChT and S1R but not VAChT (thick arrow). Paraffin sections; scale bar = 30 μm except upper row in which bar = 50 μm.

DISCUSSION

Dynein processing and localization varies in different cell types and clusters in distinct subcellular organelles (24–27). In the central nervous system, dyneins are largely localized at the axon terminals (27). Dynein assembly is modulated by a heterogeneous group of DNAAFs that act, in most instances, in combination with particular chaperones to promote cytoplasmic pre-assembly of dyneins (28–33). Mutations in certain DNAAFs such as *NADYX1C1*, *ZYYND10*, *C11orf70* (encoding CFAP300: cilia and flagella associated protein 300), and *PIH1D3*result in abnormal dynein assembly (30, 34–40). Likewise, mutations in *DNAAF1* result in abnormal assembly of cilia in respiratory epithelia, infertility, altered cardiac laterality, and polycystic kidney (20–22).

The present study identifies the presence of LRRC50-immunoreactive boutons at the surface of motor neurons of the

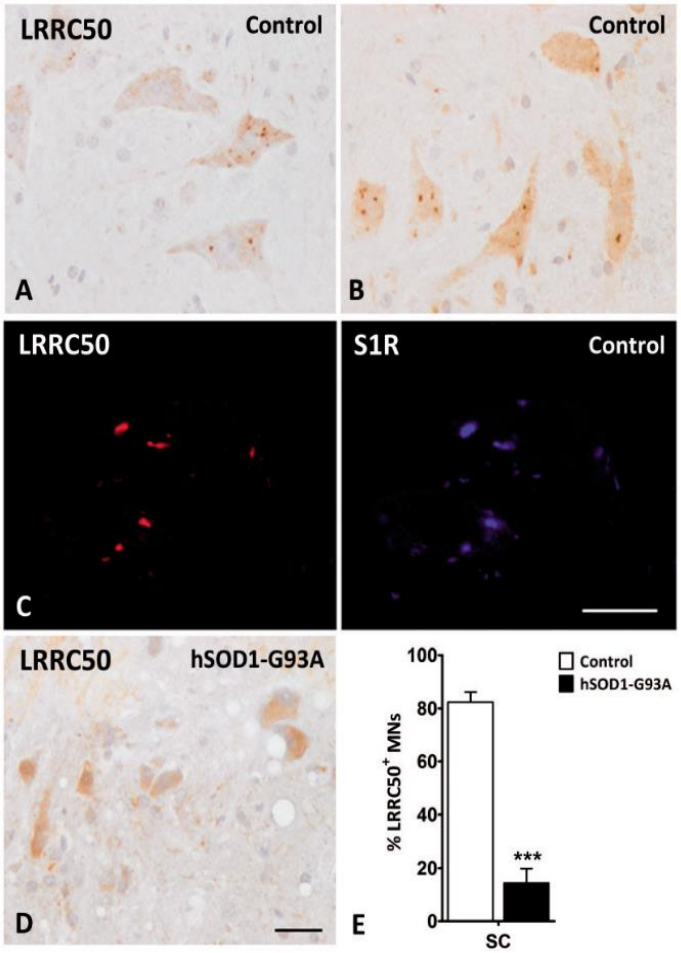

FIGURE 4. LRRC50-immunoreactive boutons in motor neurons of the spinal cord in mice. **(A, B)** LRRC-50 immunoreactivity is found in cytoplasmic structures in control mice. **(C)** Double-labeling immunofluorescence and confocal microscopy depicts close proximity and partial colocalization of LRRC50 (green) and S1R (red) immunoreactivity. **(D)** LRRC50 immunoreactivity is almost depleted in motor neurons in *hSOD1-G93A* transgenic mice aged 150 days (clinical stage). **(E)** Quantification of motor-neurons with LRRC50-positive structures is significantly reduced in transgenic mice when compared with wild type littermates. Unpaired *t*-test: ***$p < 0.001$. Paraffin sections; scale bars: **A**, **B**, **D**, bar = 25 μm; **C** = 15 μm.

SC and motor nuclei of the brain stem in humans and mice, which are identified as C-boutons on the basis of single immunohistochemistry, and double- and triple-labeling immunofluorescence and confocal microscopy. C-boutons are pre-synaptic terminals of cholinergic interneurons localized in the SC and in most of the motor nuclei of the cranial nerves excepting the oculomotor nuclei of the brainstem (41–47). They contain VAChT and synaptic vesicle markers, and are in contact with postsynaptic components including M2 muscarinic receptors and S1R; neuregulin 1-ErB retrograded signaling is also differentially compartmentalized in C-type boutons (43, 46–49). Cholinergic interneurons modulate motor neuron activity through C-boutons (43–45, 50). On the basis of the present findings, LRRC50 may be considered a component of C-boutons involved in dynein assembly and retrograde axonal transport.

In agreement with our previous gene transcription observations, *DNAAF1* mRNA expression is reduced in the SC anterior horn in sALS cases. Reduced *DNAAF1* mRNA expression can be the result of mere motor neuron demise. However, LRRC50 immunoreactivity is drastically reduced at the surface of the remaining spinal and bulbar motor neurons, in parallel with reduced numbers of C-boutons, in sALS.

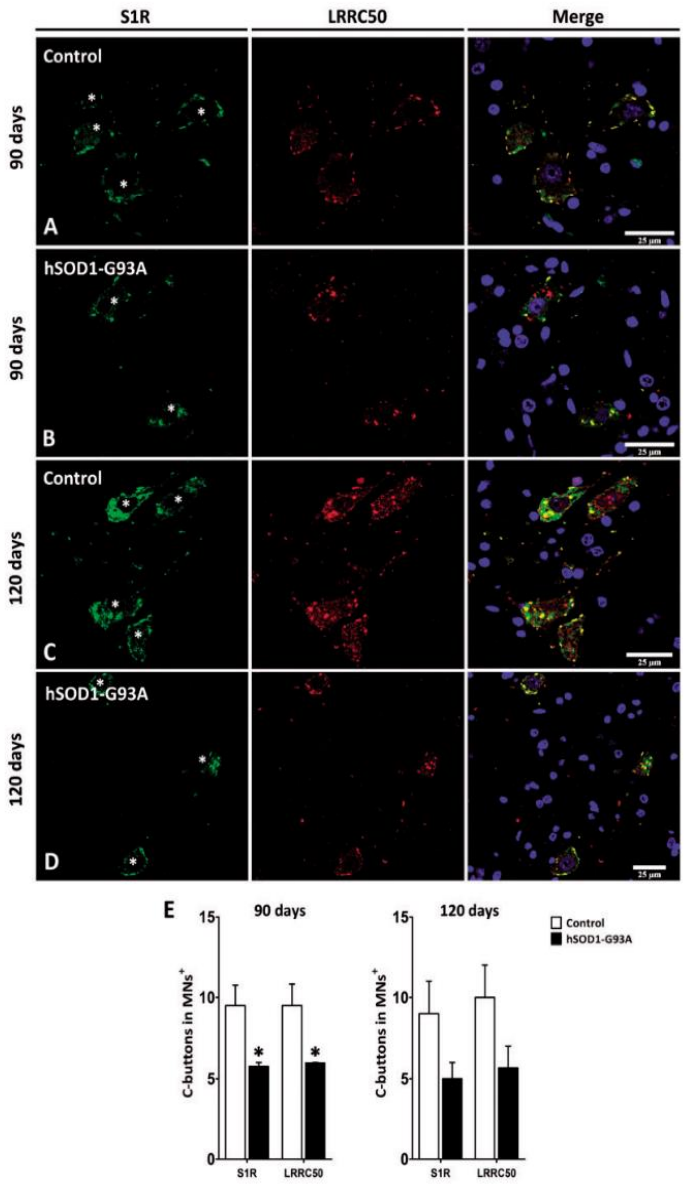

FIGURE 5. LRRC50 (red) and S1R (green) immunoreactivity in motor-neurons of the ventral horn of the spinal cord in control and *hSOD1-G93A* transgenic mice aged 90 **(A, B)** and 120 **(C, D)** days. LRRC50 and S1R immunoreactivity is decreased in transgenic animals when compared with controls **(A–D)**, although some LRRC50- and S1R-positive structures are still present in neurons in transgenic mice. Asterisks indicate the localization of the cytoplasm of motor neurons. **(E)** Quantitative studies show a significant decrease in the number of LRRC50- and S1R-immunoreactive structures in transgenic mice aged 90 days (preclinical stage) and a trend at the age of 120 days when compared with control littermates. Unpaired *t*-test: *$p < 0.05$. Paraffin sections; scale bar = 25 μm.

Therefore, LRRC50 reduction is not the mere reflection of motor neuron demise but a reduction in the number of LRRC50-immunoreactive boutons in the remaining motor neurons in sALS.

This decline occurs independently of the aberrant formation of TDP-43-immunoreactive inclusions in certain motor neurons in classical sALS (7, 8). This decline neither corelates with the appearance of dynein-dynactin-immunoreactive deposits in motor neurons, which are also not related with skein-like inclusions, in the SC in sALS (51). However, LRRC50 reduction in C-boutons is accompanied by perinuclear LRRC50 immunoreactivity in some remaining motor neurons thus suggesting some kind of alteration in the transport of this protein.

Loss of cholinergic synapses in the SC motor-neurons in sALS was reported many years ago (52). That pioneering observation was not studied further in humans but was partially refuted in SOD1 transgenic mice (53, 54). This is due in part to the different markers used to detect C-boutons in SOD1 transgenic mice. A significant increase in the number of NRG1-positive boutons was observed at the beginning of the symptomatic stage which was followed by a marked decrease at end stages of the disease. A similar pattern occurred for VAChT boutons, but some motor-neurons depleted of VAChT-immunoreactive boutons showed high numbers of NRG1-positive dots (46). Our present observations show a marked reduction in LRRC50-immunoreactive boutons in motor neurons of the ventral horn in *hSOD1-G93A* transgenic mice aged 150 days which is accompanied by a parallel decrease in, but not the absence of, S1R-immunoreactive boutons. The presence of the remaining S1R seems to be protective of motor neurons, as the knocking-out of S1R in *hSOD1-G93A* transgenic mice exacerbates motor neuron disease progression in these animals (55). Early pre-symptomatic alterations in C-boutons has been reported in SOD1(G93A) tg mice (56). Interestingly, viral-mediated delivery of type III-NRG1 to the SC restores the number of C-boutons and extends the survival time of SOD1-ALS mice (57).

Our combined study in human sALS not linked to SOD1 mutations and in transgenic mice bearing high copy numbers of the mutated form of human SOD1 show common responses regarding C-boutons in motor neurons. The number of LRRC50-immunoreactive structures is decreased in motor neurons in both paradigms. To learn whether observed alterations in ALS are early or late events, transgenic mice at preclinical, early clinical and late clinical stages were examined. A decrease in LRRC50 immunoreactivity occurs at preclinical stages in hSOD1-G93A transgenic mice, suggesting that LRRC50 alteration is an early event in the course of the disease. A trend to decrease is observed at the age of 120; lack of significance can be due to the relative low number of animals examined or to a transient attempt to compensation. However, a significant decrease is manifested at the age of 150 days.

The pattern of C-bouton response in sALS and Tg mice differs from that seen after nerve peripheral nerve axotomy in mice. Reduced expression of VAChT and NRG1 immunoreactivity together with a reduction in size of C-boutons starting at 24 hours is followed by practical recovery by 30 days postlesion (47, 58). Therefore, the changes observed here in motor neuron disease are hardly due to peripheral axotomy.

Whether LRRC50 in motor neurons is essential for the maintenance of C-boutons cannot be addressed by neuropathological approach. Yet this is an important point for understanding the role of this protein in motor neuron maintenance and neurodegeneration.

ACKNOWLEDGMENTS

We wish to thank B. Torrejón Escribano for technical help with the confocal microscopy and T. Yohannan for editorial assistance.

REFERENCES

1. Maday S, Twelvetrees AE, Moughamian AJ, et al. Axonal transport: Cargo-specific mechanisms of motility and regulation. Neuron 2014;84: 292–309
2. Hirokawa N, Niwa S, Tanaka Y. Molecular motors in neurons: Transport mechanisms and roles in brain function, development and disease. Neuron 2010;68:610–38
3. Roberts AJ, Kon T, Knight PJ, et al. Functions and mechanics of dynein motor proteins. Nat Rev Mol Cell Biol 2013;14:713–26
4. Vallee RB, McKenney RJ, Ori-McKenney KM. Multiple modes of cytoplasmic dynein regulation. Nat Cell Biol 2012;14:224–30
5. Carter AP. Crystal clear insights into how the dynein motor moves. J. Cell Sci 2013;126:705–13
6. Jaarsma D, Hoogenraad CC. Cytoplasmic dynein and its regulatory proteins in Golgi pathology in nervous system disorders. Front Neurosci 2015;9:e397
7. Strong MJ, Hortobágyi T, Okamoto K, et al. Amyotrophic lateral sclerosis, primary lateral sclerosis, and spinal muscular atrophy. In: Dickson DW, Weller RO, eds. Neurodegeneration: The Molecular Pathology of Dementia and Movement Disorders. 2nd edn. Oxford: Wiley-Blackwell 2011:418–33
8. Ince PG, Highley JR, Wharton SB. Motor neuron disorders. In: Love S, Budka H, Ironside JW, Perry A, eds. Greenfield's Neuropathology. 9th edn. Boca Raton: CRC Press, Taylor and Francis Group 2015:817–48
9. LaMonte BH, Wallace KE, Holloway BA, et al. Disruption of dynein/dynactin inhibits axonal transport in motor neurons causing late-onset progressive degeneration. Neuron 2002;34:715–27
10. Hafezparast M, Klocke R, Ruhrberg C, et al. Mutations in dynein link motor neuron degeneration to defects in retrograde transport. Science 2003;300:808–12
11. Münch C, Sedlmeier R, Meyer T, et al. Point mutations of the p150 subunit of dynactin (DCTN1) gene in ALS. Neurology 2004;63:724–6
12. Bruijn LI, Miller TM, Cleveland DW. Unraveling the mechanisms involved in motor neuron degeneration in ALS. Annu Rev Neurosci 2004; 27:723–49
13. Ligon LA, LaMonte BH, Wallace KE, et al. Mutant superoxide dismutase disrupts cytoplasmic dynein in motor neurons. NeuroReport 2005;16: 533–6
14. Levy JR, Holzbaur E. Cytoplasmic dynein/dynactin function and dysfunction in motor neurons. Int J Dev Neurosci 2006;24:103–11
15. Teuling E, van Dis V, Wulf PS, et al. A novel mouse model with impaired dynein/dynactin function develops amyotrophic lateral sclerosis (ALS)-like features in motor neurons and improves lifespan in SOD1-ALS mice. Hum Mol Genet 2008;17:2849–62
16. Deng W, Garrett C, Dombert B, et al. Neurodegenerative mutation in cytoplasmic dynein alters its organization and dynein-dynactin and dynein-kinesin interactions. J Biol Chem 2010;285:39922–34
17. Kuźma-Kozakiewicz M, Chudy A, Kaźmierczak B, et al. Dynactin deficiency in the CNS of humans with sporadic ALS and mice with genetically determined motor neuron degeneration. Neurochem Res 2013;38: 2463–73
18. Ikenaka K, Kawai K, Katsuno M, et al. Dnc-1/dynactin 1 knockdown disrupts transport of autophagosomes and induces motor neuron degeneration. PLoS One 2013;8:e54511

19. Andrés-Benito P, Moreno J, Aso E, et al. Amyotrophic lateral sclerosis, gene deregulation in the anterior horn of the spinal cord and frontal cortex area 8: Implications in frontotemporal lobar degeneration. Aging 2017;9:823–51
20. Van Rooijen E, Giles RH, Voest EE, et al. LRRC50, a conserved ciliary protein implicated in polycystic kidney disease. J Am Soc Nephrol 2008; 19:1128–38
21. Loges NT, Olbrich H, Becker-Heck A, et al. Deletions and point mutations of LRRC50 cause primary ciliary dyskinesia due to dynein arm defects. Am J Hum Genet 2009;85:883–9
22. Hartill VL, van de Hoek G, Patel MP, et al. DNAAF1 links heart laterality with the AAA+ ATPase RUVBL1 and ciliary intraflagellar transport. Hum Mol Genet 2018;27:529–45
23. Andrés-Benito P, Domínguez R, Colomina MJ, et al. YKL40 in sporadic amyotrophic lateral sclerosis: Cerebrospinal fluid levels as a prognosis marker of disease progression. Aging (Albany NY) 2018;10:2367–82
24. Vancoillie G, Lambert J, Mulder A, et al. Cytoplasmic dynein colocalizes with melanosomes in normal human melanocytes. Br J Dermatol 2000; 143:298–306
25. Chuang JZ, Milner TA, Sung CH. Subunit heterogeneity of cytoplasmic dynein: Differential expression of 14 kDa dynein light chains in rat hippocampus. J Neurosci 2001;21:5501–12
26. Jha R, Surrey T. Regulation of processive motion and microtubule localization of cytoplasmic dynein. Biochem Soc Trans 2015;43:48–57
27. Twelvetrees AE, Pernigo S, Sanger A, et al. The dynamic localization of cytoplasmic dynein in neurons is driven by kinesin-1. Neuron 2016;90: 1000–15
28. Omran H, Kobayashi D, Olbrich H, et al. Ktu/PF13 is required for cytoplasmic pre-assembly of axonemal dyneins. Nature 2008;456:611–6
29. Kott E, Duquesnoy P, Copin B, et al. Loss of zinc finger MYND-type containing 10 (zmynd10) affects cilia integrity and axonemal localization of dynein arms, resulting in ciliary dysmotility, polycystic kidney and scoliosis in medaka (*Oryzias latipes*). Dev Biol 2017;430:69–79
30. Tarkar A, Loges NT, Slagle CE, et al. DYX1C1 is required for axonemal dynein assembly and ciliary motility. Nat Genet 2013;45:995–1003
31. Inaba Y, Shinohara K, Botilde Y, et al. Transport of the outer dynein arm complex to cilia requires a cytoplasmic protein Lrrc6. Genes Cells 2016; 21:728–39
32. Jaffe KM, Grimes DT, Schottenfeld-Roames J, et al. c21orf59/kurly controls both cilia motility and polarization. Cell Rep 2016;14:1841–9
33. Mali GR, Yeyati PL, Mizuno S, et al. ZMYND10 functions in a chaperone relay during axonemal dynein assembly. eLife 2018;7:e34389
34. Moore DJ, Onoufriadis A, Shoemark A, et al. Mutations in ZMYND10, a gene essential for proper axonemal assembly of inner and outer dynein arms in humans and flies, cause primary ciliary dyskinesia. Am J Hum Genet 2013;93:346–56
35. Zariwala MA, Gee HY, Kurkowiak M, et al. ZMYND10 is mutated in primary ciliary dyskinesia and interacts with LRRC6. Am J Hum Genet 2013;93:336–45
36. Kurkowiak M, Ziętkiewicz E, Greber A, et al. ZMYND10-mutation analysis in Slavic patients with primary ciliary dyskinesia. PLoS One 2016; 11:e0148067
37. Cho KJ, Noh SH, Han SM, et al. ZMYND10 stabilizes intermediate chain proteins in the cytoplasmic pre-assembly of dynein arms. PLoS Genet 2018;14:e1007316
38. Höbean IM, Hjeij R, Olbrich H, et al. Mutations in C11orf70 cause primary ciliary dyskinesia with randomization of left/right body asymmetry due to defects of outer and inner dynein arms. Am J Hum Genet 2018; 102:973–84
39. Fassad MR, Shoemark A, le Borgne P, et al. C11orf70 mutations disrupting the intraflagellar transport-dependent assembly of multiple axonemal dyneins cause primary ciliary dyskinesia. Am J Hum Genet 2018;102: 956–72
40. Olcese C, Patel MP, Shoemark A, et al. X-linked primary ciliary dyskinesia due to mutations in the cytoplasmic axonemal dynein assembly factor PIH1D3. Nat Commun 2017;8:14279
41. Conradi S. Ultrastructure and distribution of neuronal and glial elements on the surface of the proximal part of a motoneuron dendrite, as analyzed by serial sections. Acta Physiol Scand Suppl 1969;332:49–64
42. Hellstrom J, Arvidsson U, Elde R, et al. Differential expression of nerve terminal protein isoforms in VAChT-containing varicosities of the spinal cord ventral horn. J Comp Neurol 1999;411:578–90
43. Miles GB, Hartley R, Todd AJ, et al. Spinal cholinergic interneurons regulate the excitability of motoneurons during locomotion. Proc Natl Acad Sci U S A 2007;104:2448–53
44. Zagoraiou L, Akay T, Martin JF, et al. A cluster of cholinergic premotor interneurons modulates mouse locomotor activity. Neuron 2009;64: 645–62
45. Frank E. A new class of spinal interneurons: The origin and function of C-bouton solved. Neuron 2009;64:593–5
46. Gallart-Palau X, Tarabal O, Casanovas A, et al. Neuregulin-1 is concentrated in the postsynaptic subsurface cistern of C-bouton inputs to motoneurons and altered during motoneuron diseases. FASEB J 2014;28: 3618–32
47. Casanovas A, Salvany S, Lahoz V, et al. Neuregulin 1-ErbB module in C-bouton synapses on somatic motor neurons: Molecular compartmentation and response to peripheral nerve injury. Sci Rep 2017;7:40155
48. Hellstrom J, Oliveira ALR, Meister B, et al. Large cholinergic nerve terminals on subsets of motoneurons and their relation to muscarinic receptor type 2. J Comp Neurol 2003;460:476–86
49. Mavlyutov TA, Epstein ML, Andersen KA, et al. The sigma-1 receptor is enriched in postsynaptic sites of C-terminals in mouse motoneurons. An anatomical and behavioral study. Neuroscience 2010;167:247–55
50. Witts EC, Zagoraiou L, Miles GB. Anatomy and function of cholinergic C bouton inputs to motor neurons. J Anat 2014;224:52–60
51. Ateh DD, Hussain IK, Mustafa AH, et al. Dynein-dynactin complex subunits are differentially localized in brain and spinal cord, with selective involvement in pathological features of neurodegenerative disease. Neuropathol Appl Neurobiol 2007;34:88–94
52. Nagao M, Misawa H, Kato S, et al. Loss of cholinergic synapses on the spinal motor neurons of amyotrophic lateral sclerosis. J Neuropathol Exp Neurol 1998;57:329–33
53. Pullen AH, Athanasiou D. Increase in presynaptic territory of C-terminals on lumbar motoneurons of G93A SOD1 mice during disease progression. Eur J Neurosci 2009;29:551–61
54. Herron LR, Miles GB. Gender-specific perturbations in modulatory inputs to motoneurons in a mouse model of amyotrophic lateral sclerosis. Neuroscience 2012;226:313–23
55. Mavlyutov TA, Epstein ML, Verbny YI, et al. Lack of sigma-1 receptor exacerbates ALS progression in mice. Neuroscience 2013;240:129–34
56. Casas C, Herrando-Grabulosa M, Manzano R, et al. Early presymptomatic cholinergic dysfunction in a murine model of amyotrophic lateral sclerosis. Brain Behav 2013;3:145–58
57. Lasiene J, Komine O, Fujimori-Tonou N, et al. Neuregulin 1 confers neuroprotection in SOD1-linked amyotrophic lateral sclerosis mice via restoration of C-boutons of spinal motor neurons. Acta Neuropathol Commun 2016;4:15
58. Sumner BE. A quantitative analysis of boutons with different types of synapse in normal and injured hypoglossal nuclei. Exp Neurol 1975;49: 406–17

Article V

Gene expression profile in frontal cortex in sporadic frontotemporal lobar degeneration-TDP

Pol Andrés Benito, Ellen Gelpi, Mònica Povedano, Gabriel Santpere and Isidre Ferrer

Journal of Neuropathology and Experimental Neurology 2018 Jul 1; 77(7): 608-627.

J Neuropathol Exp Neurol
Vol. 77, No. 7, July 2018, pp. 608–627
doi: 10.1093/jnen/nly037

OXFORD

ORIGINAL ARTICLE

Gene Expression Profile in Frontal Cortex in Sporadic Frontotemporal Lobar Degeneration-TDP

Pol Andrés-Benito, MSc, Ellen Gelpi, MD, PhD, Mónica Povedano, MD, Gabriel Santpere, PhD, and Isidro Ferrer, MD, PhD

Abstract

Molecular alterations compromising key metabolic pathways are poorly understood in sporadic frontotemporal lobar degeneration with TDP-43 pathology (sFTLD-TDP). Whole-transcriptome array, RT-qPCR validation, gel electrophoresis, and Western blotting, and mitochondrial electron transport chain (ETC) activity were comparatively examined in frontal cortex (area 8) of 16 sFTLD-TDP cases and 14 controls. Assessment of 111 genes by RT-qPCR showed deregulation of 81 genes linked to neurotransmission and synapses, neuronal architecture, cytoskeleton of axons and dendrites, vesicle trafficking, purines, mitochondria, and energy metabolism in sFTLD-TDP. Western blotting studies disclosed downregulation of several mitochondrial subunits encoded by genomic DNA and MT-CO1 encoded by the mitochondrial DNA. Mitochondrial ETC activity of complexes I, IV, and V was decreased in sFTLD-TDP. These findings provide robust information about downregulation of genes involved in vital biochemical pathways and in synaptic neurotransmission which may help to increase understanding about the biochemical substrates of clinical manifestations in sFTLD-TDP.

Key Words: Energy metabolism, Frontotemporal lobar degeneration, Mitochondria, Neurotransmission, Purines, Synapses, TDP43.

INTRODUCTION

Frontotemporal dementia is a progressive neurological disorder characterized by deterioration of personality, behavior, language, and cognition, with marked individual variations, and in the majority of patients is due to frontotemporal lobar degeneration (FTLD). This term stresses the progressive loss of neurons in the frontal and temporal lobes as the cause of the principal neurological symptoms. FTLD is not a unique disease but covers several unrelated conditions: 1) FTLD-tau is identified by the abnormal tau deposition in neurons and glial cells, which in turn encompasses sporadic and genetic forms associated with mutations in *MAPT*, the gene coding for protein tau; and 2) FTLD-U, which is characterized by the presence of intraneuronal ubiquitin-immunoreactive inclusions. Subsequent studies have demonstrated the heterogeneity of FTLD-U, including FTLD-TDP-43 proteinopathy, FTLD-FUS proteinopathy, and FTLD-UPS, lacking TDP-43 and FUS inclusions (1–3).

FTLD-TDP-43 proteinopathy (FTLD-TDP) is clinically manifested by behavioral-dysexecutive disorder, primary progressive aphasia and/or motor disorders including motor neuron disease; macroscopically, by frontal and temporal atrophy, commonly symmetrical, variable involvement of the basal ganglia and substantia nigra; and microscopically, by neuron loss in the cerebral cortex, microvacuolation in the upper cortical layers, astrogliosis, and TDP-43-immunoreactive inclusions in the nucleus and/or cytoplasm of neurons and oligodendrocytes, and in neuropil threads (1–3). Some cases are sporadic (sFTLD-TDP) whereas other are genetic, often familial (fFTLD-TDP) and linked to mutations in different genes including *GRN* (progranulin), *C9ORF72* (chromosome 9 open reading frame 72), *TARDP* (TAR DNA-binding protein), *VCP* (valosin-containing protein), *CHMBP2* (charged multivesicular body protein 2), and *UBQLN* (ubiquilin 2), among others (4–6). Excepting progranulin, mutations of any of the other genes may also be causative of amyotrophic lateral sclerosis (ALS), thus suggesting ALS/FTLD-TDP within the same

From the Neuropathology, Pathologic Anatomy Service, Bellvitge University Hospital, IDIBELL, Hospitalet de Llobregat, Spain (PA-B, IF); Biomedical Network Research Center on Neurodegenerative Diseases (CIBERNED), Institute Carlos III, Hospitalet de Llobregat, Spain (PA-B, IF); Neurological Tissue Bank of the Biobanc-Hospital Clínic-Institut d'Investigacions Biomèdiques August Pi I Sunyer (IDIBAPS), Barcelona, Spain (EG); Institute of Neurology, Medical University of Vienna, Vienna, Austria (EG); Functional Unit of Amyotrophic Lateral Sclerosis (UFELA), Service of Neurology, Bellvitge University Hospital, Hospitalet de Llobregat, Spain (MP); Department of Neurobiology, Yale School of Medicine, New Haven, Connecticut (GS); Department of Experimental and Health Sciences, IBE, Institute of Evolutionary Biology, Universitat Pompeu Fabra-CSIC, Barcelona, Spain (GS); Department of Pathology and Experimental Therapeutics, University of Barcelona, Hospitalet de Llobregat, Spain (IF); and Institute of Neurosciences, University of Barcelona, Barcelona, Spain (IF).

Send correspondence to: Isidro Ferrer, MD, PhD, Department of Pathology and Experimental Therapeutics, University of Barcelona, Campus Bellvitge, c/Feixa Llarga sn, 08907 Hospitalet de Llobregat, Spain; E-mail: 8082ifa@gmail.com

This study was supported by grants from CIBERNED and PI17/00809 Institute of Health Carlos III, and cofunded by FEDER funds/European Regional Development Fund (ERDF)—a way to build Europe; ALS intra-CIBERNED project to IF; and IFI15/00035 fellowship to PA-B; grant "Retos todos unidos contra la ELA" to MP; and grant from the "Fundación Tatiana Pérez de Guzmán el Bueno, convocatoria Neurociencias 2014" to EG.

The authors have no competing interests to declare.

disease spectrum (7–9). The presence of TDP-43 inclusions in ALS together with the characteristics of TDP-43, which is phosphorylated, ubiquitinated, and truncated at the C-terminal in both conditions (10), argues in favor of these bonds.

FTLD-TDP has been subclassified into 4 different neuropathologic subgroups that roughly correlate with certain clinical symptoms and genetic substrates although with low predictive value (11, 12). Type A is characterized by numerous neuronal cytoplasmic inclusions (NCIs) and dystrophic neurites (DNs), and variable number of neuronal nuclear inclusions (NIIs) predominating in the upper cortical layers. Type B is delineated by numerous NCIs in the upper and inner cortical layers, and low numbers of DNs and NIIs. Type C is defined by predominant DNs in the upper cortical layers and rare NCIs and NIIs. Type D is characterized by predominance of NIIs, and rare NCIs and DNs (1, 11, 12).

The study of human brain tissue has been useful to unveil additional molecular alterations in FTLD-TDP (13). Complementary information has been obtained using proteomics and transcriptomics in a limited number of FTLD-TDP subtypes including those linked with *GRN* and *C9Orf72* mutations, and atypical FTLD-TDP cases (14–17). Gene expression profile has also been recently described in the frontal cortex area 8 in ALS (18) and in different brain regions in sporadic ALS and ALS linked to *C9Orf72* mutations (19). However, the molecular pathology of metabolic pathways, mitochondria and energy metabolism, synapses, and neurotransmission has not been studied in sFTLD-TDP. The present study was aimed at analyzing gene expression in frontal cortex area 8 in a series of sFTLD-TDP in parallel with controls in order to gain understanding about vulnerable pathways which can explain pathogenic aspects of the disease.

MATERIALS AND METHODS

Human Cases

Brain samples were obtained from the Brain Banks of the Institute of Neuropathology HUB-ICO-IDIBELL Biobank and the Hospital Clinic-IDIBAPS Biobank following the guidelines of the Spanish legislation on this matter and the approval of the local ethics committees. The postmortem interval between death and tissue processing was between 2 and 18 hours. One hemisphere was immediately cut into 1-cm-thick coronal sections, and selected brain areas were rapidly dissected, frozen on metal plates over dry ice, placed in individual air-tight plastic bags and stored at −80°C until use. The other hemisphere was fixed by immersion in 4% buffered formalin for 3 weeks. The neuropathological study in control and FTLD-TDP cases was carried out on 20 selected 4-µm-thick dewaxed paraffin sections of representative regions of the frontal, temporal, parietal, motor, primary visual, anterior cingulate and entorhinal cortices, hippocampus, amygdala, basal forebrain, caudate, putamen, globus pallidus, thalamus, midbrain, pons, medulla oblongata, cerebellar vermis, hilus, and cerebral white matter. These were stained with hematoxylin and eosin, Klüver-Barrera, or processed for immunohistochemistry for microglia (Iba-1, Wako, Richmond, VA), glial acidic protein ([GFAP], Dako, Gostrup, Denmark), β-amyloid (Dako, clone 6F/3D), phospho-tau (Thermo Scientific, Rockford, IL, clone AT8), α-synuclein (Novocastra, Newcastle, UK, clone KM51), TDP-43 (Abnova, Taipei, Taiwan, clone 2E2-D3), ubiquitin (Dako, Polyclonal Rabbit), and p62 (BD Biosciences, San Jose, Purified Mouse Anti-p62 LCK ligand) using EnVision+ System peroxidase (Dako), and diaminobenzidine and H_2O_2. FTLD-TDP was diagnosed following well-established criteria: frontotemporal atrophy, loss of neurons and variable spongiosis in the upper cortical layers, astrocytic gliosis, and presence of TDP-43-immunoreactive inclusions in neurons and dendrites (NCIs, NIIs, and DNs) (1, 11). The whole series included 16 sporadic cases of FTLD-TDP (71.6 ± 9.6 years; 11 men and 3 women), and 14 control cases (66.5 ± 8.8 years; 8 men and 6 women). The postmortem delay varied from 2 hours and 15 minutes to 18 hours (~5.4 ± 4.0) in the control group, and between 3 hours and 40 minutes and 16 hours (~7.5 ± 3.9) in the sFTLD-TDP group. Patients with associated pathologies of the nervous system, excepting early stages of neurofibrillary tangle pathology and mild small blood vessel disease, were not included. Age-matched control cases had not suffered from neurologic and psychiatric disorders and did not show alterations other than those permitted in diseased cases. Regarding TDP types: 11 cases were categorized as type A, 1 as type B, and 4 as type C. A summary of cases is shown in Table 1.

Biochemical studies were carried out in fresh-frozen frontal cortex area 8. Special care was taken to assess premortem and postmortem factors that might interfere with RNA processing and protein integrity (20). For this reason, all the samples were used in the study of RNA expression because RNA integrity values were suitable for RNA study, whereas 10 samples per group were used for gel electrophoresis and Western blotting of samples showing a preserved band pattern after Coomassie Blue staining. The same 10 cases per group were used in the study of mitochondrial enzymatic activities. Cases excluded were neoplastic diseases affecting the nervous system, metabolic syndrome, hypoxia, and prolonged agonic state (such as those occurring in intensive care units), as well as cases with infectious, inflammatory, and autoimmune diseases, either systemic or limited to the nervous system. Assessed samples did not bear *C9ORF72* mutations (21). No other FTLD-TDP-related genes were systematically analyzed.

RNA Purification

RNA from frozen frontal cortex area 8 was extracted following the instructions of the supplier (RNeasy Mini Kit, Qiagen, Hilden, Germany). RNA integrity and 28S/18S ratios were determined with the Agilent Bioanalyzer (Agilent Technologies, Inc., Santa Clara, CA). RNA integrity values are shown in Table 1. Samples were treated with DNase digestion, and RNA concentration was evaluated using a NanoDrop Spectrophotometer (Thermo Fisher Scientific, Waltham, MA).

Whole-Transcriptome Array and RT-qPCR Validation

Selected samples were analyzed by microarray hybridization with Human Clariom D Assay kit and GeneChip WT

TABLE 1. Summary of the 30 Cases Analyzed

Case	Sex	Age	Diagnosis	PMD	RIN	TDP43
1	M	66	Control	18 h 0 min	6.4	–
2	M	61	Control	3 h 40 min	7.0	–
3	M	62	Control	5 h 45 min	5.0	–
4	M	74	Control	6 h 40 min	7.2	–
5	M	65	Control	5 h 15 min	6.8	–
6	F	64	Control	2 h 15 min	5.0	–
7	M	63	Control	8 h 05 min	7.1	–
8	F	79	Control	3 h 35 min	6.8	–
9	F	67	Control	5 h 20 min	6.2	–
10	M	70	Control	3 h 45 min	7.2	–
11	M	52	Control	4 h 40 min	7.2	–
12	F	52	Control	5 h 45 min	5.1	–
13	F	82	Control	7 h 35 min	5.2	–
14	F	74	Control	2 h 45 min	5.7	–
15	M	76	sFTLD-TDP	5 h 0 min	6.2	A
16	F	82	sFTLD-TDP	3 h 40 min	6.4	A
17	M	71	sFTLD-TDP	4 h 0 min	6.1	A
18	F	77	sFTLD-TDP	16 h 0 min	6.9	C
19	M	73	sFTLD-TDP	5 h 0 min	6.7	C
20	M	63	sFTLD-TDP	9 h 30 min	5.0	A
21	F	77	sFTLD-TDP	7 h 39 min	7.0	A
22	M	65	sFTLD-TDP	13 h 0 min	7.4	A
23	F	88	sFTLD-TDP	6 h 30 min	5.4	A
24	M	59	sFTLD-TDP	8 h 0 min	7.4	A
25	M	58	sFTLD-TDP	4 h 0 min	7.3	A
26	M	56	sFTLD-TDP	8 h 0 min	5.0	A
27	F	84	sFTLD-TDP	6 h 0 min	5.9	B
28	M	78	sFTLD-TDP	7 h 15 min	6.7	C
29	M	66	sFTLD-TDP	5 h 15 min	7.2	A
30	M	74	sFTLD-TDP	15 h 0 min	6.4	C

sFTLD-TDP, sporadic frontotemporal lobar degeneration-TDP; F, female; M, male; PM, postmortem delay; RIN, RNA integrity number; TDP43, histological types of FTLD-TDP based on TDP-43-immunoreactive inclusions (see Materials and Methods).

Plus Reagent Kit and microarray 7000 G platform from Affymetrix (Santa Clara, CA). Preprocessing of raw data and statistical analyses were performed using bioconductor packages in R programming environment for genes (22). Complementary DNA (cDNA) was obtained using High-Capacity cDNA Reverse Transcription kit (Applied Biosystems, Foster City, CA) following the protocol of the supplier. Parallel reactions for each RNA sample were run in the absence of MultiScribe Reverse Transcriptase to assess lack of contamination of genomic DNA. Gene selection was based upon their values using a test for differential expression between 2 classes (Student *t*-test). Selected genes differentially expressed showed an absolute logarithm of fold change >0.5 combined with a p value ≤ 0.01. Table 2 shows identification numbers and names of selected TaqMan probes. Most of the tested probes corresponded to deregulated genes as revealed by microarrays; the remainder was selected to assess other key genes of the altered pathways that were not identified as deregulated in the arrays. TaqMan RT-qPCR assays were performed in duplicate for each gene on cDNA samples in 384-well optical plates using

TABLE 2. Gene Symbols and TaqMan Probes Used in Frontal Cortex Area 8 Including Normalization Probes (*GUS*-β)

Gene	TaqMan assay
ABLIM2	Hs00402222_m1
ACTLB6	Hs00211827_m1
ACTR3B	Hs01051213_m1
ACTR3C	Hs03988416_m1
AK1	Hs00176119_m1
AK2	Hs01123132_g1
AK5	Hs00952786_m1
AK7	Hs00330574_m1
AMIGO1	Hs00324802_s1
APOOL	Hs00922772_g1
APRT	Hs00975725_m1
ARPC5L	Hs00229649_m1
ATP2B3	Hs00222625_m1
ATP2B4	Hs00608066_m1
ATP4A	Hs00167575_m1
ATP5A1	Hs00900735_m1
ATP5B	Hs00969569_m1
ATP5H	Hs01046892_gH
ATP5L	Hs00538946_g1
ATP5O	Hs00426889_m1
ATP6D	Hs00371515_m1
ATP6V1A	Hs01097169_m1
BSN	Hs01109152_m1
C9ORF72	Hs00376619_m1
CALB1	Hs01077197_m1
CEP126	Hs01573778_m1
CEP41	Hs00363344_m1
CKAP2	Hs00217068_m1
COA6	Hs01372973_m1
CORO2A	Hs00185610_m1
COX7AL	Hs00190880_m1
DDN	Hs00391784_m1
DGUOK	Hs00176514_m1
ENTPD1	Hs00969559_m1
ENTPD2	Hs00154301_m1
ENTPD3	Hs00928977_m1
FASTKD2	Hs01556124_m1
FRMPD4	Hs01568794_m1
GABBR2	Hs01554996_m1
GABRA1	Hs00971228_m1
GABRA2	Hs00168069_m1
GABRA3	Hs00968130_m1
GABRB2	Hs00241451_m1
GABRB3	Hs00241459_m1
GABRD	Hs00181309_m1
GABRG2	Hs00168093_m1
GABRG3	Hs00264276_m1
GAD1	Hs01065893_m1
GAP43	Hs00967138_m1
GDAP1L1	Hs00225209_m1
GFAP	Hs00909240_m1
GRIA1	Hs00181348_m1
GRIN2A	Hs00168219_m1

(continued)

TABLE 2. Continued

Gene	TaqMan assay
GRIN2B	Hs01002012_m1
GRM5	Hs00168275_m1
GULP1	Hs01061497_m1
GUS-β	Hs00939627_m1
HOMER1	Hs01029333_m1
KIF17	Hs00325418_m1
KLC2	Hs03988192_m1
LRRC6	Hs00917168_m1
MAP1A	Hs00357973_m1
MAST3	Hs00390797_m1
MCU	Hs00293548_m1
MICU3	Hs01028469_m1
MRPL1	Hs00220322_m1
MRPS35	Hs00950427_m1
MTIF2	Hs01091373_m1
MTX3	Hs01372688_m1
NDUFA10	Hs01071117_m1
NDUFA2	Hs00159575_m1
NDUFA5	Hs00916783_m1
NDUFAF2	Hs02380072_u1
NDUFAF6	Hs00901870_m1
NDUFB10	Hs00605903_m1
NDUFB5	Hs00159582_m1
NDUFB8	Hs00428204_m1
NDUFS8	Hs00159597_m1
NME1	Hs02621161_s1
NME3	Hs01573874_g1
NME4	Hs00359037_m1
NME7	Hs00273690_m1
NRN1	Hs00213192_m1
NT5C	Hs00274359_m1
NUDT1	Hs00159343_m1
PAK5	Hs00379318_m1
PCLO	Hs00382694_m1
PLP1	Hs00166914_m1
PNP	Hs01002926_m1
POLR3B	Hs00932002_m1
PRUNE	Hs00535700_m1
PSD	Hs00160539_m1
RMND1	Hs01012514_m1
RMND2	Hs04187037_m1
RND1	Hs00205507_m1
SDHB	Hs00268117_m1
SLC17A7	Hs00220404_m1
SLC1A1	Hs00188172_m1
SLC1A2	Hs01102423_m1
SLC25A1	Hs01105608_g1
SLC25A11	Hs00185940_m1
SLC25A23	Hs01012756_m1
SLC32A1	Hs00369773_m1
SNAP25	Hs00938957_m1
SNAP91	Hs01097941_m1
SYN1	Hs00199577_m1
SYP	Hs00300531_m1
SYT1	Hs00194572_m1
TARDBP	Hs00606522_m1
TOMM70	Hs00207896_m1
UQCR11	Hs00907747_m1
UQCRB	Hs00559884_m1
VAMP1	Hs04399177_m1

(continued)

an ABI Prism 7900 Sequence Detection system (Applied Biosystems, Life Technologies, Waltham, MA). For each 10 µL TaqMan reaction, 4.5 µL cDNA was mixed with 0.5 µL 20× TaqMan Gene Expression Assays and 5 µL of 2× TaqMan Universal PCR Master Mix (Applied Biosystems). Values of *GUS*-β were used as internal controls for normalization (23). The parameters of the reactions were 50°C for 2 minutes, 95°C for 10 minutes, and 40 cycles of 95°C for 15 seconds and 60°C for 1 minute. Finally, capture of all TaqMan PCR data used the Sequence Detection Software (SDS version 2.2.2, Applied Biosystems). For the data analysis, threshold cycle (CT) values for each sample were processed to obtain the double delta CT (ΔΔCT) values. First, delta CT (ΔCT) values were calculated as the normalized CT values of each target gene in relation to the CT of endogenous controls *GUS*-β. Then, ΔΔCT values were obtained from the ΔCT of each sample minus the mean ΔCT of the population of control samples. Results were analyzed using the Student *t*-test.

RNA Purification, Retrotranscription Reaction, and RT-qPCR for Detection of 3 R and 4 R Tau Isoforms

Tau mRNA isoforms were assessed by using SYBR green quantitative RT-qPCR; 1000 ng of total RNA was used as a template. cDNA samples obtained from the retrotranscription reaction were diluted 1:20 and duplicate SYBR green PCR assays for each gene were performed. For each reaction, 2.5 µL of cDNA was mixed with 1.25 µL of forward primer 10 µM, 1.25 µL reverse primer 10 µM, and 5 µL of PowerUp SYBR Green Master Mix (Applied Biosystems). The reactions were performed following the parameters: 50°C for 2 minutes, 95°C for 10 minutes, and 40 cycles at 95°C for 15 seconds and at 60°C for 1 minute. SYBR green PCR data were captured using the Sequence Detection Software (SDS version 2.2). 3Rtau forward primer sequence: GTCCGTACTCCACCCAAGTC; 3Rtau reverse: GTTTGTAGACTATTTGCACCTTC; 4Rtau forward: GGCGGGAAGATGCAGATAA TTAAT; 4Rtau reverse: GTAGACTATTTGCACACTGCC. Parallel assays for each sample were carried out using primers for β-glucuronidase (*GUS*-β), forward: GTCTGCGGCA TTTTGTCGG; reverse: CACACGATGGCATAGGAATGG as endogenous controls. Mean fold-change values of each experimental group were analyzed by 1-way ANOVA test with post hoc Tukey by using GraphPad Prism version 5.01 (La Jolla, CA) and Statgraphics Statistical Analysis and Data Visualization Software version.1 (Warrenton, VA).

TABLE 3. List of Antibodies Used in Western Blotting

Primary antibody	Symbol	Source	Reference	Host	WB Dilution
Actin Binding LIM Protein Family Member 2	ABLIM2	Abcam	ab100926	Rabbit	1:750
ATP synthase subunit alpha, mitochondrial	ATP5	Abcam	ab110411	Mouse	1:1000
Calbindin	CALB	Swant	CB-38a	Rabbit	1:5000
Chromosome 9 open reading frame 72	C9ORF72	Abcam	ab183892	Rabbit	1:500
Cytochrome b-c1 complex subunit 2, mitochondrial	UQCRC2	Abcam	ab110411	Mouse	1:1000
Cytochrome c oxidase	MT-CO1	Abcam	ab110411	Mouse	1:1000
Gamma-aminobutyric acid Receptor Subunit beta-2	GABAARB2	Abcam	ab156000	Rabbit	1:500
Gamma-Aminobutyric Acid Type A Receptor Delta Subunit	GABRD	Abcam	ab110014	Rabbit	1:1000
Glial Fibrillary Acidic Protein	GFAP	Dako	Z0334	Rabbit	1:5000
Glutamate (NMDA) receptor subunit epsilon-1	NMDAR2A	Abcam	ab169555	Rabbit	1:250
Glutamate Decarboxylase 1	GAD1	CellSignaling	#5305	Rabbit	1:250
Glyceraldehyde-3-Phosphate Dehydrogenase	GAPDH	Abcam	ab9485	Rabbit	1:2500
Mitochondrial import receptor subunit TOM70	TOMM70	Novus biological	NBP1-87863	Rabbit	1:500
NADH dehydrogenase (ubiquinone) 1 alpha subcomplex subunit 10	NDUFA10	Antibody BCN	GTX114572	Rabbit	1:1000
NADH dehydrogenase (ubiquinone) 1 beta subcomplex subunit 10	NDUFB10	Antibody BCN	15589-1-AP	Rabbit	1:2500
NADH dehydrogenase (ubiquinone) 1 beta subcomplex subunit 8, mitochondrial	NDUFB8	Abcam	ab110411	Mouse	1:1000
NADH dehydrogenase (ubiquinone) iron-sulfur protein 8, mitochondrial	NDUFS8	Antibody BCN	GTX114119	Rabbit	1:1000
NADH-ubiquinone oxidoreductase chain 1	MT-ND1	Abcam	ab181848	Rabbit	1:1000
Postsynaptic density protein 95	PSD-95	Invitrogen	7E3-1B8	Mouse	1:1000
Succinate dehydrogenase (ubiquinone) iron-sulfur subunit, mitochondrial	SDHB	Abcam	ab110411	Mouse	1:1000
Synaptophysin	SYN	Novocastra	NCL-L-SYNAP-299	Mouse	1:1000
Synaptosome Associated Protein 25	SNAP-25	BioLegend	SMI81	Mouse	1:1000
Vesicular inhibitory amino acid transporter	VGAT	Synaptic systems	131 011	Mouse	1:1000
Voltage Dependent Anion Channel 1	VDAC1	Abcam	ab15895	Rabbit	1:500
4R TAU	4R TAU	Merck-Millipore	clone 1E1/A6	Mouse	1:50
3R TAU	3R TAU	Merck-Millipore	clone 8E6/C11	Mouse	1:500
Phospho-tau Thr181	Thr181	Cell Signalling	mAb 12885	Rabbit	1:50
Total Tau	Tau 5	Thermo-Fisher	AHB002	Mouse	1:250
TAR DNA-binding protein 43	TDP-43	Abcam	ab154047	Rabbit	1:250

Gel Electrophoresis and Western Blotting

Frozen samples of the frontal cortex area 8 were homogenized in RIPA lysis buffer (50 mM Tris/HCl buffer, pH 7.4 containing 2 mM EDTA, 0.2% Nonidet P-40, 1 mM PMSF, protease, and phosphatase inhibitor cocktails; Roche Molecular Systems, Pleasanton, CA). Homogenates were centrifuged at 14 000*g* for 20 minutes. Protein concentration was determined with the BCA method (ThermoFisher Scientific). Equal amounts of protein (12 µg) for each sample were loaded and separated by electrophoresis on 10% sodium dodecyl-sulfate polyacrylamide gel electrophoresis (SDS-PAGE) gels and transferred onto nitrocellulose membranes (Amersham, Freiburg, Germany). Nonspecific binding was blocked by incubation with 3% albumin in PBS containing 0.2% Tween for 1 hour at room temperature. After washing, membranes were incubated overnight at 4°C with 1 of primary antibodies (Table 3). Protein loading was normalized using an antibody against GAPDH (37 kDa, 1:2500, Abcam, Cambridge, UK). Membranes were then incubated for 1 hour in the appropriate HRP-conjugated secondary antibodies (1:2000, Dako, Santa Clara, CA). Immunocomplexes were revealed with chemiluminescence reagent (ECL, Amersham). Densitometric quantification was carried out with ImageLab v4.5.2 software (Bio-Rad, Hercules, CA).

Isolation of Mitochondrial-Enriched Fractions From Human Brain Tissue

Mitochondria were extracted from frozen frontal cortex (100 mg) under ice-cold conditions. Tissues were minced in ice-cold isolation buffer (IB) containing 0.25 M sucrose, 10 mmol/L Tris, and 0.5 mmol/L EDTA, pH 7.4, and then homogenized and centrifuged at 1000*g* for 10 minutes. Samples were homogenized with a micropestle using 10 vol buffer per mg of tissue and centrifuged at 1000*g* for 10 minutes at 4°C. The supernatant (S1) was conserved. The pellet was washed with 2 vol IB and centrifuged under the same conditions. The last supernatant (S2) was combined with S1, mixed, and centrifuged at 10 000*g* for 10 minutes at 4°C, resulting in the mitochondria-enriched pellet. The supernatant (S3) was discarded and the pellet was washed with 2 volumes IB and centrifuged at 10 000*g* for 10 minutes at 4°C, thereby obtaining the washed mitochondria-enriched pellet. The supernatant (S4) was discarded and the final pellet was resuspended in 1 vol IB and stored at −80°C. Protein concentration was measured using a SmartspectTMplus spectrophotometer (Bio-Rad) and the Bradford method (Merck, Darmstadt, Germany). The mitochondrial enriched fraction was used for mitochondrial enzymatic activities and for Western blotting. Protein loading (12 µg) was normalized with anti-VDAC (1:500, Abcam).

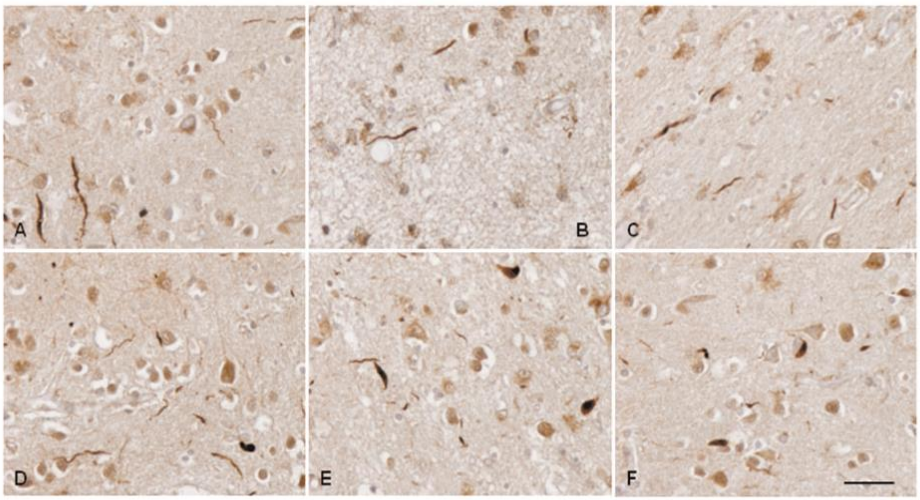

FIGURE 1. Examples of TDP-43-immunoreactive inclusions, including thin and thick dystrophic neuritis and cytoplasmic inclusions in frontal cortex area 8 in sFTLD-TDP. **(A–C)** Type C; **(D, E)** Type A; **(F)** Type B. **(A)**, **(B)**, and **(C)**, cases 18, 19, and 28, respectively; **(D)** and **(E)**, cases 23 and 25, respectively; **(F)**, case 27. Paraffin sections, hematoxylin counterstaining, scale bar = 50 μm.

The activities of mitochondrial complexes I, II, IV, and V were analyzed using commercial kits following the instructions of the suppliers (Mitochondrial complex V: Novagen, Merck Biosciences; and Mitochondrial complex I, II, and IV: Abcam). Activity of citrate synthase was evaluated as a quantitative enzyme marker for the presence of intact mitochondria using commercial kits (Abcam). About 25 μg of mitochondria extract was loaded into each well. The enzymatic activities for each mitochondrial complex were expressed as a rate of milli-optical densities per minute normalized with the citrate synthase activity.

Statistical Analysis

The normality of distribution of fold-change values was analyzed with the Kolmogorov-Smirnov test. The nonparametric Mann-Whitney test was performed to compare each group when values did not follow a normal distribution, while the unpaired *t*-test was used for normal variables. Statistical analysis and graphic design were performed with GraphPad Prism version 5.01 (La Jolla, CA). Results were analyzed with the Student *t*-test. Outliers were detected using the GraphPad software QuickCalcs ($p < 0.05$). All data were expressed as mean ± SEM and significance levels were set at $^{*}p < 0.05$, $^{**}p < 0.01$, and $^{***}p < 0.001$. Pearson's correlation coefficient was used to assess a possible linear association between 2 continuous quantitative variables.

RESULTS

Main Neuropathological Findings

All sFTLD-TDP cases presented variable neuron loss and microvacuolation in the upper cortical layers, mild astrocytic gliosis in all layers of the cortex and the presence of TDP-43-immunoreactive dystrophic neurites mainly in the upper layers accompanied or not by neuronal cytoplasmic inclusions. Neuronal intranuclear inclusions were extremely rare. About 11 cases were categorized as type A, 1 as type B, and 4 as type C (Table 1; Fig. 1). Type A was characterized by numerous NCIs and DNs in the upper cortical layers; type B by numerous NCIs in the upper and inner cortical layers; and type C by predominant DNs in the upper cortical layers. p62-immunoreactive inclusions were absent in any brain region.

Microarray Analysis

All samples had enough quality for subsequent analysis after quality control analysis. The cofactors age and gender were not relevant for the analysis. After filtering, 4851 genes were included in the analysis. The analysis to select differentially expressed genes was based on adjusting a linear model with empirical Bayes moderation of the variance. The 538 top variable genes (with nominal p values <0.01 and an absolute logarithm of the fold change ≥0.5) were represented in a heat map to illustrate common and differing gene expression patterns between control and sFTLD-TDP cases in FC (Fig. 2A). We identified 425 genes differentially expressed in sFTLD-TDP compared with controls (5 up and 420 down) (Fig. 2B). Gene Ontology (GO) database was used to highlight biological categories of differentially regulated genes. Down-regulated genes in sFTLD-TDP were involved in neurotransmission and synapsis, neuron architecture, cytoskeleton of axons and dendrites, vesicle trafficking, purine metabolism, mitochondria, and energy metabolism (Table 4). Raw data are

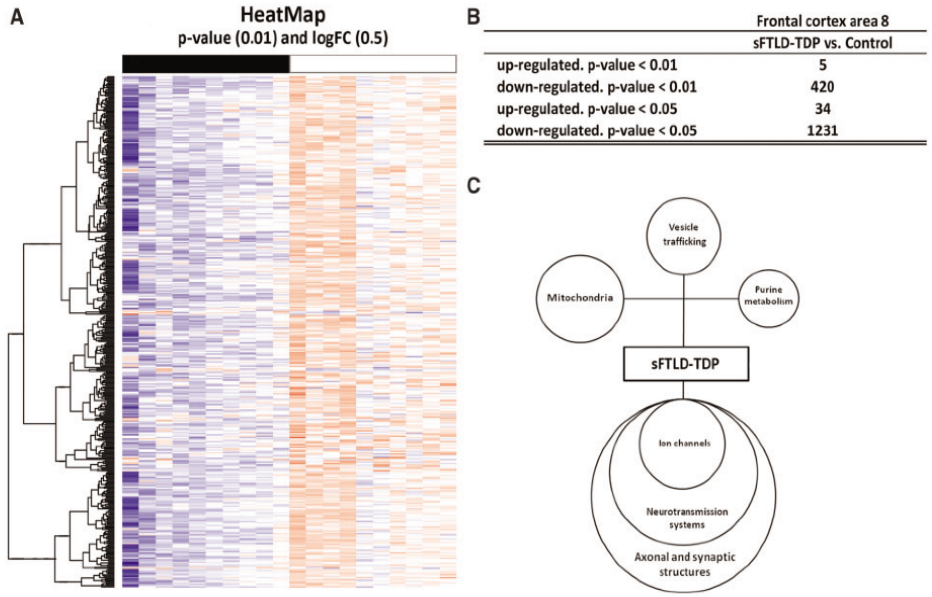

FIGURE 2. (A) Hierarchical clustering heat-map of expression intensities of mRNA array transcripts reflects differential gene expression profiles in frontal cortex area 8 in controls (red), sFTLD-TDP (blue). Differences are considered statistically significant at p value ≤ 0.01 and logFC 0.5. **(B)** Total number of significantly different expressed genes in sFTLD-TDP versus controls. **(C)** Diagram showing deregulated gene clusters in frontal cortex area 8 in sFTLD-TDP compared with controls as revealed by whole transcriptome arrays.

found in https://www.ebi.ac.uk/arrayexpress/; reference number fgsubs #218580.

Gene Expression Validation

RT-qPCR was carried out to assess the expression of 111 selected genes; 81 of them were abnormally regulated in sFTLD-TDP.

TARDBP and *C9ORF72*, and *GFAP*

TARDBP and *C9ORF72* were significantly decreased in sFTLD-TDP compared with controls ($p = 0.05$ and $p = 0.01$, respectively) (Fig. 2A). *GFAP* expression was increased ($p = 0.003$) in sFTLD-TDP (Fig. 3A).

Cytoskeleton and Neuron Architecture

The expression of 17 genes was analyzed by RT-qPCR; 12 of them showed decreased expression in sFTLD-TDP when compared with controls. *ABLIM2* ($p = 0.0001$), *ACTLB6* ($p = 0.025$), *ACTR3B* ($p = 0.002$), *ACTR3C* ($p = 0.05$), *CEP41* ($p = 0.003$), *CKAP2* ($p = 0.017$), *CORO2A* ($p = 0.05$), *KIF17* ($p = 0.003$), *MAP1A* ($p = 0.05$), *MAST3* ($p = 0.003$), *PAK5* ($p = 0.005$), and *RND1* ($p = 0.008$) showed a significant decrease in sFTLD-TDP (Fig. 3B, C).

Synapsis and Neurotransmission

The expression of 36 genes was assessed; 30 of them were downregulated in sFTLD-TDP. The expression of the following genes implicated in presynaptic and postsynaptic attachment was significantly decreased in sFTLD-TDP: *DDN* ($p = 0.04$), *FRMPD4* ($p = 0.01$), *GAP43* ($p = 0.004$), *HOMER1* ($p = 0.000$), *NRN1* ($p = 0.004$), *PCLO* ($p = 0.005$), and *PSD* ($p = 0.013$). Similarly, 15 genes involved in GABAergic and glutamatergic neurotransmission were downregulated in sFTLD-TDP: *CALB1* ($p = 0.000$), *GABBR2* ($p = 0.033$), *GABRA1* ($p = 0.004$), *GABRA2* ($p = 0.008$), *GABRA3* ($p = 0.000$), *GABRB2* ($p = 0.006$), *GABRB3* ($p = 0.002$), *GABRD* ($p = 0.024$), *GABRG2* ($p = 0.001$), *GAD1* ($p = 0.05$), *GRIA1* ($p = 0.042$), *GRIN2A* ($p = 0.048$), *GRIN2B* ($p = 0.025$), *GRM5* ($p = 0.002$), *SLC1A1* ($p = 0.02$), *SLC17A2* ($p = 0.049$), and *SLC32A1* ($p = 0.025$). Finally, a set of genes involved in synaptic vesicles were significantly deregulated in sFTLD-TDP: *GULP1* ($p = 0.001$), *SNAP25* ($p = 0.006$), *SNAP91* ($p = 0.012$), *SYN1* ($p = 0.001$), *SYP* ($p = 0.035$), and *SYT1* ($p = 0.017$) (Fig. 4).

Expression Levels of Genes Involved in Purine Metabolism

The expression of 18 genes was assessed by RT-qPCR; 9 of them were downregulated. *AK5* ($p = 0.000$), *AK7*

TABLE 4. Main Significant Clusters of Altered Genes in Frontal Cortex Area 8 in sFTLD-TDP

GO Term	Count	Size	Genes	Odds ratio	p value
Actin filament-based process	38	186	*ABLIM2, ACTN4, ACTR3B, ACTR3C, ADD2, ARHGEF2, ARPC5L, BAG4, BAIAP2, CACNA2D1, CACNB2, CAP2, CAPZA2, CDK5, CDK5R1, CORO2A, DNAJB6, EPB41L4B, FGF12, ID1, ITGB1BP1, LIMK1, MEF2C, PACSIN1, PHACTR1, PIP5K1C, PRKCZ, PTK2B, RND1, SCN1B, SCN2B, SCN3B, SDAD1, SORBS2, STC1, SYNPO, TPM2, WASF1*	1.65	6.74e-03
Action potential	15	43	*CACNA1G, CACNA1H, CACNA1I, CACNA2D1, CACNB2, DRD1, FGF12, GNAQ, KCNA1, PTPN3, SCN1B, SCN2A, SCN2B, SCN3B, SCN8A*	3.42	3.74e-04
Alternative mRNA splicing, via spliceosome	5	10	*CELF3, CELF4, RBFOX1, RBFOX2, RBFOX3*	6.30	6.82e-03
Anterograde transsynaptic signaling	63	182	*AKAP5, AMPH, BAIAP2, BTBD9, CA7, CACNA1G, CACNB1, CACNB2, CADPS, CADPS2, CDK5, CELF4, CHRM1, CLSTN3, DGKI, DLGAP1, DOC2A, DRD1, EGR3, FGF12, GABBR2, GABRB3, GABRG2, GFAP, GLRA3, GPR176, GRIN2A, GRM2, GRM5, GSK3A, HOMER1, HTR4, KCNA1, KCNQ2, KCNQ5, LRRTM1, LRRTM2, MAPK8IP2, MEF2C, NRXN3, OPRL1, PCDH8, PIP5K1C, PLK2, PNOC, PRKCG, PRKCZ, PTK2B, RASGRF1, RIMS1, RPH3A, SCN1B, SCN2B, SLC12A5, SLC17A7, SNAP25, SNAP91, STXBP1, SYN1, SYNJ1, SYP, SYT1, UNC13A*	3.65	1.90e-13
Axon	47	127	*AMIGO1, AP1S1, AP3S1, ATL1, ATP1A3, BLOC1S2, CCK, CDK5, CDK5R1, CHRM1, DAGLA, DGKI, ELK1, GABRA2, GABRG2, GAP43, GRM2, HOMER1, HPCA, INPP5F, KCNA1, KCNA3, KCNA4, KCNC2, KCNIP3, KCNQ2, LRRTM1, NEFL, NEFM, NRP1, PACSIN1, PNOC, PRKCZ, PTK2B, ROBO2, SCN1B, SCN2A, SCN8A, SERPINF1, SLC17A7, STXBP1, SYN1, SYNJ1, SYP, SYT1, UNC13A, VAMP1*	3.96	1.99e-11
Axon hillock	3	4	*CCK, PRKCZ, SERPINF1*	18.80	9.40e-03
Axon part	27	71	*AP1S1, AP3S1, BLOC1S2, CCK, CHRM1, DAGLA, DGKI, ELK1, KCNA1, KCNC2, KCNIP3, KCNQ2, NEFL, PACSIN1, PNOC, PRKCZ, ROBO2, SCN1B, SCN2A, SCN8A, SERPINF1, STXBP1, SYN1, SYNJ1, SYP, SYT1, VAMP1*	4.00	2.42e-07
Axon terminus	16	35	*AP1S1, CCK, CHRM1, DGKI, ELK1, KCNA1, KCNC2, KCNIP3, PACSIN1, PNOC, STXBP1, SYN1, SYNJ1, SYP, SYT1, VAMP1*	5.40	4.44e-06
Blood circulation	30	138	*ATP1A3, ATP2B1, CACNA1G, CACNA1H, CACNA2D1, CACNB1, CACNB2, CACNG2, CACNG3, CHRM1, CLIC2, DRD1, EHD3, FGF12, GSK3A, HMGCR, ITGB1BP1, KCND3, KCNIP1, KCNIP3, KCNIP4, KCNK1, NCALD, OPRL1, PPARG, SCN1B, SCN2B, SCN3B, STC1, TRHDE*	1.78	6.23e-03
Calcium channel complex	10	26	*CACNA1G, CACNA1H, CACNA1I, CACNA2D1, CACNB1, CACNB2, CACNG2, CACNG3, MCU, PTPA*	3.96	1.53e-03
Calcium ion binding	38	171	*ACTN4, ANXA2, CABP1, CAMKK2, CDH10, CDH12, CDH18, CDH9, CDK5R1, CLSTN3, CRTAC1, DGKB, DOC2A, EHD3, EPDR1, HPCA, KCNIP1, KCNIP3, KCNIP4, MCTP1, NCALD, NELL1, PCDH19, PCDH8, PITPNM2, PITPNM3, PPP3R1, PRSS3, RASGRP1, RCVRN, REPS2, RPH3A, SLC25A23, SLIT1, SYT1, TBC1D9, TLL1, VSNL1*	1.85	1.44e-03
Calcium ion transmembrane transporter activity	11	37	*ATP2B1, CACNA1G, CACNA1H, CACNA1I, CACNA2D1, CACNB1, CACNB2, CACNG2, CACNG3, GRIN2A, MCU*	2.68	8.89e-03
Channel activity	42	139	*CACNA1G, CACNA1H, CACNA1I, CACNA2D1, CACNB1, CACNB2, CACNG2, CACNG3, CLIC2, GABRA2, GABRA3, GABRB3, GABRG2, GABRG3, GLRA3, GRIN2A, KCNA1, KCNA3, KCNA4, KCNB2, KCNC2, KCND3, KCNIP1, KCNIP3, KCNIP4, KCNJ16, KCNJ6, KCNK1, KCNQ2, KCNQ5, KCNS2, KCNV1, MCU, NCALD, PTK2B, SCN1B, SCN2A, SCN2B, SCN3B, SCN8A, SLC17A7, TTYH3*	2.87	2.44e-07
Chemical synaptic transmission, postsynaptic	12	22	*CDK5, CELF4, DGKI, GABRB3, GRIN2A, GSK3A, MAPK8IP2, MEF2C, PRKCZ, PTK2B, RIMS1, SLC17A7*	7.65	7.33e-06

(continued)

TABLE 4. Continued

GO Term	Count	Size	Genes	Odds ratio	p value
Chloride channel complex	8	19	*CLIC2, GABRA2, GABRA3, GABRB3, GABRG2, GABRG3, GLRA3, TTYH3*	4.60	2.33e-03
Cilium	23	88	*ANKMY2, ARL6, C5orf30, CEP126, CEP41, CFAP221, DRD1, EHD3, GNAQ, GPR83, GRK4, HK1, IQUB, KIF17, KIFAP3, LRRC6, MCHR1, NAPEPLD, NME5, PRKAR1B, PRKAR2B, SSX2IP, WRAP73*	2.27	1.39e-04
Circulatory system process	30	138	*ATP1A3, ATP2B1, CACNA1G, CACNA1H, CACNA2D1, CACNB1, CACNB2, CACNG2, CACNG3, CHRM1, CLIC2, DRD1, EHD3, FGF12, GSK3A, HMGCR, ITGB1BP1, KCND3, KCNIP1, KCNIP3, KCNIP4, KCNK1, NCALD, OPRL1, PPARG, SCN1B, SCN2B, SCN3B, STC1, TRHDE*	1.78	6.23e-03
Cyclic nucleotide biosynthetic process	13	38	*CAP2, ADCY1, RUNDC3A, DRD1, PTK2B, GNAL, GRM2, GSK3A, HPCA, OPRL1*	3.31	1.13e-03
Cyclic purine nucleotide metabolic process	13	38	*CAP2, ADCY1, RUNDC3A, DRD1, PTK2B, GNAL, GRM2, GSK3A, HPCA, OPRL1*	3.31	1.13e-03
Dendrite	43	160	*AMIGO1, ARHGAP32, ARHGAP44, ARHGEF2, ATP1A3, BAIAP2, CCK, CDK5, CDK5R1, CHL1, CHRM1, DGKI, DRP2, ELK1, FRMPD4, GABRA2, GLRA3, GLRX2, GNAQ, GNG3, GRK4, GRM2, HPCA, INPP5F, KCNA1, KCNB2, KCNC2, KCND3, KCNIP1, KCNIP3, KCNK1, PCDH8, PCSK2, PLK2, PNOC, PRKAR2B, PRKCG, PTK2B, RCVRN, SLC12A5, SYN1, SYNPO, THY1*	2.42	5.82e-06
Dendrite extension	4	7	*CPNE5, RIMS1, SYT1, UNC13A*	8.38	8.91e-03
Dopamine receptor signaling pathway	5	9	*DRD1, GNAL, GNAQ, GSK3A, VPS35*	7.87	3.84e-03
GABA receptor activity	6	10	*GABBR2, GABRA2, GABRA3, GABRB3, GABRG2, GABRG3*	9.47	8.64e-04
GABA receptor complex	5	9	*GABRA2, GABRA3, GABRB3, GABRG2, GABRG3*	7.87	3.84e-03
Gamma-aminobutyric acid signaling pathway	6	10	*HTR4, GABRG3, GABRG2, GABRA3, GABRA2, GABBR2*	9.47	8.64e-04
Glutamate receptor signaling pathway	13	28	*ATP1A3, CACNG2, CACNG3, CDK5R1, GNAQ, GRIN2A, GRM2, GRM5, HOMER1, MAPK8IP2, MEF2C, PTK2B, RASGRF1*	5.53	2.93e-05
Glutamate secretion	7	15	*CCK, GRM2, RIMS1, SLC17A7, SNAP25, STXBP1, SYT1*	5.53	2.14e-03
Growth cone	13	41	*CDK5, CDK5R1, CRTAC1, GAP43, LRRTM1, NEFL, NGEF, NRP1, PTK2B, RASGRF1, SNAP25, THY1, TIAM2*	2.95	2.48e-03
Intracellular protein transport	46	237	*AKAP5, ANXA2, AP1S1, AP2S1, AP3S1, ARHGEF2, ARL6, ATG4B, BAG4, BAP1, BID, CABP1, CDK5, CDK5R1, CHML, CHRM1, DRD1, EHD3, FBXW7, GDAP1, GNAQ, GSK3A, HPCA, ITGB1BP1, KCNB2, KCNIP3, MAPK14, NAPB, NAPG, OAZ2, PPP3R1, RAB8B, RANBP1, REEP2, RFTN1, RIMS1, RPH3A, RTN2, SSX2IP, TBC1D9, TMEM30A, TOMM34, TOMM70, UBR5, VPS35, VPS36*	1.56	8.18e-03
Ion channel complex	46	96	*AMIGO1, CACNA1G, CACNA1H, CACNA1I, CACNA2D1, CACNB1, CACNB2, CACNG2, CACNG3, CLIC2, DPP6, GABRA2, GABRA3, GABRB3, GABRG2, GABRG3, GLRA3, GRIN2A, KCNA1, KCNA3, KCNA4, KCNB2, KCNC2, KCND3, KCNIP1, KCNIP3, KCNIP4, KCNJ16, KCNJ6, KCNK1, KCNQ2, KCNQ5, KCNS2, KCNV1, MCU, OLFM2, OLFM3, PTK2B, PTPA, SCN1B, SCN2A, SCN2B, SCN3B, SCN8A, SNAP25, TTYH3*	6.24	3.15e-16
Ionotropic glutamate receptor signaling pathway	4	7	*ATP1A3, CDK5R1, GRIN2A, PTK2B*	8.38	8.91e-03
Main axon	9	25	*CCK, DAGLA, KCNA1, KCNC2, KCNQ2, ROBO2, SCN1B, SCN2A, SCN8A*	3.56	4.44e-03
Mitochondrial outer membrane permeabilization	4	7	*BID, BLOC1S2, GSK3A, PPP3R1*	8.38	8.91e-03
Mitochondrial outer membrane permeabilization involved in programmed cell death	4	7	*BID, BLOC1S2, GSK3A, PPP3R1*	8.38	8.91e-03

(continued)

TABLE 4. Continued

GO Term	Count	Size	Genes	Odds ratio	p value
Modulation of synaptic transmission	27	78	*BAIAP2, BTBD9, CA7, CDK5, CELF4, CLSTN3, DGKI, DRD1, GFAP, GRIN2A, GRM2, GRM5, LRRTM1, LRRTM2, MAPK8IP2, MEF2C, PLK2, PRKCZ, PTK2B, RASGRF1, RIMS1, SNAP25, STXBP1, SYN1, SYP,* SYT1, UNC13A	3.44	2.13e-06
Neurofilament	4	6	*INA, NEFL, NEFM, NRP1*	12.60	4.28e-03
Neuron part	107	379	*ACTL6B, ACTN4, ADGRB1, AMIGO1, AMPH, AP1S1, AP3S1, ARHGAP32, ARHGAP44, ARHGEF2, ATL1, ATP1A3, ATP2B1, BAIAP2, BLOC1S2, CABP1, CADPS, CADPS2, CCK, CDK5, CDK5R1, CHL1, CHRM1, CPNE5, CRTAC1, DAGLA, DDN, DGKI, DLGAP1, DOC2A, DRP2, ELK1, ENC1, FRMPD4, GABBR2, GABRA2, GABRG2, GAP43, GLRA3, GLRX2, GNAQ, GNG3, GRIN2A, GRK4, GRM2, GRM5, HOMER1, HPCA, ICA1, INPP5F, KCNA1, KCNA3, KCNA4, KCNB2, KCNC2, KCND3, KCNIP1, KCNIP3, KCNK1, KCNQ2, LIMK1, LRRTM1, MAPK8IP2, NAPEPLD, NEFL, NEFM, NGEF, NRP1, NRSN2, NRXN3, OPRL1, PACSIN1, PCDH8, PCSK2, PDE1B, PIP5K1C, PLK2, PNOC, PRKAR2B, PRKCG, PRKCZ, PTK2B, RAP1GAP2, RASGRF1, RBFOX3, RCVRN, RIMS1, ROBO2, RPH3A, SCN1B, SCN2A, SCN8A, SERPINF1, SLC12A5, SLC17A7, SNAP25, STXBP1, SV2B, SYN1, SYNJ1, SYNPO, SYP, SYT1, THY1, TIAM2, UNC13A, VAMP1*	2.81	2.92e-15
Neuron projection	90	294	*ACTN4, AMIGO1, AP1S1, AP3S1, ARHGAP32, ARHGAP44, ARHGEF2, ATL1, ATP1A3, ATP2B1, BAIAP2, BLOC1S2, CCK, CDK5, CDK5R1, CHL1, CHRM1, CPNE5, CRTAC1, DAGLA, DDN, DGKI, DOC2A, DRP2, ELK1, FRMPD4, GABBR2, GABRA2, GABRG2, GAP43, GLRA3, GLRX2, GNAQ, GNG3, GRIN2A, GRK4, GRM2, GRM5, HOMER1, HPCA, INPP5F, KCNA1, KCNA3, KCNA4, KCNB2, KCNC2, KCND3, KCNIP1, KCNIP3, KCNK1, KCNQ2, LIMK1, LRRTM1, NEFL, NEFM, NGEF, NRP1, OPRL1, PACSIN1, PCDH8, PCSK2, PLK2, PNOC, PRKAR2B, PRKCG, PRKCZ, PTK2B, RAP1GAP2, RASGRF1, RCVRN, ROBO2, RPH3A, SCN1B, SCN2A, SCN8A, SERPINF1, SLC12A5, SLC17A7, SNAP25, STXBP1, SV2B, SYN1, SYNJ1, SYNPO, SYP, SYT1, THY1, TIAM2, UNC13A, VAMP1*	3.16	3.62e-15
Neuron projection morphogenesis	33	157	*ADCY1, ADGRB1, AMIGO1, ATL1, BAIAP2, CCK, CDK5, CDK5R1, CHL1, CLIN1, CPNE5, GAP43, HPRT1, ID1, LIMK1, MAPK8IP2, NEFL, NGEF, NRP1, NRXN3, NTN4, PACSIN1, PRKCZ, RBFOX2, RIMS1, ROBO2, SCN1B, SLIT1, STXBP1, SYT1, THY1, UNC13A, ZNF280B*	1.71	7.27e-03
Neuron remodeling	3	4	*GNAQ, NTN4, RND1*	18.80	9.40e-03
Neuronal cell body	36	130	*AMIGO1, ARHGEF2, ATP2B1, BAIAP2, CCK, CDK5, CDK5R1, CPNE5, DDN, DGKI, DRP2, ELK1, ENC1, GABRA2, GLRA3, GLRX2, GRK4, HPCA, INPP5F, KCNA1, KCNB2, KCNC2, KCNK1, MAPK8IP2, NRP1, NRSN2, PCSK2, PDE1B, PNOC, PRKAR2B, PRKCZ, PTK2B, RBFOX3, SERPINF1, SLC12A5, SYNPO*	2.50	1.69e-05
Neuron-neuron synaptic transmission	16	46	*CA7, CDK5, CLSTN3, DGKI, DRD1, GABRG2, GLRA3, GRM2, GRM5, MAPK8IP2, MEF2C, PTK2B, SLC17A7, STXBP1, SYT1, UNC13A*	4.10	5.04e-05
Neurotransmitter receptor activity	9	23	*CHRM1, DRD1, GABRA2, GABRA3, GABRB3, GABRG2, GLRA3, GRIN2A, PTK2B*	4.07	2.23e-03
Neurotransmitter secretion	16	46	*CDK5, RPH3A, RIMS1, UNC13A, PIP5K1C, MEF2C, SNAP25, STXBP1, SYN1, SYT1, DOC2A, CADPS, SYNJ1, DGKI, CADPS2, NRXN3*	3.41	2.49e-04
Node of Ranvier	4	6	*KCNQ2, SCN1B, SCN2A, SCN8A*	12.60	4.28e-03
Nonmotile primary cilium	9	25	*C5orf30, DRD1, GNAQ, GPR83, GRK4, KIF17, KIFAP3, MCHR1, NAPEPLD*	3.56	4.44e-03
Postsynapse	39	121	*ADGRB1, ARHGAP32, ARHGAP44, ATP1A3, BAIAP2, CABP1, CADPS2, CDK5, CDK5R1, CHRM1, CLSTN3, DGKI, DLGAP1, DRP2, FRMPD4, GABBR2, GABRA2, GABRA3, GABRB3, GABRG2, GABRG3, GAP43, GLRA3, GRIN2A, GRM5, GSK3A, HOMER1, HPCA, KCNC2, LRRTM1, LRRTM2, MAPK8IP2, MEF2C, PCDH8, PRKAR2B, PTK2B, SLC17A7, SYN1, SYNPO*	3.14	9.97e-08

(continued)

TABLE 4. Continued

GO Term	Count	Size	Genes	Odds ratio	p value
Postsynaptic density	17	54	*ADGRB1, ARHGAP32, BAIAP2, CABP1, CDK5, CDK5R1, CHRM1, DLGAP1, DRP2, GAP43, GRIN2A, GRM5, HOMER1, MAPK8IP2, PTK2B, SYN1, SYNPO*	2.94	6.16e-04
Potassium channel activity	16	39	*KCNA1, KCNA3, KCNA4, KCNB2, KCNC2, KCND3, KCNIP1, KCNIP3, KCNIP4, KCNJ16, KCNJ6, KCNK1, KCNQ2, KCNQ5, KCNS2, KCNV1*	4.46	2.41e-05
Potassium ion transport	25	71	*AMIGO1, ATP1A3, CAB39, DPP10, DPP6, DRD1, KCNA1, KCNA3, KCNA4, KCNB2, KCNC2, KCND3, KCNIP1, KCNIP3, KCNIP4, KCNJ16, KCNJ6, KCNK1, KCNQ2, KCNQ5, KCNS2, KCNV1, PTK2B, SLC12A5, SLC12A8*	3.52	3.60e-06
Presynapse	29	84	*AMPH, AP1S1, CADPS, CADPS2, CCK, CDK5, DGKI, DOC2A, GABRA2, GRIN2A, GRM2, ICA1, KCNA1, KCNC2, NRXN3, PCDH8, PIP5K1C, RIMS1, RPH3A, SLC17A7, SNAP25, STXBP1, SV2B, SYN1, SYNJ1, SYP, SYT1, UNC13A, VAMP1*	3.44	9.43e-07
Primary cilium	11	37	*ARL6, C5orf30, CEP41, DRD1, GNAQ, GPR83, GRK4, KIF17, KIFAP3, MCHR1, NAPEPLD*	2.68	8.98e-03
Purine nucleotide biosynthetic process	16	59	*ADCY1, AKAP5, ATP5A1, CAP2, DRD1, GABBR2, GNAL, GRM2, GSK3A, HPCA, HPRT1, NME5, OPRL1, PTK2B, RCVRN, RUNDC3A*	2.37	4.90e-03
Regulation of alternative mRNA splicing, via spliceosome	5	10	*CELF3, CELF4, RBFOX1, RBFOX2, RBFOX3*	6.30	6.82e-03
Regulation of calcium ion-dependent exocytosis	9	24	*CACNA1G, CACNA1I, CDK5, DOC2A, RIMS1, RPH3A, STXBP1, SYN1, SYT1*	3.80	3.23e-03
Regulation of ion transmembrane transport	46	125	*ACTN4, AMIGO1, CAB39, CACNA1G, CACNA1H, CACNA1I, CACNA2D1, CACNB1, CACNB2, CACNG2, CACNG3, CLIC2, DPP10, DPP6, DRD1, EHD3, FGF12, HOMER1, KCNA1, KCNA3, KCNA4, KCNB2, KCNC2, KCND3, KCNIP1, KCNIP3, KCNIP4, KCNJ16, KCNJ6, KCNQ2, KCNQ5, KCNS2, KCNV1, MAPK8IP2, MEF2C, MMP9, OPRL1, PTK2B, PTPN3, RASGRF1, SCN1B, SCN2A, SCN2B, SCN3B, SCN8A, THY1*	3.91	4.16e-11
Regulation of neurotransmitter levels	23	64	*CADPS, CADPS2, CDK5, DAGLA, DGKI, DOC2A, DRD1, GABRA2, GFAP, MEF2C, NRXN3, PDE1B, PIP5K1C, RIMS1, RPH3A, SLC17A7, SNAP25, STXBP1, SV2B, SYN1, SYNJ1, SYT1, UNC13A*	3.63	5.98e-06
Regulation of nucleotide biosynthetic process	13	37	*ADCY1, AKAP5, CAP2, DRD1, GABBR2, GNAL, GRM2, GSK3A, HPCA, OPRL1, PTK2B, RCVRN, RUNDC3A*	3.45	8.49e-04
Regulation of nucleotide metabolic process	15	49	*ADCY1, AKAP5, CAP2, DRD1, GABBR2, GNAL, GRM2, GSK3A, HPCA, OPRL1, PTK2B, RCVRN, RUNDC3A, SLC25A23, TIGAR*	2.81	1.76e-03
Regulation of purine nucleotide biosynthetic process	13	39	*CAP2, ADCY1, RUNDC3A, DRD1, PTK2B, GNAL, GRM2, GSK3A, HPCA, OPRL1*	3.18	1.49e-03
Regulation of synapse assembly	10	27	*ADGRB1, ADGRB2, AMIGO1, CLSTN3, LRRTM1, LRRTM2, MEF2C, NRXN3, ROBO2, SLIT1*	3.73	2.17e-03
Regulation of synapse organization	11	36	*ADGRB1, ADGRB2, AMIGO1, CLSTN3, FRMPD4, LRRTM1, LRRTM2, MEF2C, NRXN3, ROBO2, SLIT1*	2.79	7.18e-03
Regulation of synapse structure or activity	11	36	*ADGRB1, ADGRB2, AMIGO1, CLSTN3, FRMPD4, LRRTM1, LRRTM2, MEF2C, NRXN3, ROBO2, SLIT1*	2.79	7.18e-03
Regulation of synaptic plasticity	18	43	*BAIAP2, CDK5, DGKI, DRD1, GFAP, GRIN2A, GRM5, LRRTM1, LRRTM2, MEF2C, PLK2, PRKCZ, PTK2B, RASGRF1, SNAP25, STXBP1, SYP, UNC13A*	4.63	5.26e-06
Regulation of transmembrane transport	47	129	*ACTN4, AMIGO1, CAB39, CACNA1G, CACNA1H, CACNA1I, CACNA2D1, CACNB1, CACNB2, CACNG2, CACNG3, CLIC2, DPP10, DPP6, DRD1, EHD3, FGF12, HOMER1, KCNA1, KCNA3, KCNA4, KCNB2, KCNC2, KCND3, KCNIP1, KCNIP3, KCNIP4, KCNJ16, KCNJ6, KCNQ2, KCNQ5, KCNS2, KCNV1, MAPK8IP2, MEF2C, MMP9, OAZ2, OPRL1, PTK2B, PTPN3, RASGRF1, SCN1B, SCN2A, SCN2B, SCN3B, SCN8A, THY1*	3.86	3.79e-11

(continued)

TABLE 4. Continued

GO Term	Count	Size	Genes	Odds ratio	p value
Regulation of vesicle-mediated transport	27	120	*ACTN4, ANXA2, AP2S1, BTBD9, CACNA1G, CACNA1I, CADPS2, CDK5, DOC2A, INPP5F, LRRTM1, LRRTM2, NRP1, PACSIN1, PPARG, PRKCG, RAB27B, RIMS1, RINT1, RPH3A, SCFD1, SNAP91, STXBP1, SYN1, SYT1, TBC1D9, VSNL1*	1.86	5.74e-03
Somatodendritic compartment	54	205	*AMIGO1, ARHGAP32, ARHGAP44, ARHGEF2, ATP1A3, ATP2B1, BAIAP2, CCK, CDK5, CDK5R1, CHL1, CHRM1, CPNE5, DDN, DGKI, DRP2, ELK1, ENC1, FRMPD4, GABRA2, GLRA3, GLRX2, GNAQ, GNG3, GRK4, GRM2, HPCA, INPP5F, KCNA1, KCNB2, KCNC2, KCND3, KCNIP1, KCNIP3, KCNK1, MAPK8IP2, NRP1, NRSN2, PCDH8, PCSK2, PDE1B, PLK2, PNOC, PRKAR2B, PRKCG, PRKCZ, PTK2B, RBFOX3, RCVRN, SERPINF1, SLC12A5, SYN1, SYNPO, THY1*	2.39	6.48e-07
Synapse	68	222	*ADGRB1, AMPH, AP1S1, ARHGAP32, ARHGAP44, ATP1A3, ATP2B1, BAIAP2, CABP1, CADPS, CADPS2, CCK, CDK5, CDK5R1, CHRM1, CLSTN3, DDN, DGKI, DLGAP1, DOC2A, DRP2, FRMPD4, GABBR2, GABRA2, GABRA3, GABRB3, GABRG2, GABRG3, GAP43, GLRA3, GRIN2A, GRM2, GRM5, GSK3A, HOMER1, HPCA, ICA1, KCNA1, KCNC2, KCNK1, LRRTM1, LRRTM2, MAPK8IP2, MEF2C, NRXN3, OLFM2, OLFM3, PACSIN1, PCDH8, PHACTR1, PIP5K1C, PRKAR2B, PRKCG, PTK2B, RIMS1, RPH3A, SLC17A7, SNAP25, STXBP1, SV2B, SYN1, SYNJ1, SYNPO, SYP, SYT1, UNC13A, VAMP1, WASF1*	3.05	1.43e-11
Synapse assembly	12	39	*ADGRB1, ADGRB2, AMIGO1, CDK5, CLSTN3, DRD1, LRRTM1, LRRTM2, MEF2C, NRXN3, ROBO2, SLIT1*	2.82	4.75e-03
Synapse organization	18	67	*ADGRB1, ADGRB2, AMIGO1, CACNB1, CACNB2, CACNG2, CDK5, CLSTN3, DRD1, DRP2, FRMPD4, LRRTM1, LRRTM2, MEF2C, NRXN3, ROBO2, SLIT1, UNC13A*	2.34	3.25e-03
Synapse part	63	190	*ADGRB1, AMPH, AP1S1, ARHGAP32, ARHGAP44, ATP1A3, ATP2B1, BAIAP2, CABP1, CADPS, CADPS2, CCK, CDK5, CDK5R1, CHRM1, CLSTN3, DDN, DGKI, DLGAP1, DOC2A, DRP2, FRMPD4, GABBR2, GABRA2, GABRA3, GABRB3, GABRG2, GABRG3, GAP43, GLRA3, GRIN2A, GRM2, GRM5, GSK3A, HOMER1, HPCA, ICA1, KCNA1, KCNC2, LRRTM1, LRRTM2, MAPK8IP2, MEF2C, NRXN3, OLFM2, PCDH8, PIP5K1C, PRKAR2B, PRKCG, PTK2B, RIMS1, RPH3A, SLC17A7, SNAP25, STXBP1, SV2B, SYN1, SYNJ1, SYNPO, SYP, SYT1, UNC13A, VAMP1*	3.41	1.79e-12
Synaptic membrane	35	89	*ARHGAP32, ATP2B1, CABP1, CADPS2, CDK5, CHRM1, CLSTN3, DDN, DGKI, DLGAP1, DRP2, GABBR2, GABRA2, GABRA3, GABRB3, GABRG2, GABRG3, GLRA3, GRIN2A, GRM2, HOMER1, KCNA1, KCNC2, LRRTM1, LRRTM2, OLFM2, PCDH8, PRKCG, RIMS1, SNAP25, SYNJ1, SYNPO, SYP, SYT1, UNC13A*	4.28	1.28e-08
Synaptic signaling	63	182	*AKAP5, AMPH, BAIAP2, BTBD9, CA7, CACNA1G, CACNB1, CACNB2, CADPS, CADPS2, CDK5, CELF4, CHRM1, CLSTN3, DGKI, DLGAP1, DOC2A, DRD1, EGR3, FGF12, GABBR2, GABRB3, GABRG2, GFAP, GLRA3, GPR176, GRIN2A, GRM2, GRM5, GSK3A, HOMER1, HTR4, KCNA1, KCNQ2, KCNQ5, LRRTM1, LRRTM2, MAPK8IP2, MEF2C, NRXN3, OPRL1, PCDH8, PIP5K1C, PLK2, PNOC, PRKCG, PRKCZ, PTK2B, RASGRF1, RIMS1, RPH3A, SCN1B, SCN2B, SLC12A5, SLC17A7, SNAP25, SNAP91, STXBP1, SYN1, SYNJ1, SYP, SYT1, UNC13A*	3.65	1.90e-13
Synaptic transmission, glutamatergic	12	26	*CDK5, CLSTN3, DGKI, DRD1, GRM2, GRM5, MAPK8IP2, MEF2C, PTK2B, SLC17A7, SYT1, UNC13A*	5.46	6.45e-05
Synaptic vesicle	14	37	*AMPH, DGKI, DOC2A, GABRA2, GRIN2A, ICA1, RPH3A, SLC17A7, SNAP25, SV2B, SYN1, SYP, SYT1, VAMP1*	3.88	2.21e-04
Synaptic vesicle endocytosis	6	10	*CDK5, BTBD9, PIP5K1C, PACSIN1, SYT1, SYNJ1*	9.47	8.64e-04

(continued)

TABLE 4. Continued

GO Term	Count	Size	Genes	Odds ratio	p value
Synaptic vesicle exocytosis	13	34	*CADPS, CADPS2, CDK5, DOC2A, PIP5K1C, RIMS1, RPH3A, SNAP25, STXBP1, SYN1, SYNJ1, SYT1, UNC13A*	3.94	3.28e-04
Synaptic vesicle maturation	4	5	*UNC13A, SYP, STXBP1, SLC17A7*	25.20	1.60e-03
Synaptic vesicle membrane	11	22	*AMPH, DOC2A, GABRA2, ICA1, RPH3A, SLC17A7, SV2B, SYN1, SYP, SYT1, VAMP1*	6.36	5.22e-05
Synaptic vesicle priming	5	7	*CADPS, CADPS2, SNAP25, STXBP1, SYNJ1*	15.80	8.14e-04
Synaptic vesicle recycling	6	10	*CDK5, BTBD9, PIP5K1C, PACSIN1, SYT1, SYNJ1*	9.47	8.64e-04
Synaptic vesicle transport	17	42	*AP3S1, BLOC1S2, BTBD9, CADPS, CADPS2, CDK5, DOC2A, PACSIN1, PIP5K1C, RIMS1, RPH3A, SNAP25, STXBP1, SYN1, SYNJ1, SYT1, UNC13A*	4.36	1.66e-05
Terminal bouton	9	17	*AP1S1, CCK, KCNC2, STXBP1, SYN1, SYNJ1, SYP, SYT1, VAMP1*	7.14	1.47e-05
Transport vesicle	25	103	*AMPH, AP1S1, AP3S1, CNST, DDHD2, DGKI, DOC2A, GABRA2, GRIN2A, ICA1, NCALD, NRSN2, PCSK2, RAB27B, RPH3A, SCG3, SLC17A7, SNAP25, STEAP2, SV2B, SYN1, SYP, SYT1, TMEM30A, VAMP1*	2.06	2.69e-03
Voltage-gated ion channel activity	30	65	*CACNA1G, CACNA1H, CACNA1I, CACNA2D1, CACNB1, CACNB2, CACNG2, CACNG3, CLIC2, KCNA1, KCNA3, KCNA4, KCNB2, KCNC2, KCND3, KCNIP1, KCNIP3, KCNIP4, KCNJ16, KCNJ6, KCNK1, KCNQ2, KCNQ5, KCNS2, KCNV1, SCN1B, SCN2A, SCN2B, SCN3B, SCN8A*	5.64	1.91e-10

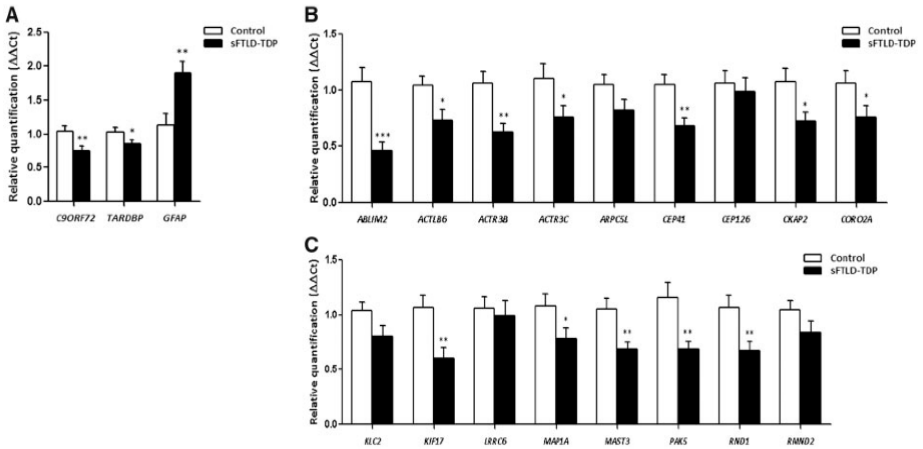

FIGURE 3. mRNA expression levels of selected deregulated genes in frontal cortex area 8 of sFTLD-TDP and controls assessed with TaqMan RT-qPCR assays. Genes coding for **(A)** proteins involved in toxic aggregates of FTLD variants and *GFAP*: **(B, C)** cytoskeleton and structural components. Significant levels set at *p < 0.05, **p < 0.01, and ***p < 0.001.

(p = 0.001), *APRT* (p = 0.001), *DGUOK* (p = 0.007), *ENTPD3* (p = 0.02), *NME1* (p = 0.03), *NME3* (p = 0.01), *NME7* (p = 0.007), and *POLR3B* (p = 0.003) were significantly deregulated in sFTLD-TDP (Fig. 5).

Protein Expression Levels of Selected Genes

Expression levels of 14 proteins not related to mitochondria and energy metabolism were assessed. C9ORF72 protein levels were significantly decreased in sFTLD-TDP (p = 0.01). However, TDP-43 levels were increased in sFTLD-TDP (p = 0.02) (Fig. 6). Significant reduction of VGAT (p = 0.04) and GAD1 (p = 0.02) levels occurred in sFTLD-TDP. A significant reduction was found in GABRD protein levels (p = 0.02), but no changes were detected in synaptophysin (SYP), NMDAR2A, GABAARB2, calbindin-28K (CALB1), and SNAP25 levels in sFTLD-TDP. GFAP levels showed a

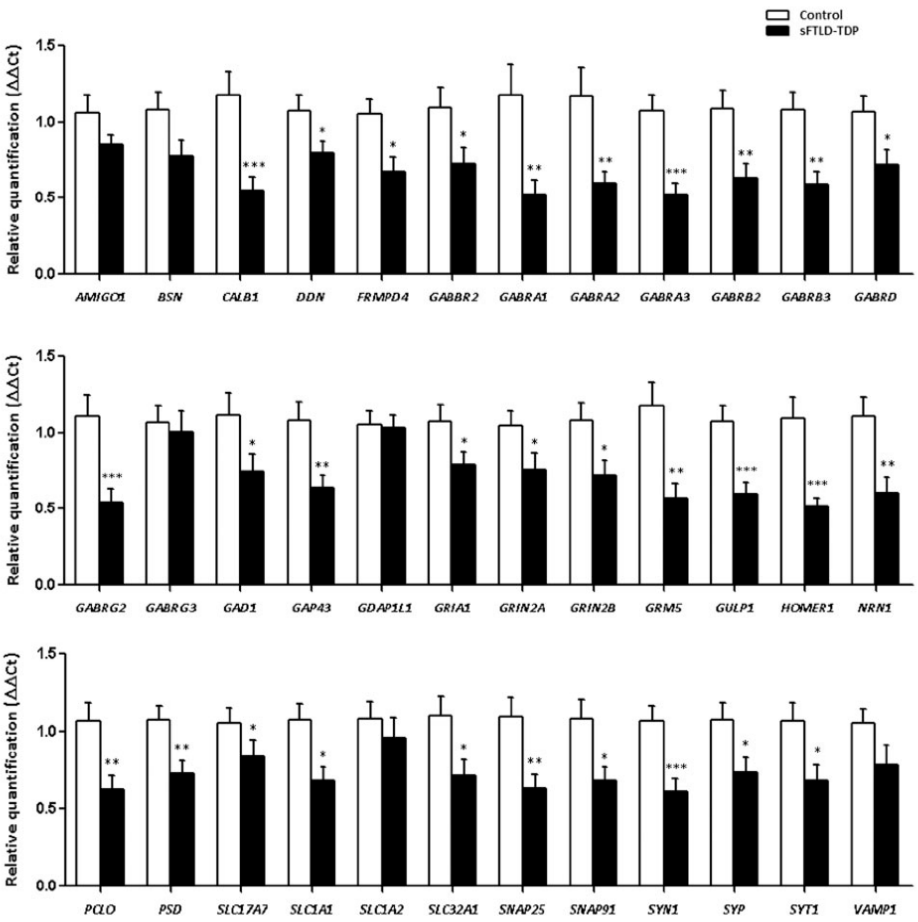

FIGURE 4. mRNA expression levels of selected deregulated genes identified by microarray analysis in frontal cortex area 8 of sFTLD-TDP and controls assessed by TaqMan RT-qPCR assays are coding for glutamatergic and GABAergic-related genes and corresponding ionotropic and metabotropic receptors, as well as synaptic cleft proteins and neurotransmission vesicles system. Significant levels set at *$p < 0.05$, **$p < 0.01$, and ***$p < 0.001$.

nonsignificant increase in sFTLD-TDP cases when compared with controls (Fig. 6).

Total TAU, 4R-TAU and 3R-TAU

To further analyze cytoskeletal anomalies, the expression levels of total TAU, 3R-TAU, and 4R-TAU were assessed using forward SYBR primer and reverse primer specific probes. Total Tau, 3R-TAU, and 4R-TAU mRNA expression levels were similar in sFTLD-TDP cases when compared with controls. In this line, 4R/3R ratio was preserved in sFTLD cases. Protein expression was studied with Western blotting. Total TAU protein levels were similar in sFTLD-TDP and controls and the ratio 4R/3R was not modified. Finally, no evidence of increased tau phosphorylation, as revealed with the phospho-tauThr181 antibody was found in sFTLD-TDP (Fig. 7).

Mitochondrial Alterations

Genes Coding for Mitochondrial Subunits and Energy Metabolism

The expression of 37 genes was assessed by RT-qPCR; 27 of them were deregulated in sFTLD-TDP. Downregulated genes encoded subunits of the electron transport chain (ETC) complexes I: *NDUFA2* ($p = 0.02$), *NDUFA5* ($p = 0.05$), *NDUFA10* ($p = 0.016$), *NDUFAF2* ($p = 0.02$), *NDUFAF6* ($p = 0.04$), *NDUFB5* ($p = 0.016$), *NDUFB8* ($p = 0.017$), and *NDUFB10* ($p = 0.025$); subunits of complex IV: *COX7A2L*

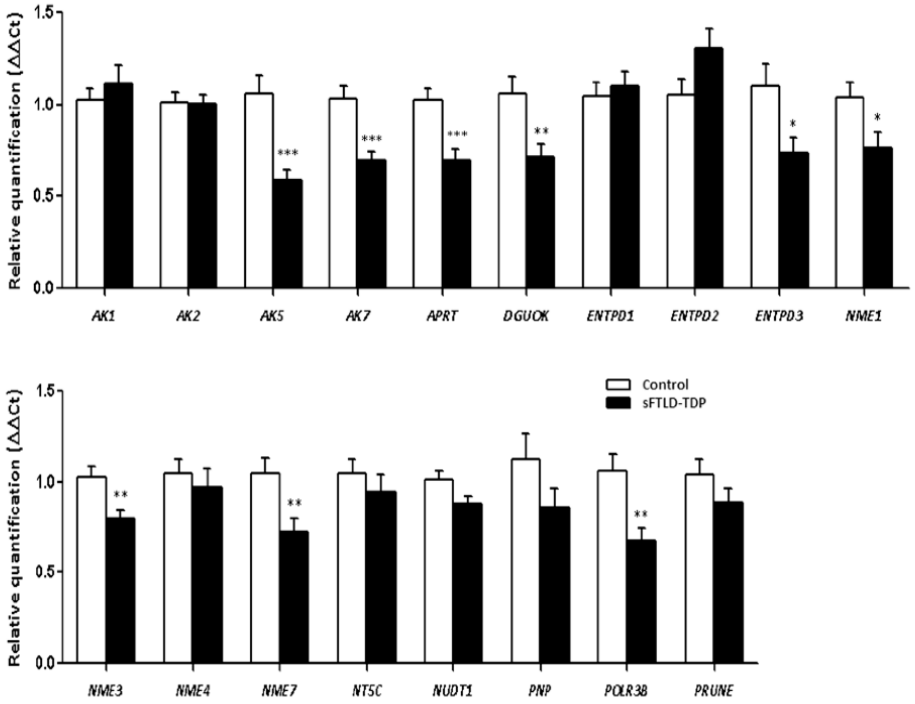

FIGURE 5. mRNA expression levels of selected deregulated genes identified by microarray analysis in frontal cortex area 8 of sFTLD-TDP and controls assessed with TaqMan RT-qPCR assays coding for purines metabolism. Significant levels set at *$p < 0.05$, **$p < 0.01$, and ***$p < 0.001$.

($p = 0.02$) and *COA6* ($p = 0.02$); and complex V: *ATP5O* ($p = 0.015$), *ATP5A1* ($p = 0.03$), and *ATP5B* ($p = 0.04$). In addition, several genes involved in energy metabolism were downregulated in sFTLD-TDP including *ATP2B3* ($p = 0.03$), *ATP2B4* ($p = 0.04$), *ATP6D* ($p = 0.02$), *ATP6V1A* ($p = 0.002$), *FASTKD2* ($p = 0.007$), *MCU* ($p = 0.045$), *MICU3* ($p = 0.01$), *MTIF2* ($p = 0.006$), *MTX3* ($p = 0.03$), *RMND1* ($p = 0.005$), *SLC25A1* ($p = 0.01$), *SLC25A11* ($p = 0.03$), *SLC25A23* ($p = 0.03$), and *TOMM70* ($p = 0.001$) (Fig. 8A).

Mitochondria Protein Levels in Mitochondria-enriched Fractions

Decreased levels of NDUFB10 were found in sFTLD-TDP ($p = 0.04$), but not of NDUFB8, NDUFS8, NDUFA10. Protein levels of SDHB, a component of ETC complex II, were not modified in sFTLD-TDP. In contrast, UQCRC2, a component of ETC complex III, was significantly increased in sFTLD-TDP ($p = 0.03$). Levels of ATP5A were significantly decreased ($p = 0.04$). MT-CO1 levels were significantly decreased in sFTLD-TDP ($p = 0.01$) but MT-ND1 expression was preserved (Fig. 8B). In contrast to mRNA expression, TOMM70 protein levels were not significantly altered in pathological cases when compared with controls.

Mitochondrial Enzymatic Activities in Mitochondrial Enriched Fractions

The enzymatic activity of mitochondrial complexes I, IV, and V was significantly reduced in sFTLD-TDP cases when compared with controls ($p = 0.04$, $p = 0.03$, and $p = 0.05$, respectively) (Fig. 8C).

DISCUSSION

Gene transcription profiles are analyzed in the frontal cortex area 8 in sFTLD cases with typical neuropathology including TDP-43-immunoreactive inclusions mainly in the form of cortical neurites and intracytoplasmic inclusions. Cases in this series had reduced *TARDBP* mRNA expression and increased levels of TDP-43 protein, and reduced expression of C9Orf72 mRNA and protein. Opposite expression of TDP mRNA and protein may be related to translational modifications. These are further accompanied by posttranslational modifications of TDP-43 (10). Decreased C9Orf72 mRNA and protein was not expected and further studies are needed to elucidate C9Orf72 loss of function in sFTLD-TDP not linked to *C9ORF72* mutations.

The present study using whole-transcriptome microarray hybridization showed downregulation of several genes in

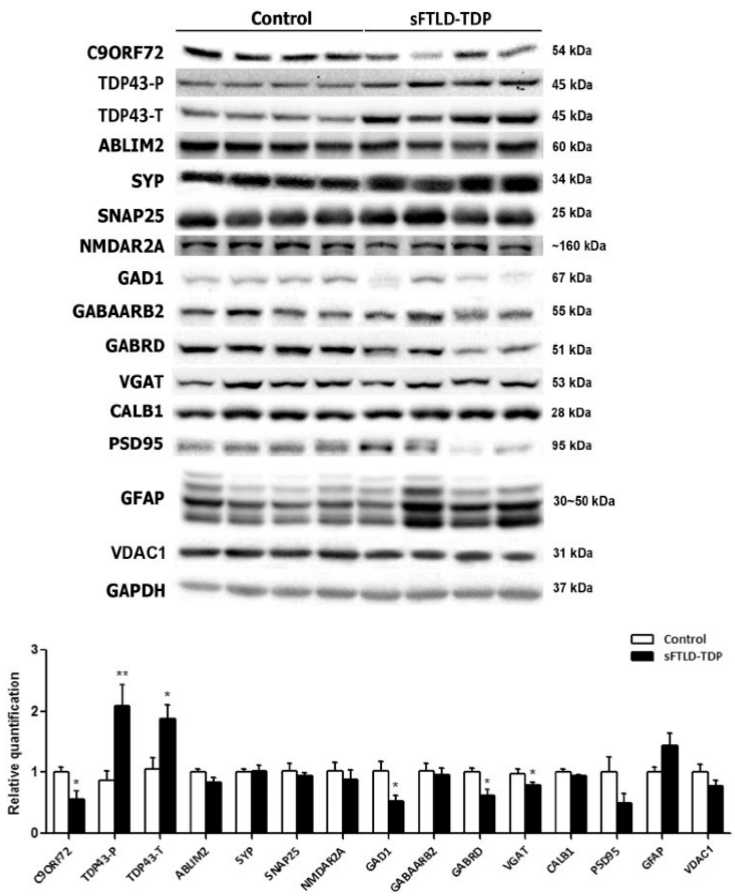

FIGURE 6. Gel electrophoresis and Western blotting of proteins involved in toxic aggregates in FTLD, GABAergic, and glutamatergic neurotransmission systems, synaptic vesicles, cytoskeleton, neuroinflammation, and mitochondria. Significant levels set at $^{*}p < 0.05$, $^{**}p < 0.01$, and $^{***}p < 0.001$.

the frontal cortex area 8 in sFTLD-TDP clustered in pathways involved in neurotransmission and synapsis, neuronal architecture, cytoskeleton of axons and dendrites, vesicle trafficking, purine metabolism, mitochondria, and energy metabolism. Microarray observations were further validated by RT-qPCR of selected genes from predicted altered pathways after searching on Gene Ontology (GO) database, using 111 probes; the expression of 81 genes was significantly deregulated in this cortical region in sFTLD-TDP when compared with controls. Expression levels of 24 proteins were analyzed by Western blotting; levels of 8 proteins were altered in sFTLD-TDP. Neurotransmission was markedly affected in sFTLD-TDP involving downregulated gene expression of glutamate decarboxylase, several types and subunits of ionotropic and metabotropic glutamate and GABA receptors, neuronal vesicular and soluble glutamate transporters, and various synaptic proteins, together with loss of calbindin expression. This provides robust support to preliminary observations showing decreased numbers, amputation, and proximal swellings of dendritic branches and loss of synaptic spine pyramidal cells, and loss of calbindin-immunoreactive neurons and atrophy of remaining neurons in layers II and III of the frontal cortex in FTLD (24). Protein expression studies showing decreased levels of synaptic markers are also in line with previous observations demonstrating reduced levels of several synaptic and presynaptic plasma membrane proteins in the frontal cortex, but not in the posterior parietal cortex assessed in parallel, in FTLD (25).

In contrast to the marked decrease in the expression of cytoskeletal and synaptic markers, tau mRNA and protein levels were preserved in the present series, and tau phosphorylation was not increased in sFTLD-TDP. This is in contrast with

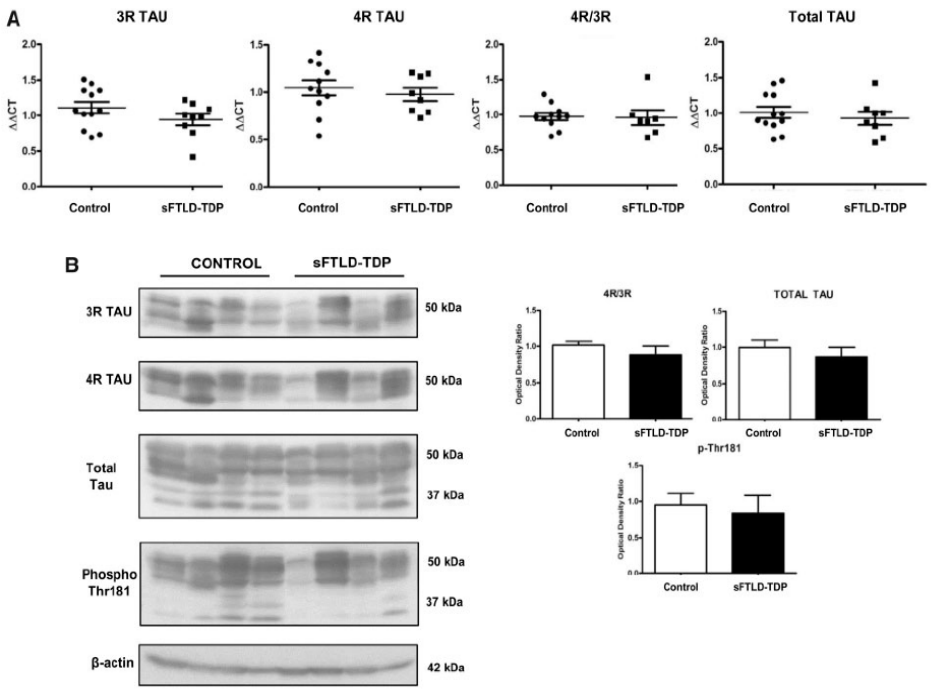

FIGURE 7. (A) mRNA expression levels of total TAU, 3R-TAU, and 4R-TAU in the frontal cortex area 8 in control and sFTLD-TDP. No significant differences are observed and the ratio 4R/3R is similar in sFTLD and controls. **(B)** Similarly, no differences in TAU protein expression and 4R/3R are seen in sFTLD-TDP cases and controls. Phospho-tau levels, as revealed with the phospho-tau-specific Thr181 antibody, are similar in control and sFTLD-TDP.

early reports pointing to decreased tau protein levels in FTLD with ubiquitin inclusions (presumably FTLD-TDP), which suggested that FTLD-U may be a novel "inverse" tauopathy because of the reduced levels of tau (26, 27). Reduced tau mRNA and protein levels have been reported in FTLD-TDP linked to GRN mutations but not in other FTLD-TDP subtypes including sporadic FTLD-TDP and FTLD-TDP-C9ORF72 (28).

Mitochondrial alterations compromise mRNA expression of several subunits of the mitochondrial complexes. Moreover, they are accompanied by altered protein expression of several subunits and with reduced activity of complexes I, IV, and V in sFTLD-TDP. Importantly, in addition to mitochondrial subunits encoded by genomic DNA, expression levels of MT-CO1 encoded by mitochondrial DNA are reduced in sFTLD-TDP. Therefore, mitochondrial alterations in sFTLD-TDP have both genomic and mitochondrial components. Other genes involved in energy metabolism are downregulated as well, thus indicating functional energy metabolism failure in sFTLD-TDP. Gene-specific mitochondrial dysfunction has been described in human fibroblasts bearing mutations in *TARDBP* and *C9ORF72* (29). Mitochondrial dysfunction has also been documented in a transgenic knock-in mouse model for TDP-43 (30). Therefore, mitochondrial alterations seem to be common to different forms of sFTLD-TDP and fFTLD-TDP.

Purines and pyrimidines are components of a large number of key molecules. The primary purines adenine and guanosine, and pyrimidines cytosine, thymidine, and uracyl, are the core of DNA, RNA, nucleosides, and nucleotides involved in energy transfer (ATP, GTP) and coenzymes (NADH, FADH2) (31, 32). Alterations in the expression of genes encoding enzymes of purine metabolism may interfere with numerous metabolic processes in sFTLD-TDP.

It can be argued that differences in the percentage of neurons, astrocytes, oligodendroglia, and microglia lie beyond distinct patterns of gene expression, protein levels, and mitochondrial enzymatic activities in sFTLD-TDP. Certainly, neuron loss, spongiosis in the upper cortical layers and variable astrocytic gliosis are typical morphological alterations in sFTLD-TDP (1–3). Present findings complement morphological observations by biochemical data that identify damage of particular components of vital molecular pathways and essential modulators of synaptic transmission.

Previous studies have shown differential gene expression in frontal cortex between 6 cases of FTLD-U

A

	Gene symbol	Gene name	Control	sFTLD-TDP
Complex I	*NDUFA2*	NADH:Ubiquinone Oxidoreductase Subunit A2	1,03 ± 0,07	0,77 ± 0,07*
	NDUFA5	NADH:Ubiquinone Oxidoreductase Subunit A5	1,03 ± 0,07	0,78 ± 0,09*
	NDUFA10	NADH:Ubiquinone Oxidoreductase Subunit A10	1,03 ± 0,06	0,75 ± 0,04***
	NDUFAF6	NADH:Ubiquinone Oxidoreductase Complex Assembly Factor 6	1,02 ± 0,07	0,79 ± 0,08*
	NDUFAF2	NADH:Ubiquinone Oxidoreductase Complex Assembly Factor 2	1,05 ± 0,09	0,76 ± 0,07*
	NDUFB5	NADH:Ubiquinone Oxidoreductase Subunit B5	1,02 ± 0,06	0,76 ± 0,08*
	NDUFB8	NADH:Ubiquinone Oxidoreductase Subunit B8	1,04 ± 0,08	0,77 ± 0,07*
	NDUFB10	NADH:Ubiquinone Oxidoreductase Subunit B10	1,03 ± 0,07	0,78 ± 0,07*
	NDUFS8	NADH:Ubiquinone Oxidoreductase Subunit S8	1,03 ± 0,07	0,92 ± 0,10
Complex II	*SDHB*	Succinate Dehydrogenase Complex Iron Sulfur Subunit B	1,03 ± 0,07	0,87 ± 0,08
Complex III	*UQCR11*	Ubiquinol-Cytochrome C Reductase, Complex III Subunit XI	1,04 ± 0,08	0,83 ± 0,09
	UQCRB	Ubiquinol-Cytochrome C Reductase Binding Protein	1,07 ± 0,11	0,78 ± 0,11
Complex IV	*COX7AL*	Cytochrome C Oxidase Subunit 7A	1,03 ± 0,07	0,76 ± 0,08*
	COA6	Cytochrome c oxidase assembly factor 6	1,04 ± 0,09	0,73 ± 0,09*
Complex V	*ATP5H*	ATP Synthase, H+ Transporting, Mitochondrial Fo Complex Subunit D	1,03 ± 0,07	0,81 ± 0,08
	ATP5L	ATP Synthase, H+ Transporting, Mitochondrial Fo Complex Subunit G	1,03 ± 0,06	0,85 ± 0,09
	ATP5O	ATP Synthase, H+ Transporting, Mitochondrial F1 Complex, O Subunit	1,04 ± 0,08	0,74 ± 0,08*
	ATP5A1	ATP Synthase, H+ Transporting, Mitochondrial F1 Complex, Alpha Subunit 1	1,07 ± 0,11	0,75 ± 0,09*
	ATP5B	ATP Synthase, H+ Transporting, Mitochondrial F1 Complex, Beta Polypeptide	1,09 ± 0,13	0,76 ± 0,09*
Indirect components of ETC	*ATP2B3*	ATPase Plasma Membrane Ca2+ Transporting 3	1,05 ± 0,09	0,74 ± 0,1*
	ATP2B4	ATPase Plasma Membrane Ca2+ Transporting 4	1,05 ± 0,09	0,78 ± 0,09*
	ATP4A	ATPase H+/K+ Transporting Alpha Subunit	1,15 ± 0,15	1,14 ± 0,17
	ATP6D	ATPase H+ Transporting V0 Subunit D1	1,03 ± 0,06	0,78 ± 0,08*
	ATP6V1A	ATPase H+ Transporting V1 Subunit A	1,12 ± 0,15	0,57 ± 0,08**
Mitochondrial structure	*APOOL*	Apolipoprotein O like	1,02 ± 0,06	0,96 ± 0,10
	FASTKD2	FAST kinase domains 2	1,04 ± 0,07	0,74 ± 0,07**
	MCU	Mitochondrial calcium uniporter	1,05 ± 0,09	0,78 ± 0,09*
	MICU3	Mitochondrial calcium uptake family member 3	1,03 ± 0,06	0,71 ± 0,09**
	MRPL1	Mitochondrial ribosomal protein L1	1,03 ± 0,07	0,83 ± 0,09
	MRPS35	Mitochondrial ribosomal protein S35	1,04 ± 0,09	0,84 ± 0,08
	MTIF2	Mitochondrial translational initiation factor 2	1,04 ± 0,08	0,74 ± 0,06**
	MTX3	Metaxin 3	1,04 ± 0,08	0,79 ± 0,07*
	RMND1	Required for meiotic nuclear division 1 homolog	1,04 ± 0,08	0,70 ± 0,08**
	SLC25A1	Solute carrier family 25 member 1	1,10 ± 0,13	0,61 ± 0,11**
	SLC25A11	Solute carrier family 25 member 11	1,04 ± 0,08	0,77 ± 0,08*
	SLC25A23	Solute carrier family 25 member 23	1,03 ± 0,07	0,78 ± 0,08*
	TOMM70	Translocase of outer mitochondrial membrane 70	1,07 ± 0,11	0,62 ± 0,07***

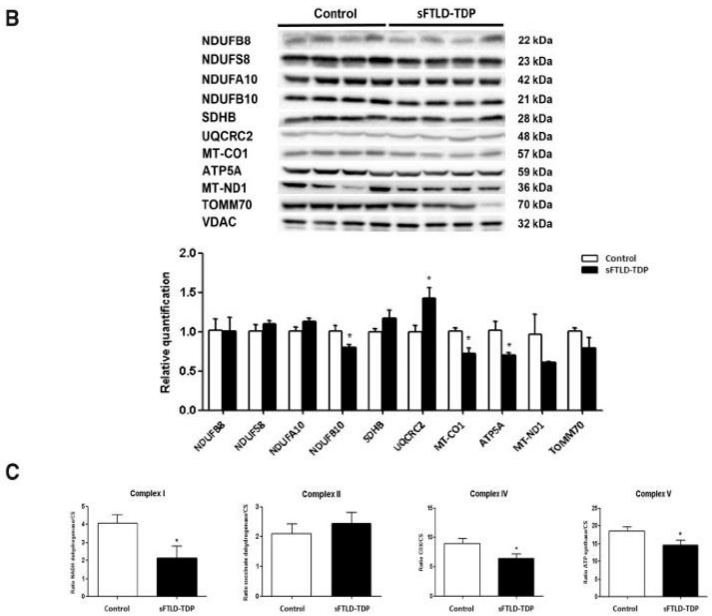

FIGURE 8. (A) mRNA expression levels of selected deregulated genes identified by microarray analysis in the frontal cortex area 8 of sFTLD-TDP and controls assessed with TaqMan RT-qPCR assays coding for subunits of the mitochondrial respiratory chain and proteins linked to energy metabolism. **(B)** Protein levels in control and sFTLD-TDP of subunits encoded by genomic DNA of mitochondrial complexes I (NDUFA10, NDUFB10, NDUFS8, NDUFB8), II (SDHB), III (UQCRC2), and V (ATP5A); encoded by mitochondrial DNA of complex I (MT-ND1) and complex IV (MTCO1); and TOMM10 normalized with voltage-dependent anion channel (VDAC). Diagrams show quantitative values of all assessed cases. **(C)** Mitochondrial enzymatic activities in complex I, II, IV, and V in control and FTLD. All the mitochondrial activities are corrected with citrate synthase activity. Significant levels set at $*p < 0.05$, $**p < 0.01$, and $***p < 0.001$.

(FTLD-TDP), 3 of them bearing *GRN* mutations, and 4 FTLD-MND (linked to motor neuron disease) cases. RT-qPCR validated the deregulation of dynein, annexinA2, and myeloid differentiation primary response in FTLD-U (14). Another study examined 7 FTLD-U cases linked to *GRN* mutations and 10 FTLD-U cases without *GRN* mutations (15).

A distinct molecular phenotype was identified for *GRN*+ FTLD-U when compared with *GRN*-FTLD-U subtypes. Validation by RT-qPCR was assessed for 16 genes; deregulated biological processes associated with *GRN*-FTLD-U were lipid metabolism, MAPK signaling pathways, and transport (15). A recent study in the cerebellum and frontal cortex in sALS and ALS linked to *C9ORF72* mutations has shown 57 genes in cerebellum and 32 genes in frontal cortex abnormally expressed in both c9ALS and sALS; however, the number of deregulated genes in C9ORF72 sALS cases was double than in sALS thus further suggesting differences between different forms of ALS (19).

Comparison between present findings and our previous observations in frontal cortex area 8 in sALS (18), using the same methods, is worth stressing since most of downregulated genes in sFTLD-TDP are upregulated in the frontal cortex area 8 in sALS cases without dementia (18). This suggests a primary response to synaptic and neurotransmission disturbances of frontal cortex area 8 at preclinical stages of frontal degeneration in sALS. Reduced expression of genes encoding actin, actin-related members, kinesin, and microtubule-associated protein further supports cytoskeletal damage in sALS and sFTLD-TDP.

Conclusions

Whole transcriptome arrays and bioinformatics processing followed by RT-qPCR expression of 111 genes shows deregulation of 81 genes involved in cytoskeleton and neuron structure, neurotransmitters, receptors, transporters and synaptic proteins, components of mitochondrial function and energy metabolism, enzymes involved in purine metabolism and RNA splicing in sFTLD-TDP. Western blotting of selected proteins further supports alterations of these pathways at translational level. Finally, altered mitochondrial activity of several mitochondrial complexes is demonstrated by enzymatic assays.

ACKNOWLEDGMENTS

We are indebted to the Neurological Tissue Bank of the IDIBAPS Biobank, Barcelona, Spain, for sample and data procurement. Microarrays were carried out at the High Technology Unit (UAT), Vall d'Hebron Research Institute (VHIR), Barcelona, Spain. We wish to thank F. Briansó, Unit of Statistics and Bioinformatics, VHIR, for the preliminary bioinformatics processing of data, and T. Yohannan for editorial help.

REFERENCES

1. Hortobagyi T, Cairns NJ, Amyotrophic lateral sclerosis and frontotemporal lobar degeneration. In: Kovacs Gabor G, eds. Neuropathology of Neurodegenerative Diseases: A Practical Guide. Cambridge: Cambridge University Press 2015:209–48
2. Lashley T, Roher JD, Mead S, et al. Review: an update on clinical, genetic and pathological aspects of frontotemporal lobar degenerations. Neuropathol Appl Neurobiol 2015;41:858–81
3. Mann DMA, Snowden JS. Frontotemporal lobar degeneration: pathogenesis, pathology and pathways to phenotype. Brain Pathol 2017;27: 723–36
4. Olszewska DA, Lonergan R, Fallon EM, et al. Genetics of frontotemporal dementia. Curr Neurol Neurosci Rep 2016;16:107
5. Pottier C, Ravenscroft TA, Sanchez-Contreras M, et al. Genetics of FTLD: Overview and what else we can expect from genetic studie. J Neurochem 2016;138:32–53
6. Rainero I, Rubino E, Michelerio A, et al. Recent advances in the molecular genetics of frontotemporal lobar degeneration. Funct Neurol 2017;32: 7–16
7. Geser F, Martinez-Lage M, Robinson J, et al. Clinical and pathological continuum of multisystem TDP-43 proteinopathies. Arch Neurol 2009; 66:180–9
8. Cruts M, Gijselinck I, Van Langenhove T, et al. Current insights into the C9orf72 repeat expansion diseases of the FTLD/ALS spectrum. Trends Neurosci 2013;36:450–99
9. Renton AE, Chiò A, Traynor BJ. State of play in amyotrophic lateral sclerosis genetics. Nat Neurosci 2014;17:17–23
10. Neumann M, Sampathu DM, Kwong LK, et al. Ubiquitinated TDP-43 in frontotemporal lobar degeneration and amyotrophic lateral sclerosis. Science 2006;314:130–3
11. Mackenzie IR, Neumann M, Baborie A, et al. A harmonized classification system for FTLD-TDP pathology. Acta Neuropathol 2011;122: 111–3
12. Alafuzoff I, Pikkarainen M, Neumann M, et al. Neuropathological assessments of the pathology in frontotemporal lobar degeneration with TDP43-positive inclusions: An inter-laboratory study by the BrainNet Europe consortium. J Neural Transm (Vienna) 2015;122:957–72
13. Mackenzie IR, Neumann M. Molecular neuropathology of frontotemporal dementia: Insights into disease mechanisms from postmortem studies. J Neurochem 2016;138:54–70
14. Mishra M, Paunesku T, Woloschak GE, et al. Gene expression analysis of frontotemporal lobar degeneration of the motor neuron disease type with ubiquitinated inclusions. Acta Neuropathol 2007;114:81–94
15. Chen-Plotkin AS, Geser F, Plotkin JB, et al. Variations in the progranulin gene affect global gene expression in frontotemporal lobar degeneration. Hum Mol Genet 2008;17:1349–62
16. Martins-de-Souza D, Guest PC, Mann DM, et al. Proteomic analysis identifies dysfunction in cellular transport, energy, and protein metabolism in different brain regions of atypical frontotemporal lobar degeneration. J Proteome Res 2012;11:2533–43
17. Evers BM, Rodriguez-Navas C, Tesla RJ, et al. Lipidomic and transcriptomic basis of lysosomal dysfunction in progranulin deficiency. Cell Rep 2017;20:2565–74
18. Andrés-Benito P, Moreno J, Aso E, et al. Amyotrophic lateral sclerosis, gene deregulation in the anterior horn of the spinal cord and frontal cortex area 8: Implications in frontotemporal lobar degeneration. Aging 2017;9:823–51
19. Prudencio M, Belzil VV, Batra R, et al. Distinct brain transcriptome profiles in C9orf72-associated and sporadic ALS. Nat Neurosci 2015;8: 251175–82
20. Ferrer I, Martinez A, Boluda S, et al. Brain banks: Benefits, limitations and cautions concerning the use of post-mortem brain tissue for molecular studies. Cell Tissue Bank 2008;9:181–94
21. van der Zee J, Gijselinck I, Dillen L, et al. A pan-European study of the C9orf72 repeat associated with FTLD: Geographic prevalence, genomic instability, and intermediate repeats. Hum Mutat 2013;34:363–73
22. Gentleman RC, Carey VJ, Bates DM, et al. Bioconductor: Open software development for computational biology and bioinformatics. Genome Biol 2004;5:R80
23. Barrachina M, Castaño E, Ferrer I. TaqMan PCR assay in the control of RNA normalization in human post-mortem brain tissue. Neurochem Int 2006;49:276–84
24. Ferrer I. Dementia of frontal lobe type and amyotrophy. Behav Neurol 1992;5:87–96
25. Ferrer I. Neurons and their dendrites in frontotemporal dementia. Dement Geriatr Cogn Disord 1999;10(Suppl 1):55–60
26. Zhukareva V, Sundarraj S, Mann D, et al. Selective reduction of soluble tau proteins in sporadic and familial frontotemporal dementias: An international follow-up study. Acta Neuropathol 2003;105:469–76
27. Zhukareva V, Vogelsberg-Ragaglia V, Van Deerlin VM, et al. Loss of brain tau defines novel sporadic and familial tauopathies with frontotemporal dementia. Ann Neurol 2001;49:165–75
28. Papegaey A, Eddarkaoui S, Deramecourt V, et al. Reduced Tau protein expression is associated with frontotemporal degeneration with progranulin mutation. Acta Neuropathol Commun 2016;4:74

29. Onesto E, Colombrita C, Gumina V, et al. Gene-specific mitochondria dysfunctions in human TARDP and C9ORF72 fibroblasts. Acta Neuropathol Commun 2016;4:47
30. Stribl C, Samara A, Trümbach D, et al. Mitochondrial dysfunction and decrease in body weight of a transgenic knock-in mouse model for TDP-43. J Biol Chem 2014;289:10769–84
31. Ipata PL, Camici M, Micheli V, et al. Metabolic network of nucleosides in the brain. Curr Top Med Chem 2011;11:902–22
32. Ansoleaga B, Jové M, Schlüter A, et al. Deregulation of purine metabolism in Alzheimer's disease. Neurobiol Aging 2015;36:68–80

Article VI

Combined transcriptomics and proteomics in frontal cortex area 8 in frontotemporal lobar degeneration linked to *C9ORF72* expansion

Pol Andrés Benito, Ellen Gelpi, Mònica Povedano, Karina Ausín, Joaquín Fernández Irigoyen, Enrique Santamaría and Isidre Ferrer

Journal of Alzheimer's Disease. 2019; 68(3): 1287-1307.

Journal of Alzheimer's Disease 68 (2019) 1287–1307
DOI 10.3233/JAD-181123
IOS Press

Combined Transcriptomics and Proteomics in Frontal Cortex Area 8 in Frontotemporal Lobar Degeneration Linked to *C9ORF72* Expansion

Pol Andrés-Benito[a,b], Ellen Gelpi[c,d], Mónica Povedano[g], Karina Ausín[h,i], Joaquín Fernández-Irigoyen[h,i], Enrique Santamaría[h,i] and Isidro Ferrer[a,b,e,f,*]
[a]*Neuropathology, Pathologic Anatomy Service, Bellvitge University Hospital - Bellvitge Biomedical Research Institute (IDIBELL), Hospitalet de Llobregat, Spain*
[b]*Biomedical Network Research Center on Neurodegenerative Diseases (CIBERNED), Institute of Health Carlos III, Hospitalet de Llobregat, Spain*
[c]*Neurological Tissue Bank of the Biobanc-Hospital Clínic-Institut d'Investigacions Biomèdiques August Pi i Sunyer (IDIBAPS), Barcelona, Spain*
[d]*Institute of Neurology, Medical University of Vienna, Vienna, Austria*
[e]*Department of Pathology and Experimental Therapeutics, University of Barcelona, Hospitalet de Llobregat, Spain*
[f]*Institute of Neurosciences, University of Barcelona, Barcelona, Spain*
[g]*Functional Unit of Amyotrophic Lateral Sclerosis (UFELA), Service of Neurology, Bellvitge University Hospital, Hospitalet de Llobregat, Spain*
[h]*IDISNA, Navarra Institute for Health Research, Pamplona, Spain*
[i]*Clinical Neuroproteomics group and Proteored-ISCIII, Proteomics Unit, Navarrabiomed, Department of Health, Public University of Navarra, Pamplona, Spain*

Accepted 31 January 2019

Abstract.
Background: Frontotemporal lobar degeneration with TDP-43 immunoreactive inclusions (FTLD-TDP) may appear as sporadic (sFTLD-TDP) or linked to mutations in various genes including expansions of the non-coding region of *C9ORF72* (c9FTLD).
Objective: Analysis of differential mRNA and protein expression in the frontal cortex in c9FLTD and evaluation with previous observations in frontal cortex in sFTLD-TDP and amyotrophic lateral sclerosis with TDP-43 inclusions.
Methods: Microarray hybridization and mass spectrometry-based quantitative proteomics followed by RT-qPCR, gel electrophoresis, and western blotting in frontal cortex area 8 in 19 c9FTLD cases and 14 age- and gender-matched controls.
Results: Microarray hybridization distinguish altered gene transcription related to DNA recombination, RNA splicing regulation, RNA polymerase transcription, myelin synthesis, calcium regulation, and ubiquitin-proteasome system in c9FTLD; proteomics performed in the same tissue samples pinpoints abnormal protein expression involving apoptosis, inflammation,

*Correspondence to: Prof. Isidro Ferrer, Department of Pathology and Experimental Therapeutics, University of Barcelona, Campus Bellvitge, c/Feixa Llarga sn, 08907 L'Hospitalet de Llobregat, Spain. Tel.: +34 93 4035808; E-mail: 8082ifa@gmail.com.

ISSN 1387-2877/19/$35.00

metabolism of amino acids, metabolism of carbohydrates, metabolism of membrane lipid derivatives, microtubule dynamics, morphology of mitochondria, neuritogenesis, neurotransmission, phagocytosis, receptor-mediated endocytosis, synthesis of reactive oxygen species, and calcium signaling in c9FTLD.

Conclusion: Transcriptomics and proteomics, as well as bioinformatics processing of derived data, reveal similarly altered pathways in the frontal cortex in c9FTLD, but different RNAs and proteins are identified by these methods. Combined non-targeted '-omics' is a valuable approach to deciphering altered molecular pathways in FTLD provided that observations are approached with caution when assessing human postmortem brain samples.

Keywords: C9ORF72, frontotemporal lobar degeneration, FTLD-TDP, gene expression, proteomics

INTRODUCTION

Frontotemporal lobar degeneration with TDP-43 inclusions (FTLD-TDP) is manifested by behavioral-dysexecutive disorder, primary progressive aphasia, and/or motor disorders including motor neuron disease due to frontal and temporal atrophy, as well as variable involvement of the basal ganglia, substantia nigra, and spinal cord. Neuron loss in the cerebral cortex, microvacuolation in the upper cortical layers, astrogliosis, and TDP-43-immunoreactive inclusions in the nucleus and/or cytoplasm of neurons and oligodendocytes and in neuropil threads, are the main microscopical alterations [1–4]. Some cases are sporadic (sFTLD-TDP) whereas others are genetic, often familial (fFTLD-TDP) and linked to mutations in various genes including *GRN* (progranulin), *C9ORF72* (chromosome 9 open reading frame 72), *TARDP* (TAR DNA-binding protein), *VCP* (valosin-containing protein), *CHMBP2* (charged multivesicular body protein 2), and *UBQLN* (ubiquilin 2), among others [4, 5–8]. The presence of TDP-43 inclusions in amyotrophic lateral sclerosis (ALS), together with the fact that mutations in the same genes, excepting *GRN*, may be causative of ALS, suggests that ALS and FTLD-TDP are within the same disease spectrum [9–13].

C9ORF72 expansions produce haploinsufficiency of C9*orf*72 protein, RNA foci sequestering of various RNA-binding proteins, dipeptide repeat protein inclusions probably sequestering additional proteins, abnormal protein binding, TDP-43 aggregation and loss of function, nucleocytoplasmic transport defects, RNA mis-splicing, DNA damage, abnormal stress granule dynamics, and altered autophagy, among others [8, 14–41].

Complementary information has been gained from the application of transcriptomics and proteomics in FTLD-TDP and ALS [42–45] but studies including FTLD linked to *C9ORF72* expansion (c9FTLD) are scarce [46]. The present study was designed to gain understanding about c9FTLD pathogenesis by using microarray hybridization and mass spectrometry-based quantitative proteomics in frontal cortex area 8 postmortem samples. Data were then processed using bioinformatics methods to identify altered molecular pathways and their interactions. Finally, data obtained in c9FTLD were compared with those previously obtained in the same cortical region in sFTLD-TDP and sALS.

MATERIAL AND METHODS

Human cases

Postmortem fresh-frozen frontal cortex (FC) (Brodmann area 8) samples were obtained from the Institute of Neuropathology HUB-ICO-IDIBELL Biobank and the Hospital Clinic-IDIBAPS Biobank following the guidelines of Spanish legislation on this matter and approval of the local ethics committees. The postmortem interval between death and tissue processing was between 2 and 18 h. One hemisphere was immediately cut in coronal sections, 1 cm thick, and selected areas of the encephalon were rapidly dissected, frozen on metal plates over dry ice, placed in individual air-tight plastic bags, and stored at –80°C until use for biochemical studies. The other hemisphere was fixed by immersion in 4% buffered formalin for 3 weeks for morphological studies. FTLD-TDP cases were diagnosed following well-established criteria [1]. All cases bore *C9ORF72* repeat expansion (more than 30 intronic hexanucleotide repeats). TDP-43-immunoreactive inclusions were found in the frontal cortex in every case; these were neuronal cytoplasmic inclusions mainly in layer II but also in the deeper layers in some cases, together with dystrophic neurites corresponding to types A and B [47], and sequential pattern II-III [48]. Patients with associated pathologies, including middle or late stages of Alzheimer's and Parkinson's diseases, and those with

vascular diseases, neoplastic disorders affecting the nervous system, metabolic syndrome, hypoxia, and prolonged axonal states such as those occurring in intensive care units, were excluded. The whole series included 19 familial cases of fFTLD associated with *C9ORF72* mutation, henceforth named c9FTLD for practical purposes (mean age 70 years; 10 men and 9 women), and 14 cases (mean age 67 years; 8 men and 6 women) not suffering from neurologic or psychiatric diseases, and without abnormalities in the neuropathologic examination, which were assessed in parallel as age-matched controls (Table 1). Details of the clinical symptoms were very brief in the accompanying data provided with the brain samples used for study. Apathy, loss of empathy, disinhibition, executive dysfunction, memory loss, hallucinations, and delusions were common, often accompanied by motor neuron disease; parkinsonism and progressive aphasia were reported in some cases.

Table 1
Summary of the thirty-three cases analyzed, including frontal cortex area 8 of 14 controls and 19 fFTLD cases. c9FTLD, familial FTLD linked to C9orf72 expansion; F, female; M, male; PMD, postmortem delay (hours, minutes); RIN, RNA integrity number

Case	Sex	Age	Diagnosis	PMD	RIN
1	M	66	Control	18 h 00 min	6.4
2	M	61	Control	03 h 40 min	7.0
3	M	62	Control	05 h 45 min	5.0
4	M	74	Control	06 h 40 min	7.2
5	M	65	Control	05 h 15 min	6.8
6	F	64	Control	02 h 15 min	5.0
7	M	63	Control	08 h 05 min	7.1
8	F	79	Control	03 h 35 min	6.8
9	F	67	Control	05 h 20 min	6.2
10	M	70	Control	03 h 45 min	7.2
11	M	52	Control	04 h 40 min	7.2
12	F	52	Control	05 h 45 min	5.1
13	F	82	Control	07 h 35 min	5.2
14	F	74	Control	02 h 45 min	5.7
15	M	69	c9FTLD	11 h 30 min	6.5
16	F	69	c9FTLD	13 h 15 min	5.4
17	M	68	c9FTLD	02 h 30 min	6.8
18	M	61	c9FTLD	07 h 45 min	6.9
19	M	66	c9FTLD	15 h 15 min	7.9
20	F	55	c9FTLD	03 h 15 min	8.7
21	M	69	c9FTLD	05 h 00 min	6.1
22	F	75	c9FTLD	17 h 30 min	7.5
23	F	92	c9FTLD	09 h 15 min	7.1
24	F	58	c9FTLD	11 h 00 min	8.4
25	F	66	c9FTLD	11 h 30 min	8,1
26	M	73	c9FTLD	15 h 30 min	6.2
27	F	69	c9FTLD	12 h 30 min	5.9
28	F	57	c9FTLD	03 h 40 min	7.2
29	M	80	c9FTLD	12 h 00 min	8.0
30	F	57	c9FTLD	08 h 00 min	6.9
31	M	88	c9FTLD	05 h 00 min	7.3
32	M	69	c9FTLD	05 h 45 min	7.1
33	M	80	c9FTLD	08 h 30 min	6.5

RNA purification

RNA from frozen frontal cortex area 8 was extracted following the instructions of the supplier (RNeasy Mini Kit, Qiagen® GmbH, Hilden, Germany). RNA integrity and 28S/18S ratios were determined with the Agilent Bioanalyzer (Agilent Technologies Inc, Santa Clara, CA, USA) to assess RNA quality combined with DNase digestion to avoid extraction and later amplification of genomic DNA, and the RNA concentration was evaluated using a NanoDrop™ Spectrophotometer (Thermo Fisher Scientific, Waltham, MA, USA). RIN values are shown in Table 1. Special care was taken to assess premortem and postmortem factors which may interfere with RNA processing [49].

Microarray hybridization

Samples were analyzed by microarray hybridization with Human Clariom™ D Assay kit and GeneChip WT Plus Reagent Kit, and microarray 7000G platform from Affymetrix® (Affymetrix, Santa Clara, CA, USA) with a capacity to detect more than 540,000 transcripts. Preprocessing of raw data and statistical analyses were performed using bioconductor packages in an R programming environment for genes [50] which enabled data preprocessing for differential gene expression analysis and enrichment analysis. Gene selection was based upon their values using a test for differential expression between two classes (Student's *t*-test). Genes differentially expressed showed an absolute fold change >2.0 in combination with a p-value ≤ 0.05.

RT and q-PCR

Complementary DNA (cDNA) preparation used the High-Capacity cDNA Reverse Transcription kit (Applied Biosystems, Foster City, CA, USA) following the protocol provided by the supplier. Parallel reactions for each RNA sample were run in the absence of MultiScribe Reverse Transcriptase to assess the lack of contamination of genomic DNA. TaqMan RT-qPCR assays were performed in duplicate for each gene on cDNA samples in 384-well optical plates using an ABI Prism 7900 Sequence Detection System (Applied Biosystems). For each 10 µL TaqMan reaction, 4.5 µL cDNA was mixed with 0.5 µL 20× TaqMan Gene Expression Assays and 5 µL of 2× TaqMan Universal PCR

Table 2
Genes, gene symbols, and TaqMan probes used for the study of gene expression including probe for normalization (*GUS*-β)

Gene	Full name	Reference
C9ORF72	*Chromosome 9 Open Reading Frame 72*	Hs00376619_m1
CNP	*2′,3′-Cyclic Nucleotide 3′ Phosphodiesterase*	Hs00263981_m1
DDX3Y	*DEAD-Box Helicase 3 Y-Linked*	Hs00190539_m1
EIF1AY	*Eukaryotic Translation Initiation Factor 1A Y-Linked*	Hs01040047_m1
GPN2	*GPN-Loop GTPase 2*	Hs00216252_m1
GUS-β	*β-glucuronidase*	Hs00939627_m1
MAG	*Myelin Associated Glycoprotein*	Hs01114387_m1
MAL	*Mal, T-Cell Differentiation Protein*	Hs00360838_m1
MBP	*Myelin Basic Protein*	Hs00921945_m1
MOBP	*Myelin-Associated Oligodendrocyte Basic Protein*	Hs01094434_m1
MOG	*Myelin Oligodendrocyte Glycoprotein*	Hs01555268_m1
MYRF	*Myelin Regulatory Factor*	Hs00973739_m1
NG2	*Neural/glial antigen 2*	Hs00426981_m1
OLIG1	*Oligodendrocyte Transcription Factor 1*	Hs00744293_s1
OLIG2	*Oligodendrocyte Lineage Transcription Factor 2*	Hs00377820_m1
PLP1	*Proteolipid Protein 1*	Hs00166914_m1
SCARNA2	*Small Cajal Body-Specific RNA 2*	Hs04232660_s1
SOX-10	*SRY-Box 10*	Hs00366918_m1
TARDBP	*TAR DNA Binding Protein*	Hs00606522_m1
UBR5	*Ubiquitin Protein Ligase E3 Component N-Recognin 5*	Hs00210750_m1

Master Mix (Applied Biosystems) [51]. Table 2 shows identification numbers and names of selected TaqMan probes. Values for glucuronidase-β (*GUS*-β) were used as internal controls for normalization. The selection of this housekeeping gene was based on previous data showing its low vulnerability in the brain in several human neurodegenerative diseases [52]. The parameters of the reactions were 50°C for 2 min, 95°C for 10 min, and 40 cycles of 95°C for 15 s, and 60°C for 1 min. Finally, all TaqMan PCR data were captured with Sequence Detection Software (SDS version 2.2.2, Applied Biosystems). The double-delta cycle threshold (ΔΔCT) method was used to analyze the data. Results were analyzed using Student's *t*-test [50].

Proteomic analysis

Sample preparation for proteomic analysis

Frozen samples of frontal cortex from eight c9FTLD and eight controls of the same case series were homogenized in lysis buffer containing 7 M urea, 2 M thiourea, and 50 mM DTT. The homogenates were spun down at 100,000 ×g for 1 h at 15°C. Protein concentration was measured in the supernatants with the Bradford assay kit (Biorad, Hercules, CA, USA).

Label free LC-MS/MS

The protein extract for each sample was diluted in Laemmli sample buffer and loaded into a 0.75 mm thick polyacrylamide gel with a 4% stacking gel cast over a 12.5% resolving gel. The run was stopped as soon as the front entered 3 mm into the resolving gel so that the whole proteome became concentrated in the stacking/resolving gel interface. Bands were stained with Coomassie Brilliant Blue and excised from the gel. Protein enzymatic cleavage (20 μg) was carried out with trypsin (1:20, w/w, Promega, Madison, WI, USA) at 37°C for 16 h. Purification and concentration of peptides was performed using C18 Zip Tip Solid Phase Extraction (Millipore, Burlington, MA, USA). Peptide mixtures were separated by reverse phase chromatography using an Eksigent nanoLC ultra 2D pump fitted with a 75 μm ID column (Eksigent 0.075 × 250). Samples were first loaded for desalting and concentration into a 0.5 cm length 100 μm ID pre-column packed with the same chemistry as the separating column. Mobile phases were 100% water, 0.1% formic acid (FA) (buffer A), and 100% acetonitrile 0.1% FA (buffer B). Column gradient was developed in a two-step gradient from 5% B to 25% B for 210 min and 25%B to 40% B for 30 min. The column was equilibrated in 95% B for 9 min and 5% B for 14 min. During the entire process, pre-column was in line with column, and the flow maintained all along the gradient at 300 nl/min. Eluting peptides from the column were analyzed using an AB Sciex 5600 Triple-TOF system (Sciex). Information data were acquired upon a survey scan performed in a mass range from 350 m/z up to 1,250 m/z in a scan time of 250 ms. The top 35 peaks were selected for fragmentation. Minimum accumulation time for MS/MS was set at 100 ms, yielding a total cycle time

of 3.8 s. Product ions were scanned in a mass range from 230 m/z up to 1,500 m/z and excluded for further fragmentation for 15 s.

Peptide identification and quantification

MS/MS data acquisition was performed using Analyst 1.7.1 (Sciex) and spectra files were processed through Protein Pilot Software (v.5.0-Sciex) using Paragon™ algorithm (v.4.0.0.0) for database search and Progroup™ for data grouping, and then searched against the concatenated target-decoy UniProt proteome reference Human database (Proteome ID: UP000005640, 70902 proteins, December 2015). False discovery rate was identified using a nonlineal fitting method [53], and displayed results were those reporting a 1% global false discovery rate or better. The peptide quantification was performed using the Progenesis LC–MS software (version 2.0.5556.29015, Nonlinear Dynamics, Newcastle, UK). Using the accurate mass measurements from full survey scans in the TOF detector and the observed retention times, runs were aligned to compensate for between-run variations in our nanoLC separation system. To this end, all runs were aligned to a reference run automatically chosen by the software, and a master list of features considering m/z values and retention times was generated. The quality of these alignments was manually supervised with the help of quality scores provided by the software. The peptide identifications were exported from Protein Pilot software and imported into Progenesis LC-MS software, where they were matched to the respective features. Output data files were managed using Perseus Software for subsequent statistical analyses and representation [54]. Proteins identified by site (identification based only on a modification), reverse proteins (identified by decoy database), and potential contaminants were filtered out. Proteins quantified with at least two unique peptides, a *p*-value lower than 0.05 and an absolute fold change of <0.77 (downregulation) or >1.3 (upregulation) in linear scale, were considered to be significantly differentially expressed. MS raw data and search results files were deposited in the ProteomeXchange Consortium (http://proteomecentral.proteomexchange.org) via the PRIDE partner repository with the dataset identifiers PXD011713.

Proteome bioinformatic analysis

The specifically dysregulated regulatory/metabolic networks identified in c9FTLD were analyzed with the use of QIAGEN's Ingenuity® Pathway Analysis (IPA) (QIAGEN Redwood City, CA, USA, http://www.qiagen.com/ingenuity). This software comprises curated information from databases of experimental and predictive origin, enabling discovery of highly represented functions, pathways, and interactome networks.

Gel electrophoresis and immunoblotting

Brain samples were homogenized in RIPA lysis buffer (50 mM Tris/HCl buffer, pH 7.4 containing 2 mM EDTA, 0.2% Nonidet P-40, 1 mM PMSF, protease, and phosphatase inhibitor cocktails, Roche Molecular Systems, Basel, Switzerland). The homogenates were centrifuged for 15 min at 13,000 rpm. Protein concentrations were determined with the BCA method (Thermo Fisher). Equal amounts of protein (12 μg) for each sample were loaded and separated by electrophoresis on sodium dodecyl sulfate polyacrylamide gel electrophoresis (SDS-PAGE) (10%) gels and transferred onto nitrocellulose membranes (Amersham, Freiburg, Germany). Non-specific bindings were blocked by incubation in 3% albumin in PBS containing 0.2% Tween for 1 h at room temperature. After washing, membranes were incubated overnight at 4°C with the antibody against C9orf72 (rabbit polyclonal used at a dilution of 1:1,000; ab183982, Abcam, Cambridge, UK), TDP43-T (rabbit polyclonal used at dilution of 1:250; ab154047, Abcam), SNAP25 (mouse monoclonal used at dilution of 1:1000, SMI81, BioLegend, San Diego, CA, USA), CAMMKIIa (mouse monoclonal diluted 1:1,000; 13-7300, Zymed, MA, USA) and CAMMKIV (mouse monoclonal diluted 1:1,000; c28420, BD Biosciences, NJ, USA). Protein loading was monitored using an antibody against β-actin (mouse monoclonal diluted 1:30,000; A5316, Sigma, St. Louis, MO, USA). Membranes were then incubated for 1h in the appropriate HRP-conjugated secondary antibody (1:2,000 Agilent), and immunocomplexes were revealed by chemiluminescence reagent (ECL, Freiburg, Germany). Densitometric quantification was carried out with ImageLab software (Biorad). Bands were normalized to β-actin. Seven cases per group were analyzed.

Statistical analysis

The normality of distribution of fold change values was analyzed with the Kolmogorov-Smirnov test. The non-parametric Mann-Whitney test was performed to compare each group when values

did not follow a normal distribution, whereas the unpaired *t*-test was used for normal variables. Statistical analysis and graphic design were performed with GraphPad Prism version 5.01 (La Jolla, CA, USA). Outliers were detected using the GraphPad software QuickCalcs ($p<0.05$). The data were expressed as mean ± SEM, and significance levels were set at $^{*}p<0.05$, $^{**}p<0.01$, $^{***}p<0.001$.

RESULTS

Microarray analysis

Cofactors age, gender, RIN value, and postmortem delay were not relevant for the analysis. After filtering, 4,851 genes were included in the analysis. Gene expression in control and c9FTLD cases, with *p*-values equal to or lower than 0.05 and absolute fold change logarithm equal to or greater than 0.5, is represented in a heat-map (Fig. 1A). Forty-eight genes were differentially expressed in frontal cortex area 8 of c9FTLD when compared with controls (11 upregulated, 37 downregulated). Using GO database, we identified clusters of deregulated genes related to DNA recombination, RNA splicing regulation, RNA polymerase transcription, and centriole (Fig. 1B). Deregulated genes are listed in Table 3. In addition to reported clusters, genes linked to myelin synthesis, calcium regulation, and ubiquitin-protesome system were also deregulated. Microarray details: https://www.ebi.ac.uk/arrayexpress/; reference number fgsubs #218580.

Gene validation

Aberrant accumulation of hyper-phosphorylated TDP43 and toxic aggregates of C9orf72 are common hallmarks in c9FTLD. mRNA levels of *TARDBP and C9ORF72* were evaluated with RT-qPCR. *C9ORF72* mRNA expression was significantly decreased in c9FTLD when compared with controls ($p=0.003$), in line with the results of the array

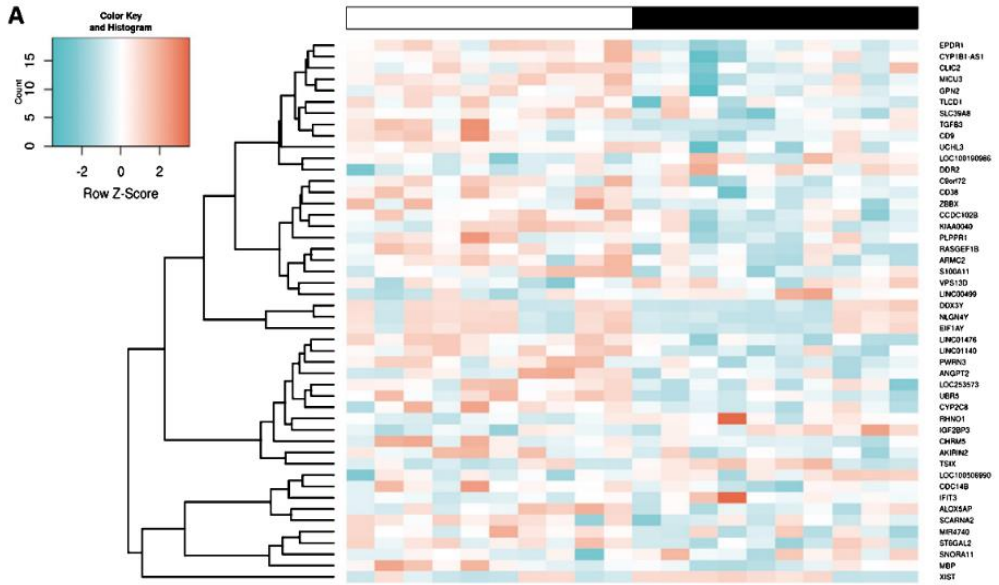

B

GO Term	Count	Size	Genes	Odds ratio	p-value
DNA recombination	7	36	H2AFX, PSMC3IP, RHNO1, RMI1, SFR1, TFRC, XRCC4	3.63	0.006660
regulation of RNA splicing	5	21	AGGF1, CELF6, CLK2, RBM10, SRSF5	4.67	0.008800
centriole	5	20	CEP290, CEP41, IFT88, POC5, TUBD1	4.99	0.00707
RNA polymerase II transcriptio	5	21	ERCC2, GTF2H3, MED14, STAT3, TAF4B	4.67	0.00808

Fig. 1. Microarray analysis. A) Hierarchical clustering heat-map of expression intensities of mRNA array transcripts in frontal cortex area 8 in c9FTLD compared with controls. B) GO database identifies clusters of deregulated genes in c9FTLD. Genes differentially expressed show an absolute fold change >2.0 in combination with a *p*-value ≤ 0.05.

Table 3
Deregulated genes in FC of c9FTLD cases

Gene ID	Coding protein	Deregulation	*FC*	*p*
NLGN4Y	Neuroligin 4 Y-Linked	Down	–1.66	0.016
DDX3Y	DEAD-Box Helicase 3 Y-Linked	Down	–1.42	0.040
EIF1AY	Eukaryotic Translation Initiation Factor 1A Y-Linked	Down	–1,16	0.020
CHRM5	Cholinergic Receptor Muscarinic 5	Down	–0.90	0.010
PWRN3	Prader-Willi Region Non-Protein Coding RNA 3	Down	–0.73	0.002
MICU3	Mitochondrial Calcium Uptake Family Member 3	Down	–0.73	0.002
MBP	Myelin Basic Protein	Down	–0.68	0.044
PLPPR1	Phospholipid Phosphatase Related 1	Down	–0.70	0.043
CD38	CD38 Molecule	Down	–0.64	0.005
LINC01476	Long Intergenic Non-Protein Coding RNA 1476	Down	–0.60	0.001
C9orf72	Chromosome 9 Open Reading Frame 72	Down	–0.60	0.006
UBR5	Ubiquitin Protein Ligase E3 Component N-Recognin 5	Down	–0.60	0.000
KIAA0040	Uncharacterized Protein KIAA0040	Down	–0,60	0.029
ALOX5AP	Arachidonate 5-Lipoxygenase Activating Protein	Down	–0.59	0.032
TGFB3	Transforming Growth Factor Beta 3	Down	–0.59	0.030
CD9	CD9 Molecule	Down	–0.58	0.048
CCDC102B	Coiled-Coil Domain Containing 102B	Down	–0.57	0.011
LOC253573	Uncharacterized LOC253573	Down	–0.57	0.005
EPDR1	Ependymin Related 1	Down	–0.57	0.001
ZBBX	Zinc Finger B-Box Domain Containing	Down	–0.57	0.040
CYP2C8	Cytochrome P450 Family 2 Subfamily C Member 8	Down	–0.57	0.015
CLIC2	Chloride Intracellular Channel 2	Down	–0.56	0.015
ST6GAL2	ST6 Beta-Galactoside Alpha-2,6-Sialyltransferase 2	Down	–0.56	0.024
RASGEF1B	RasGEF Domain Family Member 1B	Down	–0.54	0.030
MIR4740	Hsa-Mir-4740	Down	–0.53	0.034
ANGPT2	Angiopoietin 2	Down	–0.53	0.027
S100A11	S100 Calcium Binding Protein A11	Down	–0.53	0.036
UCHL3	Ubiquitin C-Terminal Hydrolase L3	Down	–0.53	0.027
TLCD1	Calfacilitin	Down	–0.52	0.024
ARMC2	Armadillo Repeat Containing 2	Down	–0.52	0.014
CYP1B1-AS1	CYP1B1 Antisense RNA 1 (Non-Protein Coding)	Down	–0.52	0.024
LINC01140	Long Intergenic Non-Protein Coding RNA 1140	Down	–0.52	0.004
GPN2	GPN-Loop GTPase 2	Down	–0.52	0.015
AKIRIN2	Akirin 2	Down	–0.52	0.007
SLC39A8	Solute Carrier Family 39 (Metal Ion Transporter), Member 8	Down	–0.51	0.031
SCARNA2	Small Cajal Body-Specific RNA 2	Down	–0.50	0.027
CDC14B	Cell Division Cycle 14B	Down	–0.50	0.044
LOC100506990	Uncharacterized LOC100506990	Up	0.51	0.036
VPS13D	Vacuolar Protein Sorting 13 Homolog D	Up	0.51	0.016
LINC00499	Long Intergenic Non-Protein Coding RNA 499	Up	0.52	0.011
DDR2	Discoidin Domain Receptor Tyrosine Kinase 2	Up	0.54	0.017
RHNO1	RAD9-HUS1-RAD1 Interacting Nuclear Orphan 1	Up	0.55	0.018
IFIT3	Interferon Induced Protein With Tetratricopeptide Repeats 3	Up	0.55	0.034
IGF2BP3	Insulin-like Growth Factor 2 MRNA Binding Protein 3	Up	0.55	0.024
LOC100190986	Uncharacterized LOC100190986	Up	0.56	0.034
SNORA11	Small Nucleolar RNA, H/ACA Box 11	Up	0.57	0.048
TSIX	TSIX Transcript, XIST Antisense RNA	Up	0.67	0.021
XIST	X Inactive Specific Transcript	Up	2.22	0.043

(Fig. 2A). *TARDBP* mRNA levels were not significant altered in c9FTLD when compared with controls ($p = 0.15$).

Significant increase in *UBR5* ($p = 0.03$) and *DD3XY* ($p = 0.026$) mRNAs was confirmed by RT-qPCR. Expression levels of *SCARNA2* ($p = 0.83$), *EIF1AY* ($p = 0.36$), and *GPN2* ($p = 0.76$), although reduced in the array, were preserved when assessed with RT-qPCR (Fig. 2B).

MBP mRNA expression was significantly decreased in c9FTLD ($p = 0.05$) (Fig. 2C). To further extend knowledge about genes linked to myelin and oligodendrocytes, RT-qPCR revealed reduced expression of *MAG* ($p = 0.036$), *MAL* ($p = 0.02$), *MOBP* ($p = 0.025$), and *MOG* ($p = 0.05$) in c9FTLD when compared with controls (Fig. 2C). However, the expression of *OLIG1* ($p = 0.17$), *OLIG2* ($p = 0.40$), *SOX10* ($p = 0.33$), *NG2* ($p = 0.34$), *MYRF*

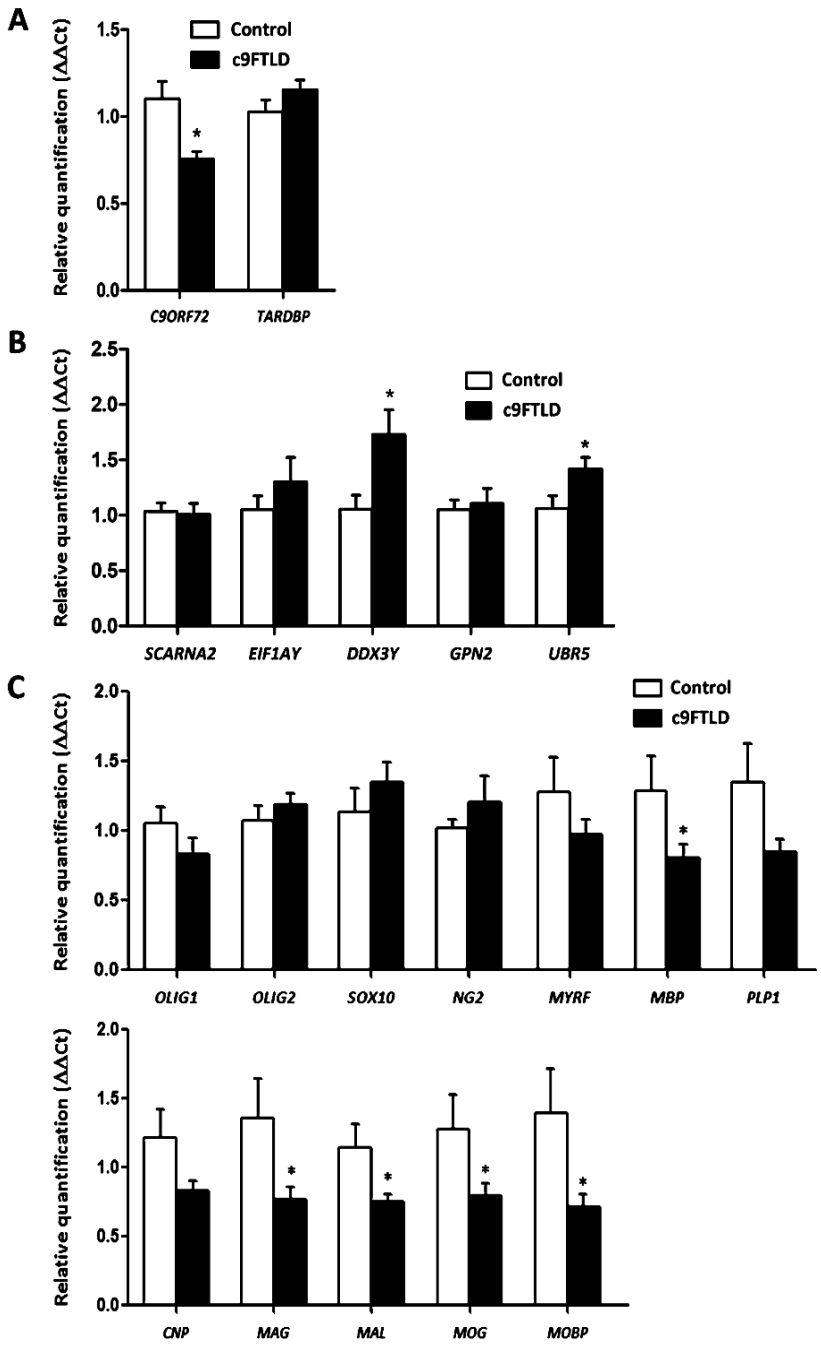

Fig. 2. mRNA expression of selected genes in c9FTLD. A) Expression levels of genes *C9ORF72* and *TARDBP*. B) Relative expression levels of genes linked to DNA/RNA regulation mechanisms. C) Expression levels of genes coding for myelin and oligodendrocyte proteins. The significance level is set at $^{*}p < 0.05$.

($p=0.23$), *CNP* ($p=0.065$), and *PLP1* ($p=0.07$) was not altered in c9FTLD (Fig. 2C). None of these genes, excepting *MBP*, was identified as deregulated in the arrays.

Cortical proteostatic impairment in c9FTLD

To probe additional molecular disturbances in frontal cortex (area 8) from c9FTLD cases with respect to neurologically intact controls, a label-free MS-based approach was used. Postmortem delay was not relevant for the study. Among 3,909 identified proteins, the differential frontal cortex site-specific proteomic signature was composed of 130 proteins (40 downregulated and 90 upregulated) in c9FTLD cases when compared with controls. A heat-map representing the fold-change of identified proteins with associated *p*-values from the pair-wise quantitative comparisons, and a Volcano plot showing the distribution of differentially expressed proteins in c9FTLD and controls, are depicted in Fig. 3. Deregulated proteins are listed in Table 4.

Cortical deregulated pathways in c9FTLD

To enhance the analytical outcome of proteomic experiments, differential proteome datasets were functionally analyzed across specific biological functions using IPA software. Bioinformatic analysis revealed clusters categorized under the terms apoptosis, inflammation, metabolism of amino acids, metabolism of carbohydrates, metabolism of membrane lipid derivatives, microtubule dynamics, morphology of mitochondria, neuritogenesis, neurotransmission, phagocytosis, receptor-mediated endocytosis, and synthesis of reactive oxygen species as altered pathways in c9FTLD (Table 5). Additional integrative network unveiled disruptions in calcium signalling (NECAB1, CAMMKK2 and CNTN2), calmodulin function, and vesicle release (CLSTN1) (Fig. 4 and Table 4). Moreover, the protein interactome map showed deregulation of cross-linkers between DNA/RNA regulation systems and ubiquitin-proteasome systems, suggesting an imbalance in cellular transcription processes and protein degradation mechanisms in c9FTLD (Fig. 4).

Monitoring the frontal cortical expression of specific protein mediators in c9FTLD

In order to partially validate the results obtained by LC-MS/MS, western-blotting was used as an orthogonal technique. To complement our study, total TDP43 protein levels were increased in c9FTLD when compared with controls ($p=0.02$). C9orf72 long isoform was significantly reduced ($p=0.04$) whereas C9orf72 short isoform was significantly increased ($p=0.000$) in c9FTLD (Fig. 5). In

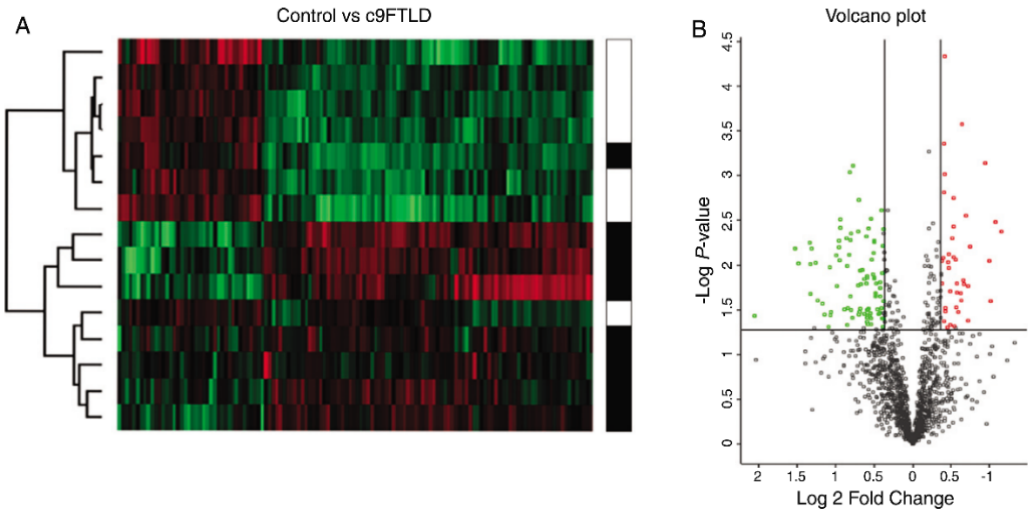

Fig. 3. Differentially expressed proteins in frontal cortex area 8 in c9FTLD. A) Heat map representing the fold-change of identified proteins with associated *p*-values from the pair-wise quantitative comparisons with controls. Significantly upregulated proteins in c9FTLD between pair-wise comparisons are labelled in green, and significantly downregulated proteins are labelled in red. B) Volcano plot of differentially expressed proteins.

Table 4
Deregulated proteins in c9FTLD compared with controls

Gene	Protein name	Uniprot	Deregulation	FC	*p*
RAP1GAP	Rap1 GTPase-activating protein 1	X6R8W7	Down	0.77	0.01
CLIP2	CAP-Gly domain-containing linker protein 2	Q9UDT6	Down	0.77	0.02
SUGT1	Protein SGT1 homolog	Q9Y2Z0	Down	0.76	0.00
AAK1	AP2-associated protein kinase 1	Q2M2I8	Down	0.76	0.01
DYNC1LI1	Cytoplasmic dynein 1 light intermediate chain 1	Q9Y6G9	Down	0.76	0.00
PRKCB	Protein kinase C beta type	P05771	Down	0.75	0.00
PRKCG	Protein kinase C gamma type	P05129	Down	0.75	0.04
CLTC	Clathrin heavy chain 1	Q00610	Down	0.75	0.00
GAS7	Growth arrest-specific protein 7	O60861	Down	0.74	0.03
NPTX1	Neuronal pentraxin-1	Q15818	Down	0.74	0.03
ARHGEF2	Rho guanine nucleotide exchange factor 2	Q92974	Down	0.73	0.05
INA	Internexin Neuronal Intermediate Filament Protein Alpha	Q16352	Down	0.73	0.01
PUF60	Poly(U)-binding-splicing factor PUF60	Q9UHX1	Down	0.72	0.01
ATL1	Atlastin-1	Q8WXF7	Down	0.72	0.01
CNTN2	Contactin-2	A0A1W2PQ11	Down	0.72	0.02
GLTP	Glycolipid transfer protein	Q9NZD2	Down	0.71	0.05
PRRT2	Proline-rich transmembrane protein 2	Q7Z6L0	Down	0.70	0.00
AIDA	Axin interactor, dorsalization-associated protein	Q96BJ3	Down	0.69	0.00
CCDC6	Coiled-coil domain-containing protein 6	Q16204	Down	0.69	0.00
NCKIPSD	NCK-interacting protein with SH3 domain	Q9NZQ3	Down	0.69	0.05
PLD3	Phospholipase D3	Q8IV08	Down	0.69	0.01
RABL6	Rab-like protein 6	Q3YEC7	Down	0.68	0.01
INF2	Inverted formin-2	Q27J81	Down	0.68	0.03
AGL	Glycogen debranching enzyme	P35573	Down	0.67	0.03
APOE	Apolipoprotein E	P02649	Down	0.67	0.02
CAMKK2	Calcium/calmodulin-dependent protein kinase kinase 2	Q96RR4	Down	0.67	0.02
GPRIN1	G protein-regulated inducer of neurite outgrowth 1	Q7Z2K8	Down	0.65	0.02
OPTN	Optineurin	Q96CV9	Down	0.65	0.02
POR	NADPH—cytochrome P450 reductase	P16435	Down	0.64	0.00
ABLIM2	Actin-binding LIM protein 2	Q6H8Q1	Down	0.63	0.02
NECAB1	N-terminal EF-hand calcium-binding protein 1	Q8N987	Down	0.63	0.01
UGGT1	UDP-glucose:glycoprotein glucosyltransferase 1	Q9NYU2	Down	0.62	0.00
STRN4	Striatin-4	Q9NRL3	Down	0.61	0.04
DNAJC11	DnaJ homolog subfamily C member 11	Q9NVH1	Down	0.61	0.02
CLSTN1	Calsyntenin-1	O94985	Down	0.59	0.01
BAG6	Large proline-rich protein BAG6	P46379	Down	0.52	0.00
SLC2A3	Solute carrier family 2, facilitated glucose transporter member 3	P11169	Down	0.50	0.01
SEC24B	Protein transport protein Sec24B	O95487	Down	0.49	0.03
ANK3	Ankyrin-3	Q12955	Down	0.47	0.00
WDR47	WD repeat-containing protein 47	O94967	Down	0.45	0.00
CPNE1	Copine-1	Q99829	Up	1.30	0.03
GAPDH	Glyceraldehyde-3-phosphate dehydrogenase	P04406	Up	1.30	0.00
PHB	Prohibitin	P35232	Up	1.30	0.04
ADH5	Alcohol dehydrogenase class-3	P11766	Up	1.31	0.04
IDH1	Isocitrate dehydrogenase [NADP] cytoplasmic	O75874	Up	1.31	0.01
MSN	Moesin	P26038	Up	1.31	0.05
CNDP2	Cytosolic non-specific dipeptidase	Q96KP4	Up	1.32	0.01
ACAA2	3-ketoacyl-CoA thiolase, mitochondrial	P42765	Up	1.33	0.00
PSMA6	Proteasome subunit alpha type-6	P60900	Up	1.33	0.03
HPX	Hemopexin	P02790	Up	1.34	0.02
PSMA4	Proteasome subunit alpha type-4	P25789	Up	1.34	0.03
SERPINB6	Serpin B6	P35237	Up	1.34	0.02
TARDBP	TAR DNA-binding protein 43	Q13148	Up	1.34	0.02
BRSK1	Serine/threonine-protein kinase BRSK1	Q8TDC3	Up	1.36	0.03
ECH1	Delta(3,5)-Delta(2,4)-dienoyl-CoA isomerase, mitochondrial	Q13011	Up	1.37	0.03
PACSIN2	Protein kinase C and casein kinase substrate in neurons protein 2	Q9UNF0	Up	1.38	0.02
PPT1	Palmitoyl-protein thioesterase 1	P50897	Up	1.39	0.02
RAB7A	Ras-related protein Rab-7a	P51149	Up	1.40	0.02
REPS1	RalBP1-associated Eps domain-containing protein 1	Q96D71	Up	1.40	0.02
ALDH9A1	4-trimethylaminobutyraldehyde dehydrogenase	P49189	Up	1.41	0.01

(*Continued*)

Table 4
(*continued*)

Gene	Protein name	Uniprot	Deregulation	FC	*p*
COPS2	COP9 signalosome complex subunit 2	P61201	Up	1.41	0.01
ECI2	Enoyl-CoA delta isomerase 2, mitochondrial	O75521	Up	1.41	0.01
EEF1A1	Elongation factor 1-alpha 1	P68104	Up	1.41	0.01
FHL1	Four and a half LIM domains protein 1 (Fragment)	Q5JXI8	Up	1.42	0.01
MPI	Mannose-6-phosphate isomerase	P34949	Up	1.43	0.01
CTSD	Cathepsin D	P07339	Up	1.45	0.01
CUTA	Protein CutA	O60888	Up	1.45	0.05
LHPP	Phospholysine phosphohistidine inorganic pyrophosphate phosphatase	Q9H008	Up	1.45	0.00
CSRP1	Cysteine and glycine-rich protein 1	P21291	Up	1.46	0.04
NUDT21	Cleavage and polyadenylation specificity factor subunit 5	O43809	Up	1.46	0.03
CLIC4	Chloride intracellular channel protein 4	Q9Y696	Up	1.47	0.04
LMNA	Prelamin-A/C	P02545	Up	1.49	0.03
SELENBP1	Selenium-binding protein 1	Q13228	Up	1.49	0.00
MTHFD1	C-1-tetrahydrofolate synthase, cytoplasmic	P11586	Up	1.50	0.03
PNPO	Pyridoxine-5′-phosphate oxidase	Q9NVS9	Up	1.50	0.04
SKP1	S-phase kinase-associated protein 1	P63208	Up	1.50	0.05
DNPEP	Aspartyl aminopeptidase	Q9ULA0	Up	1.51	0.01
FBXO2	F-box only protein 2	Q9UK22	Up	1.51	0.01
HDHD2	Haloacid dehalogenase-like hydrolase domain-containing protein 2	Q9H0R4	Up	1.51	0.04
PEBP1	Phosphatidylethanolamine-binding protein 1	P30086	Up	1.51	0.04
SMS	Spermine synthase	P52788	Up	1.51	0.03
SRI	Sorcin	P30626	Up	1.51	0.00
PSAT1	Phosphoserine aminotransferase	Q9Y617	Up	1.52	0.02
ANXA5	Annexin A5	P08758	Up	1.54	0.03
PHGDH	D-3-phosphoglycerate dehydrogenase	O43175	Up	1.54	0.01
GSTM5	Glutathione S-transferase Mu 5	P46439	Up	1.55	0.04
PLCD1	1-phosphatidylinositol 4,5-bisphosphate phosphodiesterase delta-1	P51178	Up	1.57	0.01
HSPB1	Heat shock protein beta-1	P04792	Up	1.60	0.03
NAXD	ATP-dependent (S)-NAD(P)H-hydrate dehydratase	Q8IW45	Up	1.60	0.02
PRDX2	Peroxiredoxin-2	P32119	Up	1.60	0.01
TPPP3	Tubulin polymerization-promoting protein family member 3	Q9BW30	Up	1.61	0.03
SOD2	Superoxide dismutase [Mn], mitochondrial	P04179	Up	1.62	0.04
COPS8	COP9 signalosome complex subunit 8	Q99627	Up	1.63	0.00
CUL3	Cullin-3	A0A087WTG3	Up	1.63	0.00
CYCS	Cytochrome c	P99999	Up	1.63	0.02
PKM	Pyruvate kinase PKM	P14618	Up	1.71	0.00
TMLHE	Trimethyllysine dioxygenase, mitochondrial	Q9NVH6	Up	1.72	0.04
PSMA5	Proteasome subunit alpha type-5	P28066	Up	1.74	0.03
ARL3	ADP-ribosylation factor-like protein 3	P36405	Up	1.75	0.00
GSTP1	Glutathione S-transferase P	P09211	Up	1.75	0.02
HBA1	Hemoglobin subunit alpha	P69905	Up	1.75	0.01
CD81	CD81 antigen	P60033	Up	1.77	0.00
PRDX1	Peroxiredoxin-1	Q06830	Up	1.77	0.01
NIT2	Omega-amidase NIT2	Q9NQR4	Up	1.79	0.03
AK1	Adenylate kinase isoenzyme 1	P00568	Up	1.81	0.01
GSTM2	Glutathione S-transferase	E9PHN6	Up	1.81	0.05
AK3	GTP:AMP phosphotransferase AK3, mitochondrial	Q9UIJ7	Up	1.82	0.01
FMOD	Fibromodulin	Q06828	Up	1.85	0.03
BLVRB	Flavin reductase (NADPH)	P30043	Up	1.91	0.00
NAE1	NEDD8-activating enzyme E1 regulatory subunit	Q13564	Up	1.92	0.00
PRDX6	Peroxiredoxin-6	P30041	Up	1.93	0.01
HBB	Hemoglobin subunit beta	P68871	Up	1.94	0.01
NDUFB10	NADH dehydrogenase [ubiquinone] 1 beta subcomplex subunit 10	O96000	Up	1.94	0.01
DNAH8	Dynein heavy chain 8, axonemal	Q96JB1	Up	1.98	0.02
IGKC	Immunoglobulin kappa constant	P01834	Up	1.99	0.01
ANXA2	Annexin A2	P07355	Up	2.09	0.03
ANXA1	Annexin A1	P04083	Up	2.10	0.04
LGALS1	Galectin-1	P09382	Up	2.12	0.01
EIF3I	Eukaryotic translation initiation factor 3 subunit I	Q13347	Up	2.13	0.05
SPTBN1	Spectrin beta chain, non-erythrocytic 1	Q01082	Up	2.22	0.04

(*Continued*)

Table 4
(*continued*)

Gene	Protein name	Uniprot	Deregulation	FC	*p*
PGLS	6-phosphogluconolactonase	O95336	Up	2.26	0.03
COTL1	Coactosin-like protein	Q14019	Up	2.35	0.03
MYL6	Myosin light polypeptide 6	P60660	Up	2.39	0.01
SNPH	Syntaphilin	O15079	Up	2.48	0.01
SPR	Sepiapterin reductase	P35270	Up	2.51	0.01
HBD	Hemoglobin subunit delta	P02042	Up	2.52	0.01
PGAM2	Phosphoglycerate mutase 2	P15259	Up	2.52	0.02
IAH1	Isoamyl acetate-hydrolyzing esterase 1 homolog	Q2TAA2	Up	2.80	0.01
IGHG2	Immunoglobulin heavy constant gamma 2	P01859	Up	2.88	0.01
H2AFX	Histone H2AX	P16104	Up	4.17	0.04

Table 5
Main biofunctions of abnormally expressed proteins in frontal cortex area 8 in c9FTLD

Functional terms	*p*	Proteins
Apoptosis	0.000	PEBP1, PHGDH, PPT1, LGALS1, BAG6, PHB, SRI, PKM, CYCS, PRDX1, EIF3I, H2AFX, LMNA, SPTBN1, PRDX6, POR, GSTM5, PRKCB, CLIC4, ADH5, NAE1, PRDX2, GSTP1, CTSD, OPTN, CUL3, TARDBP, GAS7, PLCD1, EEF1A1, PUF60, SLC2A3, CLTC, NPTX1, MSN, ANXA5, ANXA2, CCDC6, ANXA1, HSPB1, SOD2, RABL6, GAPDH, APOE, SELENBP1, FMOD, PRKCG
Inflammation	0.000	PHGDH, PPT1, LGALS1, PHB, PKM, PRDX1, POR, PRDX6, CPNE1, PRKCB, PRDX2, GSTP1, CTSD, OPTN, IGKC, EEF1A1, MSN, ANXA5, HBB, ANXA1, SOD2, APOE, GAPDH, HPX, SELENBP1, COTL1, CD81
Metabolism of amino acids	0.000	PHGDH, MTHFD1, CNDP2, NIT2, PKM, IDH1, SMS
Metabolism of carbohydrate	0.000	AGL, PLCD1, EEF1A1, CLTC, PKM, ANXA1, PRDX6, MPI, PRKCB, CAMKK2, GAPDH, PRDX2, APOE, IDH1, OPTN
Metabolism of membrane lipid derivative	0.004	PRDX6, POR, PLCD1, EEF1A1, PPT1, PRKCB, PRDX2, APOE, ANXA1
Microtubule dynamics	0.000	PHGDH, CSRP1, ATL1, CLSTN1, PKM, SPTBN1, PRKCB, CAMKK2, ARL3, OPTN, CD81, GAS7, BRSK1, EEF1A1, PACSIN2, MSN, RAP1GAP, NCKIPSD, CNTN2, ANK3, HSPB1, ARHGEF2, APOE, GAPDH, GPRIN1
Morphology of mitochondria	0.003	SOD2, SNPH, GAPDH, INF2, AK1
Neuritogenesis	0.000	BRSK1, CSRP1, LGALS1, NPTX1, RAP1GAP, SNPH, CNTN2, ANK3, SPTBN1, APOE, CAMKK2, GPRIN1, GAS7, TARDBP
Neurotransmission	0.005	NPTX1, CLSTN1, PRKCB, FBXO2, SRI, SNPH, APOE, PRKCG, ANK3
Phagocytosis	0.001	RAB7A, CLTC, ANXA5, MSN, CLIC4, PRKCB, RAP1GAP, PRKCG, ANXA1
Receptor-mediated endocytosis	0.001	PACSIN2, PPT1, CLTC, REPS1, NAE1, APOE
Synthesis of reactive oxygen species	0.000	PHB, ANXA2, HBB, PRDX1, ANXA1, HSPB1, PRDX6, SOD2, PRKCB, PRDX2, APOE, IDH1, GSTP1

addition, one synaptic protein, SNAP25, and two proteins linked with the calcium/calmodulin-dependent (CaM) kinase cascade were selected for validation. SNAP25 was significantly decreased ($p = 0.02$), and CaMKII and CaMKIV protein levels were significantly reduced, in c9FTLD when compared with controls ($p = 0.05$ and $p = 0.03$, respectively) (Fig. 5).

DISCUSSION

This study analyzes differential mRNA and protein expression in frontal cortex area 8 in 19 fFTLD cases linked to C9ORF72 expansion (c9FTLD) and 14 age- and gender-matched controls using microarray hybridization and 7000G platform technology from Affymetrix® and quantitative proteomics using LC-MS/MS, respectively. mRNA expression for selected genes was validated with RT-qPCR, and protein levels with gel electrophoresis and western blotting.

Regarding TDP-43 and C9orf72, major pathologic components in c9FTLD, *TARDBP* mRNA expression was preserved but total TDP-43 protein showed increased levels in c9FTLD when compared with controls. This is in accordance with the abnormal deposition of this protein in intracellular inclusions and threads characteristic of this disease. In contrast, *C9ORF72* mRNA expression was significantly decreased in c9FTLD. However, the C9orf72 long isoform was significantly reduced and the C9orf72 short isoform significantly increased in c9FTLD. Reduced C9ORF72 protein levels were found in previous reports [55–58]. The functional implications of the reduced levels of the long C9orf72 isoform are not known, but quantitative mass spectrometry-based proteomics used to identify interacting proteins

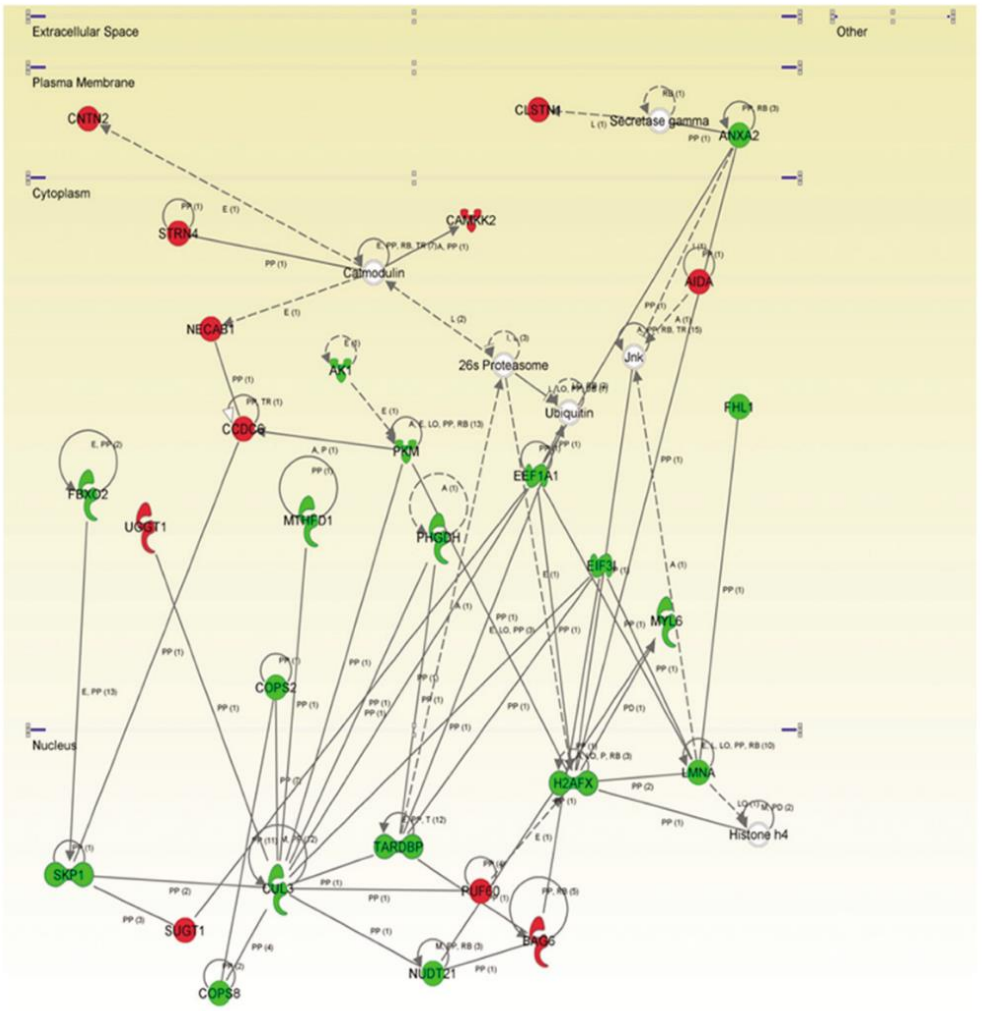

Fig. 4. High-scoring protein interactome map of differentially expressed proteins in the frontal cortex in c9FTLD. Visual representation of the relationships between differentially expressed proteins and functional interactors. Downregulated proteins are highlighted in red and upregulated proteins in green. Continuous and discontinuous lines represent direct and indirect interactions, respectively.

in motor neurons has shown that the long isoform complex stabilizes SMCR8, a protein which acts as an autophagic regulator [59, 60]. Therefore, reduced levels of the long isoform may interfere with normal autophagy and lysosomal processing [60]. C9orf72 also binds to several proteins including members of the Rab family, endoplasmic reticulum and synapses; nuclear and cytoplasmic transport, endoplasmic reticulum stress, and altered synaptic function have all been reported in association with pathogenic *C9ORF72* expansions [21, 22, 26, 28, 35, 39, 61].

The present study reveals altered gene transcription related to DNA recombination, RNA splicing regulation, RNA polymerase transcription, myelin synthesis, calcium regulation, and ubiquitin-proteasome system in c9FTLD. Proteomics performed in the same tissue samples identifies altered protein expression linked to apoptosis, inflammation, metabolism of amino acids, metabolism

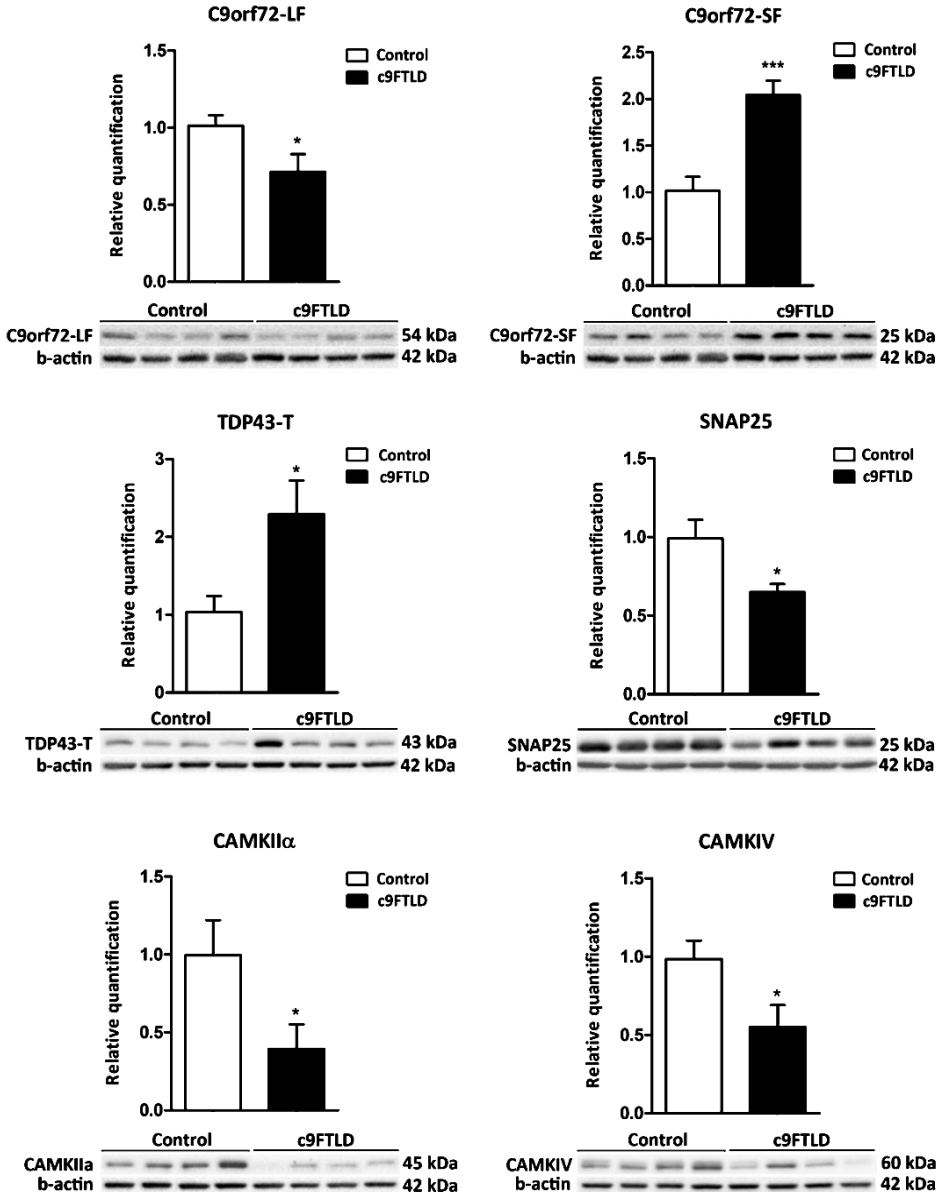

Fig. 5. Gel electrophoresis and western blotting to C9orf72 isoforms, and total TDP-43, CAMKIIa, and CAMKIV in frontal cortex area 8 in c9FTLD and controls. The protein expression of C9orf72 long isoform (54 kDa) is reduced in parallel with the increased protein level of the C9orf72 short isoform (25 kDa). Total protein levels of TDP-43 are significantly increased in c9FTLD. CAMKII and CAMKIV protein levels are significantly decreased. $^{*}p < 0.05$ and $^{***}p < 0.001$.

of carbohydrates, metabolism of membrane lipid derivatives, microtubule dynamics, morphology of mitochondria, neuritogenesis, neurotransmission, phagocytosis, receptor-mediated endocytosis, synthesis of reactive oxygen species, and calcium signaling in c9FTLD.

Genes and proteins do not match in the two lists of deregulated mRNAs and proteins in c9FTLD

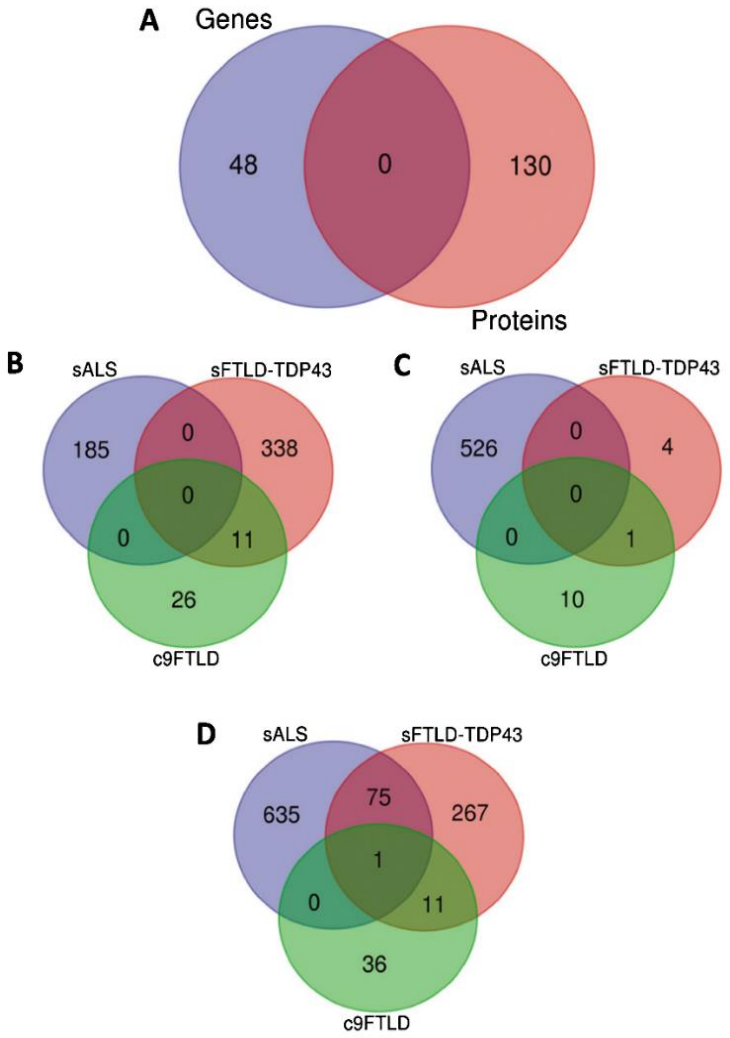

Fig. 6. A) Venn's diagram comparing transcriptomics and proteomics profile in c9FTLD based on the present observations. B–D) Overlap of the transcriptomic profiles obtained in the frontal cortex area 8 in sALS, sFTLD-TDP, and c9FTLD based on the present observations and our previous studies cited in [45] and [51]. B) Venn's diagram of downregulated genes in sALS, sFTLD, and c9FTLD. C) Venn's diagram of upregulated genes in sALS, sFTLD, and c9FTLD. D) Venn's diagram of total deregulated genes in sALS, sFTLD, and c9FTLD.

(Fig. 6A). However, a protein interactome map constructed using the IPA software shows deregulation of cross-linkers between DNA/RNA regulation systems and ubiquitin-proteasome systems, suggesting an imbalance in cellular transcription processes and protein degradation mechanisms, which makes sense in light of gene transcription observations of the main contributors to the pathogenesis of neurodegenerative diseases with abnormal protein aggregates, and it is particularly in line with the function of TDP-43 and C9orf72.

Together, this combined transcriptomics-proteomics analysis supports the list of separately reported altered pathways linked to *C9ORF72* mutations, including those involved in DNA recombination and transcription, RNA splicing, endoplasmic reticulum and mitochondria, synaptic transmission, protein degradation, calcium home-

ostasis, and inflammation [35, 37–39, 41, 61–66]. Additional alterations involve altered metabolism of amino acids and carbohydrates, membrane lipid derivatives, and microtubule dynamics, and synthesis of reactive oxygen species. Links between oxidative and endoplasmic reticulum stress, TDP-43, and docosahexaenoic acid have been described in the spinal cord in ALS [67–69] but information is lacking about c9FTLD. Moreover, oxidative damage has been assessed and proven in FTLD-TDP [70], but no special focus on c9FTLD was provided in that study.

An interesting deregulated cluster is composed of genes linked to several miRNAs, nuclear RNAs and long non-coding RNAs, including MIR4740, the small nucleolar RNA (SCARNA2), and long non-coding RNAs such as X-inactive specific transcript (XIST) and the long intergenic non-coding RNAs LINC1476, LINC1140, and LINC00499. miRNAS participate in a large number of variegated processes covering mRNA silencing and regulation of gene transcription [71, 72]. SCARNA2 localizes to Cajal bodies, the process of binding of its box C/D being modulated by coilin [73]. Long intergenic non-coding RNAs are mainly localized in the nucleus where they modulate chromatin and genome architecture, in addition to RNA stabilization and transcription regulation [74]. XIST is localized in the X-chromosome and participates in the inactivation of chromosome X [75]. The consequences of XIST deregulation in C9orf72 remains elusive.

Our previous studies using a similar transcriptomics approach in frontal cortex area 8 in sFTLD-TDP have shown down-deregulation of genes linked to neurotransmission and synapses, neuronal architecture, cytoskeleton of axons and dendrites, vesicle trafficking, purines, mitochondria, and energy metabolism [45]. Additional protein and enzymatic studies have revealed altered mitochondrial function and oxidative phosphorylation [45]. Using the same methods, we observed upregulated gene clusters in frontal cortex area 8 in sALS involving neurotransmission, synaptic proteins, and vesicle trafficking, and downregulated genes clustering into oligodendrocyte function and myelin-related proteins [51]. Venn's diagrams serve to illustrate downregulated and upregulated genes shared in these diseases: sALS, sFTLD-TDP, and c9FTLD (Fig. 6B–D).

Curiously, some downregulated clusters related mainly to synapses and neurotransmission in frontal cortex in sFTLD-TDP were upregulated in frontal cortex in sALS without dementia [45, 51]. The present observations in c9FTLD reveal some commonalities with sFTLD-TDP in altered clusters but not in particular genes. Downregulation of genes linked to oligodendrocytes and myelin in frontal cortex area 8 is shared in c9FTLD and sALS.

Recent studies have shown oligodendrocytes as key players in neurodegenerative diseases with abnormal protein aggregates [76]. Oligodendrogliopathy is common in sALS and FTLD-TDP. Phosphorylated-TDP-43-immunoreactive oligodendroglial inclusions are found, in addition to spinal cord motor neurons, in the motor, sensory and premotor cortex, but not in the corpus callosum, cingulum or lateral tracts of the spinal cord [77]. TDP-43 oligodendroglial inclusions are common in the deep layers of the cerebral cortex and white matter in FTLD-TDP [78]. The functional effects of oligodendroglial TDP-43 inclusions are not known, but present findings indicate altered oligodendroglial gene expression in the frontal cortex in c9FTLD. Particular features are linked to C9orf72 hexanucleotide repeat expansion [79, 80], and TDP-43-dependent or TDP-43-independent oligodendroglial dysfunction might be a characteristic trait linked to C9orf72 hexanucleotide repeat expansion.

In contrast, although astrocytes play key pathogenic roles in ALS [81], TDP-43-immunoreactive inclusions are rare in sALS and FTLD-TDP [82].

Commonalities and discrepancies are also seen when comparing the transcriptome of the frontal cortex in sALS with no mutations and ALS linked to C9orf72 mutations (c9ALS) [83]. The number and type of deregulated genes in c9ALS was approximately double that seen in sALS. For example, alteration of the unfolded protein response and intracellular protein transport were identified from genes differentially upregulated in c9ALS but not in sALS, whereas alterations in oxidative phosphorylation, cytoskeleton, and synaptic transmission were predominant in frontal cortex in sALS [83]. These data in frontal cortex in sALS roughly correlate with our observations in the sALS/sFTLD-TDP spectrum [45, 51] although the lack of information regarding the cognitive status of patients in the c9ALS/sALS comparative study does not permit further analogies between the separate series. That study was performed using RNA-sequencing methods [83], which uses high-throughput sequencing to document all transcripts in contrast to microarrays which quantify a set of predetermined sequences. Therefore, RNA-seq is presumably more robust than our microarrays approach, and may account for differences in the

results obtained by these different strategies. However, focusing on c9ALS and present observations in c9FTLD, altered RNA splicing and ubiquitin-proteasome system are identified in both studies.

Comparisons with other studies performed in different types of FTLD-TDP show disparate results. One gene expression analysis in fFTLD linked to *GRN* mutations identified abnormal regulated processes associated with lipid metabolism, MAPK signaling pathway, and transport [43], while lysosomal dysfunction was identified in another [44]. Another study recognized synapse-, cytoskeletal/filament-, microtubule/axon-, and proteasome-related pathways in FTLD-TDP when compared with controls, and cytoskeletal protein-, mitochondria/energy-, synapse-, microtubule/axon-, and ubiquitin-proteasome-associated deregulation when comparing FTLD-TDP with FTLD associated with motor neuron disease [42]. Common mechanisms occur within the FTLD-ALS spectrum [84]. However, weighted co-expression network proteomic analysis has recently revealed 15 modules of co-expressed proteins, eight of which differed significantly across the ALS-FTD disease spectrum [46]. Interestingly, a module enriched with astrocyte and microglia proteins was significantly increased in the frontal cortex in ALS cases carrying the C9orf72 mutation compared to sporadic ALS cases, suggesting that the genetic expansion is associated with inflammation in the brain [46]. Increased levels of proteins linked to inflammation are also identified in the frontal cortex in C9orf72 in our study. The present dual-omic approach, like the majority of molecular studies carried out in the postmortem human brain, is based on the relative abundance of particular mRNAs and proteins or ratios of two absolute concentrations (fold-change) representing concentrations relative to reference samples. Moreover, the agonal state and postmortem delay may differentially interfere with transcription and protein synthesis/degradation. Therefore, when analyzing postmortem brain samples, a non-steady-state condition is always the real scenario. This statement is important when assessing transcripts and proteins separately, but it is especially crucial when analyzing RNA and protein correlations of particular genes in human postmortem brain [85–87]. Moreover, distinct cell populations are usually mingled, and rates and scales of RNA and corresponding encoded proteins may be cell type-dependent. These facts, together with particular characteristics of samples, and differences in the procedures and methods, may account for the non-homogeneous results in different laboratories. Although the original samples are the same in the present series, and the identified altered pathways are similar and complementary using a combination of transcriptomics and proteomics, it is worth stressing that different RNAs and proteins are identified by these methods. Combined non-targeted '-omics' seems to be a valuable approach to deciphering altered molecular pathways in FTLD provided that observations are viewed cautiously when assessing human postmortem brain samples.

ACKNOWLEDGMENTS

We wish to thank Valle de Hebron Institute of Research (VHIR) Whole-transcriptome array platform for their help in the arrays, and T. Yohannan for editorial assistance.

This study was supported by grants from CIBERNED and PI17/00809 Institute of Health Carlos III, and co-funded by FEDER funds/European Regional Development Fund (ERDF) – a way to build Europe; ALS intra-CIBERNED project to IF; IFI15/00035 fellowship to PA-B; "Retos todos unidos contra la ELA" and "Proyecto DGeneración conexiones con sentido" to MP; and grant from the "Fundación Tatiana Pérez de Guzmán el Bueno, convocatoria Neurociencias 2014" to EG. Additional support came from grants from the Department of Economic Development of the Government of Navarra (Ref. PC025, PC081-82) to ES. The Proteomics Unit of Navarrabiomed is a member of Proteored, PRB3-ISCIII, and is supported by grant PT17/0019, of the PE I+D+i 2013-2016 to JFI, funded by ISCIII and ERDF.

Authors' disclosures available online (https://www.j-alz.com/manuscript-disclosures/18-1123r2).

REFERENCES

[1] Hortobagyi T, Cairns NJ (2015) Amyotrophic lateral sclerosis and frontotemporal lobar degeneration. In *Neuropathology of neurodegenerative diseases: A practical guide*, Kovacs GG, ed. Cambridge University Press, Cambridge, pp. 209-248.

[2] Lashley T, Roher JD, Mead S, Revesz T (2015) Review: An update on clinical, genetic and pathological aspects of frontotemporal lobar degenerations. *Neuropathol Appl Neurobiol* **41**, 858-881.

[3] Mann DMA, Snowden JS (2017) Frontotemporal lobar degeneration: Pathogenesis, pathology and pathways to phenotype. *Brain Pathol* **27**, 723-736.

[4] Van Mossevelde S, Engelborghs S, van der Zee J, Broeckhoven C (2018) Genotype-phenotype links in fron-

totemporal lobar degeneration. *Nature Rev Neurol* **14**, 363-378.

[5] Olszewska DA, Lonergan R, Fallon EM, Lynch T (2016) Genetics of frontotemporal dementia. *Curr Neurol Neurosci Rep* **16**, 107.

[6] Pottier C, Ravenscroft TA, Sánchez-Contreras M, Rademakers R (2016) Genetics of FTLD: Overview and what else we can expect from genetic studies. *J Neurochem* **138**, 32-53.

[7] Rainero I, Rubino E, Michelerio A, D'Agata F, Gentile S, Pinessi L (2017) Recent advances in the molecular genetics of frontotemporal lobar degeneration. *Funct Neurol* **32**, 7-16.

[8] Neumann M, Mackenzie IRA (2019) Neuropathology of non-tau frontotemporal lobar degeneration. *Neuropathol Appl Neurobiol* **45**, 19-40.

[9] Neumann M, Sampathu DM, Kwong LK, Truax AC, Micsenyi MC, Chou TT, Bruce J, Schuck T, Grossman M, Clark CM, McCluskey LF, Miller BL, Masliah E, Mackenzie IR, Feldman H, Feiden W, Kretzschmar HA, Trojanowski JQ, Lee VM (2006) Ubiquitinated TDP-43 in frontotemporal lobar degeneration and amyotrophic lateral sclerosis. *Science* **314**, 130-133.

[10] Geser F, Martinez-Lage M, Robinson J, Uryu K, Neumann M, Brandmeir NJ, Xie SX, Kwong LK, Elman L, McCluskey L, Clark CM, Malunda J, Miller BL, Zimmerman EA, Qian J, Van Deerlin V, Grossman M, Lee VM, Trojanowski JQ (2009) Clinical and pathological continuum of multisystem TDP-43 proteinopathies. *Arch Neurol* **66**, 180-189.

[11] DeJesús-Hernández M, Mackenzie IR, Boeve BF, Boxer AL, Baker M, Rutherford NJ, Nicholson AM, Finch NA, Flynn H, Adamson J, Kouri N, Wojtas A, Sengdy P, Hsiung GY, Karydas A, Seeley WW, Josephs KA, Coppola G, Geschwind DH, Wszolek ZK, Feldman H, Knopman DS, Petersen RC, Miller BL, Dickson DW, Boylan KB, Graff-Radford NR, Rademakers R (2011) Expanded GGG GCC hexanucleotide repeat in non-coding region of C9ORF72 causes chromosome 9p-linked FTD and ALS. *Neuron* **72**, 245-256.

[12] Cruts M, Gijselinck I, Van Langenhove T, Van der Zee J, Van Broeckhoven C (2013) Current insights into the C9orf72 repeat expansion diseases of the FTLD/ALS spectrum. *Trends Neurosci* **36**, 450-499.

[13] Renton AE, Chiò A, Traynor BJ (2014) State of play in amyotrophic lateral sclerosis genetics. *Nat Neurosci* **17**, 17-23.

[14] Stewart H, Rutherford NJ, Briemberg H, Krieger C, Cashman N, Fabros M, Baker M, Fok A, DeJesús-Hernández M, Eisen A, Rademakers R, Mackenzie IR (2012) Clinical and pathological features of amyotrophic lateral sclerosis caused by mutation in the C9ORF72 gene on chromosome 9p. *Acta Neuropathol* **123**, 409-417.

[15] Boeve BF, Boylan KB, Graff-Radford NR, DeJesus-Hernandez M, Knopman DS, Pedraza O, Vemuri P, Jones D, Lowe V, Murray ME, Dickson DW, Josephs KA, Rush BK, Machulda MM, Fields JA, Ferman TJ, Baker M, Rutherford NJ, Adamson J, Wszolek ZK, Adeli A, Savica R, Boot B, Kuntz KM, Gavrilova R, Reeves A, Whitwell J, Kantarci K, Jack CR Jr, Parisi JE, Lucas JA, Petersen RC, Rademakers R (2012) Characterization of frontotemporal dementia GCC repeat expansion in C9ORF72. *Brain* **135**, 765-783.

[16] Gendron TF, Bieniek KF, Zhang YJ, Jansen-West K, Ash PE, Caulfield T, Daughrity L, Dunmore JH, Castanedes-Casey M, Chew J, Cosio DM, van Blitterswijk M, Lee WC, Rademakers R, Boylan KB, Dickson DW, Petrucelli L (2013) Antisense transcripts of the expanded C9ORF72 hexanucleotide repeat form nuclear RNA foci and undergo repeat-associated non-ATG translation in c9FTD/ALS. *Acta Neuropathol* **126**, 829-844.

[17] Lee YB, Chen HJ, Peres JN, Gomez-Deza J, Attig J, Stalekar M, Troakes C, Nishimura AL, Scotter EL, Vance C, Adachi Y, Sardone V, Miller JW, Smith BN, Gallo JM, Ule J, Hirth F, Rogelj B, Houart C, Shaw CE (2013) Hexanucleotide repeats in ALS/FTD form length-dependent RNA foci, sequester RNA binding proteins, and are neurotoxic. *Cell Rep* **5**, 1178-1186.

[18] Donnelly CJ, Zhang PW, Pham JT, Haeusler AR, Mistry NA, Vidensky S, Daley EL, Poth EM, Hoover B, Fines DM, Maragakis N, Tienari PJ, Petrucelli L, Traynor BJ, Wang J, Rigo F, Bennett CF, Blackshaw S, Sattler R, Rothstein JD (2013) RNA toxicity from the ALS/FTD C9ORF72 expansion is mitigated by antisense intervention. *Neuron* **80**, 415-428.

[19] Sareen D, O'Rourke JG, Meera P, Muhammad AK, Grant S, Simpkinson M, Bell S, Carmona S, Ornelas L, Sahabian A, Ornelas L, Sahabian A, Gendron T, Petrucelli L, Baughn M, Ravits J, Harms MB, Rigo F, Bennett CF, Otis TS, Svendsen CN, Baloh RH (2013) Targeting RNA foci in iPSC-derived motor neurons from ALS patients with a C9ORF72 repeat expansion. *Sci Transl Med* **5**, 208ra149.

[20] Mizielinska S, Lashley T, Norona FE, Clayton EL, Ridler CE, Fratta P, Isaacs AM (2013) C9orf72 frontotemporal lobar degeneration is characterised by frequent neuronal sense and antisense RNA foci. *Acta Neuropathol* **126**, 845-857.

[21] May S, Hornburg D, Schludi MH, Arzberger T, Rentzsch K, Schwenk BM, Grasser FA, Mori K, Kremmer E, Banzhaf-Strathmann, Mann M, Meissner F (2014) C9orf72 FTLD/ALS-associated Gly-Ala dipeptide repeat proteins cause neuronal toxicity and Unc119 sequestration. *Acta Neuropathol* **128**, 485-503.

[22] Zhang YJ, Jansen-West K, Xu YF, Gendron TF, Bieniek KF, Lin WL, Sasaguri H, Caulfield T, Hubbard J, Daughrity L, Chew J, Belzil VV, Prudencio M, Stankowski JN, Castanedes-Casey M, Whitelaw E, Ash PE, DeTure M, Rademakers R, Boylan KB, Dickson DW, Petrucelli L (2014) Aggregation-prone c9FTD/ALS poly(GA) RANtranslated proteins cause neurotoxicity by inducing ER stress. *Acta Neuropathol* **128**, 505-524.

[23] Wen X, Tan W, Westergard T, Krishnamurthy K, Markandaiah SS, Shi Y, Lin S, Shneider NA, Monaghan J, Pandey UB, Pasinelli P, Ichida JK, Trotti D (2014) Antisense proline-arginine RAN dipeptides linked to C9ORF72-ALS/FTD form toxic nuclear aggregates that initiate in vitro and in vivo neuronal death. *Neuron* **84**, 1213-1225.

[24] Cooper-Knock J, Walsh MJ, Higginbottom A, Robin Highley J, Dickman MJ, Edbauer D, Ince PG, Wharton SB, Wilson SA, Kirby J Wharton SB, Wilson SA, Kirby J, Hautbergue GM, Shaw PJ (2014) Sequestration of multiple RNA recognition motif-containing proteins by C9orf72 repeat expansions. *Brain* **137**, 2040-2051.

[25] Kwon I, Xiang S, Kato M, Wu L, Theodoropoulos P, Wang T, Kim J, Yun J, Xie Y, McKnight SL (2014) Poly-dipeptides encoded by the C9orf72 repeats bind nucleoli, impede RNA biogenesis, and kill cells. *Science* **345**, 1139-1145.

[26] Freibaum BD, Lu Y, Lopez-Gonzalez R, Kim NC, Almeida S, Lee KH, Badders N, Valentine M, Miller BL, Wong PC, Petrucelli L, Kim HJ, Gao FB, Taylor JP (2015) GGG GCC

repeat expansion in C9orf72 compromises nucleocytoplasmic transport. *Nature* **525**, 129-133.

[27] Tao Z, Wang H, Xia Q, Li K, Li K, Jiang X, Xu G, Wang G, Ying Z (2015) Nucleolar stress and impaired stress granule formation contribute to C9orf72 RAN translation-induced cytotoxicity. *Hum Mol Genet* **24**, 2426-2441.

[28] Jovicic A, Mertens J, Boeynaems S, Bogaert E, Chai N, Yamada SB, Paul JW 3rd, Sun S, Herdy JR, Bieri G, Kramer NJ, Gage FH, Van Den Bosch L, Robberecht W, Gitler AD (2015) Modifiers of C9orf72 dipeptide repeat toxicity connect nucleo-cytoplasmic transport defects to FTD/ALS. *Nat Neurosci* **18**, 1226-1229.

[29] Schludi MH, May S, Grasser FA, Rentzsch K, Kremmer E, Kupper C, Klopstock T, Arzberger T, German Consortium for Frontotemporal Lobar Degeneration, Bavarian Brain Banking (2015) Distribution of dipeptide repeat proteins in cellular models and C9orf72 mutation cases suggests link to transcriptional silencing. *Acta Neuropathol* **130**, 537-555.

[30] Porta S, Kwong LK, Trojanowski JQ, Lee VM (2015) Drosha inclusions are new components of dipeptide-repeat protein aggregates in FTLD-TDP and ALS C9orf72 expansion cases. *J Neuropathol Exp Neurol* **74**, 380-387.

[31] Todd TW, Petrucelli L (2016) Insights into the pathogenic mechanisms of chromosome 9 open reading frame 72 (C9orf72) repeat expansions. *J Neurochem* **138**, 145-162.

[32] Cooper-Knock J, Higginbottom A, Stopford MJ, Highley JR, Ince PG, Wharton SB, Pickering-Brown S, Kirby J, Hautbergue GM, Shaw PJ (2015) Antisense RNA foci in the motor neurons of C9ORF72-ALS patients are associated with TDP-43 proteinopathy. *Acta Neuropathol* **130**, 63-75.

[33] Xiao S, MacNair L, McLean J, McGoldrick P, McKeever P, Soleimani S, Keith J, Zinman L, Rogaeva E, Robertson J (2016) C9orf72 isoforms in amyotrophic lateral sclerosis and frontotemporal lobar degeneration. *Brain Res* **1647**, 43-49.

[34] Zhang YJ, Gendron TF, Grima JC, Sasaguri H, Jansen-West K, Xu YF, Katzman RB, Gass J, Murray ME, Shinohara M, Lin WL, Garrett A, Stankowski JN, Daughrity L, Tong J, Perkerson EA, Yue M, Chew J, Castanedes-Casey M, Kurti A, Wang ZS, Liesinger AM, Baker JD, Jiang J, Lagier-Tourenne C, Edbauer D, Cleveland DW, Rademakers R, Boylan KB, Bu G, Link CD, Dickey CA, Rothstein JD, Dickson DW, Fryer JD, Petrucelli L (2016) C9ORF72 poly(GA) aggregates sequester and impair HR23 and nucleocytoplasmic transport proteins. *Nat Neurosci* **19**, 668-677.

[35] Gao FB, Almeida S, López-González R (2017) Dysregulated molecular pathways in amyotrophic lateral sclerosis–frontotemporal dementia spectrum disorder. *EMBO J* **36**, 2931-2950.

[36] DeJesús-Hernández M, Finch NA, Wang X, Gendron TF, Bieniek KF, Heckman MG, Vasilevich A, Murray ME, Rousseau L, Weesner R, Lucido A, Parsons M, Chew J, Josephs KA, Parisi JE, Knopman DS, Petersen RC, Boeve BF, Graff-Radford NR, de Boer J, Asmann YW, Petrucelli L, Boylan KB, Dickson DW, van Blitterswijk M, Rademakers R (2017) In-depth clinico-pathological examination of RNA foci in a large cohort of C9ORF72 expansion carriers. *Acta Neuropathol* **134**, 255-269.

[37] Budini M, Buratti E, Morselli E, Criollo A (2017) Autophagy and its impact on neurodegenerative diseases: New roles for TDP-43 and C9orf72. *Front Mol Neurosci* **10**, 170.

[38] Ji YJ, Ugolino J, Brady NR, Hamacher-Brady A, Wang J (2017) Systemic deregulation of autophagy upon loss of ALS- and FTD-linked C9orf72. *Autophagy* **13**, 1254-1255.

[39] Vatsavayai SC, Nana AL, Yokoyama JS, Seeley WW (2019) C9orf72-FTD/ALS pathogenesis: Evidence from human neuropathological studies. *Acta Neuropathol* **137**, 1-26.

[40] Zhang Y, Burberry A, Wang JY, Sandoe J, Ghosh S, Udeshi ND, Svinkina T, Mordes DA, Mok J, Charlton M, Li QZ, Carr SA, Eggan K (2018) The C9orf72-interacting protein Smcr8 is a negative regulator of autoimmunity and lysosomal exocytosis. *Genes Dev* **32**, 929-943.

[41] Herrmann D, Parlato R (2018) C9orf72-associated neurodegeneration in ALS-FTD: Breaking new ground in ribosomal RNA and nucleolar dysfunction. *Cell Tissue Res* **373**, 351-360.

[42] Mishra M, Paunesku T, Woloschak GE, Siddique T, Zhu LJ, Lin S, Greco K, Bigio EH (2007) Gene expression analysis of frontotemporal lobar degeneration of the motor neuron disease type with ubiquitinated inclusions. *Acta Neuropathol* **114**, 81-94

[43] Chen-Plotkin AS, Geser F, Plotkin JB, Clark CM, Kwong LK, Yuan W, Grossman M, Van Deerlin VM, Trojanowski JQ, Lee VM (2008) Variations in the progranulin gene affect global gene expression in frontotemporal lobar degeneration. *Hum Mol Genet* **17**, 1349-1362.

[44] Evers BM, Rodríguez-Navas C, Tesla RJ, Prange-Kiel J, Wasser CR, Yoo KS, McDonald J, Cenik B, Ravenscroft TA, Plattner F, Rademakers R, Yu G, White CL 3rd, Herz J (2017) Lipidomic and transcriptomic basis of lysosomal dysfunction in progranulin deficiency. *Cell Rep* **20**, 2565-2574.

[45] Andrés-Benito P, Gelpi E, Povedano M, Santpere G, Ferrer I (2018) Gene expression profile in frontal cortex in sporadic frontotemporal lobar degeneration-TDP. *J Neuropathol Exp Neurol* **77**, 608-627.

[46] Umoh ME, Dammer EB, Dai J, Duong DM, Lah JJ, Levey AI, Gearing M, Glass JD, Seyfried NT (2018) A proteomic network approach across the ALS-FTD disease spectrum resolves clinical phenotypes and genetic vulnerability in human brain. *EMBO Mol Med* **10**, 48-62.

[47] Mackenzie IR, Neumann M, Baborie A, Sampathu DM, Du Plessis D, Jaros E, Perry RH, Trojanowski JQ, Mann DM, Lee VM (2011) A harmonized classification system for FTLD-TDP pathology. *Acta Neuropathol* **122**, 111-113.

[48] Brettschneider J, Del Tredici K, Irwin DJ, Grossman M, Robinson JL, Toledo JB, Fang L, Van Deerlin VM, Ludolph AC, Lee VM, Braak H, Trojanowski JQ (2014) Sequential distribution of pTDP-43 pathology in behavioral variant frontotemporal dementia (bvFTD). *Acta Neuropathol* **127**, 423-439.

[49] Durrenberger PF, Fernando S, Kashefi SN, Ferrer I, Hauw JJ, Seilhean D, Smith C, Walker R, Al-Sarraj S, Troakes C, Palkovits M, Kasztner M, Huitinga I, Arzberger T, Dexter DT, Kretzschmar H, Reynolds R (2010) Effects of antemortem and postmortem variables on human brain mRNA quality: A BrainNet Europe study. *J Neuropathol Exp Neurol* **69**, 70-81.

[50] Gentleman RC, Carey VJ, Bates DM, Bolstad B, Dettling M, Dudoit S, Ellis B, Gautier L, Ge Y, Gentry J, Hornik K, Hothorn T, Huber W, Iacus S, Irizarry R, Leisch F, Li C, Maechler M, Rossini AJ, Sawitzki G, Smith C, Smyth G, Tierney L, Yang JY, Zhang J (2004). Bioconductor: Open software development for computational biology and bioinformatics. *Genome Biol* **5**, R80.

[51] Andrés-Benito P, Moreno J, Aso E, Povedano M, Ferrer I (2017) Amyotrophic lateral sclerosis, gene deregulation in the anterior horn of the spinal cord and frontal cortex area

8: Implications in frontotemporal lobar degeneration. *Aging* **9**, 823-851.

[52] Durrenberger PF, Fernando FS, Magliozzi R, Kashefi SN, Bonnert TP, Ferrer I, Seilhean D, Nait-Oumesmar B, Schmitt A, Gebicke-Haerter PJ, Falkai P, Grünblatt E, Palkovits M, Parchi P, Capellari S, Arzberger T, Kretzschmar H, Roncaroli F, Dexter DT, Reynolds R (2012) Selection of novel reference genes for use in the human central nervous system: A BrainNet Europe Study. *Acta Neuropathol* **124**, 893-903.

[53] Tang WH, Shilov IV, Seymour SL (2008) Nonlinear fitting method for determining local false discovery rates from decoy database searches. *J Proteome Res* **7**, 3661.

[54] Tyanova S, Temu T, Sinitcyn P, Carlson A, Hein MY, Geiger T, Mann M, Cox J (2016) The Perseus computational platform for comprehensive analysis of (prote)omics data. *Nature Methods* **13**, 731-740.

[55] Belzil VV, Bauer PO, Prudencio M, Gendron TF, Stetler CT, Yan IK, Pregent L,Daughrity L, Baker MC, Rademakers R, Boylan K, Patel TC, Dickson DW, Petrucelli L (2013) Reduced C9orf72 gene expression in c9FTD/ALS is caused by histone trimethylation, an epigenetic event detectable in blood. *Acta Neuropathol* **126**, 895-905.

[56] Ciura S, Lattante S, Le Ber I, Latouche M, Tostivint H, Brice A, Kabashi E (2013) Loss of function of C9orf72 causes motor deficits in a zebrafish model of amyotrophic lateral sclerosis. *Ann Neurol* **74**, 180-187.

[57] Xi Z, Zinman L, Moreno D, Schymick J, Liang Y, Sato C, Zheng Y, Ghani M, Dib S, Keith J, Robertson J, Rogaeva E (2013) Hypermethylation of the CpG island near the G4C2 repeat in ALS with a C9orf72 expansion. *Am J Hum Genet* **92**, 981-989.

[58] Waite AJ, Baumer D, East S, Neal J, Morris HR, Ansorge O, Blake DJ (2014) Reduced C9orf72 protein levels in frontal cortex of amyotrophic lateral sclerosis and frontotemporal degeneration brain with the C9ORF72 hexanucleotide repeat expansion. *Neurobiol Aging* **35**, 1779.e5-1779.e13.

[59] Jung J, Behrends C (2017) Multifaceted role of SMCR8 as autophagy regulator. *Small GTPases* **1**, 1-9.

[60] Zhang YJ, Gendron TF, Ebbert MTW, O'Raw AD, Yue M, Jansen-West K, Zhang X, Prudencio M, Chew J, Cook CN, Daughrity LM, Tong J, Song Y, Pickles SR, Castanedes-Casey M, Kurti A, Rademakers R2, Oskarsson B, Dickson DW, Hu W, Gitler AD, Fryer JD, Petrucelli L (2018) Poly(GR) impairs protein translation and stress granule dynamics in C9orf72-associated frontotemporal dementia and amyotrophic lateral sclerosis. *Nat Med* **24**, 1136-1142.

[61] Frick P, Sellier C, Mackenzie IRA, Cheng CY, Tahraoui-Bories J, Martinat C, Pasterkamp RJ, Prudlo J, Edbauer D, Oulad-Abdelghani M, Feederle R, Charlet-Berguerand N, Neumann M (2018) Novel antibodies reveal presynaptic localization of C9orf72 protein and reduced protein levels in C9orf72 mutation carriers. *Acta Neuropathol Commun* **6**, 72.

[62] Kaus A, Sareen D (2015) ALS Patient stem cells for unveiling disease signatures of motoneuron susceptibility: Perspectives on the deadly mitochondria, ER stress and calcium triad. *Front Cell Neurosci* **9**, 448.

[63] Dafinca R, Scaber J, Ababneh N, Lalic T, Weir G, Christian H, Vowles J, Douglas AG, Fletcher-Jones A, Browne C, Nakanishi M, Turner MR, Wade-Martins R, Cowley SA, Talbot K (2016) 9orf72 hexanucleotide expansions are associated with altered endoplasmic reticulum calcium homeostasis and stress granule formation in induced pluripotent stem cell-derived neurons from patients with amyotrophic lateral sclerosis and frontotemporal dementia. *Stem Cells* **34**, 2063-2078.

[64] Palluzzi F, Ferrari R, Graziano F, Novelli V, Rossi G, Galimberti D, Rainero I, Benussi L, Nacmias B, Bruni AC, Cusi D, Salvi E, Borroni B, Grassi M (2017) A novel network analysis approach reveals DNA damage, oxidative stress and calcium/cAMP homeostasis-associated biomarkers in frontotemporal dementia. *PLoS One* **12**, e0185797.

[65] Lau DHW, Hartopp N, Welsh NJ, Mueller S, Glennon EB, Mórotz GM, Annibali A, Gomez-Suaga P, Stoica R, Paillusson S, Miller CCJ (2018) Disruption of ER-mitochondria signalling in fronto-temporal dementia and related amyotrophic lateral sclerosis. *Cell Death Dis* **9**, 327.

[66] Evans CS, Holzbaur ELF (2019) Autophagy and mitophagy in ALS. *Neurobiol Dis* **122**, 35-40.

[67] Ayala V, Granado-Serrano AB, Cacabelos D, Naudí A, Ilieva EV, Boada J, Caraballo-Miralles V, Lladó J, Ferrer I, Pamplona R, Portero-Otin M (2011) Cell stress induces TDP-43 pathological changes associated with ERK1/2 dysfunction: Implications in ALS. *Acta Neuropathol* **122**, 259-270.

[68] Cacabelos D, Ayala V, Granado-Serrano AB, Jové M, Torres P, Boada J, Cabré R, Ramírez-Núñez O, Gonzalo H, Soler-Cantero A, Serrano JC, Bellmunt MJ, Romero MP, Motilva MJ, Nonaka T, Hasegawa M, Ferrer I, Pamplona R, Portero-Otín M (2016) Interplay between TDP-43 and docosahexaenoic acid-related processes in amyotrophic lateral sclerosis. *Neurobiol Dis* **88**, 148-160.

[69] Ilieva EV, Ayala V, Jové M, Dalfó E, Cacabelos D, Povedano M, Bellmunt MJ, Ferrer I, Pamplona R, Portero-Otín M (2007) Oxidative and endoplasmic reticulum stress interplay in sporadic amyotrophic lateral sclerosis. *Brain* **130**, 3111-3123.

[70] Martínez A, Carmona M, Portero-Otin M, Naudí A, Pamplona R, Ferrer I (2008) Type-dependent oxidative damage in frontotemporal lobar degeneration: Cortical astrocytes are targets of oxidative damage. *J Neuropathol Exp Neurol* **67**, 1122-1136.

[71] Ambros V (2004) The functions of animal microRNAs. *Nature* **431**, 350-355.

[72] Bartel DP (2004) MicroRNAs: Genomics, biogenesis, mechanism, and function. *Cell* **116**, 281-297.

[73] Enwerem II, Wu G, Yu YT, Hebert MD (2015) Cajal body proteins differentially affect the processing of box C/D scaRNPs. *PLoS One* **10**, e0122348.

[74] Ransohoff JD, Wei Y, Khavari PA (2018) The functions and unique features of long intergenic non-coding RNA. *Nat Rev Mol Cell Biol 19*, 143-157.

[75] Chow JC, Yen Z, Ziesche SM, Brown CJ (2005) Silencing of the mammalian X chromosome. *Annu Rev Genom Hum Genet* **6**, 69-92.

[76] Ferrer I (2018) Oligodendrogliopathy in neurodegenerative diseases with abnormal protein aggregates: The forgotten partner. *Progr Neurobiol* **169**, 24-54.

[77] Neumann M, Kwong LK, Truax AC, Vanmassenhove B, Kretzschmar HA, Van Deerlin VM, Clark CM, Grossman M, Miller BL, Trojanowski JQ, Lee VM (2007) TDP-43-positive white matter pathology in frontotemporal lobar degeneration with ubiquitin-positive inclusions. *J Neuropathol Exp Neurol* **66**, 177-183.

[78] Fatima M, Tan R, Halliday GM, Kril JJ (2015) Spread of pathology in amyotrophic lateral sclerosis: Assessment of phosphorylated TDP-43 along axonal pathways. *Acta Neuropathol Commun* **3**, 47.

[79] Bigio EH (2011) C9ORF72, the new gene on the block, causes C9FTD/ALS: New insights provided by neuropathology. *Acta Neuropathol* **122**, 653-655.

[80] Bigio EH (2012) Motor neuron disease: The C9orf72 hexanucleotide repeat expansion in FTD and ALS. *Nat Rev Neurol* **8**, 249-250.

[81] Ferrer I (2017) Diversity of astroglial responses across human neurodegenerative disorders and brain aging. *Brain Pathol* **27**, 645-674.

[82] Kovacs GG, Lee VM, Trojanowski JQ (2017) Protein astrogliopathies in human neurodegenerative diseases and aging. *Brain Pathol* **27**, 675-690.

[83] Prudencio M, Belzil VV, Batra R, Ross CA, Gendron TF, Pregent LJ, Murray ME, Overstreet KK, Piazza-Johnston AE, Desaro P, Bieniek KF, DeTure M, Lee WC, Biendarra SM, Davis MD, Baker MC, Perkerson RB, van Blitterswijk M, Stetler CT, Rademakers R, Link CD, Dickson DW, Boylan KB, Li H, Petrucelli L (2015) Distinct brain transcriptome profiles in C9orf72-associated and sporadic ALS. *Nat Neurosci* **8**, 251175-251182.

[84] Conlon EG, Fagegaltier D, Agius P, Davis-Porada J, Gregory J, Hubbard I, Kang K, Kim D; New York Genome Center ALS Consortium, Phatnani H, Kwan J, Sareen D, Broach JR, Simmons Z, Arcila-Londono X, Lee EB, Van Deerlin VM, Shneider NA, Fraenkel E, Ostrow LW, Baas F, Zaitlen N, Berry JD, Malaspina A, Fratta P, Cox GA, Thompson LM, Finkbeiner S, Dardiotis E, Miller TM, Chandran S, Pal S, Hornstein E, MacGowan DJ, Heiman-Patterson T, Hammell MG, Patsopoulos NA, Dubnau J, Nath A, Phatnani H, Shneider NA, Manley JL (2018) Unexpected similarities between C9ORF72 and sporadic forms of ALS/FTD suggest a common disease mechanism. *Elife* **13**, 7.

[85] Vogel C, Marcotte EM (2012) Insights into the regulation of protein abundance from proteomic and transcriptomic analyses. *Nat Rev Genet* **13**, 227-232.

[86] Marguerat S, Schmidt A, Codlin S, Chen W, Aebersold R, Bähler J (2012) Quantitative analysis of fission yeast transcriptomes and proteomes in proliferating and quiescent cells. *Cell* **151**, 671-683.

[87] Liu Y, Beyer A, Aebersold R (2016) On the dependency of cellular protein levels on mRNA abundance. *Cell* **165**, 535-550.

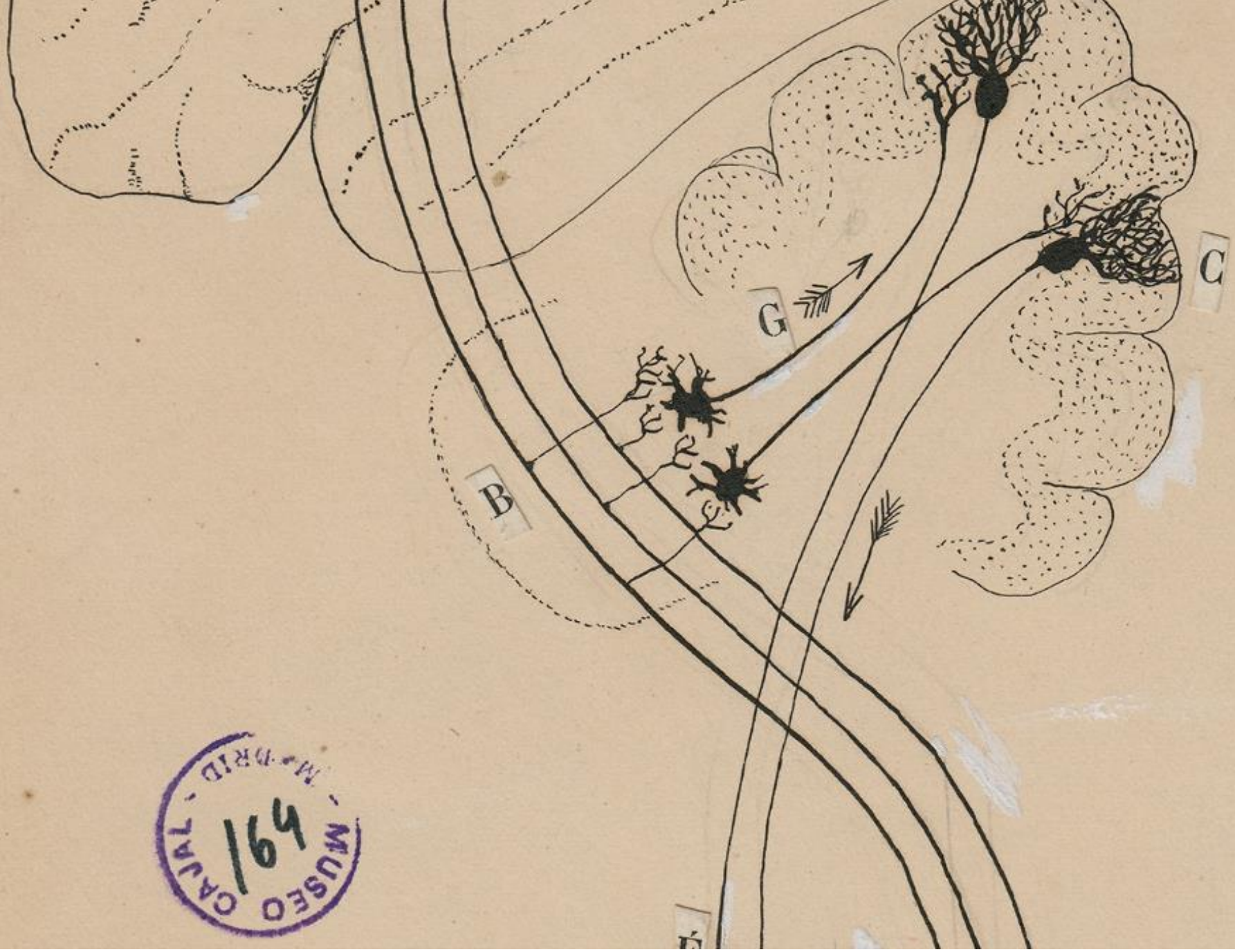

DISCUSSION

4. Discussion

In the present thesis, we have examined several molecular alterations underlying distinct TDP-43 proteinopathies within the ALS-FTLD spectrum in frontal cortex area 8 and in the anterior horn of spinal cord.

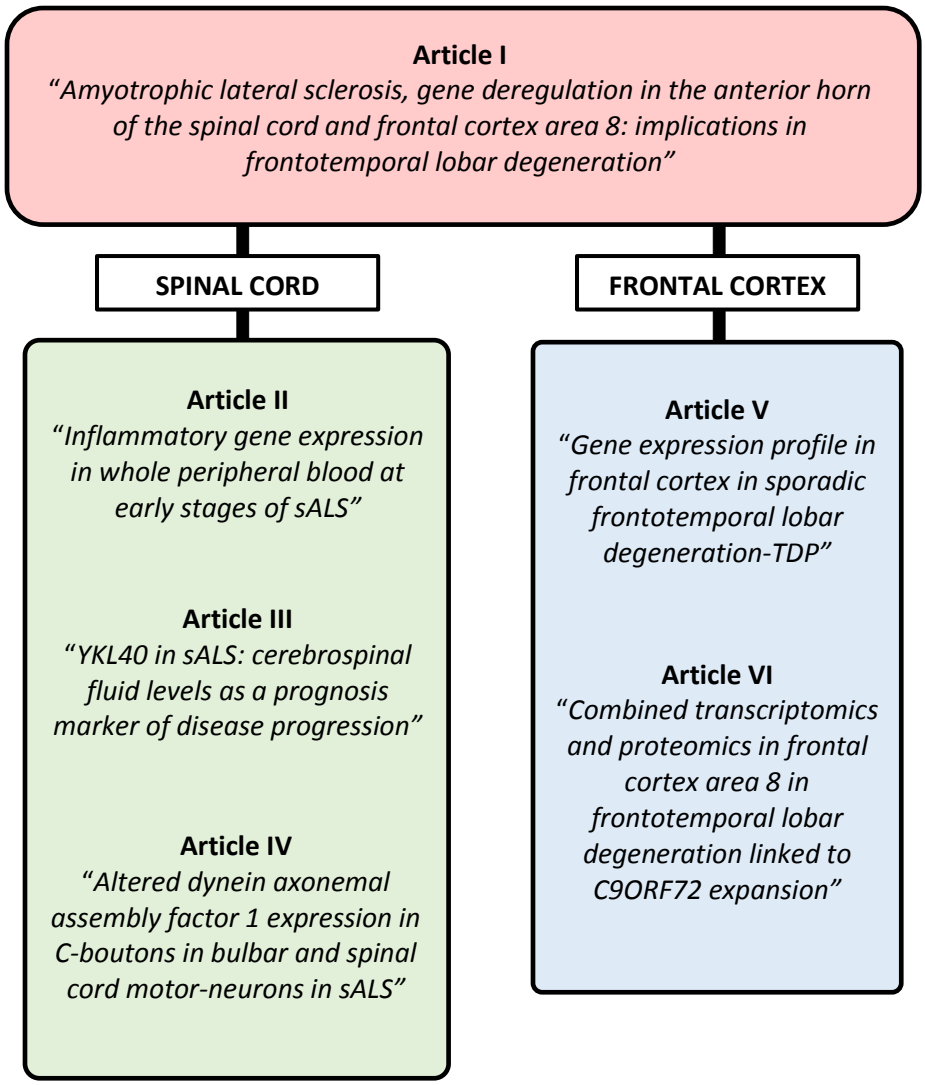

Figure 22. Flowchart showing the connections between the results included in the present thesis

4.1. Transcriptomic study of molecular alterations associated to ALS in spinal cord and frontal cortex area 8

As shown in Figure 22, the starting point of this thesis was the publication of the manuscript "*Amyotrophic lateral sclerosis, gene deregulation in the anterior horn of the spinal cord and frontal cortex area 8: implications in frontotemporal lobar degeneration*". In this study, we studied the whole-transcriptomic profiles of frontal cortex area 8 and the anterior horn of the spinal cord in sALS patients without cognitive impairment and concluded that transcriptomic profiles in sALS are region-dependent. Whole transcriptome arrays showed that major up-regulated clusters in the anterior horn were related with innate inflammatory and adaptative inflammatory responses; genes involved in homeostasis and ion transport formed a small up-regulated group. The major group of down-regulated genes in the anterior horn was linked to the neuronal cytoskeleton. In contrast, the majority of differentially up-regulated transcripts in sALS in frontal cortex area 8 were linked with neurotransmission, ion channels and ion transport, synapses, and axon and dendrite maintenance. Down-regulated genes in frontal cortex area 8 were linked to oligodendrocyte development and function, myelin regulation, and membrane lipid metabolism.

Altered gene expression was validated by RT-qPCR in 58 of 66 assessed genes. These observations extended the list of genes that are de-regulated in the anterior horn of the spinal cord, and they provided, for the first time, robust evidence of gene de-regulation in frontal cortex area 8 in sALS without cognitive impairment. Additionally, increased inflammatory response in the anterior horn and increased expression of selected neurotransmitter markers in frontal cortex were assessed using immunohistochemistry and western blotting, respectively.

Gene validations indicated up-regulation of several genes involved in inflammatory response in the anterior horn of the spinal cord in sALS. *AIF1* and *CD68* genes coding for reactive microglial proteins were highly up-regulated in this region. In addition, high levels of transcripts coding for Toll-like receptors (TLRs) expressed in glial cells (Arroyo *et al.*, 2011), whose activation, in turn, activates phagocytosis (Iribarren *et al.*, 2005; Chen *et al.*, 2006; Tahara *et al.*, 2006) and pro-inflammatory responses (Facci *et al.*, 2014), were up-regulated as well. Moreover, up-regulation of genes coding for pro-inflammatory effectors was found in the anterior horn of the spinal cord, involving interleukin-1B (*IL1B*), interleukin-10 (*IL10*), interleukin-10RA (*IL10RA*), interleukin-10RB (*IL10RB*), tumor necrosis factor alpha (*TNFA*), catepsin C and S, (*CTSC* and *CTSS*, respectively), major histocompatibility complex, class II, DR beta 1/5 (*HLA-DRB-1/5*), programmed cell death 1 ligand 2 (*PDCD1LG2*), interferon-gamma (*INFG*) and interleukin-33 (*IL33*), among others. This general view was in contrast with certain astrocitary markers, such as glial fibrillary acidic protein and voltage dependent anion channel, in which levels of mRNA were not modified. Moreover, *IL6* mRNA, which encodes one specific pro-inflammatory cytokine with regenerative and anti-inflammatory activities in particular settings (Simpson *et al.*, 1997; Locksley *et al.*, 2001; Schellera *et al.*, 2011; Pal *et al.*, 2014), was not modified.

Increased inflammatory response in the anterior horn of the spinal cord was further documented by immunohistochemistry, showing increased expression of IBA-1, CD68, HLADRB1 and HLA-DRB5 in reactive microglia. Reactive microglia had a round, amoeboid morphology and is localized, as expected, in the anterior horn, and the lateral and anterior pyramidal tracts. IL-10 and TNF-α were mainly localized in neurons of the spinal cord, and their expression was increased in remaining motor neurons of the spinal cord in sALS. In contrast, the different localization of microglial markers and IL-10 and TNF-α in neurons

pointed to a cross-talk between microglia and neurons in sALS. GFAP immunoreactivity was clearly increased in reactive astrocytes, as already reported in classical neuropathological studies.

In the anterior horn of the spinal cord, RTq-PCR results confirmed the reduced expression of axonemal genes identified in microarrays. The expression levels of genes coding for dynein heavy chain components and dynein assembly factors (DNAAF1) were down-regulated, thus suggesting impairment of motor ATPases involved in the transport of various cellular cargoes by 'walking' along cytoskeletal microtubules towards the minus-end of the microtubule (Asai and Brokaw, 1993; Chapelin *et al*., 1997; McKenney *et al*., 2014). However, mRNA levels of *NEFH*, which codes for neurofilament heavy polypeptide protein (Figlewicz *et al.*, 1994) and acts as a rail for this kind of transport, were preserved in ALS.

Regarding frontal cortex area 8, validations indicated up-regulation of neurotransmission-related genes and synaptic cleft genes. Genes involved in glutamatergic and GABAergic transmission were up-regulated in the frontal cortex in sALS. This applies to genes encoding the ionotropic glutamate receptor AMPA 1 (*GRIA1*), glutamate ionotropic receptor NMDA type subunit 2A (*GRIN2A*), the glutamate ionotropic receptor NMDA type subunit 2B (*GRIN2B*) and glutamate metabotropic receptor 5 (*GRM5*). Regarding the GABAergic system, *GAD1*, coding for glutamate decarboxylase 1, a rate-limiting enzyme that acts in the decarboxylation of glutamate essential for the conversion reaction of GABA from glutamate, was up-regulated, as were *GABRA1*, *GABRD* and *GABRB2*, which code for different subunits of ionotropic GABA-A receptors. *GABBR2,* that codes for the metabotropic receptor component gamma-aminobutyric acid type B receptor subunit 2 and forms

heterodimers with GABBR1, resulting in the formation of the G-protein coupled receptor for GABA, was also up-regulated (Burmakina *et al.*, 2014).

In line with increased expression of neurotransmitter-related genes, several genes encoding molecules linked to the synaptic cleft were also up-regulated in sALS, including:

- *BSN*: Bassoon, a pre-synaptic cytoskeletal matrix (PCM) protein acting as a scaffolding protein and essential for the regulation of neurotransmitter release in a subset of synapses (Hallermann *et al*., 2010; Davydova *et al*., 2014).
- *PCLO*: Piccolo protein, a component of the PCM assembled in the active zone of neurotransmitter release (Fenster *et al.,* 2000; Fenster and Garner, 2002).
- *FRMPD4*: PSD-95-interacting regulator of spine morphogenesis protein, which regulates dendritic spine morphogenesis and is required for the maintenance of excitatory synaptic transmission (Matosin *et al.*, 2016).
- *DDN* and *NRN1*: dendrin and neuritin 1 proteins, respectively, which are involved in the remodeling of the postsynaptic cytoskeleton and neuritic outgrowth (Naeve *et al.,* 1997; Kremerskothen *et al.,* 2006; Shimada *et al.,* 2016).

Moreover, de-regulation of neurotransmitters and receptors was further supported by the demonstration of a significant increase in the protein levels of GluR-1 and a tendency to increase in those of GABAAB2 in frontal cortex area 8 in sALS when compared with controls. It is worth stressing that only a few antibodies of the eight assessed were suitable for western blotting.

As an important regional difference related to neurotransmission and excitotoxicity, the expression of glutamate transporters was markedly different in the anterior horn of the spinal cord and frontal cortex area 8. *SLC1A2* and *SLC17A7* mRNA expression was significantly decreased in the anterior horn of the spinal cord, whereas *SLC1A2* was significantly increased in frontal cortex area 8. *SLC1A2* encodes the solute carrier family 1 member 2 or excitatory amino acid transporter 2 (EAAT2) which clears glutamate from the extracellular space at synapses in the central nervous system. Immunohistochemistry showed decreased SLC1A2 protein expression in the membrane of neurons and neuropil of the anterior horn in sALS. *SLC17A7* encodes the vesicular glutamate transporter 1 (VGLUT1) which is a vesicle-bound, sodium-dependent phosphate glutamate transporter expressed in the synaptic vesicles. Decreased expression of these proteins is linked to increased excitotoxity, which is postulated as a primary factor triggering motor neuron degeneration in sALS (Rothstein, 1995 and 2009).

Finally, the expression of several myelin-related genes and oligodendrocyte genes was down-regulated in frontal cortex area 8:

- *MYRF*: Myelin transcription factor regulates oligodendrocyte differentiation and is required for central nervous system myelination (Cahoy *et al.*, 2008; Emery *et al*., 2009; Koenning *et al*., 2012; Li *et al.*, 2013).
- *OLIG2*: The basic loop-helix protein OLIG2 mediates motor neuron and oligodendrocyte differentiation (Lederer *et al.*, 2007; Sun *et al*., 2011).
- *SOX10*: High mobility group protein SOX10 modulates myelin protein transcription (Leblanc *et al*., 2007; Li *et al.,* 2007).
- *NKX2.2*: NKX2.2 homeodomain transcription factor is a key regulator of oligodendrocyte differentiation (Zhu *et al.*, 2014).

- *TF*: Transferrin participates in the early stages of myelination (Connor, 1994; Erikson *et al.*, 1997).
- *PLP1*: Proteolipid protein 1 plays a role in the compaction, stabilization and maintenance of myelin sheaths, as well as in oligodendrocyte development and axonal survival (Diehl *et al*., 1986; Griffiths *et al*., 1998).
- *MBP*: Myelin basic protein is the second most abundant myelin-associated protein, constituting about 30% of the total myelin proteins (Marty *et al.,* 2002).
- *MOBP*: Myelin-associated oligodendrocyte basic protein constitutes the third most abundant protein in CNS myelin and acts by compacting and stabilizing myelin sheaths (Montague *et al.*, 2006).
- *MOG*: Myelin oligodendrocyte glycoprotein is a cell surface marker of oligodendrocyte maturation (Roth *et al.*, 1995).
- *MAG*: Myelin-associated glycoprotein is a type I membrane protein and member of the immunoglobulin superfamily involved in the process of myelination and certain myelin-neuron cell-cell interactions (Lossos *et al*., 2015).
- *MAL*: Mal T-cell differentiation protein is involved in myelin biogenesis (Kim *et al*., 1995).
- *CNP1*: 2',3'-cyclic nucleotide 3' phosphodiesterase participates in early oligodendrocyte differentiation and myelination (Kasama-Yoshida *et al*., 1997; Lappe-Siefke *et al*., 2003; Kursula, 2008).

RTq-PCR gene validation, western blotting and immunohistochemestry results further confirm genetic de-regulation and protein level alterations in studied regions.

4.2. Inflammatory alterations associated to ALS

Based on the data obtained in this first work, one block of the subsequent studies was oriented toward searching for novel molecular alterations and candidate biomarkers, taking into account the reported alterations in the inflammatory response pathways and axonal transport components in the anterior horn of the spinal cord. Concretely, the second work of this thesis, entitled "*Inflammatory gene expression in whole peripheral blood at early stages of sporadic amyotrophic lateral sclerosis*", was focused on the study of early inflammatory alterations in whole peripheral blood of sALS cases.

Inflammation involving microglial cells, macrophages, T cells, astrocytes and neurons, and mediated by a plethora of mediators of the immune response, occurs in the anterior horn of the spinal cord and, to a lesser extent, in other brain regions in ALS (Sta *et al*., 2011; McCombe and Henderson, 2011; Philips and Robberecht, 2011; Evans *et al*., 2013; Hooten *et al.*, 2015; Komine and Yamanaka, 2015; Puentes *et al.*, 2016; Liu and Wang, 2017; Article I). However, peripheral inflammatory responses are common, but poorly defined, in human neurodegenerative diseases. Several studies have focused on inflammatory responses in spinal cord and blood in sALS (Graves *et al*., 2004; Henkel *et al*., 2004; Shi *et al*., 2007; Casula *et al*., 2011; Sta *et al*., 2011; Rentzos *et al*., 2012; Johann *et al.*, 2015; Puentes *et al*., 2016; Article I). We aimed to gaining information about inflammatory gene expression profiles in whole blood in a series of sALS patients at the beginning of clinical symptoms and not treated with riluzole to avoid bias related to treatment.

Our observations complement data from previous studies and point to the activation of mechanisms facilitating extravasation of white blood cells (WBC) to target organs. Neutrophil recruitment was supported by increased

expression of leukocyte adhesion molecules, chemokines and cytokines (Ley, 2002; Nathan, 2006). Increased expression of *ITGB2* and a tendency of *ICAM1* to increase in blood suggest that adhesion and trans-endothelial migration of leukocytes were facilitated in sALS (Smith *et al.*, 1989; Lefort and ley, 2012; Hua, 2013). Selectin 1, encoded by *SELL*, participates in leukocytes' binding to endothelial cells and facilitates migration of WBC (Ley *et al.*, 2007; Marki *et al.*, 2015); *SELL* expression showed a tendency to increase in sALS. Increased expression of *MMP9* observed in sALS favors degradation of extracellular matrix components and facilitation of leukocyte migration. MMP9 is usually secreted in conjunction with TIMP-1, a specific inhibitor, which controls its proteolytic activity (Kurzepa *et al.*, 2014). A balance between MMP9 and TIMP-1 proteins regulates excessive tissue degradation in chronic inflammation (Amalinei *et al.*, 2010). In contrast, other effectors involved in cell extravasation were not modified in WBC of sALS. mRNA expression levels of cathepsins, also involved in extracellular matrix degradation (Fonović and Turk, 2014), were not modified in blood of ALS cases when compared with blood samples from controls. Expression levels of *CCL2* and *CCL3*, the products of which modulate monocyte attraction (Paavola *et al.*, 1998; Sanadgol *et al.*, 2016), were not modified in sALS. Finally, increased *INPP5D* mRNA expression favored a negative regulation of myeloid cell proliferation (Hakim *et al.*, 2012).

Regarding the state of lymphocyte cells, reduced expression of *CCR5*, *CCL5* and *CXCR5* supports reduced activation of B-cells (Le *et al.*, 2004). *CCL5* and *CCR5* encode T-cell chemo-attractant and regulatory molecules (Siveke and Hamann, 1998; Rabin *et al.*, 1999). The product of *CD2* expressed in T-cells modulates T-cell proliferation (The *et al.*, 1997), whereas the product of *TRBC1* is implicated in T-cell activation (MacLean and Gibson, 1997). Our observations showed decreased expression of *CD2*, coding for CD2 molecule, *TRBC1*, coding for T-cell receptor beta constant 1; in addition to decreased

expression of *CD8* mRNA, coding for CD8 molecule, and preserved *CD4* mRNA expression, coding for CD4 molecule; both T-cell markers as well. Reduced mRNA expression of these markers suggests inhibition of T-cell signaling. However, additional studies are needed to elucidate these discrepancies in larger series.

As to pro- and anti-inflammatory cytokines, results indicated down-regulation of these molecules in sALS. Toll-like receptors are involved in the initiation of the inflammatory process (Trinchieri and Sher, 2007). Reduced levels of *TLR3* accompanied by a tendency to increased *TLR4* and *TLR2* mRNA expression pointed to ambiguous activation signaling by Toll-like receptors. *TGFB2, IL10* and *IL6* mRNAs were down-regulated, and *IL10RA* and *TNFA* had tendency to decrease in blood in sALS when compared with controls. Expression levels of *IL10RB*, *TGFB1*, *IL1*β, *IL6ST*, *INFG* and *VEGFA* were not modified in sALS. Expression levels of assessed colony-stimulating receptors and *CSF3R* did not differ from control values. Only increased expression levels were reported in *TNFR1S* mRNA.

With the aim of assessing our results at a clinical level, correlation studies were performed. Positive correlation between *MMP9* and age, and negative correlation between age and *CCL5*, *CCR5*, and *TRBC1,* were observed in sALS but not in controls. No correlation was found between present observations and first clinical manifestation, gender and disease progression. Therefore, the present findings have little prognostic value. There was only positive correlation between *TNFA* mRNA expression and creatinin kinase (CK) levels. Although *TNFA* mRNA expression in blood was lower in sALS cases when compared with controls, higher *TNFA* mRNA values correlated with higher CK protein levels. This observation pointed to the possibility of a link between *TNFA* and muscular damage in sALS.

Previous studies showed that muscular pathology is accompanied by increased expression of systemic inflammatory markers (Lu *et al.*, 2016). Moreover, increased expression of inflammatory markers, including IL-1β and TNF-α, has been found in the skeletal muscle at symptomatic and end-stages of SOD1(G93A) transgenic mice (Van Dyke *et al.*, 2016). However, these individual data are not sufficient to allow us to advance any definitive conclusion. Transcriptome studies at early clinical stages in SOD1(G93A) transgenic mice in spinal cord, muscle and sciatic nerve have shown common deregulated pathways associated with T cell activation, two with macrophage activation and one pathway with genes involved in co-stimulatory regulation of the adaptive and innate immune systems; but blood did not show representation of these altered pathways (Lincecum *et al.*, 2010).

Thus, these results point to involvement of peripheral blood cells in the inflammatory response in the spinal cord in ALS. Present observations showed systemic inflammatory responses linked to extravasation of leukocytes and remodeling of extracellular matrix at early stages of sALS.

Following our interest on improve the knowledge about the involvement of inflammatory mechanisms in ALS pathogenesis, the third work presented in this thesis, entitled "*YKL40 in sporadic amyotrophic lateral sclerosis: cerebrospinal fluid levels as a prognosis marker of disease progression,*" was focused on studying the neuroinflammatory response in the central nervous system. Specifically, we evaluated the astrocitary molecule YKL40 in the anterior horn of the spinal cord and frontal cortex area 8 of sporadic ALS cases and its possible role as a disease biomarker.

Increased levels of selected inflammatory markers are found in blood and serum in ALS, suggesting systemic inflammatory responses which roughly

correlate with disease progression (Zhang *et al*., 2005; Shi *et al*., 2007; Cereda *et al*., 2008; Mantovani *et al*., 2009; Rentzos *et al*., 2012; Henkel *et al*., 2013; Sidaway, 2017; Zhao *et al*., 2017). All these observations strongly support a role for inflammation in the pathogenesis of sALS. However, the identification of a biomarker of inflammation with practical prognosis value has been limited because of individual variation and variations between methods and laboratories.

Previous studies of ALS showed YKL40 mRNA up-regulation in the motor cortex (Sanfilippo *et al.*, 2017) and increased YKL40 protein levels in the CSF correlating with disease progression (Illán-Gala *et al*., 2017; Thompson *et al*., 2018). Regarding brain tissue, our present observations showed significant YKL40 mRNA up-regulation in the anterior horn of the spinal cord and frontal cortex area 8, accompanied by significantly increased YKL40 protein levels in the frontal cortex and a tendency to increased YKL40 in the spinal cord in sALS. Importantly, YKL40 was expressed in astrocytes, in agreement with other observations (Bonneh-Barkay *et al*., 2010; Bonneh-Barkay *et al*., 2012; Wiley *et al*., 2015; Ferrer, 2017; Llorens *et al.*, 2017; Querol-Vilaseca *et al*., 2017), but in contrast to another description ascribing YKL40 expression to brain macrophages (Thompson *et al.*, 2018).

Up-regulation and increased YKL40 expression occcur in parallel with increased levels of microglia markers in the spinal cord but not in the frontal cortex area in sALS, and with increased GFAP protein levels in the spinal cord and frontal cortex but not with GFAP mRNA up-regulation in these regions.

Based on these findings, increased YKL40 protein levels in the CSF mirror YKL40 changes in the central nervous system, and they can be interpreted as the consequence of YKL40 delivery of astrocytes to the CSF. Unfortunately, no

analysis of a possible correlation between YKL40 brain and spinal cord values, or disease progression/survival, was feasible in the present series because of the lack of sufficient clinical data. However, YKL40 CSF values negatively correlated with patient survival, indicating that higher YKL40 in the CSF likely occurs in patients with rapid disease progression.

We do not know at this time what the functional implications of elevated YKL40 expression in ALS and other neurological diseases are. Nor do we know whether YKL40, even considering this particular chitinase as a marker of astrocyte inflammation, has beneficial or deleterious effects. In this line, chi3l1 KO mice have increased astrocytic responses (GFAP staining) and increased IBA1 microglial expression when compared with wild-type animals following traumatic brain injury, suggesting that YKL40 limits the extent of astroglial and microglial neuroinflammation (Wiley *et al*., 2015). If this is the case then increased YKL40 expression *per se* would not be dangerous but rather a manifestation of increased beneficial response in the face of a more aggressive facet of ALS in a subgroup of patients.

Previous studies showed increased levels of neurofilaments in the CSF of ALS cases (Oeckl *et al.*, 2016; Weydt *et al*., 2016; Steinacker *et al*., 2016; Feneberg *et al*., 2018). NF heavy chain levels in CSF are negatively correlated with disease duration and ALS-FRS-R slope, and NF-L light chain levels in CSF are negatively correlated with disease duration. Thus, NF heavy and light chain levels have potential use as markers of neural degeneration in ALS (Xu *et al*., 2016; Rossi *et al.*, 2018). Increased NF-L levels in the CSF are not specific for the disease, but they are more likely useful as measures of disease progression (Xu *et al*., 2016; Rossi *et al.*, 2018). In the present work, YKL40 levels in the CSF were assessed in parallel with levels of NF light chain. As expected, our results were in line with previous observations by other authors; NF-light chain levels

were significantly increased in ALS and levels negatively correlated with disease progression and ALS-FRS-R slope in our series.

Thus, the present findings in this third work reveal that YKL40 and NF-L levels in CSF constitute a valuable combination of biomarkers for improving accuracy in the prognosis of patients with sALS.

4.3. Alterations in axonal transport and dynein assembly in ALS

Finally, as to altered pathways in the anterior horn of the spinal cord of sALS post-mortem tissue, the fourth paper included in the present thesis, entitled "*Altered dynein axonemal assembly factor 1 expression in C-boutons in bulbar and spinal cord motor-neurons in sporadic amyotrophic lateral sclerosis,*" describes for the first time novel specific changes in dynein-mediated axonal transport mechanisms.

Neuronal retrograde transport, mediated by dyneins, is required to maintain homeostasis by removing aging proteins and organelles from the distal axon for degradation and recycling of components (Roberts *et al*., 2013; Maday *et al*., 2014). Dynein processing and localization varies in different cell types and clusters in distinct subcellular organelles (Vancoillie *et al.*, 2000; Chuang *et al*., 2001; Jha and Surrey, 2015; Twelvetrees *et al.*, 2016). In the central nervous system, dyneins are largely localized at the axon terminals (Twelvetrees *et al.*, 2016) and their assembly is modulated by a heterogeneous group of dynein axonemal assembly factor DNAAFs that act, in most instances, in combination with particular chaperones to promote cytoplasmic pre-assembly of dyneins (Omran *et al.*, 2008; Tarkar *et al.,* 2013; Inaba *et al*., 2016; Jaffe *et al*., 2016; Kott *et al.,* 2017; Mali *et al.*, 2018). Our study carefully examines the role of

DNAAF1 gene and the encoded protein, leucine-rich repeat-containing protein 50 (LRRC50), in motor-neurons and in the context of sALS.

In agreement with our previous gene transcription results (Article I), *DNAAF1* mRNA expression was reduced in the spinal cord anterior horn in sALS cases. Reduced *DNAAF1* mRNA expression can be the result of mere motor neuron demise. However, LRRC50 immunoreactivity was drastically reduced at the surface of the remaining spinal and bulbar motor neurons in parallel with reduced numbers of C-boutons in sALS. Our study identified the presence of LRRC50-immunoreactive boutons at the surface of motor neurons of the spinal cord and motor nuclei of the brain stem in humans and mice; these are identified as C-boutons on the basis of single immunohistochemistry, and double- and triple-labeling immunofluorescence and confocal microscopy. C-boutons are pre-synaptic terminals of cholinergic interneurons, which modulate motor neuron activity. They are localized in the spinal cord and in most of the motor nuclei of the cranial nerves excepting the oculomotor nuclei of the brainstem (Conradi, 1969; Hellstrom *et al.*, 1999; Miles *et al*., 2007; Frank, 2009; Zagoraiou *et al*., 2009; Gallart-Palau *et al*., 2014; Casanovas *et al*., 2017). They contain VAChT and synaptic vesicle markers, and are in contact with postsynaptic components including M2 muscarinic receptors and S1R; neuregulin 1-ErB retrograded signaling is also differentially compartmentalized in C-type boutons (Miles *et al*., 2007; Mavlyutov *et al*., 2010; Gallart-Palau *et al*., 2014; Casanovas *et al*., 2017). Therefore, LRRC50 reduction is not the mere reflection of motor neuron demise but a reduction in the number of LRRC50-immunoreactive boutons in the remaining motor neurons in sALS.

This decline occurs independently of the aberrant formation of TDP-43-immunoreactive inclusions in certain motor neurons in classical sALS (Strong

et al., 2011; Ince *et al.*, 2015). Nor does this decline correlate with the appearance of dynein-dynactin-immunoreactive deposits in motor neurons, which are neither related with skein-like inclusions, in the spinal cord in sALS (Ateh *et al.*, 2007). However, LRRC50 reduction in C-boutons was accompanied by perinuclear LRRC50 immunoreactivity in some remaining motor neurons, suggesting some kind of alteration in the transport of this protein.

Loss of cholinergic synapses in the spinal cord motor-neurons in sALS was reported many years ago (Nagao *et al*., 1998). This pioneering observation was partially refuted in SOD1 transgenic mice (Pullen and Athanasiou, 2009; Herron and Miles, 2012), due, in part, to different markers used to detect C-boutons in SOD1 transgenic mice. A significant increase in the number of VAChT-positive boutons is observed at the beginning of the symptomatic stage, which is followed by a marked decrease at the final stages of the disease. Our present observations showed a marked reduction in LRRC50-immunoreactive boutons in motor neurons of the ventral horn in *hSOD1-G93A* transgenic mice aged 150 days, which was accompanied by a parallel decrease in S1R-immunoreactive boutons. The presence of the remaining S1R seems to be protective of motor neurons, as the knocking-out of S1R in *hSOD1-G93A* transgenic mice exacerbates motor neuron disease progression (Casas *et al.*, 2013). Early pre-symptomatic alterations in C-boutons have also been reported in SOD1(G93A) transgenic mice (Mavlyutov *et al*., 2013).

Our combined study in human sALS not linked to SOD1 mutations and in transgenic mice bearing high copy numbers of the mutated form of human SOD1 showed common responses regarding C-boutons in motor neurons. The number of LRRC50-immunoreactive structures was decreased in motor neurons in both paradigms. To learn whether observed alterations in ALS are

early or late events, transgenic mice at pre-clinical, early clinical and late clinical stages were examined. A decrease in LRRC50 immunoreactivity occured at preclinical stages in hSOD1-G93A transgenic mice, suggesting that LRRC50 alteration is an early event in the course of the disease. Moreover, a trend to decrease was observed at the age of 120 days and a significant decrease was manifested at the age of 150 days.

Comparing, the pattern of C-bouton response in sALS and Tg mice differs from that seen after nerve peripheral nerve axotomy in mice. Reduced expression of VAChT and NRG1 immunoreactivity together with a reduction in size of C-boutons starting at 24 hours is followed by practical recovery by 30 days postlesion (Sumner, 1975; Casanovas *et al.*, 2017). Therefore, the changes observed here in motor neuron disease are hardly due to peripheral axotomy.

However, whether LRRC50 in motor neurons is essential for the maintenance of C-boutons cannot be addressed by neuropathological approach. Yet this is an important point for understanding the role of this protein in motor neuron maintenance and neurodegeneration.

4.4. Molecular alterations underlying cognitive impairment in frontotemporal lobar degeneration TDP-43

The second block of this thesis was focused on the study of molecular alterations in frontal cortex area 8 underlying sporadic and familial forms of FTLD-TDP pathology, and their comparison with those observed in frontal cortex area 8 of sALS. The first study included in this block is entitled "*Gene expression profile in frontal cortex in sporadic frontotemporal lobar degeneration-TDP.*"

This manuscript was based on whole-transcriptome microarray hybridization and showed down-regulation of several genes in frontal cortex area 8 in sFTLD-TDP clustered in pathways involved in neurotransmission and synapsis, neuronal architecture, cytoskeleton of axons and dendrites, vesicle trafficking, purine metabolism, mitochondria and energy metabolism. 111 selected genes from predicted altered pathways based on Gene Ontology (GO) database were validated by RT-qPCR. The expression of 81 genes was significantly deregulated in this cortical region in sFTLD-TDP when compared with controls. From those, 24 coded proteins were analyzed with western blotting and 8 of them resulted altered in sFTLD-TDP. Our results demonstrated that neurotransmission is markedly affected in sFTLD-TDP since several of the down-regulated genes were related to glutamate decarboxylase, several types and subunits of ionotropic and metabotropic glutamate and GABA receptors, neuronal vesicular and soluble glutamate transporters, and various synaptic proteins, together with loss of calbindin expression. This provides robust support to preliminary morphological observations using the Golgi method and calbindin immunohistochemistry showing decreased numbers, amputation, and proximal swellings of dendritic branches and loss of synaptic spine pyramidal cells, and loss of calbindin-immunoreactive neurons with atrophy of remaining neurons in layers II and III of the frontal cortex in FTLD (Ferrer, 1992). Protein expression studies showing decreased levels of synaptic markers are also in line with previous observations demonstrating reduced levels of several synaptic and presynaptic plasma membrane proteins in the frontal cortex, but not in the posterior parietal cortex assessed in parallel, in FTLD (Ferrer, 1999).

In contrast to the marked decrease in the expression of cytoskeletal and synaptic markers, tau mRNA and protein levels were preserved in the present series, and tau phosphorylation was not increased in sFTLD-TDP. This is in

contrast with early reports pointing to decreased tau protein levels in FTLD with ubiquitin inclusions (presumably FTLD-TDP), which suggested that FTLD-U could be a novel 'inverse' tauopathy because of the reduced levels of tau (Zhukareva *et al*., 2001; Zhukareva *et al*., 2003). Reduced tau mRNA and protein levels have been reported in FTLD-TDP linked to GRN mutations but not in other FTLD-TDP subtypes such as sporadic FTLD-TDP and FTLD-TDP-C9ORF72 (Papegaey *et al*., 2016).

Mitochondrial alterations compromise mRNA expression of several subunits of the mitochondrial complexes. Moreover, they were accompanied by altered protein expression of several subunits and with reduced activity of complexes I, IV, and V in sFTLD-TDP. Importantly, in addition to mitochondrial subunits encoded by genomic DNA, expression levels of MT-CO1 encoded by mitochondrial DNA were reduced in sFTLD-TDP. Therefore, mitochondrial alterations in sFTLD-TDP have both genomic and mitochondrial components. Other genes involved in energy metabolism were down-regulated as well, indicating functional energy metabolism failure in sFTLD-TDP. Gene-specific mitochondrial dysfunction has been described in human fibroblasts bearing mutations in TARDBP and C9ORF72 (Onesto *et al.*, 2016). Mitochondrial dysfunction has also been documented in a transgenic knock-in mouse model for TDP-43 (Stribl *et al*., 2014). Therefore, mitochondrial alterations seem to be common to different forms of sFTLD-TDP and fFTLD-TDP.

Purines and pyrimidines are components of a large number of key molecules. The primary purines adenine and guanosine, and pyrimidines cytosine, thymidine, and uracyl, are the core of DNA, RNA, nucleosides, and nucleotides involved in energy transfer (ATP, GTP) and coenzymes (NADH, FADH2) (Ipata *et al.*, 2011; Ansoleaga *et al.*, 2015). Alterations in the expression of genes encoding enzymes of purine metabolism may interfere with numerous

metabolic processes in sFTLD-TDP. It can be argued that differences in the percentage of neurons, astrocytes, oligodendroglia and microglia lie beyond distinct patterns of gene expression, protein levels, and mitochondrial enzymatic activities in sFTLD-TDP. Certainly, neuron loss, spongiosis in the upper cortical layers and variable astrocytic gliosis are typical morphological alterations in sFTLD-TDP (Hortobagyi *et al.,* 2015; Lashley *et al*., 2015; Mann and Snowden, 2017). Present findings complement morphological observations with biochemical data that identify damage of particular components of vital molecular pathways and essential modulators of synaptic transmission.

Comparison of the present findings with our previous observations in frontal cortex area 8 in sALS using the same methods shows that most down-regulated genes in sFTLD-TDP are up-regulated in frontal cortex area 8 in sALS cases without dementia (Article I). This suggests a primary response linked to synaptic and neurotransmission disturbances in frontal cortex area 8 at preclinical stages of frontal degeneration in sALS (sALS cases without apparent cognitive impairment), which may decay with disease progression and dementia in FTLD-TDP. Reduced expression of genes encoding actin, actin-related members, kinesin and microtubule-associated protein further suggest cytoskeletal damage in sALS and sFTLD-TDP.

Finally, the last part of the second block of this thesis was focused on the study entitled "*Combined transcriptomics and proteomics in frontal cortex area 8 in frontotemporal lobar degeneration linked to C9ORF72 expansion,*" in which mRNA and protein expression in frontal cortex area 8 was analyzed in fFTLD-TDP cases linked to *C9ORF72* expansion (c9FTLD).

This study revealed altered gene transcription related to DNA recombination, RNA splicing regulation, RNA polymerase transcription, myelin synthesis, calcium regulation and ubiquitin-proteasome system in c9FTLD. Proteomics performed in the same tissue samples identified altered protein expression linked to apoptosis, inflammation, metabolism of amino acids, metabolism of carbohydrates, metabolism of membrane lipid derivatives, microtubule dynamics, morphology of mitochondria, neuritogenesis, neurotransmission, phagocytosis, receptor-mediated endocytosis, synthesis of ROS, and calcium signaling in c9FTLD.

Genes and proteins did not match in the two lists of deregulated mRNAs and proteins in c9FTLD. However, a protein interactome map constructed using the IPA software showed deregulation of cross-linkers between DNA/RNA regulation systems and ubiquitin-proteasome systems, suggesting an imbalance in cellular transcription processes and protein degradation mechanisms, which makes sense in light of gene transcription observations of the main contributors to the pathogenesis of neurodegenerative diseases with abnormal protein aggregates. This is in line with the function of TDP-43 and C9orf72. Together, this combined transcriptomics-proteomics analysis supported the list of separately reported altered pathways linked to *C9orf72* mutations, including those involved in DNA recombination and transcription, RNA splicing, endoplasmic reticulum and mitochondria, synaptic transmission, protein degradation, calcium homeostasis, and inflammation (Kaus and Sareen, 2015; Dafinca *et al.*, 2016; Budini *et al.*, 2017; Gao *et al.*, 2017; Palluzzi *et al.*, 2017; Frick *et al.*, 2018; Hermann and Parlato, 2018; Lau *et al.*, 2018; Evans and Holzbaur, 2019). Additional alterations involved altered metabolism of amino acids and carbohydrates, membrane lipid derivatives, and microtubule dynamics, and synthesis of reactive oxygen species. Links between oxidative and endoplasmic reticulum stress, TDP-43, oxidative stress

damage and docosahexaenoic acid have previously been reported in the spinal cord in ALS, and in frontal cortex in FTLD-TDP (Ilieva *et al.*, 2007; Martinez *et al.*, 2008; Ayala *et al.*, 2011a).

Regarding TDP-43 and C9orf72, major pathologic components in c9FTLD, TARDBP mRNA expression was preserved but total TDP-43 protein showed increased levels in c9FTLD when compared with controls. This is in accordance with the abnormal deposition of this protein in intracellular inclusions and threads characteristic of this disease. In contrast, *C9orf72* mRNA expression was significantly decreased in c9FTLD. However, the C9orf72 long isoform was significantly reduced and the C9orf72 short isoform significantly increased in c9FTLD. Reduced C9ORF72 protein levels were found in previous reports (Belzil *et al*., 2013a; Ciura *et al.*, 2013; Xi *et al.*, 2013; Waite *et al.*, 2014). The functional implications of the reduced levels of the long C9orf72 isoform are not known, but quantitative mass spectrometry-based proteomics used to identify interacting proteins in motor neurons has shown that the long isoform complex stabilizes SMCR8, a protein which acts as an autophagic regulator (Jung and Behrends, 2017; Zhang *et al*., 2018). Therefore, reduced levels of the long isoform may interfere with normal autophagy and lysosomal processing (Zhang *et al*., 2018). C9orf72 also binds to several proteins including members of the Rab family, endoplasmic reticulum and synapses; nuclear and cytoplasmic transport, endoplasmic reticulum stress and altered synaptic function have all been reported in association with pathogenic C9ORF72 expansions (May *et al*., 2014; Zhang *et al*., 2014; Freibaum *et al*., 2015; Jovicic *et al*., 2015; Gao *et al*., 2017; Frick *et al.*, 2018; Vatsavayai *et al.*, 2019).

An interesting deregulated cluster is composed of genes linked to several miRNAs, nuclear RNAs and long non-coding RNAs, including *MIR4740*, the

small nucleolar RNA (*SCARNA2*), and long noncoding RNAs such as X-inactive specific transcript (*XIST*) and the long intergenic non-coding RNAs *LINC1476*, *LINC1140*, and *LINC00499*. miRNAS participate in a large number of variegated processes including mRNA silencing and regulation of gene transcription (Ambros, 2004; Bartel, 2004). SCARNA2 localizes to Cajal bodies, the process of binding of its box C/D being modulated by coilin (Enwerem *et al*., 2015). Long intergenic non-coding RNAs are mainly localized in the nucleus where they modulate chromatin and genome architecture, in addition to RNA stabilization and transcription regulation (Ransohoff *et al.*, 2018). XIST is localized in the X-chromosome and participates in the inactivation of chromosome X (Chow *et al*., 2005). The consequences of XIST deregulation in C9orf72 remain elusive.

Our studies using a similar transcriptomics approach in frontal cortex area 8 in sFTLD-TDP have shown down-deregulation of genes linked to neurotransmission and synapses, neuronal architecture, cytoskeleton of axons and dendrites, vesicle trafficking, purines, mitochondria, and energy metabolism. Additional protein and enzymatic studies have revealed altered mitochondrial function and oxidative phosphorylation. Using the same methods, we observed up-regulated gene clusters in frontal cortex area 8 in sALS involving neurotransmission, synaptic proteins, and vesicle trafficking, and down-regulated genes clustering into oligodendrocyte function and myelin-related proteins. Curiously, some down-regulated clusters related mainly to synapses and neurotransmission in frontal cortex in sFTLD-TDP were up-regulated in frontal cortex in sALS without dementia. The present observations in c9FTLD reveal some commonalities with sFTLD-TDP in altered clusters but not in particular genes. Down-regulation of genes linked to oligodendrocytes and myelin in frontal cortex area 8 is shared in c9FTLD and sALS.

Recent studies have shown oligodendrocytes as key players in neurodegenerative diseases with abnormal protein aggregates (Ferrer, 2018). Oligodendrogliopathy is common in sALS and FTLD-TDP. Phosphorylated-TDP-43-immunoreactive oligodendroglial inclusions are found in, in addition to spinal cord motor neurons, the motor, sensory and premotor cortex, but not the corpus callosum, cingulum or lateral tracts of the spinal cord (Neumann *et al.*, 2007). TDP-43 oligodendroglial inclusions are common in the deep layers of the cerebral cortex and white matter in FTLD-TDP (Fatima *et al.*, 2015). The functional effects of oligodendroglial TDP43 inclusions are not known, but present findings indicate altered oligodendroglial gene expression in the frontal cortex in c9FTLD. Particular features are linked to C9orf72 hexanucleotide repeat expansion (Bigio, 2011, 2012), and TDP-43-dependent or TDP43-independent oligodendroglial dysfunction might be a characteristic trait linked to C9orf72 hexanucleotide repeat expansion. In contrast, although astrocytes play key pathogenic roles in ALS (Ferrer, 2017), TDP-43-immunoreactive inclusions are rare in sALS and FTLD-TDP (Kovacs *et al.*, 2017).

Comparisons with other studies performed in different types of FTLD-TDP showed disparate results. One gene expression analysis in fFTLD linked to GRN mutations identified abnormal regulated processes associated with lipid metabolism, MAPK signaling pathway, and transport (Chen-Plotkin *et al.*, 2008), while lysosomal dysfunction was identified in another (Evers *et al.*, 2017). Another study recognized synapse-, cytoskeletal/filament-, microtubule/axon-, and proteasome-related pathways in FTLD-TDP when compared with controls, and cytoskeletal protein-, mitochondria/energy-, synapse-, microtubule/axon-, and ubiquitin-proteasome-associated deregulation when comparing FTLD-TDP with FTLD associated with motor neuron disease (Mishra *et al.*, 2007). Common mechanisms occur within the

FTLD-ALS spectrum (Conlon *et al.*, 2018). However, weighted co-expression network proteomic analysis has recently revealed 15 modules of co-expressed proteins, eight of which differed significantly across the ALS-FTD disease spectrum. Interestingly, a module enriched with astrocyte and microglia proteins was significantly increased in the frontal cortex in ALS cases carrying the C9orf72 mutation compared to sporadic ALS cases, suggesting that the genetic expansion is associated with inflammation in the brain (Umoh *et al.*, 2018). Increased levels of proteins linked to inflammation were also identified in the frontal cortex in C9orf72 in our study.

The present dual 'omics' approach, like the majority of molecular studies carried out in the *post-mortem* human brain, is based on the relative abundance of particular mRNAs and proteins or ratios of two absolute concentrations (fold-change) representing concentrations relative to reference samples. Moreover, the agonal state and postmortem delay may differentially interfere with transcription and protein synthesis/degradation. Therefore, when analyzing postmortem brain samples, a non-steady-state condition is always the real scenario. This statement is important when assessing transcripts and proteins separately, but it is especially critical when analyzing RNA and protein correlations of particular genes in human postmortem brain (Marguerat *et al.*, 2012; Vogel and Marcotte, 2012; Liu *et al.*, 2016).

Moreover, distinct cell populations are usually mingled, and rates and scales of RNA and corresponding encoded proteins may be cell type-dependent. These facts, together with particular characteristics of samples, and differences in the procedures and methods, may account for the non-homogeneous results in different laboratories. Although the original samples are the same in the present series, and the identified altered pathways are

similar and complementary using a combination of transcriptomics and proteomics, it is worth stressing that different RNAs and proteins were identified by these methods. Combined nontargeted '-omics' seems to be a valuable approach to deciphering altered molecular pathways in FTLD provided that observations are viewed cautiously when assessing human postmortem brain samples.


B
F
E
G
g
D

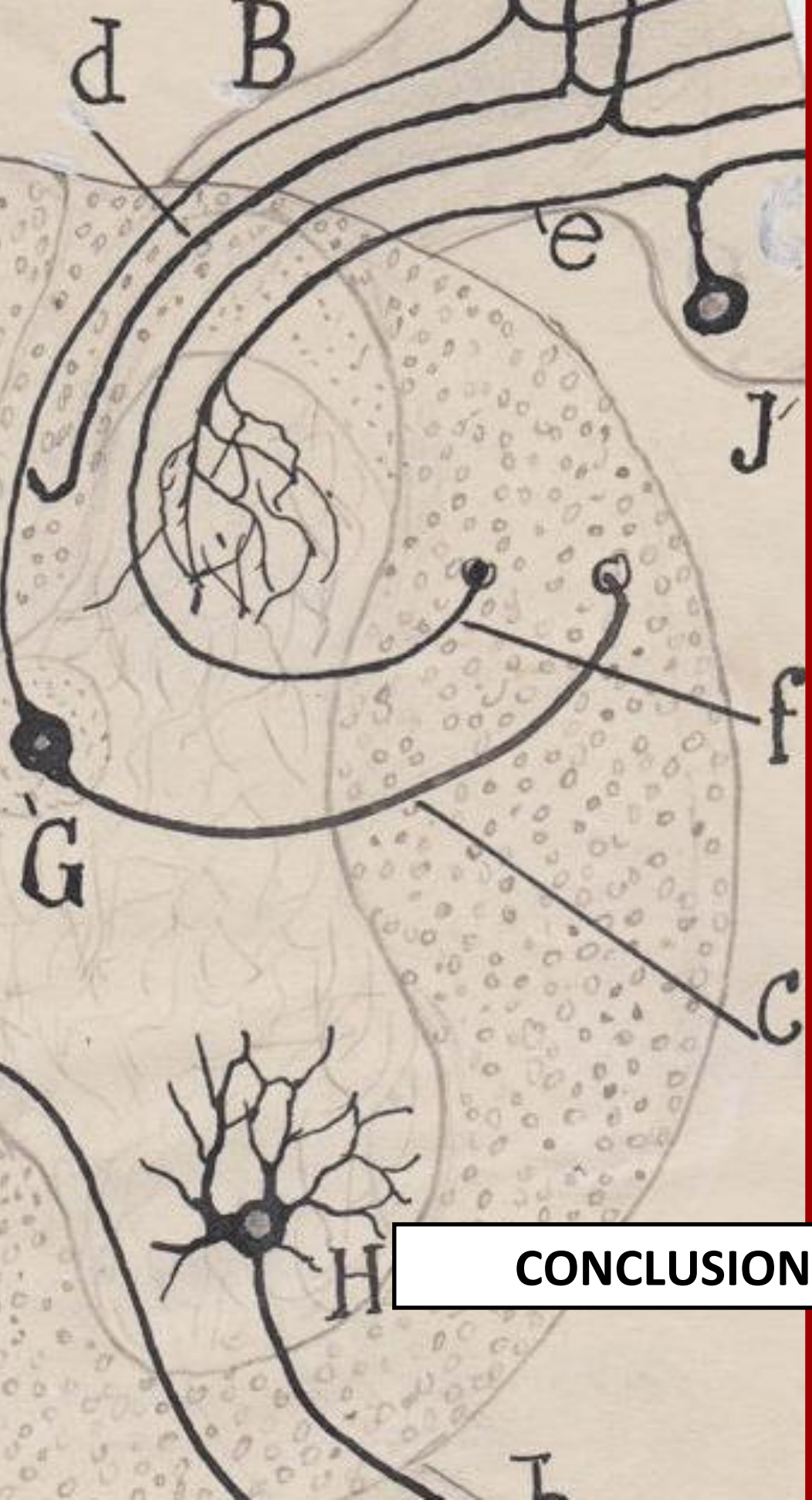

CONCLUSIONS

5. Conclusions

I. Altered regulation of transcription is observed in sALS in a region-dependent manner in frontal cortex area 8 and the anterior horn of the spinal cord in the same cases.

II. The expression of synaptic and neurotransmission related genes is up-regulated, whereas myelin and lipid related genes are down-regulated in frontal cortex area 8 in sALS cases without apparent cognitive impairment. In contrast, in the spinal cord, most up-regulated genes belong to inflammatory response, whereas the main down-regulated genes are involved in axonal transport.

III. Alterations in the regulation of transcription related to synapses and neurotransmission in frontal cortex area 8 in the absence of overt clinical symptoms of cognitive impairment are particularly important to identify early molecular alterations in frontal cortex within the spectrum of ALS/FTLD-TDP.

IV. Inflammatory markers analysis in peripheral whole-blood shows a complex scenario at early clinical stages of sALS, including, on the one hand, up-regulation of genes whose products are involved in leukocyte extravasation and extracellular matrix remodeling, and, on the other, down-regulation of chemokines, anti- and pro-inflammatory cytokines, and lymphocyte modulators.

V. Increased YKL40 levels in the CSF are not disease-specific but are a good biomarker of sALS progression. Co-detection of YKL40 and NF-L levels in CSF offers a valuable combination of biomarkers for

improving accuracy in determining the prognosis of patients with sALS.

VI. LRRC50 is described for the first time in motor-neurons and is a component of C-boutons involved in dynein assembly and retrograde axonal transport.

VII. LRRC50-immunoreactive boutons are reduced in the remaining motor neurons in the anterior horn of the spinal cord, and motor nuclei of the vagus and hippoglossus nerves in sALS. Interestingly, oculomotor nuclei of the brainstem, which are not affected in sALS, do not have LRRC50-positive boutons.

VIII. Transgenic mice bearing high copy numbers of the mutated form of human SOD1 show decreased numbers of LRRC50-immunoreactive boutons at early, preclinical stages of the disease, highlighting decreased LRRC50-immunoreactive structures as an early event in ALS pathogenesis.

IX. Marked decrease in the expression of genes coding for cytoskeletal and neurotransmission components is found in sFTLD-TDP. In contrast, tau mRNA and protein levels are preserved, and tau phosphorylation is not increased in sFTLD-TDP.

X. Impairment of mitochondrial activity affecting several mitochondrial complexes, as well as down-regulation of selected genes and reduced proteins implicated in mitochondrial function and energy metabolism, occurs in the frontal cortex of sFTLD-TDP.

XI. Comparing results in frontal cortex area 8 in sALS and sFTLD-TDP, most down-regulated genes in sFTLD-TDP are up-regulated in frontal cortex area 8 in sALS cases without dementia. This suggests a primary response to synaptic and neurotransmission disturbances in frontal cortex area 8 at preclinical stages of frontal degeneration in sALS which decays with disease progression and dementia.

XII. c9FTLD transcriptomic study in frontal cortex area 8 reveals altered gene transcription related to DNA/RNA mechanisms, myelin synthesis, calcium regulation and ubiquitin-proteasome system.

XIII. c9FTLD proteomics performed in the same tissue samples identifies altered protein expression linked to apoptosis, inflammation, synaptic structure and function, morphology of mitochondria, endocytosis mechanisms and synthesis of ROS.

XIV. Down-regulated clusters related mainly to synapses and neurotransmission in frontal cortex in sFTLD-TDP are up-regulated in frontal cortex in sALS without dementia. c9FTLD reveal some commonalities within the spectrum of sFTLD-TDP in altered clusters but not in specific genes. Additionally, down-regulation of genes linked to oligodendrocytes and myelin in frontal cortex area 8 is shared in c9FTLD and sALS.


C
B

REFERENCES

References

Abbott NJ, Ronnback L, Hansson E. (**2006**). Astrocyte-endothelial interactions at the blood-brain barrier. *Nat Rev Neurosci*. Jan; 7(1): 41-53.

Abe K, Itoyama Y, Sobue G, Tsuji S, Aoki M, Doyu M, et al. (**2014**). Confirmatory double-blind, parallel-group, placebo-controlled study of efficacy and safety of edaravone (MCI-186) in amyotrophic lateral sclerosis patients. *Amyotroph. Lateral Scler. Frontotemporal Degener*. 15: 610–617.

Abhinav K, Stanton B, Johnston C, Hardstaff J, Orrell RW, Howard R, Clarke J, Sakel M, Ampong MA, Shaw CE, Leigh PN, Al-Chalabi A. (**2007**). Amyotrophic lateral sclerosis in South-East England: a population-based study. The South-East England register for amyotrophic lateral sclerosis (SEALS Registry). *Neuroepidemiology*. 29(1-2):44-8.

Afifi AK, Aleu FP, Goodgold J, MacKay B. (**1966**). Ultrastructure of atrophic muscle in amyotrophic lateral sclerosis. *Neurology*. May; 16(5):475-81.

Ahmed Z, Mackenzie IR, Hutton ML, Dickson DW. (**2007**). Progranulin in frontotemporal lobar degeneration and neuroinflammation. *J Neuroinflammation*. Feb 11; 4: 7.

Al-Chalabi, Hardiman O, Kiernan MC, Chiò A, Rix-Brooks B, Van den Berg LH. (**2016**) Amyotrophic lateral sclerosis: moving towards a new classification system. *Lancet Neurol.* Oct; 15(11): 1182-94.

Al-Chalabi A, Jones A, Troakes C, King A, Al-Sarraj S, Van den Berg LH. (**2012**). The genetics and neuropathology of amyotrophic lateral sclerosis. *Acta Neuropathol*. Sep; 124(3): 339-52.

ALS CNTF Treatment Study Group. (**1995**). A phase I study of recombinant human ciliary neurotrophic factor (rHCNTF) in patients with amyotrophic lateral sclerosis. The ALS CNTF Treatment Study (ACTS) Phase I-II Study Group. *Clin. Neuropharmacol.* 18: 515–532.

ALS CNTF Treatment Study Group (**1996**). A double-blind placebo-controlled clinical trial of subcutaneous recombinant human ciliary neurotrophic factor (rHCNTF) in amyotrophic lateral sclerosis. *Neurology* 46: 1244–1244.

Alves-Rodrigues A, Gregori L, Figueiredo-Pereira ME. (**1998**). Ubiquitin, cellular inclusions and their role in neurodegeneration. *Trends Neurosci*. Dec; 21(12): 516-20.

Amalinei C, Caruntu ID, Giuşca SE, Balan RA. (**2010**). Matrix metalloproteinases involvement in pathologic conditions. *Rom J Morphol Embryol*. 51: 215–28.

Ambros V, Bartel B, Bartel DP, Burge CB, Carrington JC, Chen X, Dreyfuss G, Eddy SR, Griffiths-Jones S, Marshall M, Matzke M, Ruvkun G, Tuschl T. (**2003**). A uniform system for microRNA annotation. *RNA-Publ. RNA Soc*. Mar; 9(3): 277-9.

Ambros V. (**2004**). The functions of animal microRNAs. *Nature* 431: 350-355.

Amick J. and Ferguson SM. (**2017**). C9orf72: At the intersection of lysosome cell biology and neurodegenerative disease. *Traffic*. May; 18(5): 267-276.

Anderson P. and Ivanov, P. (**2014**). tRNA fragments in human health and disease. *FEBS Lett*. 2014 Nov 28; 588(23): 4297-304.

Ansoleaga B, Jove M, Schluter A, et al. (**2015**). Deregulation of purine metabolism in Alzheimer's disease. *Neurobiol Aging* 36: 68–80.

Appel SH, Zhao W, Beers DR, Henkel JS. (**2011**). The microglial-motoneuron dialogue in ALS. *Acta Myol.* 2011 Jun; 30(1): 4-8.

Arancibia-Carcamo L. and Attwell D. (**2014**). The node of Ranvier in CNS pathology. *Acta Neuropathol*. Aug; 128(2): 161-75.

Araque A, Carmignoto G, Haydon PG. (**2001**). Dynamic signaling between astrocytes and neurons. *Annu Rev Physiol*. 63: 795–813.

Araque A. (**2008**). Astrocytes process synaptic information. *Neuron Glia Biol.* Feb; 4(1): 3-10.

Arias E. and Cuervo AM. (**2011**). Chaperone-mediated autophagy in protein quality control. *Curr. Opin. Cell Biol*. Apr; 23(2): 184-9.

Armon C. (**2018**). ALS 1996 and Beyond: New Hopes and Challenges. A manual for patients, families and friends. Fourth Edition. Loma Linda, CA, USA. *LLU Department of Neurology*

Arroyo DS, Soria JA, Gaviglio EA, Rodriguez-Galan MC, Iribarren P. (**2011**). Toll-like receptors are key players in neurodegeneration. *Int Immunopharmacol*. 2011; 11:1415–21.

Asai DJ. and Brokaw CJ. (**1993**). Dynein heavy chain isoforms and axonemal motility. *Trends Cell Biol*. 3: 398–402.

Ash PE, Bieniek KF, Gendron TF, Caulfield T, Lin WL, Dejesus-Hernandez M, van Blitterswijk MM, Jansen-West K, Paul JW 3rd, Rademakers R, Boylan KB, Dickson DW, Petrucelli L. (**2013**) Unconventional translation of C9ORF72 GGGGCC expansion generates insoluble polypeptides specific to c9FTD/ALS. 2013. *Neuron*. Feb 20; 77(4): 639-46.

Aswathy PM, Jairani PS, Mathuranath PS. (**2010**). Genetics of frontotemporal lobar degeneration. *Annals of Indian Academy of Neurology*, 13 (Suppl 2): S55–S62.

Atanasio A, Decman V, White D, Ramos M, Ikiz B, Lee HC, Siao CJ, Brydges S, LaRosa E, Bai Y, Fury W, Burfeind P, Zamfirova R, Warshaw G, Orengo J, Oyejide A, Fralish M, Auerbach W, Poueymirou W, Freudenberg J, Gong G, Zambrowicz B, Valenzuela D, Yancopoulos G, Murphy A, Thurston G, Lai KM. (**2016**). C9orf72 ablation causes immune dysregulation characterized by leukocyte expansion, autoantibody production, and glomerulonephropathy in mice. *Sci. Rep*. 6: 23204.

Ateh DD, Hussain IK, Mustafa AH, et al. (**2007**). Dynein-dynactin complex subunits are differentially localized in brain and spinal cord, with selective involvement in pathological features of neurodegenerative disease. *Neuropathol Appl Neurobiol* 34: 88–94.

Atkin JD, Farg MA, Turner BJ, Tomas D, Lysaght JA, Nunan J, Rembach A, Nagley P, Beart PM, Cheema SS, Horne MK. (**2006**). Induction of the unfolded protein response in familial amyotrophic lateral sclerosis and association of protein-disulfide isomerase with superoxide dismutase 1. *J Biol Chem*. Oct 6; 281(40): 30152-65.

Atsumi T. (**1981**). The ultrastructure of intramuscular nerves in amyotrophic lateral sclerosis. *Acta Neuropathol*. 55(3): 193-8.

Ayala V, Granado-Serrano AB, Cacabelos D, Naudi A, Ilieva EV, Boada J, Caraballo-Miralles V, Llado J, Ferrer I, Pamplona R, Portero-Otin M. (**2011a**). Cell stress induces TDP-43 pathological changes associated with ERK1/2 dysfunction: Implications in ALS. *Acta Neuropathol* 122: 259-270.

Ayala YM, De Conti L, Avendaño-Vázquez SE, Dhir A, Romano M, D'Ambrogio A, Tollervey J, Ule J, Baralle M, Buratti E, Baralle FE. (**2011b**). TDP-43 regulates its mRNA levels through a negative feedback loop. *EMBO J*. Jan 19; 30(2):277-88.

Ayala YM, Zago P, D'Ambrogio A, Xu YF, Petrucelli L, Buratti E, Baralle FE. (**2008**). Structural determinants of the cellular localization and shuttling of TDP-43. *J Cell Sci*. Nov 15; 121(Pt 22): 3778-85.

Babst M, Katzmann DJ, Estepa-Sabal EJ, Meerloo T, Emr SD. (**2002**). Escrt-III: an endosome-associated heterooligomeric protein complex required for mvb sorting. *Dev Cell*. Aug; 3(2): 271-82.

Bachoo RM, Kim RS, Ligon KL, Maher EA, Brennan C, Billings N, Chan S, Li C, Rowitch DH, Wong WH, DePinho RA. (**2004**). Molecular diversity of astrocytes with implications for neurological disorders. *Proc Natl Acad Sci USA*. Jun 1; 101(22): 8384-9.

Baker M, Mackenzie IR, Pickering-Brown SM, Gass J, Rademakers R, Lindholm C, Snowden J, Adamson J, Sadovnick AD, Rollinson S, Cannon A, Dwosh E, Neary D, Melquist S, Richardson A, Dickson D, Berger Z, Eriksen J, Robinson T, Zehr C, Dickey CA, Crook R, McGowan E, Mann D, Boeve B, Feldman H, Hutton M. (**2006**). Mutations in progranulin cause tau-negative frontotemporal dementia linked to chromosome 17. *Nature*. Aug 24; 442 (7105): 916-9.

Balendra R. and Isaacs AM. (**2018**). C9orf72-mediated ALS and FTD: multiple pathways to disease. *Nat Rev Neurol*. Sep; 14(9): 544–558.

Balsa E, Marco R, Perales-Clemente E, Szklarczyk R, Calvo E, Landázuri MO, Enríquez JA. (**2012**). NDUFA4 is a subunit of complex IV of the mammalian electron transport chain. *Cell Metab*. Sep 5; 16(3): 378-86.

Bang J, Spina S, Miller BL. (**2015**). Frontotemporal dementia. *Lancet*. Oct 24; 386(10004): 1672-82.

Bannwarth S, Ait-El-Mkadem S, Chaussenot A, Genin EC, Lacas-Gervais S, Fragaki K, Berg-Alonso L, Kageyama Y, Serre V, Moore DG, Verschueren A, Rouzier C, Le Ber I, Augé G, Cochaud C, Lespinasse F, N'Guyen K, de Septenville A, Brice A, Yu-Wai-Man P, Sesaki H, Pouget J, Paquis-Flucklinger V. (**2014**). A mitochondrial origin for frontotemporal dementia and amyotrophic lateral sclerosis through CHCHD10 involvement. *Brain*. Aug; 137(Pt 8): 2329-45..

Barber SC, Mead RJ, Shaw PJ. (**2006**). Oxidative stress in ALS: a mechanism of neurodegeneration and a therapeutic target. *Biochim Biophys Acta*. Nov-Dec; 1762(11-12): 1051-67.

Bardehle S, Kruger M, Buggenthin F, Schwausch J, Ninkovic J, Clevers H, Snippert HJ, Theis FJ, Meyer-Luehmann M, Bechmann I, Dimou L, Gotz M. (**2013**). Live imaging of astrocyte responses to acute injury reveals selective juxta vascular proliferation. *Nat. Neurosci.* Mar; 16(5): 580–586.

Barker HV, Niblock M, Lee YB, Shaw CE, Gallo JM. (**2017**). RNA Misprocessing in C9orf72-Linked Neurodegeneration. *Frontiers in cellular neuroscience*, 1: 195.

Barmada SJ and Finkbeiner S. (**2010**). Pathogenic TARDBP mutations in amyotrophic lateral sclerosis and frontotemporal dementia: disease-associated pathways. *Rev. Neurosci.*, 21(4):251-72.

Barmada SJ, Skibinski G, Korb E, Rao EJ, Wu JY, Finkbeiner S. (**2010**). Cytoplasmic mislocalization of TDP-43 is toxic to neurons and enhanced by a mutation associated with familial amyotrophic lateral sclerosis. *J. Neurosci*. Jan 13; 30(2):639-49.

Barres BA, Hart IK, Coles HS, Burne JF, Voyvodic JT, Richardson WD, Raff MC. (**1992**). Cell death and control of cell survival in the oligodendrocyte lineage. *Cell*. Jul 10; 70(1): 31-46.

Bartel DP. (**2004**). MicroRNAs: Genomics, biogenesis, mechanism, and function. *Cell* 116: 281-297.

Battistini S, Giannini F, Greco G, Bibbò G, Ferrera L, Marini V, Causarano R, Casula M, Lando G, Patrosso MC, Caponnetto C, Origone P, Marocchi A, Del Corona A, Siciliano G, Carrera P, Mascia V, Giagheddu M, Carcassi C, Orrù S, Garrè C, Penco S. (**2005**). SOD1 mutations in amyotrophic lateral sclerosis. Results from a multicenter Italian study. *J Neurol*. Jul; 252(7): 782-8.

Baumann N. and Pham-Dinh D. (**2001**). Biology of oligodendrocyte and myelin in the mammalian central nervous system. *Physiol. Rev.* Apr; 81(2): 871-927.

Bäumer D, Hilton D, Paine SM, Turner MR, Lowe J, Talbot K, Ansorge O. (**2010**). Juvenile ALS with basophilic inclusions is a FUS proteinopathy with FUS mutations. *Neurology*. Aug 17; 75(7): 611–618.

Bayer TA. (**2013**) Proteinopathies, a core concept for understanding and ultimately treating degenerative disorders?. *Eur Neuropsychopharmacol*. 25 (5): 713-724.

Beal MF, Ferrante RJ, Browne SE, Matthews RT, Kowall NW, Brown RH Jr. (**1997**). Increased 3-nitrotyrosine in both sporadic and familial amyotrophic lateral sclerosis. *Ann. Neurol*. Oct; 42(4): 644-54.

Beaulieu JM, Robertson J, Julien JP. (**1999**). Interactions between peripherin and neurofilaments in cultured cells: disruption of peripherin assembly by the NF-M and NF-H subunits. *Biochem Cell Biol*. 77(1): 41-5.

Beers DR, Zhao W, Liao B, Kano O, Wang J, Huang A, Appel SH, Henkel JS. (**2011**). Neuroinflammation modulates distinct regional and temporal clinical responses in ALS mice. *Brain Behav Immun*. Jul; 25(5): 1025-35.

Belly A, Moreau-Gachelin F, Sadoul R, Goldberg Y. (**2005**). Delocalization of the multifunctional RNA splicing factor TLS/FUS in hippocampal neurones: Exclusion from the nucleus and accumulation in dendritic granules and spine heads. *Neurosci Lett*. 379: 152–7.

Belzil VV, Bauer PO, Prudencio M, Gendron TF, Stetler CT, Yan IK, Pregent L,Daughrity L, Baker MC, Rademakers R, Boylan K, Patel TC, Dickson DW, Petrucelli L. (**2013a**). Reduced C9orf72 gene expression in c9FTD/ALS is caused by histone trimethylation, an epigenetic event detectable in blood. *Acta Neuropathol* 126: 895-905.

Belzil VV, Gendron TF, Petrucelli L. (**2013b**). RNA-mediated toxicity in neurodegenerative disease. *Mol Cell Neurosci*. Sep; 56: 406-19.

Ben Halevy D, Peretti D, Dahan N. (**2008**). The VAP protein family: from cellular functions to motor neuron disease. *Trends Cell Biol.* Jun; 18(6): 282-90.

Bendotti C, Calvaresi N, Chiveri L, Prelle A, Moggio M, Braga M, Silani V, De Biasi S. (**2001**). Early vacuolization and mitochondrial damage in motor neurons of FALS mice are not associated with apoptosis or with changes in cytochrome oxidase histochemical reactivity. *J Neurol Sci*. Oct 15; 191(1-2): 25-33.

Bendotti C, Marino M, Cheroni C, Fontana E, Crippa V, Poletti A, De Biasi S. (**2012**). Dysfunction of constitutive and inducible ubiquitin-proteasome system in amyotrophic lateral sclerosis: implication for protein aggregation and immune response. *Prog. Neurobiol*. May; 97(2): 101-26.

Bennett ML, Bennett FC, Liddelow SA, Ajami B, Zamanian JL, Fernhoff NB, Mulinyawe SB, Bohlen CJ, Adil A, Tucker A, Weissman IL, Chang EF, Li G, Grant GA, Hayden Gephart MG, Barres BA. (**2016**). New tools for studying microglia in the mouse and human CNS. *Proc Natl Acad Sci USA*. Mar 22; 113(12): E1738-46.

Bensimon G, Lacomblez L, Meininger V. [ALS/Riluzole Study Group]. (**1994**). A controlled trial of riluzole in amyotrophic lateral sclerosis. *N. Engl. J. Med*. Mar 3; 330(9): 585-91.

Bensimon G, Lacomblez L, Delumeau JC, Bejuit R, Truffinet P, Meininger V. (**2002**). A study of riluzole in the treatment of advanced stage or elderly patients with amyotrophic lateral sclerosis. *J. Neurol*. 249: 609-615.

Bentmann E, Haass C, Dormann D. (**2013**). Stress granules in neurodegeneration--lessons learnt from TAR DNA binding protein of 43 kDa and fused in sarcoma. *FEBS J*. Sep; 280(18): 4348-70.

Bento-Abreu A, Van Damme P, Van Den Bosch L, Robberecht W. The neurobiology of amyotrophic lateral sclerosis. *Eur. J. Neurosci*. Jun; 31(12): 2247-65.

Bergami M, Santi S, Formaggio E, Cagnoli C, Verderio C, Blum R, Berninger B, Matteoli M, Canossa M. (**2008**). Uptake and recycling of pro-BDNF for transmitter-induced secretion by cortical astrocytes. *J Cell Biol*. Oct 20; 183(2): 213-21.

Berliocchi L, Bano D, Nicotera P. (**2005**). Ca2+ signals and death programmes in neurons. *Philos Trans R Soc Lond B Biol Sci*. Dec 29; 360(1464): 2255-8.

Berry JD, Shefner JM, Conwit R, Schoenfeld D, Keroack M, Felsenstein D, et al. (**2013**). Design and initial results of a multi-phase randomized trial of ceftriaxone in amyotrophic lateral sclerosis. *PLoS ONE* 8:e61177.

Bertram L. and Tanzi RE. (**2005**). The genetic epidemiology of neurodegenerative disease. *J. Clin. Invest.* Jun 1; 115(6): 1449–1457.

Betteridge DJ. (**2000**). What is oxidative stress? *Metabolism*. Feb; 49 (2 Suppl 1):3-8.

Bezawork-Geleta A, Rohlena J, Dong L, Pacak K, Neuzil J. (**2017**). Mitochondrial Complex II: At the Crossroads. *Trends Biochem Sci*. Apr; 42(4): 312-325. doi: 10.1016/j.tibs.2017.01.003.

Bigio EH, Wu JY, Deng HX, Bit-Ivan EN, Mao Q, Ganti R, Peterson M, Siddique N, Geula C, Siddique T, Mesulam M. (**2013**). Inclusions in frontotemporal lobar degeneration with TDP-43 proteinopathy (FTLD-TDP) and amyotrophic lateral sclerosis (ALS), but not FTLD with FUS proteinopathy (FTLD-FUS), have properties of amyloid. *Acta Neuropathol*. Mar; 125(3):463-5.

Bigio EH. (**2011**). C9ORF72, the new gene on the block, causes C9FTD/ALS: New insights provided by neuropathology. *Acta Neuropathol* 122: 653-655.

Bigio EH. (**2012**). Motor neuron disease: the C9orf72 hexanucleotide repeat expansion in FTD and ALS. *Nat Rev Neurol*. Apr 10; 8(5): 249-50.

Bilsland LG, Sahai E, Kelly G, Golding M, Greensmith L, Schiavo G. (**2010**). Deficits in axonal transport precede ALS symptoms in vivo. *Proc Natl Acad Sci USA*. Nov 23; 107(47): 20523-8.

Birsoy K, Wang T, Chen WW, Freinkman E, Abu-Remaileh M, Sabatini DM. (**2015**). An essential role of the mitochondrial electron transport chain in cell proliferation is to enable aspartate synthesis. *Cell*. Jul 30; 162(3): 540-51.

Black DL. (**2003**). Mechanisms of alternative pre-messenger RNA splicing. *Annu Rev Biochem*. 72: 291-336.

Blasco H, Corcia P, Pradat PF, Bocca C, Gordon PH, Veyrat-Durebex C, Mavel S, Nadal-Desbarats L, Moreau C, Devos D, Andres CR, Emond P. (**2013**). Metabolomics in cerebrospinal fluid of patients with amyotrophic lateral sclerosis: an untargeted approach via high-resolution mass spectrometry. *J Proteome Res*. Aug 2; 12(8): 3746-54.

Blokhuis AM, Groen EJ, Koppers M, van den Berg LH, Pasterkamp RJ. (**2013**). Protein aggregation in amyotrophic lateral sclerosis. Acta Neuropathol. Jun; 125(6): 777-94.

Boche D, Perry VH, Nicoll JA. (**2013**). Review: activation patterns of microglia and their identification in the human brain. *Neuropathol Appl Neurobiol*. Feb; 39(1): 3-18.

Boeynaems S, Bogaert E, Kovacs D, Konijnenberg A, Timmerman E, Volkov A, Guharoy M, De Decker M, Jaspers T, Ryan VH, Janke AM, Baatsen P, Vercruysse T, Kolaitis RM, Daelemans D, Taylor JP, Kedersha N, Anderson P, Impens F, Sobott F, Schymkowitz J, Rousseau F, Fawzi NL, Robberecht W, Van Damme P, Tompa P, Van Den Bosch L. (**2017**). Phase separation of C9orf72 dipeptide repeats perturbs stress granule dynamics. *Mol. Cell* Mar 16; 65(6): 1044-1055.e5.

Bogen IL, Risa Ø, Haug KH, Sonnewald U, Fonnum F, Walaas SI. (**2008**). Distinct changes in neuronal and astrocytic amino acid neurotransmitter metabolism in mice with reduced numbers of synaptic vesicles. *J Neurochem*. Jun 1; 105(6): 2524-34.

Boillée S, Vande Velde C, Cleveland DW. (**2006**). ALS: a disease of motor neurons and their nonneuronal neighbors. *Neuron*. Oct 5; 52(1): 39-59.

Bonneh-Barkay D, Bissel SJ, Kofler J, Starkey A, Wang G, Wiley CA. (**2012**). Astrocyte and macrophage regulation of YKL-40 expression and cellular response in neuroinflammation. *Brain Pathol*. 22: 530–46.

Bonneh-Barkay D, Zagadailov P, Zou H, Niyonkuru C, Figley M, Starkey A, Wang G, Bissel SJ, Wiley CA, Wagner AK. (**2010**). YKL-40 expression in traumatic brain injury: an initial analysis. *J Neurotrauma.* 27: 1215–23.

Borchelt DR, Guarnieri M, Wong PC, Lee MK, Slunt HS, Xu ZS, Sisodia SS, Price DL, Cleveland DW. (**1995**). Superoxide dismutase 1 subunits with mutations linked to familial amyotrophic lateral sclerosis do not affect wild-type subunit function. *J. Biol. Chem*. Feb 17; 270(7): 3234-8.

Borasio GD, Robberecht W, Leigh PN, Emile J, Guiloff RJ, Jerusalem F, et al. (**1998**). A placebo-controlled trial of insulin-like growth factor-I in amyotrophic lateral sclerosis. European ALS/IGF-I Study Group. *Neurology* 51: 583–586.

Borchelt DR, Wong PC, Becher MW, Pardo CA, Lee MK, Xu ZS, Thinakaran G, Jenkins NA, Copeland NG, Sisodia SS, Cleveland DW, Price DL, Hoffman PN. (**1998**). Axonal transport of mutant superoxide dismutase 1 and focal axonal abnormalities in the proximal axons of transgenic mice. *Neurobiol Dis*. Jul; 5(1): 27-35.

Borthwick GM, Johnson MA, Ince PG, Shaw PJ, Turnbull DM. (**1999**). Mitochondrial enzyme activity in amyotrophic lateral sclerosis: implications for the role of mitochondria in neuronal cell death. *Ann Neurol*. Nov; 46(5): 787-90.

Bosco DA, Lemay N, Ko HK, Zhou H, Burke C, Kwiatkowski TJ Jr, Sapp P, McKenna-Yasek D, Brown RH Jr, Hayward LJ. (**2010a**). Mutant FUS proteins that cause amyotrophic lateral sclerosis incorporate into stress granules. *Hum Mol Genet*. Nov 1; 19(21): 4160-75.

Bosco DA, Morfini G, Karabacak NM, Song Y, Gros-Louis, F, Pasinelli, P, Goolsby, H, Fontaine BA, Lemay N, McKenna-Yasek D, Frosch MP, Agar JN, Julien JP, Brady ST, Brown RH. (**2010b**). Wild-type and mutant SOD1 share an aberrant conformation and a common pathogenic pathway in ALS. *Nat Neurosci*. Nov; 13(11): 1396–1403.

Bose JK, Wang IF, Hung L, Tarn WY, Shen CK. (**2008**). TDP-43 overexpression enhances exon 7 inclusion during the survival of motor neuron pre-mRNA splicing. *J Biol Chem*. Oct 24; 283(43): 28852-9.

Bott NT, Radke A, Stephens ML, Kramer JH. (**2014**). Frontotemporal dementia: diagnosis, deficits and management. *Neurodegener Dis Manag*. 4(6): 439-54.

Bouzier-Sore AK, Merle M, Magistretti PJ, Pellerin L. (**2002**). Feeding active neurons: (Re)emergence of a nursing role for astrocytes. *J Physiol Paris*. Apr-Jun; 96(3-4): 273-82.

Bowling AC, Schulz JB, Brown RH Jr. Beal MF. (**1993**). Superoxide dismutase activity, oxidative damage, and mitochondrial energy metabolism in familial and sporadic amyotrophic lateral sclerosis. *J Neurochem*. Dec; 61(6): 2322-5.

Boxer AL, Gold M, Huey E, Gao FB, Burton EA, Chow T, Kao A, Leavitt BR, Lamb B, Grether M, Knopman D, Cairns NJ, Mackenzie IR, Mitic L, Roberson ED, Van Kammen D, Cantillon M, Zahs K, Salloway S, Morris J, Tong G, Feldman H, Fillit H, Dickinson S, Khachaturian Z, Sutherland M, Farese R, Miller BL, Cummings J. (**2012**). Frontotemporal degeneration, the next therapeutic frontier: molecules and animal models for frontotemporal degeneration drug development. *Alzheimers Dement*. Mar; 9(2): 176-88.

Bozik ME, Mitsumoto H, Brooks BR, Rudnicki SA, Moore DH, Zhang B, et al. (**2014**). A post hoc analysis of subgroup outcomes and creatinine in the phase III clinical trial (EMPOWER) of dexpramipexole in ALS. *Amyotroph. Lateral Scler. Front. Degener*. 15 406–413.

Braakman I. and Bulleid NJ. (**2011**). Protein folding and modification in the mammalian endoplasmic reticulum. *Annu Rev Biochem*. 80: 71-99.

Bradl M. and Lassmann H. (**2010**). Oligodendrocytes: biology and pathology. *Acta Neuropathol*. Jan; 119(1): 37-53.

Bradley WG. (**1995**). A phase I/II study of recombinant brain-derived neurotrophic in patients with ALS. *Ann. Neurol*. 38: 971.

Brandmeir NJ, Geser F, Kwong LK, Zimmerman E, Qian J, Lee VM, Trojanowski JQ. (**2008**). Severe subcortical TDP-43 pathology in sporadic frontotemporal lobar degeneration with motor neuron disease. *Acta Neuropathol*. Jan; 115(1):123-31.

Brettschneider J, Arai K, Del Tredici K, Toledo JB, Robinson JL, Lee EB, Kuwabara S, Shibuya K, Irwin DJ, Fang L, Van Deerlin VM, Elman L, McCluskey L, Ludolph AC, Lee VM, Braak H, Trojanowski JQ. (**2014a**). TDP-43 pathology and neuronal loss in amyotrophic lateral sclerosis spinal cord. *Acta Neuropathol*. Sep; 128(3): 423-37.

Brettschneider J, Del Tredici K, Irwin DJ, Grossman M, Robinson JL, Toledo JB, Fang L, Van Deerlin VM, Ludolph AC, Lee VM, Braak H, Trojanowski JQ. (**2014b**). Sequential distribution of pTDP-43 pathology in behavioral variant frontotemporal dementia (bvFTD). *Acta Neuropathol*. Mar; 127(3): 423-439.

Brettschneider J, Del Tredici K, Toledo JB, Robinson JL, Irwin DJ, Grossman M, Suh E, Van Deerlin VM, Wood EM, Baek Y, Kwong L, Lee EB, Elman L, McCluskey L, Fang L, Feldengut S, Ludolph AC, Lee VM, Braak H, Trojanowski JQ. (**2013**). Stages of pTDP-43 pathology in amyotrophic lateral sclerosis. *Ann Neurol.* Jul; 74(1): 20-38.

Breuer AC, Atkinson MB. (**1988**). Fast axonal transport alterations in amyotrophic lateral sclerosis (ALS) and in parathyroid hormone (PTH)-treated axons. *Cell Motil Cytoskeleton*. 10(1-2): 321-30.

Breuer AC, Lynn MP, Atkinson MB, Chou SM, Wilbourn AJ, Marks KE, Culver JE, Fleegler EJ. (**1987**). Fast axonal transport in amyotrophic lateral sclerosis: an intra-axonal organelle traffic analysis. *Neurology*. May; 37(5): 738-48.

Brooks BR, et al., from World Federation of Neurology (WFN) research group on neuromuscular diseases. (**1994**). El Escorial World Federation of Neurology Criteria for the Diagnosis of Amyotrophic Lateral Sclerosis. *Journal of the Neurological Sciences*. 124 (Suppl.): 96-107.

Brooks BR, et al., from World Federation of Neurology (WFN) research group on neuromuscular diseases. (**2001**). El Escorial revisited: Revised criteria for the diagnosis of Amyotrophic Lateral Sclerosis. *ALS and other motor neuron disorders*. 1 (5): 293-299.

Bruijn LI, Becher MW, Lee MK, Anderson KL, Jenkins NA, Copeland NG, Sisodia SS, Rothstein JD, Borchelt DR, Price DL, Cleveland DW. (**1997**). ALS-linked SOD1 mutant G85R mediates damage to astrocytes and promotes rapidly progressive disease with SOD1-containing inclusions. *Neuron*. Feb; 18(2): 327-38.

Bruijn LI, Miller TM, Cleveland DW. (**2004**). Unraveling the mechanisms involved in motor neuron degeneration in ALS. *Annu Rev Neurosci*. 27: 723-49.

Budini M, Buratti E, Morselli E, Criollo A. (**2017**). Autophagy and its impact on neurodegenerative diseases: New roles for TDP-43 and C9orf72. *Front Mol Neurosci* 10: 170.

Bundesen LQ, Scheel TA, Bregman BS, Kromer LF. (**2003**). Ephrin-B2 and EphB2 regulation of astrocyte-meningeal fibroblast interactions in response to spinal cord lesions in adult rats. *J Neurosci.* Aug 27; 23(21):7789-800.

Buratti E, Brindisi A, Giombi M, Tisminetzky S, Ayala YM, Baralle FE. (**2005**). TDP-43 binds heterogeneous nuclear ribonucleoprotein A/B through its C-terminal tail: an important region for the inhibition of cystic fibrosis transmembrane conductance regulator exon 9 splicing. *J Biol Chem*. Nov 11; 280(45): 37572-84.

Buratti E, De Conti L, Stuani C, Romano M, Baralle M, Baralle F. (**2010**). Nuclear factor TDP-43 can affect selected microRNA levels. *FEBS journal*. May; 277(10): 2268-81.

Buratti E, Dörk T, Zuccato E, Pagani F, Romano M, Baralle FE. (**2001**). Nuclear factor TDP-43 and SR proteins promote in vitro and in vivo CFTR exon 9 skipping. *EMBO J*. Apr 2; 20(7):1774-84.

Burmakina S, Geng Y, Chen Y, Fan QR. (**2014**). Heterodimeric coiled-coil interactions of human GABAB receptor. *Proc Natl Acad Sci USA*. 111: 6958–63.

Burton PR. and Paige JL. (**1981**). Polarity of axoplasmic microtubules in the olfactory nerve of the frog. *Proc Natl Acad Sci USA*. May; 78(5): 3269-73.

Byrne S, Heverin M, Elamin M, Walsh C, Hardiman O. (**2014**). Intermediate repeat expansion length in C9orf72 may be pathological in amyotrophic lateral sclerosis. *Amyotroph. Lateral Scler. Frontotemporal Degener*. Mar; 15(1-2): 148-50.

Cahoy JD, Emery B, Kaushal A, Foo LC, Zamanian JL, Christopherson KS, Xing Y, Lubischer JL, Krieg PA, Krupenko SA, Thompson WJ, Barres BA. (**2008**). A transcriptome database for astrocytes, neurons, and oligodendrocytes: A new resource for understanding brain development and function. *J Neurosci*. Jan 2; 28(1): 264-78.

Cairns NJ, Neumann M, Bigio EH, Holm IE, Troost D, Hatanpaa KJ, Foong C, White CL 3rd, Schneider JA, Kretzschmar HA, Carter D, Taylor-Reinwald L, Paulsmeyer K, Strider J, Gitcho M, Goate AM, Morris JC, Mishra M, Kwong LK, Stieber A, Xu Y, Forman MS, Trojanowski JQ, Lee VM, Mackenzie IR. (**2007**). TDP-43 in familial and sporadic frontotemporal lobar degeneration with ubiquitin inclusions. *Am J Pathol*. Jul; 171(1): 227-40.

Campbell GR, Ziabreva I, Reeve AK, Krishnan KJ, Reynolds R, Howell O, Lassmann H, Turnbull DM, Mahad DF. (**2010**). Mitochondrial DNA deletions and neurodegeneration in multiple sclerosis *Ann. Neurol.* Mar; 69(3): 481-92. doi: 10.1002/ana.22109.

Carey J (Editor). (**2002**). Brain facts: a primer on the brain and nervous system. 4th edition. *The society for Neuroscience*. Washington (DC). USA.

Carpenter S. (**1968**). Proximal axonal enlargement in motor neuron disease. *Neurology*. Sep; 18(9): 841-51.

Carrell R.W. and Lomas D.A. (**1997**). Conformational disease. *Lancet*, 350(9071):134-8. doi: 10.1016/S0140-6736(97)02073-4.

Carriedo SG, Sensi SL, Yin HZ, Weiss JH. (**2000**). AMPA exposures induce mitochondrial Ca(2+) overload and ROS generation in spinal motor neurons in vitro. *J Neurosci.* Jan 1; 20(1): 240-50. doi: 10.1523/JNEUROSCI.20-01-00240.2000.

Casanovas A, Salvany S, Lahoz V, et al. (**2017**). Neuregulin 1-ErbB module in C-bouton synapses on somatic motor neurons: Molecular compartmentation and response to peripheral nerve injury. *Sci Rep* 7: 40155.

Casas C, Herrando-Grabulosa M, Manzano R, et al. (**2013**). Early presymptomatic cholinergic dysfunction in a murine model of amyotrophic lateral sclerosis. *Brain Behav* 3: 145–58.

Casula M, Iyer AM, Spliet WG, Anink JJ, Steentjes K, Sta M, et al. (**2011**). Toll-like receptor signaling in amyotrophic lateral sclerosis spinal cord tissue. *Neuroscience* 179:233–43.

Cereda C, Baiocchi C, Bongioanni P, Cova E, Guareschi S, Metelli MR, Rossi B, Sbalsi I, Cuccia MC, Ceroni M. (**2008**). TNF and sTNFR1/2 plasma levels in ALS patients. *J Neuroimmunol*. 194: 123–31.

Chandel NS. (**2010**). Mitochondrial complex III: an essential component of universal oxygen sensing machinery?. *Respir Physiol Neurobiol*. Dec 31; 174(3): 175–181.

Chandra K, Salman AS, Mohd A, Rajpoot S, Ali KN. (**2015**). Protection against FCA induced oxidative stress induced DNA damage as a model of arthritis and in vitro anti-arthritic potential of costus speciosus rhizome extract. *Int. J. Pharmacognosy and Phytochem. Res*. 7(2): 383–389.

Chang NC, Hung SI, Hwa KY, Kato I, Chen JE, Liu CH, Chang AC. (**2001**). A macrophage protein, Ym1, transiently expressed during inflammation is a novel mammalian lectin. *J Biol Chem*. May 18; 276(20): 17497-506.

Chapelin C, Duriez B, Magnino F, Goossens M, Escudier E, Amselem S. (**1997**). Isolation of several human axonemal dynein heavy chain genes: genomic structure of the catalytic site, phylogenetic analysis and chromosomal assignment. *FEBS Lett*. 412: 325–30.

Chattopadhyay M. and Valentine JS. (**2009**). Aggregation of copper-zinc superoxide dismutase in familial and sporadic ALS. *Antioxid Redox Signal*. Jul; 11(7): 1603-14.

Chen HJ, Mitchell JC, Novoselov S, Miller J, Nishimura AL, Scotter EL, Vance CA, Cheetham ME, Shaw CE. (**2016**). The heat shock response plays an important role in TDP-43 clearance: Evidence for dysfunction in amyotrophic lateral sclerosis. *Brain*. May; 139(Pt 5): 1417-32.

Chen K, Iribarren P, Hu J, Chen J, Gong W, Cho EH, Lockett S, Dunlop NM, Wang JM. (**2006**). Activation of Tolllike receptor 2 on microglia promotes cell uptake of Alzheimer disease-associated amyloid β peptide. *J Biol Chem.* 281: 3651–59.

Chen S, Sayana P, Zhang X, Le W. (**2013**). Genetics of amyotrophic lateral sclerosis: an update. *Mol Neurodegener*. Aug 13; 8: 28.

Cheney RE. and Baker JP. (**1999**). Guidebook to the cytoskeletal and motor proteins. Myosins, divergent. *Trends Cell Biol*. 4(2) p65: 453-456.

Chen-Plotkin AS, Geser F, Plotkin JB, Clark CM, Kwong LK, Yuan W, Grossman M, Van Deerlin VM, Trojanowski JQ, LeeVM. (**2008**). Variations in the progranulin gene affect global gene expression in frontotemporal lobar degeneration. *Hum Mol Genet*. 17: 1349-1362.

Chew J, Gendron TF, Prudencio M, Sasaguri H, Zhang YJ, Castanedes-Casey M, Lee CW, Jansen-West K, Kurti A, Murray ME, Bieniek KF, Bauer PO, Whitelaw EC, Rousseau L, Stankowski JN, Stetler C, Daughrity LM, Perkerson EA, Desaro P, Johnston A, Overstreet K, Edbauer D, Rademakers R, Boylan KB, Dickson DW, Fryer JD, Petrucelli L. (**2015**). *C9ORF72* repeat expansions in mice cause TDP-43 pathology, neuronal loss, and behavioral deficits. *Science*. Jun 5; 348(6239):1151-4.

Chiu AY, Zhai P, Dal Canto MC, Peters TM, Kwon YW, Prattis SM, Gurney ME. (**1995**). Age-dependent penetrance of disease in a transgenic mouse model of familial amyotrophic lateral sclerosis. *Mol Cell Neurosci*. Aug; 6(4): 349-62.

Choi DW. (**1988**). Glutamate neurotoxicity and diseases of the nervous system. *Neuron*. Oct; 1(8): 623-34.

Chomyn A, Mariottini P, Cleeter MW, Ragan CI, Matsuno-Yagi A, Hatefi Y, Doolittle RF, Attardi G. (**1985**). Six unidentified reading frames of human mitochondrial DNA encode components of the respiratory-chain NADH dehydrogenase. *Nature*. Apr 18-24; 314(6012): 592-7.

Chow JC, Yen Z, Ziesche SM, Brown CJ. (**2005**). Silencing of the mammalian X chromosome. *Annu Rev Genom Hum Genet.* 6: 69-92.

Chow TW, Miller BL, Hayashi VN, Geschwind DH. (**1999**). Inheritance of frontotemporal dementia. *Arch Neurol*. Jul; 56(7): 817-22.

Chrast R, Saher G, Nave KA, Verheijen MH. (**2011**). Lipid metabolism in myelinating glial cells: lessons from human inherited disorders and mouse models. *J. Lipid Res*. Mar; 52(3): 419-34.

Chuang JZ, Milner TA, Sung CH. (**2001**). Subunit heterogeneity of cytoplasmic dynein: Differential expression of 14 kDa dynein light chains in rat hippocampus. *J Neurosci* 21: 5501–12.

Ciura S, Lattante S, Le Ber I, Latouche M, Tostivint H, Brice A, Kabashi E. (**2013**). Loss of function of C9orf72 causes motor deficits in a zebrafish model of amyotrophic lateral sclerosis. *Ann. Neurol*. Aug; 74(2): 180-7.

Clancy S. and Brown W. (**2008**). Translation: DNA to mRNA to Protein. *Nature Education*. 1(1): 101.

Clark JA, Yeaman EJ, Blizzard CA, Chuckowree JA, Dickson TC. (**2016**). A case for microtubule vulnerability in amyotrophic lateral sclerosis: altered dynamics during disease. *Front Cell Neurosci*. Sep 13; 10:204.

Cobley JN, Fiorello ML, Bailey DM. (**2018**). 13 reasons why the brain is susceptible to oxidative stress. *Redox Biol*. May; 15: 490-503.

Cohen TJ, Lee VM, Trojanowski JQ. (**2011**). TDP-43 functions and pathogenic mechanisms implicated in TDP-43 proteinopathies. *Trends Mol. Med*. Nov; 17(11):659-67.

Collard JF, Cote F, Julien JP. (**1995**). Defective axonal transport in a transgenic mouse model of amyotrophic lateral sclerosis. *Nature*. May 4; 375(6526): 61-4.

Colombrita C, Zennaro E, Fallini C, Weber M, Sommacal A, Buratti E, Silani V, Ratti A. (**2009**). TDP-43 is recruited to stress granules in conditions of oxidative insult. *J Neurochem*. Nov; 111(4): 1051-61.

Colton CA. (**2009**). Heterogeneity of microglial activation in the innate immune response in the brain. *J Neuroimmune Pharmacol*. Dec; 4(4): 399-418.

Conlon EG, Fagegaltier D, Agius P, Davis-Porada J, Gregory J, Hubbard I, Kang K, Kim D; NewYork Genome Center ALS Consortium, Phatnani H,Kwan J, Sareen D, Broach JR, Simmons Z, Arcila-Londono X, Lee EB, Van Deerlin VM, Shneider NA, Fraenkel E, Ostrow LW, Baas F, Zaitlen N, Berry JD, Malaspina A, Fratta P, Cox GA, Thompson LM, Finkbeiner S, Dardiotis E, Miller TM, Chandran S, Pal S, Hornstein E, MacGowan DJ, Heiman-Patterson T, Hammell MG, Patsopoulos NA, Dubnau J, Nath A, Phatnani H, Shneider NA, Manley JL. (**2018**). Unexpected similarities between C9ORF72 and sporadic forms of ALS/FTD suggest a common disease mechanism. *Elife* 13: 7.

Connor JR. (**1994**). Iron acquisition and expression of iron regulatory proteins in the developing brain: manipulation by ethanol exposure, iron deprivation and cellular dysfunction. *Dev Neurosci.* 16:233– 47.

Conradi S. (**1969**). Ultrastructure and distribution of neuronal and glial elements on the surface of the proximal part of a motoneuron dendrite, as analyzed by serial sections. *Acta Physiol Scand* Suppl 332:49–64

Cooper GM. and Hausman RE. (**2006**). The Cell: A molecular approach, 4th Edition. Washington DC and Sunderland (MA), USA. *ASM Press* and *Sinauer Associates*.

Cozzolino M. and Carrì MT. (**2012**). Mitochondrial dysfunction in ALS. *Prog Neurobiol*. May; 97(2): 54-66.

Cruts M, Gijselinck I, van der Zee J, Engelborghs S, Wils H, Pirici D, Rademakers R, Vandenberghe R, Dermaut B, Martin JJ, van Duijn C, Peeters K, Sciot R, Santens P, De Pooter T, Mattheijssens M, Van den Broeck M, Cuijt I, Vennekens K, De Deyn PP, Kumar-Singh S, Van Broeckhoven C. (**2006**). Null mutations in progranulin cause ubiquitin-positive frontotemporal dementia linked to chromosome 17q21. *Nature*. Aug 24; 442 (7105): 920-4.

Cudkowicz M, Bozik ME, Ingersoll EW, Miller R, Mitsumoto H, Shefner J, et al. (**2011**). The effects of dexpramipexole (KNS-760704) in individuals with amyotrophic lateral sclerosis. *Nat. Med.* 17: 1652–1656.

Cudkowicz M, Shefner J, Consortium N. (**2013**). STAGE 3 Clinical Trial of Ceftriaxone in Subjects with ALS (S36.001). Available at: http://www.neurology.org/content/80/7_Supplement/S36.001.abstract [accessed June 6, 2016].

Cudkowicz ME, Shefner JM, Schoenfeld DA, Zhang H, Andreasson KI, Rothstein JD, et al. (**2006**). Trial of celecoxib in amyotrophic lateral sclerosis. *Ann. Neurol*. 60: 22-31.

Cudkowicz ME, van den Berg LH, Shefner JM, Mitsumoto H, Mora JS, Ludolph A, et al. (**2013**). Dexpramipexole versus placebo for patients with amyotrophic lateral sclerosis (EMPOWER): a randomised, double-blind, phase 3 trial. *Lancet Neurol*. 12: 1059–1067.

Cuervo AM. (**2011**). Chaperone-mediated autophagy: Dice's'wild' idea about lysosomal selectivity. *Nat. Rev. Mol. Cell Biol*. Jul 13; 12(8): 535-41.

Curti D, Malaspina A, Facchetti G, Camana C, Mazzini L, Tosca P, Zerbi F, Ceroni M. (**1996**). Amyotrophic lateral sclerosis: oxidative energy metabolism and calcium homeostasis in peripheral blood lymphocytes. *Neurology*. Oct; 47(4): 1060-4.

D'Ambrogio A, Buratti E, Stuani C, Guarnaccia C, Romano M, Ayala YM, Baralle FE. (**2009**). Functional mapping of the interaction between TDP-43 and hnRNP A2 in vivo. *Nucleic Acids Res*. Jul; 37(12): 4116-26.

Dafinca R, Scaber J, Ababneh N, Lalic T, Weir G, Christian H, Vowles J, Douglas AG, Fletcher-Jones A, Browne C, Nakanishi M, Turner MR, Wade-Martins R, Cowley SA, Talbot K. (**2016**). C9orf72 hexanucleotide expansions are associated with altered endoplasmic reticulum calcium homeostasis and stress granule formation in induced pluripotent stem cell-derived neurons from patients with amyotrophic lateral sclerosis and frontotemporal dementia. *Stem Cells*. Aug; 34(8): 2063-78.

Dal Canto MC. and Gurney ME. (**1995**). Neuropathological changes in two lines of mice carrying a transgene for mutant human Cu, Zn SOD, and in mice overexpressing wild type human SOD: a model of familial amyotrophic lateral sclerosis (FALS). *Brain Res.* Apr 3; 676(1): 25-40.

Damiano M, Starkov AA, Petri S, Kipiani K, Kiaei M, Mattiazzi M, Flint Beal M, Manfredi G. (**2006**). Neural mitochondrial Ca2+ capacity impairment precedes the onset of motor symptoms in G93A Cu/Zn superoxide dismutase mutant mice. *J Neurochem*. Mar; 96(5): 1349-61.

Danysz W. and Parsons CG. (**2003**). The NMDA receptor antagonist memantine as a symptomatological and neuroprotective treatment for Alzheimer's disease: preclinical evidence. *Int J Geriatr Psychiatry*. Sep; 18(Suppl 1): S23-32.

Davalos D, Grutzendler J, Yang G, Kim JV, Zuo Y, Jung S, Littman DR, Dustin ML, Gan WB. (**2005**). ATP mediates rapid microglial response to local brain injury in vivo. *Nat Neurosci*. Jun; 8(6): 752-8. doi: 10.1038/nn1472.

Davidson Y, Kelley T, Mackenzie IR, Pickering-Brown S, Du Plessis D, Neary D, Snowden JS, Mann DM. (**2007**). Ubiquitinated pathological lesions in frontotemporal lobar degeneration contain the TAR DNA-binding protein, TDP-43. *Acta Neuropathol* May; 113(5): 521-33.

Davidson YS, Barker H, Robinson AC, Thompson JC, Harris J, Troakes C, Smith B, Al-Saraj S, Shaw C, Rollinson S, Masuda-Suzukake M, Hasegawa M, Pickering-Brown S, Snowden JS, Mann DM. (**2014**). Brain distribution of dipeptide repeat proteins in frontotemporal lobar degeneration and motor neurone disease associated with expansions in C9ORF72. *Acta Neuropathol. Commun*. Jun 20; 2: 70.

Davidson YS, Robinson AC, Liu X, Wu D, Troakes C, Rollinson S, Masuda-Suzukake M, Suzuki G, Nonaka T, Shi J, Tian J, Hamdalla H, Ealing J, Richardson A, Jones M, Pickering-Brown S, Snowden JS, Hasegawa M, Mann DM. (**2016**). Neurodegeneration in frontotemporal lobar degeneration and motor neurone disease associated with expansions in C9orf72 is linked to TDP-43 pathology and not associated with aggregated forms of dipeptide repeat proteins. *Neuropath. Appl. Neurobiol*. Apr; 42(3): 242-54.

Davis RE. and Williams M. (**2012**). Mitochondrial function and dysfunction: an update. *J Pharmacol Exp Ther*. Sep; 342(3): 598-607.

Davydova D, Marini C, King C, Klueva J, Bischof F, Romorini S, Montenegro-Venegas C, Heine M, Schneider R, Schröder MS, Altrock WD, Henneberger C, Rusakov DA, et al. (**2014**). Bassoon specifically controls presynaptic P/Q-type Ca(2+) channels via RIM-binding protein. *Neuron*. 82:181–94.

Dawson MR, Polito A, Levine JM, Reynolds R. (**2003**). NG2-expressing glial progenitor cells: an abundant and widespread population of cycling cells in the adult rat CNS. *Mol. Cell. Neurosci*. Oct; 24(2): 476-88.

Dawson TM, Golde TE, Lagier-Tourenne C. (**2018**). Animal models of neurodegenerative diseases. *Nat Neurosci*. Oct; 21(10): 1370-1379.

Dawson VL, Dawson TM, London ED, Bredt DS, Snyder SH. (**1991**). Nitric oxide mediates glutamate neurotoxicity in primary cortical cultures. *Proc Natl Acad Sci USA*. Jul 15; 88(14): 6368–6371.

de Carvalho M, Pinto S, Costa J, Evangelista T, Ohana B, Pinto A. (**2010**). A randomized, placebo-controlled trial of memantine for functional disability in amyotrophic lateral sclerosis. *Amyotroph. Lateral Scler*. 11: 456–460

De Conti L, Akinyi MV, Mendoza-Maldonado R, Romano M, Baralle M, Buratti E. (**2015**). TDP-43 affects splicing profiles and isoform production of genes involved in the apoptotic and mitotic cellular pathways. *Nucleic acids research* 43(18): 8990–9005.

REFERENCES

De Vos KJ. and Hafezparast M. (**2017**). Neurobiology of axonal transport defects in motor neuron diseases: Opportunities for translational research? *Neurobiol. Dis*. Sep; 105: 283-299.

DeJesus-Hernandez M, Mackenzie IR, Boeve BF, Boxer AL, Baker M, Rutherford NJ, Nicholson AM, Finch NA, Flynn H, Adamson J, Kouri N, Wojtas A, Sengdy P, Hsiung GY, Karydas A, Seeley WW, Josephs KA, Coppola G, Geschwind DH, Wszolek ZK, Feldman H, Knopman DS, Petersen RC, Miller BL, Dickson DW, Boylan KB, Graff-Radford NR, Rademakers R. (**2011**). Expanded GGGGCC hexanucleotide repeat in noncoding region of C9ORF72 causes chromosome 9p-linked FTD and ALS. *Neuron*. Oct 20; 72(2): 245-56.

DeKosky ST, Ikonomovic MD, Gandy S. (**2010**). Traumatic brain injury - football, warfare and long-term effects. *N. Engl. J. Med.*, Sep 30; 363(14):1293-6.

Del Río Hortega P. (**1922**). ¿Son homologables la glía de escasas radiaciones y las células de Schwann? *Bol. Soc. Esp. Biol*. 10(I): 25–28.

Del Río Hortega P. (**1928**). Tercera aportación al conocimiento morfológico e interpretación funcional de la oligodendroglía. *Mem. Real Soc. Esp. Hist. Nat*. 14: 5–122.

Del Rio-Hortega P. (**1919**). El tercer elemento de los centros nerviosos. *Bio Soc Esp Biol*. IX: 69-129.

Del Río-Hortega P. (**1921**). La glía de escasa radiaciones (oligodendroglia). *Trab. Lab. Histol. Patol.* 1(15): 1-43.

Deng HX, Shi Y, Furukawa Y, Zhai H, Fu R, Liu E, Gorrie GH, Khan MS, Hung WY, Bigio EH, Lukas T, Dal Canto MC, O'Halloran TV, Siddique T. (**2006**). Conversion to the amyotrophic lateral sclerosis phenotype is associated with intermolecular linked insoluble aggregates of SOD1 in mitochondria. *Proc Natl Acad Sci USA*. May 2; 103(18): 7142-7147.

Devasagayam TP, Tilak JC, Boloor KK, Sane KS, Ghaskadbi SS, Lele RD (**2004**). Free radicals and antioxidants in human health: current status and future prospects. *J Assoc Physicians India*. Oct; 52: 794-804.

Dickerson BC. (**2016**). Hodges' Frontotemporal Dementia. 2nd edition. Cambridge, UK. *Ed. Cambridge.*

Dickson DW, Josephs KA, Amador-Ortiz. C (**2007**). TDP-43 in differential diagnosis of motor neuron disorders. *Acta Neuropathol* Jul; 114(1): 71-9.

Diehl HJ, Schaich M, Budzinski RM, Stoffel W. (**1986**). Individual exons encode the integral membrane domains of human myelin proteolipid protein. *Proc Natl Acad Sci USA*. 83: 9807–11.

Dormann D, Rodde R, Edbauer D, Bentmann E, Fischer I, Hruscha A, Than ME, Mackenzie IR, Capell A, Schmid B, Neumann M, Haass C. (**2010**). ALS-associated fused in sarcoma (FUS) mutations disrupt transportin-mediated nuclear import. *EMBO J.* Aug 18; 29(16): 2841-57.

Dringen R, Gutterer JM, Hirrlinger J. (**2000**). Glutathione metabolism in brain metabolic interaction between astrocytes and neurons in the defense against reactive oxygen species. *Eur J Biochem.* Aug; 267(16): 4912-6.

Dupuis L, Dengler R, Heneka MT, Meyer T, Zierz S, Kassubek J, et al. (**2012**). A randomized, double blind, placebo-controlled trial of pioglitazone in combination with riluzole in amyotrophic lateral sclerosis. *PLoS ONE* 7:e37885.

Dykens JA. (**1994**). Isolated cerebral and cerebellar mitochondria produce free radicals when exposed to elevated CA2+ and Na+: implications for neurodegeneration. *J Neurochem*. Aug; 63(2): 584-91.

Ellison D, Love S, Chimelli LMC, Harding B, Lowe J, Vinters HV, Brandner S, Yon W. (**2012**). Neuropathology: a reference text of CNS pathology. Third Edition. Missouri, USA. *Elsevier Health Sciences (Mosby Ltd).*

Elman LB and McCluskey L. (**2012**). Clinical features of amyotrophic lateral sclerosis and other forms of motor neuron disease. *UpToDate*, Wolters Kluwer Health.

Elman LB, McCluskey L, Grossman M. (**2008**). Motor neuron disease and frontotemporal lobar degeneration: a tale of two disorders linked to TDP-43. *Neurosignals*. 16(1):85-90.

Emery B, Agalliu D, Cahoy JD, Watkins TA, Dugas JC, Mulinyawe SB, Ibrahim A, Ligon KL, Rowitch DH, Barres BA. (**2009**). Myelin gene regulatory factor is a critical transcriptional regulator required for CNS myelination. *Cell.* Jul 10; 138(1): 172-85.

Enwerem II, Wu G, Yu YT, Hebert MD. (**2015**). Cajal body proteins differentially affect the processing of box C/D scaRNPs. *PLoS One* 10: e0122348.

Erikson KM, Pinero DJ, Connor JR, Beard JL. (**1997**). Regional brain iron, ferritin and transferrin concentrations during iron deficiency and iron repletion in developing rats. *J Nutr*. 127:2030–38.

Ernster L. and Schatz G. (**1981**). Mitochondria: a historical review. *J Cell Biol*. Dec; 91(3 Pt 2): 227s-255s. doi:10.1083/jcb.91.3.227s.

Evans CS. and Holzbaur ELF. (**2019**) Autophagy and mitophagy in ALS. *Neurobiol Dis* 122: 35-40.

Evans MC, Couch Y, Sibson N, Turner MR. (**2013**). Inflammation and neurovascular changes in amyotrophic lateral sclerosis. *Mol Cell Neurosci*. 53: 34–41.

Evers BM, Rodrıguez-Navas C, Tesla RJ, Prange-Kiel J, Wasser CR, Yoo KS, McDonald J, Cenik B, Ravenscroft TA, Plattner F, Rademakers R, Yu G, White CL 3rd, Herz J. (**2017**). Lipidomic and transcriptomic basis of lysosomal dysfunction in progranulin deficiency. *Cell Rep* 20: 2565-2574.

Facci L, Barbierato M, Marinelli C, Argentini C, Skaper SD, Giusti P. (**2014**). Toll-like receptors 2, -3 and -4 prime microglia but not astrocytes across central nervous system regions for ATP-dependent interleukin-1β release. *Sci Rep*. 4: 6824.

Farg MA, Sundaramoorthy V, Sultana JM, Yang S, Atkinson RA, Levina V, Halloran MA, Gleeson PA, Blair IP, Soo KY, King AE, Atkin JD. (**2014**). C9ORF72, implicated in amytrophic lateral sclerosis and frontotemporal dementia, regulates endosomal trafficking. *Hum Mol Genet*. Jul 1; 23(13): 3579-95.

Fatima M, Tan R, Halliday GM, Kril JJ. (**2015**). Spread of pathology in amyotrophic lateral sclerosis: assessment of phosphorylated TDP-43 along axonal pathways. *Acta Neuropathol*. *Commun.* Jul 28; 3:47.

Fawcett JW. and Asher RA. (**1999**). The glial scar and central nervous system repair. *Brain Res Bull*. Aug; 49(6): 377-91.

Feiguin F, Godena VK, Romano G, D'Ambrogio A, Klima R, Baralle FE. (**2009**). Depletion of TDP-43 affects Drosophila motoneurons terminal synapsis and locomotive behavior. *FEBS Lett*. 583: 1586–92.

Feneberg E, Oeckl P, Steinacker P, Verde F, Barro C, Van Damme P, Gray E, Grosskreutz J, Jardel C, Kuhle J, Koerner S, Lamari F, Amador MD, et al. (**2018**). Multicenter evaluation of neurofilaments in early symptom onset amyotrophic lateral sclerosis. *Neurology*. 90: e22–30.

Fenster SD and Garner CC. (**2002**). Gene structure and genetic localization of the PCLO gene encoding the presynaptic active zone protein Piccolo. *Int J Dev Neurosci*. 20:161–71.

Fenster SD, Chung WJ, Zhai R, Cases-Langhoff C, Voss B, Garner AM, Kaempf U, Kindler S, Gundelfinger ED, Garner CC. (**2000**). Piccolo, a presynaptic zinc finger protein structurally related to bassoon. *Neuron*. 25: 203 – 14.

Ferguson TA and Elman LB. (**2007**). Clinical presentation and diagnosis of amyotrophic lateral sclerosis. *NeuroRehabilitation.* 22(6):409-16.

Fernández-Vizarra E. and Zeviani M. (**2015**). Nuclear gene mutations as the cause of mitochondrial complex III deficiency. *Front Genet*. Apr 9; 6:134.

Ferraiuolo L., Kirby J, Grierson AJ, Sendtner M, Shaw PJ. (**2011**). Molecular pathways of motor neuron injury in amyotrophic lateral sclerosis. *Nat. Rev. Neurol*. Nov; 7(11): 616-30.

Ferrante KL, Shefner J, Zhang H, Betensky R, O'Brien M, Yu H, et al. (**2005**). Tolerance of high-dose (3,000 mg/day) coenzyme Q10 in ALS. *Neurology* 65:1834-1836.

Ferrante RJ, Browne SE, Shinobu LA, Bowling AC, Baik MJ, MacGarvey U, Kowall NW, Brown RH Jr, Beal MF. (**1997**). Evidence of increased oxidative damage in both sporadic and familial amyotrophic lateral sclerosis. *J. Neurochem*. Nov; 69(5): 2064-74.

Ferrari R, Kapogiannis D, Huey ED, Momeni P. (**2011**). FTD and ALS: a tale of two diseases. *Curr Alzheimer Res.* May; 8(3): 273-94.

Ferrer I. (**1992**). Dementia of frontal lobe type and amyotrophy. *Behav Neurol*. 5: 87–96.

Ferrer I. (**1999**). Neurons and their dendrites in frontotemporal dementia. *Dement Geriatr Cogn Disord*. 10 (Suppl 1): 55–60.

Ferrer I. (**2017**). Diversity of astroglial responses across human neurodegenerative disorders and brain aging. *Brain Pathol*. 27: 645-674.

Ferrer I. (**2018**). Oligodendrogliopathy in neurodegenerative diseases with abnormal protein aggregates: The forgotten partner. *Prog Neurobiol.* Oct; 169: 24-54.

Fields RD. and Stevens-Graham B. (**2002**). New insights into neuron-glia communication. *Science*. Oct 18; 298(5593): 556-62.

Figlewicz DA, Krizus A, Martinoli MG, Meininger V, Dib M, Rouleau GA, Julien JP. (**1994**). Variants of the heavy neurofilament subunit are associated with the development of amyotrophic lateral sclerosis. *Hum Mol Genet.* 3: 1757–61.

Fitzmaurice PS, Shaw IC, Kleiner HE, Miller RT, Monks TJ, Lau SS, Mitchell JD, Lynch PG. (**1996**). Evidence for DNA damage in amyotrophic lateral sclerosis. *Muscle Nerve*. Jun; 19(6): 797-8.

Fonović M. and Turk B. (**2014**). Cysteine cathepsins and extracellular matrix degradation. *Biochim Biophys Acta*. 1840:2560–70.

Forman MS, Farmer J, Johnson JK, Clark CM, Arnold SE, Coslett HB, Chatterjee A, Hurtig HI, Karlawish JH, Rosen HJ, Van Deerlin V, Lee VM, Miller BL, Trojanowski JQ, Grossman M. (**2006**). Frontotemporal dementia: clinicopathological correlations. *Ann Neurol*. Jun; 59(6): 952-62.

Forman MS, Mackenzie IR, Cairns NJ, Swanson E, Boyer PJ, Drachman DA, Jhaveri BS, Karlawish JH, Pestronk A, Smith TW, Tu PH, Watts GD, Markesbery WR, Smith CD, Kimonis VE. (**2006**). Novel ubiquitin neuropathology in frontotemporal dementia with valosin-containing protein gene mutations. *J Neuropathol Exp Neurol*. Jun; 65(6): 571-81.

Fornai F, Longone P, Cafaro L, Kastsiuchenka O, Ferrucci M, Manca ML, et al. (**2008**). Lithium delays progression of amyotrophic lateral sclerosis. *Proc. Natl. Acad. Sci. U.S.A.* 105: 2052–2057.

Foth BJ, Goedecke MC, Soldati D. (**2006**). New insights into myosin evolution and classification. *Proc. Natl. Acad. Sci. USA*. Mar 7; 103(10): 3681-6.

Frago LM. and Chowen JA. (**2017**). Involvement of Astrocytes in Mediating the Central Effects of Ghrelin. *Int J Mol Sci.* Mar; 18(3): 536.

Frank E. (**2009**). A new class of spinal interneurons: The origin and function of C-bouton solved. *Neuron* 64: 593–5.

Frank-Cannon TC, Alto LT, McAlpine FE, Tansey MG. (**2009**). Does neuroinflammation fan the flame in neurodegenerative diseases? *Mol Neurodegener*. Nov 16; 4: 47.

Fray AE, Ince PG, Banner SJ, Milton ID, Usher PA, Cookson MR, Shaw PJ. (**1998**). The expression of the glial glutamate transporter protein EAAT2 in motor neuron disease: an immunohistochemical study. *Eur J Neurosci*. Aug; 10(8): 2481-9.

Freibaum BD, Lu Y, Lopez-Gonzalez R, Kim NC, Almeida S, Lee KH, Badders N, Valentine M, Miller BL, Wong PC, Petrucelli L, Kim HJ, Gao FB, Taylor JP. (**2015**). GGG GCC repeat expansion in C9orf72 compromises nucleocytoplasmic transport. *Nature* 525: 129-133.

Frey D, Schneider C, Xu L, Borg J, Spooren W, Caroni P. (**2000**). Early and selective loss of neuromuscular synapse subtypes with low sprouting competence in motoneuron diseases. *J Neurosci*. Apr 1; 20(7): 2534-42.

Frick P, Sellier C, Mackenzie IRA, Cheng CY, Tahraoui-Bories J, Martinat C, Pasterkamp RJ, Prudlo J, Edbauer D, Oulad-Abdelghani M, Feederle R, Charlet-Berguerand N, Neumann M. (**2018**). Novel antibodies reveal presynaptic localization of C9orf72 protein and reduced protein levels in C9orf72 mutation carriers. *Acta Neuropathol Commun* 6: 72.

Friedman JR. and Nunnari J. (**2014**). Mitochondrial form and function. *Nature.* Jan 16; 505(7483): 335-43.

Friedman LK. (**2006**). Calcium: a role for neuroprotection and sustained adaptation. *Mol Interv*. Dec; 6(6): 315-29.

Fujii R, Okabe S, Urushido T, Inoue K, Yoshimura A, Tachibana T, Nishikawa T, Hicks GG, Takumi T. (**2005**). The RNA binding protein TLS is translocated to dendritic spines by mGluR5 activation and regulates spine morphology. *Curr Biol*. Mar 29; 15(6): 587-93. doi: 10.1016/j.cub.2005.01.058 10.1016/j.cub.2005.01.058.

Fujita K, Yamauchi M, Shibayama K, Ando M, Honda M, Nagata Y. (**1996**). Decreased cytochrome c oxidase activity but unchanged superoxide dismutase and glutathione peroxidase activities in the spinal cords of patients with amyotrophic lateral sclerosis. *J Neurosci Res*. Aug 1; 45(3): 276-81.

Fujita Y, Mizuno Y, Takatama M, Okamoto K. (**2008**). Anterior horn cells with abnormal TDP-43 immunoreactivities show fragmentation of the Golgi apparatus in ALS. *J Neurol Sci* Jun 15; 269(1-2): 30-4.

Gallart-Palau X, Tarabal O, Casanovas A, et al. (**2014**). Neuregulin-1 is concentrated in the postsynaptic subsurface cistern of C-bouton inputs to motoneurons and altered during motoneuron diseases. *FASEB J* 28: 3618–32.

Gami P, Murray C, Schottlaender L, Bettencourt C, De Pablo Fernandez E, Mudanohwo E, Mizielinska S, Polke JM, Holton JL, Isaacs AM, Houlden H, Revesz T, Lashley T. (**2015**). A 30-unit hexanucleotide repeat expansion in C9orf72 induces

pathological lesions with dipeptide-repeat proteins and RNA foci, but not TDP-43 inclusions and clinical disease. *Acta Neuropathol.* Oct; 130(4): 599-601.

Gao FB, Almeida S, Lopez-Gonzalez R. (**2017**). Dysregulated molecular pathways in amyotrophic lateral sclerosis–frontotemporal dementia spectrum disorder. *EMBO J.* 36: 2931-2950.

Gendron TF and Petrucelli L. (**2011**). Rodent models of TDP-43 proteinopathy: investigating the mechanisms of TDP-43-mediated neurodegeneration. *J Mol Neurosci*. Nov; 45(3): 486-99.

Gendron TF, Bieniek KF, Zhang YJ, Jansen-West K, Ash PE, Caulfield T, Daughrity L, Dunmore JH, Castanedes-Casey M, Chew J, Cosio DM, van Blitterswijk M, Lee WC, Rademakers R, Boylan KB, Dickson DW, Petrucelli L. (**2013**). Antisense transcripts of the expanded C9ORF72 hexanucleotide repeat form nuclear RNA foci and undergo repeat-associated non-ATG translation in c9FTD/ALS. *Acta Neuropathol*. Dec; 126(6): 829-44.

Genin EC, Plutino M, Bannwarth S, Villa E, Cisneros-Barroso E, Roy M, Ortega-Vila, B, Fragaki, K., Lespinasse F, Pinero-Martos E, Augé G, Moore D, Burté F, Lacas-Gervais S, Kageyama Y, Itoh K, Yu-Wai-Man P, Sesaki H, Ricci JE, Vives-Bauza C, Paquis-Flucklinger V. (**2015**). CHCHD10 mutations promote loss of mitochondrial cristae junctions with impaired mitochondrial genome maintenance and inhibition of apoptosis. *EMBO Mol. Med*. Jan; 8(1): 58–72.

Geser F, Martinez-Lage M, Robinson J, Uryu K, Neumann M, Brandmeir NJ, Xie SX, Kwong LK, Elman L, McCluskey L, Clark CM, Malunda J, Miller BL, Zimmerman EA, Qian J, Van Deerlin V, Grossman M, Lee VM, Trojanowski JQ. (**2009**). Clinical and pathological continuum of multisystem TDP-43 proteinopathies. *Arch Neurol*. Feb; 66(2): 180-9.

Geser F, Prvulovic D, O'Dwyer L, Hardiman O, Bede P, Bokde AL, Trojanowski JQ, Hampel H. (**2011**). On the development of markers for pathological TDP-43 in amyotrophic lateral sclerosis with and without dementia. *Prog Neurobiol.* Dec; 95(4): 649–662.

Gijselinck I, Van Broeckhoven C, Cruts M. (**2008**). Granulin mutations associated with frontotemporal lobar degeneration and related disorders: an update. *Hum Mutat*. Dec; 29(12): 1373-86.

Gijselinck I, Van Langenhove T, van der Zee J, Sleegers K, Philtjens S, Kleinberger G, Janssens J, Bettens K, Van Cauwenberghe C, Pereson S, Engelborghs S, Sieben A, De Jonghe P, Vandenberghe R, Santens P, De Bleecker J, Maes G, Bäumer V, Dillen L, Joris G, Cuijt I, Corsmit E, Elinck E, Van Dongen J, Vermeulen S, Van den Broeck M, Vaerenberg C, Mattheijssens M, Peeters K, Robberecht W, Cras P, Martin JJ, De Deyn PP, Cruts M, Van Broeckhoven C. (**2012**). A C9orf72 promoter repeat expansion in a Flanders-Belgian cohort with disorders of the frontotemporal lobar degeneration-amyotrophic lateral sclerosis spectrum: a gene identification study. *Lancet Neurol*. Jan; 11(1): 54-65.

Ginhoux F, Lim S, Hoeffel G, Low D, Huber T. (**2013**). Origin and differentiation of microglia. *Front Cell Neurosci*. Apr 17; 7:45.

Giordana MT, Piccinini M, Grifoni S, De Marco G, Vercellino M, Magistrello M, Pellerino A, Buccinnà B, Lupino E, Rinaudo MT. (**2010**). TDP-43 redistribution is an early event in sporadic amyotrophic lateral sclerosis. *Brain Pathol*. Mar; 20(2): 351-60.

Glick D, Barth S, Macleod KF. (**2010**). Autophagy: cellular and molecular mechanisms. *J. Pathol*. May; 221(1): 3-12.

Glickman MH. and Ciechanover A. (**2002**) The Ubiquitin-Proteasome Proteolytic Pathway: Destruction for the Sake of Construction. *Physiol. Rev*. Apr; 82(2): 373-428.

Godena, VK, Romano G, Romano M, Appocher C, Klima R, Buratti E, Baralle FE, Feiguin F. (**2011**). TDP-43 regulates Drosophila neuromuscular junctions growth by modulating Futsch/MAP1B levels and synaptic microtubules organization. *PloS one*. 6(3): e17808.

Goetz CG. (**2000**). Amyotrophic lateral sclerosis: early contributions of Jean-Martin Charcot. *Muscle Nerve*. Mar; 23(3): 336-43.

Golgi C. (**1873**). On structure of the gray matter of the brain. *Gazzetta Medica Italiana-Lombardia*. 33(6): 244–6.

Golgi C. (**1903**). (Vol. I-III). Opera Omnia. *Hoepli Editore*. Milano, (Italy).

Gomez-Deza J, Lee YB, Troakes C, Nolan M, Al-Sarraj S, Gallo JM, Shaw CE. (**2015**). Dipeptide repeat protein inclusions are rare in the spinal cord and almost absent from motor neurons in C9ORF72 mutant amyotrophic lateral sclerosis and are unlikely to cause their degeneration. *Acta Neuropathol. Commun*. Jun 25; 3:38.

Gordon P, Moore D, Miller R, Florence J, Verheijde J, Doorish C, et al. (**2007**). Efficacy of minocycline in patients with amyotrophic lateral sclerosis: a phase III randomised trial. *Lancet Neurol.* 6: 1045-1053.

Gordon PH, Doorish C, Montes J, Mosley RL, Mosely RL, Diamond B, et al. (**2006**). Randomized controlled phase II trial of glatiramer acetate in ALS. *Neurology* 66 1117–1119.

Gordon PH, Moore DH, Gelinas DF, Qualls C, Meister ME, Werner J, et al. (**2004**). Placebo-controlled phase I/II studies of minocycline in amyotrophic lateral sclerosis. *Neurology* 62: 1845–1847.

Gordon S. (**2003**). Alternative activation of macrophages. *Nat Rev Immunol*. Jan; 3(1): 23-35. doi: 10.1038/nri978.

Graffmo KS, Forsberg K, Bergh J, Birve A, Zetterström P, Andersen PM, Marklund SL, Brännström T. (**2012**). Expression of wild-type human superoxide dismutase-1 in mice causes amyotrophic lateral sclerosis. *Hum. Mol. Genet.* Jan 1; 22(1): 51-60.

Graves MC, Fiala M, Dinglasan LA, Liu NQ, Sayre J, Chiappelli F, et al. (**2004**). Inflammation in amyotrophic lateral sclerosis spinal cord and brain is mediated by activated macrophages, mast cells and T cells. *Amyotroph Lateral Scler Other Motor Neuron Disord.* 5: 213–9.

Greenway MJ, Andersen PM, Russ C, Ennis S, Cashman S, Donaghy C, Patterson V, Swingler R, Kieran D, Prehn J, Morrison KE, Green A, Acharya KR, Brown RH Jr, Hardiman O. (**2006**). ANG mutations segregate with familial and 'sporadic' amyotrophic lateral sclerosis. *Nat Genet*. Apr; 38(4): 411-3.

Griffiths I, Klugmann M, Anderson T, Yool D, Thomson C, Schwab MH, Schneider A, Zimmermann F, McCulloch M, Nadon N, Nave KA. (**1998**). Axonal swellings and degeneration in mice lacking the major proteolipid of myelin. *Science.* 280: 1610–13.

Groeneveld GJ, Veldink JH, van der Tweel I, Kalmijn S, Beijer C, de Visser M, et al. (**2003**). A randomized sequential trial of creatine in amyotrophic lateral sclerosis. *Ann. Neurol*. 53: 437–445.

Guo H, Lai L, Butchbach ME, Stockinger MP, Shan X, Bishop GA, Lin CL. (**2003**). Increased expression of the glial glutamate transporter EAAT2 modulates excitotoxicity and delays the onset but not the outcome of ALS in mice. *Hum Mol Genet*. Oct 1; 12(19): 2519-32.

Gurney ME, Pu H, Chiu AY, Dal Canto MC, Polchow CY, Alexander DD, Caliendo J, Hentati A, Kwon YW, Deng HX. (**1994**). Motor neuron degeneration in mice that express a human Cu, Zn superoxide dismutase mutation. *Science*. Jun 17; 264(5166): 1772-5.

Hafezparast M, Klocke R, Ruhrberg C, Marquardt A, Ahmad-Annuar A, Bowen S, Lalli G, Witherden AS, Hummerich H, Nicholson S, Morgan PJ, Oozageer R, Priestley JV, Averill S, King VR, Ball S, Peters J, Toda T, Yamamoto A, Hiraoka Y, Augustin M, Korthaus D, Wattler S, Wabnitz P, Dickneite C, Lampel S, Boehme F, Peraus G, Popp A, Rudelius M, Schlegel J, Fuchs H, Hrabe de Angelis M, Schiavo G, Shima DT, Russ AP, Stumm G, Martin JE, Fisher EM. (**2003**). Mutations in dynein link motor neuron degeneration to defects in retrograde transport. *Science*. May 2; 300(5620): 808-12.

Haidet-Phillips AM, Hester ME, Miranda CJ, Meyer K, Braun L, Frakes A, Song S, Likhite S, Murtha MJ, Foust KD, Rao M, Eagle A, Kammesheidt A, Christensen A, Mendell JR, Burghes AH, Kaspar BK. (**2011**). Astrocytes from familial and sporadic ALS patients are toxic to motor neurons. *Nat Biotechnol*. Aug 10; 29(9): 824-8.

Hakim S, Bertucci MC, Conduit SE, Vuong DL, Mitchell CA. (**2012**). Inositol polyphosphate phosphatases in human disease. *Curr Top Microbiol Immunol*. 362:247–314.

Hall ED, Oostveen JA, Gurney ME. (**1998**). Relationship of microglial and astrocytic activation to disease onset and progression in a transgenic model of familial ALS. *Glia*. Jul; 23(3): 249-56.

Hallermann S, Fejtova A, Schmidt H, Weyhersmüller A, Silver RA, Gundelfinger ED, Eilers J. (**2010**). Bassoon speeds vesicle reloading at a central excitatory synapse. *Neuron*. 68: 710–23.

Hammer RP, Tomiyasu U, Scheibel AB. (**1979**). Degeneration of the human Betz cell due to amyotrophic lateral sclerosis. *Exp Neurol.* Feb; 63(2): 336-46.

Hart MN, Cancilla PA, Frommes S, Hirano A. (**1977**). Anterior horn cell degeneration and Bunina-type inclusions associated with dementia. *Acta Neuropathol.* Jun 15; 38(3): 225-8.

Hasegawa M. (**2017**). FTLD-TDP-43 and FTLD-FUS. *Alzheimers Dement*. Jul; 13(7): P892.

He L. and Hannon GJ. (**2004**). MicroRNAs: small RNAs with a big role in gene regulation. *Nat. Rev. Genet*. 5 Jul; 5(7): 522-31.

He Z, Ong CH, Halper J, Bateman A. (**2003**). Progranulin is a mediator of the wound response. *Nat Med*. Feb; 9(2): 225-9.

He Z. and Bateman A. (**2003**). Progranulin (granulin-epithelin precursor, PC-cell-derived growth factor, acrogranin) mediates tissue repair and tumorigenesis. *J Mol Med (Berl)*. Oct; 81(10): 600-12.

Heiman-Patterson TD, Sher RB, Blankenhorn EA, Alexander G, Deitch JS, Kunst CB, Maragakis N, Cox G. (**2011**). Effect of genetic background on phenotype variability in transgenic mouse models of amyotrophic lateral sclerosis: a window of opportunity in the search for genetic modifiers. *Amyotroph Lateral Scler.* Mar; 12(2): 79-86.

Hellstrom J, Arvidsson U, Elde R, et al. (**1999**). Differential expression of nerve terminal protein isoforms in VAChT-containing varicosities of the spinal cord ventral horn. *J Comp Neurol* 411: 578–90.

Hendrickx DAE, van Eden CG, Schuurman KG, Hamann J, Huitinga I. (**2017**). Staining of HLA-DR, Iba1 and CD68 in human microglia reveals partially overlapping expression depending on cellular morphology and pathology. *J Neuroimmunol*. Aug 15; 309: 12-22.

Henkel JS, Beers DR, Wen S, Rivera AL, Toennis KM, Appel JE, Zhao W, Moore DH, Powell SZ, Appel SH. (**2013**). Regulatory T-lymphocytes mediate amyotrophic lateral sclerosis progression and survival. *EMBO Mol Med*. 5: 64–79.

Henkel JS, Engelhardt JI, Siklós L, Simpson EP, Kim SH, Pan T, et al. (**2004**). Presence of dendritic cells, MCP-1, and activated microglia/macrophages in amyotrophic lateral sclerosis spinal cord tissue. *Ann Neurol* 55: 221–35.

Herrmann D. and Parlato R. (**2018**). C9orf72-associated neurodegeneration in ALS-FTD: Breaking newground in ribosomal RNA and nucleolar dysfunction. *Cell Tissue Res* 373: 351-360.

Herron LR. and Miles GB. (**2012**). Gender-specific perturbations in modulatory inputs to motoneurons in a mouse model of amyotrophic lateral sclerosis. *Neuroscience* 226: 313–23.

Hershko A. and Ciechanover A. (**1998**). The ubiquitin system. *Annu Rev Biochem*. 67: 425-79.

Hetz C, Thielen P, Matus S, Nassif M, Court F, Kiffin R, Martinez G, Cuervo AM, Brown RH, Glimcher LH. (**2009**). XBP-1 deficiency in the nervous system protects against amyotrophic lateral sclerosis by increasing autophagy. *Genes Dev*. Oct 1; 23(19): 2294-306.

Hicks GG, Singh N, Nashabi A, Mai S, Bozek G, Klewes L, Arapovic D, White EK, Koury MJ, Oltz EM, Van Kaer L, Ruley HE. (**2000**). Fus deficiency in mice results in defective B-lymphocyte development and activation, high levels of chromosomal instability and perinatal death. *Nat Genet*. Feb; 24(2): 175-9.

Higashi S, Kabuta T, Nagai Y, Tsuchiya Y, Akiyama H, Wada K. (**2013**). TDP-43 associates with stalled ribosomes and contributes to cell survival during cellular stress. *J Neurochem*. Jul; 126(2): 288-300.

Hipp MS, Park SH, Hartl FU. (**2014**). Proteostasis impairment in protein-misfolding and -aggregation diseases. *Trends Cell Biol.* Sep; 24(9): 506-14.

Hirokawa N, Niwa S, Tanaka Y. (**2010**). Molecular motors in neurons: transport mechanisms and roles in brain function, development, and disease. *Neuron*. Nov 18; 68(4): 610-38.

Hirokawa N, Noda Y, Tanaka Y, Niwa S. (**2009**). Kinesin superfamily motor proteins and intracellular transport. *Nat Rev Mol Cell Biol*. Oct; 10(10): 682-96.

Hirokawa N, Sato-Yoshitake R, Kobayashi N, Pfister KK, Bloom GS, Brady ST. (**1991**). Kinesin associates with anterogradely transported membranous organelles in vivo. *J Cell Biol*. Jul; 114(2): 295-302.

Hirokawa N, Sato-Yoshitake R, Yoshida T, Kawashima T. (**1990**). Brain dynein (MAP1C) localizes on both anterogradely and retrogradely transported membranous organelles in vivo. *J Cell Biol*. Sep; 111(3): 1027-37.

Hirokawa N. (**1998**). Kinesin and dynein superfamily proteins and the mechanism of organelle transport. *Science*. Jan 23; 279(5350): 519-26.

Hirokawa N. and Noda Y. (**2008**). Intracellular transport and kinesin superfamily proteins, KIFs: Structure, function, and dynamics. *Physiol Rev*. Jul; 88(3): 1089-118.

Hirtz D, Thurman DJ, Gwinn-Hardy K, Mohamed M, Chaudhuri AR, Zalutsky R. (**2007**). How common are the "common" neurologic disorders? *Neurology*. Jan 30; 68(5): 326-37.

Hodges JR, Davies R, Xuereb J, Kril J, Halliday G. (**2003**). Survival in frontotemporal dementia. *Neurology*. Aug 12; 61(3): 349-54.

Hodges JR. and Patterson K. (**2007**). Semantic dementia: a unique clinicopathological syndrome. *Lancet Neurol*. Nov; 6(11): 1004-14.

Holm IE, Englund E, Mackenzie IR, Johannsen P, Isaacs AM. (**2007**). A reassessment of the neuropathology of frontotemporal dementia linked to chromosome 3. *J Neuropathol Exp Neurol*. Oct; 66(10): 884-91.

Holmøy T. (**2008**). T cells in amyotrophic lateral sclerosis. *Eur J Neuro*l. Apr; 15(4): 360-6.

Hooten KG, Beers DR, Zhao W, Appel SH. Protective and toxic neuroinflammation in amyotrophic lateral sclerosis. *Neurotherapeutics*. 2015; 12:364–75.

Hortobagyi T. and Cairns NJ. (**2015**). Amyotrophic lateral sclerosis and frontotemporal lobar degeneration. In: Kovacs Gabor G, eds. Neuropathology of Neurodegenerative Diseases: A Practical Guide. *Cambridge: Cambridge University Press*: 209–48.

Hosler BA, Siddique T, Sapp PC, Sailor W, Huang MC, Hossain A, Daube JR, Nance M, Fan C, Kaplan J, Hung WY, McKenna-Yasek D, Haines JL, Pericak-Vance MA, Horvitz HR, Brown RH Jr. (**2000**). Linkage of familial amyotrophic lateral sclerosis with frontotemporal dementia to chromosome 9q21-q22. *JAMA*. Oct 4; 284(13): 1664-9.

Howland DS, Liu J, She Y, Goad B, Maragakis NJ, Kim B, Erickson J, Kulik J, DeVito L, Psaltis G, DeGennaro LJ, Cleveland DW, Rothstein JD. (**2002**). Focal loss of the glutamate transporter EAAT2 in a transgenic rat model of SOD1 mutant mediated amyotrophic lateral sclerosis (ALS). *Proc Natl Acad Sci USA.* Feb 5; 99(3): 1604-9.

Hristovska, I. and Pascual O. (**2016**). Deciphering resting microglial morphology and process motility from a synaptic prospect. *Front Integr Neurosci*. Jan 19; 9: 73.

Hu R, Cai WQ, Wu XG, Yang Z. (**2007**). Astrocyte-derived estrogen enhances synapse formation and synaptic transmission between cultured neonatal rat cortical neurons. *Neuroscience*. Feb 23; 144(4): 1229-40.

Hua S. (**2013**). Targeting sites of inflammation: intercellular adhesion molecule-1 as a target for novel inflammatory therapies. *Front Pharmacol.* 4: 127.

Hung CW, Chen YC, Hsieh WL, Chiou SH, Kao CL. (**2010**). Ageing and neurodegenerative diseases. *Ageing Res Rev*. 9 Suppl 1:S36-46.

Hyman AA, Weber CA, Jülicher F. (**2014**). Liquid-liquid phase separation in biology. *Annu. Rev. Cell Dev. Biol*. 30, 39–58.

Ikenaka K, Katsuno M, Kawai K, Ishigaki S, Tanaka F, Sobue G. (**2012**). Disruption of axonal transport in motor neuron diseases. *Int J Mol Sci*. 13(1): 1225-38.

Ilieva EV, Ayala V, Jove M, Dalfo E, Cacabelos D, Povedano M, Bellmunt MJ, Ferrer I, Pamplona R, Portero-Otin M. (**2007**). Oxidative and endoplasmic reticulum stress interplay in sporadic amyotrophic lateral sclerosis. *Brain* 130: 3111-3123.

Illán-Gala I, Alcolea D, Montal V, Dols O, Muñoz L, de Luna N, Turón-Sans J, Cortés-Vicente E, Sánchez-Saudinós B, Subirana A, Sala I, Blesa R, Clarimón J, et al. (**2017**). CSF sAPPβ, YKL-40, and NfL along the ALS-FTD spectrum. *Neurology*. 89:178-88.

Inaba Y, Shinohara K, Botilde Y, et al. (**2016**). Transport of the outer dynein arm complex to cilia requires a cytoplasmic protein Lrrc6. *Genes Cells* 21: 728–39.

Ince PG, Highley JR, Wharton SB. (**2015**). Motor neuron disorders. In: Love S, Budka H, Ironside JW, Perry A, eds. Greenfield's Neuropathology. 9th edn. Boca Raton: CRC Press, Taylor and Francis Group. 817–48.

Ince PG, Stout N, Shaw P, Slade J, Hunziker W, Heizmann CW, Baimbridge KG. (**1993**). Parvalbumin and calbindin D-28k in the human motor system and in motor neuron disease. *Neuropathol Appl Neurobiol*. Aug; 19(4):291-9.

Ipata PL, Camici M, Micheli V, et al. (**2011**). Metabolic network of nucleosides in the brain. *Curr Top Med Chem*. 11: 902–22.

Iribarren P, Zhou Y, Hu J, Le Y, Wang JM. Role of formyl peptide receptor-like 1 (FPRL1/FPR2) in mononuclear phagocyte responses in Alzheimer disease. (**2005**) *Immunol Res*. 31:165–76.

Isaacs JD, Dean AF, Shaw CE, Al-Chalabi A, Mills KR, Leigh PN. (**2007**). Amyotrophic lateral sclerosis with sensory neuropathy: part of a multisystem disorder? *J Neurol Neurosurg Psychiatry*. Jul; 78(7): 750-3. doi: 10.1136/jnnp.2006.098798.

Ishibashi T, Dakin KA, Stevens B, Lee PR, Kozlov SV, Stewart CL, Fields RD. (**2006**). Astrocytes promote myelination in response to electrical impulses. *Neuron*. Mar 16; 49(6): 823-32.

Izumikawa K, Nobe Y, Yoshikawa H, Ishikawa H, Miura Y, Nakayama H, Nonaka T, Hasegawa M, Egawa N, Inoue H, Nishikawa K, Yamano K, Simpson RJ, Taoka M, Yamauchi Y, Isobe T Takahashi N. (**2017**). TDP-43 stabilises the processing intermediates of mitochondrial transcripts. *Scientific reports.* 7(1): 7709.

Jaarsma D, Haasdijk ED, Grashorn JA, Hawkins R, van Duijn W, Verspaget HW, London J, Holstege JC. (**2000**). Human Cu/Zn superoxide dismutase (SOD1) overexpression in mice causes mitochondrial vacuolization, axonal degeneration, and premature motoneuron death and accelerates motoneuron disease in mice expressing a familial amyotrophic lateral sclerosis mutant SOD1 *Neurobiol Dis*. Dec; 7(6 Pt B): 623-43.

Jaarsma D. (**2006**). Swelling and vacuolisation of mitochondria in transgenic SOD1–ALS mice: a consequence of supranormal SOD1 expression? *Mitochondrion*. Feb; 6(1): 48-9; author reply 50-1.

Jaffe KM, Grimes DT, Schottenfeld-Roames J, et al. (**2016**). c21orf59/kurly controls both cilia motility and polarization. *Cell Rep* 14: 1841–9.

Jahn O, Tenzer S, Werner HB. (**2009**). Myelin proteomics: molecular anatomy of an insulating sheath. *Mol. Neurobiol*. Aug; 40(1): 55-72.

Jäkel S. and Dimou L. (**2017**). Glial cells and their function in the adult brain: A journey through the history of their ablation. *Front Cell Neurosci*. Feb 13; 11: 24.

Jawdat O, Statland JM, Barohn RJ, Katz JS, Dimachkie MM. (**2015**). Amyotrophic lateral sclerosis regional variants (Brachial Amyotrophic Diplegia, Leg Amyotrophic Diplegia and Isolated Bulbar Amyotrophic Lateral Sclerosis). *Neurol Clin.* Nov; 33(4): 775–785.

Jellinger KA. (**2010**). Basic mechanisms of neurodegeneration: a critical update. *J Cell Mol Med*. 14(3):457-87.

Jha R. and Surrey T. (**2015**). Regulation of processive motion and microtubule localization of cytoplasmic dynein. *Biochem Soc Trans.* 43: 48–57.

Jiang YM, Yamamoto M, Kobayashi Y, Yoshihara T, Liang Y, Terao S, Takeuchi H, Ishigaki S, Katsuno M, Adachi H, Niwa J, Tanaka F, Doyu M, Yoshida M, Hashizume Y, Sobue G. (**2005**). Gene expression profile of spinal motor neurons in sporadic amyotrophic lateral sclerosis. *Ann. Neurol.* Feb; 57(2): 236-51.

Jiang YM, Yamamoto M, Tanaka F, Ishigaki S, Katsuno M, Adachi H, Niwa J, Doyu M, Yoshida M, Hashizume Y, Sobue G. (**2007**). Gene expressions specifically detected in motor neurons (dynactin-1, early growth response 3, acetyl-coa transporter, death receptor 5, and cyclin c) differentially correlate to pathologic markers in sporadic amyotrophic lateral sclerosis. *J. Neuropathol. Exp. Neurol*. Jul; 66(7): 617-27.

Johann S, Heitzer M, Kanagaratnam M, Goswami A, Rizo T, Weis J, et al. (**2015**). NLRP3 inflammasome is expressed by astrocytes in the SOD1 mouse model of ALS and in human sporadic ALS patients. *Glia*. 63: 2260–73.

Johnson JK, Diehl J, Mendez MF, Neuhaus J, Shapira JS, Forman M, Chute DJ, Roberson ED, Pace-Savitsky C, Neumann M, Chow TW, Rosen HJ, Forstl H, Kurz A, Miller BL. (**2005**). Frontotemporal lobar degeneration: demographic characteristics of 353 patients. *Arch Neurol*. Jun; 62(6): 925-30.

Johnston JA, Dalton MJ, Gurney ME, Kopito RR. (**2000**). Formation of high molecular weight complexes of mutant Cu, Zn-superoxide dismutase in a mouse model for familial amyotrophic lateral sclerosis. *Proc Natl Acad Sci USA*. Nov 7; 97(23): 12571-6.

Jonckheere AI, Smeitink JA, Rodenburg RJ. (**2012**). Mitochondrial ATP synthase: architecture, function and pathology. *J Inherit Metab Dis*. Mar; 35(2): 211-25.

Josephs KA, Stroh A, Dugger B, Dickson DW. (**2009**). Evaluation of subcortical pathology and clinical correlations in FTLD-U subtypes. *Acta Neuropathol*. Sep; 118(3): 349-58.

Jovicic A, Mertens J, Boeynaems S, Bogaert E, Chai N, Yamada SB, Paul JW 3rd, Sun S, Herdy JR, Bieri G, Kramer NJ, Gage FH, Van Den Bosch L, Robberecht W, Gitler AD. (**2015**). Modifiers of C9orf72 dipeptide repeat toxicity connect nucleo-cytoplasmic transport defects to FTD/ALS. *Nat Neurosci* 18: 1226-1229.

Julien JP. (**1997**). Neurofilaments and motor neuron disease. *Trends Cell Biol*. Jun; 7(6): 243-9.

Jung J. and Behrends C. (**2017**). Multifaceted role of SMCR8 as autophagy regulator. *Small GTPases* 1: 1-9.

Kabashi E, Agar JN, Strong MJ, Durham HD. (**2012**). Impaired proteasome function in sporadic amyotrophic lateral sclerosis. *Amyotroph. Lateral Scler*. Jun; 13(4): 367-71.

Kamiya R. (**2002**). Functional diversity of axonemal dyneins as studied in Chlamydomonas mutants. *Int. Rev. Cytol*. 219: 115-55.

Kang SH, Li Y, Fukaya M, Lorenzini I, Cleveland DW, Ostrow LW, Rothstein JD, Bergles DE. (**2013**). Degeneration and impaired regeneration of gray matter oligodendrocytes in amyotrophic lateral sclerosis. *Nat Neurosci*. May; 16(5): 571-9.

Karki S. and Holzbaur EL. (**1999**). Cytoplasmic dynein and dynactin in cell division and intracellular transport. *Curr. Opin. Cell Biol.* Feb; 11(1):45-53.

Kasama-Yoshida H, Tohyama Y, Kurihara T, Sakuma M, Kojima H, Tamai Y. (**1997**). A comparative study of 2', 3'- cyclic-nucleotide 3'-phosphodiesterase in vertebrates: cDNA cloning and amino acid sequences for chicken and bullfrog enzymes. *J Neurochem*. 69: 1335–42.

Kasarskis EJ, Shefner JM, Miller R. (**1999**). A controlled trial of recombinant methionyl human BDNF in ALS: the BDNF study group (phase III). *Neurology* 52: 1427-1433.

Kassubek J, Unrath A, Huppertz HJ, Lulé D, Ethofer T, Sperfeld AD, Ludolph AC. (**2005**). Global brain atrophy and corticospinal tract alterations in ALS, as investigated by voxel-based morphometry of 3-D MRI. *Amyotroph Lateral Scler Other Motor Neuron Disord*. Dec; 6(4): 213-20.

Kaufmann P, Thompson JLP, Levy G, Buchsbaum R, Shefner J, Krivickas LS, et al. (**2009**). Phase II trial of CoQ10 for ALS finds insufficient evidence to justify phase III. *Ann. Neurol*. 66: 235–244.

Kaus A. and Sareen D. (**2015**). ALS Patient stem cells for unveiling disease signatures of motoneuron susceptibility: Perspectives on the deadly mitochondria, ER stress and calcium triad. *Front Cell Neurosci* 9: 448.

Kawahara Y. and Mieda-Sato A. (**2012**). TDP-43 promotes microRNA biogenesis as a component of the Drosha and Dicer complexes. *Proc Natl Acad Sci USA*. Feb 28; 109(9): 3347-52.

Kawamata T, Akiyama H, Yamada T, McGeer PL. (**1992**). Immunologic reactions in amyotrophic lateral sclerosis brain and spinal cord tissue. *Am J Pathol*. Mar; 140(3): 691-707.

Kawamura Y, Dyck PJ, Shimono M, Okazaki H, Tateishi J, Doi HJ. (**1981**). Morphometric comparison of the vulnerability of peripheral motor and sensory neurons in amyotrophic lateral sclerosis. *J. Neuropathol Exp Neurol*. Nov; 40(6): 667-75.

Kettenmann H, Kirchhoff F, Verkhratsky A. (**2013**). Microglia: new roles for the synaptic stripper. *Neuron*. Jan 9; 77(1): 10-8.

Kiernan MC, Vucic S, Cheah BC, Turner MR, Eisen A, Hardiman O, Burrell JR, Zoing MC (**2011**). "Amyotrophic lateral sclerosis." *Lancet.* Mar 12; 377(9769): 942-55.

Kim SU. and de Vellis J. (**2005**). Microglia in health and disease. *J Neurosci Res*. Aug 1; 81(3): 302-13.

Kim T, Fiedler K, Madison DL, Krueger WH, Pfeiffer SE. (**1995**). Cloning and characterization of MVP17: a developmentally regulated myelin protein in oligodendrocytes. *J Neurosci Res*. 42: 413–22.

Kim VN, Han J, Siomi MC. (**2009**). Biogenesis of small RNAs in animals. *Nat. Rev. Mol. Biol*. Feb; 10(2): 126-39.

King AE, Woodhouse A, Kirkcaldie MTK, Vickers JC. (**2016**). Excitotoxicity in ALS: Overstimulation, or overreaction? *Exp Neurol*. Jan; 275 Pt 1:162-71.

Kipps CM, Hodges JR, Fryer TD, Nestor PJ. (**2009**). Combined magnetic resonance imaging and positron emission tomography brain imaging in behavioural variant frontotemporal degeneration: refining the clinical phenotype. *Brain*. Sep; 132(Pt 9): 2566-78.

Kirkinezos IG, Bacman SR, Hernandez D, Oca-Cossio J, Arias LJ, Perez-Pinzon MA, Bradley WG, Moraes CT. (**2005**). Cytochrome c association with the inner mitochondrial membrane is impaired in the CNS of G93A-SOD1 mice. *J. Neurosci*. Jan 5; 25(1): 164-72.

Kluckova K, Bezawork-Geleta A, Rohlena J, Dong L, Neuzil J. (**2013**). Mitochondrial complex II, a novel target for anti-cancer agents. *Biochim Biophys Acta*. May; 1827(5): 552-64.

Koenning M, Jackson S, Hay CM, Faux C, Kilpatrick TJ, Willingham M, Emery B. (**2012**). Myelin gene regulatory factor is required for maintenance of myelin and mature oligodendrocyte identity in the adult CNS. *J Neurosci.* 32: 12528–42.

Koga H. and Cuervo AM. (**2011**). Chaperone-mediated autophagy dysfunction in the pathogenesis of neurodegeneration. *Neurobiol. Dis*. Jul; 43(1): 29-37.

Komine O. and Yamanaka K. (**2015**). Neuroinflammation in motor neuron disease. *Nagoya J Med Sci*. Nov; 77(4): 537-49.

Kott E, Duquesnoy P, Copin B, et al. (**2017**). Loss of zinc finger MYND-type containing 10 (zmynd10) affects cilia integrity and axonemal localization of dynein arms, resulting in ciliary dysmotility, polycystic kidney and scoliosis in medaka (Oryzias latipes). *Dev Biol* 430: 69–79.

Kovacs GG, Botond G, Budka H. (**2010**). Protein coding of neurodegenerative dementias: the neuropathological basis of biomarker diagnostics. *Acta Neuropathol*. 119(4):389-408.

Kovacs GG, Lee VM, Trojanowski JQ. (**2017**). Protein astrogliopathies in human neurodegenerative diseases and aging. *Brain Pathol.* 27: 675-690.

Kovacs GG. (**2016**). Molecular pathological classification of neurodegenerative diseases: Turning towards precision medicine. *Int J Mol Sci*. Feb 2; 17(2). pii: E189.

Kramer DM, Roberts AG, Muller F, Cape J, Bowman MK. (**2004**). Q-cycle bypass reactions at the Qo site of the cytochrome bc1 (and related) complexes. *Meth. Enzymol*. 382: 21–45.

Kremerskothen J, Kindler S, Finger I, Veltel S, Barnekow A. (**2006**). Postsynaptic recruitment of Dendrin depends on both dendritic mRNA transport and synaptic anchoring. *J Neurochem*. 2006; 96:1659–66.

Kumar DR, Aslinia F, Yale SH, Mazza JJ. (**2011**). Jean-Martin Charcot: The Father of Neurology. *Clin Med Res.* Mar; 9(1): 46–49.

Kuroda S, Ishizu H, Kawai K, Otsuki S. (**1990**). Bunina bodies in dendrites of patients with amyotrophic lateral sclerosis. *Acta Med Okayama.* Feb; 44(1): 41-5.

Kursula P. (**2001**). The current status of structural studies on proteins of the myelin sheath. *Int. J. Mol. Med.* Nov; 8(5): 475-9.

Kursula P. (**2008**). Structural properties of proteins specific to the myelin sheath. *Amino Acids*, Feb; 34(2): 175-85.

Kurzepa J, Madro A, Czechowska G, Kurzepa J, Celiński K, Kazmierak W, et al. (**2014**). Role of MMP-2 and MMP-9 and their natural inhibitors in liver fibrosis, chronic pancreatitis and non-specific inflammatory bowel diseases. *Hepatobiliary Pancreat Dis Int.* 13: 570–9.

Kushner PD, Stephenson DT, Wright S. (**1991**). Reactive astrogliosis is widespread in the subcortical white matter of amyotrophic lateral sclerosis brain. *J Neuropathol Exp Neurol*. May; 50(3):263-77.

Kwan AC, Dombeck DA, Webb WW. (**2008**). Polarized microtubule arrays in apical dendrites and axons. *Proc Natl Acad Sci USA*. Aug 12; 105(32):11370-5.

Kwon I, Xiang S, Kato M, Wu L, Theodoropoulos P, Wang T, Kim J, Yun J, Xie Y, McKnight SL. (**2014**). Poly-dipeptides encoded by the C9orf72 repeats bind nucleoli, impede RNA biogenesis, and kill cells. *Science*. Sep 5; 345(6201): 1139-45.

Lacomblez L, Bensimon G, Douillet P, Doppler V, Salachas F, Meininger V. (**2004**). Xaliproden in amyotrophic lateral sclerosis: early clinical trials. *Amyotroph. Lateral Scler. Other Motor Neuron Disord*. 5: 99–106.

Lacomblez L, Bensimon G, Leigh PN, Guillet P, Meininger V. [Amyotrophic Lateral Sclerosis/Riluzole Study Group II]. (**1996**). Doseranging study of riluzole in amyotrophic lateral sclerosis. *Lancet*. May 25; 347(9013): 1425-31.

Lai EC, Felice KJ, Festoff BW, Gawel MJ, Gelinas DF, Kratz R, et al. (**1997**). Effect of recombinant human insulin-like growth factor-I on progression of ALS. A placebo-controlled study. The North America ALS/IGF-I Study Group. *Neurology* 49: 1621-1630.

Lagier-Tourenne C, Baughn M, Rigo F, Sun S, Liu P, Li HR, Jiang J, Watt AT, Chun S, Katz M, Qiu J, Sun Y, Ling SC, Zhu Q, Polymenidou M, Drenner K, Artates JW, McAlonis-Downes M, Markmiller S, Hutt KR, Pizzo DP, Cady J, Harms MB, Baloh RH, Vandenberg SR, Yeo GW, Fu XD, Bennett CF, Cleveland DW, Ravits J. (**2013**). Targeted degradation of sense and antisense C9orf72 RNA foci as therapy for ALS and frontotemporal degeneration. *Proc. Natl. Acad. Sci. USA*. Nov 19; 110(47): E4530-9.

Lagier-Tourenne C, Polymenidou M, Cleveland DW. (**2010**). TDP-43 and FUS/TLS: emerging roles in RNA processing and neurodegeneration. *Hum Mol Genet*. Apr 15; 19(R1): R46-64.

Lagier-Tourenne C. and Cleveland DW. (**2009**). Rethinking ALS: the FUS about TDP-43. *Cell.* Mar 20; 136(6):1001-4.

Lanson NA Jr and Pandey UB. (**2012**). FUS-related proteinopathies: lessons from animal models. *Brain Res.* Jun 26; 1462: 44-60.

Lappe-Siefke C, Goebbels S, Gravel M, Nicksch E, Lee J, Braun PE, Griffiths IR, Nave KA. Disruption of Cnp1 uncouples oligodendroglial functions in axonal support and myelination. *Nat Genet*. 2003; 33:366–74.

Lashley T, Roher JD, Mead S, et al. (**2015**). Review: an update on clinical, genetic and pathological aspects of frontotemporal lobar degenerations. *Neuropathol Appl Neurobiol* 41: 858–81.

Lattante S, Ciura S, Rouleau GA, Kabashi E. (**2015**). Defining the genetic connection linking amyotrophic lateral sclerosis (ALS) with frontotemporal dementia (FTD). *Trends Genet*. May; 31(5): 263-73.

Lau DHW, Hartopp N, Welsh NJ, Mueller S, Glennon EB, Morotz GM, Annibali A, Gomez-Suaga P, Stoica R, Paillusson S, Miller CCJ. (**2018**). Disruption of ER-mitochondria signalling in fronto-temporal dementia and related amyotrophic lateral sclerosis. *Cell Death Dis* 9: 327.

Lauria G, Campanella A, Filippini G, Martini A, Penza P, Maggi L, et al. (**2009**). Erythropoietin in amyotrophic lateral sclerosis: a pilot, randomized, double-blind, placebo-controlled study of safety and tolerability. *Amyotroph. Lateral Scler*. 10 410–415.

Lawrence CJ, Dawe RK, Christie KR, Cleveland DW, Dawson SC, Endow SA, Goldstein LS, Goodson HV, Hirokawa N, Howard J, Malmberg RL, McIntosh JR, Miki H, Mitchison TJ, Okada Y, Reddy AS, Saxton WM, Schliwa M, Scholey JM, Vale RD, Walczak CE, Wordeman L. (**2004**). A standardized kinesin nomenclature. *J Cell Biol*. Oct 11; 167(1): 19-22.

Le Masson G, Przedborski S, Abbott LF. (**2014**). A computational model of motor neuron degeneration. *Neuron*. Aug 20; 83(4): 975–988.

Le Y, Zhou Y, Iribarren P, Wang J. (**2004**). Chemokines and chemokine receptors: their manifold roles in homeostasis and disease. *Cell Mol Immunol*. 1: 95–104.

LeBlanc SE, Ward RM, Svaren J. (**2007**). Neuropathyassociated Egr2 mutants disrupt cooperative activation of myelin protein zero by Egr2 and Sox10. *Mol Cell Biol*. 27: 3521–29.

Lederer CW, Torrisi A, Pantelidou M, Santama N, Cavallaro S. (**2007**). Pathways and genes differentially expressed in the motor cortex of patients with sporadic amyotrophic lateral sclerosis. *BMC Genomics*. 8:26.

Lee DY. and McMurray CT. (**2014**).Trinucleotide expansion in disease: why is there a length threshold? *Curr Opin Genet Dev*. Jun; 26: 131-40.

Lee HG, Zhu X, Casadesus G, Pallàs M, Camins A, O'Neill MJ, Nakanishi S, Perry G, Smith MA. (**2009**). The effect of mGluR2 activation on signal transduction pathways and neuronal cell survival. *Brain Res*. Jan 16; 1249: 244-50.

Lee KH, Zhang P, Kim HJ, Mitrea DM, Sarkar M, Freibaum BD, Cika J, Coughlin M, Messing J, Molliex A, Maxwell BA, Kim NC, Temirov J, Moore J, Kolaitis RM, Shaw TI, Bai B, Peng J, Kriwacki RW, Taylor JP. (**2016**). C9orf72 dipeptide repeats impair the assembly, dynamics and function of membrane-less organelles. *Cell* Oct 20; 167(3): 774-788.e17.

Lee WL, Kaiser MA, Cooper JA. (**2005**). The offloading model for dynein function: differential function of motor subunits. *J Cell Biol.* Jan 17; 168(2): 201-7.

Lee Y, Morrison BM, Li Y, Lengacher S, Farah MH, Hoffman PN, Liu Y, Tsingalia A, Jin L, Zhang PW, Pellerin L, Magistretti PJ, Rothstein JD. (**2012**) Oligodendroglia metabolically support axons and contribute to neurodegeneration. *Nature*. Jul 26; 487(7408): 443-8.

Lefort CT, Ley K. (**2012**). Neutrophil arrest by LFA-1 activation. *Front Immunol.* 3: 157. doi:10.3389/fimmu.2012.00157.

Lenaz G, Bovina C, D'Aurelio M, Fato R, Formiggini G, Genova ML, Giuliano G, Merlo Pich M, Paolucci U, Parenti Castelli G, Ventura B. (**2002**). Role of mitochondria in oxidative stress and ageing. *Ann. N. Y. Acad. Sci.* Apr; 959: 199-213.

Lenglet T, Lacomblez L, Abitbol JL, Ludolph A, Mora JS, Robberecht W, et al. (**2014**). A phase II-III trial of olesoxime in subjects with amyotrophic lateral sclerosis. *Eur. J. Neurol*. 21: 529–536.

Levine TP, Daniels RD, Gatta AT, Wong LH, Hayes MJ. (**2013**). The product of C9orf72, a gene strongly implicated in neurodegeneration, is structurally related to DENN Rab-GEFs. *Bioinformatics*. Feb 15; 29(4): 499-503.

Ley K, Laudanna C, Cybulsky MI, Nourshargh S. (**2007**). Getting to the site of inflammation: the leukocyte adhesion cascade updated. *Nat Rev Immunol*. 7: 678–89.

Ley K. (**2002**). Integration of inflammatory signals by rolling neutrophils. *Immunol Rev*. 186:8–18.

Leybaert L. (**2005**). Neurobarrier coupling in the brain: A partner of neurovascular and neurometabolic coupling? *J Cereb Blood Flow Metab*. Jan; 25(1): 2-16.

Leyva JA, Bianchet MA, Amzel LM. (**2003**). Understanding ATP synthesis: structure and mechanism of the F1-ATPase. *Mol Membr Biol*. Jan-Mar; 20(1): 27-33.

Li H, Lu Y, Smith HK, Richardson WD. (**2007**). Olig1 and Sox10 interact synergistically to drive myelin basic protein transcription in oligodendrocytes. *J Neurosci*. 27: 14375–82.

Li L, Zhang X, Le W. (**2008**). Altered macroautophagy in the spinal cord of SOD1 mutant mice. *Autophagy*. Apr; 4(3): 290-3.

Li W, Reeb AN, Lin B, Subramanian P, Fey EE, Knoverek CR, French RL, Bigio EH, Ayala YM. (**2017**). Heat Shock-induced Phosphorylation of TAR DNA-binding Protein 43 (TDP-43) by MAPK/ERK Kinase Regulates TDP-43 Function. *J Biol Chem.* Mar 24; 292(12): 5089–5100. doi:10.1074/jbc.M116.753913.

Li Z, Park Y, Marcotte EM. (**2013**). A Bacteriophage tailspike domain promotes self-cleavage of a human membrane-bound transcription factor, the myelin regulatory factor MYRF. *PLoS Biol*. 11:e1001624.

Liao B, Zhao W, Beers DR, Henkel JS, Appel SH. (**2012**). Transformation from a neuroprotective to a neurotoxic microglial phenotype in a mouse model of ALS. *Exp Neurol*. Sep; 237(1): 147-52.

Liberto CM, Albrecht PJ, Herx LM, Yong VW, Levison SW. (**2004**). Pro-regenerative properties of cytokine-activated astrocytes. *J Neurochem*. Jun; 89(5): 1092-100.

Ligon LA, LaMonte BH, Wallace KE, Weber N, Kalb RG, Holzbaur EL. (**2005**). Mutant superoxide dismutase disrupts cytoplasmic dynein in motor neurons. *Neuroreport*. Apr 25; 16(6): 533-6.

Lincecum JM, Vieira FG, Wang MZ, Thompson K, De Zutter GS, Kidd J, et al. (**2010**). From transcriptome analysis to therapeutic anti-CD40L treatment in the SOD1 model of amyotrophic lateral sclerosis. *Nat Genet*. 42: 392–9.

Ling SC, Polymenidou M, Cleveland DW. (**2013**). Converging mechanisms in ALS and FTD: disrupted RNA and protein homeostasis. *Neuron*. Aug 7; 79(3): 416-38.

Liu EY, Cali CP, Lee EB. (**2017**). RNA metabolism in neurodegenerative disease. *Dis Model Mech*. May 1; 10(5): 509-518.

Liu J. and Wang F. (**2017**). Role of neuroinflammation in Amyotrophic Lateral Sclerosis: Cellular mechanisms and therapeutic implications. *Front Immunol.* Aug 21; 8:1005.

Liu Y, Beyer A, Aebersold R. (**2016**). On the dependency of cellular protein levels on mRNA abundance. *Cell* 165: 535-550.

Liu Z, Hu X, Cai J, Liu B, Peng X, Wegner M, Qiu M. (**2007**). Induction of oligodendrocyte differentiation by Olig2 and Sox10: evidence for reciprocal interactions and dosage-dependent mechanisms. *Dev. Biol.* Feb 15; 302(2): 683-93.

Liu-Yesucevitz L, Bilgutay A, Zhang YJ, Vanderweyde T, Citro A, Mehta T, Zaarur N, McKee A, Bowser R, Sherman M, Petrucelli L, Wolozin B. (**2010**). Tar DNA binding protein-43 (TDP-43) associates with stress granules: analysis of cultured cells and pathological brain tissue. *PloS one*, 5(10), e13250.

Llorens F, Thüne K, Tahir W, Kanata E, Diaz-Lucena D, Xanthopoulos K, Kovatsi E, Pleschka C, Garcia-Esparcia P, Schmitz M, Ozbay D, Correia S, Correia Â, et al. (**2017**). YKL-40 in the brain and cerebrospinal fluid of neurodegenerative dementias. *Mol Neurodegener*. 12: 83.

Lobsiger CS and Cleveland DW. (**2009**). Neurofilaments: Organization and function in neurons, *Encyclopedia of Neuroscience*. Academic Press (Ed). pp: 433-436.

Locksley RM, Killeen N, Lenardo MJ. (**2001**). The TNF and TNF receptor superfamilies: integrating mammalian biology. *Cell*. 104:487–501.

Logroscino G, Traynor BJ, Hardiman O, Chiò A, Mitchell D, Swingler RJ, Millul A, Benn E, Beghi E [EURALS]. (**2010**). Incidence of amyotrophic lateral sclerosis in Europe. *J Neurol Neurosurg Psychiatry*. Apr; 81(4): 385-90.

Lomen-Hoerth C, Anderson T, Miller B. (**2002**). The overlap of amyotrophic lateral sclerosis and frontotemporal dementia. *Neurology*. Oct 8; 59(7): 1077-9.

Lossos A, Elazar N, Lerer I, Schueler-Furman O, Fellig Y, Glick B, Zimmerman BE, Azulay H, Dotan S, Goldberg S, Gomori JM, Ponger P, Newman JP, et al. (**2015**). Myelin-associated glycoprotein gene mutation causes Pelizaeus-Merzbacher disease-like disorder. *Brain*. 138: 2521–36.

Lu CH, Allen K, Oei F, Leoni E, Kuhle J, Tree T, et al. (**2016**). Systemic inflammatory response and neuromuscular involvement in amyotrophic lateral sclerosis. *Neurol Neuroimmunol Neuroinflamm.* 3:e244.

Lü, JM, Lin PH, Yao Q, Chen C. (**2009**). Chemical and molecular mechanisms of antioxidants: experimental approaches and model systems. *Journal of cellular and molecular medicine*. 14(4): 840-60.

Lundgaard I, Osório MJ, Kress B, Sanggaard S, Nedergaard M. (**2013**). White matter astrocytes in health and disease. *Neuroscience*. Sep 12; 276: 161-73.

Luquin N, Yu B, Saunderson RB, Trent RJ, Pamphlett R. (**2009**). Genetic variants in the promoter of TARDBP in sporadic amyotrophic lateral sclerosis. *Neuromuscul Disord*. Oct; 19(10): 696-700..

Mackenzie IR and Feldman HH. (**2005**). Ubiquitin immunohistochemistry suggests classic motor neuron disease, motor neuron disease with dementia, and frontotemporal dementia of the motor neuron disease type represent a clinicopathologic spectrum. *J Neuropathol Exp Neurol*. Aug; 64(8):730-9.

Mackenzie IR, Arzberger T, Kremmer E, Troost D, Lorenzl S, Mori K, Weng SM, Haass C, Kretzschmar HA, Edbauer D, Neumann M. (**2013**). Dipeptide repeat protein pathology in C9ORF72 mutation cases: clinico-pathological correlations. *Acta Neuropathol*. Dec; 126(6): 859-79.

Mackenzie IR, Baborie A, Pickering-Brown S, Du Plessis D, Jaros E, Perry RH, Neary D, Snowden JS, Mann DM. (**2006a**). Heterogeneity of ubiquitin pathology in frontotemporal lobar degeneration: classification and relation to clinical phenotype. *Acta Neuropathol*. Nov; 112(5): 539-49.

Mackenzie IR, Baker M, Pickering-Brown S, Hsiung GY, Lindholm C, Dwosh E, Gass J, Cannon A, Rademakers R, Hutton M, Feldman HH. (**2006b**). The neuropathology of frontotemporal lobar degeneration caused by mutations in the progranulin gene. *Brain*. Nov; 129(Pt 11): 3081-90.

Mackenzie IR, Neumann M, Baborie A, Sampathu DM, Du Plessis D, Jaros E, Perry RH, Trojanowski JQ, Mann DM, Lee VM. (**2011**). A harmonized classification system for FTLD-TDP pathology. *Acta Neuropathol*. Jul; 122(1): 111-3.

MacLean SJ. and Gibson DM. (**1997**). Identification of a predominant sequence variant of the T-cell receptor TCRBC1 gene. *Immunogenetics* 45: 223–5.

Maday S, Twelvetrees AE, Moughamian AJ, Holzbaur EL. (**2014**). Axonal transport: cargo-specific mechanisms of motility and regulation. *Neuron*. Oct 22; 84(2): 292-309.

Magrané J, Sahawneh MA, Przedborski S, Estévez ÁG, Manfredi G. (**2012**) Mitochondrial dynamics and bioenergetic dysfunction is associated with synaptic alterations in mutant SOD1 motor neurons. *J Neurosci*. Jan 4; 32(1): 229-42.

Magrané J. and Manfredi G. (**2009**). Mitochondrial function, morphology, and axonal transport in amyotrophic lateral sclerosis. *Antioxid Redox Signal*. Jul; 11(7): 1615-26.

Mahad D, Ziabreva I, Lassmann H, Turnbull D. (**2008**). Mitochondrial defects in acute multiple sclerosis lesions. Jul; 131(Pt 7): 1722-35.

Mali GR, Yeyati PL, Mizuno S, et al. (**2018**). ZMYND10 functions in a chaperone relay during axonemal dynein assembly. *eLife* 7:e34389.

Mancuso R, Oliván S, Mancera P, Pastén-Zamorano A, Manzano R, Casas C, Osta R, Navarro X. (**2012a**). Effect of genetic background on onset and disease progression in the SOD1-G93A model of amyotrophic lateral sclerosis. *Amyotroph Lateral Scler*. May; 13(3): 302-10.

Mancuso R, Oliván S, Rando A, Casas C, Osta R, Navarro X. (**2012b**). Sigma-1R agonist improves motor function and motoneuron survival in ALS mice. *Neurotherapeutics* Oct; 9(4): 814-26.

Manev H, Favaron M, Guidotti A, Costa E. (**1989**). Delayed increase of Ca2+ influx elicited by glutamate: role in neuronal death. *Mol Pharmacol*. Jul; 36(1): 106–112.

Mann DM, Rollinson S, Robinson A, Bennion Callister J, Thompson JC, Snowden JS, Gendron T, Petrucelli L, Masuda-Suzukake M, Hasegawa M, Davidson Y, Pickering-Brown S. (**2013**). Dipeptide repeat proteins are present in the p62 positive inclusions in patients with frontotemporal lobar degeneration and motor neurone disease associated with expansions in C9ORF72. *Acta Neuropathol. Commun*. Oct 14; 1:68.

Mann DMA. and Snowden JS. (**2017**). Frontotemporal lobar degeneration: pathogenesis, pathology and pathways to phenotype. *Brain Pathol*. 27: 723–36.

Mansilla N, Racca S, Gras DE, Gonzalez DH, Welchen E. (**2018**). The complexity of mitochondrial complex IV: an update of cytochrome C oxidase biogenesis in plants. *Int J Mol Sci*. Feb 27; 19(3). pii: E662.

Mantovani S, Garbelli S, Pasini A, Alimonti D, Perotti C, Melazzini M, Bendotti C, Mora G. (**2009**). Immune system alterations in sporadic amyotrophic lateral sclerosis patients suggest an ongoing neuroinflammatory process. *J Neuroimmunol*. 210: 73–79.

Maragakis NJ, Dykes-Hoberg M, Rothstein JD. (**2004**). Altered expression of the glutamate transporter EAAT2b in neurological disease. *Ann Neurol*. Apr;55(4): 469-77.

Marangi G and Traynor BJ. (**2015**). Genetic causes of amyotrophic lateral sclerosis: new genetic analysis methodologies entailing new opportunities and challenges. *Brain Res*. May 14; 1607: 75-93.

Marguerat S, Schmidt A, Codlin S, Chen W, Aebersold R, Bahler J. (**2012**). Quantitative analysis of fission yeast transcriptomes and proteomes in proliferating and quiescent cells. *Cell* 151: 671-683.

Marinelli C, Bertalot T, Zusso M, Skaper SD, Giusti P. (**2016**). Systematic review of pharmacological properties of the oligodendrocyte lineage. *Front. Cell. Neurosci*. Feb 12; 10: 27.

Marki A, Esko JD, Pries AR, Ley K. (**2015**). Role of the endothelial surface layer in neutrophil recruitment. *J Leukoc Biol*. 98: 503–15.

Martin LJ, Liu Z, Chen K, Price AC, Pan Y, Swaby JA, Golden WC. (**2007**). Motor neuron degeneration in amyotrophic lateral sclerosis mutant superoxide dismutase-1 transgenic mice: mechanisms of mitochondriopathy and cell death. *J Comp Neurol*. Jan 1; 500(1): 20-46.

Martin LJ. (**2007**). Transgenic mice with human mutant genes causing Parkinson's disease and amyotrophic lateral sclerosis provide common insight into mechanisms of motor neuron selective vulnerability to degeneration. *Rev Neurosci*. 18(2): 115-36.

Martinez A, Carmona M, Portero-Otin M, Naudi A, Pamplona R, Ferrer I. (**2008**). Type-dependent oxidative damage in frontotemporal lobar degeneration: Cortical astrocytes are targets of oxidative damage. *J Neuropathol Exp Neurol* 67: 1122-1136.

Martinez FO, Helming L, Gordon S. (**2009**). Alternative activation of macrophages: an immunologic functional perspective. *Annu Rev Immunol*. 27: 451-83.

Marty MC, Alliot F, Rutin J, Fritz R, Trisler D, Pessac B. (**2002**). The myelin basic protein gene is expressed in differentiated blood cell lineages and in hemopoietic progenitors. *Proc Natl Acad Sci USA*. 99: 8856– 61.

Matosin N, Green MJ, Andrews JL, Newell KA, Fernandez-Enright F. (**2016**). Possibility of a sex-specific role for a genetic variant in FRMPD4 in schizophrenia, but not cognitive function. *Neuroreport*. 27: 33–38.

Mattson MP, Gnthrie PB, Kater SB. (**1989**). A role for Na+-dependent Ca++ extrusion in protection against neuronal excitotoxicity. *FASEB J*. 3: 2519-2526.

Mavlyutov TA, Epstein ML, Andersen KA, et al. (**2010**). The sigma-1 receptor is enriched in postsynaptic sites of C-terminals in mouse motoneurons. An anatomical and behavioral study. *Neuroscience* 167: 247–55.

May S, Hornburg D, Schludi MH, Arzberger T, Rentzsch K, Schwenk BM, Grässer FA, Mori K, Kremmer E, Banzhaf-Strathmann J, Mann M, Meissner F, Edbauer D. (**2014**). C9orf72 FTLD/ALS-associated Gly-Ala dipeptide repeat proteins cause neuronal toxicity and Unc119 sequestration. *Acta Neuropathol*. Oct; 128(4): 485-503.

McCombe PA. and Henderson RD. (**2011**). The role of immune and inflammatory mechanisms in ALS. *Curr Mol Med*. Apr; 11(3): 246-54.

McEwen ML, Sullivan PG, Rabchevsky AG, Springer JE. (**2011**).Targeting mitochondrial function for the treatment of acute spinal cord injury. *Neurotherapeutics*. Apr; 8(2): 168-79.

McKenney RJ, Huynh W, Tanenbaum ME, Bhabha G, Vale RD. (**2014**). Activation of cytoplasmic dynein motility by dynactin-cargo adapter complexes. *Science*. 345: 337–41.

McMillian MK, Thai L, Hong JS, O'Callaghan JP, Pennypacker KR. (**1994**). Brain injury in a dish: A model for reactive gliosis. *Trends Neurosci*. Apr; 17(4): 138-42.

Meininger V, Bensimon G, Bradley WR, Brooks B, Douillet P, Eisen AA, et al. (**2004**). Efficacy and safety of xaliproden in amyotrophic lateral sclerosis: results of two phase III trials. *Amyotroph. Lateral Scler. Other Motor Neuron Disord*. 5: 107-117.

Meininger V, Drory VE, Leigh PN, Ludolph A, Robberecht W, Silani V. (**2009**). Glatiramer acetate has no impact on disease progression in ALS at 40 mg/day: a double-blind, randomized, multicentre, placebo-controlled trial. *Amyotroph. Lateral Scler*. 10 378–383.

Miki H, Setou M, Kaneshiro K, Hirokawa N. (**2001**). All kinesin superfamily protein, KIF, genes in mouse and human. *Proc. Natl. Acad. Sci. USA*. Jun 19; 98(13): 7004-11.

Miki Y, Mori F, Seino Y, Tanji K, Yoshizawa T, Kijima H, Shoji M, Wakabayashi K. (**2018**). Colocalization of Bunina bodies and TDP-43 inclusions in a case of sporadic amyotrophic lateral sclerosis with Lewy body-like hyaline inclusions. *Neuropathology*. Oct; 38(5): 521-528.

Miles GB, Hartley R, Todd AJ, et al. (**2007**). Spinal cholinergic interneurons regulate the excitability of motoneurons during locomotion. *Proc Natl Acad Sci USA*. 104: 2448–53.

Millecamps S, Robertson J, Lariviere R, Mallet J, Julien JP. (**2006**). Defective axonal transport of neurofilament proteins in neurons overexpressing peripherin. *J Neurochem*. Aug; 98(3): 926-38.

Miller R, Bradley W, Cudkowicz M, Hubble J, Meininger V, Mitsumoto H, et al. (**2007a**). Phase II/III randomized trial of TCH346 in patients with ALS. *Neurology* 69: 776–784.

Miller R, Bryan W, Munsat T. (**1993**). Safety, tolerability and pharmacokinetics of recombinant human ciliary neurotrophic factor (rhCNTF) in patients with amyotrophic lateral sclerosis (ALS). *Ann. Neurol*. 34:241.

Miller RG, Block G, Katz JS, Barohn RJ, Gopalakrishnan V, Cudkowicz M, et al. (**2015**). Randomized phase 2 trial of NP001-a novel immune regulator: Safety and early efficacy in ALS. *Neurol. Neuroimmunol. Neuroinflammation* 2:e100.

Miller RG, Petajan JH, Bryan WW, Armon C, Barohn RJ, Goodpasture JC, et al. (**1996**). A placebo-controlled trial of recombinant human ciliary neurotrophic (rhCNTF) factor in amyotrophic lateral sclerosis. rhCNTF ALS Study Group. *Ann. Neurol.* 39: 256–260.

Miller RG, Zhang R, Block G, Katz J, Barohn R, Kasarskis E, et al. (**2014**). NP001 regulation of macrophage activation markers in ALS: A phase I clinical and biomarker study. *Amyotroph. Lateral Scler. Front. Degener*. 15: 601–609.

Mishra M, Paunesku T, Woloschak GE, Siddique T, Zhu LJ, Lin S, Greco K, Bigio EH. (**2007**). Gene expression analysis of frontotemporal lobar degeneration of the motor neuron disease type with ubiquitinated inclusions. *Acta Neuropathol* 114: 81-94.

Mitchell P. (**1961**). Coupling of phosphorylation to electron and hydrogen transfer by a chemi-osmotic type of mechanism. *Nature*. Jul 8; 191: 144-8.

Mizielinska S, Grönke S, Niccoli T, Ridler CE, Clayton EL, Devoy A, Moens T, Norona FE, Woollacott IOC, Pietrzyk J, Cleverley K, Nicoll AJ, Pickering-Brown S, Dols J, Cabecinha M, Hendrich O, Fratta P, Fisher EMC, Partridge L, Isaacs AM. (**2014**). C9orf72 repeat expansions cause neurodegeneration in Drosophila through arginine-rich proteins. *Science*. Sep 5; 345(6201): 1192-1194.

Mizielinska S, Lashley T, Norona FE, Clayton EL, Ridler CE, Fratta P, Isaacs AM. (**2013**). C9orf72 frontotemporal lobar degeneration is characterised by frequent neuronal sense and antisense RNA foci. *Acta Neuropathol*. Dec; 126(6): 845-57.

Mizuno Y, Fujita Y, Takatama M, Okamoto K. (**2011**). Peripherin partially localizes in Bunina bodies in amyotrophic lateral sclerosis. *J. Neurol. Sci.* Mar 15; 302(1-2): 14-8.

Mizusawa H. (**1993**). Hyaline and Skein-like Inclusions in Amyotrophic Lateral Sclerosis. *Neuropathology*. 13 (3):201–208.

Mizushima N. and Komatsu M. (**2011**). Autophagy: renovation of cells and tissues. *Cell*. Nov 11; 147(4): 728-41. doi: 10.1016/j.cell.2011.10.026.

Momeni P, Rogaeva E, Van Deerlin V, Yuan W, Grafman J, Tierney M, Huey E, Bell J, Morris CM, Kalaria RN, van Rensburg SJ, Niehaus D, Potocnik F, Kawarai T, Salehi-Rad S, Sato C, St George-Hyslop P, Hardy J. (**2006**). Genetic variability in CHMP2B and frontotemporal dementia. *Neurodegener Dis*. 3(3): 129-33. doi: 10.1159/000094771.

Montague P, McCallion AS, Davies RW, Griffiths IR. (**2006**). Myelin-associated oligodendrocytic basic protein: a family of abundant CNS myelin proteins in search of a function. *Dev Neurosci*. 28: 479–87. doi: 10.1159/000095110.

Mori F, Tanji K, Zhang HX, Nishihira Y, Tan CF, Takahashi H, Wakabayashi K. (**2008**). Maturation process of TDP-43-positive neuronal cytoplasmic inclusions in amyotrophic lateral sclerosis with and without dementia. *Acta Neuropathol*. Aug; 116(2): 193-203. doi: 10.1007/s00401-008-0396-9.

Mori K, Weng SM, Arzberger T, May S, Rentzsch K, Kremmer E, Schmid B, Kretzschmar HA, Cruts M, Van Broeckhoven C, Haass C, Edbauer D. (**2013**). The C9orf72 GGGGCC repeat is translated into aggregating dipeptide-repeat proteins in FTLD/ALS. *Science*. Mar 15; 339(6125): 1335-8.

Morimoto N, Nagai M, Ohta Y, Miyazaki K, Kurata T, Morimoto M, Murakami T, Takehisa Y, Ikeda Y, Kamiya T, Abe K. (**2007**). Increased autophagy in transgenic mice with a G93A mutant SOD1 gene. *Brain Res*. Sep 5; 1167: 112-7.

Morrison BM, Li Y, Lengacher S, Farah MH, Hoffman PN, Liu Y, Tsingalia A, Jin L, Zhang PW, Pellerin L, Magistretti PJ, Rothstein JD. (**2012**). Oligodendroglia metabolically support axons and contribute to neurodegeneration. *Nature.* Jul 26; 487(7408): 443-8. doi: 10.1038/nature11314.

Morrison KE, Dhariwal S, Hornabrook R, Savage L, Burn DJ, Khoo TK, et al. (**2013**). Lithium in patients with amyotrophic lateral sclerosis (LiCALS): a phase 3 multicentre, randomised, double-blind, placebo-controlled trial. *Lancet Neurol*. 12: 339–345.

Moumen A, Virard I, Raoul C. (**2011**). Accumulation of wildtype and ALS-linked mutated VAPB impairs activity of the proteasome. *PLoS One*. 6(10):e26066.

Mount CW. and Monje M. (**2017**). Wrapped to Adapt: Experience-Dependent Myelination. *Neuron*. Aug 16; 95(4): 743-756.

Mourelatos Z, Gonatas NK, Stieber A, Gurney ME, Dal Canto MC. (**1996**). The Golgi apparatus of spinal cord motor neurons in transgenic mice expressing mutant Cu,Zn superoxide dismutase becomes fragmented in early, preclinical stages of the disease. *Proc Natl Acad Sci USA*. May 28; 93(11): 5472-7.

Münch C, Sedlmeier R, Meyer T, Homberg V, Sperfeld AD, Kurt A, Prudlo J, Peraus G, Hanemann CO, Stumm G, Ludolph AC. (**2004**). Point mutations of the p150 subunit of dynactin (DCTN1) gene in ALS. *Neurology*. Aug 24; 63(4): 724-6.

Munoz DG, Greene C, Perl DP, Selkoe DJ. (**1988**). Accumulation of phosphorylated neurofilaments in anterior horn motoneurons of amyotrophic lateral sclerosis patients. *J Neuropathol Exp Neurol*. Jan; 47(1): 9-18.

Murphy J, Henry R, Lomen-Hoerth C. (**2007a**). Establishing subtypes of the continuum of frontal lobe impairment in amyotrophic lateral sclerosis. *Arch Neurol.* Mar; 64(3): 330-4.

Murphy JM, Henry RG, Langmore S, Kramer JH, Miller BL, Lomen-Hoerth C. (**2007b**). Continuum of frontal lobe impairment in amyotrophic lateral sclerosis. *Arch Neurol.* Apr; 64(4): 530-4.

Murphy MP. (**2009**). How mitochondria produce reactive oxygen species. *Biochem J*. Jan 1; 417(1): 1-13.

Naeve GS, Ramakrishnan M, Kramer R, Hevroni D, Citri Y, Theill LE. (**1997**). Neuritin: a gene induced by neural activity and neurotrophins that promotes neuritogenesis. *Proc Natl Acad Sci USA*. 94:2648–53.

Nagao M, Misawa H, Kato S, et al. (**1998**). Loss of cholinergic synapses on the spinal motor neurons of amyotrophic lateral sclerosis. *J Neuropathol Exp Neurol* 57: 329–33.

Nagy D, Kato T, Kushner PD. (**1994**). Reactive astrocytes are widespread in the cortical gray matter of amyotrophic lateral sclerosis. *J Neurosci Res*. Jun 15; 38(3): 336-47.

Nathan C. (**2006**). Neutrophils and immunity: challenges and opportunities. *Nat Rev Immunol.* 6:173–82.

Nave KA. (**2010a**). Myelination and support of axonal integrity by glia. *Nature*. Nov 11; 468(7321): 244-52.

Nave KA. (**2010b**). Myelination and the trophic support of long axons. *Nat. Rev. Neurosci*. Apr; 11(4): 275-83.

Neumann M, Kwong LK, Truax AC, Vanmassenhove B, Kretzschmar HA, Van Deerlin VM, Clark CM, Grossman M, Miller BL, Trojanowski JQ, Lee VM. (**2007**). TDP-43-positive white matter pathology in frontotemporal lobar degeneration with ubiquitin-positive inclusions. *J Neuropathol Exp Neurol*. 66: 177-183.

Neumann M, Sampathu DM, Kwong LK, Truax AC, Micsenyi MC, Chou TT, Bruce J, Schuck T, Grossman M, Clark CM, McCluskey LF, Miller BL, Masliah E, Mackenzie IR, Feldman H, Feiden W, Kretzschmar HA, Trojanowski JQ, Lee VM. (**2006**). Ubiquitinated TDP-43 in frontotemporal lobar degeneration and amyotrophic lateral sclerosis. Science. Oct 6; 314(5796):130-3.

Ng AS, Rademakers R, Miller BL. (**2015**). Frontotemporal dementia: a bridge between dementia and neuromuscular disease. *Ann N Y Acad Sci.* Mar; 1338: 71-93.

Niebroj-Dobosz I, Rafalowska J, Fidzianska A, Gadamski R, Grieb P. (**2007**). Myelin composition of spinal cord in a model of amyotrophic lateral sclerosis (ALS) in SOD1G93A transgenic rats. *Folia Neuropathol*. 45(4): 236-41.

Nihei K, McKee AC, Kowall NW. (**1993**). Patterns of neuronal degeneration in the motor cortex of amyotrophic lateral sclerosis patients. *Acta Neuropathol*. 86(1): 55-64.

Nijholt DA, De Kimpe L, Elfrink HL, Hoozemans JJ, Scheper W. (**2011**). Removing protein aggregates: the role of proteolysis in neurodegeneration. *Curr Med Chem*. 18(16):2459-76.

Nimmerjahn A, Kirchhoff F, Helmchen F. (**2005**). Resting microglial cells are highly dynamic surveillants of brain parenchyma *in vivo*. *Science*. May 27; 308(5726): 1314-8.

Nimse SB and Pal D. (**2015**). Free radicals, natural antioxidants, and their reaction mechanisms. *RSC Adv*., 5, 27986.

Nishihira Y, Tan CF, Toyoshima Y, Yonemochi Y, Kondo H, Nakajima T, Takahashi H. (**2009**). Sporadic amyotrophic lateral sclerosis: Widespread multisystem degeneration with TDP-43 pathology in a patient after long-term survival on a respirator. *Neuropathology*. Dec 29(6):689-96.

Nishimura AL, Mitne-Neto M, Silva HC, Richieri-Costa A, Middleton S, Cascio D, Kok F, Oliveira JR, Gillingwater T, Webb J, Skehel P, Zatz M. (**2004**). A mutation in the vesicle-trafficking protein vapb causes late-onset spinal muscular atrophy and amyotrophic lateral sclerosis. *Am J Hum Genet*. Nov; 75(5): 822–831.

Niwa J, Yamada S, Ishigaki S, Sone J, Takahashi M, Katsuno M, Tanaka F, Doyu M, Sobue G. (**2007**). Disulfide bond mediates aggregation, toxicity, and ubiquitylation of familial amyotrophic lateral sclerosis-linked mutant SOD1. *J Biol Chem*. Sep 21; 282(38): 28087-95.

Nolan M, Talbot K, Ansorge O. (**2016**). Pathogenesis of FUS-associated ALS and FTD: insights from rodent models. *Acta Neuropathol Commun*. Sep 6; 4(1): 99.

Nonneman A, Robberecht W, Van Den Bosch L. (**2014**). The role of oligodendroglial dysfunction in amyotrophic lateral sclerosis. *Neurodegener Dis Manag*. 4(3): 223-39.

Nover L, Scharf KD, Neumann D. (**1989**). Cytoplasmic heat shock granules are formed from precursor particles and are associated with a specific set of mRNAs. *Mol Cell Biol*. Mar; 9(3):1298-308.

Oeckl P, Jardel C, Salachas F, Lamari F, Andersen PM, Bowser R, de Carvalho M, Costa J, van Damme P, Gray E, Grosskreutz J, Hernández-Barral M, Herukka SK, et al. (**2016**). Multicenter validation of CSF neurofilaments as diagnostic biomarkers for ALS. *Amyotroph Lateral Scler Frontotemporal Degener*. 17: 404–13.

Okamoto K, Hirai S, Amari M, Watanabe M, Sakurai A. (**1993**). Bunina bodies in amyotrophic lateral sclerosis immunostained with rabbit anti-cystatin C serum. *Neurosci Lett*. Nov 12; 162(1-2): 125-8.

Okamoto K, Mizuno Y, Fujita Y. (**2008**). Bunina bodies in amyotrophic lateral sclerosis. *Neuropathology*, 28(2): 109-115.

Olney JW. (**1969**). Brain lesions, obesity, and other disturbances in mice treated with monosodium glutamate. *Science*. May; 164 (3880): 719–721.

Olney JW. (**1978**). Neurotoxicity of excitatory amino acids. In: kainic acid as a tool in neurobiology. 95-121. EG McGeer (Eds). Raven Press, New York.

Omran H, Kobayashi D, Olbrich H, et al. (**2008**). Ktu/PF13 is required for cytoplasmic pre-assembly of axonemal dyneins. *Nature* 456: 611–6.

Onesto E, Colombrita C, Gumina V, Borghi MO, Dusi S, Doretti A, Fagiolari G, Invernizzi F, Moggio M, Tiranti V, Silani V, Ratti A. (**2016**). Gene-specific mitochondria dysfunctions in human TARDBP and C9ORF72 fibroblasts. *Acta Neuropathol Commun*. May 5; 4(1): 47.

O'Rourke JG, Bogdanik L, Yáñez A, Lall D, Wolf AJ, Muhammad AK, Ho R, Carmona S, Vit JP, Zarrow J, Kim KJ, Bell S, Harms MB4, Miller TM4, Dangler CA, Underhill DM, Goodridge HS, Lutz CM, Baloh RH. (**2016**). C9orf72 is required for proper macrophage and microglial function in mice. *Science*. 351, 1324–1329.

Paavola CD, Hemmerich S, Grunberger D, Polsky I, Bloom A, Freedman R, et al. (**1998**). Monomeric monocyte chemoattractant protein-1 (MCP-1) binds and activates the MCP-1 receptor CCR2B. *J Biol Chem* 273: 33157–65.

Pal M, Febbraio MA, Whitham M. (**2014**). From cytokine to myokine: the emerging role of interleukin-6 in metabolic regulation. *Immunol Cell Biol*. 92:331–39.

Palluzzi F, Ferrari R, Graziano F, Novelli V, Rossi G, Galimberti D, Rainero I, Benussi L, Nacmias B, BruniAC, Cusi D, Salvi E, Borroni B, Grassi M. (**2017**). A novel network analysis approach reveals DNA damage, oxidative stress and calcium/cAMP homeostasis-associated biomarkers in frontotemporal dementia. *PLoS One* 12: e0185797.

Palumbo J, Sakata T, Tanaka M, Akimoto M. (**2016**). "Sustained efficacy for up to 12 months in an active extension of a phase III study of edaravone (MCI-186) for treatment of amyotrophic lateral sclerosis (ALS) (P3.190)," in Poster Presented at: AAN 2016 Annual Meeting Vancouve, BC.

Papegaey A, Eddarkaoui S, Deramecourt V, et al. (**2016**). Reduced Tau protein expression is associated with frontotemporal degeneration with progranulin mutation. *Acta Neuropathol Commun*. 4:74.

Parkinson N, Ince PG, Smith MO, Highley R, Skibinski G, Andersen PM, Morrison KE, Pall HS, Hardiman O, Collinge J, Shaw PJ, Fisher EM, MRC Proteomics in ALS Study., FReJA Consortium. (**2006**). ALS phenotypes with mutations in CHMP2B (charged multivesicular body protein 2B). *Neurology*. Sep 26; 67(6): 1074-7.

Parpura V. and Verkhratsky A. (**2012**). Astrocytes revisited: concise historic outlook on glutamate homeostasis and signaling. *Croat Med J.* Dec; 53(6): 518–528.

Pascuzzi RM, Shefner J, Chappell AS, Bjerke JS, Tamura R, Chaudhry V, et al. (**2010**). A phase II trial of talampanel in subjects with amyotrophic lateral sclerosis. Amyotroph. Lateral Scler. 11 266–271.

Pasinelli P and Brown RH. (**2006**). Molecular biology of amyotrophic lateral sclerosis: insights from genetics. *Nat Rev Neurosci*. Sep; 7(9): 710-23.

Pastula DM, Moore DH, Bedlack RS. (**2012**). Creatine for amyotrophic lateral sclerosis/motor neuron disease. *Cochrane database Syst. Rev*. 12:CD005225.

Pérez-Cerdá F, Sánchez-Gómez MV, Matute C. (**2015**). Pío del Río Hortega and the discovery of the oligodendrocytes. *Front Neuroanat*. Jul 7; 9: 92.

Pesiridis GS, Lee VM, Trojanowski JQ. (**2009**). Mutations in TDP-43 link glycine-rich domain functions to amyotrophic lateral sclerosis. *Hum Mol Genet*. Oct 15; 18(R2): R156–R162.

Peters OM, Ghasemi M, Brown RH. (**2015**). Emerging mechanisms of molecular pathology in ALS. *J. Clin. Invest*. May; 125(5): 1767-79.

Petros TJ, Williams SE, Mason CA. (**2006**). Temporal regulation of EphA4 in astroglia during murine retinal and optic nerve development. *Mol Cell Neurosci*. May-Jun; 32(1-2):49-66.

Petrov D, Mansfield C, Moussy A, Hermine, O. (**2017**). ALS Clinical Trials Review: 20 Years of Failure. Are We Any Closer to Registering a New Treatment? *Front Aging Neurosci.* 9: 68.

Pfister KK, Fisher EM, Gibbons IR, Hays TS, Holzbaur EL, McIntosh JR, Porter ME, Schroer TA, Vaughan KT, Witman GB, King, SM, Vallee RB. (**2005**). Cytoplasmic dynein nomenclature. *J Cell Biol*. Nov 7; 171(3): 411–413.

Philips T. and Rothstein JD. (**2015**). Rodent Models of Amyotrophic Lateral Sclerosis. *Curr Protoc Pharmacol*. Jun 1; 69:5.67.1-21.

Philips T, Bento-Abreu A, Nonneman A, Haeck W, Staats K, Geelen V, Hersmus N, Küsters B, Van Den Bosch L, Van Damme P, Richardson WD, Robberecht W. (**2013**). Oligodendrocyte dysfunction in the pathogenesis of amyotrophic lateral sclerosis. *Brain*. Feb; 136(Pt 2): 471-82.

Philips T. and Robberecht W. (**2011**). Neuroinflammation in amyotrophic lateral sclerosis: role of glial activation in motor neuron disease. *Lancet Neurol*. Mar; 10(3): 253-63.

Philips T. and Rothstein JD. (**2014**). Glial cells in amyotrophic lateral sclerosis. *Exp Neurol*. Dec; 262PB: 111–120.

Phukan J, Pender NP, Hardiman O. (**2007**). Cognitive impairment in amyotrophic lateral sclerosis. *Lancet Neurol.* Nov; 6(11): 994-1003.

Piao YS, Wakabayashi K, Kakita A, Yamada M, Hayashi S, Morita T, Ikuta F, Oyanagi K, Takahashi H. (**2003**). Neuropathology with clinical correlations of sporadic amyotrophic lateral sclerosis: 102 autopsy cases examined between 1962 and 2000. *Brain Pathol*, Jan; 13(1): 10-22.

Picher-Martel V, Valdmanis PN, Gould PV, Julien JP, Dupré N. (**2016**). From animal models to human disease: a genetic approach for personalized medicine in ALS. *Acta Neuropathol Commun*. Jul 11;4(1):70.

Piepers S, Veldink JH, De Jong SW, Van Der Tweel I, Van Der Pol WL, Uijtendaal EV, et al. (**2009**). Randomized sequential trial of valproic acid in amyotrophic lateral sclerosis. *Ann. Neurol*. 66: 227–234.

Pocock JM and Piers TM. (**2018**). Modelling microglial function with induced pluripotent stem cells: an update. *Nat Rev Neurosci*. Aug; 19(8): 445-452.

Poliak S. and Peles E. (**2003**). The local differentiation of myelinated axons at nodes of Ranvier. *Nat. Rev. Neurosci.* Dec; 4(12): 968-80.

Polymenidou M. and Cleveland DW. (**2011**). The seeds of neurodegeneration: prion-like spreading in ALS. *Cell*. Oct 28; 147(3): 498-508.

Pontieri FE, Ricci A, Pellicano C, Benincasa D, Buttarelli FR. (**2005**). Minocycline in amyotrophic lateral sclerosis: a pilot study. Neurol. Sci. 26 285–287.

Pratt AJ, Shin DS, Merz GE, Rambo RP, Lancaster WA, Dyer KN, Borbat PP, Poole FL 2nd, Adams MW, Freed JH, Crane BR, Tainer JA, Getzoff ED. (**2014**). Aggregation propensities of superoxide dismutase G93 hotspot mutants mirror ALS clinical phenotypes. *Proc Natl Acad Sci USA*. Oct 28; 111(43): E4568-76.

Prentice H, Modi JP, Wu JY. (**2015**). Mechanisms of neuronal protection against excitotoxicity, endoplasmic reticulum stress, and mitochondrial dysfunction in stroke and neurodegenerative diseases. *Oxid Med Cell Longev*. 2015:964518.

Przedborski S, Vila M, Jackson-Lewis VR. (**2003**). Introduction: Neurodegeneration: What is it and where are we? *J Clin Invest*. 2003; 111(1):3-10.

Puentes F, Malaspina A, Van Noort JM, Amor S. (**2016**). Non-neuronal cells in ALS: role of glial, immune cells and blood-CNS barriers. *Brain Pathol* 26: 248–57.

Pullen AH. and Athanasiou D. (**2009**). Increase in presynaptic territory of C-terminals on lumbar motoneurons of G93A SOD1 mice during disease progression. *Eur J Neurosci* 29: 551–61.

Puls I, Oh SJ, Sumner CJ, Wallace KE, Floeter MK, Mann EA, Kennedy WR, Wendelschafer-Crabb G, Vortmeyer A, Powers R, Finnegan K, Holzbaur EL, Fischbeck KH, Ludlow CL. (**2005**). Distal spinal and bulbar muscular atrophy caused by dynactin mutation. *Ann Neurol*. May; 57(5): 687-94.

Pun S, Santos AF, Saxena S, Xu L, Caroni P. (**2006**). Selective vulnerability and pruning of phasic motoneuron axons in motoneuron disease alleviated by CNTF. *Nat Neurosci*. Mar; 9(3): 408-19.

Purves D, Augustine GJ, Fitzpatrick D, Katz LC, LaMantia AS, McNamara JO and Williams SM. (**2001**). Neuroscience. 2nd edition. Sunderland, MA, USA. *Sinauer Associates*.

Querol-Vilaseca M, Colom-Cadena M, Pegueroles J, San Martín-Paniello C, Clarimon J, Belbin O, Fortea J, Lleó A. (**2017**). YKL-40 (Chitinase 3-like I) is expressed in a subset of astrocytes in Alzheimer's disease and other tauopathies. *J Neuroinflammation*. 14: 118.

Rabin RL, Park MK, Liao F, Swofford R, Stephany D, Farber JM. (**1999**). Chemokine receptor responses on T cells are achieved through regulation of both receptor expression and signaling. *J Immunol*. 162: 3840–50.

Rabinovici GD. and Miller BL. (**2010**). Frontotemporal lobar degeneration: epidemiology, pathophysiology, diagnosis and management. *CNS drugs*. May; 24(5): 375-98.

Rademakers R, Neumann M, Mackenzie IR. (**2012**). Advances in understanding the molecular basis of frontotemporal dementia. *Nat Rev Neurol*. Aug; 8(8): 423-34.

Raes G, Noël W, Beschin A, Brys L, de Baetselier P, Hassanzadeh GH. (**2002**). FIZZ1 and Ym as tools to discriminate between differentially activated macrophages. *Dev Immunol*. Sep; 9(3): 151-9.

Ramon y Cajal S. (**1909**). Histologie du système nerveux de l'homme et des vertébrés. Maloine, Paris. ISBN: 9788400005986.

Ransohoff JD, Wei Y, Khavari PA. (**2018**). The functions and unique features of long intergenic non-coding RNA. *Nat Rev Mol Cell Biol*. 19, 143-157.

Ransohoff RM. and Brown MA. (**2012**). Innate immunity in the central nervous system. *J Clin Invest*. Apr; 122(4): 1164-71.

Ransohoff RM. and Perry VH. (**2009**). Microglial physiology: unique stimuli, specialized responses. *Annu Rev Immunol*. 27: 119-45.

Rasband MN. (**2011**). Composition, assembly, and maintenance of excitable membrane domains in myelinated axons. *Semin. Cell Dev. Biol*. Apr; 22(2): 178-84.

Rasband MN. (**2016**). Glial contributions to neural function and disease. *Mol Cell Proteomics*. Feb 1; 15(2): 355-361.

Rascovsky K, Hodges JR, Knopman D, Mendez MF, Kramer JH, Neuhaus J, van Swieten JC, Seelaar H, Dopper EG, Onyike CU, Hillis AE, Josephs KA, Boeve BF, Kertesz A, Seeley WW, Rankin KP, Johnson JK, Gorno-Tempini ML, Rosen H, Prioleau-Latham CE, Lee A, Kipps CM, Lillo P, Piguet O, Rohrer JD, Rossor MN, Warren JD, Fox NC, Galasko D, Salmon DP, Black SE, Mesulam M, Weintraub S, Dickerson BC, Diehl-Schmid J, Pasquier F, Deramecourt V, Lebert F, Pijnenburg Y, Chow TW, Manes F, Grafman J, Cappa SF, Freedman M, Grossman M, Miller BL. (**2011**). Sensitivity of revised diagnostic criteria for the behavioural variant of frontotemporal dementia. *Brain*. Sep; 134(Pt 9): 2456-77.

Ratnavalli E, Brayne C, Dawson K, Hodges JR. (**2002**). The prevalence of frontotemporal dementia. *Neurology*. 2002 Jun 11; 58(11): 1615-21.

Reaume AG, Elliott JL, Hoffman EK, Kowall NW, Ferrante RJ, Siwek DF, Wilcox HM, Flood DG, Beal MF, Brown Jr. RH, Scott RW, Snider WD. (**1996**). Motor neurons in Cu/Zn superoxide dismutase-deficient mice develop normally but exhibit enhanced cell death after axonal injury. *Nat. Genet.* May; 13(1): 43-7.

Reck-Peterson SL. (**2015**). Dynactin revealed. *Nat Struct Mol Biol*. May; 22(5): 359-60.

Renton AE, Majounie E, Waite A, Simón-Sánchez J, Rollinson S, Gibbs JR, Schymick JC, Laaksovirta H, van Swieten JC, Myllykangas L, Kalimo H, Paetau A, Abramzon Y, Remes AM, Kaganovich A, Scholz SW, Duckworth J, Ding J, Harmer DW, Hernandez DG, Johnson JO, Mok K, Ryten M, Trabzuni D, Guerreiro RJ, Orrell RW, Neal J, Murray A, Pearson J, Jansen IE, Sondervan D, Seelaar H, Blake D, Young K, Halliwell N, Callister JB, Toulson G, Richardson A, Gerhard A, Snowden J, Mann D, Neary D, Nalls MA, Peuralinna T, Jansson L, Isoviita VM, Kaivorinne AL, Hölttä-Vuori M, Ikonen E, Sulkava R, Benatar M, Wuu J, Chiò A, Restagno G, Borghero G, Sabatelli M; ITALSGEN Consortium, Heckerman D, Rogaeva E, Zinman L, Rothstein JD, Sendtner M, Drepper C, Eichler EE, Alkan C, Abdullaev Z, Pack SD, Dutra A, Pak E, Hardy J, Singleton A, Williams NM, Heutink P, Pickering-Brown S, Morris HR, Tienari PJ, Traynor BJ. (**2011**). A hexanucleo-tide repeat expansion in C9ORF72 is the cause of chromosome 9p21-linked ALS-FTD. *Neuron*. Oct 20; 72(2): 257-68.

Rentzos M, Evangelopoulos E, Sereti E, Zouvelou V, Marmara S, Alexakis T, Evdokimidis I. (**2012**). Alterations of T cell subsets in ALS: a systemic immune activation? *Acta Neurol Scand*. 125: 260–64.

Ringholz GM, Appel SH, Bradshaw M, Cooke NA, Mosnik DM, Schulz PE. (**2005**). Prevalence and patterns of cognitive impairment in sporadic ALS. *Neurology*. Aug 23; 65(4): 586-90.

Rizzo F, Riboldi G, Salani S, Nizzardo M, Simone C, Corti S, Hedlund E. (**2014**). Cellular therapy to target neuroinflammation in amyotrophic lateral sclerosis. *Cell Mol Life Sci*. 71(6): 999-1015.

Robberecht W and Philips T. (**2013**). The changing scene of amyotrophic lateral sclerosis. *Nat Rev Neurosci*. Apr; 14(4): 248-64.

Roberson ED, Hesse JH, Rose KD, Slama H, Johnson JK, Yaffe K, Forman MS, Miller CA, Trojanowski JQ, Kramer JH, Miller BL. (**2005**). Frontotemporal dementia progresses to death faster than Alzheimer disease. *Neurology*. Sep 13; 65(5): 719-25.

Roberts AJ, Kon T, Knight PJ, Sutoh K, Burgess SA. (**2013**). Functions and mechanics of dynein motor proteins. *Nat Rev Mol Cell Biol*. Nov; 14(11): 713-26.

Roberts BR, Tainer JA, Getzoff ED, Malencik DA, Anderson SR, Bomben VC, Meyers KR, Karplus PA, Beckman JS. (**2007**). Structural characterization of zinc-deficient human superoxide dismutase and implications for ALS. *J. Mol. Biol.* Nov 2; 373(4): 877-90.

Rohrer JD, Rossor MN, Warren JD. (**2010**). Syndromes of nonfluent primary progressive aphasia: a clinical and neurolinguistic analysis. *Neurology*. Aug 17; 75(7): 603-10.

Rosen DR, Siddique T, Patterson D, Figlewicz DA, Sapp P, Hentati A, Donaldson D, Goto J, O'Regan JP, Deng HX, Rahmani Z, Krizus A, McKenna-Yasek D, Cayabyab A, Gaston SM, Berger R, Tanzi RE, Halperin JJ, Herzfeldt B, Van den Bergh R, Hung WY, Bird T, Deng G, Mulder DW, Smyth C, Laing NG, Soriano E, Pericak–Vance MA, Haines J, Rouleau GA, Gusella JS, Horvitz HR, Brown RH Jr. (**1993**). Mutations in Cu/Zn superoxide dismutase gene are associated with familial amyotrophic lateral sclerosis. *Nature*. Mar 4; 362(6415):59-62.

Rosenfeld J, King RM, Jackson CE, Bedlack RS, Barohn RJ, Dick A, et al. (**2008**). Creatine monohydrate in ALS: effects on strength, fatigue, respiratory status and ALSFRS. *Amyotroph. Lateral Scler*. 9: 266–272.

Rosenfeld J. (**2001**). "Creatine monohydrate in amyotrophic lateral sclerosis: preliminary results," in Proceedings of the American Academy of Neurology Annual Meeting Philadelphia, PA.

Rossi D, Volanti P, Brambilla L, Colletti T, Spataro R, La Bella V. (**2018**). CSF neurofilament proteins as diagnostic and prognostic biomarkers for amyotrophic lateral sclerosis. *J Neurol*. 265: 510–21.

Roth MP, Malfroy L, Offer C, Sevin J, Enault G, Borot N, Pontarotti P, Coppin H. (**1995**). The human myelin oligodendrocyte glycoprotein (MOG) gene: complete nucleotide sequence and structural characterization. *Genomics*. 28: 241–50.

Rothstein JD, Dykes-Hoberg M, Pardo CA, Bristol LA, Jin L, Kuncl RW, Kanai Y, Hediger MA, Wang Y, Schielke JP, Welty DF. (**1996**). Knockout of glutamate transporters reveals a major role for astroglial transport in excitotoxicity and clearance of glutamate. *Neuron*. Mar; 16(3): 675-86.

Rothstein JD, Patel S, Regan MR, Haenggeli C, Huang YH, Bergles DE, Jin L, Dykes Hoberg M, Vidensky S, Chung DS, Toan SV, Bruijn LI, Su ZZ, Gupta P, Fisher PB. (**2005**). β-Lactam antibiotics offer neuroprotection by increasing glutamate transporter expression. Nature. Jan 6; 433(7021): 73-7.

Rothstein JD, Van KM, Levey AI, Martin LJ, Kuncl RW. (**1995**). Selective loss of glial glutamate transporter GLT-1 in amyotrophic lateral sclerosis. *Ann Neurol*. Jul; 38(1): 73-84.

Rothstein JD. (**1995**). Excitotoxic mechanisms in the pathogenesis of amyotrophic lateral sclerosis. *Adv Neurol*. 68: 7–20.

Rothstein JD. (**2009**). Current hypotheses for the underlying biology of amyotrophic lateral sclerosis. *Ann Neurol*. (Suppl 1); 65:S3–9.

Rowland LP and Shneider NA. (**2001**). Amyotrophic lateral sclerosis. *N Engl J Med.*; May 31; 344(22): 1688-700.

Rowland LP. (**1998**). Diagnosis of amyotrophic lateral sclerosis. *J Neurol Sci*. Oct; 160 Suppl. 1:S6-24.

Rowland LP. (**2001**). "How amyotrophic lateral sclerosis got its name: the clinical-pathologic genius of Jean-Martin Charcot". *Arch. Neurol.* Mar; 58(3): 512-5.

Ruegsegger C. and Saxena S. (**2016**). Proteostasis impairment in ALS. *Brain Res*. Oct 1; 1648(Pt B): 571-579.

Saberi S, Stauffer JE, Schulte DJ, Ravits J. (**2015**). Neuropathology of amyotrophic lateral sclerosis and its variants. *Neurol Clin.* Nov; 33(4): 855-76

Saher G. and Stumpf SK. (**2015**). Cholesterol in myelin biogenesis and hypomyelinating disorders. *Biochim. Biophys. Acta*. Aug; 1851(8): 1083-94.

Sakata T, Palumbo J, Akimoto M, Tanaka M. (**2016**). A long-term safety and efficacy extension study of patients diagnosed with amyotrophic lateral sclerosis (ALS) and treated with edaravone (MCI-186) (P3.192). *Neurology* 86: (Suppl. P3.192).

Sampathu DM, Neumann M, Kwong LK, Chou TT, Micsenyi M, Truax A, Bruce J, Grossman M, Trojanowski JQ, Lee VM. (**2006**). Pathological heterogeneity of frontotemporal lobar degeneration with ubiquitin-positive inclusions delineated by ubiquitin immunohistochemistry and novel monoclonal antibodies. *Am J Pathol.* Oct; 169(4): 1343-52.

Sanadgol N, Golab F, Mostafaie A, Mehdizadeh M, Abdollahi M, Sharifzadeh M, et al. (**2016**). Ellagic acid ameliorates cuprizone-induced acute CNS inflammation via restriction of microgliosis and down-regulation of CCL2 and CCL3 pro-inflammatory chemokines. *Cell Mol Biol* 62: 24–30. doi:10.14715/cmb/2016.62.12.5.

Sanai N, Tramontin AD, Quinones-Hinojosa A, Barbaro NM, Gupta N, Kunwar S, Lawton MT, McDermott MW, Parsa AT, Manuel-Garcia Verdugo J, Berger MS, Alvarez-Buylla A. (**2004**). Unique astrocyte ribbon in adult human brain contains neural stem cells but lacks chain migration. *Nature*. Feb 19; 427(6976): 740-4.

Sanfilippo C, Longo A, Lazzara F, Cambria D, Distefano G, Palumbo M, Cantarella A, Malaguarnera L, Di Rosa M. (**2017**). CHI3L1 and CHI3L2 overexpression in motor cortex and spinal cord of sALS patients. *Mol Cell Neurosci*. 85:162–69.

Sapp PC, Hosler BA, McKenna-Yasek D, Chin W, Gann A, Genise H, Gorenstein J, Huang M, Sailer W, Scheffler M, Valesky M, Haines JL, Pericak-Vance M, Siddique T, Horvitz HR, Brown RH Jr. (**2003**). Identification of two novel loci for dominantly inherited familial amyotrophic lateral sclerosis. *Am J Hum Genet*. Aug; 73(2): 397-403.

Sardiello M, Palmieri M, di Ronza A, Medina DL, Valenza M, Gennarino VA, Di Malta C, Donaudy F, Embrione V, Polishchuk RS, Banfi S, Parenti G, Cattaneo E, Ballabio A. (**2009**). A gene network regulating lysosomal biogenesis and function. *Science*. Jul 24; 325(5939): 473-7.

Sasaki S and Maruyama S. (**1994**). Immunocytochemical and ultrastructural studies of the motor cortex in amyotrophic lateral sclerosis. *Acta Neuropathol*. 87(6): 578-85.

Sasaki S, Komori T, Iwata M. (**2000**). Excitatory amino acid transporter 1 and 2 immunoreactivity in the spinal cord in amyotrophic lateral sclerosis. *Acta Neuropathol*. Aug; 100(2): 138-44.

Sasaki S, Yamane K, Sakuma H, Maruyama S. (**1989**). Sporadic motor neuron disease with Lewy body-like hyaline inclusions. *Acta Neuropathol*; 78(5): 555-60.

Sasaki S. (**2011**) Autophagy in spinal cord motor neurons in sporadic amyotrophic lateral sclerosis. *J. Neuropathol. Exp. Neurol*. May; 70(5): 349-59.

Sasaki S. and Iwata M. (**1996**). Impairment of fast axonal transport in the proximal axons of anterior horn neurons in amyotrophic lateral sclerosis. *Neurology*. Aug; 47(2): 535-40.

Sasaki S. and Iwata M. (**2007**). Mitochondrial alterations in the spinal cord of patients with sporadic amyotrophic lateral sclerosis. *J. Neuropathol. Exp. Neurol*. Jan; 66(1): 10-6.

Sayre LM, Smith MA, Perry G. (**2011**) Chemistry and biochemistry of oxidative stress in neurodegenerative disease. *Curr Med Chem*. Jun; 8(7): 721-38.

Sazanov LA, Peak-Chew SY, Fearnley IM, Walker JE. (**2000**). Resolution of the membrane domain of bovine complex I into subcomplexes: implications for the structural organization of the enzyme. *Biochemistry*. Jun 20; 39(24): 7229-35.

Schagger H, Link TA, Engel WD, Von Jagow G. (**1986**). Isolation of the eleven protein subunits of the bc1 complex grom beef heart. *Methods Enzymol*. 126: 224–237.

Schellera J, Chalarisb A, Schmidt-Arrasb D, Rose-Johnb S. (**2011**). The pro- and anti-inflammatory properties of the cytokine interleukin-6. *Biochim Biophys Acta Mol. Cell Res*. 1813: 878–88.

Schiffer D, Cordera S, Cavalla P, Migheli A. (**1996**). Reactive astrogliosis of the spinal cord in amyotrophic lateral sclerosis. *J Neurol Sci*. 139 (Suppl): 27–33.

Schludi MH, May S, Grässer FA, Rentzsch K, Kremmer E, Küpper C, Klopstock T, Arzberger T, Edbauer D. (**2015**). Distribution of dipeptide repeat proteins in cellular models and C9orf72 mutation cases suggests link to transcriptional silencing. *Acta Neuropathol*. 4, 537–555. Oct; 130(4): 537-55.

Schmitt S, Castelvetri LC, Simons M. (**2015**). Metabolism and functions of lipids in myelin. *Biochim. Biophys. Acta*. Aug; 1851(8): 999-1005.

Schroer TA. (**2004**). Dynactin. *Annual Review of Cell and Developmental Biology*. Nov; 20: 759–79.

Schubert, Antón LC, Gibbs J, Norbury CC, Yewdell JW, Bennink JR. (**2000**). Rapid degradation of a large fraction of newly synthesized proteins by proteasomes. *Nature*, 404: 770-774.

Scotter EL, Vance C, Nishimura AL, Lee YB, Chen HJ, Urwin H, Sardone V, Mitchell JC, Rogelj B, Rubinsztein DC, Shaw CE. (**2014**). Differential roles of the ubiquitin proteasome system and autophagy in the clearance of soluble and aggregated TDP-43 species. *J. Cell Sci*. Mar 15; 127(Pt 6): 1263-78.

Sellier C, Campanari ML, Julie Corbier C, Gaucherot A, Kolb-Cheynel I, Oulad-Abdelghani M, Ruffenach F, Page A, Ciura S, Kabashi E, Charlet-Berguerand N. (**2016**). Loss of C9ORF72 impairs autophagy and synergizes with polyQ Ataxin-2 to induce motor neuron dysfunction and cell death. *EMBO J*. Jun 15; 35(12): 1276-97.

Sephton CF, Cenik B, Cenik BK, Herz, J, Yu G. (**2012**). TDP-43 in CNS development and function: clues to TDP-43-associated neurodegeneration. *Biological Chemistry*. 393(7): 589–594.

Sephton CF, Cenik C, Kucukural A, Dammer EB, Cenik B, Han Y, Dewey CM, Roth FP, Herz J, Peng J, Moore MJ, Yu G. (**2011**). Identification of neuronal RNA targets of TDP-43-containing ribonucleoprotein complexes. *J Biol Chem*. Jan 14; 286(2): 1204-15.

Seri B, Garcia-Verdugo JM, McEwen BS, Alvarez-Buylla A. (**2001**). Astrocytes give rise to new neurons in the adult mammalian hippocampus. *J Neurosci*. Sep 15; 21(18): 7153-60.

Sharma LK, Lu J, Bai Y. (**2009**). Mitochondrial respiratory complex I: structure, function and implication in human diseases. *Curr Med Chem*. 16(10): 1266-77.

Shaw PJ and Eggett CJ. (**2000**). Molecular factors underlying selective vulnerability of motor neurons to neurodegeneration in amyotrophic lateral sclerosis. J. Neurol., Mar; 247 Suppl. 1: I17-27.

Shaw PJ, Ince PG, Falkous G, Mantle D. (**1995**). Oxidative damage to protein in sporadic motor neuron disease spinal cord. *Ann. Neurol*. Oct; 38(4): 691-5.

Shaw PJ. and Ince PG. (**1997**). Glutamate, excitotoxicity and amyotrophic lateral sclerosis. *J Neurol.* May; 244 Suppl 2:S3-14.

Shefner JM, Cudkowicz ME, Schoenfeld D, Conrad T, Taft J, Chilton M, et al. (**2004**). A clinical trial of creatine in ALS. *Neurology*. 63: 1656-1661.

Shefner JM, Wolff AA, Meng L, Bian A, Lee J, Barragan D, et al. (**2016**). A randomized, placebo-controlled, double-blind phase IIb trial evaluating the safety and efficacy of tirasemtiv in patients with amyotrophic lateral sclerosis. *Amyotroph. Lateral Scler. Frontotemporal Degener*. 17:426-435.

Shen WC, Li HY, Chen GC, Chern Y, Tu PH. (**2015**). Mutations in the ubiquitin-binding domain of OPTN/optineurin interfere with autophagy-mediated degradation of misfolded proteins by a dominant-negative mechanism. *Autophagy*. Apr 3; 11(4): 685-700.

Shi N, Kawano Y, Tateishi T, Kikuchi H, Osoegawa M, Ohyagi Y, Kira J. (**2007**). Increased IL-13-producing T cells in ALS: positive correlations with disease severity and progression rate. *J Neuroimmunol.* 182: 232–35.

Shibata N, Nagai R, Uchida K, Horiuchi S, Yamada S, Hirano A, Kawaguchi M, Yamamoto T, Sasaki S, Kobayashi M. (**2001**). Morphological evidence for lipid peroxidation and protein glycoxidation in spinal cords from sporadic amyotrophic lateral sclerosis patients. *Brain Res*. Oct 26; 917(1): 97-104.

Shih AY, Johnson DA, Wong G, Kraft AD, Jiang L, Erb H, Johnson JA, Murphy TH. (**2003**). Coordinate regulation of glutathione biosynthesis and release by Nrf2-expressing glia potently protects neurons from oxidative stress. *J Neurosci*. Apr 15; 23(8): 3394-406.

Shimada T, Yoshida T, Yamagata K. (**2016**). Neuritin mediates activity-dependent axonal branch formation in part via FGF signaling. *J Neurosci*. 36:4534–48.

Shobha K, Alladi PA, Nalini A, Sathyaprabha TN, Raju TR. (**2010**). Exposure to CSF from sporadic amyotrophic lateral sclerosis patients induces morphological transformation of astroglia and enhances GFAP and S100beta expression. *Neurosci Lett*. Mar 31; 473(1): 56-61.

Sidaway P. (**2017**). Motor neuron disease: peripheral immune cell levels correlate with disease progression in ALS. *Nat Rev Neurol*. 13: 708.

Siegel GJ, Agranoff BW, Wayne Albers R, Fisher SK, Uhler MD. (**2011**). Basic Neurochemistry: Molecular, Cellular and Medical Aspects. 8th edition. Cambridge, MA, USA. Academic Press.

Siekevitz P. (**1957**). Powerhouse of the cell. *Scientific American*. 197(1): 131–140.

Sievers J, Parwaresch R, Wottge HU. (**1994**). Blood monocytes and spleen macrophages differentiate into microglia-like cells on monolayers of astrocytes: morphology. *Glia*. Dec; 12(4): 245-58.

Siklos L, Engelhardt J, Harati Y, Smith RG, Joo F, Appel SH. (**1996**). Ultrastructural evidence for altered calcium in motor nerve terminals in amyotropic lateral sclerosis. *Ann Neurol*. Feb; 39(2): 203-16.

Simons M. and Trotter J. (**2007**). Wrapping it upthe cell biology of myelination. *Curr. Opin. Neurobiol.* Oct; 17(5): 533-40.

Simpson RJ, Hammacher A, Smith DK, Matthews JM, Ward LD. (**1997**). Interleukin-6: structure-function relationships. *Protein Sci.* 6:929–55.

Sirohi D. and Kuhn RJ. (**2017**). Can an FDA-Approved Alzheimer's Drug Be Repurposed for Alleviating Neuronal Symptoms of Zika Virus?. *M Bio*. Jun 27; 8(3). pii: e00916-17.

Siveke JT. and Hamann A. (**1998**). T helper 1 and T helper 2 cells respond differentially to chemokines. *J Immunol.* 160: 550–4.

Skibinski G, Parkinson NJ, Brown JM, Chakrabarti L, Lloyd SL, Hummerich H, Nielsen JE, Hodges JR, Spillantini MG, Thusgaard T, Brandner S, Brun A, Rossor MN, Gade A, Johannsen P, Sørensen SA, Gydesen S, Fisher EM, Collinge J. (**2005**). Mutations in the endosomal ESCRTIII-complex subunit CHMP2B in frontotemporal dementia. *Nat Genet*. Aug; 37(8): 806-8.

Skovronsky DM, Lee VM, Trojanowski JQ. (**2006**). Neurodegenerative diseases: new concepts of pathogenesis and their therapeutic implications. *Annu Rev Pathol*.; 1:151-70.

Smith CW, Marlin SD, Rothlein R, Toman C, Anderson DC. (**1989**). Cooperative interactions of LFA-1 and MAC-1 with intercellular adhesion molecule-1 in facilitating adherence and transendothelial migration of human neutrophils in vitro. *J Clin Invest* 83: 2008–17.

Sofroniew MV. (**2005**). Reactive astrocytes in neural repair and protection. *Neuroscientist*. Oct; 214(7): 630-41.

Sofroniew MV. (**2014**). Astrogliosis. *Cold Spring Harb Perspect Biol*. Nov 7; 7(2): a020420.

Son JH, Shim JH, Kim KH, Ha JY, Han JY. (**2012**). Neuronal autophagy and neurodegenerative diseases. *Exp Mol Med*. Feb 29; 44(2): 89-98.

Sorenson EJ, Windbank AJ, Mandrekar JN, Bamlet WR, Appel SH, Armon C, et al. (**2008**). Subcutaneous IGF-1 is not beneficial in 2-year ALS trial. *Neurology* 71: 1770–1775.

Sreedharan J, Blair IP, Tripathi VB, Hu X, Vance C, Rogelj B, Ackerley S, Durnall JC, Williams KL, Buratti E, Baralle F, de Belleroche J, Mitchell JD, Leigh PN, Al-Chalabi A, Miller CC, Nicholson G, Shaw CE. (**2008**). TDP-43 mutations in familial and sporadic amyotrophic lateral sclerosis. *Science*. Mar 21; 319(5870): 1668-72.

Sta M, Sylva-Steenland RM, Casula M, de Jong JM, Troost D, Aronica E, et al. (**2011**). Innate and adaptive immunity in amyotrophic lateral sclerosis: evidence of complement activation. *Neurobiol Dis*. 42: 211–20.

Stein M, Keshav S, Harris N, Gordon S. (**1992**). Interleukin 4 potently enhances murine macrophage mannose receptor activity: a marker of alternative immunologic macrophage activation. *J Exp Med*. Jul 1; 176(1): 287-92.

Steinacker P, Feneberg E, Weishaupt J, Brettschneider J, Tumani H, Andersen PM, von Arnim CA, Böhm S, Kassubek J, Kubisch C, Lulé D, Müller HP, Muche R, et al. Neurofilaments in the diagnosis of motoneuron diseases: a prospective study on 455 patients. *J Neurol Neurosurg Psychiatry*. 2016; 87:12–20.

Stepanova T, Slemmer J, Hoogenraad CC, Lansbergen G, Dortland B, De Zeeuw CI, Grosveld F, Van Cappellen G, Akhmanova A, Galjart N. (**2003**). Visualization of microtubule growth in cultured neurons via the use of EB3-GFP (end-binding protein 3-green fluorescent protein). *J Neurosci*. Apr 1; 23(7): 2655-64.

Stephens B, Guiloff RJ, Navarrete R, Newman P, Nikhar N, Lewis P. (**2006**). Widespread loss of neuronal populations in the spinal ventral horn in sporadic motor neuron disease. A morphometric study. *J Neurol Sci.* May 15; 244(1-2): 41-58.

Stribl C, Samara A, Trumbach D, et al. (**2014**). Mitochondrial dysfunction and decrease in body weight of a transgenic knock-in mouse model for TDP-43. *J Biol Chem* 289: 10769–84.

Ström AL, Gal J, Shi P, Kasarskis EJ, Hayward LJ, Zhu H. (**2008**). Retrograde axonal transport and motor neuron disease. *J Neurochem*. Jul; 106(2): 495–505.

Strong MJ, Hortobágyi T, Okamoto K, et al. (**2011**). Amyotrophic lateral sclerosis, primary lateral sclerosis, and spinal muscular atrophy. In: Dickson DW, Weller RO, eds. Neurodegeneration: The Molecular Pathology of Dementia and Movement Disorders. 2nd edn. Oxford: Wiley-Blackwell. 418–33.

Strong MJ, Volkening K, Hammond R, Yang W, Strong W, Leystra-Lantz C, Shoesmith C. (**2007**). TDP43 is a human low molecular weight neurofilament (hNFL) mRNA-binding protein. *Mol Cell Neurosci*. 35 (2): 320–7.

Strong MJ. (**2008**). The syndromes of frontotemporal dysfunction in amyotrophic lateral sclerosis. *Amyotroph Lateral Scler*. Dec; 9(6):323-38..

Sullivan PM, Zhou X, Robins AM, Paushter DH, Kim D, Smolka MB, Hu F. (**2016**). The ALS/FTLD associated protein C9orf72 associates with SMCR8 and WDR41 to regulate the autophagy-lysosome pathway. *Acta Neuropathol Commun*. May 18; 4(1): 51.

Sun Y, Meijer DH, Alberta JA, Mehta S, Kane MF, Tien AC, Fu H, Petryniak MA, Potter GB, Liu Z, Powers JF, Runquist IS, Rowitch DH, Stiles CD. (**2011**). Phosphorylation state of Olig2 regulates proliferation of neural progenitors. *Neuron*. 2011; 69:906–17.

Sumner BE. (**1975**). A quantitative analysis of boutons with different types of synapse in normal and injured hypoglossal nuclei. *Exp Neurol* 49: 406–17.

Swartz JR, Miller BL, Lesser IM, Darby AL. (**1997**). Frontotemporal dementia: treatment response to serotonin selective reuptake inhibitors. *J Clin Psychiatry*. May; 58 (5): 212–6.

Swerdlow RH, Parks JK, Cassarino DS, Trimmer PA, Miller SW, Maguire DJ, Sheehan JP, Maguire RS, Pattee G, Juel VC, Phillips LH, Tuttle JB, Bennett JP Jr, Davis RE, Parker WD Jr. (**1998**). Mitochondria in sporadic amyotrophic lateral sclerosis. *Exp. Neurol.* Sep; 153(1): 135-42.

Tahara K, Kim HD, Jin JJ, Maxwell JA, Li L, Fukuchi K. (**2006**). Role of toll-like receptor signalling in Abeta uptake and clearance. *Brain*. 2006; 129:3006–19.

Takalo M, Salminen A, Soininen H, Hiltunen M, Haapasalo A. (**2013**). Protein aggregation and degradation mechanisms in neurodegenerative diseases. *Am. J. Neurodegener. Dis*. 2(1): 1-14.

Takeuchi R, Tada M, Shiga A, Toyoshima Y, Konno T, Sato T, Nozaki H, Kato T, Horie M, Shimizu H, Takebayashi H, Onodera O, Nishizawa M, Kakita A, Takahashi H. (**2016**). Heterogeneity of cerebral TDP-43 pathology in sporadic amyotrophic lateral sclerosis: Evidence for clinico-pathologic subtypes. *Acta Neuropathol Commun*. Jun 23; 4(1): 61.

Tan RH, Shepherd CE, Kril JJ, McCann H, McGeachie A, McGinley C, Affleck A, Halliday GM. (**2013**). Classification of FTLD-TDP cases into pathological subtypes using antibodies against phosphorylated and non-phosphorylated TDP43. *Acta Neuropathol Commun*. 1(1): 33.

Tan SY and Shigaki D. (**2007**). Jean-Martin Charcot (1825-1893): pathologist who shaped modern neurology. *Singapore Med J.* May; 48(5): 383-4.

Tanaka M, Sakata T, Palumbo J, Akimoto M. (**2016a**). A 24-week, phase III, double-blind, parallel-group study of edaravone (MCI-186) for treatment of amyotrophic lateral sclerosis (ALS) (P3.189). *Neurology* 86: (Suppl. P3.189).

Tanaka M, Sakata T, Palumbo J, Akimoto M. (**2016b**). A double-blind, parallel-group, placebo-controlled, 24-week, exploratory study of edaravone (MCI-186) for the treatment of advanced amyotrophic lateral sclerosis (ALS) (P3.191). *Neurology.* 86: (Suppl. P3.191).

Tarkar A, Loges NT, Slagle CE, et al. (**2013**). DYX1C1 is required for axonemal dynein assembly and ciliary motility. *Nat Genet* 45: 995–1003.

Taylor JP, Brown RH, Cleveland DW. (**2016**). Decoding ALS: from genes to mechanism. *Nature* Nov 10; 539(7628): 197-206.

Teva (**2010**). News Release. Available at: http://ir.tevapharm.com/phoenix.zhtml?c=73925&p=irol-newsArticle&ID=1555496.

Thaxton C, Pillai AM, Pribisko AL, Dupree JL, Bhat MA. (**2011**). Nodes of Ranvier act as barriers to restrict invasion of flanking paranodal domains in myelinated axons. *Neuron*. Jan 27; 69(2): 244-57.

The SO, Killeen N, Tarakhovsky A, Littman DR, The HS. (**1997**). CD2 regulates the positive selection and function of antigen-specific CD4-CD8 T cells. *Blood* 89: 1308–18.

Thompson AG, Gray E, Thézénas ML, Charles PD, Evetts S, Hu MT, Talbot K, Fischer R, Kessler BM, Turner MR. (**2018**). Cerebrospinal fluid macrophage biomarkers in amyotrophic lateral sclerosis. *Ann Neurol*. 2018; 83:258–68.

Thorpe JR, Tang H, Atherton J, Cairns NJ. (**2008**). Fine structural analysis of the neuronal inclusions of frontotemporal lobar degeneration with TDP-43 proteinopathy. *J Neural Transm*. Dec; 115(12): 1661-71.

Tollervey JR, Curk T, Rogelj B, Briese M, Cereda M, Kayikci M, König J, Hortobágyi T, Nishimura AL, Zupunski V, Patani R, Chandran S, Rot G, Zupan B, Shaw CE, Ule J. (**2011**). Characterizing the RNA targets and position-dependent splicing regulation by TDP-43. *Nat Neurosci*. Apr; 14(4):452-8.

Tomanek L. (**2015**). Proteomic responses to environmentally induced oxidative stress. *J Exp Biol*. Jun; 218(Pt 12): 1867-79.

Tomiyama M, Kimura T, Maeda T, Tanaka H, Furusawa K, Kurahashi K, Matsunaga M. (**2001**). Expression of metabotropic glutamate receptor mRNAs in the human spinal cord: implications for selective vulnerability of spinal motor neurons in amyotrophic lateral sclerosis. *J Neurol Sci*. Aug 15; 189(1-2): 65-9.

Trinchieri G and Sher A. (**2007**). Cooperation of toll-like receptor signals in innate immune defence. *Nat Rev Immunol*. 7: 179–90.

Tu PH, Raju P, Robinson KA, Gurney ME, Trojanowski JQ, Lee VM. (**1996**). Transgenic mice carrying a human mutant superoxide dismutase transgene develop neuronal cytoskeletal pathology resembling human amyotrophic lateral sclerosis lesions. *Proc Natl Acad Sci USA*. Apr 2; 93(7): 3155-60.

Turner BJ and Talbot K. (**2008**). Transgenics, toxicity and therapeutics in rodent models of mutant SOD1-mediated familial ALS. *Prog Neurobiol*. May; 85(1): 94-134.

Turner MR, Brockington A, Scaber J, Hollinger H, Marsden R, Shaw PJ, Talbot K. (**2010**). Pattern of spread and prognosis in lower limb-onset ALS. *Amyotroph Lateral Scler*. Aug; 11(4): 369-73.

Turner MR, Hardiman O, Benatar M, Brooks BR, Chio A, de Carvalho M, Ince PG, Lin C, Miller RG, Mitsumoto H, Nicholson G, Ravits J, Shaw PJ, Swash M, Talbot K, Traynor BJ, Van den Berg LH, Veldink JH, Vucic S, Kiernan MC. (**2013**). Controversies and priorities in amyotrophic lateral sclerosis. *Lancet Neurol*. Mar; 12(3): 310-22.

Twelvetrees AE, Pernigo S, Sanger A, et al. (**2016**). The dynamic localization of cytoplasmic dynein in neurons is driven by kinesin-1. *Neuron* 90: 1000–15.

Umoh ME, Dammer EB, Dai J, Duong DM, Lah JJ, Levey AI, Gearing M, Glass JD, Seyfried NT. (**2018**). A proteomic network approach across the ALS-FTD disease spectrum resolves clinical phenotypes and genetic vulnerability in human brain. *EMBO Mol Med.* 10: 48-62.

Urushitani, Kurisu J, Tsukita K, Takahashi R. (**2002**). Proteasomal inhibition by misfolded mutant superoxide dismutase 1 induces selective motor neuron death in familial amyotrophic lateral sclerosis. *J Neurochem*. Dec; 83(5): 1030-42.

Valdmanis PN, Rouleau GA. (**2008**). Genetics of familial amyotrophic lateral sclerosis. *Neurology*. Jan 8; 70(2): 144-52.

Van Blitterswijk M, DeJesus-Hernandez M, Rademakers R. (**2012**). How do C9ORF72 repeat expansions cause amyotrophic lateral sclerosis and frontotemporal dementia: can we learn from other noncoding repeat expansion disorders? *Curr Opin Neurol*. Dec; 25(6): 689-700.

Van Damme P, Dewil M, Robberecht W, Van Den Bosch L. (**2005**). Excitotoxicity and amyotrophic lateral sclerosis. *Neurodegener Dis*. (3-4): 147-59.

Van Damme P, Robberecht W, Van Den Bosch L. (**2017**). Modelling amyotrophic lateral sclerosis: progress and possibilities. *Dis Model Mech*. May 1; 10(5): 537-549.

Van den Bosch L, Van Damme P, Bogaert E, Robberecht W. (**2006**). The role of excitotoxicity in the pathogenesis of amyotrophic lateral sclerosis. *Biochim Biophys Acta*. Nov-Dec; 1762(11-12): 1068-82.

Van der Zee J, Gijselinck I, Dillen L, Van Langenhove T, Theuns J, Engelborghs S, et al. (**2013**). A pan-European study of the C9orf72 repeat associated with FTLD: geographic prevalence, genomic instability, and intermediate repeats. *Hum. Mutat*. Feb; 34(2): 363-73.

Van Dyke JM, Smit-Oistad IM, Macrander C, Krakora D, Meyer MG, Suzuki M. (**2016**). Macrophage-mediated inflammation and glial response in the skeletal muscle of a rat model of familial amyotrophic lateral sclerosis (ALS). *Exp Neurol*. 277: 275–82.

Vance C, Al-Chalabi A, Ruddy D, Smith BN, Hu X, Sreedharan J, Siddique T, Schelhaas HJ, Kusters B, Troost D, Baas F, de Jong V, Shaw CE. (**2006**). Familial amyotrophic lateral sclerosis with frontotemporal dementia is linked to a locus on chromosome 9p13.2-21.3. *Brain*. Apr; 129(Pt 4): 868-76.

Vance C, Rogelj B, Hortobágyi T, De Vos KJ, Nishimura AL, Sreedharan J, Hu X, Smith B, Ruddy D, Wright P, Ganesalingam J, Williams KL, Tripathi V, Al-Saraj S, Al-Chalabi A, Leigh PN, Blair IP, Nicholson G, de Belleroche J, Gallo JM, Miller CC, Shaw CE. (**2009**). Mutations in FUS, an RNA processing protein, cause familial amyotrophic lateral sclerosis type 6. *Science*. Feb 27; 323(5918): 1208-1211.

Vance C, Scotter EL, Nishimura AL, Troakes C, Mitchell JC, Kathe C, Urwin H, Manser C, Miller CC, Hortobágyi T, Dragunow M, Rogelj B, Shaw CE. (**2013**). ALS mutant FUS disrupts nuclear localization and sequesters wild-type FUS within cytoplasmic stress granules. *Hum Mol Genet*. Jul 1; 22(13): 2676-88.

Vancoillie G, Lambert J, Mulder A, et al. (**2000**). Cytoplasmic dynein colocalizes with melanosomes in normal human melanocytes. *Br J Dermatol.* 143: 298–306.

Vande Velde C, McDonald KK, Boukhedimi Y, McAlonis-Downes M, Lobsiger CS, Bel Hadj S, Zandona A, Julien JP, Shah SB, Cleveland DW. (**2011**) Misfolded SOD1 associated with motor neuron mitochondria alters mitochondrial shape and distribution prior to clinical onset. *PLoS One*. 6(7): e22031.

Varin A. and Gordon S. (**2009**). Alternative activation of macrophages: immune function and cellular biology. *Immunobiology*. 214(7): 30-41.

Vatsavayai SC, Nana AL, Yokoyama JS, Seeley WW. (**2019**) C9orf72-FTD/ALS pathogenesis: Evidence from human neuropathological studies. *Acta Neuropathol* 137: 1-26.

Vaughan KT. and Vallee RB. (**1995**). Cytoplasmic dynein binds dynactin through a direct interaction between the intermediate chains and p150Glued. *J Cell Biol*. Dec; 131 (6 Pt 1): 1507–16.

Velours J, Paumard P, Soubannier V, Spannagel C, Vaillier J, Arselin G, Graves PV. (**2000**). Organisation of the yeast ATP synthase F(0):a study based on cysteine mutants, thiol modification and cross-linking reagents. *Biochim Biophys Acta*. May 31; 1458 (2–3): 443–56.

Verma A. (**2011**). Altered RNA metabolism and amyotrophic lateral sclerosis. *Annals of Indian Academy of Neurology*. 14(4): 239-44.

Verstraete E, Veldink JH, Huisman MHB, Draak T, Uijtendaal EV, van der Kooi AJ, et al. (**2012**). Lithium lacks effect on survival in amyotrophic lateral sclerosis: a phase IIb randomised sequential trial. *J. Neurol. Neurosurg. Psychiatry* 83: 557–564.

Vogel C. and Marcotte EM. (**2012**). Insights into the regulation of protein abundance from proteomic and transcriptomic analyses. *Nat Rev Genet* 13: 227-232.

Volkening K, Leystra-Lantz C, Yang W, Jaffee H, Strong MJ. (**2009**). Tar DNA binding protein of 43 kDa (TDP-43), 14-3-3 proteins and copper/zinc superoxide dismutase (SOD1) interact to modulate NFL mRNA stability. Implications for altered RNA processing in amyotrophic lateral sclerosis (ALS). *Brain Res.* Dec 11; 1305:168-82.

Von Bartheld CS, Bahney J, Herculano-Houzel S. (**2016**). The search for true numbers of neurons and glial cells in the human brain: A review of 150 years of cell counting. *J Comp Neurol*. Dec 15; 524(18): 3865-3895.

Waite AJ, Baumer D, East S, Neal J, Morris HR, Ansorge O, Blake DJ. (**2014**). Reduced C9orf72 protein levels in frontal cortex of amyotrophic lateral sclerosis and frontotemporal degeneration brain with the C9ORF72 hexanucleotide repeat expansion. *Neurobiol Aging* 35: 1779.e5-1779.e13.

Walker LC. and LeVine H. 3rd. (**2000**). The cerebral proteopathies. *Neurobiol. Aging.* Jul-Aug; 21(4): 559-61.

Wallace DC. (**2013**). A mitochondrial bioenergetic etiology of disease. *J Clin Invest*. Apr; 123(4): 1405-12.

Walz W. (**2000**). Controversy surrounding the existence of discrete functional classes of astrocytes in adult gray matter. *Glia*. Aug; 31(2): 95-103.

Wang HY, Wang IF, Bose J, Shen CK. (**2004**). Structural diversity and functional implications of the eukaryotic TDP gene family. *Genomics*. Jan; 83(1): 130-139.

Wang IF, Wu LS, Chang HY, Shen CK. (**2008**). TDP-43, the signature protein of FTLD-U, is a neuronal activity-responsive factor. *J. Neurochemistry*. May; 105 (3): 797–806.

Wang X. and Michaelis EK. (**2010**). Selective neuronal vulnerability to oxidative stress in the brain. *Front Aging Neurosci.* 2, 12.

Warren JD, Rohrer JD, Rossor MN. (**2013**). Clinical review. Frontotemporal dementia. *BMJ*. Aug 6; 347: f4827.

Watts GD, Wymer J, Kovach MJ, Mehta SG, Mumm S, Darvish D, Pestronk A, Whyte MP, Kimonis VE. (**2004**). Inclusion body myopathy associated with Paget disease of bone and frontotemporal dementia is caused by mutant valosin-containing protein. *Nat Genet*. Apr; 36(4): 377-81.

Webster CP, Smith EF, Bauer CS, Moller A, Hautbergue GM, Ferraiuolo L, Myszczynska MA, Higginbottom A, Walsh MJ, Whitworth AJ, Kaspar BK, Meyer K, Shaw PJ, Grierson AJ, De Vos KJ. (**2016**).The C9orf72 protein interacts with Rab1a and the ULK1 complex to regulate initiation of autophagy. EMBO J. Aug 1; 35(15): 1656-76.

Webster CP, Smith EF, Shaw PJ, De Vos KJ. (**2017**). Protein homeostasis in amyotrophic lateral sclerosis: Therapeutic opportunities? *Front Mol Neurosci.* May 2; 10:123.

Wen X, Tan W, Westergard T, Krishnamurthy K, Markandaiah SS, Shi Y, Lin S, Shneider NA, Monaghan J, Pandey UB, Pasinelli P, Ichida JK, Trotti D5. (**2014**). Antisense proline-arginine RAN dipeptides linked to C9ORF72-ALS/FTD form toxic nuclear aggregates that initiate in vitro and in vivo neuronal death. *Neuron*. Dec 17; 84(6): 1213-25.

Weydt P, Oeckl P, Huss A, Müller K, Volk AE, Kuhle J, Knehr A, Andersen PM, Prudlo J, Steinacker P, Weishaupt JH, Ludolph AC, Otto M. (**2016**). Neurofilament levels as biomarkers in asymptomatic and symptomatic familial amyotrophic lateral sclerosis. *Ann Neurol*. 79: 152–58.

Wiedemann FR, Manfredi G, Mawrin C, Beal MF, Schon EA. (**2002**). Mitochondrial DNA and respiratory chain function in spinal cords of ALS patients. *J. Neurochem*. Feb; 80(4): 616-25.

Wiedemann FR, Winkler K, Kuznetsov AV, Bartels C, Vielhaber S, Feistner H, Kunz WS. (**1998**). Impairment of mitochondrial function in skeletal muscle of patients with amyotrophic lateral sclerosis. *J Neurol Sci*. 156(1): 65-72.

Wiemerslage L. and Lee D. (**2016**). Quantification of mitochondrial morphology in neurites of dopaminergic neurons using multiple parameters. *J Neurosci Methods*. Mar 15; 262: 56-65.

Wiley CA, Bonneh-Barkay D, Dixon CE, Lesniak A, Wang G, Bissel SJ, Kochanek PM. (**2015**). Role for mammalian chitinase 3-like protein 1 in traumatic brain injury. *Neuropathology*. 35: 95–106.

Wilhelmsson U, Bushong EA, Price DL, Smarr BL, Phung V, Terada M, Ellisman MH, Pekny M. (**2006**). Redefining the concept of reactive astrocytes as cells that remain within their unique domains upon reaction to injury. *Proc. Natl. Acad. Sci. USA*. Nov 14; 103(46): 17513-8.

Williamson TL. and Cleveland DW. (**1999**). Slowing of axonal transport is a very early event in the toxicity of ALS-linked SOD1 mutants to motor neurons. *Nat Neurosci.* Jan; 2(1): 50-6.

Wojcik C, Rowicka M, Kudlicki A, Nowis D, McConnell E, Kujawa M, DeMartino GN. (**2006**). Valosin-containing protein (p97) is a regulator of endoplasmic reticulum stress and of the degradation of N-end rule and ubiquitin-fusion degradation pathway substrates in mammalian cells. *Mol Biol Cell*. Nov; 17(11): 4606-18.

Wong PC, Pardo CA, Borchelt DR, Lee MK, Copeland NG, Jenkins NA, Sisodia SS, Cleveland DW, Price DL. (**1995**). An adverse property of a familial ALS-linked SOD1 mutation causes motor neuron disease characterized by vacuolar degeneration of mitochondria. *Neuron*. Jun; 14(6): 1105-16.

Xi Z, Zinman L, Moreno D, Schymick J, Liang Y, Sato C, Zheng Y, Ghani M, Dib S, Keith J, Robertson J, Rogaeva E. (**2013**). Hypermethylation of the CpG island near the G4C2 repeat in ALS with a C9orf72 expansion. *Am J Hum Genet.* 92: 981-989.

Xia D, Esser L, Tang WK, Zhou F, Zhou Y, Yu L, Yu CA. (**2013**). Structural analysis of cytochrome bc1 complexes: implications to the mechanism of function. *Biochim. Biophys. Acta*. Nov-Dec; 1827(11-12): 1278-94.

Xia Q, Wang H, Hao Z, Fu C, Hu Q, Gao F, Ren H, Chen D, Han J, Ying Z, Wang G. (**2006**). TDP-43 loss of function increases TFEB activity and blocks autophagosome lysosome fusion. *EMBO J.* Jan 18; 35(2): 121-42.

Xie Z. and Klionsky DJ. (**2007**). Autophagosome formation: core machinery and adaptations. *Nat Cell Biol*. Oct; 9(10): 1102-9.

Xu Z, Henderson RD, David M, McCombe PA. (**2016**). Neurofilaments as biomarkers for amyotrophic lateral sclerosis: A systematic review and meta-analysis. *PLoS One*. 11:e0164625.

Yamaguchi H, Kidachi Y, Umetsu H, Ryoyama K. (**2008**). Differentiation of serum-free mouse embryo cells into an astrocytic lineage is associated with the asymmetric production of early neural, neuronal and glial markers. *Biol Pharm Bull*. May; 31(5): 1008-12.

Yamamoto M, Koga Y, Ohtaki E, Nonaka I. (**1989**). Focal cytochrome c oxidase deficiency in various neuromuscular diseases. *J. Neurol. Sci.* Jun; 91(1-2): 207-13.

Yamanaka K, Sasagawa Y, Ogura T. (**2012**). Recent advances in p97/VCP/Cdc48 cellular functions. *Biochim. Biophys. Acta*. Jan; 1823(1): 130-7.

Yim MB, Chock PB, Stadtman ER. (**1990**). Copper, zinc superoxide dismutase catalyzes hydroxyl radical production from hydrogen peroxide. *Proc. Natl. Acad. Sci. USA*. Jul; 87(13): 5006–5010.

Yoshino H. and Kimura A. (**2006**). Investigation of the therapeutic effects of edaravone, a free radical scavenger, on amyotrophic lateral sclerosis (Phase II study). *Amyotroph. Lateral Scler*. 7 241–245.

Zagoraiou L, Akay T, Martin JF, et al. (**2009**). A cluster of cholinergic premotor interneurons modulates mouse locomotor activity. *Neuron* 64: 645–62.

Zhang D, Iyer LM, He F, Aravind L. (**2012**). Discovery of novel DENN proteins: implications for the evolution of eukaryotic intracellular membrane structures and human disease. *Front Genet*. Dec 13; 3:283.

Zhang R, Gascon R, Miller RG, Gelinas DF, Mass J, Hadlock K, Jin X, Reis J, Narvaez A, McGrath MS. (**2005**). Evidence for systemic immune system alterations in sporadic amyotrophic lateral sclerosis (sALS). *J Neuroimmunol*. 159: 215–24.

Zhang X, Li L, Chen S, Yang D, Wang Y, Zhang X, Wang Z, Le W. (**2011**). Rapamycin treatment augments motor neuron degeneration in SOD1(G93A) mouse model of amyotrophic lateral sclerosis. *Autophagy*. Apr; 7(4): 412-25.

Zhang Y, Chen K, Sloan SA, Bennett ML, Scholze, AR, O'Keeffe S, Phatnani HP, Guarnieri P, Caneda C, Ruderisch N, Deng S, Liddelow SA, Zhang C, Daneman R, Maniatis T, Barres BA, Wu JQ. (**2014**). An RNA-sequencing transcriptome and splicing database of glia, neurons, and vascular cells of the cerebral cortex. *J Neurosci*. Sep 3; 34(36): 11929–11947.

Zhang YJ, Gendron TF, Ebbert MTW, O'Raw AD, Yue M, Jansen-West K, Zhang X, Prudencio M, Chew J, Cook CN, Daughrity LM, Tong J, Song Y, Pickles SR, Castanedes-Casey M, Kurti A, Rademakers R, Oskarsson B, Dickson DW, Hu W, Gitler AD, Fryer JD, Petrucelli L. (**2018**). Poly(GR) impairs protein translation and stress granule dynamics in C9orf72-associated frontotemporal dementia and amyotrophic lateral sclerosis. *Nat Med.* 24: 1136-1142.

Zhang YJ, Jansen-West K, Xu YF, Gendron TF, Bieniek KF, Lin WL, Sasaguri H, Caulfield T, Hubbard J, Daughrity L, Chew J, Belzil VV, Prudencio M, Stankowski JN, Castanedes-Casey M, Whitelaw E, Ash PE, DeTure M, Rademakers R, Boylan KB, Dickson DW, Petrucelli L. (**2014**). Aggregation-prone c9FTD/ALS poly(GA) RAN translated proteins cause neurotoxicity by inducing ER stress. *Acta Neuropathol.* 128: 505-524.

Zhang YJ, Xu YF, Cook C, Gendron TF, Roettges P, Link CD, Lin WL, Tong J, Castanedes-Casey M, Ash P, Gass J, Rangachari V, Buratti E, Baralle F, Golde TE, Dickson DW, Petrucelli L. (**2009**). Aberrant cleavage of TDP-43 enhances aggregation and cellular toxicity. *Proc Natl Acad Sci USA*. 106(18):7607–12.

Zhang YJ, Xu YF, Dickey CA, Buratti E, Baralle F, Bailey R, Pickering-Brown S, Dickson D, Petrucelli L. (**2007**). Progranulin mediates caspase-dependent cleavage of TAR DNA binding protein-43. *J Neurosci*. Sep 26; 27(39): 10530-4.

Zhao W, Beers DR, Appel SH. (**2013**). Immune-mediated mechanisms in the pathoprogression of amyotrophic lateral sclerosis. *J Neuroimmune Pharmacol*. Sep; 8(4): 888-99.

Zhao W, Beers DR, Hooten KG, Sieglaff DH, Zhang A, Kalyana-Sundaram S, Traini CM, Halsey WS, Hughes AM, Sathe GM, Livi GP, Fan GH, Appel SH. (**2017**). Characterization of gene expression phenotype in amyotrophic lateral sclerosis monocytes. *JAMA Neurol*. 2017; 74: 677–85.

Zhu J, Nathan C, Jin W, Sim D, Ashcroft GS, Wahl SM, Lacomis L, Erdjument-Bromage H, Tempst P, Wright CD, Ding A. (**2002**). Conversion of proepithelin to epithelins: roles of SLPI and elastase in host defense and wound repair. *Cell*. Dec 13; 111(6): 867-78.

Zhu Q, Zhao X, Zheng K, Li H, Huang H, Zhang Z, Mastracci T, Wegner M, Chen Y, Sussel L, Qiu M. (**2014**). Genetic evidence that Nkx2.2 and Pdgfra are major determinants of the timing of oligodendrocyte differentiation in the developing CNS. *Development*. 141: 548–55.

Zhukareva V, Sundarraj S, Mann D, et al. (**2003**). Selective reduction of soluble tau proteins in sporadic and familial frontotemporal dementias: An international follow-up study. *Acta Neuropathol*. 105: 469–76.

Zhukareva V, Vogelsberg-Ragaglia V, Van Deerlin VM, et al. (**2001**). Loss of brain tau defines novel sporadic and familial tauopathies with frontotemporal dementia. *Ann Neurol* 49: 165–75.

Zu T, Liu Y, Bañez-Coronel M, Reid T, Pletnikova O, Lewis J, Miller TM, Harms MB, Falchook AE, Subramony SH, Ostrow LW, Rothstein JD, Troncoso JC, Ranum LP. (**2013**). RAN proteins and RNA foci from antisense transcripts in C9ORF72 ALS and frontotemporal dementia. *Proc. Natl. Acad. Sci. USA.* Dec 17; 110(51): E4968-77.

Zwingmann C, Richter-Landsberg C, Brand A, Leibfritz D. (**2000)**. NMR spectroscopic study on the metabolic fate of [3-(13)C]alanine in astrocytes, neurons, and cocultures: Implications for glia-neuron interactions in neurotransmitter metabolism. *Glia* 32: 286–303.

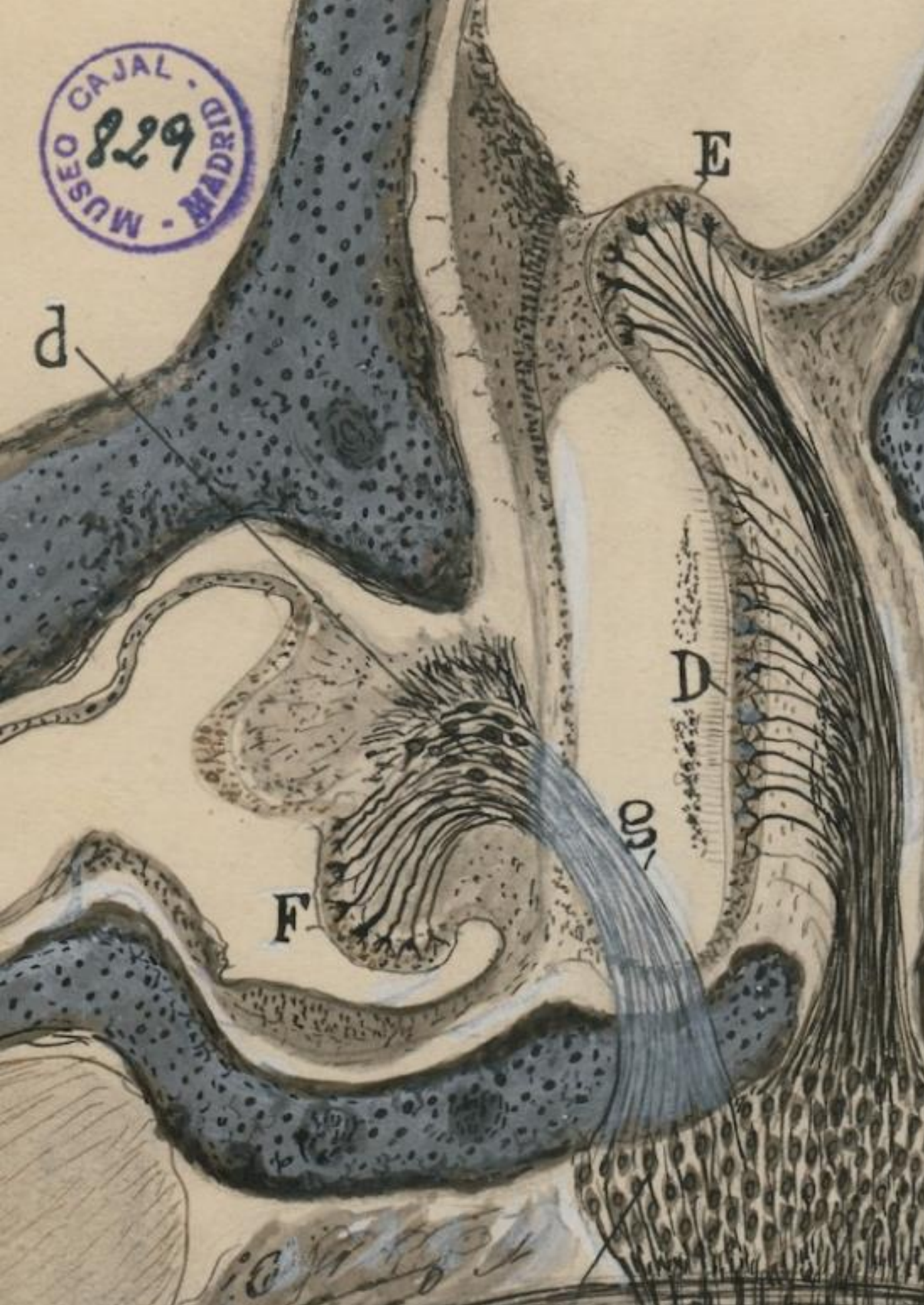

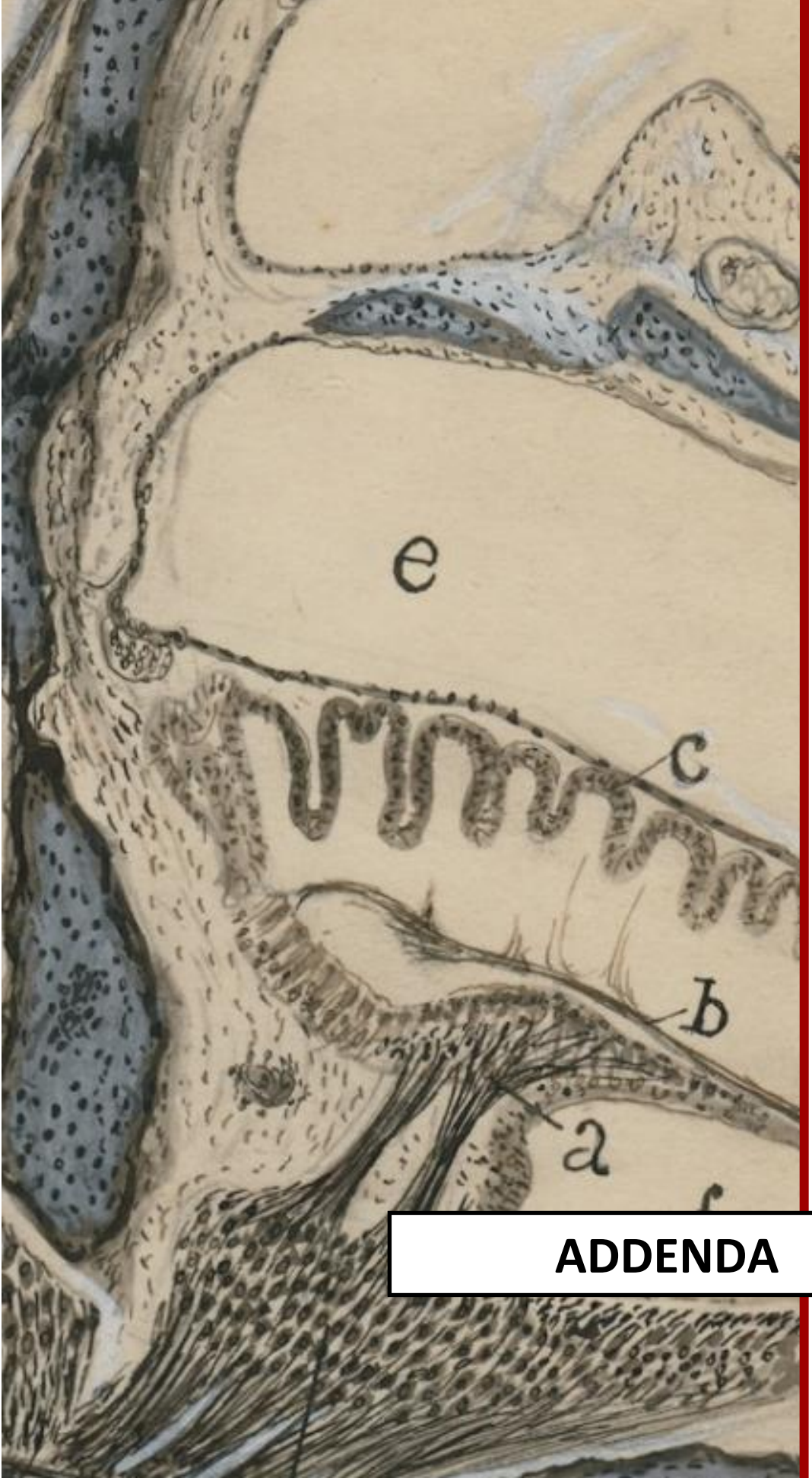

ADDENDA

Additionally, during the PhD student period, the author has also contributed in the following publications:

Cannabinoid receptor 2 participates in Aβ processing in a mouse model of Alzheimer's disease but plays a minor role in the therapeutic properties of a cannabis-based medicine

Aso E, Andrés-Benito P, Carmona M, Moreno J, Maldonado R, Ferrer I.

Journal Alzheimer's Disease. 2016 Feb 6; 2016, 51 (2): 489-500.
doi: 10.3233/JAD-150913.

ABSTRACT

The endogenous cannabinoid system represents a promising therapeutic target to modify neurodegenerative pathways linked to Alzheimer's disease (AD). The aim of the present study was to evaluate the specific contribution of CB2 receptor to the progression of AD-like pathology and its role in the positive effect of a cannabis-based medicine (1:1 combination of Δ9-tetrahidrocannabinol and cannabidiol) previously demonstrated to be beneficial in the AβPP/PS1 transgenic model of the disease. A new mouse strain was generated by crossing AβPP/PS1 transgenic mice with CB2 knockout mice. Results show that lack of CB2 exacerbates cortical Aβ deposition and increases the levels of soluble Aβ40. However, CB2 receptor deficiency does not affect the viability of AβPP/PS1 mice, does not accelerate their memory impairment, does not modify tau hyperphosphorylation in dystrophic neurites associated to Aβ plaques, and does not attenuate the positive cognitive effect induced by the cannabis-based medicine in these animals. These findings suggest a minor role for the CB2 receptor in the therapeutic effect of the cannabis-based medicine in AβPP/PS1 mice, but also constitute evidence of a link between CB2 receptor and Aβ processing.

KEYWORDS: Alzheimer's disease; AβPP/PS1 mice; amyloid; cannabinoid receptor 2; cognitive impairment; tau; therapy; Δ9-tetrahidrocannabinol and cannabidiol

PMID: 26890764

Delineating the efficacy of a cannabis-based medicine at advanced stages of dementia in a murine model

Aso E, Andrés-Benito P, Ferrer I.

Journal Alzheimer's Disease. 2016 Oct 4; 54 (3): 903-912.
doi: 10.3233/JAD-160533.

ABSTRACT

Previous reports have demonstrated that the combination of Δ9-tetrahydrocannabinol (Δ9-THC) and cannabidiol (CBD) botanical extracts, which are the components of an already approved cannabis-based medicine, reduce the Alzheimer-like phenotype of AβPP/PS1 transgenic mice when chronically administered during the early symptomatic stage. Here, we provide evidence that such natural cannabinoids are still effective in reducing memory impairment in AβPP/PS1 mice at advanced stages of the disease but are not effective in modifying the Aβ processing or in reducing the glial reactivity associated with aberrant Aβ deposition as occurs when administered at early stages of the disease. The present study also demonstrates that natural cannabinoids do not affect cognitive impairment associated with healthy aging in wild-type mice. The positive effects induced by Δ9-THC and CBD in aged AβPP/PS1 mice are associated with reduced GluR2/3 and increased levels of GABA-A Rα1 in cannabinoid-treated animals when compared with animals treated with vehicle alone.

KEYWORDS: Advanced stages; Alzheimer's disease; cannabidiol; dementia; Δ9-tetrahydrocannabinol
PMID: 27567873

Transcriptional network analysis in frontal cortex in Lewy body diseases with focus on dementia with Lewy bodies

Santpere G and Garcia-Esparcia P, Andres-Benito P, Lorente-Galdós B, Navarro A, Ferrer I.

Brain Pathol. 2017 Mar 21, 28(3):315-333.
doi: 10.1111/bpa.12511.

ABSTRACT

The present study investigates global transcriptional changes in frontal cortex area 8 in incidental Lewy Body disease (iLBD), Parkinson disease (PD) and Dementia with Lewy bodies (DLB). We identified different coexpressed gene sets associated with disease stages, and gene ontology categories enriched in gene modules and differentially expressed genes including modules or gene clusters correlated to iLBD comprising upregulated dynein genes and taste receptors, and downregulated innate inflammation. Focusing on DLB, we found modules with genes significantly enriched in functions related to RNA and DNA production, mitochondria and energy metabolism, purine metabolism, chaperone and protein folding system and synapses and neurotransmission (particularly the GABAergic system). The expression of more than fifty selected genes was assessed with real time quantitative polymerase chain reaction. Our findings provide, for the first time, evidence of molecular cortical alterations in iLBD and involvement of several key metabolic pathways and gene hubs in DLB which may underlie cognitive impairment and dementia.

KEYWORDS: GABA; Lewy body diseases; axonema; cerebral cortex; chaperones; dementia with Lewy bodies; dynein; mitochondria; neurotransmission; purine metabolism; synapses; taste receptors; transcriptome.

PMID: 28321951

Locus coeruleus at asymptomatic early and middle Braak stages of neurofibrillary tangle pathology

Andrés-Benito P, Fernández-Dueñas V, Carmona M, Escobar LA, Torrejón B, Aso E, Ciruela F, Ferrer I.

Neuropathol Appl Neurobiol. 2017 Aug; 43 (5): 373-392.
doi: 10.1111/nan.12386.

ABSTRACT

AIMS: The present study analyses molecular characteristics of the locus coeruleus (LC) and projections to the amygdala and hippocampus at asymptomatic early and middle Braak stages of neurofibrillary tangle (NFT) pathology. METHODS: Immunohistochemistry, whole-transcriptome arrays and RT-qPCR in LC and western blotting in hippocampus and amygdala in a cohort of asymptomatic individuals at stages I-IV of NFT pathology were used. RESULTS: NFTs in the LC increased in parallel with colocalized expression of tau kinases, increased neuroketal adducts and decreased superoxide dismutase 1 in neurons with hyperphosphorylated tau and decreased voltage-dependent anion channel in neurons containing truncated tau were found. These were accompanied by increased microglia and AIF1, CD68, PTGS2, IL1β, IL6 and TNF-α gene expression. Whole-transcriptome arrays revealed upregulation of genes coding for proteins associated with heat shock protein binding and genes associated with ATP metabolism and downregulation of genes coding for DNA-binding proteins and members of the small nucleolar RNAs family, at stage IV when compared with stage I. Tyrosine hydroxylase (TH) immunoreactivity was preserved in neurons of the LC, but decreased TH and increased α2A adrenergic receptor protein levels were found in the hippocampus and the amygdala. CONCLUSIONS: Complex alteration of several metabolic pathways occurs in the LC accompanying NFT formation at early and middle asymptomatic stages of NFT pathology. Dopaminergic/noradrenergic denervation and increased expression of α2A adrenergic receptor in the hippocampus and amygdala occur at first stage of NFT pathology, suggesting compensatory activation in the face of decreased adrenergic input occurring before clinical evidence of cognitive impairment and depression.

KEYWORDS: Alzheimer's disease; amygdala; hippocampus; locus coeruleus; transcriptome; α2A adrenergic receptor
PMID: 27567873

MicroRNA expression in the locus coeruleus, entorhinal cortex, and hippocampus at early and middle stages of braak neurofibrillary tangle pathology

Llorens F and Thüne K and Andrés-Benito P, Tahir W, Ansoleaga B, Hernández-Ortega K, Martí E, Zerr I, Ferrer I.

J. Mol. Neurosci. 2017 Oct; 63(2): 206-215.
doi: 10.1007/s12031-017-0971-4.

ABSTRACT

The present study analyzes by RT-qPCR the expression of microRNA (miRNA)-27a-3p, miRNA-124-3p, miRNA-132-3p, and miRNA-143-3p in the locus coeruleus (LC), entorhinal cortex (EC), CA1 region of the hippocampus (CA1), and dentate gyrus (DG) of middle-aged (MA) individuals with no brain lesions and of cases at Braak and Braak stages I-II and II-IV of neurofibrillary tangle (NFT) pathology. The most affected region is the LC in which miRNA-27a-3p, miRNA-124-3p, and miRNA-143-3p show a trend to increase at stages I-II and are significantly up-regulated at stages III-IV when compared with MA. Only miRNA-143-3p is up-regulated in the EC at stages III-IV when compared with MA and with stages I-II. No modifications in the expression levels of miRNA-27a-3p, miRNA-124-3p, miRNA-132-3p, and miRNA-143-3p are found in CA1 at any stage, whereas miRNA-124-3p is significantly down-regulated in DG at stages I-II. Accompanying in situ hybridization reveals miRNA-27a-3p, miRNA-124-3p, and miRNA-143-3 localization in neurons, indicating that changes in miRNA expression are not a direct effect of changes in the numbers of neurons and glial cells. Present observations show for the first time important miRNA de-regulation in the LC at the first stages of NFT. Since the LC is the main noradrenergic input to the cerebral cortex, key regulator of mood and depression, and one of the first nuclei affected in aging and Alzheimer's disease (AD), these findings provide insights for additional study of the LC in aging and AD.

KEYWORDS: Alzheimer disease; Entorhinal cortex; Hippocampus; Locus coeruleus; MicroRNA; Neurofibrillary tangle pathology
PMID: 28871468

Altered regulation of KIAA0566, and katanin signalling expression in the locus coeruleus with neurofibrillary tangle pathology

Andrés-Benito P, Delgado-Morales R, Ferrer I.

Front. Cell Neurosci. 2018 May 17; 12:131.
doi: 10.3389/fncel.2018.00131.

ABSTRACT

The locus coeruleus (LC), which contains the largest group of noradrenergic neurons in the central nervous system innervating the telencephalon, is an early and constantly vulnerable region to neurofibrillary tangle (NFT) pathology in aging and Alzheimer's disease (AD). The present study using whole genome bisulfite sequencing and Infinium Human Methylation 450 BeadChip was designed to learn about DNA methylation profiles in LC with age and NFT pathology. This method identified decreased DNA methylation of Katanin-Interacting Protein gene (KIAA0566) linked to age and presence of NFT pathology. KIAA0566 mRNA expression demonstrated with RT-qPCR significantly decreased in cases with NFT pathology. Importantly, KIAA0566 immunoreactivity was significantly decreased only in LC neurons with NFTs, but not in neurons without tau pathology when compared with neurons of middle-aged individuals. These changes were accompanied by a similar pattern of selective p80-katanin reduced protein expression in neurons with NFTs. In contrast, p60-katanin subunit expression levels in the neuropil were similar in MA cases and cases with NFT pathology. Since katanin is a major microtubule-severing protein and KIAA0566 binds and interacts with katanin, de-regulation of the katanin-signaling pathway may have implications in the regulation of microtubule homeostasis in LC neurons with NFTs, thereby potentially interfering with maintenance of the cytoskeleton and transport.

KEYWORDS: Alzheimer's disease; KIAA0556; katanin; locus coeruleus; methylation; microtubules; neurofibrillary tangles
PMID: 29867364

Altered gene transcription in astrocytes and oligodendrocytes in frontal cortex in Creutzfeldt-Jakob disease MM1 and VV2

Andrés-Benito P, Domínguez-González M, Ferrer I.

Prion 2018 Jul 15. 12(3-4):216-225.
doi: 10.1080/19336896.2018.1500076.

ABSTRACT

Targeted expression of genes coding for proteins specific to astrocytes, oligodendrocytes and myelin was performed in frontal cortex area 8 of Creutzfeldt-Jakob disease methionine/methionine and valine/valine (CJD MM1 and VV2, respectively) compared with controls. GFAP (glial fibrillary acidic protein) mRNA was up-regulated whereas SLC1A2 (solute carrier family 1 member 2, coding for glutamate transporter 1: GLT1), AQ4 (aquaporin 4), MPC1 (mitochondrial pyruvate carrier 1) and UCP5 (mitochondrial uncoupled protein 5) mRNAs were significantly down-regulated in CJD MM1 and CJD VV2, and GJA1 (connexin 43) in CJD VV2. OLIG1 and OLIG2 (oligodendocyte transcription factor 1 and 2, respectively), SOX10 (SRY-Box10) and oligodendroglial precursor cell (OPC) marker NG2 (neuronal/glial antigen) 2 were preserved, but GALC (coding for galactosylceramidase), SLC2A1 (solute carrier family 2 member 1: glucose transporter member 1: GLUT1) and MCT1 (monocarboxylic acid transporter 1) mRNA expression levels were significantly reduced in CJD MM1 and CJD VV2. Expression levels of most genes linked to myelin were not altered in the cerebral cortex in CJD. Immunohistochemistry to selected proteins disclosed individual variations but GFAP, Olig-2, AQ4 and GLUT1 correlated with mRNA levels, whereas GLT1 was subjected to individual variations. However, MPC1, UCP5 and MCT1 decrease was more closely related to the respective reduced neuronal immunostaining. These observations support the idea that molecular deficits linked to energy metabolism and solute transport in astrocytes and oligodendrocytes, in addition to neurons, are relevant in the pathogenesis of cortical lesions in CJD.

KEYWORDS: Creutzfeldt-Jakob disease; astrocytes; astrogliopathy; energy metabolism; myelin; oligodendrocytes; oligodendrogliopathy; prion diseases
PMID: 30009661

PPARγ agonist-loaded PLGA-PEG nanocarriers as a potential treatment for Alzheimer's disease: *in vitro* and *in vivo* studies

Silva-Abreu M, Calpena AC, Andrés-Benito P, Aso E, Roig D, Espina M, García ML, Ferrer I, Romero IA, Male D.

Int. J. Nanomedicine. 2018 Sep 20; 13:5577-5590.
doi: 10.2147/IJN.S171490. IF: 4.30

ABSTRACT

OBJECTIVE: The first aim of this study was to develop a nanocarrier that could transport the peroxisome proliferator-activated receptor agonist, pioglitazone (PGZ) across brain endothelium and examine the mechanism of nanoparticle transcytosis. The second aim was to determine whether these nanocarriers could successfully treat a mouse model of Alzheimer's disease (AD). METHODS: PGZ-loaded nanoparticles (PGZ-NPs) were synthesized by the solvent displacement technique, following a factorial design using poly (lactic-co-glycolic acid) polyethylene glycol (PLGA-PEG). The transport of the carriers was assessed in vitro, using a human brain endothelial cell line, cytotoxicity assays, fluorescence-tagged nanocarriers, fluorescence-activated cell sorting, confocal and transmission electron microscopy. The effectiveness of the treatment was assessed in APP/PS1 mice in a behavioral assay and by measuring the cortical deposition of β-amyloid. RESULTS: Incorporation of PGZ into the carriers promoted a 50x greater uptake into brain endothelium compared with the free drug and the carriers showed a delayed release profile of PGZ in vitro. In the doses used, the nanocarriers were not toxic for the endothelial cells, nor did they alter the permeability of the blood-brain barrier model. EM indicated that the nanocarriers were transported from the apical to the basal surface of the endothelium by vesicular transcytosis. An efficacy test carried out in APP/PS1 transgenic mice showed a reduction of memory deficit in mice chronically treated with PGZ-NPs. Deposition of β-amyloid in the cerebral cortex, measured by immunohistochemistry and image analysis, was correspondingly reduced. CONCLUSION: PLGA-PEG nanocarriers cross brain endothelium by transcytosis and can be loaded with a pharmaceutical agent to effectively treat a mouse model of AD.

KEYWORDS: APP/PS1 transgenic mouse; Alzheimer's disease; blood-brain barrier; brain endothelium; nanoparticle; pioglitazone
PMID: 30271148

Genetic deletion of CB1 cannabinoid receptors exacerbates the Alzheimer-like symptoms in a transgenic animal model

Aso E, Andrés-Benito P, Ferrer I.

Biochemical Pharmacology. 2018 Nov; 157: 210-216.
doi: 10.1016/j.bcp.2018.08.007.

ABSTRACT

Activating CB1 cannabinoid receptor has been demonstrated to produce certain therapeutic effects in animal models of Alzheimer's disease (AD). In this study, we evaluated the specific contribution of CB1 receptor to the progression of AD-like pathology in double transgenic APP/PS1 mice. A new mouse strain was generated by crossing APP/PS1 transgenic mice with CB1 knockout mice. Genetic deletion of CB1 drastically reduced the survival of APP/PS1 mice. In spite that CB1 mutant mice bearing the APP/PS1 transgene developed normally, they suddenly died within the first two months of life likely due to spontaneous seizures. This increased mortality could be related to an imbalance in the excitatory/inhibitory transmission in the hippocampus as suggested by the reduced density of inhibitory parvalbumin positive neurons observed in APP/PS1 mice lacking CB1 receptor at 7 weeks of age. We also evaluated the AD-like phenotype of APP/PS1 mice heterozygous for the CB1 deletion at 3 and 6 months of age. The memory impairment associated to APP/PS1 transgene was accelerated in these mice. Neither the soluble levels of Aβ or the density of Aβ plaques were modified in APP/PS1 mice heterozygous for CB1 deletion at any age. However, the reduction in CB1 receptor expression decreased the levels of PSD-95 protein in APP/PS1 mice, suggesting a synaptic dysfunction in these animals that could account for the acceleration of the memory impairment observed. In summary, our results suggest a crucial role for CB1 receptor in the progression of AD-related pathological events.

KEYWORDS: APP/PS1 mice; Alzheimer's disease; Amyloid; Cannabinoid receptor 1; Cognitive impairment
PMID: 30096288

Wnt signaling alterations in the human spinal cord of ALS cases: spotlight on Fz2, Fz5 and Wnt5a

González-Fernández C, González P, Andrés-Benito P, Ferrer I, Rodríguez FJ.

Mol. Neurobiology. 2019 Mar 28.
doi: 10.1007/s12035-019-1547-9.

ABSTRACT

Amyotrophic lateral sclerosis (ALS) is a fatal neurodegenerative disorder with no cure, and elucidation of the mechanisms mediating neuronal death in this neuropathology is crucial to develop effective treatments. It has recently been demonstrated in animal models that the Wnt family of proteins is involved in this neuropathology, although its potential involvement in case of humans is almost unknown. We analyzed the expression of Wnt signaling components in healthy and ALS human spinal cords by quantitative RT-PCR, and we found that most Wnt ligands, modulators, receptors, and co-receptors were expressed in healthy controls. Moreover, we observed clear alterations in the mRNA expression of different components of this family of proteins in human spinal cord tissue from ALS cases. Specifically, we detected a significant increase in the mRNA levels of Wnt3, Wnt4, Fz2, and Fz8, together with several non-significant increases in the mRNA expression of other genes such as Wnt2b, Wnt5a, Fz3, Lrp5, and sFRP3. Based on these observations and on previous reports of studies performed in animal models, we evaluated with immunohistochemistry the protein expression patterns of Fz2 and Fz5 receptors and their main ligand Wnt5a in control samples and ALS cases. No substantial changes were observed in Fz5 protein expression pattern in ALS samples. However, we detected an increase in the amount of Fz2+ astrocytes in the borderline between gray and white matter at the ventral horn in ALS samples. Finally, Wnt5a expression was observed in neurons and astrocytes in both control and ALS samples, although Wnt5a immunolabeling in astroglial cells was significantly increased in ALS spinal cords in the same region where changes in Fz2 were observed. Altogether, these observations strongly suggest that the Wnt family of proteins, and more specifically Fz2 and Wnt5a, might be involved in human ALS pathology.

KEYWORDS: ALS; Frizzled; Human; Spinal cord; Wnt
PMID: 30924074

Involvement of oligodendrocytes in Tau seeding and spreading in tauopathies

Ferrer I, Aguiló García M, Carmona M, Andrés-Benito P, Torrejón-Escribano B, Garcia-Esparcia P, Del Rio JA.

Front. Aging Neurosci. 2019 May 28; 11:112
doi: 10.3389/fnagi.2019.00112.

ABSTRACT

INTRODUCTION: Human tau seeding and spreading occur following intracerebral inoculation into different gray matter regions of brain homogenates obtained from tauopathies in transgenic mice expressing wild or mutant tau, and in wild-type (WT) mice. However, little is known about tau propagation following inoculation in the white matter. OBJECTIVES: The present study is geared to learning about the patterns of tau seeding and cells involved following unilateral inoculation in the corpus callosum of homogenates from sporadic Alzheimer's disease (AD), primary age-related tauopathy (PART: neuronal 4Rtau and 3Rtau), pure aging-related tau astrogliopathy (ARTAG: astroglial 4Rtau with thorn-shaped astrocytes TSAs), globular glial tauopathy (GGT: 4Rtau with neuronal tau and specific tau inclusions in astrocytes and oligodendrocytes, GAIs and GOIs, respectively), progressive supranuclear palsy (PSP: 4Rtau with neuronal inclusions, tufted astrocytes and coiled bodies), Pick's disease (PiD: 3Rtau with characteristic Pick bodies in neurons and tau containing fibrillar astrocytes), and frontotemporal lobar degeneration linked to P301L mutation (FTLD-P301L: 4Rtau familial tauopathy). METHODS: Adult WT mice were inoculated unilaterally in the lateral corpus callosum with sarkosyl-insoluble fractions or with sarkosyl-soluble fractions from the mentioned tauopathies; mice were killed from 4 to 7 months after inoculation. Brains were fixed in paraformaldehyde, embedded in paraffin and processed for immunohistochemistry. RESULTS: Tau seeding occurred in the ipsilateral corpus callosum and was also detected in the contralateral corpus callosum. Phospho-tau deposits were found in oligodendrocytes similar to coiled bodies and in threads. Moreover, tau deposits co-localized with active (phosphorylated) tau kinases p38 and ERK 1/2, suggesting active tau phosphorylation of murine tau. TSAs, GAIs, GOIs, tufted astrocytes, and tau-containing fibrillar astrocytes were not seen in any case. Tau deposits were

often associated with slight myelin disruption and the presence of small PLP1-immunoreactive globules and dots in the ipsilateral corpus callosum 6 months after inoculation of sarkosyl-insoluble fractions from every tauopathy. CONCLUSIONS: Seeding and spreading of human tau in the corpus callosum of WT mice occurs in oligodendrocytes, thereby supporting the idea of a role of oligodendrogliopathy in tau seeding and spreading in the white matter in tauopathies. Slight differences in the predominance of threads or oligodendroglial deposits suggest disease differences in the capacity of tau seeding and spreading among tauopathies.

KEYWORDS: Tau, tauopathies, seeding and spreading, AD, ARTAG, GGT, PiD
PMID: 31191295

Cannabidiol-enriched extract reduced the cognitive impairment but not the epileptic seizures of a Lafora's disease animal model

Aso E, Andrés-Benito P, Grau-Escolano J, Caltana L, Brusco A, Sanz P, Ferrer I.

Cannabis and Cannabinoid Research. 27 Jun 2019.
doi: 10.1089/can.2019.0005.

ABSTRACT

Lafora disease (LD) is a rare form of progressive infantile epilepsy in which a rapid neurological deterioration occurs as the disease advances, leading the patients to a vegetative state and then death, usually within the first decade of disease onset. Based on the capacity of the endogenous cannabinoid system (ECS) to modulate several cellular processes commonly altered in many neurodegenerative processes, as well as the antiepileptic properties of certain natural cannabinoids, the aim of the present study was to evaluate the role of the ECS in LD progression and to test whether a natural cannabis extract highly enriched in cannabidiol (CBD) might be effective in curbing the pathological phenotype of malin knockout (KO) mice as an animal model of LD. Our results reveal for the first time that alterations in the ECS occur during the evolution of LD, mainly at the level of CB1, CB2 and GPR55 receptors expression, and that a CBD-enriched extract is able to reduce the cognitive impairment exhibited by malin KO mice. However, in contrast to what has previously been reported for other kinds of refractory epilepsy in childhood, the CBD-enriched extract does not reduce the severity of the epileptic seizures induced in this animal model of LD.

KEYWORDS: Cannabidiol, Cognitive impairment, Epilepsy, Phytocannabinoids
PMID:

Relevance of host tau in tau seeding and spreading in tauopathies

Ferrer I, Zelaya MV, Aguiló García M, Carmona M, López-González I, Andrés-Benito P, Lidón L, Gavín R, Garcia-Esparcia P, Del Rio JA.

Brain Pathol. (Accepted 26/06/2019)
doi:

ABSTRACT

Introduction: Human tau seeding and spreading occur following intracerebral inoculation of brain homogenates obtained from tauopathies in transgenic mice expressing natural or mutant tau, and in wild-type (WT) mice. Objectives: The present study was geared to learning about the patterns of tau seeding, the cells involved, and the characteristics of tau following intracerebral inoculation of homogenates from primary age-related tauopathy (PART: neuronal 4Rtau and 3Rtau), aging-related tau astrogliopathy (ARTAG: astrocytic 4Rtau), and globular glial tauopathy (GGT: 4Rtau with neuronal deposits and specific tau inclusions in astrocytes and oligodendrocytes). Methods: Young and adult WT mice were inoculated unilaterally in the hippocampus or in the lateral corpus callosum with sarkosyl-insoluble fractions from PART, ARTAG, and GGT cases, and were killed at variable periods of three to seven months. Brains were processed for immunohistochemistry in paraffin sections. Results: Tau seeding occurred in the ipsilateral hippocampus and corpus callosum and spread to the septal nuclei, periventricular hypothalamus and contralateral corpus callosum, respectively. Tau deposits were mainly found in neurons, oligodendrocytes, and threads; the deposits were diffuse or granular, composed of phosphorylated tau, tau with abnormal conformation, and 3Rtau and 4Rtau independently of the type of tauopathy. Truncated tau at the aspartic acid 421 and ubiquitination were absent. Tau deposits had the characteristics of pre-tangles. A percentage of intracellular tau deposits co-localized with active (phosphorylated) tau kinases p38 and ERK 1/2. Conclusions: Seeding and spreading of human tau into the brain of WT mice involves neurons and glial cells, mainly oligodendrocytes, thereby supporting the idea of a primary role of oligodendrogliopathy, together with neuronopathy, in the progression of tauopathies. Human tau inoculation modifies murine tau metabolism with the production and deposition of 3Rtau and 4Rtau, and by activation of specific tau kinases in affected cells. Key words: tau, tauopathies, primary age-related

tauopathy, aging-related tau astrogliopathy, globular glial tauopathy, seeding, spreading.

KEYWORDS: tau, tauopathies, primary age-related tauopathy, aging-related tau astrogliopathy, globular glial tauopathy, seeding, spreading.
PMID:

Nuclear lipidome is altered in amyotrophic lateral sclerosis: a preliminary study

Ramirez-Nuñez O, Jové M, Torres P, Sol J, Fontdevila L, Romero-Guevara R, Ayala V, Rossi C, Boada J, Povedano M, Andrés-Benito P, Ferrer I, Pamplona R, Portero-Otín M.

Under revision. (Submitted 25/06/2019)

ABSTRACT

In this pilot study, we show that nuclei in spinal cord from ALS patients exhibit a differential lipidomic signature. Among the differential lipid species we could annotate 41 potential identities. These comprise membrane-bound lipids such as phosphatidylethanolamines -including plasmalogens- and phosphatidylcholines but also other lipid classes such as glycosphingolipids, diacylglycerols, and triacylglycerides (potentially present as nuclear lipid droplets). These results were orthogonally validated by showing loss of alkyldihydroxyacetonephosphate synthase (AGPS), a key peroxisomal enzyme in plasmalogen synthesis, both in ALS necropsy samples, in human motor neurons derived from iPSC from ALS patients and in hSOD-G93A transgenic mice. Further, diacylglycerol content changes were associated to ALS-linked variations in related-enzymes, such as phospholipase C βI (PLCβI), the source of nuclear diacylglycerol, and protein kinase CβII (PKCβII), whose function partially depends on nuclei concentration of diacylglycerol. These results point out for not only a role of nuclear membrane lipids but also to lipids present in the nucleoplasm, suggesting an undisclosed role for this part of the subcellular lipidome in ALS pathophysiology.

KEYWORDS: lipidomic, peroxisome, nuclear envelope, amyotrophic lateral sclerosis

PMID: XXXX

A non-canonical senescence profile in the spinal cord of the ALS model hSOD1-G93A

Torres P, Anerillas C, Encinas M, Povedano M, Andrés-Benito P, Ferrer I, Ayala V, Pamplona R, Portero-Otín M

Under revision. (Submitted 08/05/2019)

The present study was addressed to explore cellular senescence mechanisms and senescence-associated secretory phenotype (SASP) markers in the familial amyotrophic lateral sclerosis (ALS) transgenic mouse model hSOD1-G93A. We evaluate senescence biomarkers, including p16 and p21 by reverse-transcriptase quantitative PCR (RT-qPCR), immunofluorescence (IF) and immunohistochemistry (IHC), as well as senescence associated beta galactosidase (SA-beta-gal) activity in the lumbar spinal cords (LSC) of this model. We also quantified the mRNA levels of SASP markers and its association with the potential dysfunction of TAR-DNA binding of 43 kDa (TDP-43). Our results show an atypical senescence-profile in LSC from transgenic mice, with an increase of p16 and p21 mRNA and protein levels in glial cells with a mostly cytoplasmic pattern, without the canonical increase of SA-beta-gal activity. Consistent with enhanced SASP, there is an increase of Il1a and Il6. TDP43 splicing activity is compromised in this ALS model and it is significantly associated with the p16 mRNA increase. Globally, our findings support the existence of a non-canonical profile of senescence biomarkers in the LSC of the ALS model hSOD1-G93A.

KEYWORDS: Cell senescence; amyotrophic lateral sclerosis; motor neuron; cryptic exon; senescenceassociated secretory phenotype; cell cycle
PMID: XXXX

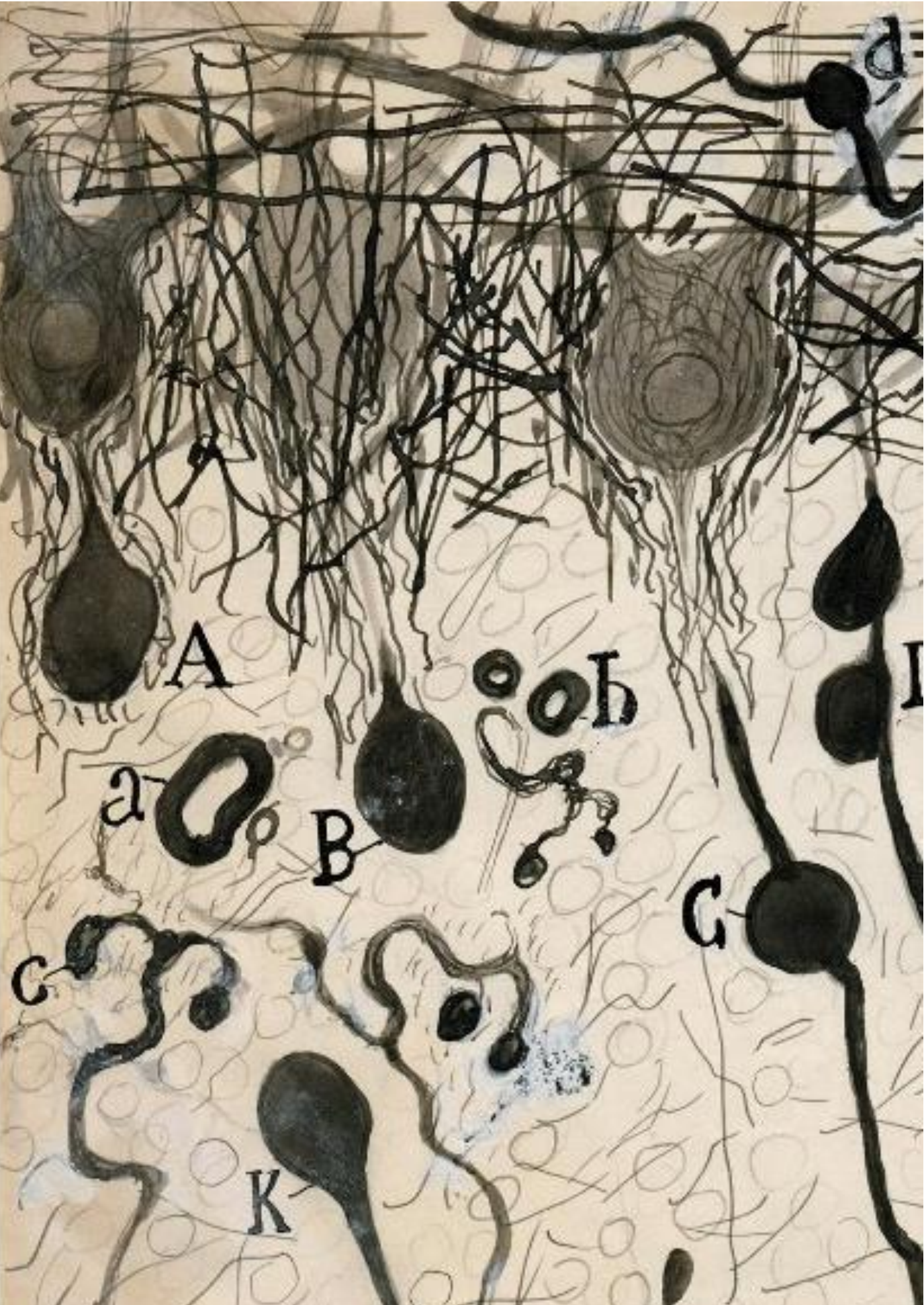
d
A
b
a
B
c
C
K

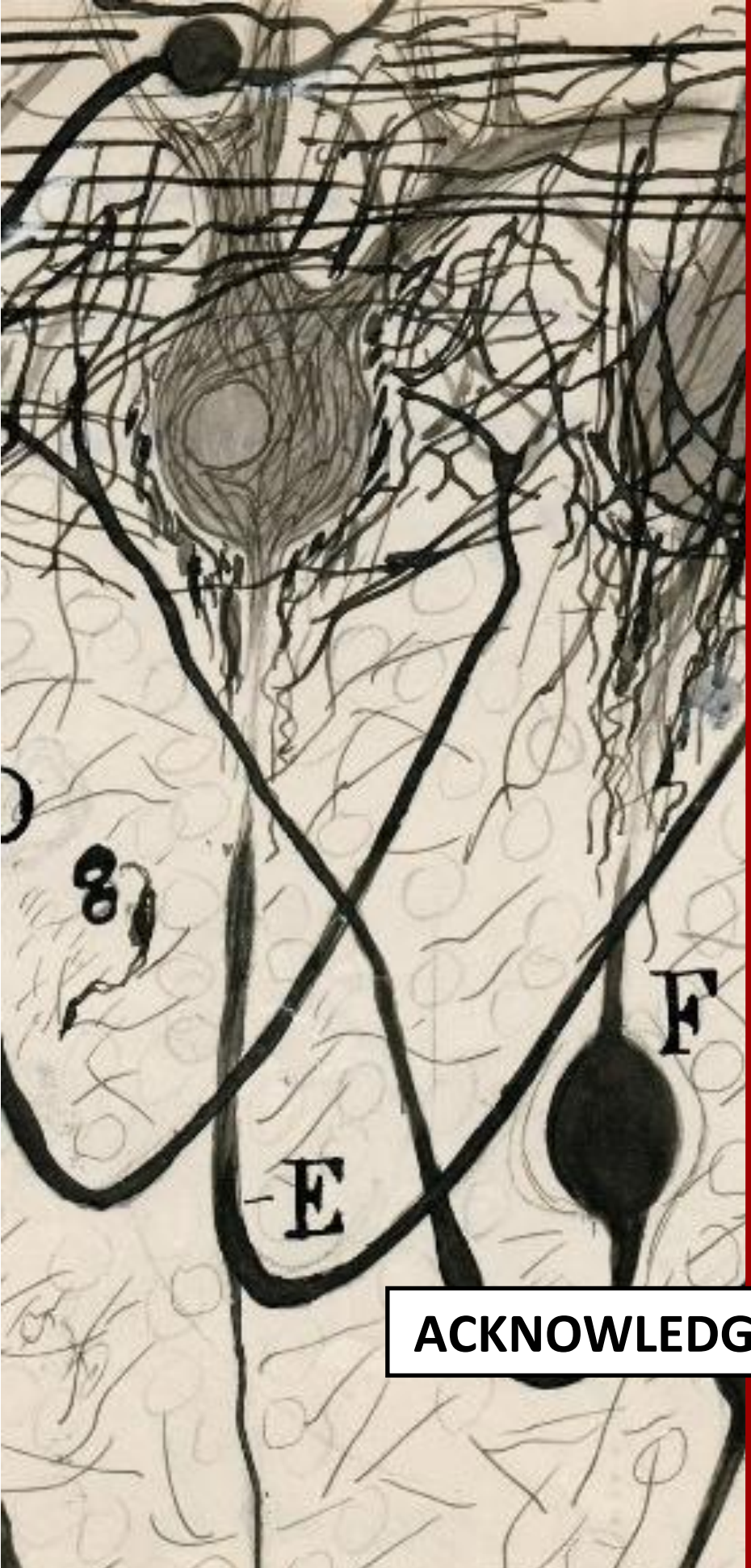

ACKNOWLEDGEMENTS

Acknowledgements